Magneplane International • Massachusetts Institute of Technology
United Engineers and Constructors • Raytheon Equipment Division
Failure Analysis Associates • Bromwell & Carrier
Beech Aircraft Corporation • Process Systems International

SYSTEM CONCEPT DEFINITION REPORT

for the

NATIONAL MAGLEV INITIATIVE

Volume 2

3.2.1. SYSTEM DESCRIPTION - VEHICLE
3.2.2. SYSTEM DESCRIPTION - MAGWAY
3.2.3. SYSTEM DESCRIPTION - SYSTEMWIDE
INDEX

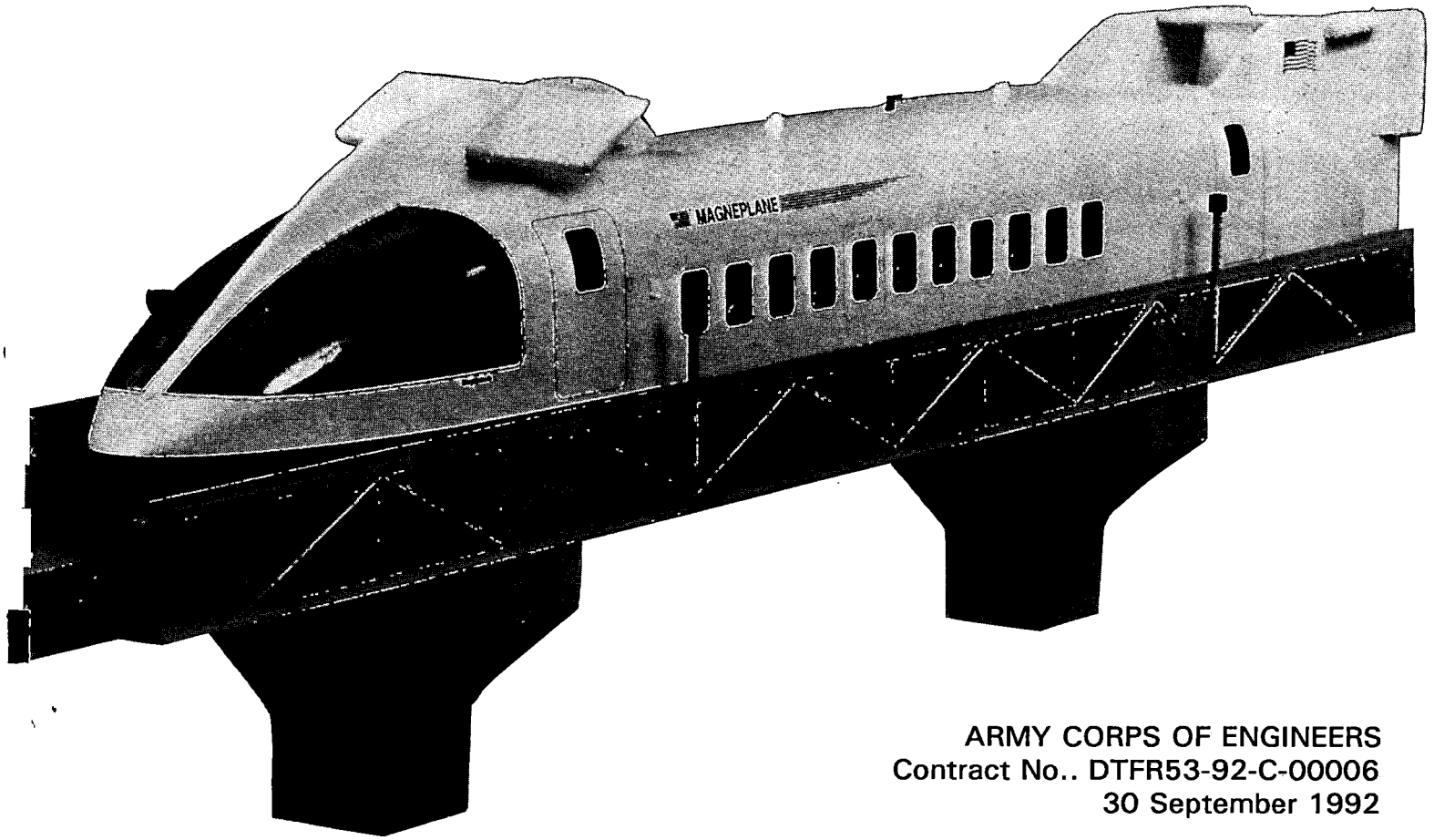

ARMY CORPS OF ENGINEERS
Contract No.. DTFR53-92-C-00006
30 September 1992

Magneplane International, Inc.
Jet Aviation Terminal, Hanscom Field West
Bedford, Massachusetts 01730
phone: 617 274 8750; fax: 617 274 8747

INDEX TO VOLUMES

LIMITED RIGHTS NOTICE

(a) These data are submitted with limited rights under Government contract No. DTFR53-92-C-00006. These data may be reproduced and used by the Government with the express limitation that they will not, without written permission of the Contractor, be used for purposes of manufacture nor disclosed outside the Government; except that the Government may disclose these data outside the Government for the following purposes, provided that the Government makes such disclosure subject to prohibition against further use and disclosure:

(i) This data shall be available, in whole or in part, for use within the Government for the purpose of analysis, and future system acquisition planning. This data may be combined with other data to form a unified system performance definition or acquisition plan. The data may then be made available to other members of the Government or potential non-Government sources which possess a bona fide interest in the Maglev program. This includes the incorporation of said data into future acquisitions for Maglev system development or any other procurement. The data may also be made available for review and comment by private sources commissioned by the Government.

(ii) Review and comment by private sources commissioned by the Government.

(b) This Notice shall be marked on any reproduction of these data, in whole or in part.

(End of notice)

3.2.1. SYSTEM DESCRIPTION - VEHICLE

CONTENTS

FIGURES

3.2.1.a. LEVITATION SYSTEM

3.2.1.a.1. MAGNET DESIGN & CONFIGURATION

3.2.1.a.1.1. COIL ARRANGEMENT IN BOGIES

A cross-sectional sketch of the vehicle, together with the levitation and propulsion coil modules, is shown in Figure 1. Each bogie has two levitation coil modules of two coils each and one propulsion module with six coils in it. The relative position of the levitation and propulsion coils has been chosen to partially reduce stray field effects.

The operating clearance between the vehicle and magway at the design point of 150 m/s is 0.15 m. The magway aluminum sheets are each nominally 1.5 m wide and 0.02 m thick. The space around the centerline for the synchronous drive windings is nominally 1.4 m. The magway sheets extend beyond the 1.5 meter dimension shown to allow for a tilt of +/- 3 deg, plus banking requirements.

The approximate dimensions for the 140 passenger vehicle, which has a total weight of 50,000 kg, are shown in Figure 2. Passengers are in a central cabin and two levitation/propulsion bogies are used. Figure 3 is a similar sketch for a 45 passenger vehicle with a total weight of 25,000 kg. It also uses two bogies, each with two levitation coil modules of two coils each and one propulsion module with six coils in it.

A schematic of the present baseline dimensions for coils in a bogie, together with the amp-turns required for the 140 passenger vehicle are shown in Figure 4. The levitation coils are excited with opposing polarity so that each levitation module of two coils forms a quadrupole to help reduce the stray fields. This sketch represents the forward bogie, which has the propulsion coils shifted forward of the levitation coils to help reduce the stray fields in the passenger section of the vehicle. The rear bogie is identical, but rotated 180 degrees so that the propulsion coils "trail" the levitation coils, again to reduce the stray fields in the passenger section.

The above information concerning the number of coils per bogie, etc for each vehicle is summarized in Figure 5. In addition it indicates the number of independent circuits chosen as a baseline. For example, levitation coils will be designed to be electrically independent and have separate cryostats for each coil in each module for redundancy. This will be coupled with other design constraints (eg-low ratio of operating current to critical current) to assure that loss of levitating action in one coil in a module does not cause a total loss of module lift. On the other hand, all propulsion coils in a bogie will be in series electrically and in a common cryostat. This will allow a savings in weight and heat load on the cryogenic system, while retaining some propulsion capability for the vehicle even if one module becomes inoperative, because there is still a propulsion module in the other bogie.

3.2.1.a.1.2. COIL-MAGWAY INTERACTION SUMMARY

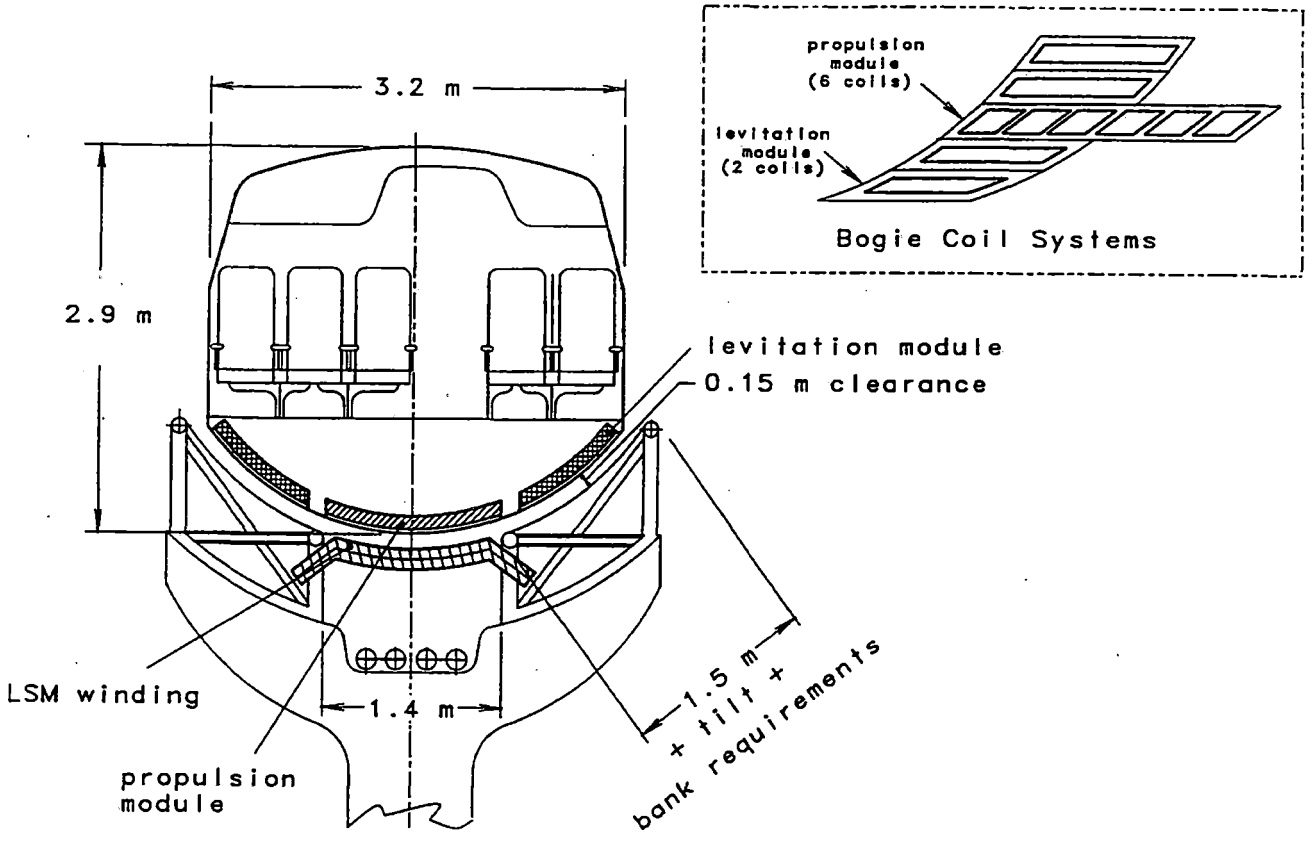

Figure 1 Vehicle cross-section sketch (4-14-92) - dimensions approximate

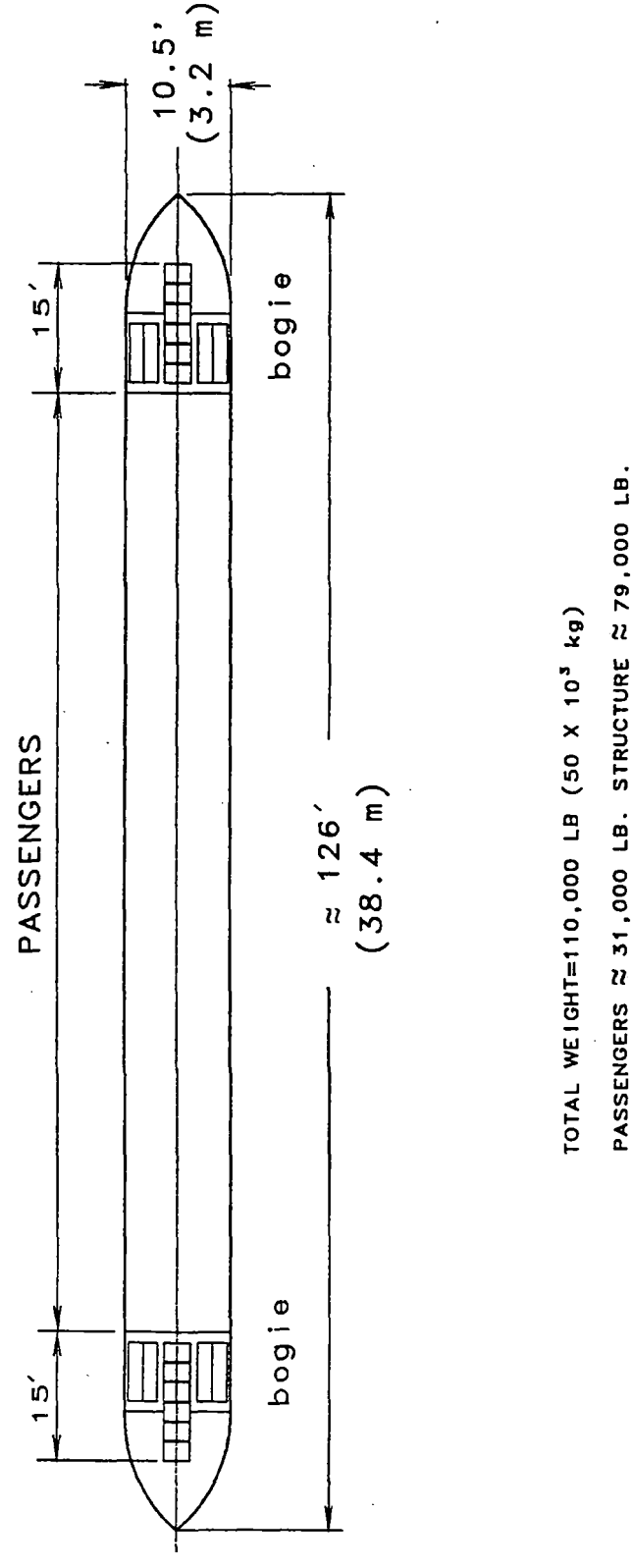

Figure 2 Baseline vehicle outline (140 passengers) - dimensions approximate

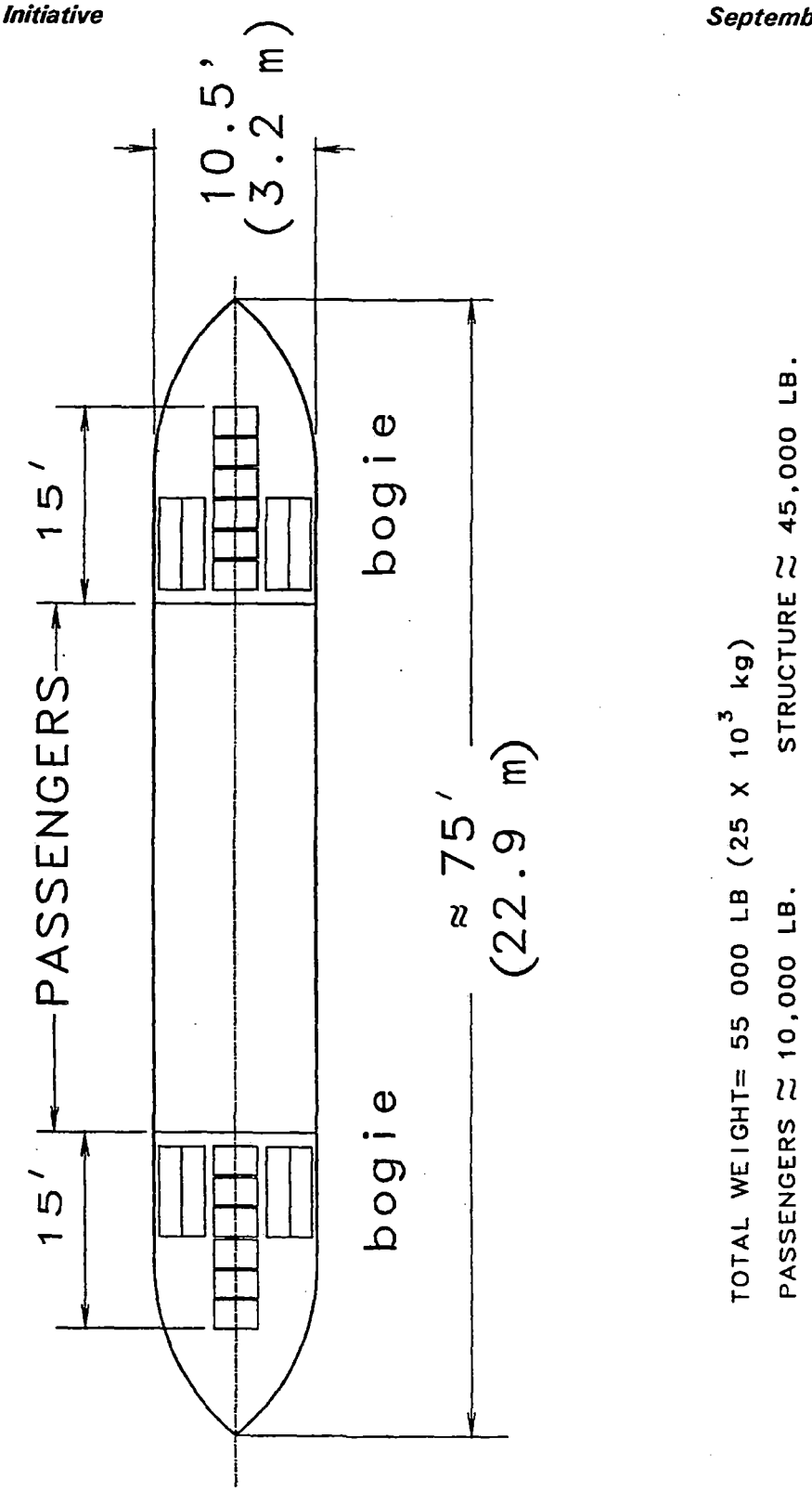

Figure 3 Baseline vehicle outline (45 passengers) - dimensions approximate

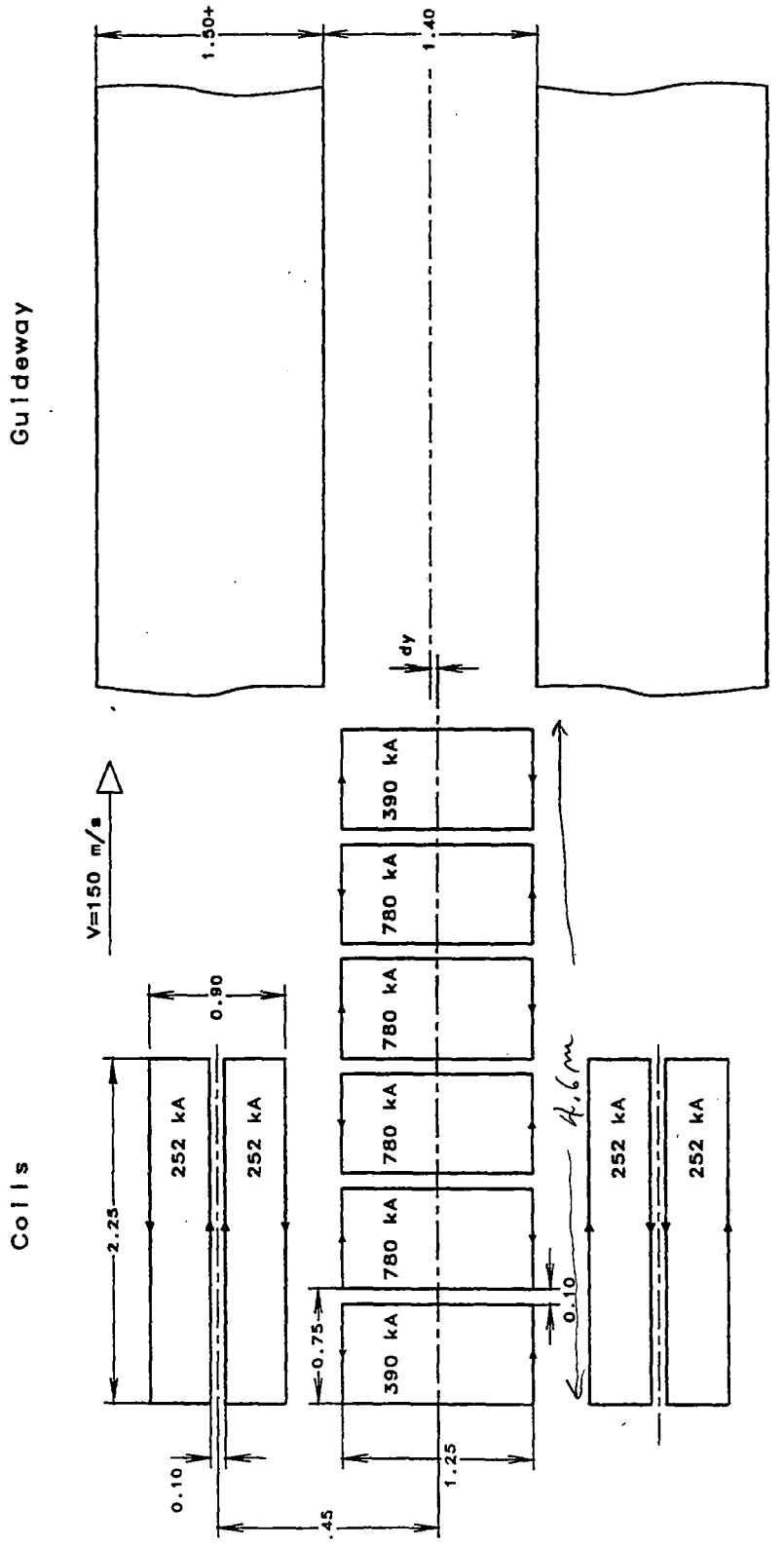

Figure 4 Schematic of coil and magway for forward bogie

Number of Passengers	140	45
Overall Vehicle Length, [m]	38.4	22.9
Number of Bogies	2	2
Levitation Coil System		
Number of Modules per Bogie	2	2
Number of Coils per Module	2	2
Total Levitation Coils	8	8
Independent Coil Circuits	8	8
Propulsion Coils		
Number of Modules per Bogie	1	1
Number of Coils per Module	6	6
Total Propulsion Coils	12	12
Independent Coil Circuits	2	2
LSM Propulsion Windings in Guideway		
Material	Aluminum	Aluminum
Phases	3	3
Wavelength, [m]	1.5	1.5

Figure 5 Vehicle levitation, propulsion, and guidance coil configuration

Figure 6 shows the eddy current pattern induced in the magway sheets due to the motion of the forward bogie ~~toward the right~~ as shown. The eddy currents are primarily due to the two quadrupole levitation modules, although small induced currents along the forward inside edges of the sheets are visible because of proximity of the longitudinal turns in the propulsion coils.

The previous figure assumed bogie motion with the centerline of the vehicle coincident with the centerline of the magway. Wind gusts or "g" forces may tend to shift the bogie off center in the magway, in which case the propulsion coils will create a restoring force. This is illustrated in Figure 7 which shows the eddy current pattern induced in the sheets due to bogie motion with the centerline of bogie and magway displaced laterally by 0.1m. The change in pattern for the levitation coils is evident as well as the strong influence of the propulsion coils which produce the restoring force or "keel effect". These restoring forces have been computed and used in the dynamic models for the vehicle. In later design phases, we can tailor the required stiffness somewhat by altering the spacing between magway sheets or changing the geometry of the propulsion coil end turns. For example, the end turns could be formed away from the magway edge, using a so-called saddle coil geometry, if lower restoring forces are found to be desirable.

The eddy current pattern in the magway sheets is related to the load footprint of the levitation modules normal to the magway. The previous figures imply that the lift load is somewhat more concentrated under the longitudinal, central legs of the coil pair in each levitation module. This pattern moves along the magway with the speed of the vehicle.

The magway sheets also experience a load parallel to their surface in the direction of motion due to the electromagnetic drag. This component of the load per module is much smaller in magnitude than the normal load (which produces lift). The drag loads are primarily located where the transverse eddy currents are strongest, that is, under the transverse turns of the levitation coils.

There is one module (six coils) in each bogie which will interact with the synchronous windings in the magway. These will produce a load on the synchronous windings in the vicinity of the bogie that is opposite to the direction of motion. This load also moves with the speed of the vehicle and must be transmitted to the magway through the fasteners which hold the synchronous windings to the magway. This load is equal to the sum of the electromagnetic drag, frictional drag, and aerodynamic drag on the vehicle divided by the number of bogies.

In addition to the above usual operating loads, there will be transverse wind loads and dynamic "g" loads on the vehicle. These lateral and vertical loads will also be transmitted to the magway through the footprints of the levitation modules.

3.2.1.a.1.3. MODULE CHARACTERISTICS

Overall characteristics for the superconducting coil systems on the vehicle for lift and propulsion are summarized in Figure 8 and Figure 9, respectively. Two columns are given in each table to summarize features for the 140 and 45 passenger vehicles.

The vehicle weights are different by a factor of two, but Figure 8 indicates that the total weight per vehicle for lift modules is essentially the same. This arises because we have chosen to use the same coil overall "footprint" size for each vehicle as a reasonable approach for development. This then leads to a small change in coil weight, but cryostat weights that are virtually the same. Since the cryostat weights

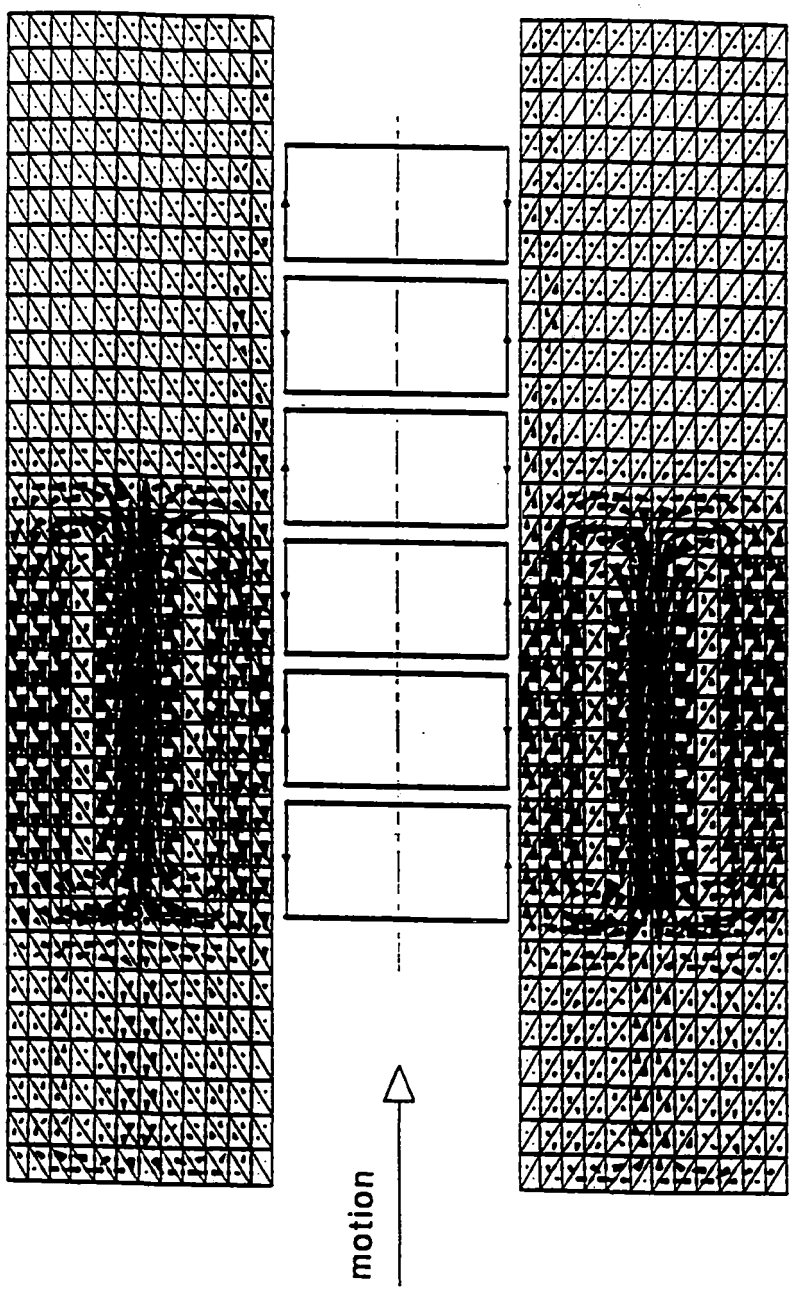

Figure 6 Eddy currents induced in magway sheets due to motion of forward bogie with aligned vehicle and magway centerlines

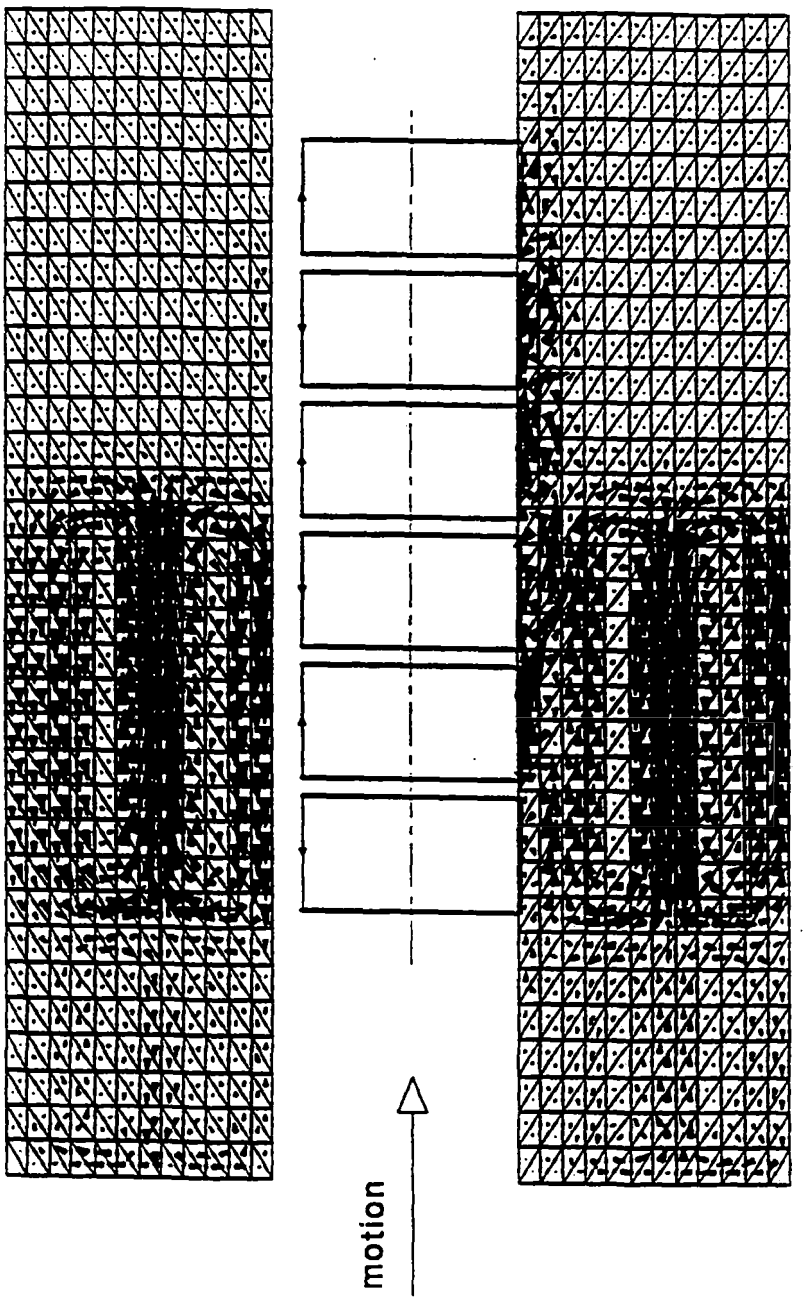

Figure 7 Eddy currents induced in magway sheets due to motion of forward bogie with vehicle and magway centerlines displaced 0.1 m (note keel effect from propulsion coils)

No. of Passengers	140	45
Total Lift Required, [N]	605055	302528
Number of Lift Modules	4	4
Module Characteristics		
Lift per Module, [N]	151,264	75,632
No. Coils per Module	2	2
Per Coil Length, [m]	2.25	2.25
Per Coil Width, [m]	0.425	0.425
Electrical Characteristics		
AT per coil per module, [A]	251,702	177,980
Conductor current density, [A/m^2]	2.44E+08	3.20E+08
Winding packing factor	0.69	0.69
Winding current density, [A/m^2]	1.68E+08	2.21E+08
Winding cross-sectional area, [m^2]	0.001495	0.000806
Inductance/N^2, 1 coil, [H]	3.1E-06	3.1E-06
Mutual Ind/N^@, 2 coils, [H]	4.38E-07	4.38E-07
Stored Energy per Module, [J]	2.24E+05	1.12E+05
Max Flux Density at Winding, [T]	3.30	2.33
Weights		
Winding density, [Kg/m^3]	4780	4780
Weight per coil per module, [Kg]	38	21
Weight of Coils in Module, [Kg]	76	41
Weight of Cold Structure, [Kg]	114	114
Dewar, supports, etc,, [Kg]	455	455
Total Wt per module, [Kg]	645	609
Total Wt per Vehicle, [Kg]	2579	2438

Figure 8 SC coil module characteristics for lift coil system

No. of Passengers	140	45
Total Amp Turns Required, [A]	7.80E+06	5.23E+06
Module Characteristics		
Number of Propulsion Modules	2	2
No. Coils per Module	6	6
Per Coil Length, [m]	0.75	0.75
Per Coil Width, [m]	1.2	1.2
Electrical Characteristics		
AmpTurns per End Coil per Module, [A]	390,000	261,300
AmpTurns per Mid Coil per Module, [A]	780000	522600
Conductor current density, [A/m^2]	1.68E+08	2.80E+08
Winding packing factor	0.69	0.69
Winding current density, [A/m^2]	1.16E+08	1.93E+08
End Coil Winding cross-sect area, [m^2]	0.003364	0.001352
Mid Coil Winding cross-sect area, [m^2]	0.006729	0.002705
Stored Energy per Module, [J]	2.86E+06	1.28E+06
Max Flux Density at Winding, [T]	5.05	2.80
Weights		
Winding density, [Kg/m^3]	4780	4780
Weight per end coil per module, [Kg]	63	25
Weight per mid coil per module, [Kg]	125	50
Weight of Coils in Module, [Kg]	627	252
Weight of Cold Structure, [Kg]	300	180
Dewar, supports, etc,, [Kg]	606	606
Total Wt per module, [Kg]	1533	1038
Total Wt per Vehicle, [Kg]	3067	2076

Figure 9 SC coil module characteristics for propulsion coil system

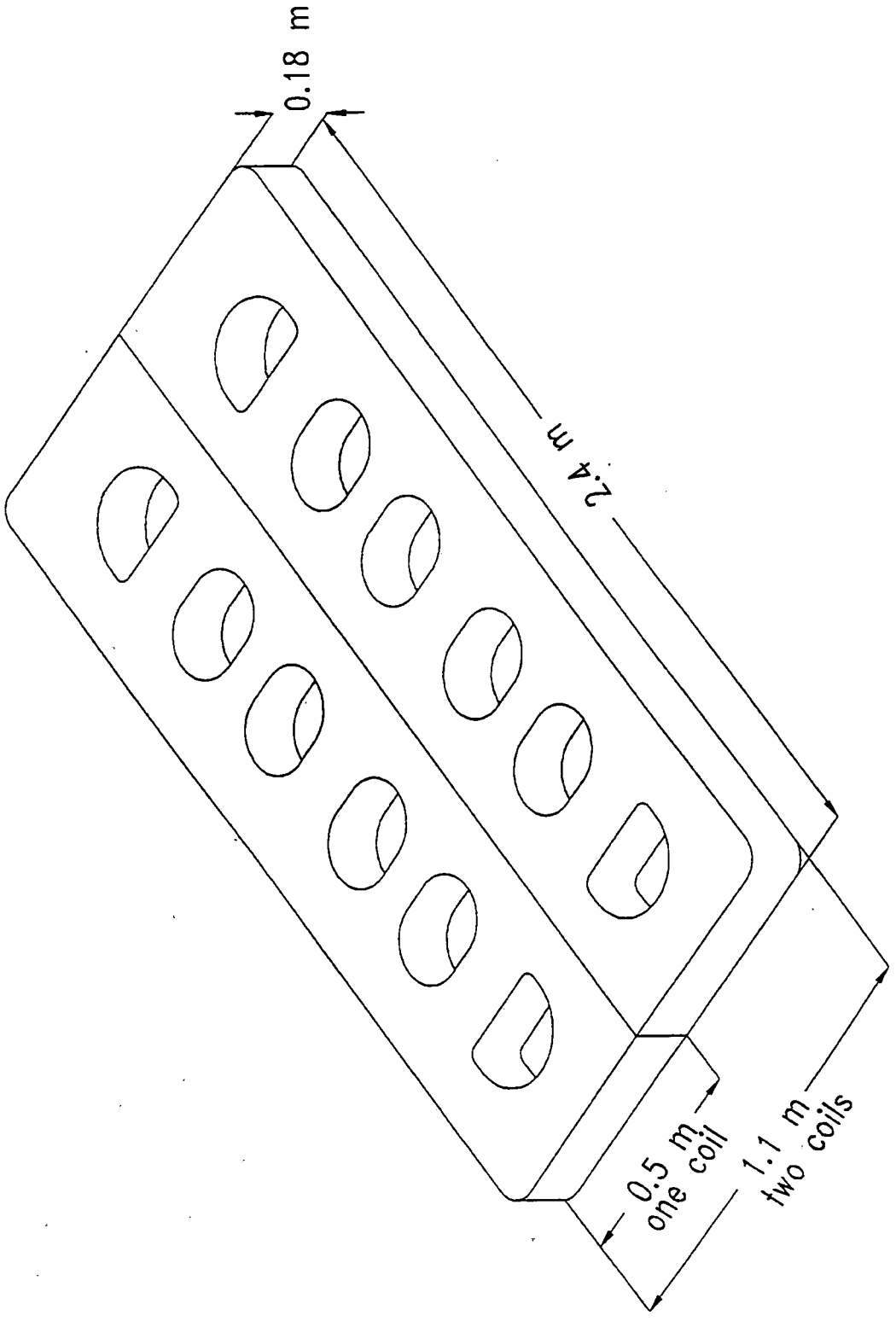

Figure 10 Levitation module features

are dominant for the levitation systems, there is little difference in weight for this subsystem for the two vehicles.

Figure 9, on the other hand, shows that the propulsion coil modules for the 140 passenger vehicle weigh approximately 50% more than the modules for the 45 passenger vehicle. We have again chosen identical coil "footprint" dimensions, in this case to be consistent with magway synchronous winding features. However, for the propulsion coils, the windings are a significant weight component. There is a substantially different amp-turn requirement and field level for the two vehicles, even though the cryostat weights are essentially the same.

Figure 10 shows an external view of a levitation module. The basic package is 2.4 m long, 1.1 m wide and 0.18 m thick. The outer vessel is the room temperature portion of the cryostat and is constructed from aluminum plate nominally 9.5 mm (0.375 in) thick. The vehicle mounts will be on the surface of the wide plate with suitable stiffeners to carry the main load to the location on the wall where the cold mass supports are anchored internally.

The twelve penetrations through the cryostat also pass through the center of the coils. The walls of the penetrations help to stiffen and support the wide flat plates of the cryostat outer vessel against the resultant loads due to the external atmospheric pressure and the vacuum within the vessel.

Figure 11 is a view of the module with the top cover plate and thermal radiation shield removed to show the internal components. The vehicle mounts will pass the load to the cold mass supports, which, in turn, pass the loads to the coil support frame that is within the thermal radiation shield. The purpose of the latter is to intercept thermal radiation at a temperature intermediate between the ambient temperature of the cryostat and the cold coil system within and thus reduce the heat load on the cryogenic system. The radiation shield is also carried by the cold mass supports, which will be described in more detail in a later figure.

Another view, with sections, is shown in Figure 12. Because of the high operating current density, the winding cross section is relatively small. This, coupled with an efficient structural and cold mass support system, allows the distance from the centerline of the coil winding to the outside of the cryostat to be relatively small. In this case we estimate that this can be 0.05 m. No current leads are shown into the vessel because we propose a "leadless" system to be described in a later section.

A better view of one of the cold mass supports is shown in Figure 13. It consists of a sequence of nested tubes to give a long thermal path from the connection to the vehicle mounts at room temperature to the coil at low temperature. The innermost tube spans the distance across the coil form/structure.

The coil form and structure are of fiber reinforced plastic and support the winding which consists of a cable-in-conduit conductor (described later). This type of conductor and the FRP support structure reduce the eddy current heat load at low temperature which can be generated due to any vibration induced relative motion of the coil within the cryostat and/or thermal radiation shield. The conductor is insulated, wound on a form, removed, externally insulated with a ground wrap and mounted on the FRP coil form for assembly to the cryostat. The winding cross section is relatively small and implies that variations from assumed requirements for levitation capability or variations in conductor properties from the values assumed could be compensated by increasing or decreasing the amp turns without a major impact on module size or overall weight.

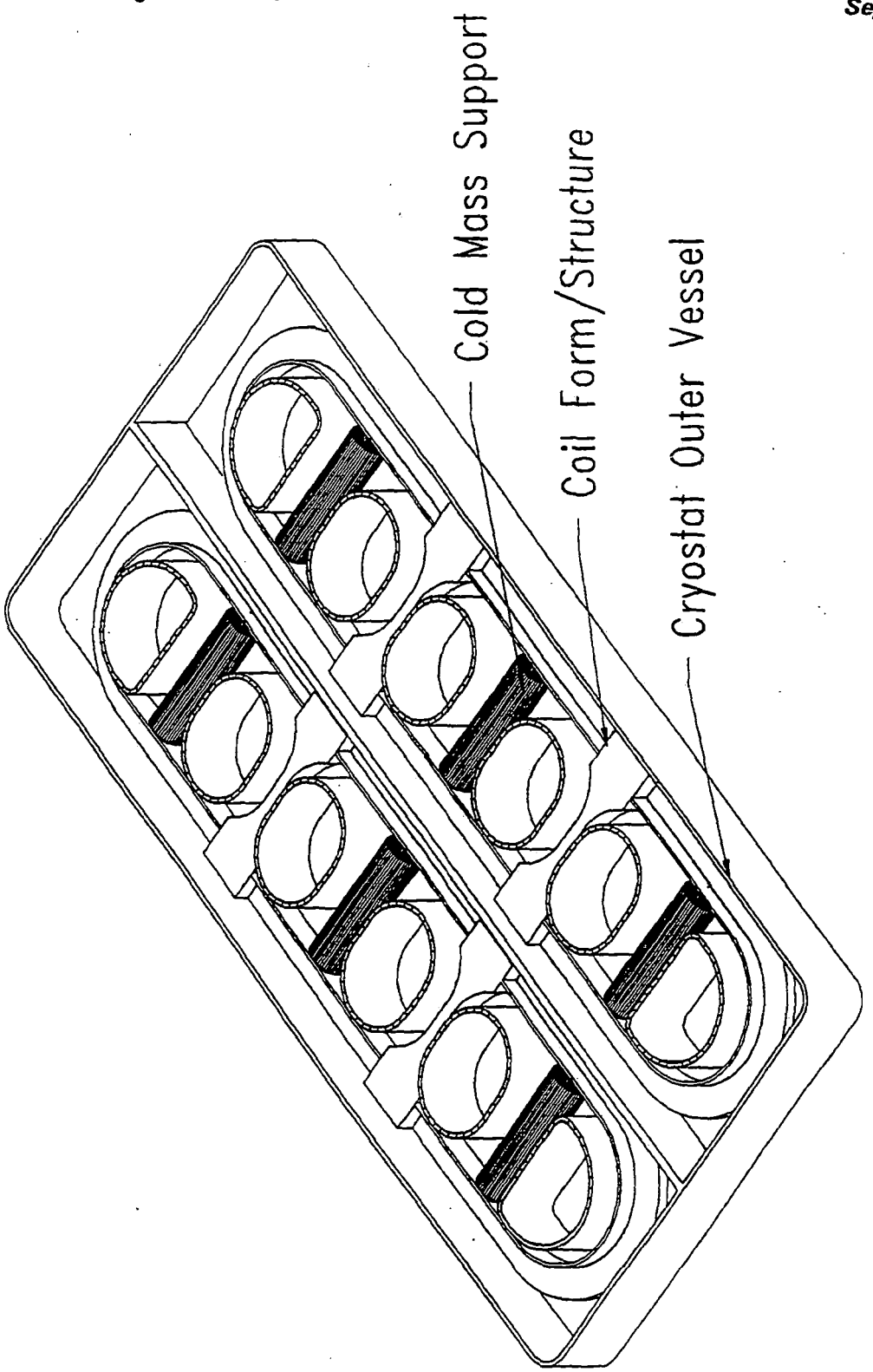

Figure 11 Levitation module with cryostat and thermal radiation shield removed

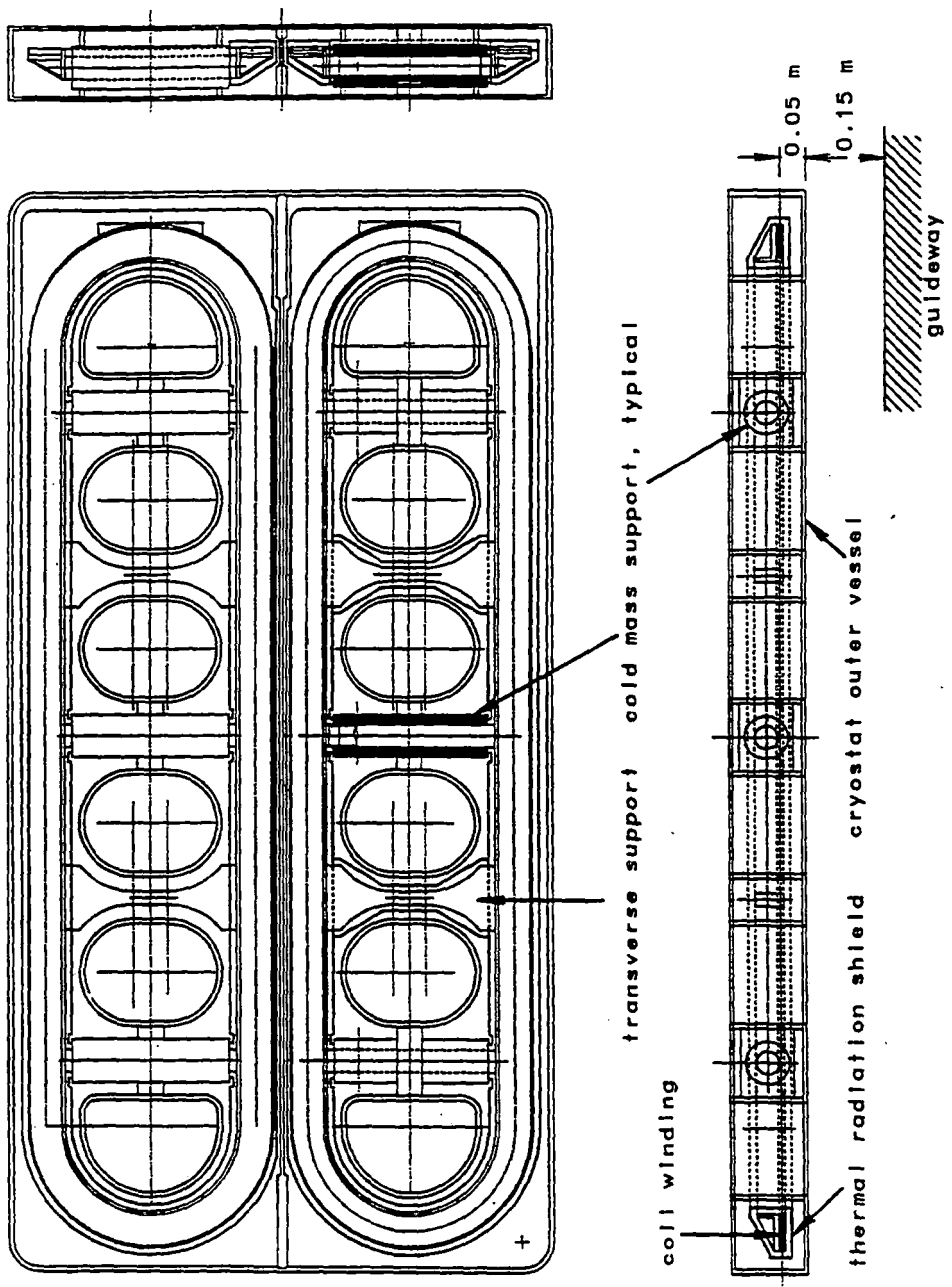

Figure 12 Major components of levitation coil module

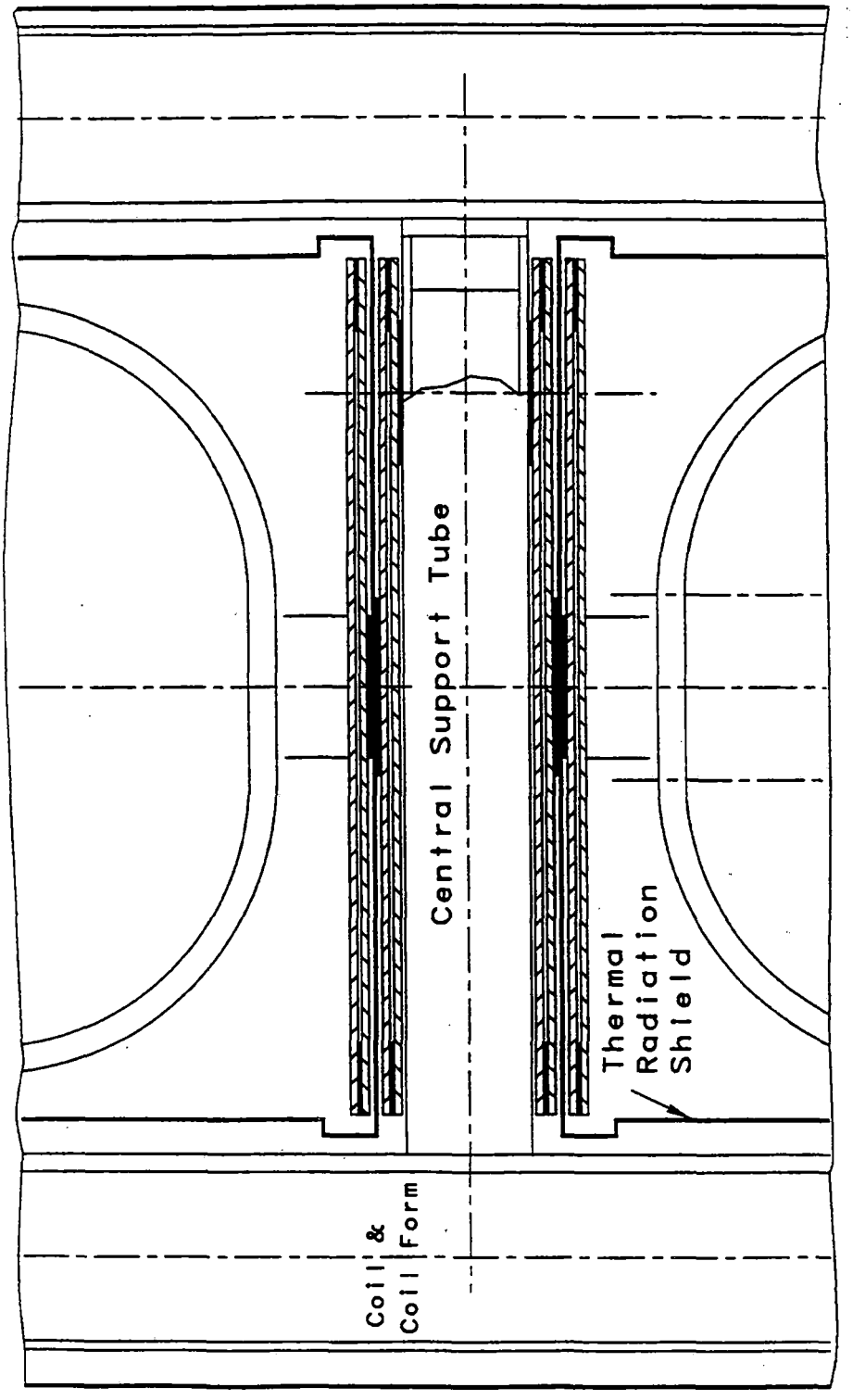

Figure 13 Cold mass support detail

An overall view of a propulsion module is shown in Figure 14. The package is approximately 4.6 m long, 1.5 m wide and 0.2 m thick and is constructed from aluminum in a manner similar to that described for the levitation modules. Figure 15 shows the module with the cryostat cover and thermal radiation shield removed to show the twelve cold mass supports that carry loads to the six propulsion coils from the mounts which are not shown. The latter can be located anywhere on the outer vessel surface with suitable stiffeners to transmit the loads to the point where the cold mass supports are anchored internally.

A sectional view of the propulsion module is shown in Figure 16. This shows that the coil cross-sections are a relatively small portion of the transverse section and that the two end coils have about half the cross-section of the central six coils. This was done to achieve a more favorable current distribution for shielding of stray fields without losing the required interaction with the synchronous windings in the magway for thrust generation. There may also be some benefit related to the voltage distribution in the magway windings. A more optimum solution may be possible from both standpoints and will be investigated in future design iterations.

3.2.1.a.1.4. STRUCTURAL DESIGN

A plan view outlining one of the two coils in a levitation module is shown in Figure 17 together with vectors representing the local force distribution in N/m. Note that there is a large attraction between the two coils in the module, as well as a tendency for the electromagnetic loads to spread the windings. Figure 19 is an isometric view of one of the two coils in a levitation module with vectors illustrating the distribution of lift force at high speed. Note that it is concentrated along the longitudinal leg adjacent to the other coil in the levitation coil pair.

Figure 18 shows the finite element model for the levitation coil, together with the nodal forces. At zero speed, the only loads would be the internal loads of electromagnetic origin and, since there is no lift, forces on opposite sides of the long legs would be in the plane of the coil and in-line. In the figure, which is done for high speed where maximum lift is generated, the loads on the long legs are still almost in line, but have a small upward component for lift. This illustrates that the internal electromagnetic loads dominate the lift and drag forces, hence a large fraction of prior experience with superconducting magnets is directly applicable to maglev.

Results for finite element analyses are shown in Figure 20 and in Figure 21 for a lift coil and for a cold mass support, respectively. They indicate reasonable levels of stress and displacement for this stage of design, thus supporting our estimates for feasibility and weight.

Figure 20 (top) shows vertical displacement contours. The source of the vertical displacements is not just the lift but also the rotation of the coil support frame due to internal Lorentz loads. Membranes bridge from straight leg to straight leg. Three nested shell type support cylinders connect the coil to the chassis. They are located in the open regions between membranes and ends of the race track. The support they provide is modeled with displacement constraints. The shell is assumed to be a 1/4 inch thick fiberglass reinforced epoxy and the low modulus of the frame contributes to the magnitude of the displacements.

Figure 20 (bottom) shows the Von Mises stresses in the shell. The peak stress is 110 MPa and occurs in the curved cantilevered ends. If necessary, this could be reduced by local reinforcement at higher stress locations. Weight could also be saved by thinning of the shell at regions of lower stress.

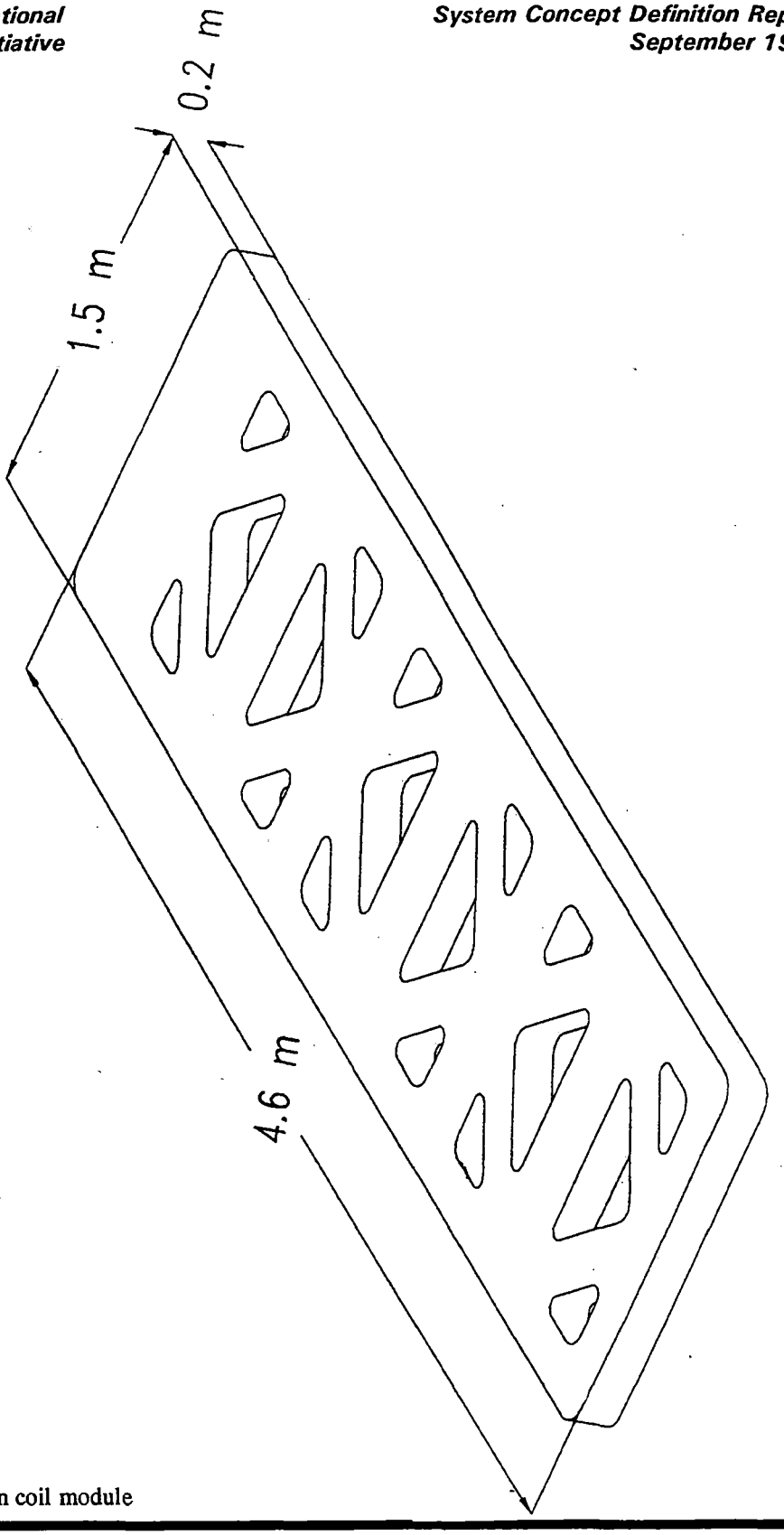

Figure 14 Propulsion coil module

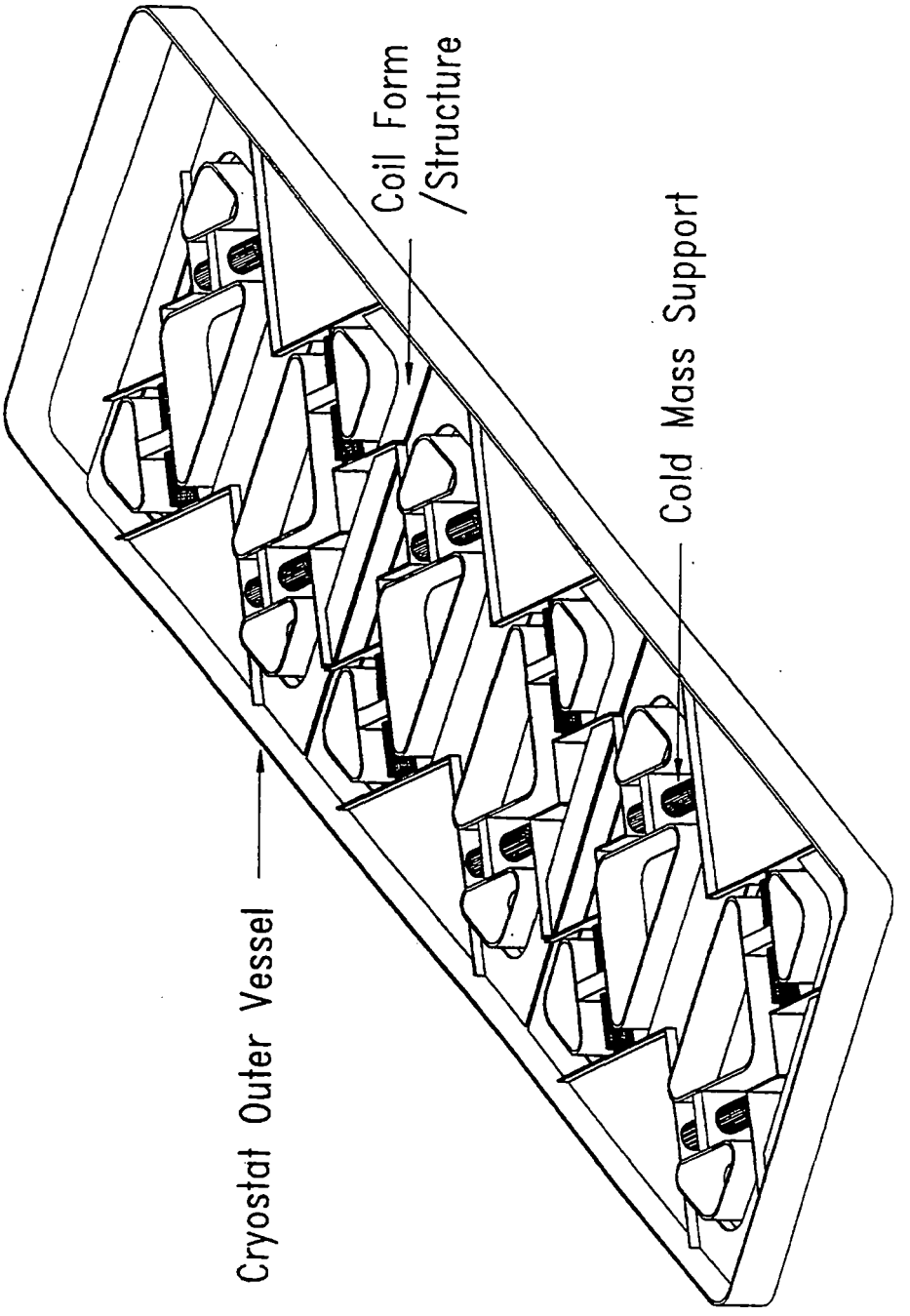

Figure 15 Major components of propulsion coil module with cryostat and radiation shield removed

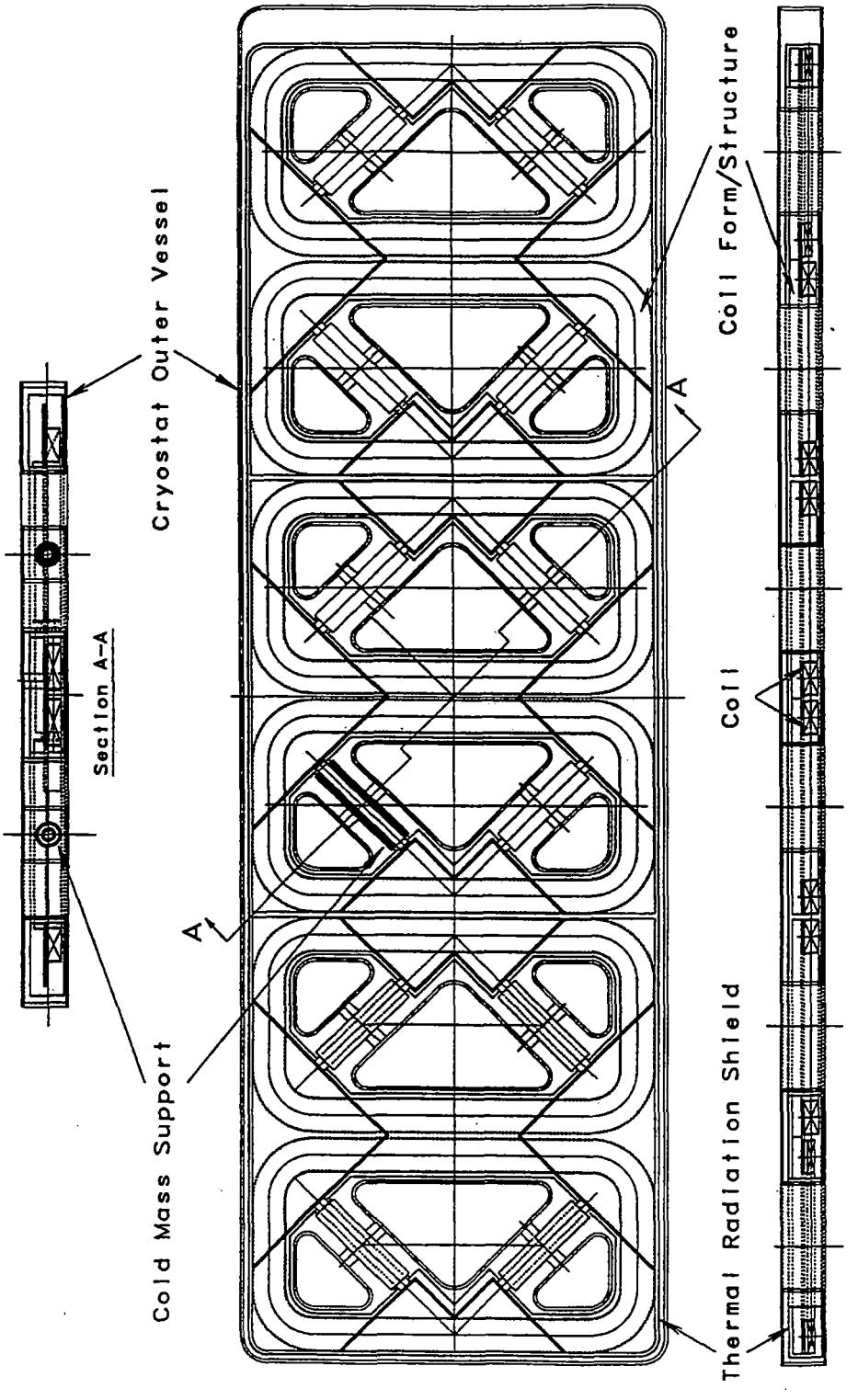

Figure 16 Major components of propulsion coil module

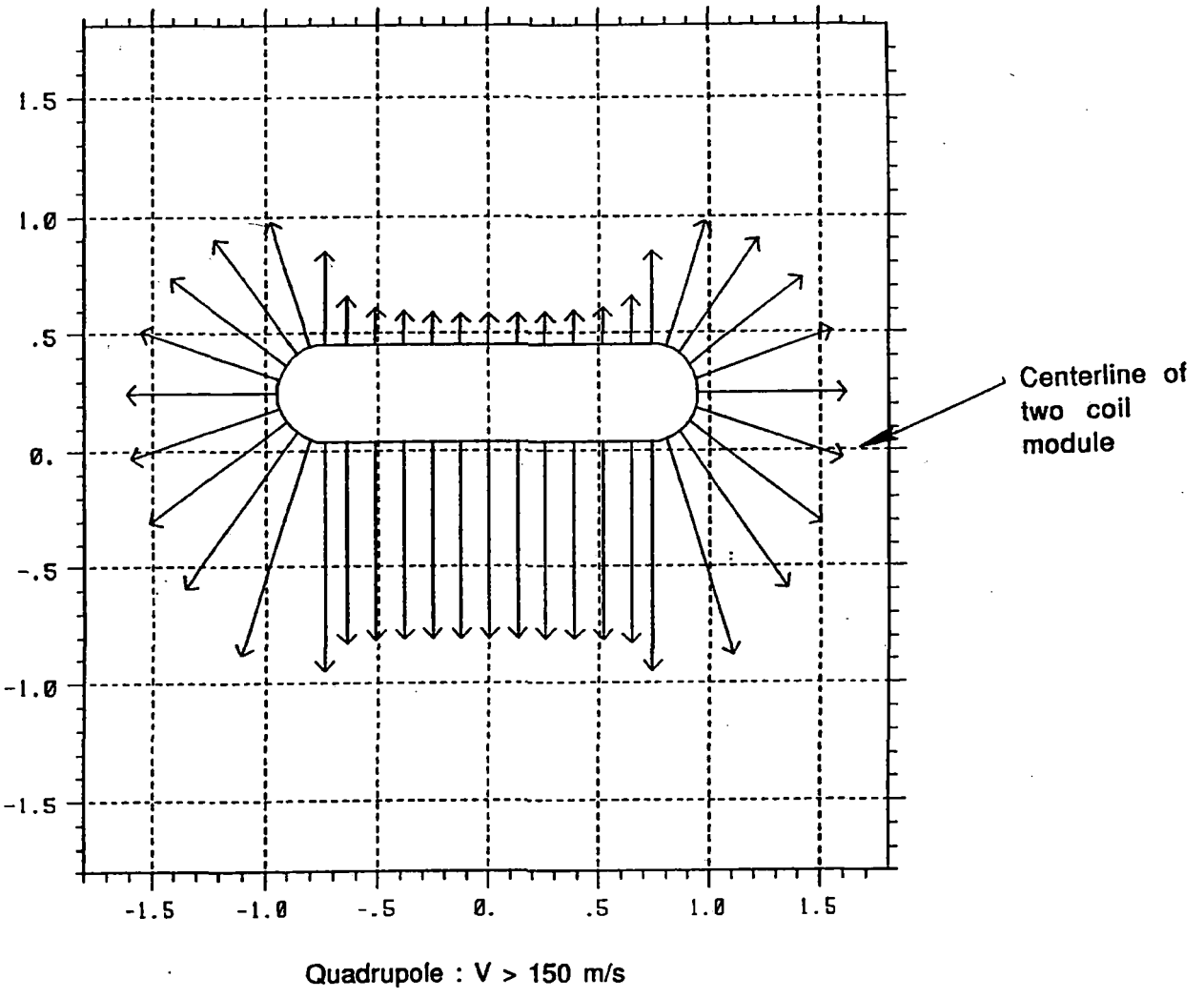

Figure 17 Plan view of force distribution (N/m) in one of the two coils in a levitation module at high speed

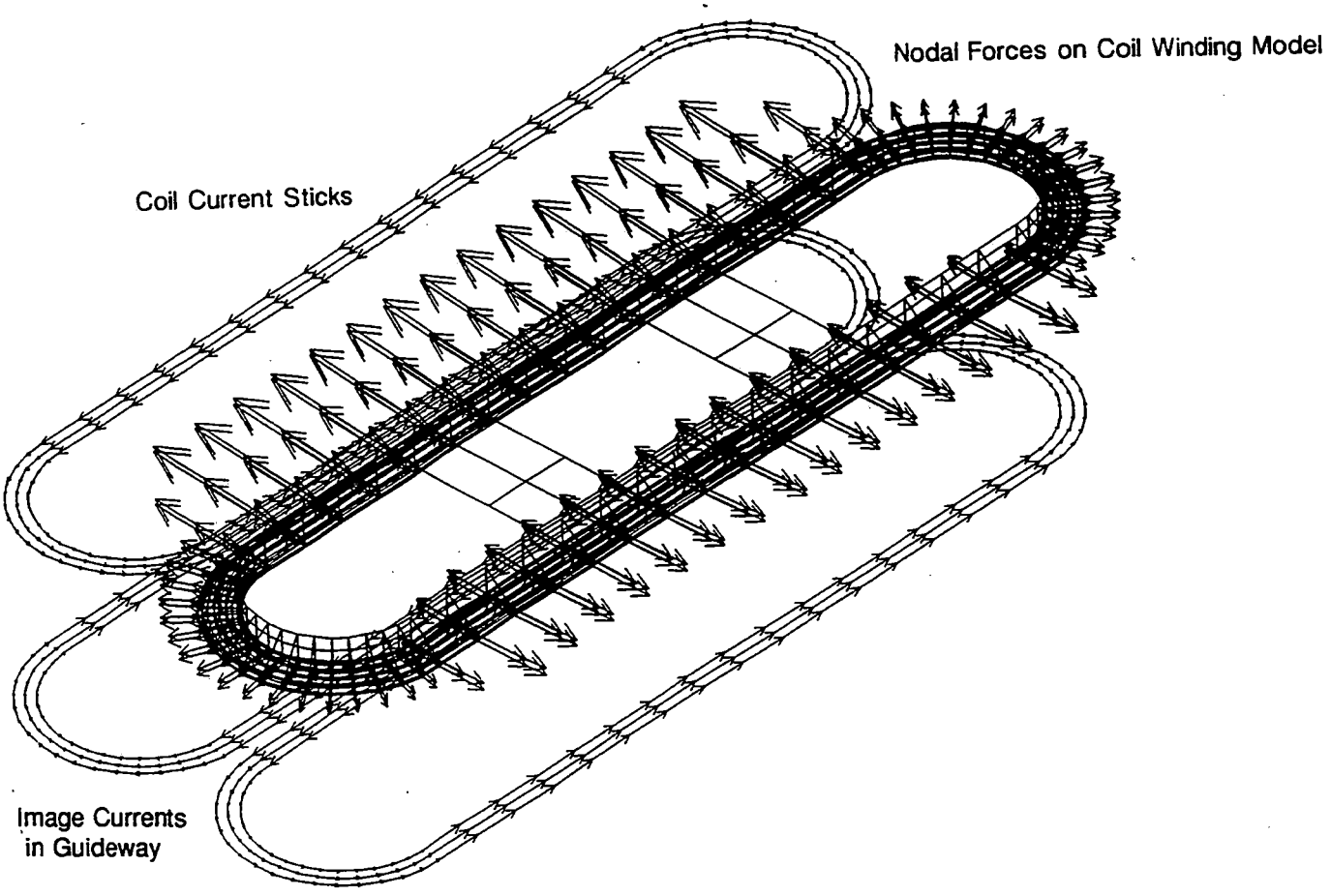

Figure 18 Nodal force distribution on finite element model of coil in levitation module

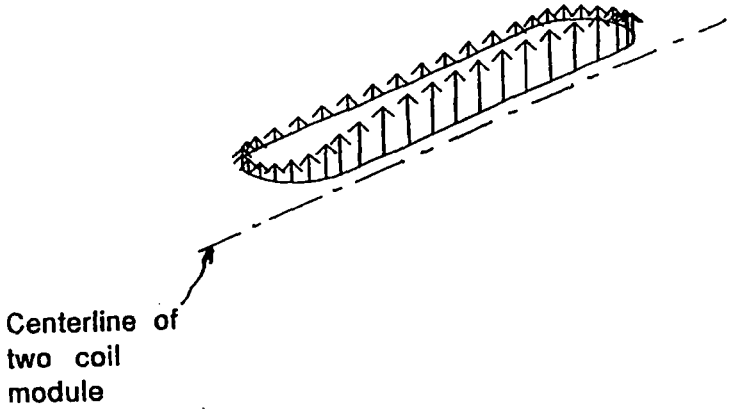

Figure 19 Lift force distribution on one of two coils in a levitation module at high speed (quadrupole: V > 150 m/s)

Figure 21 (top) is a finite element model of a representative nested shell support cylinder. Lateral loads are applied which correspond to the lift force. The lower figure shows the displacements (magnified for clarity) and the resulting peak Tresca Stress of 8 ksi.

Preliminary structural analyses have also been carried out for the propulsion coils. In this case, it can be shown that the loads in the propulsion coils are also dominated by the internal loads of electromagnetic origin and not by the thrust interaction with the magway. They are illustrated in Figure 22 as nodal forces on the finite element model. Specifically, Figure 22 shows the model used to obtain Lorentz forces on the outer two coils of the propulsion coils. Stress and displacement results for this case are shown in Figure 23 and are at a reasonable level for this stage in the conceptual design process. In the model in Figure 23, the coils are supported by a case which is connected to the coil via gapped elements. The case was modeled with 1/4-inch thick stainless steel sheet. The results indicate that the case could be lightened. The coil stresses are for the "smeared" conductor (local stresses in the conduit would be higher). The diagonally oriented support cylinders are modeled with displacement constraints.

3.2.1.a.1.5. CONDUCTOR SELECTION

The superconductor configuration selected for both the levitation and propulsion coils on the vehicle is a cable-in-conduit-conductor (CICC) as illustrated by the sample in the photograph in Figure 25. It consists of multiple strands (eg-27 in the figure) of multi-filament Nb_3Sn, which are formed into a cable, then enclosed in a steel conduit. The conduit serves as the channel for the working fluid which is supercritical helium. This eliminates the need for the usual cold helium vessel that surrounds the entire coil and that can be the source of a high heat load due to induced eddy currents if the cold vessel vibrates during operation.

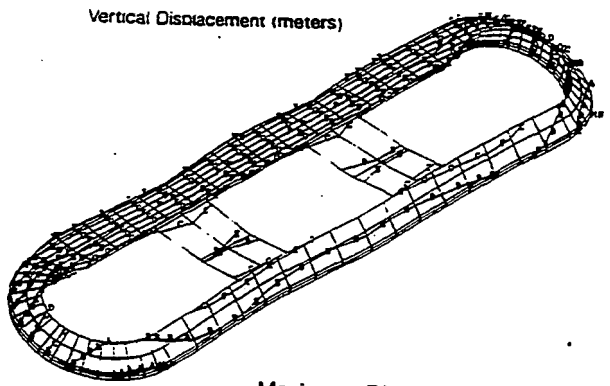

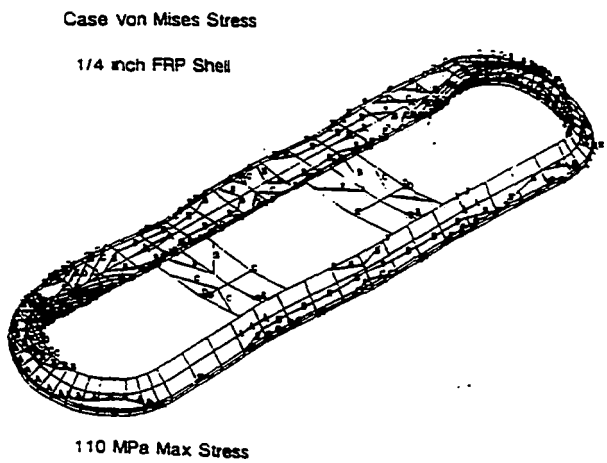

Figure 20 Preliminary stress and displacement results

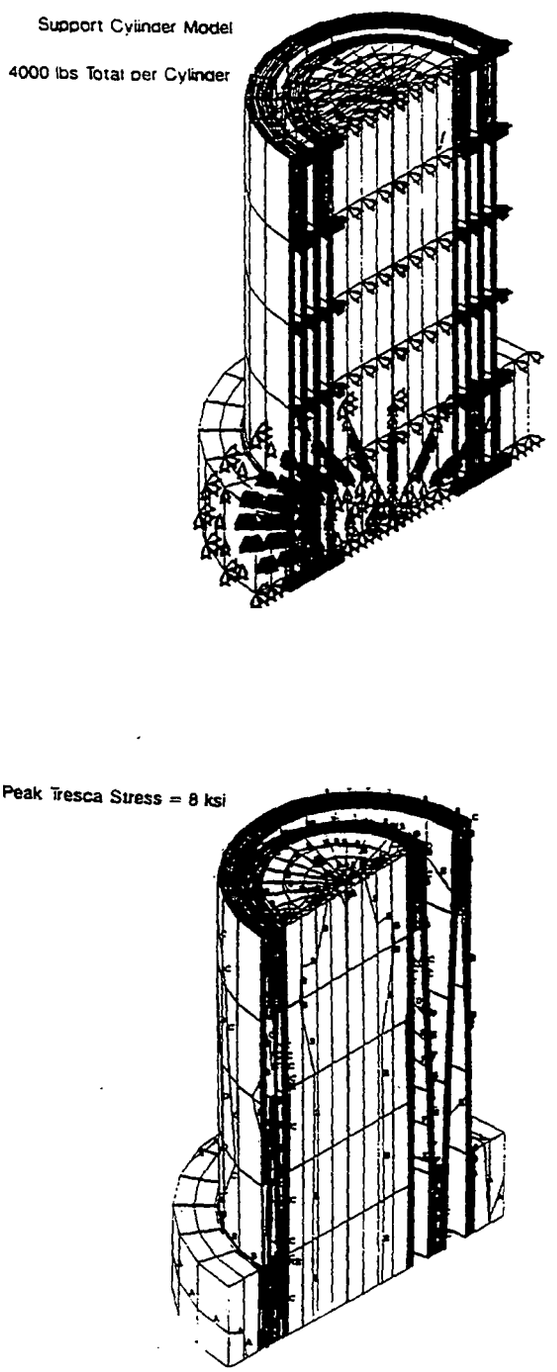

Figure 21 FEA of cold mass support cylinder

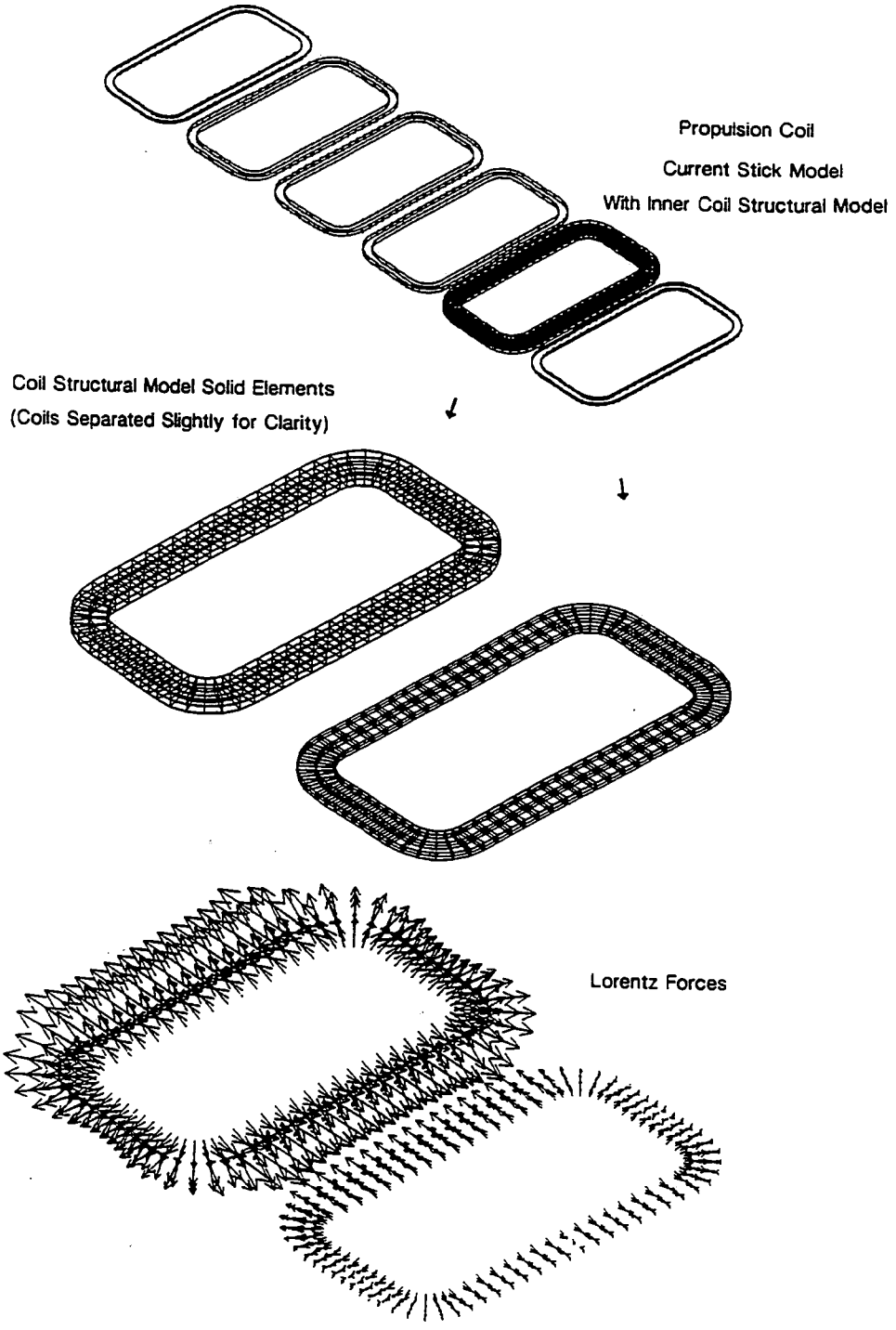

Figure 22 Nodal force distribution on finite element model of propulsion coils

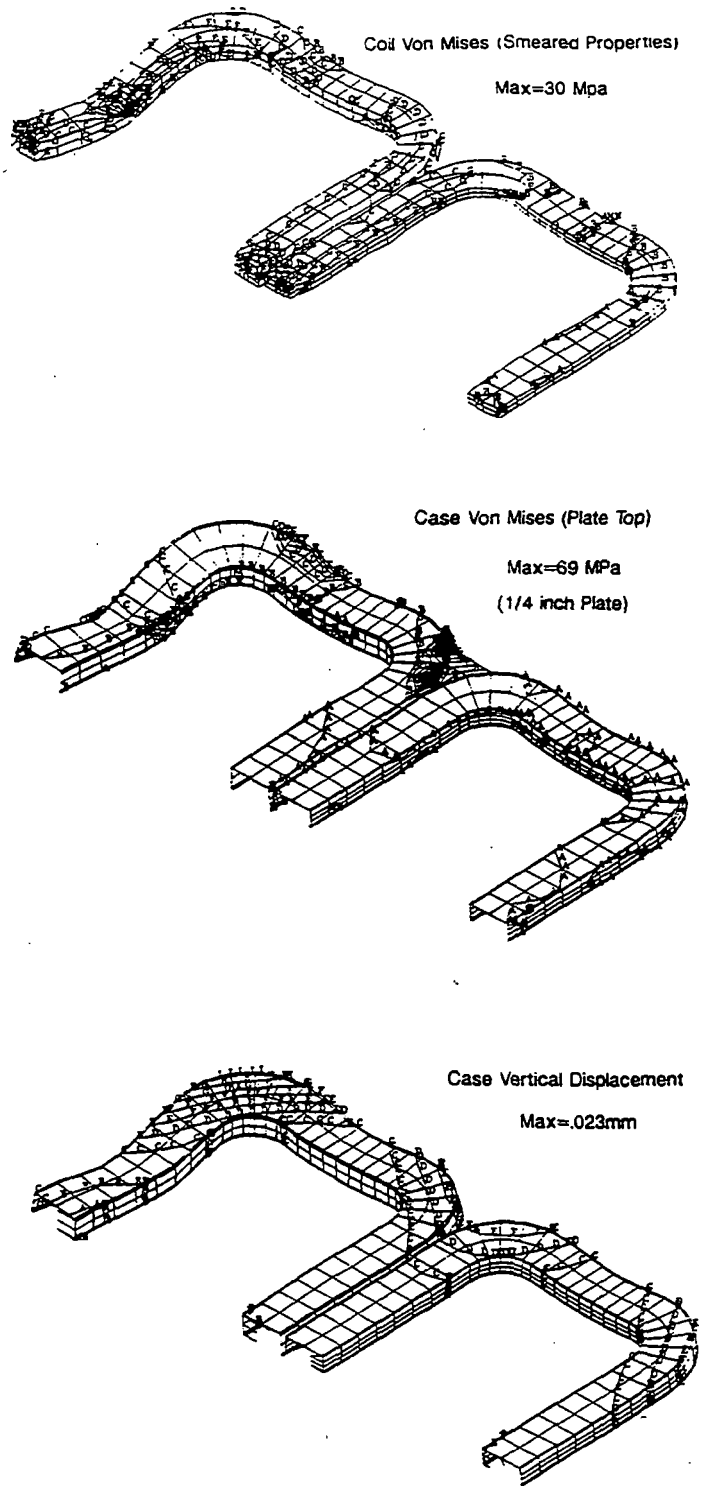

Figure 23 Preliminary stress and displacement results for propulsion coils

Conductor Type	Cable-in-Conduit
Sheath Material	304 SS
Wall Thickness	0.38 mm (0.015")
Outer Dimensions Inner Dimensions	4.95x4.95 mm (0.195x0.195") 4.2x4.2 mm (0.165x0.165")
Strand Material	Nb_3Sn with Cu
Number of Strands	27
Strand Diameter	0.71 mm (0.028")
Strand Area	10.69 mm^2 (1.66e-2 in^2)
Cable Space Area	17.64 mm^2 (2.72e-2 in^2)
Helium Area	6.95 mm^2 (1.06e-2 in^2)
Void Fraction	39%

Figure 24 Preliminary characteristics of maglev conductor

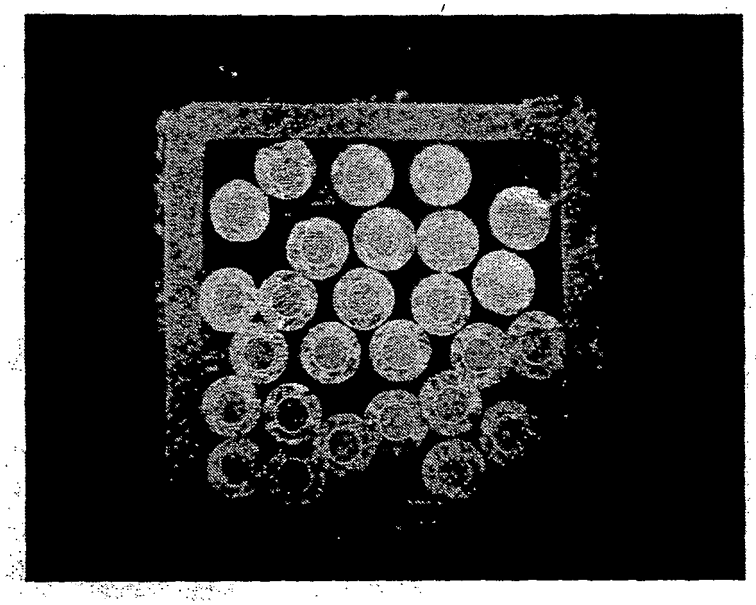

Figure 25 Sample 6000 ampere cable-in-conduit conductor consisting of 27 strands of multifilamentary copper-stabilized superconductor in a stainless steel sheath (full size is 0.2 in^2)

Analytical & experimental investigations in the fusion program have demonstrated the advantages of the Cable-in-Conduit-Conductor (CICC) approach from the operational stability standpoint. A preliminary study concerning the advantages of using this type of conductor in maglev applications has also been performed.[1] The study showed that CICC conductors have an order of magnitude higher energy margin for stability against disturbances than epoxy impregnated windings. Furthermore, it was shown that Nb_3Sn has a much higher energy margin than NbTi at a given temperature. In view of these results we have selected the CICC approach as the baseline conductor configuration for this program.

The CICC in Figure 25 has an outside dimension of about 5x5 mm (0.2x0.2 in). The characteristics of the conductor are summarized in Figure 24. This conductor was selected for illustration purposes because it had been manufactured for another program and was available, hence, it is feasible. However, it was not intended for this application and could be optimized. We will assume that we can scale it up or down in size as we require and achieve the same overall current density. This is correct to first order since it is a cable of conductors and an adjustment to current capacity can be made by adding or subtracting strands in the cable or filaments in the individual conductors. It is also possible to adjust the size of the

[1]R.J. Thome, et al, "Application of Cable-in-Conduit-Conductor to MAGLEV Magnet Systems," Final Report prepared for VNTSC under Contract no. DTFR53-91-C-00042, July, 1992.

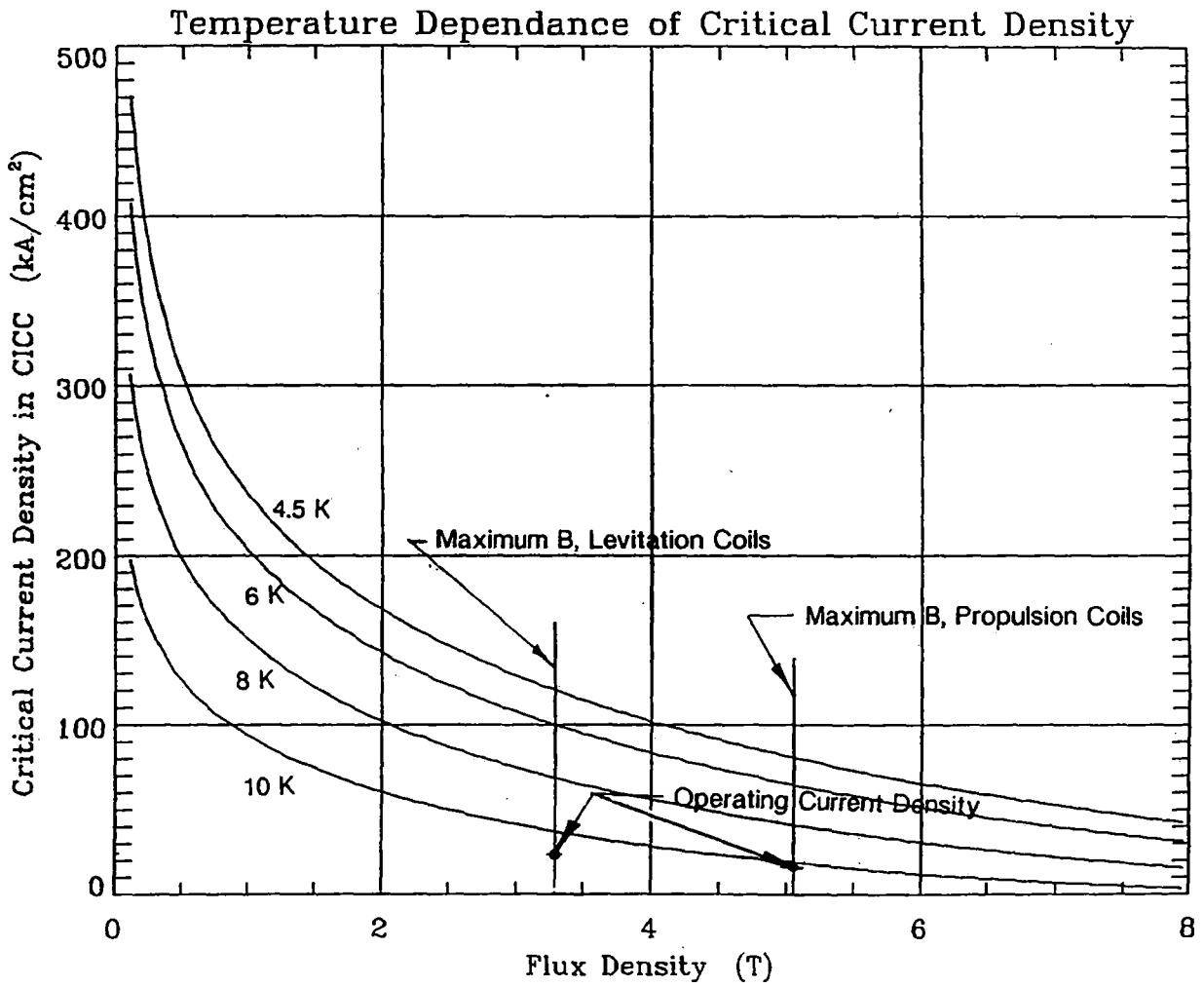

Figure 26 Design operating points of superconducting levitation and propulsion coils relative to critical surface

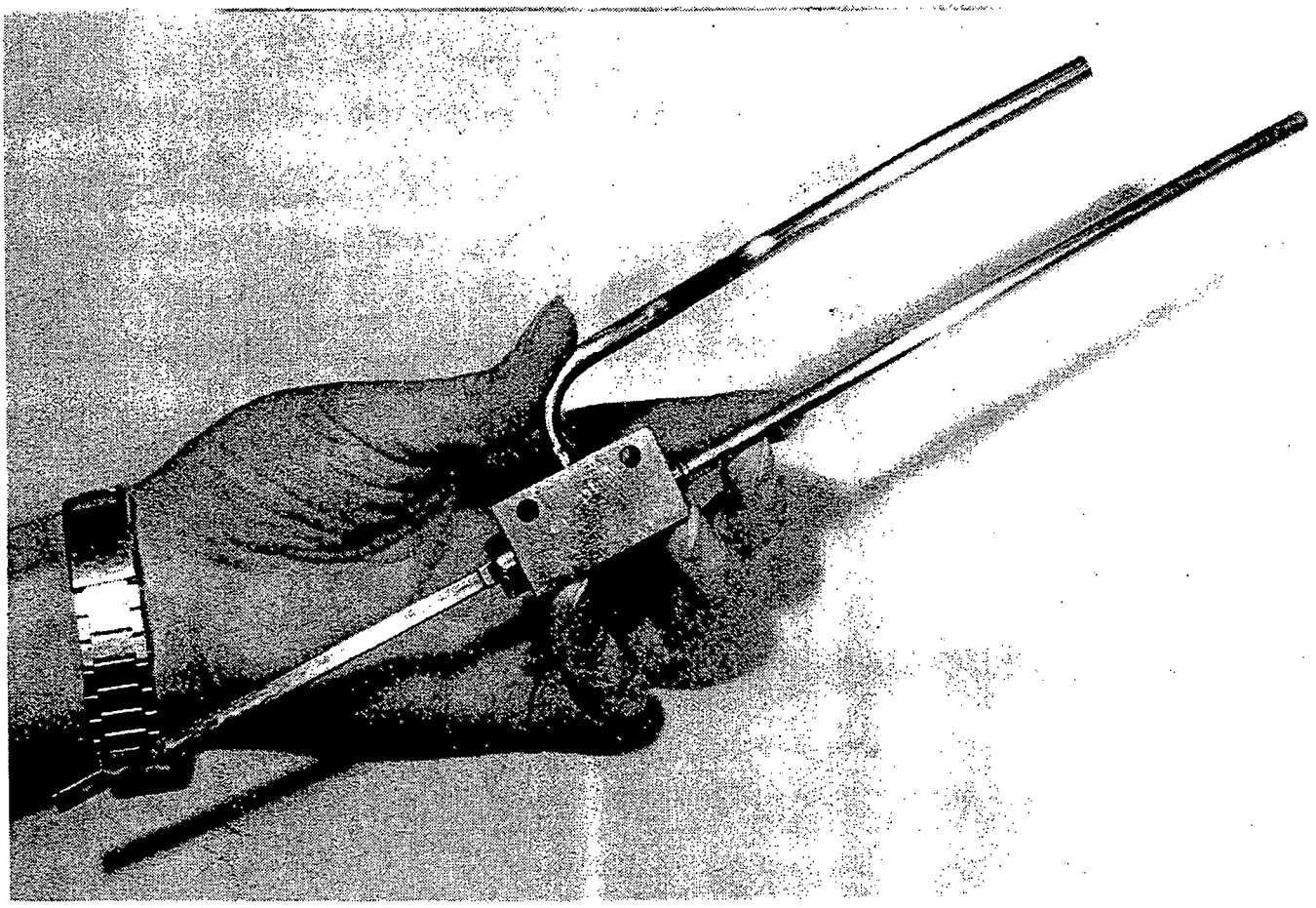

Figure 27 Typical electrical/hydraulic joint used with a cable-in-conduit contuctor

This page is blank.

latter or the ratio of matrix material to superconductor. Minor variations in Nb_3Sn CICC capability from those assumed will have a minor impact on coil module weight or other general features. Note, however, that the conductor shown could be used for this design, in which case the operating current would be about 6300 A for the levitation coils and about 5400 A for the propulsion coils.

The critical current density for this conductor is shown in Figure 26 as a function of the magnetic flux density experienced by the conductor and the operating temperature. This current density is based on the current carried, divided by the outer envelope area of the conduit enclosing the cable.

The maximum flux density in the conceptual design for the levitation and propulsion coils in this study are also indicated in Figure 26. The operating current density must be selected to be a fraction of the critical current density so as to allow for stability of the conductor to operational disturbances which could take the form of temperature excursions due to cryosystem fluctuations or losses generated by the conductor under transient conditions.

The temperature and the magnetic flux density are not uniform throughout the windings in the respective coil systems. In our case, the magnetic field experienced by the levitation winding at full current will range from zero to 3.3 T and the temperature will range from 6K to a maximum of 8 K. For the propulsion coil, the maximum field is 5.05 T and the maximum temperature is also 8K. If the maximum field point and maximum temperature point in either of the windings coincide, then this would be the point of lowest margin relative to the critical current surface for the conductor. In these designs, the operating fraction of critical current density on this basis was selected to be 40%. This should be ample margin to allow for operational uncertainties at this stage of the design process, especially since the maximum temperature and field points can be designed to occur at different points in the system.

The selection of an operating temperature was done in light of the impact on conductor operating characteristics as well as system level trade-offs such as weight and auxiliary power required for the cryogenic system. The cryogenic requirements in this system are fulfilled by a refrigeration subsystem and a substantial weight reduction and power input reduction was realized by using a Nb_3Sn CICC at an operating temperature substantially higher than could be achieved with NbTi.

Figure 27 is representative of a typical electrical/hydraulic joint for a CICC such as that shown in Figure 25. The three branches of the joint-- an electric terminal (lower right branch in Figure 27), a length of conductor (lower left branch), and hydraulic tubing (upper right branch)-- meet at a stainless steel block. The hydraulic tubing serves as an inlet for the flow of supercritical helium to the winding.

3.2.1.a.1.6. SUPERCONDUCTING COIL CHARGING PROCEDURE (NO CURRENT LEADS PLUS EXTERNAL "FLUX" SUPPLY)

The method described in this section is considered proprietary and would allow superconducting coil systems used for levitation, propulsion or guidance on maglev vehicles to be charged to their operating current level without the use of current leads passing into the cryogenic vessel to the coil at low temperature from the power supply at ambient temperature. This would alleviate one of the major sources of heat load into the cryogenic vessel containing the coil system. It would also reduce the overall size of the coil/cryogenic container envelope, simplify its mounting to the vehicle, increase reliability, and allow coil charging, discharging, & recharging to be more automated for maintenance personnel.

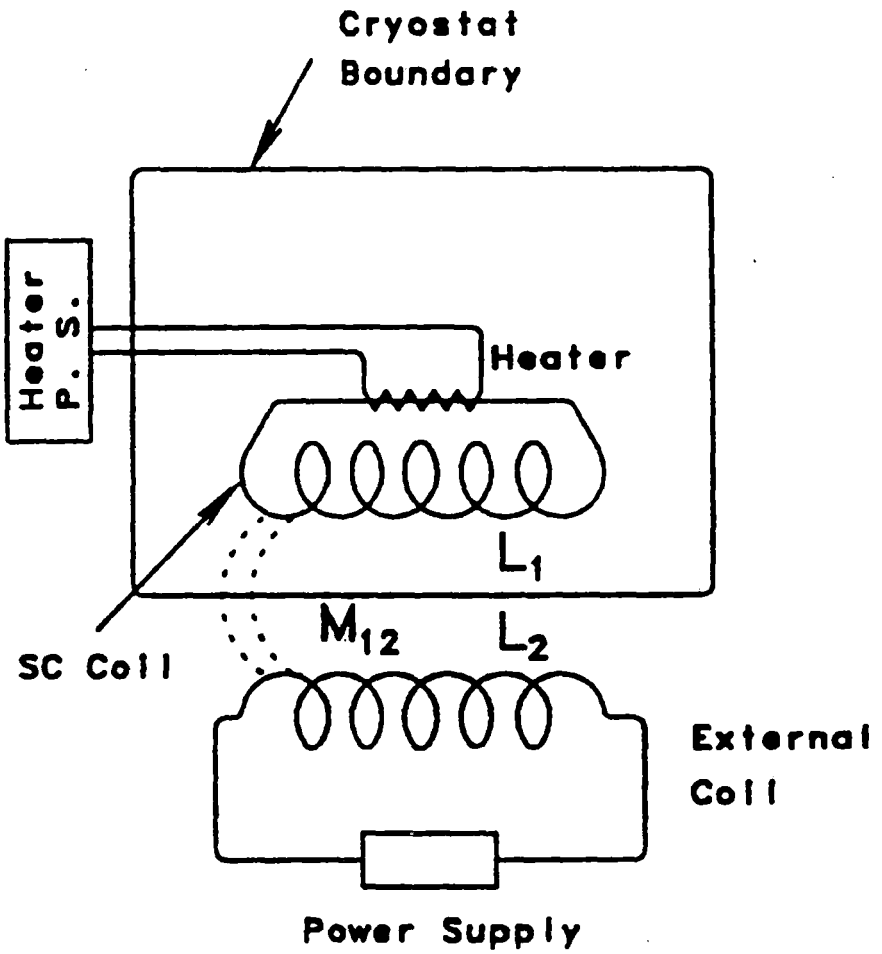

Figure 28 SC coil system with no current leads + external "flux" supply

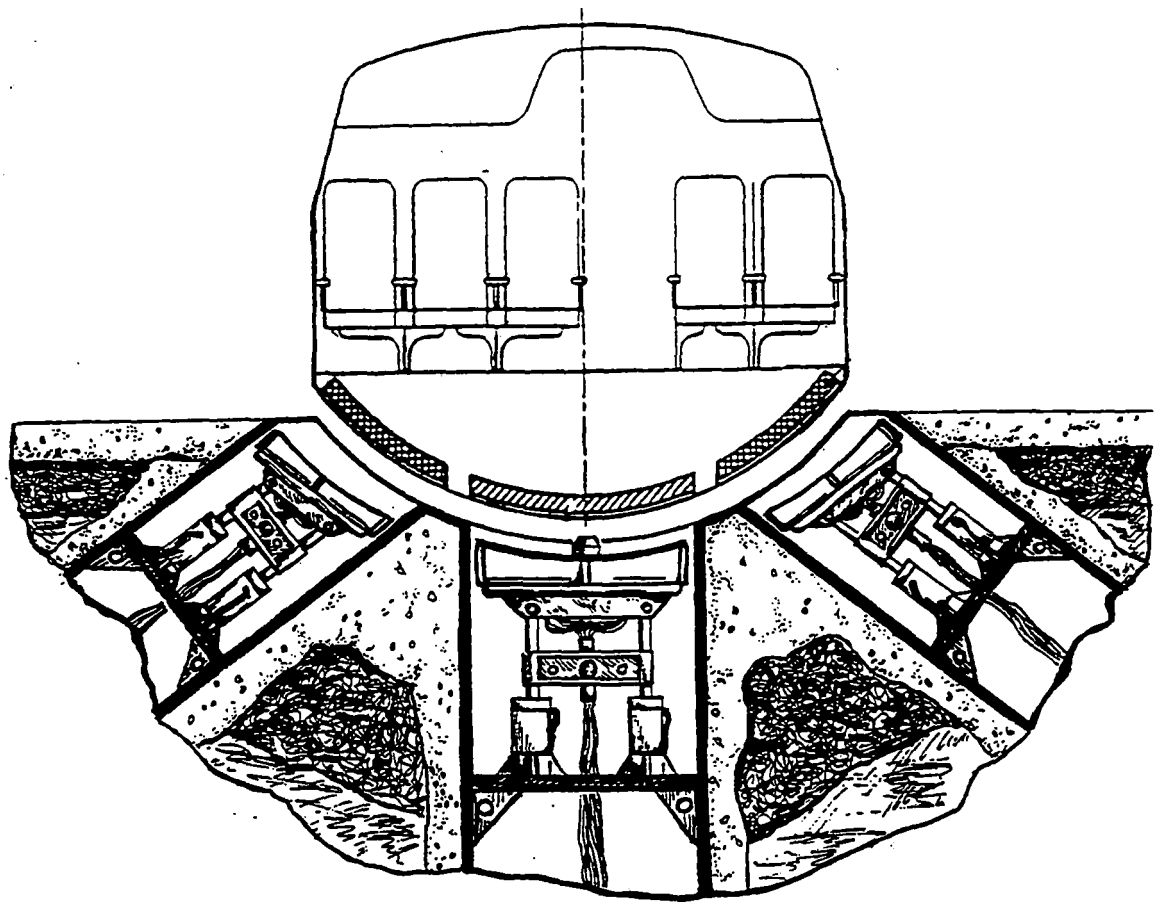

Figure 29 Cross-sectional view of a coil charging system (charging coils retracted)

Figure 28 illustrates the proposed method for charging the superconducting coils in the maglev system under consideration. It consists of a power supply which acts as an external flux supply and which is magnetically "coupled" to the superconducting coil to be charged. This baseline approach has no current leads coming through the cryostat boundary from the main superconducting coil or circuit. Taken together, the external power supply and the coil to be charged are a type of transformer. The terminals of the superconducting coil are connected together (short circuited) within the cryostat, but a length of the wire in the coil has a heater in close proximity to it. Outside the cryostat, another coil system, which may be conventional or superconducting, is brought near the superconducting coil. Both coils are assumed

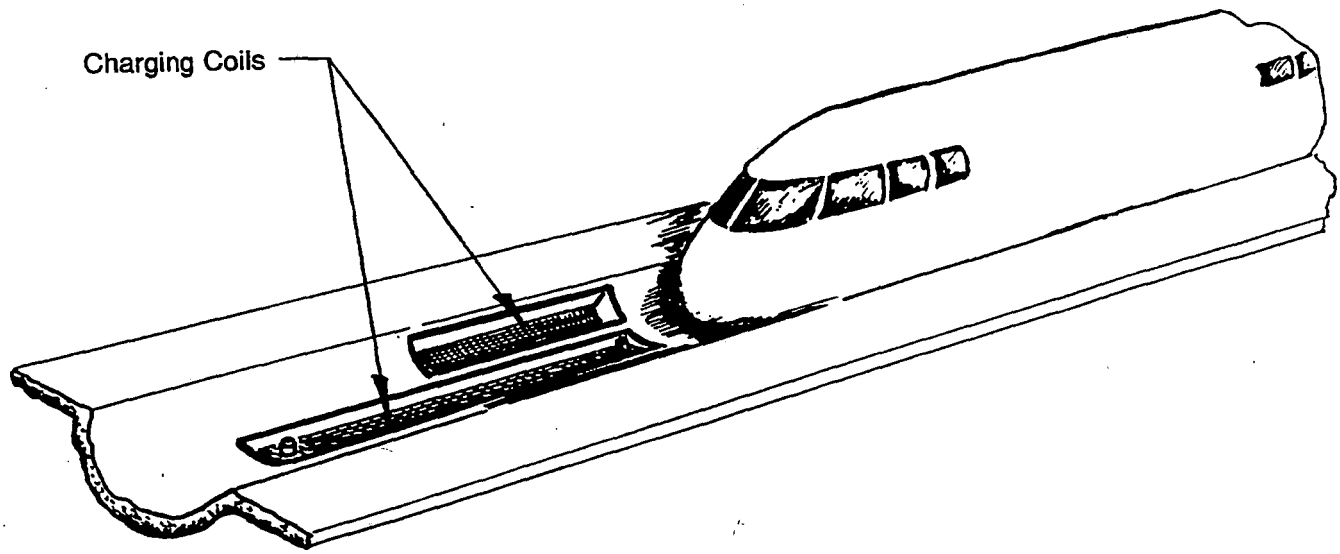

Figure 30 Possible configuration for a "turn-key" coil charging system

to be initially uncharged or in a zero current condition.

The current from the heater power supply is increased until the temperature of the main coil superconducting wire near the heater is above its critical temperature and, therefore, resistive. This becomes a resistance in series with the main coil. The current in the external coil is now raised to the necessary DC level by its power supply. During this time a small current will be induced in the main superconducting coil and will decay in time depending on circuit parameters. The heater power supply is now turned off and the main coil portion of wire allowed to regain its superconducting condition. Note that operation at this point is somewhat different than a persistent switch, for example, because the wire is not required to carry any significant current while recovering its superconducting condition as it must in cases using a persistent switch. Finally, the external coil power supply or a switch is used to discharge the external coil. This induces a current in the main superconducting coil in the cryostat by transformer action.

The principles underlying this method are straight forward and have been demonstrated in other applications. For example, it is the method used to induce the plasma current in a Tokamak (at the MIT Plasma Fusion Center and elsewhere), where the plasma is analogous to the main superconducting coil in this method and the ohmic heating transformer (coil) is analogous to the external coil system in this method. As another example, an analogous process has been used at the MIT Plasma Fusion Center to

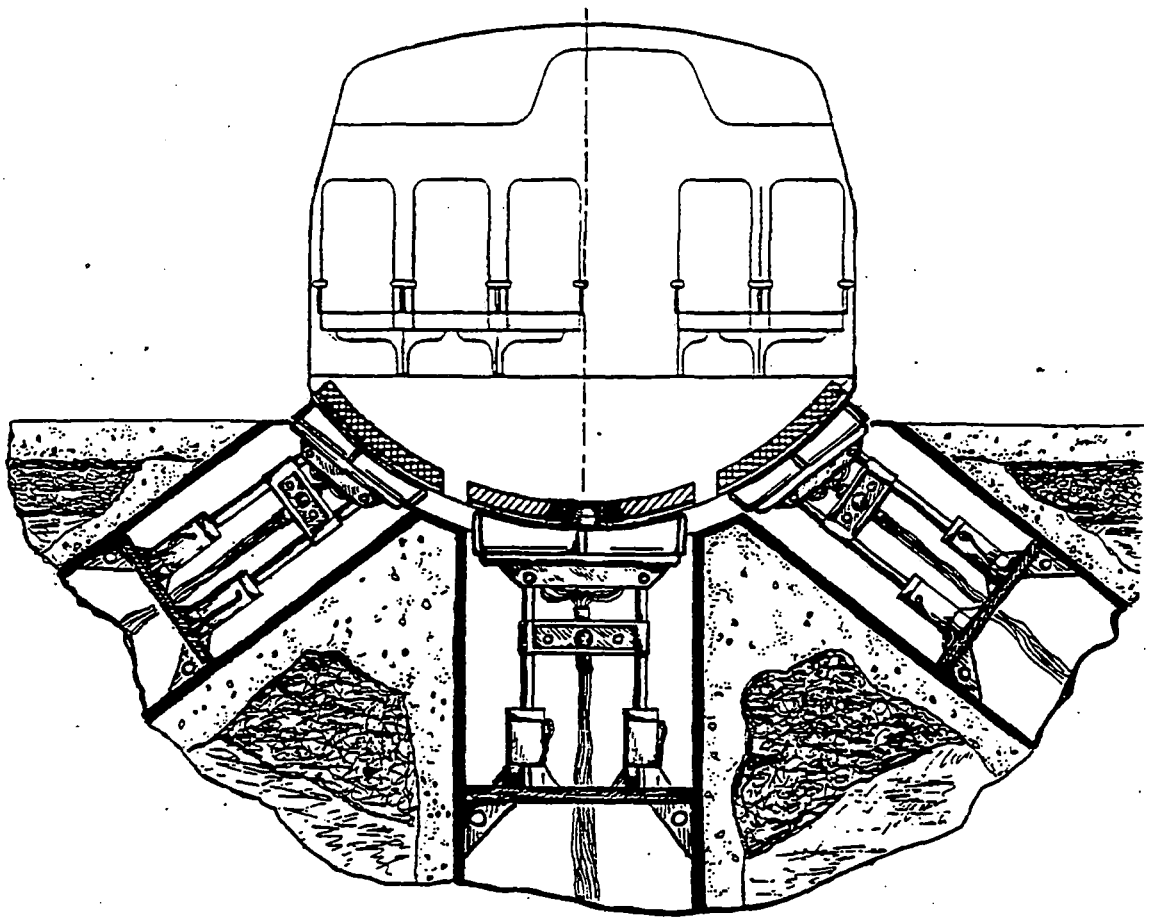

Figure 31 Cross-sectional view of coil charging system with charging coils in the charging position (extended)

induce a large current through a single turn superconducting coil to deduce the resistance of the joint.

Taking this proprietary method as the baseline charging approach for our application, we expect to produce a conceptual design in the future of a "turn-key" system that would allow all coils in a bogie to be charged simultaneously after cool down to operating temperature without the use of current leads entering into the cryostats.

Figure 30, Figure 29, and Figure 31 show various aspects of this "turn-key" charging system. Figure 30 shows a vehicle as it enters a typical charging station. Embedded in the magway is a set of electromagnetic coils that are mirror images of the levitation coils in a bogie. These embedded coils act as an external flux supply and form the primary side of the transformer-like charging system described above.

Figure 29 is a cross-sectional view of the vehicle positioned over the embedded coils of the charging station, prior to charging. In this figure, the coils within the magway are in a retracted position. The vehicle is supported on air pads (not shown) that levitate the vehicle until its superconducting magnets are energized.

During charging, the embedded coils in the magway are mechanically extended as show in Figure 31. This minimizes the gap between the charging system coils and the coils to be charged, and thereby maximizes the inductive coupling between the two sets of coils for more energy efficient charging. After charging the vehicle coils, the coils in the magway are in a discharged condition and are retracted beneath the surface.

3.2.1.a.2. CRYOGENIC REFRIGERATION SYSTEM (CRS)

3.2.1.a.2.0. CRS DESIGN CRITERIA

The CRS has been designed to meet the following major criteria:

1. Cooling of the magnets will be accomplished by a forced flow of supercritical helium through the coils.
2. The temperature of helium exiting the coils will be 8 K or less.
3. The failure or quench of one magnet should not affect other magnets.
4. The magnet coils should stay active for at least 30 minutes after power loss to the CRS.
5. Heat shields cooled by liquid nitrogen (LN2) may be used in the magnets and/or piping to reduce the heat loads at 6-8 K, if appropriate.
6. High reliability.
7. Low power consumption.
8. Minimal size and weight.

3.2.1.a.2.1. PROCESS DESIGN

3.2.1.a.2.1.1. HEAT LOADS

A preliminary thermal analysis of the magnet geometries defined by MIT leads to the results shown in Figure 32. Assumptions used in developing the table are shown in Figure 33. Heat leak calculations have been made for non-shielded and 90 K shielding (LN2), as shown. The table shows the substantial reduction in heat leak at 6-8 K achievable with the use of shields, i.e. by a factor of 5, with 90 K shielding (LN2).

Heat leaks for the cryogenic piping and valves (to be described later) have been estimated based on what has been achieved in commercial practice for both non-shielded and shielded lines.

System heat loads at the 6-8 K level and for the shields are summarized in Figure 34 and Figure 36 for 140 and 45 passenger Magneplanes, respectively. Shield coolant flows are also shown in the tables.

3.2.1.a.2.1.2. REFRIGERATION CYCLE

Magnet cooling will be accomplished by a flow of supercritical (i.e. at a pressure of approximately 3 atm) helium as it warms from about 6 K to 8 K. For the range of heat loads anticipated, and considering the other design criteria, this flow of helium coolant can best be provided by a closed-cycle helium

Configuration-->		No Shield	90 K Shld
Temperatures	Units		
Shell	K	300	300
Shield	K	-	90
Coil	K	6	6
INSULATION			
Emittance	-	0.030	0.030
Layer Density	No./cm	24	24
Degrad Factor	-	4	3
Shield Area	M^2	-	2.00
Shield k	W/cm-K	-	1.10E-06
Shield No. Lyrs.	-	-	30
Shield Heat Flux	W/cm^2	-	1.85E-04
HT to Shield	W	-	3.700
Coil Area	M^2	1.50	1.50
Coil k	W/cm-K	1.12E-06	1.87E-07
Coil No. Lyrs.	-	60	30
Coil Heat Flux	W/cm^2	1.32E-04	1.26E-05
HT to Coil	W	1.976	0.188
SUPPORTS			
Force/Coil	Lbs	20,000	20,000
Allow Stress	psi	30,000	30,000
Geom. Factor	-	2	2
Ax/Coil	cm^2	8.603	8.603
L to Shield	cm	-	5
k to Shield	W/cm-K	-	0.0061
HT to Shield	W	-	2.204
L to Coil	cm	10	5
k to Coil	W/cm-K	0.0052	0.003
HT to Coil	W	1.315	0.434
TOTALS			
HT to Coil	W	3.291	0.622
HT to Shield	W	-	5.904
No. of Coils	-	14	14
Net Shields Load	W	-	**73.951**
Coils Load @ 6-8 K	W	**46.070**	**8.706**
LN2 Flow Rate	Lbs/Hr	-	2.969
LN2 Flow Rate	Ltrs/Hr	-	1.680

Figure 32 Magnet heat leaks

INSULATION:

1. 'k' values are calculated using the NASA equation with degradation factor applied, i.e.

$$k=DF[C\,1\,(N)^{\wedge}\,1.56(Th+Tc) + C2*E(Th^{\wedge}4.67-Tc^{\wedge}4.67)/N(Th-Tc)]$$

Conductive Radiative

where

DF=Degradation Factor
C1=4.48 E-12
C2=5.40 E- 14
N=No. of layers/cm
T=Temperature, K
E=Total hemispherical emittance
k=Thermal conductivity, W/cm-K

2. Coil and shield areas are based on MIT drawing.

SUPPORTS:

1. Geometry factor attempts to account for supports in three directions.

2. Allowable stress and 'k' values are based on G-11CR properties.

Figure 33 Notes and assumptions for magnet heat leaks calculations

refrigerator using a modified Claude cycle. It is a relatively simple cycle, employing two expanders and Joule Thomson (J-T) expansion to provide the refrigeration, and is similar to the cycle used in many commercial helium refrigerator/liquefiers.

Figure 35 shows a simplified flow diagram of the cycle along with process conditions at points throughout the cycle. This is our baseline cycle. Its design heat load also assumes LN2 cooled shields for magnets, lines and valves.

Operation of the cycle is as follows: High pressure helium from the compressor flows through HX-1 where it is cooled by counter-flowing low pressure helium. The high pressure flow then splits into two streams. One stream expands partially in EXP1, is cooled in HX-3, then expands in EXP2 and is returned to the low pressure side between HX-4 and HX-5.

The other stream continues through HX-2 through HX-6 and is cooled to low temperature by the returning low pressure gas flow.

This stream then flows through the buffer tank. A portion expands to 3.5 atm in the J-T-1 valve and is supplied to the magnet coils as coolant. The remainder expands through J-T-2 and enters the return side of HX-6. The buffer tank is sized to store enough cold, high pressure helium to continue cooling the magnets for 30 minutes in the event of a loss of power supplied to the CRS. In this event, the helium from the tank, after passing through the magnet coils, would be vented to atmosphere.

Helium flow returning from the coils, from HX-6 and from EXP2 is used to cool the high pressure stream in the HX train, as shown in the flow diagrams.

Several alternatives were considered before selecting the baseline cycle depicted in Figure 35. The basic parameters for the options considered are summarized in Figure 37. The use of LN2 shielding for magnets, lines and valves substantially reduces the 6-8 K load for the refrigerator and, accordingly, the compressor power input. Thus, shielding is highly desirable.

The additional use of LN2 for refrigerator precooling leads to a much higher usage rate and does not appear to be attractive due to a larger on-board LN2 tank and increased fill times.

3.2.1.a.2.2. CRS DESIGN

A Process Flow Diagram (PFD) for the system is shown in PSI Drawing No. 8054-1335, Sheets 1 and 2. Sheet 1 shows the following major elements:

1. Helium compressor with oil cooler, after cooler and oil removal equipment, all skid mounted. Alternate configuration can be developed for bulkhead mounting of after cooler and oil removal equipment.

2. Cold box containing heat exchangers, expanders, piping and valves for the refrigerator cycle. The cold box is maintained at high vacuum for thermal insulation purposes and cold components are wrapped with multi-layer insulation (MLI).

3. Cryogenic helium storage buffer tank for emergency operation, with vacuum jacket and MLI.

4. Ambient temperature helium gas storage tank to retain part of the helium inventory when the system is warm.

5. LN2 storage tank with vacuum jacket and MLI.

Sheet 2 shows the piping and valves to distribute the helium flow and LN2 shield flow to the magnets. The helium lines to and from the magnets would also have heat shields cooled by the flowing LN2 to

	HEAT LOADS SUMMARY		
9/2/92	(No. Passengers=140)		
		No Shield	**90K Shld**
6K Loads			
20 Magnets			
AC Losses	W	20.0	20.0
Leads Conduction	W		
Insul. & Supports	W	46.1	9.0
Lines/Valves			
Supply Lines	W	19.0	9.0
Return Lines	W	19.0	9.0
12 Valves	W	12.0	6.0
Total	W	**116.1**	**53.0**
Shield Loads			
Magnets	W	-	74.0
Lines	W	-	32.0
Valves	W	-	24.0
Total	W	-	**130.0**
LN2 Flow	Lbs/Hr	-	5.22
LN2 Flow	Ltrs/Hr	-	2.95

Figure 34 Heats loads summary (140-passenger)

minimize line heat leak to the 6-8 K helium.

The baseline CRS design has one cold box (and one compressor) supplying helium to all the magnets, as the PFD's indicate. With the cold box at one end of the Magneplane, long lines are required to convey the helium to the magnets in the bogie at the other end. This is reflected in the relatively large supply and return line heat leaks shown in Figure 34 and Figure 36.

Controls for the CRS compressor and cold box would be similar to those used in commercial refrigerator/liquefier systems. Helium flow control to the magnets, including means for quench protection, merits further discussion. The concept illustrated in the PFD (PSI Drawing No. 8054-1335)

shows the magnets connected in parallel with an open/close valve on the inlet line and a check valve in

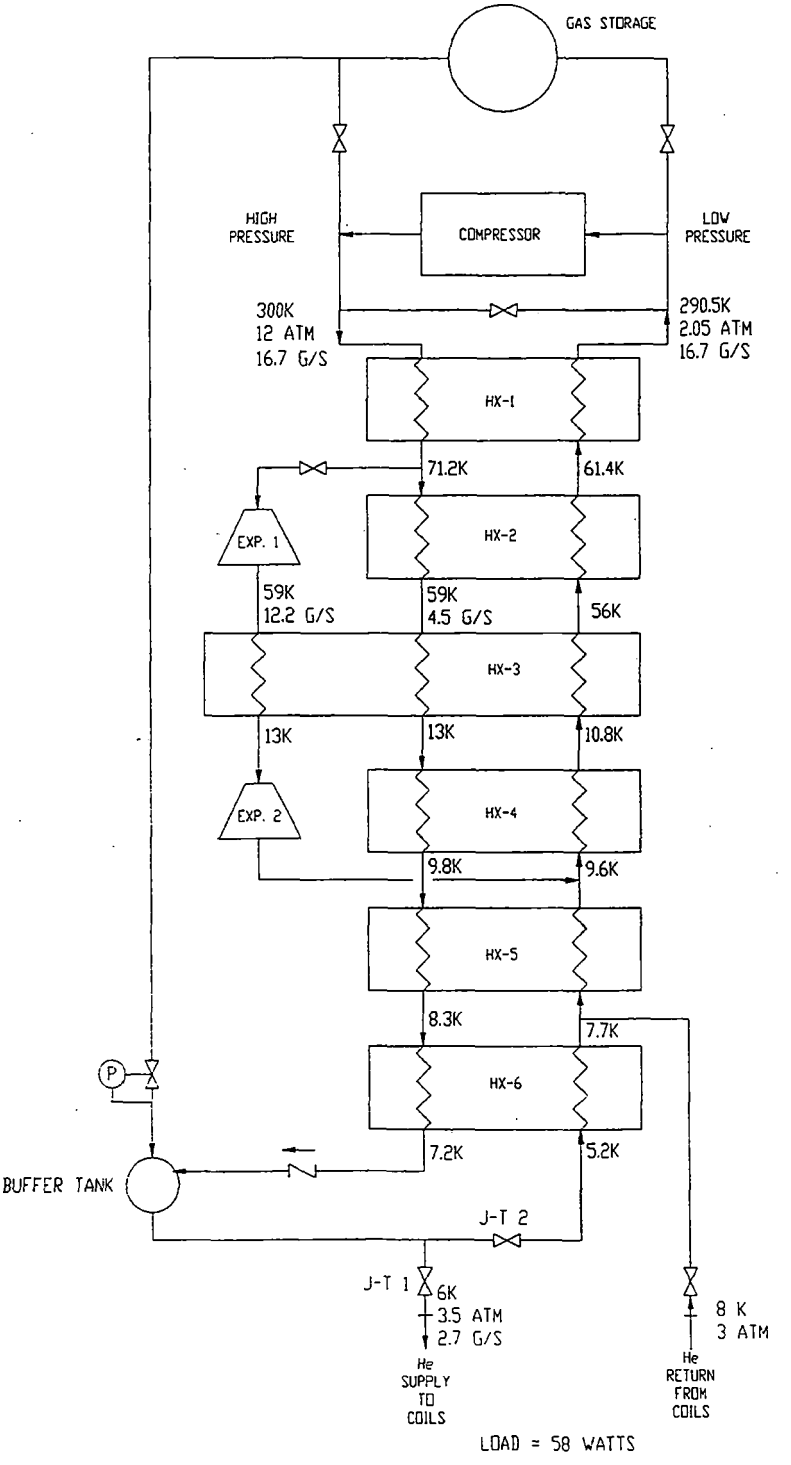

Figure 35 CRS flow diagram

	HEAT LOADS SUMMARY		
9/2/92	(No. Passengers=45)		
		No Shield	90K Shld
6K Loads			
20 Magnets			
AC Losses	W	20.0	20.0
Leads Conduction	W		
Insul. & Supports	W	46.1	9.0
Lines/Valves			
Supply Lines	W	13.0	6.5
Return Lines	W	13.0	6.5
12 Valves	W	12.0	6.0
Total	W	**104.1**	**48.0**
Shield Loads			
Magnets	W	-	74.0
Lines	W	-	22.0
Valves	W	-	24.0
Total	W	-	**120.0**
LN2 Flow	Lbs/Hr	-	4.82
LN2 Flow	Ltrs/Hr	-	2.73

Figure 36 Heat loads summary (45-passenger)

shows the magnets connected in parallel with an open/close valve on the inlet line and a check valve in the exit line of each magnet. In addition, the helium return line from each bogie has a control valve to control the return header pressure. The intent of the control system is to maintain the pressures in the helium supply and return headers nearly constant. Equal helium flow to each magnet would then be achieved by having the flow resistance of each magnet the same, with a fixed orifice for trim, if necessary. In the event of a magnet quench, the inlet valve would be closed. The expanding helium inventory in the coil would exhaust through the check valve into the return header. The return header pressure control valve would open somewhat to maintain header pressure at the set point, with the header volume as a buffer to limit the pressure transient. Transient back flow to any of the other (non-quenching) magnets would be prevented by the check valves. With the supply and return header

	CRS OPTIONS			
	Basis: 140 Passenger Magneplane			
Shield Cooling		No	LN2	LN2
Refrig. Pre-cooling		No	No	LN2
Refrigerator				
Capacity @ 6K	W	116	53	53
Compressor Electric				
Power Input	KW	110	55	35
LN2 Usage	Lbs/Day	0	125	350
LN2 Usage	Ltrs/Day	0	71	198

Figure 37 CRS options

pressures maintained more or less constant, stable coolant flow to the non-quenching magnets would be sustained. The relatively small volume of cold helium in the magnet conduit makes this possible and is an advantage of the forced flow magnet design over a pool boiling design.

The overall characteristics and salient features of the baseline CRS are summarized in Figure 38. Major components are further described in the following section.

3.2.1.a.2.3. CRS COMPONENTS

1. Expanders. PSI will employ turboexpanders in the CRS for the Magneplane. These units are compact and relatively lightweight and, when properly integrated with the CRS, are very reliable and require virtually no maintenance. They have been used in all larger capacity helium refrigerators for many years and, more recently, are being employed in smaller capacity systems. Accordingly, the baseline refrigeration cycle has been tailored to the use of two turboexpanders operating in series, as shown in the flow diagram.

The series arrangement reduces the pressure ratio across each turboexpander and increases its flow rate (as compared to two parallel expanders) which are conditions conducive to good efficiency.

System Specifications:

Cooling Capacity: 58 W at 6-8 K
Total Weight: 2500 kg (excluding cryogenic lines and valves)
Power Consumption: 69 kW
Cooling Air: TBD

Component Characteristics:

Component	Description	Envelope Dimensions (m)	Weight (kg)
Cold Box	Vertical cylinder	1.2 D x 1.7 H	700
Compressor	Skid mounted with all accessories	1.3 L x 1.0 W x 1.5 H	1,200
Cryogenic Buffer Tank	Horizontal cylinder (approx. 110 liters)	0.5 D x 1.0 L	140
Helium Gas Storage Tank	Horizontal cylinder (approx. 250 liters)	0.5 D x 1.5 L	140
Oil Cooler/ Aftercooler	Rectangular	1.5 W x 1.2 H x 0.2 D	240
Control Panel	Rectangular	1.0 H x 1.0 W x 0.5 D	80
LN2 Storage Tank	Horizontal cylinder (approx. 100 liters)	0.5 D x 1.0 L	120

Figure 38 Baseline CRS summary table

The approximate characteristics of the turboexpanders that would be compatible with the cycle requirements are shown in Figure 39. At the relatively small capacities/flow rates of interest, the units must run at extremely high rotational speeds in order to achieve a reasonable efficiency. Since the speeds are well beyond practical rotational speeds for oil bearings, gas bearings must be utilized. The use of gas bearings has other advantages in that it removes the presence of oil from this part of the system. The turboexpanders would be designs adapted from existing machines that have been built and tested. While the rotational speeds may seem high, the corresponding rotor tip velocities are well within practice. Externally pressurized, hydrostatic journal and thrust bearings will likely be used to achieve the maximum level of robustness in terms of withstanding dynamic loads. The turboexpanders for integration with the cycle would require complete design and development.

Parameter	T1	T2
pin (atm)	11.7	5.8
Tin (K)	71.2	13.0
pout (atm)	6.1	2.3
Flow (g/s)	12.24	12.24
Dia. (mm)	10	11
N (rev/sec)	6500	3700
Adiabatic Efficiency	0.75	0.75
Tout (K)	59.0	9.7
Net Refrig (W)	793	176

Envelope: Each approximately 100 mm diameter by 250 mm long

Weight: Each approximately 9 kilograms or less

Bearing Gas Flow: Each approximately 0.10 g/s at system high pressure
Figure 39 Approximate characteristics of compatible turboexpanders

An illustration of this type of turbine is shown in Figure 40. The power generated by the turbine is absorbed by means of a centrifugal blower at the other end of the rotating shaft which acts as a brake. The helium gas in the brake circuit is circulated by the blower through an air cooled heat exchanger and a throttle valve (Note: Illustration shows a water cooled heat exchanger). The heat exchanger removes from the system the heat energy equivalent to the shaft work generated by the turbine.

2. Helium Heat Exchangers. The type of heat exchanger used in PSI's commercial helium refrigerator/liquefiers is also applicable to Magneplane service, and its use is assumed in our baseline CRS design. It is relatively compact and rugged, has good performance and is inexpensive to construct. It consists of finned tubing wrapped helically around a mandrel and encased in a pressure boundary shell, as shown in Figure 41. The high pressure stream in the cycle flows inside the tube around the helical pass while the low pressure return flow passes in counter-flow over the fins in a direction parallel to the axis of the mandrel. The low pressure flow passage is confined between inner and outer stainless steel shells and headers are provided at the ends for connections to the high pressure and low pressure streams. If desired, a compact arrangement can be achieved by nesting the annular heat exchangers in the cycle one within the other, as shown in the detail of the figure.

An alternative type of exchanger which may be applicable is the conventional brazed-aluminum plate-fin

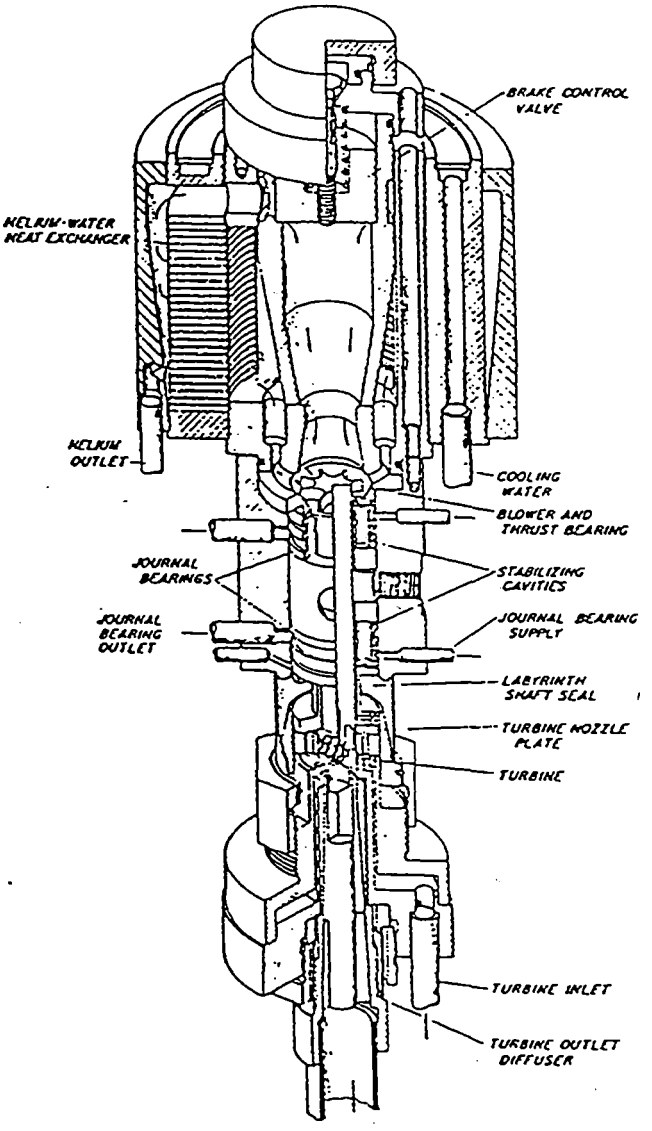

Figure 40 Gas bearing turboexpander

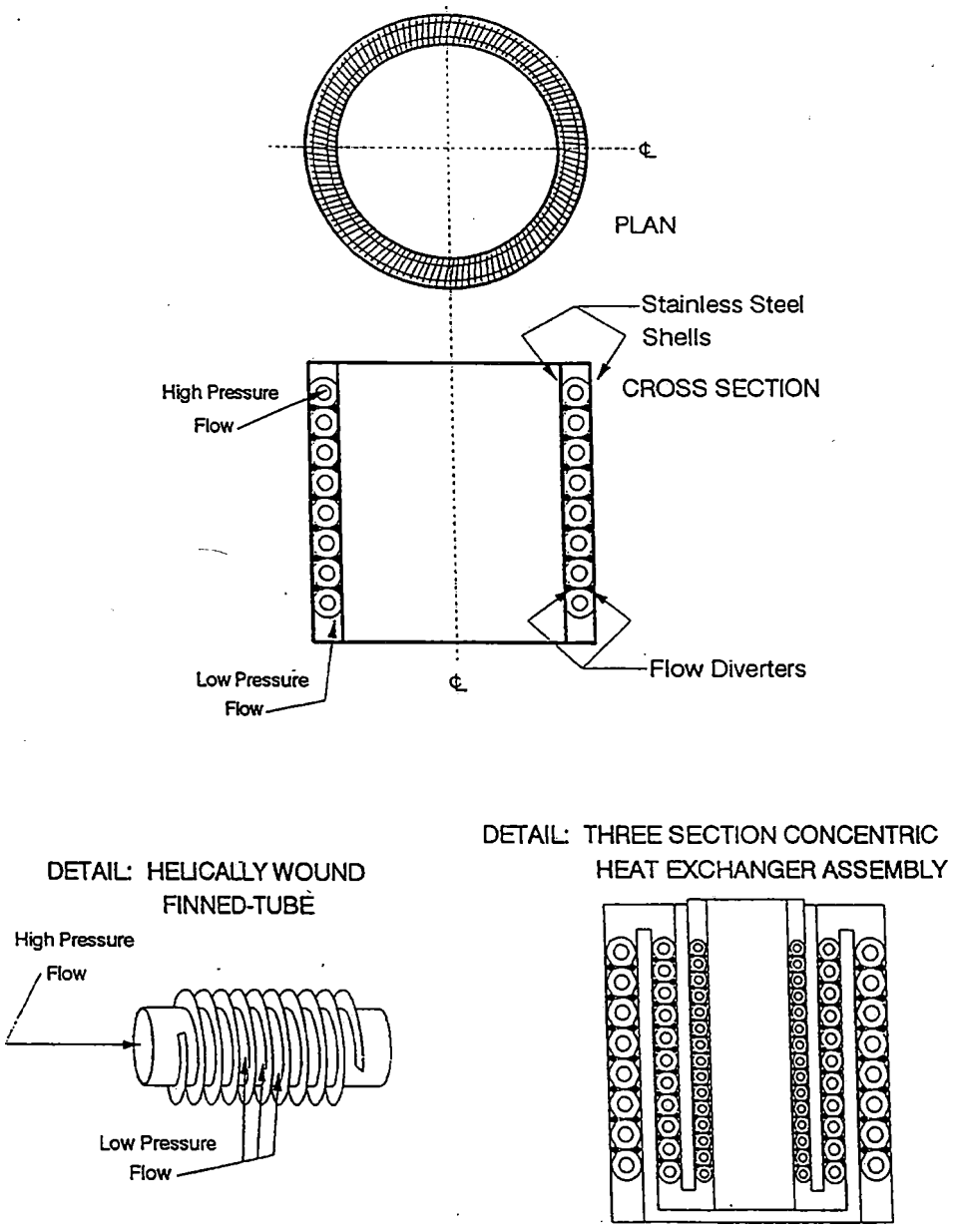

Figure 41 Finned-tube heat exchanger configuration

An alternative type of exchanger which may be applicable is the conventional brazed-aluminum plate-fin heat exchanger such as used in larger capacity refrigerator/liquefier systems. These are generally provided for much higher flow rates and tend to have long length when high effectiveness is required.

Suction pressure, atm	2.0
Discharge pressure, atm	13.5
Pressure ratio	6.75
Mass flow, g/s	16.7
Suction temperature, K	290.5
Power input, kW	55

Figure 42 Process requirements for CRS compressor

Some designs have been projected for helium refrigerators of the capacity of interest here. These designs have used long, narrow cores separated into sections with the sections placed side by side to reduce the package length. Although they may require greater volume in terms of overall package size, they may offer a weight advantage.

3. Compressor. The process requirements for the CRS compressor are listed in Figure 42. We have selected an oil-flooded, twin screw compressor for our baseline CRS design.

4. Cryogenic Lines and Valves. Cryogenic lines and valves will be vacuum jacketed with multi-layer insulation. Even so, as has been noted, the heat leaks to the 6 K helium associated with lines and valves are a significant portion of the total. To minimize these heat leaks, our baseline CRS design employs heat shielded lines and heat stationed valves with cooling for shields/stations provided by LN2 at 80-90 K. The use of heat shields/stations is common in systems where minimum heat leak is desired and the design approaches are well established. A cross-section view of an LN2 shielded transfer line concept is shown in Figure 43.

Extended-stem valves are commonly used to minimize heat leak. These can be heat stationed to further reduce heat leak by bringing the LN2 cooled shield into thermal contact with the stem bonnet part way between its warm and cold ends.

3.2.1.a.2.4. AREAS FOR DEVELOPMENT

Development activities that are required either to prove out a concept or to achieve an improvement over the baseline design include the following:

1. Turboexpanders

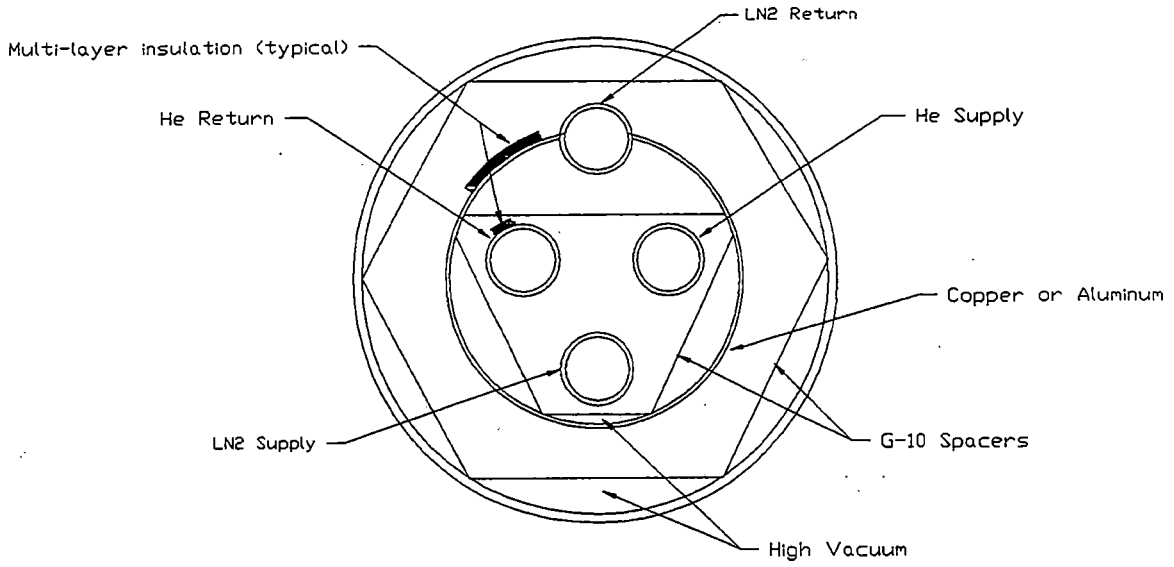

Figure 43 Vacuum-jacketed, LN2 shielded transfer line concept

Design and build prototypes for the specified process conditions and integrate with the cold box. Subject system to flow upsets and dynamic mechanical loads that are expected.

2. Regenerative Compressor

Design and build a prototype to assess performance. This type of machine offers a more compact, oil-free alternative to the oil-flooded twin screw compressor.

3. Flow Distribution/Quench Protection/Refrigeration Capacity/Control Operation

Operation of the baseline system to distribute helium flow to the parallel-connected magnets and to isolate a quenching magnet needs to be verified by test. This system would also be used to test refrigerator refrigeration capacity. This engineering test system would be equipped with additional temperature, flow and pressure instrumentation. Control system operation would be demonstrated in all modes.

4. System Reliability/Environmental Test/Maintenance Demonstration

A prototype system in the final production configuration should be tested to demonstrate reliability and verify performance in expected environmental and vibration conditions. A maintenance demonstration and verification of technical manuals can be accomplished with this unit.

3.2.1.b. PROPULSION AND BRAKING SYSTEM

The Magneplane vehicle is propelled by a *linear synchronous motor* (LSM). The LSM is a two-part system, consisting of steady-state superconducting propulsion magnets on the vehicle and an aluminum meander winding that runs along the center of the magway trough. The fields from the vehicle-based magnets interact with the continuously variable electronically controlled current in the LSM winding. The current and frequency are controlled directly by the wayside control unit, and ultimately by the global control center. Thus, *propulsion and braking control in the Magneplane system is global.*

3.2.1.b.1. THE LSM WINDING

Figure 44 shows an exploded view of a simplified three-phase LSM winding. Each phase of the winding is a rectangular pattern which proceeds down the magway away from the converter. Current returns from the far end by means of a winding which is a mirror image of the outgoing winding. Both electrical connections to each phase are at the converter end of the winding. The other two phases have the same winding pattern but are each offset by 1/3 of a pole pitch from the preceding phase.

This winding structure has several beneficial features:

1. All connections are at the converter end.
2. It has mechanical symmetry which provides strength.
3. It has electrical symmetry which generates uniform magnetic fields.

3.2.1.b.2. THE TRAVELLING MAGNETIC FIELD

Three phase power will be used to energize the magway winding. Figure 45 shows how three-phase ac power generates a travelling magnetic field. In this simplified diagram the phase conductors are shown in three distinct locations which are separated by 1/3 of a pole pitch. The currents are shown at an instant in time when the "A" phase current is at its peak. The distribution of current along the magway produces a vertical field component with an amplitude that varies sinusoidally along the x-axis. As the phase currents change with time, a sinusoidal travelling wave is generated in the positive x direction.

Thrust is produced when the vertical (z-axis) component of the magnetic field interacts with currents in the transverse conductors of the propulsion coils on the vehicle. Similarly, x-axis components of the magway magnetic field interact with the propulsion coil conductors to produce z-axis forces. As long as the available thrust exceeds the drag plus acceleration forces, the vehicle will move in synchronism

with the travelling field. Proper operation is provided by a closed-loop control system which assures that

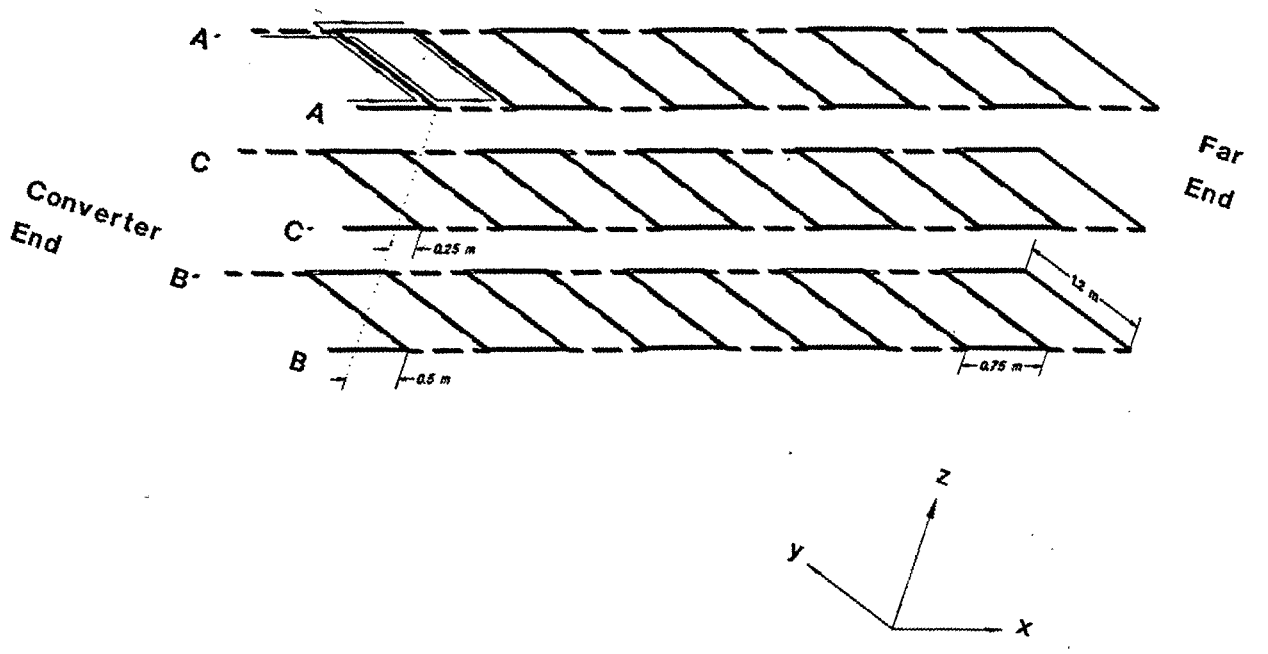

Figure 44 Exploded view of the linear synchronous motor windings

§ 3.2.1.b.

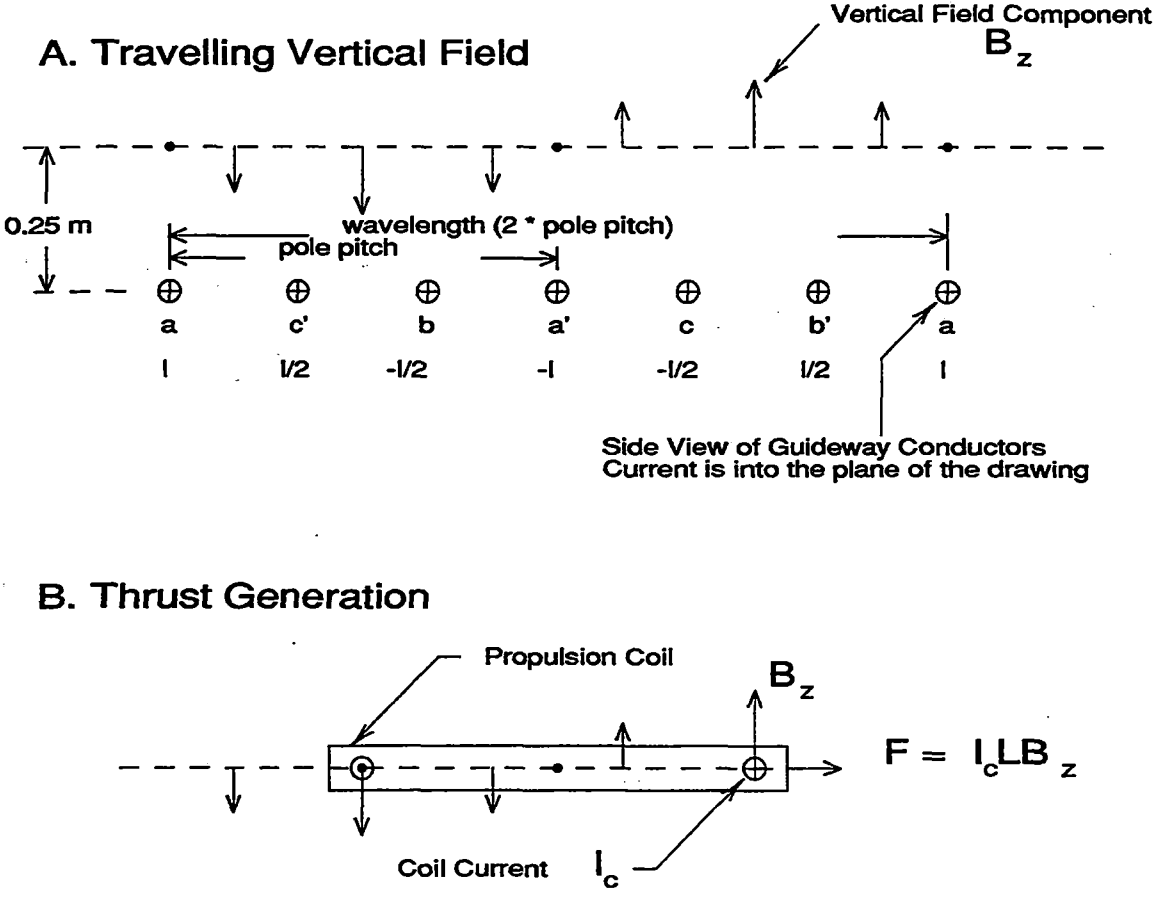

Figure 45 Linear synchronous motor operation

the vehicle is "locked" to the travelling field.

3.2.1.b.3. LSM WINDING DIMENSIONS

The width of the LSM winding was selected to use most of the 1.4 m distance between the bottom edges of the levitation sheets. Allowance has been made for the end-turns of the winding, mechanical clearance and ventilation spaces. The transverse portion of the winding, which generates the thrust, is 1.2 m wide.

The pole pitch of the winding was selected from analysis of an ideal sinusoidal magnetic field pattern. Analytic optimization in constant current operation shows that the LSM flux density at the propulsion coils is maximum when:

$$p = \pi z$$

where p is the pole pitch and z is the separation between the LSM winding and the coils. This would be $\pi/4$ or 0.7854 m for z = 0.25 m. A pole pitch of 0.75 m has been selected.

The selection of a near optimum pole pitch contributes to the overall efficiency of the system and reduces space harmonics in the travelling field.

3.2.1.b.4. PROPULSION SYSTEM FORCES

Three-dimensional magnetic field modeling was used to compute the forces that arise from the interaction between the magway field and the propulsion coils on the vehicle. The 3-dimensional model consists of a pair of propulsion coils 0.25 m above the LSM winding as shown in Figure 46. The coils were then displaced in x and y with the winding currents fixed in time. The net force acting on the coil pair was computed and scaled to represent total force on the vehicle.

Part A of Figure 47 shows how the thrust and levitation forces change when the coils are displaced in the x-axis relative to the travelling wave produced by the LSM winding. The displacement is measured as an angle such that 360° corresponds to one wavelength or twice the pole pitch. The angle is called "thrust angle" and is related to (but not equal to) the torque angle discussed in the literature on rotating synchronous machines.

The figure shows that levitation forces, as well as propulsion forces, are developed by the LSM - an important feature in the design of the Magneplane system. The thrust angle determines how much thrust and levitation are developed. Both forces are proportional to winding current at any fixed thrust angle. These two facts make it possible to use thrust angle and winding current to control thrust and levitation independently.

Modulation of the levitation force will be used for heave damping. A 20 degree range of thrust angle will provide about ± 18,000 N for damping. The nominal thrust angle of zero has been selected because nearly linear control of heave is achieved for deviations around this angle and the impact on thrust is

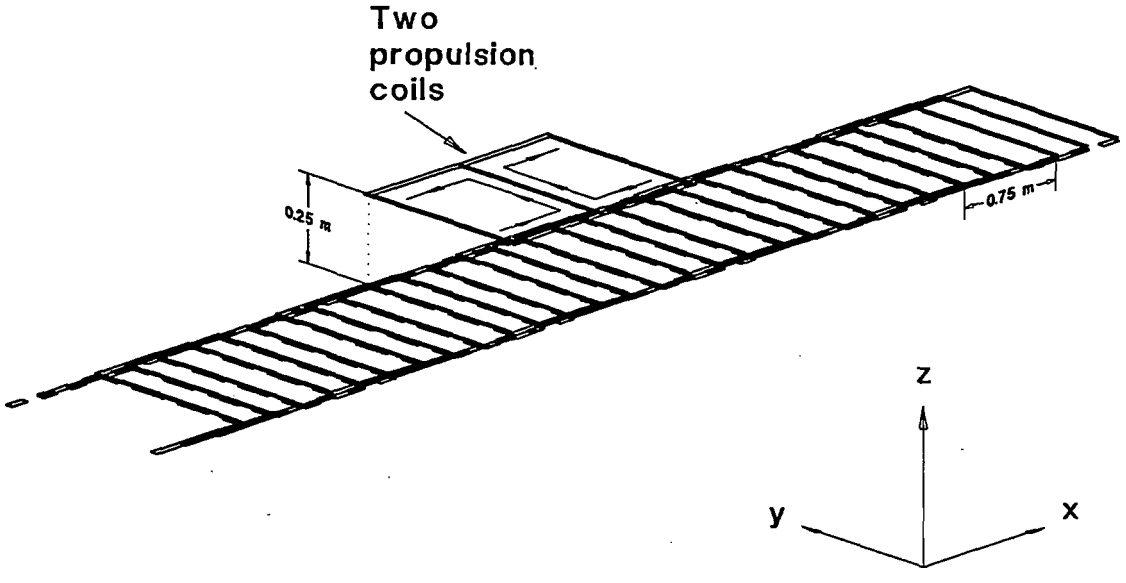

Figure 46 3D model for computing propulsion forces

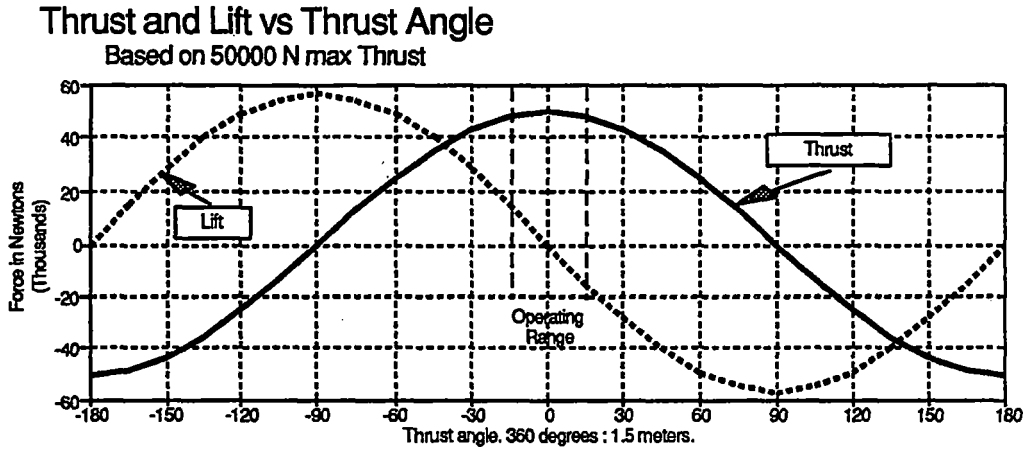

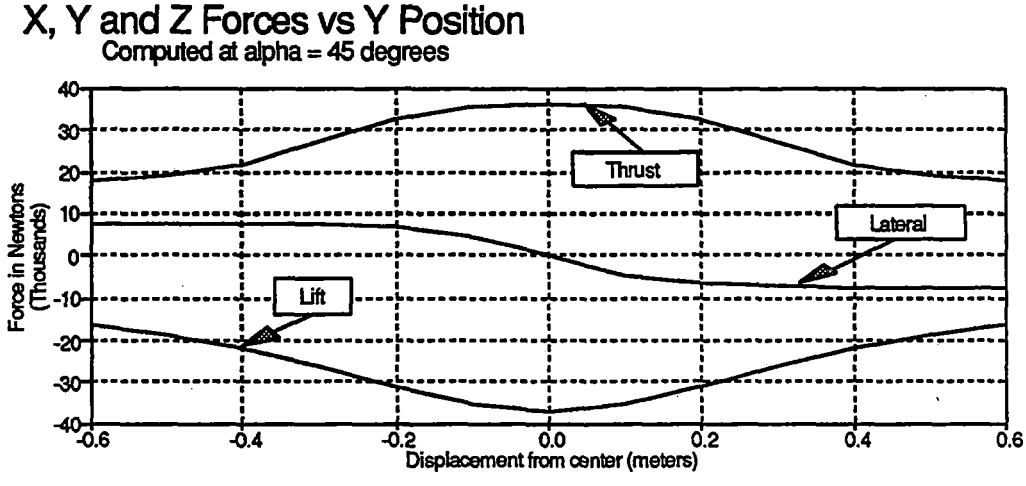

Figure 47 Propulsion forces from 3D magnetic field analysis

relatively small in this range.

Part B of Figure 47 shows how x, y, and z-axis forces are developed when the propulsion coils are displaced in the y-axis. Y-axis displacement decouples the propulsion coils from the LSM and reduces the thrust as shown. Levitation, or it opposite - attraction, pull the vehicle towards the LSM. This results in a lateral *and* vertical force component. The lateral force is stabilizing (toward the winding) when attraction is developed and destabilizing (away from the winding) when levitation is developed.

The results shown in the figure were generated at a thrust angle of 45 degrees and are based on the maximum thrust shown in Part A of the figure. The Y and Z forces at other thrust angles can be computed by solving F=K*sin(alpha) for K with alpha = 45 and then using that expression to compute the forces at other values of alpha. Thrust can be computed in a similar fashion using F=K*cos(alpha).

3.2.1.b.5. PROPULSION DESIGN SUMMARY

The baseline design of the Magneplane propulsion system has the following ratings which are based on the 140 passenger vehicle:

1. 150 m/s design speed
2. 50,000 N base thrust
3. 7.5 MW mechanical power output.

A summary of the design of the propulsion system for the 140 passenger vehicle is shown in Figure 48. All power and loss components for the baseline design are shown in the figure. The magway resistive loss is based on the nominal LSM winding resistance.

Figure 48 also shows how the Magneplane system meets the following SOW requirements.

1. 3.5% grade at operating speed. Magneplane can climb a 4% grade at 134 m/s.
2. 10% grade at reduced speed. Magneplane can climb a 10% grade at speeds up to about 90 m/s.

A design summary for the propulsion system of the 45 passenger vehicle is shown in Figure 49.

3.2.1.b.6. PROPULSION PERFORMANCE

Propulsion performance is the net effect of thrust delivered by the propulsion system and drag acting on the vehicle.

Basis data for 140 Passenger Vehicle

Design Speed	150	m/s
Thrust	50000	N
Mechanical Output Power	7.5	MW
Current	1075	A/phase
Winding Resistance	0.2	Ohms/phase

Power Budget

	Newtons	MW	%
EM Drag	14558	2.2	29.1
Aero Drag	24084	3.6	48.2
Grade Allowance	11358	1.7	22.7
Mechanical Output	50000	7.5	100.0
Mechanical Output		7.5	91.5
Guideway Resistive Loss		0.7	8.5
Total Input Power		8.2	100.0

Propulsion Efficiency

LSM Efficiency	91.5
Wayside Converter Efficiency	95.0
Substation , other losses	2.0
Total Propulsion System Efficiency	85.2

Grade Capability

Speed	50	75	100	134	150	m/s
Aero Drag	2676	6021	10704	19220	24084	N
EM Drag	39111	26735	20603	15988	14558	N
Total Drag	41787	32756	31307	35208	38642	N
Thrust @ 7.5 MW	150000	100000	75000	55970	50000	N
Total Drag	41787	32756	31307	35208	38642	N
Thrust - Drag	108213	67244	43693	20762	11358	N
Grade Capability	22	14	9	4	2	%

Figure 48 Propulsion design symmetry for 140-passenger magplane

Basis data for 45 Passenger Vehicle

Design Speed	150	m/s
Thrust	30000	N
Mechanical Output Power	4.5	MW
Current	961	A/phase
Winding Resistance	0.2	Ohms/phase

Power Budget

	Newtons	MW	%
EM Drag	7279	1.1	24.3
Aero Drag	19125	2.9	63.8
Grade Allowance	3596	0.5	12.0
Mechanical Output	30000	4.5	100.0
Mechanical Output		4.5	89.0
Guideway Resistive Loss		0.6	11.0
Total Input Power		5.1	100.0

Propulsion Efficiency

LSM Efficiency	89.0
Wayside Converter Efficiency	95.0
Substation , other losses	2.0
Total Propulsion System Efficiency	82.9

Grade Capability

Speed	50	75	100	134	150	m/s
Aero Drag	2125	4781	8500	15263	19125	N
EM Drag	19556	13367	10302	7994	7279	N
Total Drag	21681	18149	18802	23257	26404	N
Thrust @ 5.5 MW	90000	60000	45000	33582	30000	N
Total Drag	21681	18149	18802	23257	26404	N
Thrust - Drag	68319	41851	26198	10325	3596	N
Grade Capability	28	17	11	4	1	%

Figure 49 Propulsion design symmetry for 45-passenger magplane

3.2.1.b.6.1. DRAG COMPONENTS

Figure 50 shows the drag components which can act on the Magneplane vehicle in different modes of propulsion. The components are defined as follows:

Aerodynamic drag. Drag to the vehicle body travelling through air. This term includes the effect of control surfaces and wind gusts.

Landing gear friction. Landing gear friction assumes a constant coefficient of friction of 0.05. But one of the following two effects applies, depending on the magway material.

- Friction caused by the landing gear material sliding against a non-conductive magway material. No levitation force is developed and the entire vehicle weight is supported by the landing gear.

- Friction caused by the landing gear material sliding on aluminum levitation sheets. Electromagnetic lift reduces the weight supported by the landing gear and the corresponding drag term is reduced.

Electromagnetic (EM) Drag. One of the following two effects applies, depending on the propulsion mode of operation.

- *EM drag at constant height.* Electromagnetic drag caused by the levitation coils passing over the levitation sheets while the vehicle is supported at a constant height by the landing gear.

- *EM Drag at constant lift.* Electromagnetic drag caused by the levitation coils passing over the levitation sheets while the vehicle is magnetically levitated. The lift is constant but drag and height depend on vehicle speed.

Note that the drag terms have been shown over the whole speed range for illustration purposes. Some of the terms are encountered only over specific ranges of speed. For example, Magneplane operates on landing gear at low speeds so the constant height EM drag should be used rather than the constant lift EM drag.

3.2.1.b.6.2. LEVITATION MODES

The Magneplane vehicle can operate in three distinct levitation modes which are described as follows:

Mode I. Low speed operation with landing gear extended. The aluminum levitation sheets are replaced with alternate materials to eliminate low speed EM drag. Drag in this mode consists of landing gear friction plus aerodynamic drag.

Mode II. Intermediate speed operation with landing gear extended over aluminum levitation sheets. Drag in this mode consists of aerodynamic drag, EM drag at constant height and landing gear friction, which is reduced due to partial EM levitation.

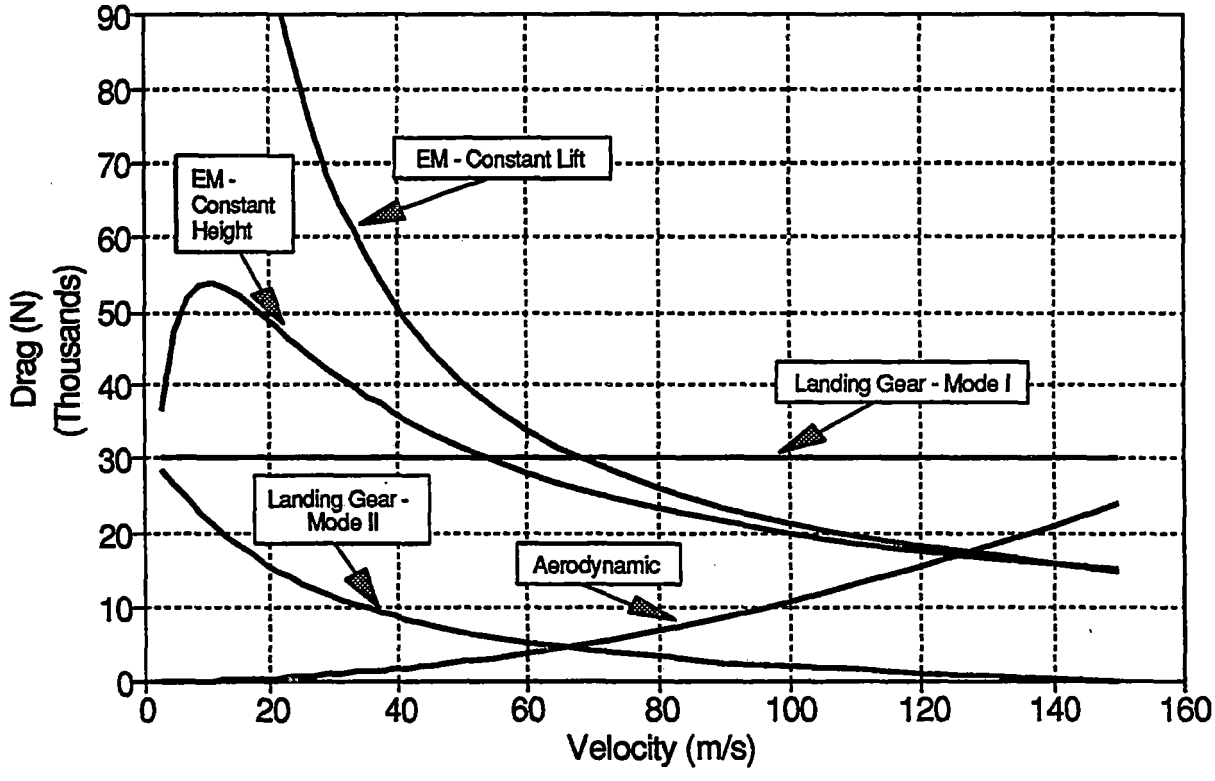

Figure 50 Drag components for 140-passenger magplane

Mode III. Normal operation, magnetically levitated. Drag consists of aerodynamic drag and EM drag, which is based on the lift/drag ratio.

3.2.1.b.6.3. DRAG AND PROPULSION ANALYSIS

EM drag components are the combined result of complex computer and manual calculations and generally cannot be represented by simple closed-form expressions. Nonetheless approximations for these and other drag terms were derived to facilitate propulsion system analysis activities during this project. The results are shown in Figure 51, where the terms are:

1. v = vehicle speed in m/s.

2. μ = landing gear coefficient of friction, 0.05.

3. FL/FD is the lift-to-drag ratio for a 2 cm levitation sheet and the specific geometry of the levitation coils. It can be approximated as:

$$FL/FD \cong -0.12686 + 0.31863v - 0.00033v^2.$$

4. W_{adj} is the total force on both levitation sheets

   - 605,505 N for the 140 passenger vehicle
   - 302,528 N for the 45 passenger vehicle

5. f_{em} is the EM drag in Mode II.

These approximations are only accurate over applicable ranges of speed. For example, the Mode II EM drag is accurate only up to about 50 m/s. Mode III terms are accurate over the range 30 to 150 m/s.

3.2.1.b.6.4. PROPULSION CAPABILITY

Propulsion capability for the 140 passenger vehicle is shown in Figure 52. The LSM operates with a constant thrust of 150,000 N up to 50 m/s and with a constant power of 7.5 MW and decreasing thrust up to 150 m/s.

Propulsion capability for the 45 passenger vehicle is shown in Figure 53. The LSM operates with a constant thrust of 150,000 N up to 50 m/s and with a constant power of 7.5 MW and decreasing thrust up to 150 m/s.

67 mph

In both figures the vehicle operates in Mode I up to 30 m/s. Then a transition occurs in which the landing gear are gradually retracted and a portion of the vehicle weight is supported magnetically. Complete EM lift occurs at 50 m/s. The vehicle is magnetically levitated in Mode III above 50 m/s. Operation during the landing gear transition is discussed in detail in section 3.2.3.i.

140-Passenger Vehicle

	MODE I	MODE II	MODE III
Aerodynamic drag	$1.0704 \cdot v^2$	$1.0704 \cdot v^2$	$1.0704 \cdot v^2$
EM Drag	0	$64{,}513\ [e^{-0.014v} - e^{-0.35v}]$	$W_{adj} / \frac{FL}{FD}$
Landing Gear Friction	$W_{adj} \cdot \mu$	$\left[W_{adj} - \left(\frac{FL}{FD} \cdot f_{em}\right)\right] \mu$	0

45-Passenger Vehicle

	MODE I	MODE II	MODE III
Aerodynamic drag	$0.85 \cdot v^2$	$0.85 \cdot v^2$	$0.85 \cdot v^2$
EM Drag	0	$32{,}256\ [e^{-0.014v} - e^{-0.35v}]$	$W_{adj} / \frac{FL}{FD}$
Landing Gear Friction	$W_{adj} \cdot \mu$	$\left[W_{adj} - \left(\frac{FL}{FD} \cdot f_{em}\right)\right] \mu$	0

Figure 51 Calculation procedure for drag components

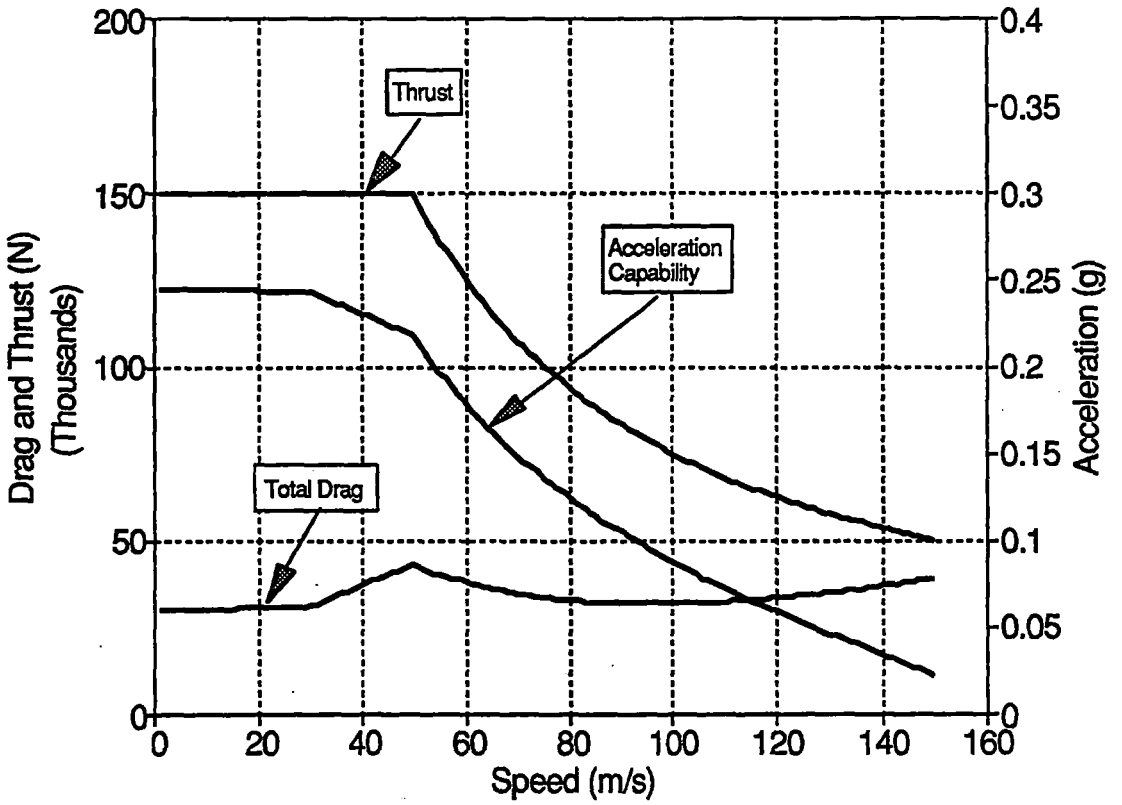

Figure 52 Propulsion characteristics for 140-passenger magplane

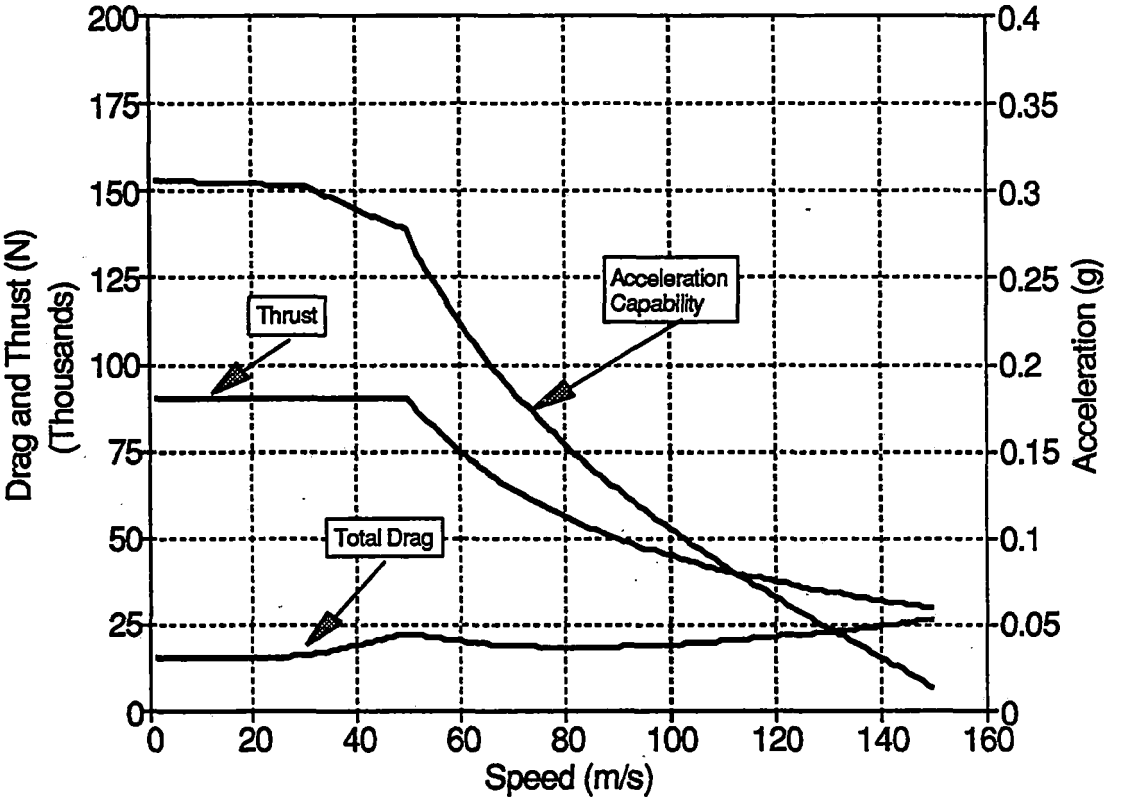

Figure 53 Propulsion characteristics for 45-passenger magplane

3.2.1.c. VEHICLE STRUCTURE AND LAYOUT

Section 3.2.1.c. contains the specifics on the vehicle fuselage, placement and weights of components, and regulatory requirements. Supplement D contains additional vehicle detail.

There are two sizes of vehicles currently under design: a 45-passenger and a 140-passenger version. A freighter variant is also under design (see Supplement D, section B).

3.2.1.c.1. SUBSYSTEMS OVERVIEW

The vehicle subsystems are listed below. Some of the subsystems are described in more detail in other parts of section 3.2.1.

3.2.1.c.1.1. SEATING:

Seating is five (5) passengers in each row, two (2) on the left side of an aisle and three (3) on the right side, a seating configuration similar to current airliner practices. The vehicle cross section showing the seating configuration is shown in Figure 54. The vehicle side view of passenger seating is shown in Figure 55. The aisle meets the criteria of FAR 25.815, which requires an aisle of 15 inches (.38 m) within 25 inches (.63 m) of the floor and 20 inches (.51 m) above this height. The cabin compartment of the 45 and 140 passenger configurations are essentially the same except for length. The 45 passenger vehicle is shown in Figure 56 and the 140 passenger vehicle is shown in Figure 57.

3.2.1.c.1.2 PASSENGER DOORS

Four (4) doors are provided, one (1) on each side at both the front and the rear. The doors are sliding and moved open and closed by an actuating system powered by compressed air.

3.2.1.c.1.3. BAGGAGE

A baggage and freight compartment is provided aft of the rear doors, which permits carry-on baggage to be deposited there by the passengers as they board the vehicle. Overhead baggage storage is also provided, similar to current passenger airliners.

3.2.1.c.1.4. EMERGENCY EGRESS

Escape hatches are provided in the passenger area similar to current aircraft practices, and a forward and rear escape hatch is provided which permits passengers to egress onto the elevated magway without ramps or other special equipment.

3.2.1.c.1.5. INTERIOR AMENITIES

Interior amenities appropriate to a commuter type vehicle will be installed, including handrails, armrests, interior panels, window estucheons, reading lights and air outlets.

3.2.1.c.1.6. CONSTRUCTION MATERIALS

The baseline vehicle structure is fabricated of advanced composite materials. The vehicle structure consists of a sandwich composite shell which is capable of carrying all design loads with an appropriate safety factor. The shell sandwich is composed of graphite epoxy or kevlar face sheets on both sides of a Nomex honeycomb core. The core thickness is approximately 1.5 inches (.04 m). Windows and door frames are integrally bonded during the sandwich layup and curing process. These materials showed an 8,000+ lb (3540 kg) weight savings in a trade study, (Supplement D, Section E) and had superior life characteristics compared to aluminum aircraft type construction. The aluminum materials did show lower initial acquisition costs and the decision to ~~change to~~ adopt non- metallic materials should await a more detailed life cycle cost analysis of the two concepts, which was beyond the scope of this study. A fine mesh of aluminum wires is bonded into the outer skin laminate to provide protection from direct lightning strikes. Other appropriate protection features such as foil groundplanes and bonding straps are provided, where appropriate, to protect the vehicle and personnel from the effects of a design lightning strike. The forward part of the vehicle shall be protected from birdstrikes. An alternate metallic vehicle structure is described in Supplement D, Section E.

3.2.1.c.1.7. CONTROL SURFACES

Active aerodynamic control surfaces are used to provide stability augmentation and ride control. Two (2) horizontal stabilators are provided at the front of the vehicle, and two (2) horizontal control surfaces are provided at the aft end. These surfaces are capable of generating both pitch and roll control forces. A vertical yaw canard is provided on the forward end and a conventional fin and rudder at the aft end (see Figure 58), which are capable of generating yaw stabilization and control forces as well as side force generation. These surfaces are actuated by a stability augmentation system described in Supplement D, Section C.

3.2.1.c.1.8. LEVITATION & PROPULSION MAGNETS

The super-cooled levitation and propulsion magnets are installed in a module on the belly at the forward and aft end of the vehicle and are removable for ease of maintenance (see Figure 59, Figure 60, and Figure 61, and section 3.2.1.a.1.). A liquid helium cryogenic system is located at the back of the vehicle. (See section 3.2.1.a.2.)

3.2.1.c.1.9. ELECTRICAL POWER

On-board electrical power is supplied by induction from the magway by means of power pick-up coils, which are located along the vehicle belly centerline, between the landing gear modules. (See Figure 59, Figure 60, and Figure 61.)

3.2.1.c.1.10. PRESSURIZATION

The cabin is pressurized when the vehicle is underway at a nominal 1/2 psi (3450 N/m^2) pressurization to protect passengers from pressure "bumps" when passing other vehicles or structures. This is a ram air pressurization system.

The nominal 1/2 psi (3450 N/m^2) cabin pressurization system is designed to limit pressure altitude changes to a 500 ft/min (2.5 m/s) rate which is consistent with aviation practices to limit passenger discomfort.

3.2.1.c.1.11. ENVIRONMENTAL SYSTEMS

Air conditioning, heating, and ventilation are provided through a system of ducts and blowers (20 CFM per occupant) (see Figure 62). Suitable air inlets, exits, heat exchangers and related ducts and components are provided to meet the passenger environmental needs.

3.2.1.c.1.12. LANDING GEAR

The landing gear consists of a system of retractable ski-type skids, supported by oleo pneumatic shock struts. The landing gear skids, when extended have a coefficient of friction of .05 and support the vehicle at speeds below the minimum levitation speed, approximately 60 mph (27 m/s) .

This set of skids is fitted with anti-friction air bearing pads, which provide for the low coefficient of friction when supplied with compressed air through a manifolding system. The landing gear uses a trailing link type suspension with a tailored oleo shock strut to provide for smooth ride qualities when the vehicle is accelerating or decelerating on the landing gear. A hydraulic retraction system is provided with uplock and downlock provisions to fix the gear in the appropriate positions. The ski/skid base incorporates features to allow it to support the vehicle in the curved magway, as well as on a flat surface as might be encountered in a station or maintenance area. The ski/skid configuration is shown in Figure 63. The anti-friction pneumatic skid pad is shown in Figure 64.

3.2.1.c.1.12.1. EMERGENCY BRAKING

While normal braking is provided by the propulsive magnets, a second set of skids is fitted with a high friction set of pads and is used for the emergency brake system. This set of skids provides for a coefficient of friction of 0.5 to 0.6 when deployed and does not have the air manifolding system. This system is fitted with a hydraulic retraction system similar to the primary landing gear and is deployed by firing an air/hydraulic accumulator.

3.2.1.c.1.13. ANTI-ICE SYSTEM

Appropriate portions of the vehicle exterior will be anti-iced or deiced, which may include control surfaces, air inlets, skid system, etc.

3.2.1.c.1.14 EXTERNAL LIGHTING

External lighting will meet criteria established by the Federal Railroad Administration.

3.2.1.c.1.15. REGULATORY REQUIREMENTS

The Magneplane vehicle shall meet criteria similar to Federal Aviation Regulation Part 25 as outlined in the following paragraphs.

3.2.1.c.1.15.1. FUNCTION AND INSTALLATION (25.1301)

All systems on the vehicle shall be installed similar to the criteria of Federal Aviation Regulation 25.1301 as follows:

Each item of installed equipment must -

(a) Be of a kind and design appropriate to its intended function;
(b) Be labeled as to its identification,function, or operating limitations, or any applicable combination of these factors;
(c) Be installed according to limitations specified for that equipment; and
(d) Function properly when installed.

3.2.1.c.1.15.2. EQUIPMENT, SYSTEMS, AND INSTALLATIONS (25.1309)

All systems on the vehicle shall meet criteria similar to FAR 1309 as follows:

(a) The equipment, systems, and installations .... must be designed to ensure that they perform their intended functions under any foreseeable operating condition.
(b) The ... systems and associated components, considered separately and in relation to other systems,must be designed so that -
(1) The occurrence of any failure condition which would prevent the continued safe flight and landing of the vehicle is extremely improbable, and
(2) The occurrence of any other failure conditions which would reduce the capability or the ability of the crew to cope with adverse operating conditions is improbable.
(c) Warning information must be provided to alert the crew to unsafe system operating conditions, and to enable them to take appropriate corrective action. Systems, controls,and associated monitoring and warning means must be designed to minimize crew errors which could create additional hazards.

3.2.1.c.1.15.2.1. SYSTEM REDUNDANCY

In addition, provisions similar to FAR Special Conditions 13 as published in the Federal Register Vol 151, 153 dated 8/8/86, shall be applicable to Magneplane as follows:

"It must be shown that there will be no single failure or probable combination of failures under any anticipated operating condition which would prevent the continued safe operation, or it shall be shown that such failures are extremely improbable."

3.2.1.c.1.15.3. HUMAN FACTOR CONSIDERATIONS

Crash requirements contained in the Statement of Work only addressed a five (5) mph (2.2 m/s) automotive type crash requirement. This does not seem adequate for a 300 mph (134 m/s) vehicle, and the aviation requirements of the Federal Aviation Regulations have been self-imposed upon the design. These requirements include:

3.2.1.c.1.15.3.1. EMERGENCY CONDITIONS GENERAL (25.561)

(a) The vehicle, although it may be damaged in emergency conditions must be designed as prescribed in this section to protect each occupant under those conditions.
(b) The structure must be designed to give each occupant every reasonable chance of escaping serious injury in a minor crash when -

(1) Proper use is made of seats, belts, and all other safety design provisions;
(3)The occupant experiences the following ultimate inertia forces acting separately relative to the surround structure:

(i) Upward, 3.0 g
(ii) Forward, 9.0 g
(iii) Sideward, 3.0 g on the airframe; and 4.0 g on the seats and their attachments.
(iv) Downward, 6.0 g
(v) Rearward, 1.5 g

(c) The supporting structure must be designed to restrain, under all loads up to those specified in Paragraph (b)(3) of this section, each item of mass that could injure an occupant if it came loose in a minor crash landing.
(d) Seats and items of mass (and their supporting structure) must not deform under any loads up to those specified in Paragraph (b)(3) of this section in any manner that would impede subsequent rapid evacuation of occupants.

3.2.1.c.1.15.3.1.1. EMERGENCY DYNAMIC CONDITIONS (VEHICLE) (25.562)

(a) The seat and restraint system in the vehicle must be designed as prescribed in this section to protect each occupant during an emergency condition when -

(1) Proper use is made of seats, safety belts, and...(other features) provided for in the design; and
(2) The occupant is exposed to loads resulting from the conditions prescribed in this section.

(b) Each seat type design approved for crew or passenger occupancy must successfully complete dynamic tests or be demonstrated by rational analysis based on dynamic tests of a similar type seat, in accordance with each of the following emergency conditions. The tests must be conducted with an occupant simulated by a 170-lb (77 kg) anthropomorphic test dummy, as defined by 49 CFR Part 572, Subpart B, or its equivalent, sitting in the normal upright position. (1) A change in downward vertical velocity (delta v) of not less than 35 feet (10 m) per second, with the ...(vehicle's)... longitudinal axis canted downward 30 degrees with respect to the horizontal plane. Peak floor deceleration must occur in not more than 0.08 seconds after impact and must reach minimum of 14 g. (2) A change in forward longitudinal velocity (delta v) of not less than 44 feet (13 m/s) per second, with the... (vehicle's)... longitudinal axis horizontal and yawed 10 degrees either right or left, whichever would cause the greatest likelihood of the upper torso restraint system (where installed), moving off the occupant's shoulder, and the vehicle level. Peak floor deceleration must occur in not more than 0.09 seconds after impact and must reach a minimum of 16 g. Where floor rails or floor fittings are used to attach the seating devices to the test fixture, the rails or fittings must be misaligned with respect to the adjacent set of rails or fittings by at least 10 degrees vertically (i.e., out of parallel) with one rolled 10 degrees.
(c) The following performance measures must not be exceeded during the dynamic tests conducted in accordance with Paragraph (b) of this section:

(1) Where upper torso straps are used for crew members, tension loads in individual straps must not exceed 1,750 pounds(795 kg). If dual straps are used for restraining the upper torso, the total strap tension loads must not exceed 2,000 pounds (909 kg).

(2) The maximum compressive load measured between the pelvis and the lumbar column of the anthropomorphic dummy must not exceed 1,500 pounds (682 kg).
(3) The upper torso restraint straps (where installed) must remain on the occupant's shoulder during the impact.
(4) The lap safety belt must remain on the occupant's pelvis during the impact.
(5) Each occupant must be protected from serious head injury under the conditions prescribed in paragraph (b) of this section. Where head contact with seats or other structure can occur, protection must be provided so that the head impact does not exceed a Head Injury Criteria of 1,000 units.
(6) Where leg injuries may result from contact with seats or structure, protection must be provided to prevent axially compressive loads exceeding 2,250 pounds (1023 kg)in each femur.
(7) The seat must remain attached at all points of attachment, although the structure may have yielded.
(8) Seats must not yield under the tests specified in Paragraphs (b)(1) and (b)(2) of this section to the extent they would impede rapid evacuation of the vehicle occupants.

3.2.1.c.1.15.3.2. DOORS (25.783)

(a) Each cabin must have at least one easily accessible external door.
(b)There must be a means to lock and safeguard each external door against opening in transit (either inadvertently by persons or as a result of mechanical failure or failure of a single structural element either during or after closure). Each external door must be openable from both the inside and the outside, even though persons may be crowded against the door on the inside of the vehicle. Inward opening doors may be used if there are means to prevent occupants from crowding against the door to an extent that would interfere with the opening of the door. The means of opening must be simple and obvious and must be arranged and marked so that it can be readily located and operated, even in darkness. Auxiliary locking devices may be used.
(c) Each external door must reasonably free from jamming as a result of fuselage deformation in a minor crash.
(e) There must be a provision for direct visual inspection of the locking mechanism to determine if external doors, for which the initial opening movement is not inward (including passenger, crew service, and cargo doors), are fully closed and locked. The provision must be discernible under operational lighting conditions by appropriate crew members using a flashlight or equivalent lighting source. In addition, there must be a visual warning means to signal the appropriate crew members if any external door is not fully closed and locked. The means must be designed such that any failure or combination of failures that would result in an erroneous closed and locked indication is improbable for doors for which the initial opening movement is not inward.
(f) External doors must have provisions to prevent the initiation of pressurization of the vehicle to an unsafe level if the door is not fully closed and locked. In addition, it must be shown by safety analysis that inadvertent opening is extremely improbable.
(g) Cargo and service doors not suitable for use as emergency exits need only meet Paragraphs (e) and (f) of this section and be safeguarded against opening in transit as a result of mechanical failure or failure of a single structural element.
(h) Each passenger entry door in the side of the fuselage must qualify as a passenger emergency exit.
(j) All lavatory doors must be designed to preclude anyone from becoming trapped inside the lavatory, and if a locking mechanism is installed, it be capable of being unlocked from the outside without the aid of special tools.

3.2.1.c.1.15.3.3. SEATS, BERTHS, SAFETY BELTS AND HARNESSES (25.785)

Seating is configured to five abreast configuration as shown in Figure 54.

Seat pitch has been established as 32 inches (.81 m), which is consistent with passenger and commuter airplane requirements (shown in Figure 55).

Seats shall meet criteria similar to the aircraft transport requirements established in FAR 25.785 as follows:

> (a) A seat must be provided for each occupant who has reached his or her second birthday.
> (b) Each seat, berth, safety belt, harness, and adjacent part of the vehicle at each station designated as occupiable must be designed so that a person making proper use of these facilities will not suffer serious injury in an emergency as a result of the inertia forces specified in 25.561 and 25.562.
> (c) Each seat or berth must be approved.
> (f) Each seat or berth, and its supporting structure, and each safety belt or harness and its anchorage must be designed for an occupant weight of 170 pounds (77 kg), considering the maximum load factors, inertia forces, and reactions among the occupant, seat, safety belt and harness for each relevant load condition (including the emergency conditions prescribed in 25.561). In addition -
>
> > (1) The structural analysis and testing of the seats, berths, and their supporting structures may be determined by assuming that the critical load in the forward, sideward, downward, upward and rearward directions (as determined from the prescribed emergency conditions) acts separately or using selected combinations of loads if the required strength in each specified direction is substantiated. The forward load factor need not be applied to safety belts for berths.
> > (3) The inertia forces specified in 25.561 must be multiplied by a factor of 1.33 (instead of the fitting factor prescribed in 25.625) in determining the strength of the attachment of each set to the structure and each belt or harness to the seat or structure.
>
> (g) Each seat at a crew station must have a restraint system... There must be a means to secure each combined restraint system when not in use to prevent interference with the operation of the vehicle and with rapid egress in an emergency.
> (i) Each safety belt must be equipped with a metal to metal latching device.
> (j) If the seat backs do not provide a firm handhold, there must be a handgrip or rail along each aisle to enable persons to steady themselves while using the aisles...
> (k) Each projecting object that would injure persons seated or moving about ... in normal flight must be padded.

3.2.1.c.1.15.3.4. STOWAGE COMPARTMENTS (25.787)

(a) Each compartment for the stowage of cargo, baggage, carry-on articles and equipment and any other stowage compartment, must be designed for its placarded maximum weight of contents and for the critical load distribution at the appropriate maximum load factors corresponding to the specified load conditions, and to the emergency conditions of 25.561(b), except that the forces specified in the emergency conditions need not be applied to compartments located below, or forward, of all occupants in the vehicle. If the vehicle has a passenger seating configuration, excluding crew seats, of 10 seats or more, each

stowage compartment in the passenger cabin, except for underseat and overhead compartments for passenger convenience, must be completely enclosed.
(b) There must be a means to prevent the contents in the compartments from becoming a hazard by shifting, under the loads specified in Paragraph (a) of this section. For stowage compartments in the passenger and crew cabin, if the means used is a latched door, the design must take into consideration the wear and deterioration expected in service.
(c) If cargo compartment lamps are installed, each lamp must be installed so as to prevent contact between lamp bulb and cargo.

3.2.1.c.1.15.3.5. RETENTION OF ITEMS OF MASS IN PASSENGER AND CREW COMPARTMENTS (25.789)

(a) Means must be provided to prevent each item of mass in a passenger or crew compartment from becoming a hazard by shifting under the appropriate maximum load factors corresponding to the specified load conditions, and to the emergency conditions of 25.561(b).
(b) Each interphone restraint system must be designed so that when subjected to the load factors specified in 25.561(b)(3), the interphone will remain in its stowed position.

3.2.1.c.1.15.3.6. PASSENGER INFORMATION SIGNS AND PLACARDS. (25.791)

(a) If smoking is to be prohibited, there must be at least one placard so stating that is legible to each person seated in the cabin. If smoking is to be allowed, and if the crew compartment is separated from the passenger compartment, there must be at least one sign notifying when smoking is prohibited. Signs which notify when smoking is prohibited must be operable by a member of the crew and, when illuminated, must be legible under all probable conditions of cabin illumination to each person seated in the cabin.
(b) Signs that notify when seat belts should be fastened and that are installed to comply with the operating rules of this chapter must be operable by a member of the crew and when illuminated, must be legible under all probable conditions of cabin illumination to each person seated in the cabin.
(c) A placard must be located on or adjacent to the door of each receptacle used for the disposal of flammable waste materials to indicate that use of the receptacle for disposal of cigarettes, etc., is prohibited.
(d) Lavatories must have "No Smoking" or "No Smoking in Lavatory" placards conspicuously located on or adjacent to each of the entry doors.
(e) Symbols that clearly express the intent of the sign or placard may be used in lieu of letters.

3.2.1.c.1.15.3.7. FLOOR SURFACES (25.793)

The floor surface of all areas which are likely to become wet in service must have slip resistant properties.

3.2.1.c..3.15.3.8. EMERGENCY EVACUATION (25.803)

(a) Each crew and passenger area must have emergency means to allow rapid evacuation ...
(c) ... it must be shown that the maximum seating capacity including the number of crew members required ... can be evacuated from the vehicle to the ground under simulated emergency conditions within 90 seconds.

Emergency exits shall be provided per FAR 25.807, two Type 1 exits on each side of the vehicle between the front and rear doors. This includes the following requirement:

> Type I. This type is a floor level exit with a rectangular opening of not less than 24 inches (.6 m) wide by 48 inches (1.22 m) high, with corner radii not greater than one-third the width of the exit.

3.2.1.c.1.15.3.9. EMERGENCY EXIT ARRANGEMENT (25.809)

The emergency exit arrangement (see Figure 65) shall meet the guidelines of FAR 25.809 as follows:

(a) Each emergency exit, including a crew emergency exit, must be a movable door or hatch in the external walls of the fuselage, allowing unobstructed opening to the outside.
(b) Each emergency exit must be openable from the inside and the outside...

Each emergency exit must be capable of being opened when there is no fuselage deformation -

> (1) With the ...vehicle... in the normal ground attitude and in each of the attitudes corresponding to collapse of one or more legs of the landing gear; and
> (2) Within 10 seconds measured from the time when the opening means is actuated to the time when the exit is fully opened.

(c) The means of opening emergency exits must be simple and obvious and may not require exceptional effort.
(f) There must be a means to lock each emergency exit and to safeguard against its opening in transit, either inadvertently by persons or as a result of mechanical failure. In addition, there must be a means for direct visual inspection of the locking mechanism by crew members to determine that each emergency exit, for which the initial opening movement is outward, is fully locked.
(g) There must be provisions to minimize the probability of jamming of the emergency exits resulting from fuselage deformation in a minor crash.

The primary emergency exits are at the forward and aft end of the vehicle, which permits evacuation onto the magway. In addition, the side opening doors provide an alternate escape path, as well as side opening escape hatches located between the doors.

which is @ 127°C !

3.2.1.c.1.15.3.10. EMERGENCY EXIT MARKING (25.811)

(a) Each passenger emergency exit, its means of access, and its means of opening must be conspicuously marked.
(b) The identity and location of each passenger emergency exit must be recognizable from a distance equal to the width of the cabin.
(c) Means must be provided to assist the occupants in locating the exits in conditions of dense smoke.
(d) The location of each passenger emergency exit must be indicated by a sign visible to occupants approaching along the main passenger aisle (or aisles). There must be -

> (1) A passenger emergency exit locator sign above the aisle (or aisles) near each passenger emergency exit, or at another overhead location if it is more practical because of low headroom, except that one sign may serve more than one exit if each exit can be seen readily from the sign;
> (2) A passenger emergency exit marking sign next to each passenger emergency exit, except that one sign may serve two such exits if they both can be seen readily from the sign; and

(3) A sign on each bulkhead or divider that prevents fore and aft vision along the passenger cabin to indicate emergency exits beyond and obscured by the bulkhead or divider, except that if this is not possible, the sign may be placed at another appropriate location.

(e) The location of the operating handle and instructions for opening exits from the inside of the airplane must be shown in the following manner:

(1) Each passenger emergency exit must have, on or near the exit, a marking that is readable from a distance of 30 inches (.76 m).

(2) Each Type I passenger emergency exit operating handle must -

(i) Be self-illuminated with an initial brightness of at least 160 microlamberts; or

(ii) Be conspicuously located and well illuminated by the emergency lighting seen in conditions of occupant crowding at the exit.

(4) Each Type I passenger emergency exit with a locking mechanism released by rotary motion of the handle must be marked -

(i) With a red arrow, with a shaft of at least three-fourths of an inch wide and a head twice the width of the shaft, extending along at least 70 degrees of arc at a radius approximately equal to three-fourths of the handle length.

(ii) So that the centerline of the exit handle is within ± 1 inch (.025 m) of the projected point of the arrow when the handle has reached full travel and has released the locking mechanism, and

(iii) With the word "open" in red letters 1 inch (.025 m) high placed horizontally near the head of the arrow.

(f) Each emergency exit that is required to be enable from the outside, and its means of opening, must be marked on the outside of the airplane. In addition, the following apply:

(1) The outside marking for each passenger emergency exit in the side of the fuselage must include a 2-inch (.05 m) colored band outlining the exit.

(2) Each outside marking including the band, must have color contrast to be readily distinguishable from the surrounding fuselage surface. The contrast must be such that if the reflectance of the darker color is 15% or less, the reflectance of the lighter color must be at least 45% "Reflectance" is the ratio of the luminous flux reflected by a body to the luminous flux it receives. When the reflectance of the darker color is greater than 15%, at lease a 30% difference between its reflectance and the reflectance of the lighter color must be provided.

3.2.1.c.1.15.3.11. EMERGENCY LIGHTING (25.812)

Emergency lighting shall be in accordance with FAR 25.812 as follows:

(a) An emergency lighting system, independent of the main lighting system must be installed. However, the sources of general cabin illumination may be common to both the emergency and the main lighting systems if the power supply to the emergency lighting system is independent of the power supply to the main lighting system. The emergency lighting system must include:

(1) Illuminated emergency exit marking and locating signs, sources of general cabin illumination, interior lighting in emergency exit areas, and floor proximity escape path marking.

(2) Exterior emergency lighting.

(b) Emergency exit signs -

(1) For vehicles that have a passenger seating configuration, excluding crew seats, of 10 seats of more must meet the following requirements:

(i) Each passenger emergency exit locator sign required by 25.811(d)(1) and each passenger emergency exit marking sign required by 25.811(d)(1) must have red letters at least 1-1/2 inches (.038 m) high on an illuminated white background, and must have an area of at least 21 square inches (.014 m^2) excluding the letters. The lighted background-to-letter contrast must be at least 10:1. The letter height to stroke-width radio may not be more than 7:1, nor less than 6:1. These signs must be internally electrically illuminated with a background brightness of at least 24 foot-lamberts and a high-to-low background contrast no greater than 3:1.

(ii) Each passenger emergency exit sign required by 25.811(d)(3) must have red letters at least 1-1/2 inches (.038 m) high on a white background having an area of at least 21 square inches (.014 m^2) excluding the letters. These signs must be internally electrically illuminated or self-illuminated by other than electrical means and must have an initial brightness of at least 400 microlamberts. The colors may be reversed in the case of a sign that is self-illuminated by other than electrical means.

(c) General illumination in the passenger cabin must be provided so that when measured along the centerline of main passenger aisle(s), and cross aisle(s) between main aisles, at seat armrest height and at 40-inch (1 m) intervals, the average illumination is not less than 0.05 foot-candle and the illumination at each 40-inch (1 m) interval is not less than 0.01 foot-candle. A main passenger aisle(s) is considered to extend along the fuselage from the most forward passenger emergency exit or cabin occupant seat, whichever is farther forward, to the most rearward passenger emergency exit or cabin occupant seat, whichever is farther aft.

(d) The floor of the passageway leading to each floor-level passenger emergency exit, between the main aisles and the exit openings, must be provided with illumination that is not less than 0.02 foot-candle measured along a line that is within 6 inches (.15 m) of and parallel to the floor and is centered on the passenger evacuation path

(e) Floor proximity emergency escape path marking must provide emergency evacuation guidance for passengers when all sources of illumination more than 4 feet (1.2 m) above the cabin aisle floor are totally obscured. In the dark of night, the floor proximity emergency escape path marking must enable each passenger to -

(1) After leaving the passenger seat, visually identify the emergency escape path along the cabin aisle floor to the first exits or pair of exits forward and aft of the seat; and

(2) Readily identify each exit from the emergency escape path by reference only to markings and visual features not more than 4 feet above the cabin floor.

(f) Except for subsystems provided in accordance with Paragraph (h) of this section that serve no more than one assist means, are independent of the vehicle's main emergency lighting system, and are automatically activated when the assist means is erected. The emergency lighting system must be designed as follows.

(1) The lights must be operable manually from the crew station and from a point in the passenger compartment that is readily accessible .....

(2) There must be a crew warning light which illuminates when power is on in the vehicle and the emergency lighting control device is not armed.

(3) The crew station control device must have an "on" "off" and "armed" position so that when armed or turned on, the lights will either light or remain lighted upon interruption (except an interruption caused by a transverse vertical separation of the fuselage during crash) of the vehicle's normal electric power. There must be a means to safeguard against inadvertent operation of the control device from the "armed" or "on" positions.

(g) Exterior emergency lighting must be provided as follows:

(i) Not less than 0.03 foot-candle (measured normal to the direction of the incident light) on a 2-square-foot (.18 m^2) area where an evacuee is likely to make his first step outside the cabin.
(i) The emergency supply to each emergency lighting unit must provide the required level of illumination for at least 10 minutes(600 s) at the critical ambient conditions.
(j) If storage batteries are used as the energy supply for the emergency lighting system, they may be recharged from the main electric power system, provided that the charging circuit is designed to preclude inadvertent battery discharge into charging circuit faults.
(k) Components of the emergency lighting system.... must be capable of normal operation after having been subjected to the inertia forces listed in 25.561(b).
(l) The emergency lighting system must be designed so that after any single transverse vertical separation of the fuselage during a minor crash -

(1) Not more than 25 percent of all electrically illuminated emergency lights required by this section are rendered inoperative, in addition to the lights that are directly damaged by the separation;
(2) Each electrically illuminated exit sign required under 25.811(d)(2) remains operative exclusive of those that are directly damaged by the separation; and
(3) At least one required exterior emergency light for each side of the vehicle remains operative exclusive of those that are directly damaged by the separation.

3.2.1.c.1.15.3.12. EMERGENCY EXIT ACCESS (25.813)

Emergency Exit Access shall be per FAR 25.813 as follows:

Each required emergency exit must be accessible to the passengers and located where it will afford an effective means of evacuation. Emergency exit distribution must be as uniform as practical, taking passenger distribution into account; however, the size and location of exits on both sides of the cabin need not be symmetrical. In addition,

(a) There must be a passageway leading from each main aisle to..... each emergency exit and between individual passenger areas. Unless there are two or more main aisles, each exit must be located so that there is passenger flow along the main aisle to that exit from both the forward and aft directions.
(b) Adequate space to allow crew member(s) to assist in the evacuation of passengers must be provided as follows:
(e) No door may be installed in any partition between passenger compartments.
(f) If it is necessary to pass through a doorway separating the passenger cabin from other areas to reach any required emergency exit from any passenger seat, the door must have a means to latch it in open position. The latching means must be able to withstand the loads imposed upon it when the door is subjected to the ultimate inertia forces, relative to the surrounding structure listed in 25.561(b).

3.2.1.c.1.15.3.13. FIRE PROTECTION (25.851)

Fire protection shall be per FAR 25.851 as follows:

A minimum of three hand fire extinguisher shall be located conveniently in passenger compartments. At least one hand fire extinguisher must be conveniently located in the compartment.

3.2.1.c.1.15.3.13.1. FIRE PROTECTION SYSTEM (25.869)

Fire protection system shall be installed per FAR 25.869 as follows:

(a) Electrical system components:

(1) Components of the electrical system must meet the applicable fire and smoke protection requirements of 25.831(c) and 25.863.

(2) Electrical cables, terminals, and equipment in designated fire zones, that are used during emergency procedures, must be at least fire resistant (there are no fire zones).

(3) Main power cables (including generator cables) in the fuselage must be designed to allow a reasonable degree of deformation and stretching without failure and must be -

(i) Isolated from flammable fluid lines; or

(ii) Shrouded by means of electrically insulated, flexible conduit, or equivalent, which is in addition to the normal cable insulation.

(4) Insulation on electrical wire and electrical cable installed in any area of the fuselage must be self-extinguishing (no fire zones).

(c) Oxygen equipment lines must -

(3) Be installed so that escaping oxygen cannot cause ignition of grease fluid, or vapor accumulations that are present in normal operation or as a result of failure or vapor accumulations that are present in normal operation or as a result of failure or malfunction of any system.

There are no flammable fluids used on the vehicle except hydraulic fluid. If desired, a non-flammable hydraulic fluid could be utilized. However, this would not seem to be merited since there are no fire zones (engine compartments) in the vehicle.

3.2.1.c.1.15.3.13.2. FLAMMABLE FLUID FIRE PROTECTION (25.863)

Flammable fluid fire protection shall be per FAR 25.863 as follows:

(a) In each area where flammable fluids or vapors might escape by leakage of a fluid system, there must be means to minimize the probability of ignition of the fluids and vapors, and the resultant hazards if ignition does occur.

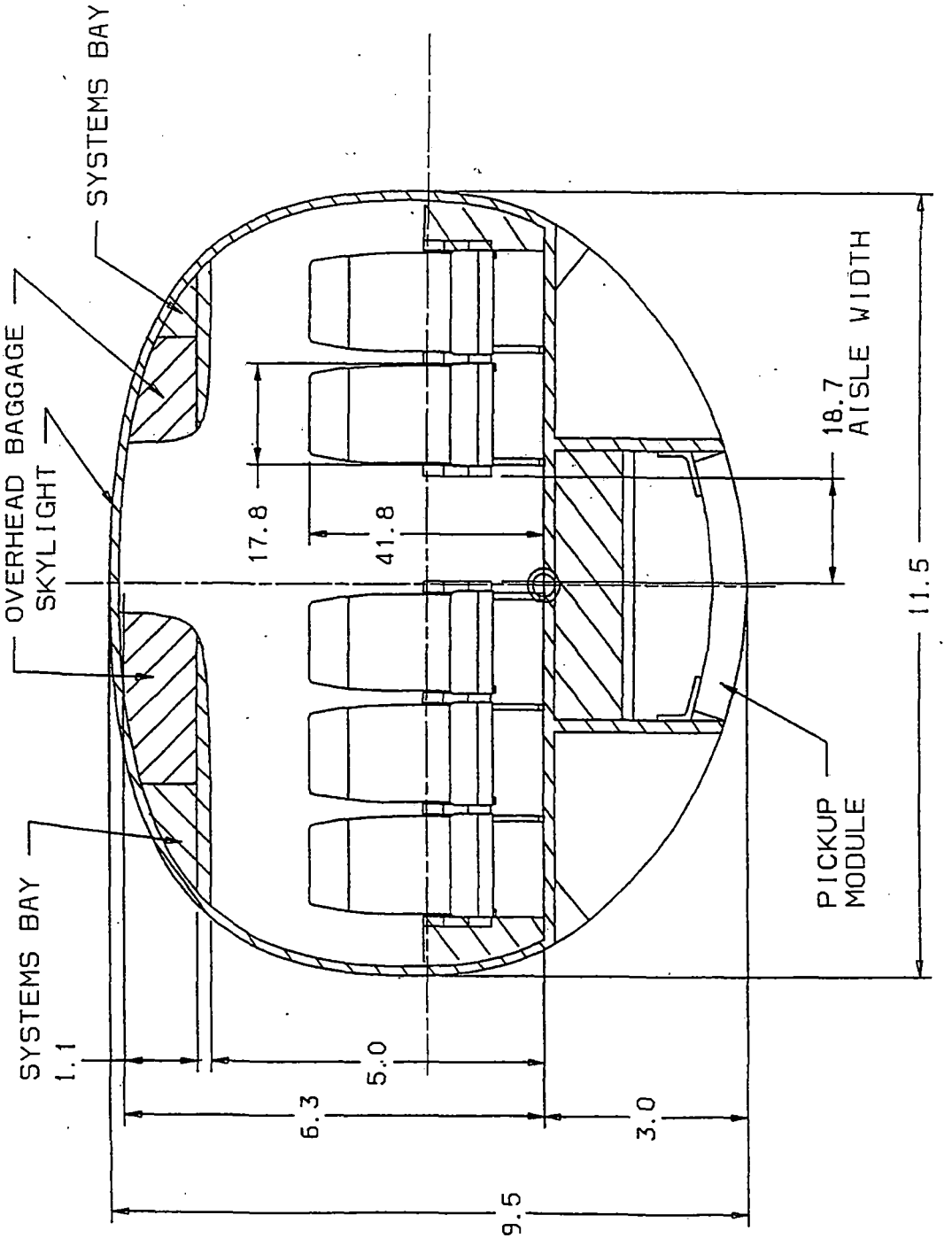

Figure 54 Magplane cabin cross section

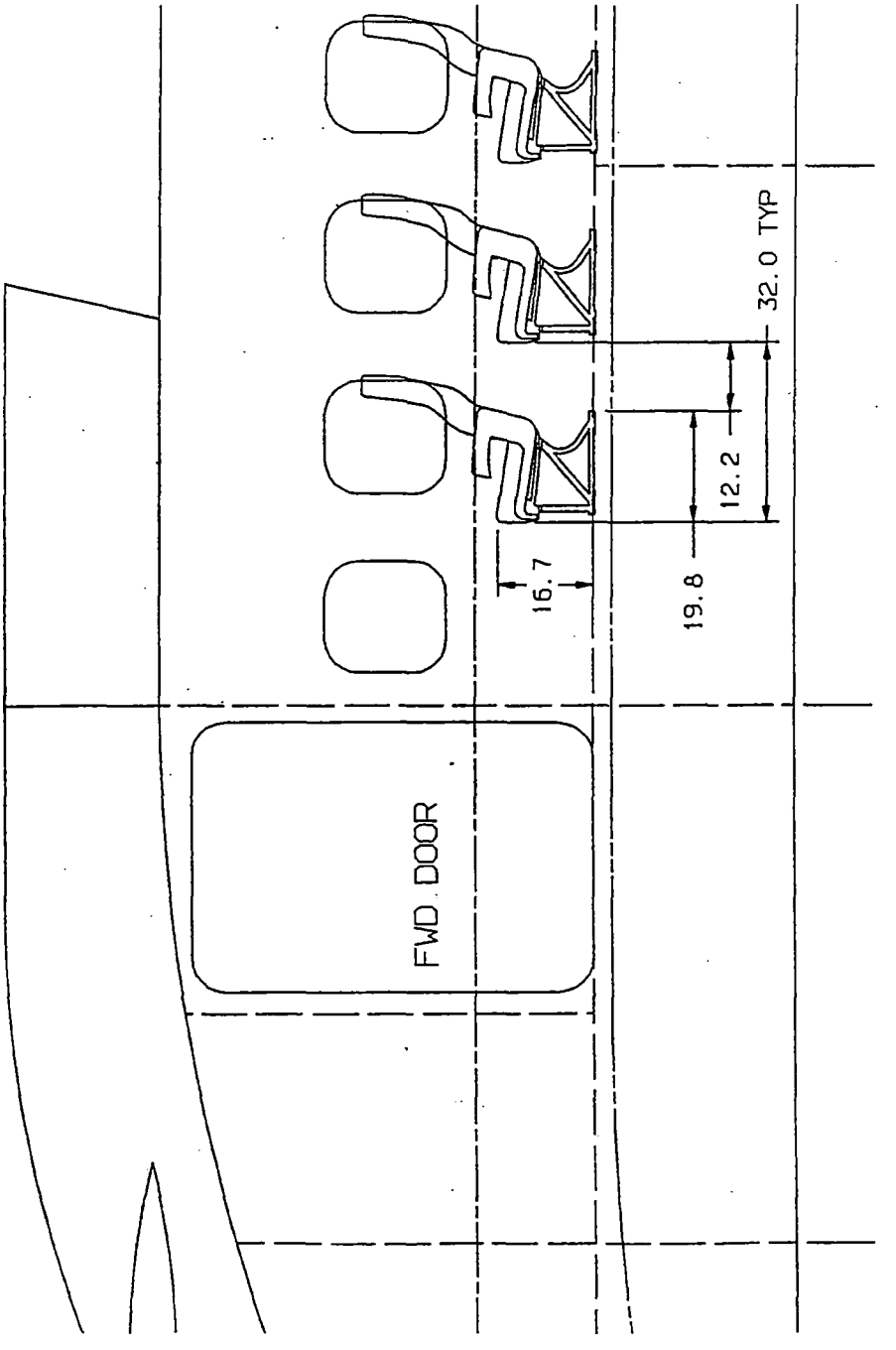

Figure 55 Side-view passenger seats

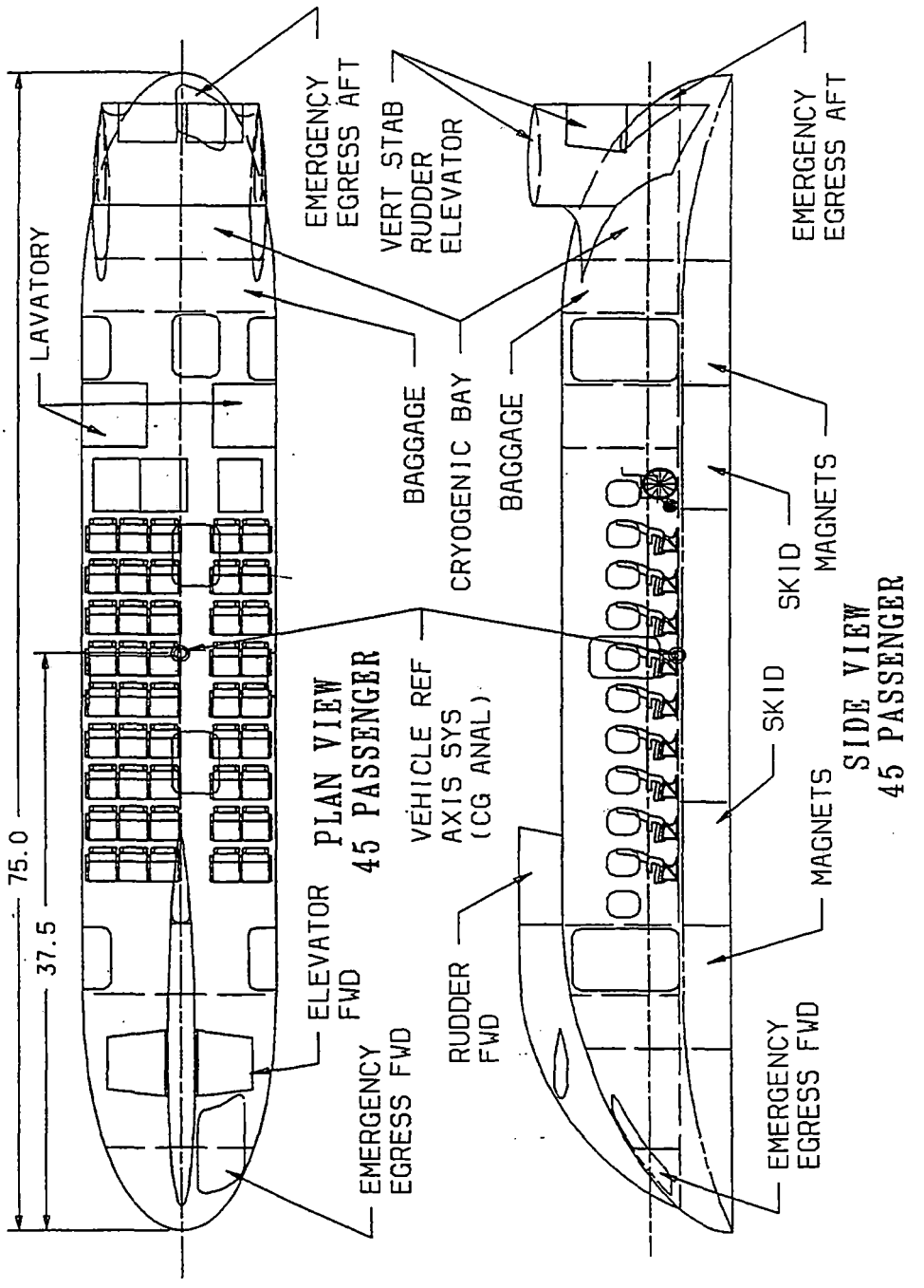

Figure 56 45 passenger magplane vehicle

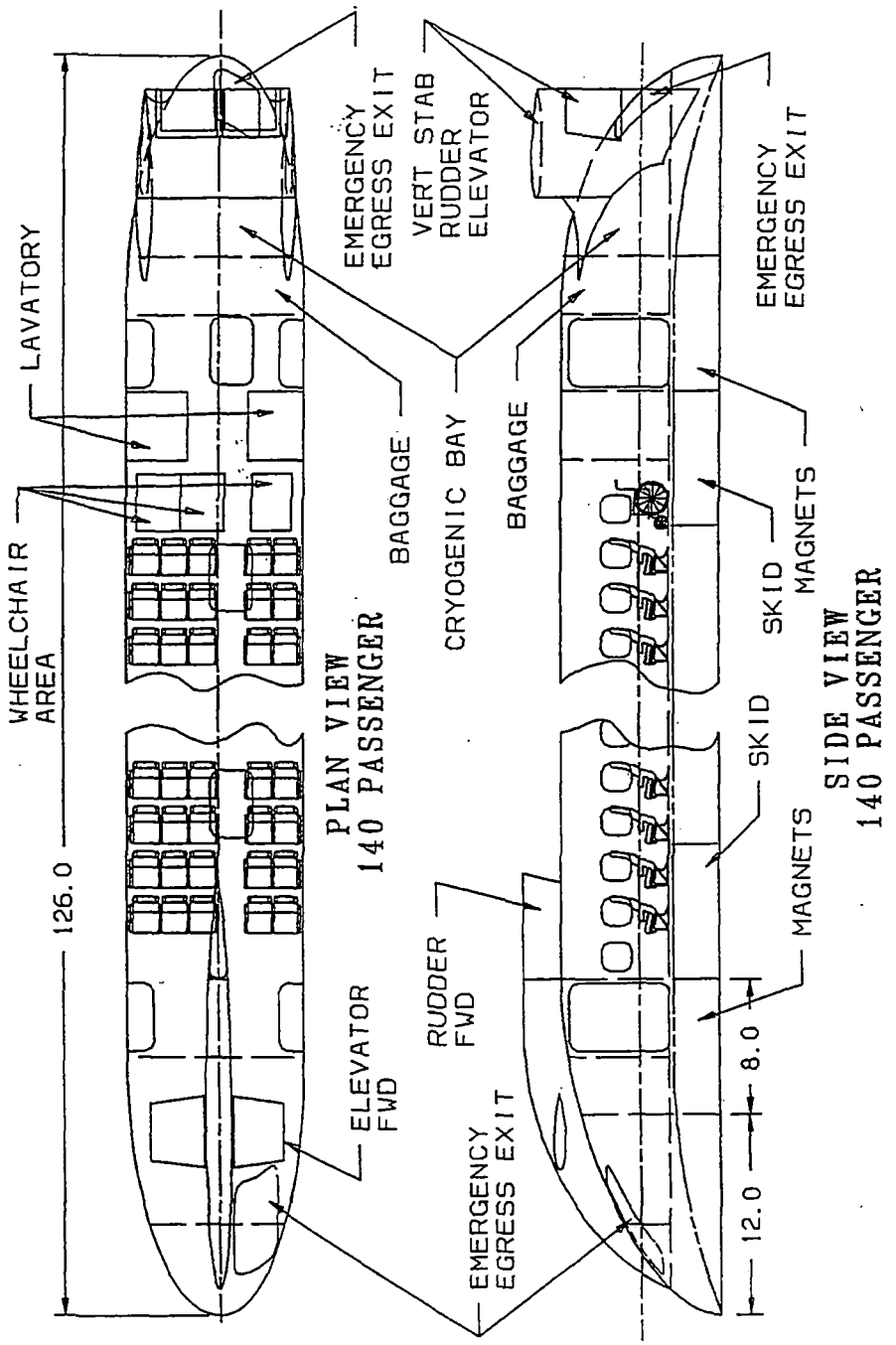

Figure 57 140 passenger magplane vehicle

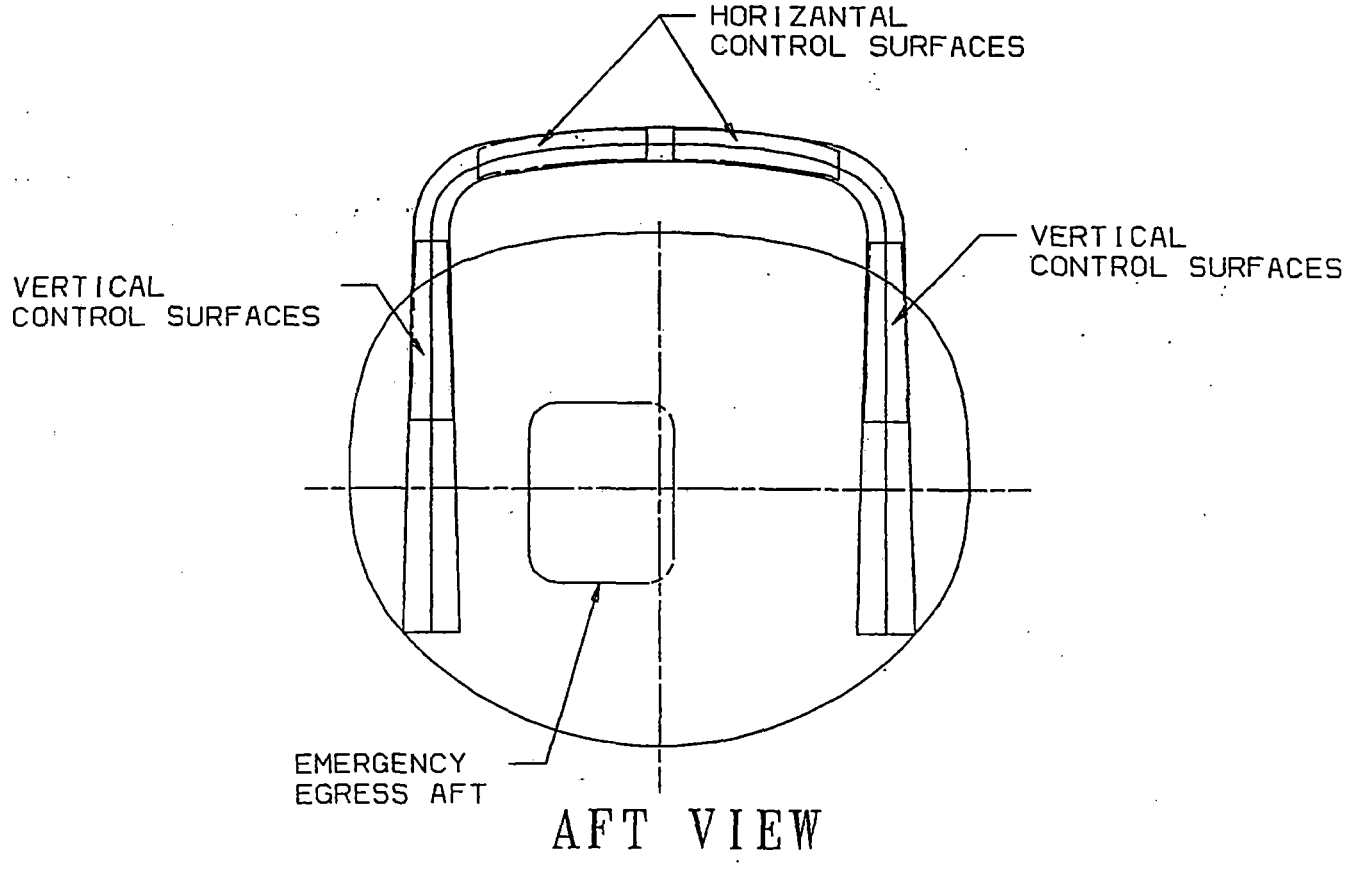

Figure 58 Aft control surface

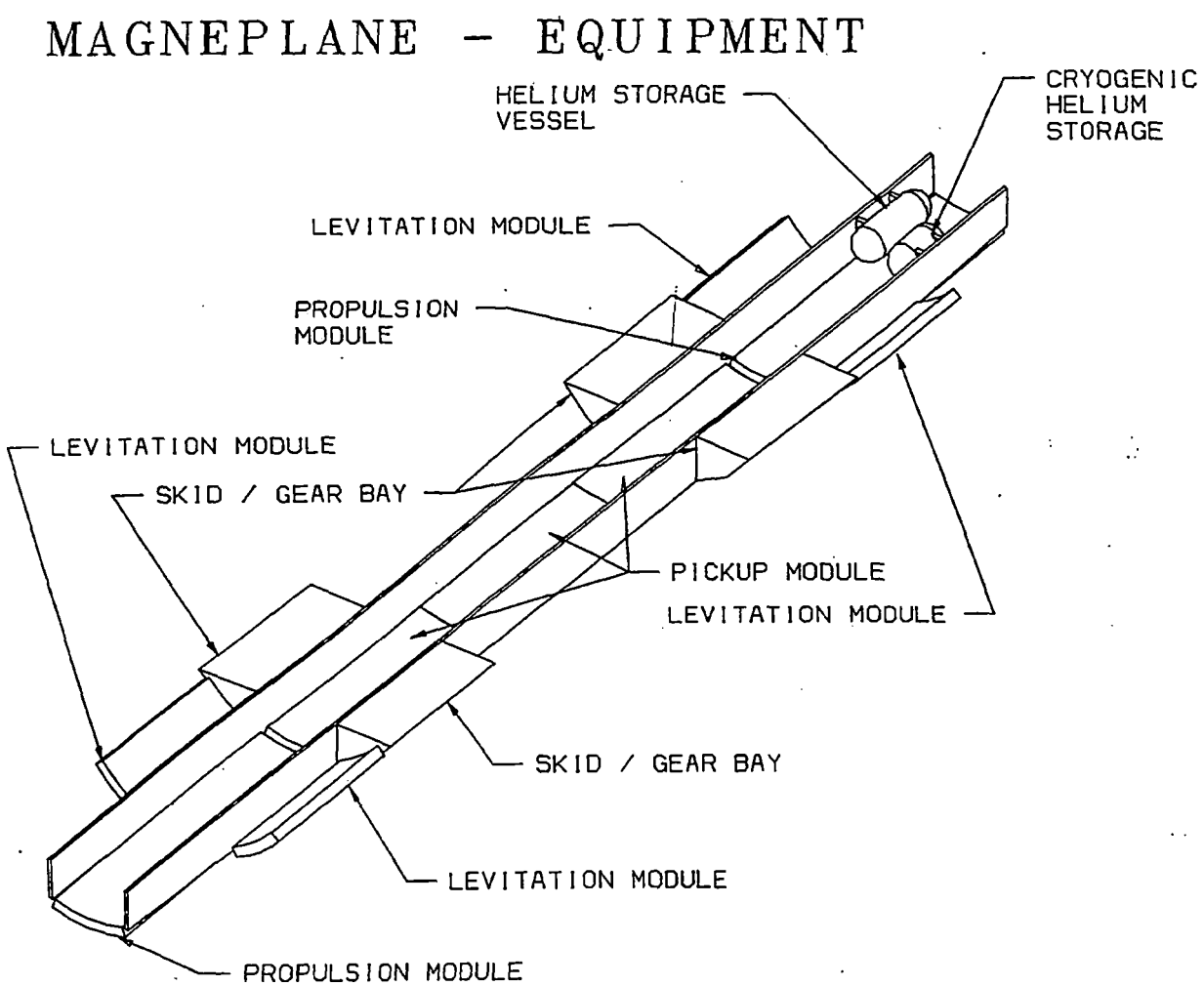

Figure 59 Cryogenics and electrical (under floor)

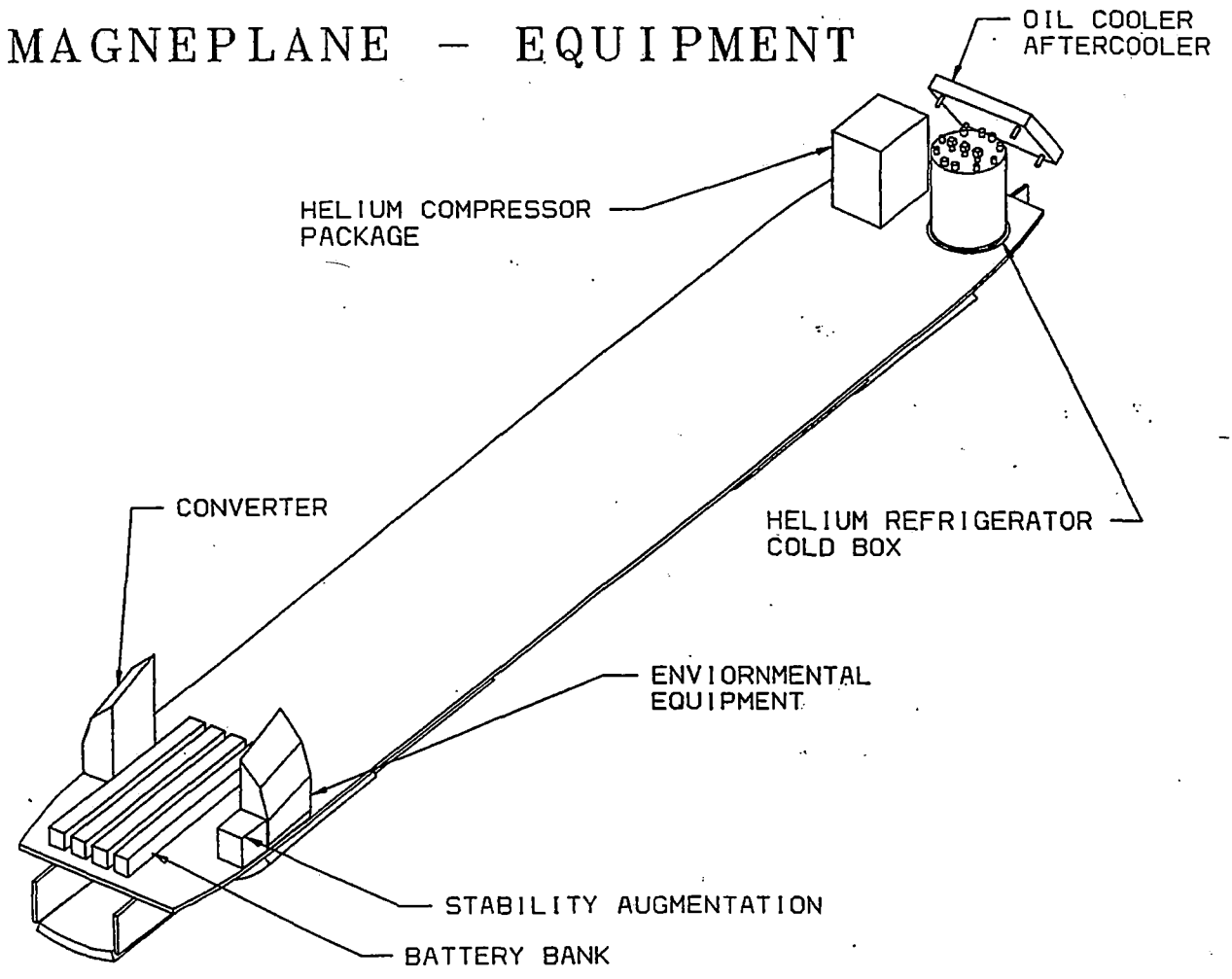

Figure 60 Cryogenics and electrical (above floor)

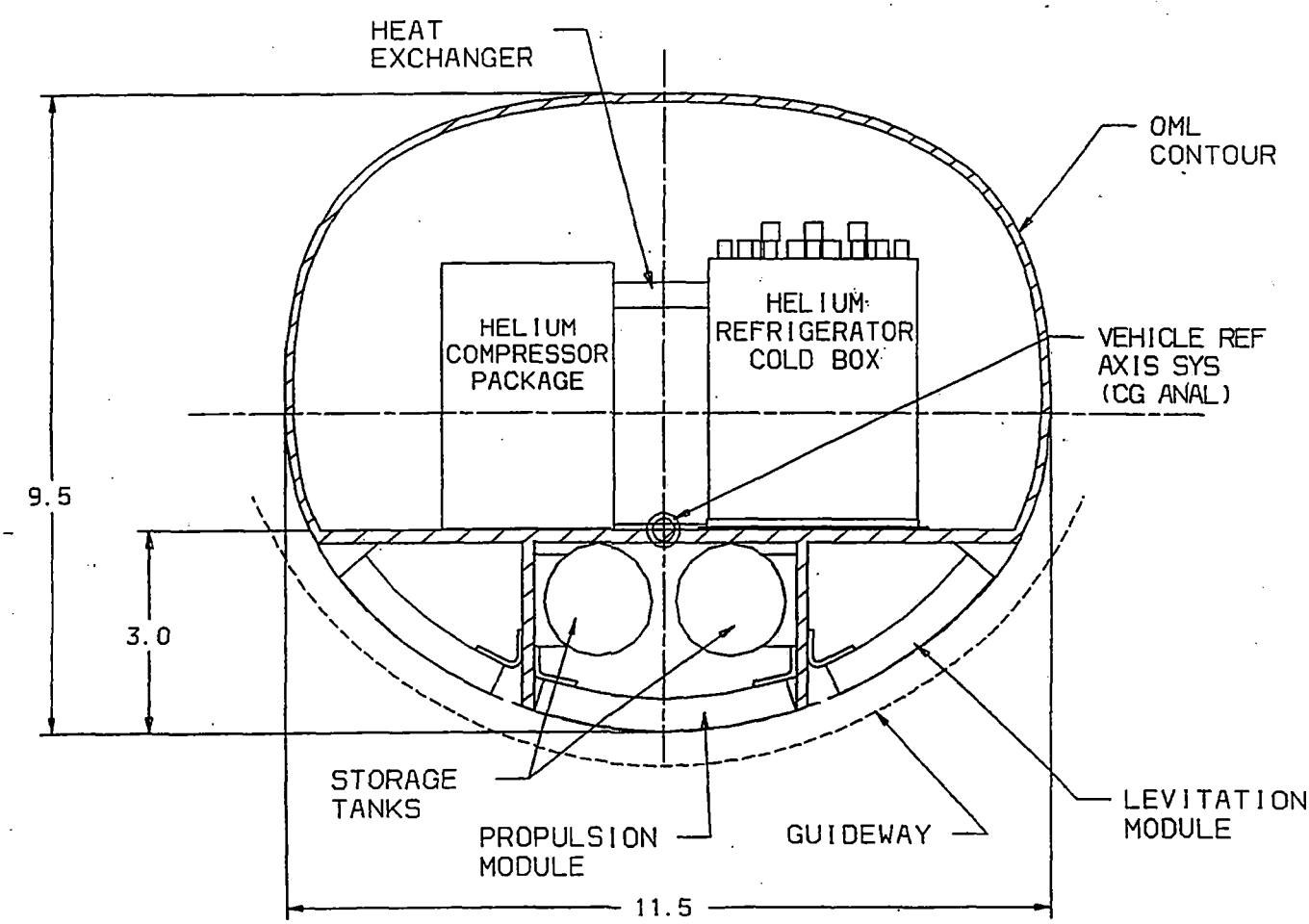

Figure 61 Cryogenics (cross section)

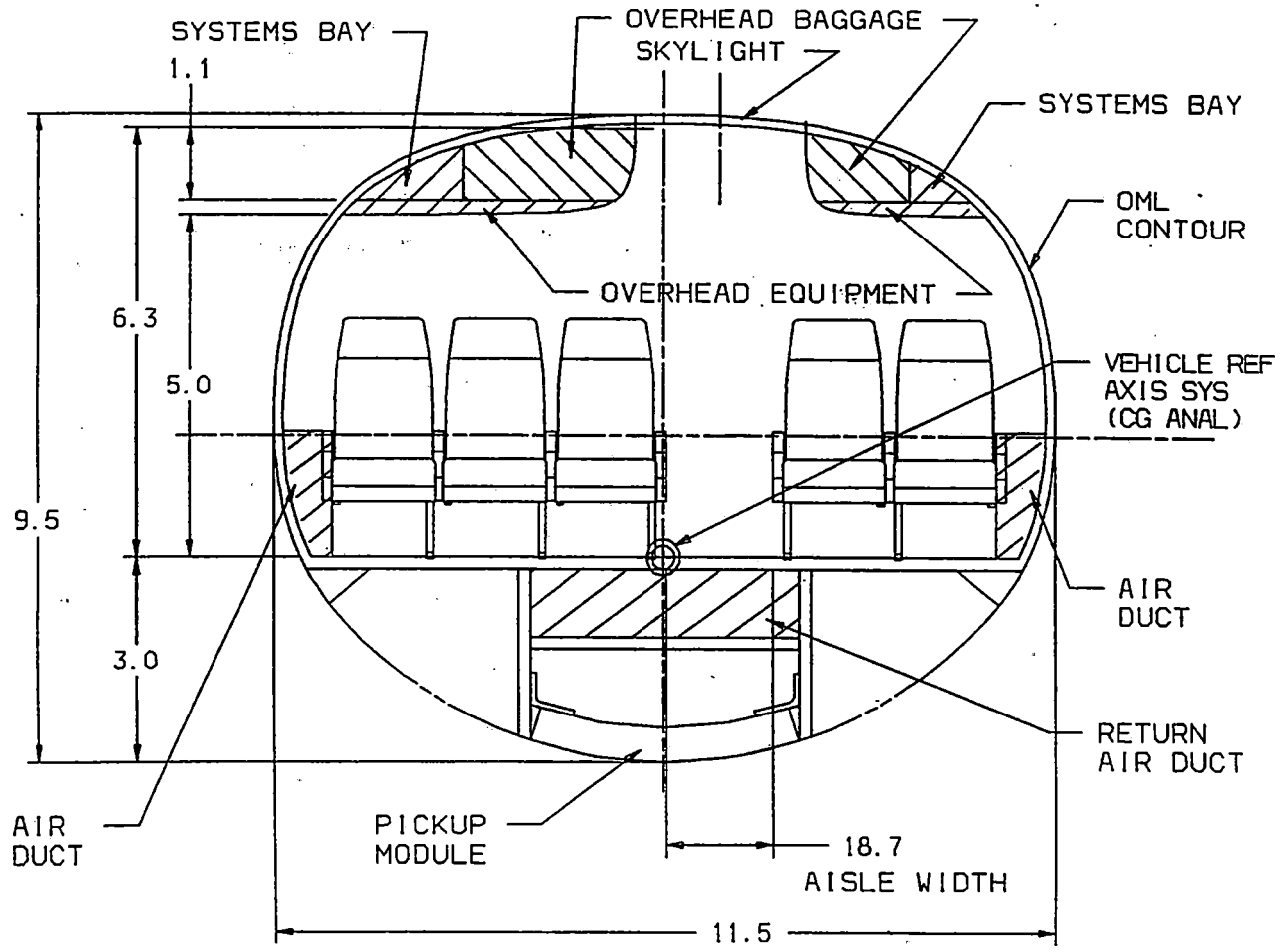

Figure 62 Air distribution system

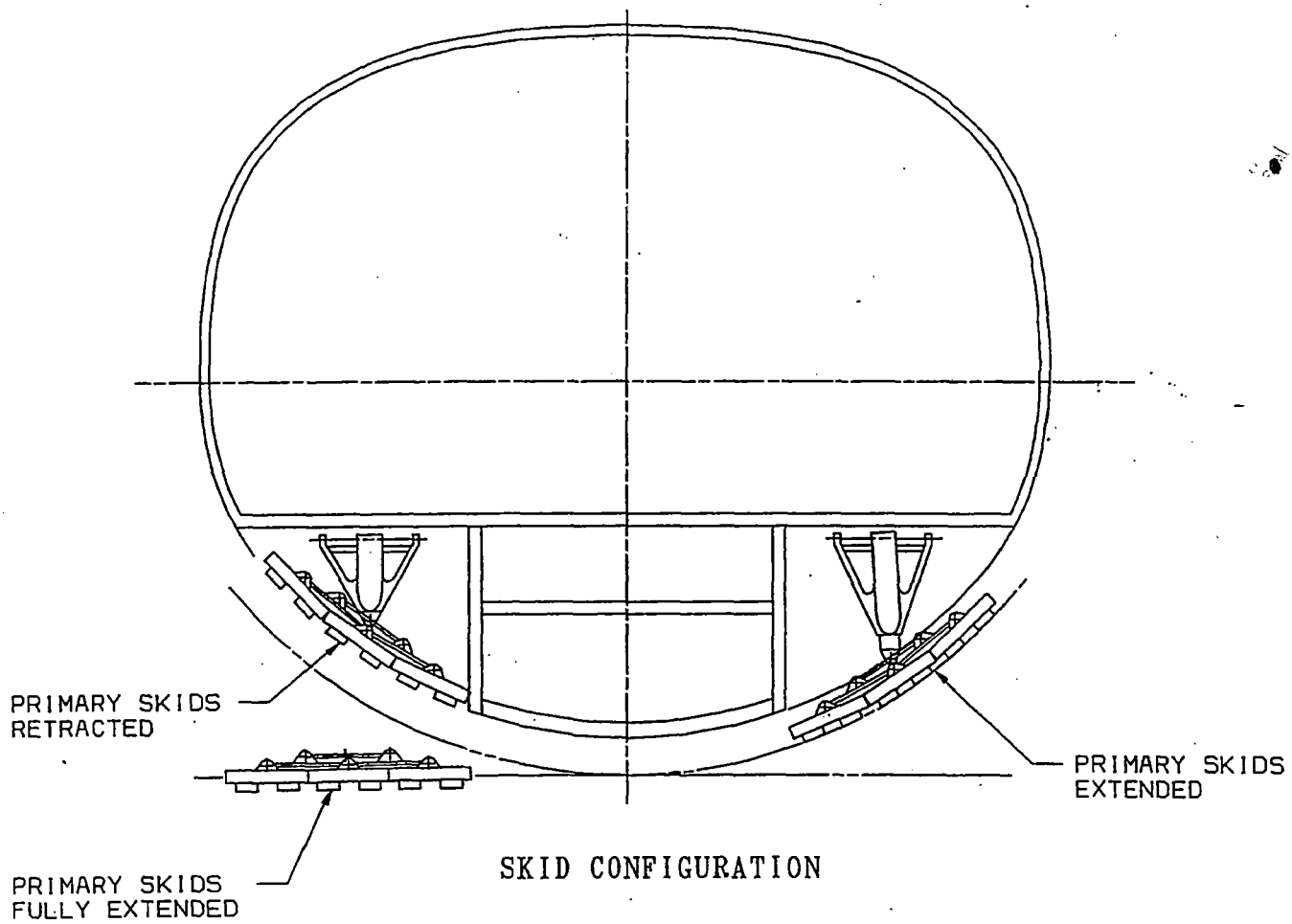

Figure 63 Ski/skid configuration

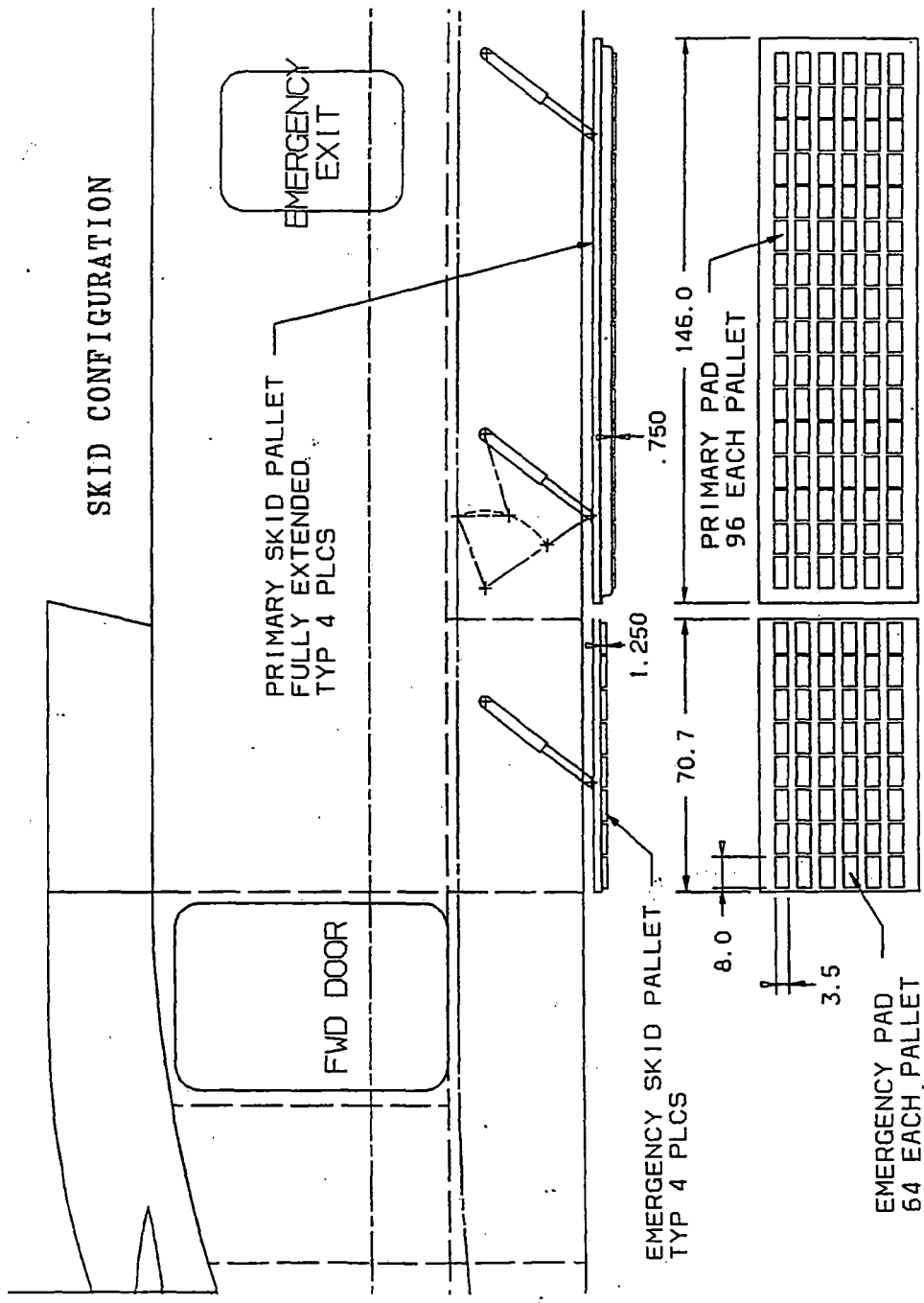

Figure 64 Anti friction pneumatic skid

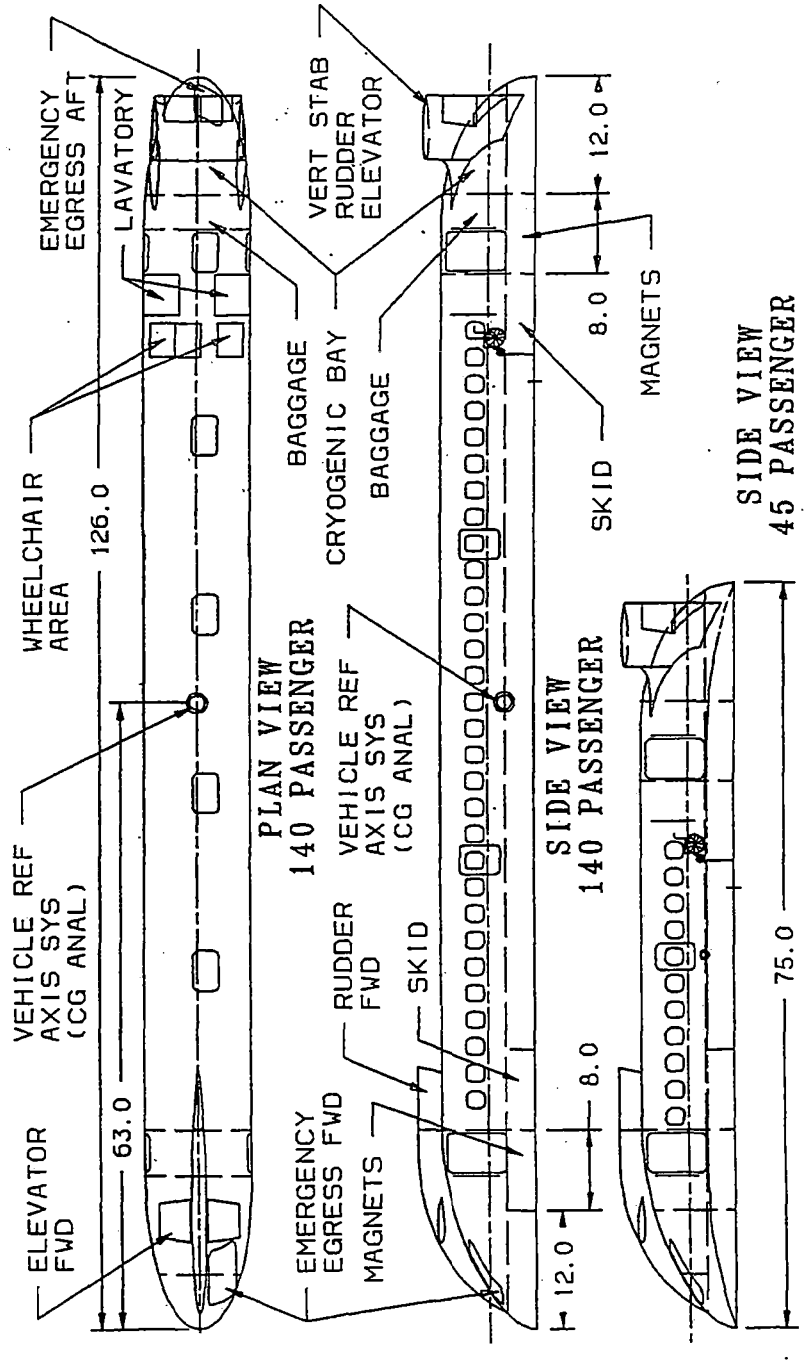

Figure 65 Emergency exit arrangements

3.2.1.c.2. STRUCTURAL INTEGRITY

The Magneplane vehicle is designed to load cases presented in Figure 66. A 50% safety factor is added to these design loads. In addition to these static loading cases, a stiffness requirement is imposed to preclude fuselage bending frequencies of less than 5 hz.

The fuselage structure is designed for a life of 60,000 hours or 25 years, an ability which has been enhanced by the composite honeycomb construction. Appropriate structural testing would be conducted to qualify the vehicles to the above criteria prior to the vehicle being certificated for passenger service.

3.2.1.c.3. MATERIAL TRADEOFFS

A comparison of fuselage structural designs based on conventional aluminum aircraft type construction and graphite epoxy advanced composite construction. These studies are contained in Supplement D, Section E and show a 28% weight savings for the composite fuselage compared to conventional metallic construction.

The baseline vehicle utilizes the composite structure for weight savings, improved fatigue and service life. During full-scale development, a detailed life cycle cost tradeoff would be conducted between the composite and metallic designs prior to committing the design to one or the other.

3.2.1.c.4. EMERGENCY SYSTEMS

Seat, safety belt and emergency evacuation criteria have been previously discussed under the Human Factors Section. The emergency evacuation criteria of Federal Aviation Regulations Part 25.803 should be imposed.

Emergency exits shall meet the criteria of FAR 25.807 as previously stated.

The emergency exit arrangement shall meet the criteria of FAR 25.809 as previously stated.

Emergency exit marking shall be in accordance with FAR 25.811.

The vehicle shall be designed for emergency crash conditions per FAR 25.561.

A megaphone and public address system shall be provided.

Appropriate system monitoring and annunciation provisions will be provided to the operator to permit him to intervene with automated functions in an emergency situation.

3.2.1.c.5. SANITARY FACILITIES

Lavatory facilities consisting of toilet and wash basin are provided in the cabin area, accessible by the passengers. Adequate consideration for use by handicapped persons shall be made and appropriate features incorporated to provide for the handicapped.

3.2.1.c.6. HANDICAPPED ACCESS

The vehicle will be designed to meet the American Disabilities Act of 1990, and shall be designed to meet the needs of those persons in wheelchairs.

3.2.1.c.7. MAIL AND HIGHER PRIORITY CARGO

A portion of the baggage area on passenger vehicles would be reserved for mail and higher priority cargo. This area would be secured and would not be accessible to passengers. These provisions would be limited to mail and higher priority packages. This area would provide for carrying of 500-lbs (227 kg) of these items on normal passenger runs.

3.2.1.c.8. FREIGHTER VARIANT

A freighter version of the Magneplane is envisioned which would be externally identical to the passenger vehicle, but which would not have seats, would have a larger door at the rear which would permit loading of palletized cargo. A floor-mounted cargo handling system would be provided. This version of the vehicle is shown in Figure 69. This version is more fully described in Supplement D, Section B.

3.2.1.c.9. WEIGHT AND BALANCE

Weight estimates for both large and small vehicle are shown in Figure 68. Balance for the large vehicle is more critical and, due to the larger payload of passengers and freight, has a larger variation in center of gravity due to the larger disposable load. The larger vehicle center of gravity limits have been initially established as follows:

Most Forward - Station 56
Most Aft - Station 70

These stations are distanced aft of the nose reference point in feet.

The large vehicle empty center of gravity is at Station 60.8 Empty weight is 66,310 lbs (30100 kg).

The most forward loading is no freight, and passenger seats full ahead of Station 60.8, and empty aft of Station 60.8. The weight and center of gravity for this loading is 80,600 lbs (36,600 kg), cg Station 56.2.

The most aft loading is with the seats ahead of Station 60.8 empty and full seats aft of this Station and 8,000 lbs (3640 kg) freight in the aft freight compartment. For this loading is the weight is 87,980 lbs (40,000 kg) with cg at Station 69.2.

The vehicle can be loaded without special considerations for loading, as it is essentially impossible to load it outside the limits.

(Note: Weight goals are tabulated in Figure 68). A more complete weight and balance estimate is found in Supplement D, Section D.

No special requirements shall be necessary to balance the vehicle during loading, other than not exceeding compartment maximum loading limits.

3.2.1.c.10. COST ESTIMATES

Estimated vehicle costs for both development and production units are shown in Figure 67. A more detailed breakdown of this estimate including rationale is found in Supplement d, Section G.

Normal Structural Load Factor

Vertical Up Acceleration	(2.5)
Vertical Down Acceleration	(1.25)
Lateral Acceleration	(1.5)
Longitudinal Acceleration	(1.5)

Emergency Structural Loads (Applied at seats)
(Load Factor)

Vertical Up Acceleration	3.0 (Applied to seat, vehicle restrained.
Vertical Down Acceleration	6.0 " " "
Rearward Acceleration	1.5 " " "
Forward Acceleration	9.0 " " "
Lateral Accel.(Airframe)	3.0 " " "
Lateral Accel.(Seats & Attach)	4.0 " " "

Note: The normal loads shall be assumed to be encountered in service. The emergency loads are assumed to be encountered only in an emergency and need not be addressed from a repeated load standpoint. The emergency loads are applicable for design of occupant protection features. Structural damage may be sustained when the emergency loads are applied as long as the failures do not jeopardize the occupants.

Figure 66 Magplane static design loads

Large Vehicle Development Cost	$ 970,213 K
Small Vehicle Development Cost	$ 607,695 K
Combined Small/Large Vehicle Dev.	$ 1,261,277 K

Small Composite Vehicle	$ 13,467 K*
Large Composite Vehicle	$ 20,221 K*
Large Metallic Vehicle	$ 15,938 K*

*Average unit cost for 100 unit production run above assumes conventional dimensional system. If metric dimensional system including fasteners is required, an additional 15% production cost is anticipated due to special handling requirements.

Figure 67 Cost Estimates

Figure 68 Weight goals

Item & No.	
(1)	Airframe
(2)	Passengers/Baggage
(2)	Freight
(3)	Interior
(4)	Heating/Air Cond.
(5)	Levitation Magnets
(6)	Propulsion Magnets
(7)	Cryogenic System
(8)	Suspension System
(9)	Shielding
(10)	Skids/Landing Gear
(11)	Controls/Stability Augmentation
(12)	Power Pick-up Coils
(13)	Battery
(14)	Converter
(15)	Miscellaneous
TOTAL	

MAGNEPLANE WEIGHT ESTIMATES-kg
(Composite Airframe)

Small Vehicle		Large Vehicle	
Weight Fractions	Weight (kg)	Weight Fractions	Weight (kg)
.18	4418	017	8202
.18	4582	.29	13950
-0-	-0-	.076	3636
.044	1091	.043	2036
.044	1091	.034	1636
.098	2438	.054	2579
.083	2076	.064	3067
.036	909	.019	909
.009	227	.005	227
.064	1604	.050	2405
.052	1309	.048	2273
.017	436	.014	654
.058	1461	.041	1948
.055	1368	.038	1804
.015	367	.010	501
.065	1614	.040	1899
1.00	25,000	1.00	47,727

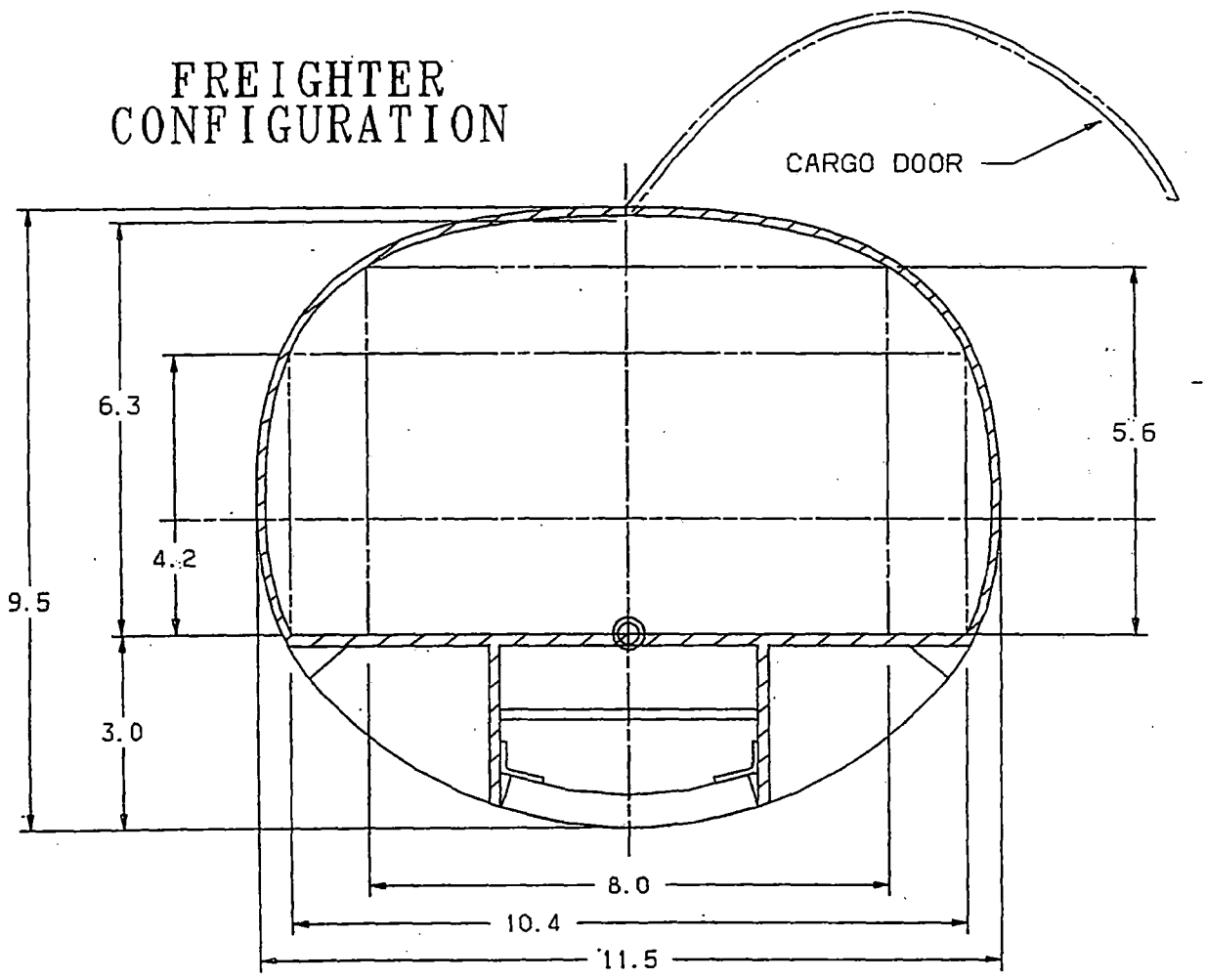

Figure 69 Magplane freighter version

3.2.1.d. MECHANICAL LEVITATION

The H-pads (high friction) and A-pads (anti-friction) are two alternate forms of mechanical levitation. H-pads are used for emergency braking, while A-pads (landing gear) are used for normal operation at low speeds.

3.2.1.d.1. A-PADS (LANDING GEAR)

The landing gear consists of a system of retractable ski-type skids, supported by oleo pneumatic shock struts. The landing gear skids, when extended have a coefficient of friction of .05 and support the vehicle at speeds below the minimum levitation speed.

This set of skids is fitted with anti-friction air bearing pads, which provide for the low coefficient of friction when supplied with compressed air through a manifolding system. The landing gear uses a trailing link type suspension with a tailored oleo shock strut to provide for smooth ride qualities when the vehicle is accelerating or decelerating on the landing gear. A hydraulic retraction system is provided with uplock and downlock provisions to fix the gear in the appropriate positions. The ski/skid base incorporates features to allow it to support the vehicle in the curved magway, as well as on a flat surface as might be encountered in a station or maintenance area. Sketches of the landing gear are shown in section 3.2.1.c.1.12.

3.2.1.d.2. H-PADS (EMERGENCY BRAKES)

While normal braking is provided by the propulsive magnets, a second set of skids is fitted with a high friction set of pads and is used for the emergency brake system. This set of skids provides for a coefficient of friction of 0.5 to 0.6 when deployed and does not have the air manifolding system. This system is fitted with a hydraulic retraction system similar to the primary landing gear and is deployed by firing an air/hydraulic accumulator.

Emergency braking is accomplished by lowering the H-pads to a point which raises the vehicle to about twice its normal support height. Under these conditions the brake mechanism will be supporting about seventy-five percent of the vehicle's weight at full speed. With the design friction coefficient of 0.6 this will provide initial deceleration of 0.45g increasing as the magnetic levitation decreases and the magnetic drag increases to about 0.6g at low speeds.

These surfaces are distributed in 8 modules (4 high friction, 4 low friction) operating at a contact bearing pressure on the magway of 69 kPa (10 psi) for the A-pads and 138 kPa (20 PSI) for the H-pads. See sections 3.2.1.c and Supplement D, Section A for descriptions of the locations of the skids and brakes.

Full characterization of the applicability and durability of the proposed materials for the purposes outlined is not available but will be the subject of early verification testing. Preliminary information shows that heat dissipation and temperature rise associated with emergency brake deployment is acceptable as shown in Figure 70 and Figure 71. Durability of materials, wear and tear on the magway and operational characteristics at high speed need to be established.

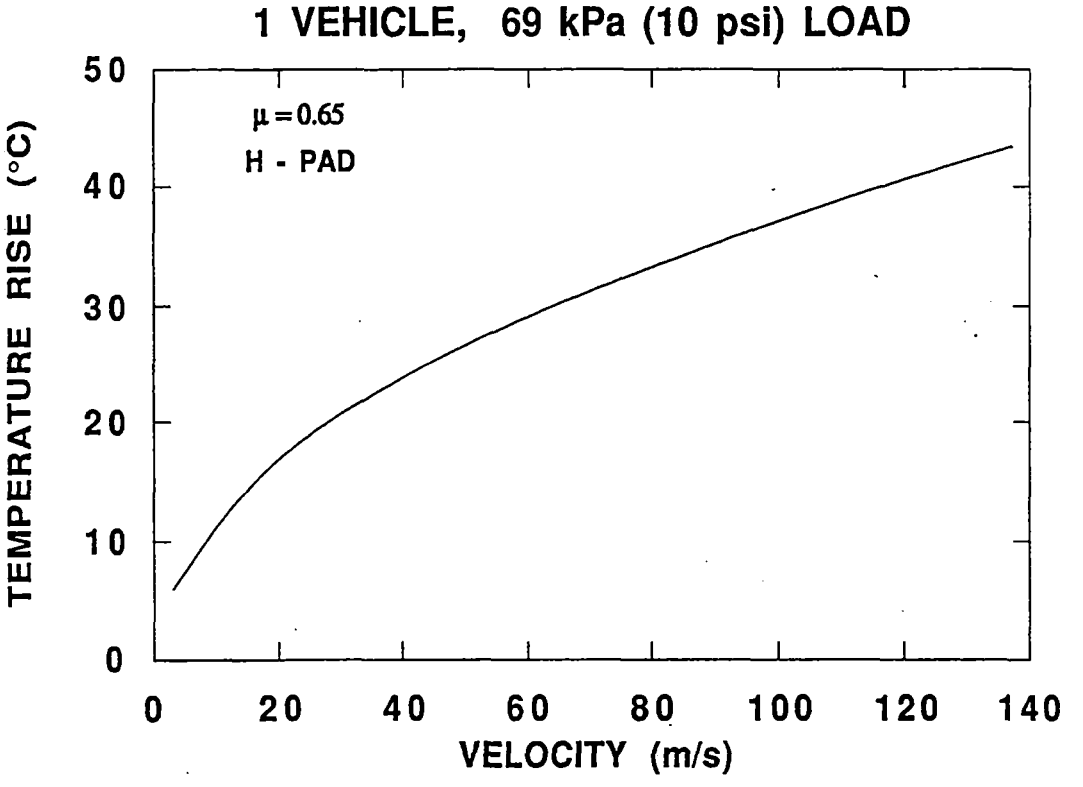

Figure 70 Temperature rise in magway surface due to passage of one vehicle on its emergency brakes

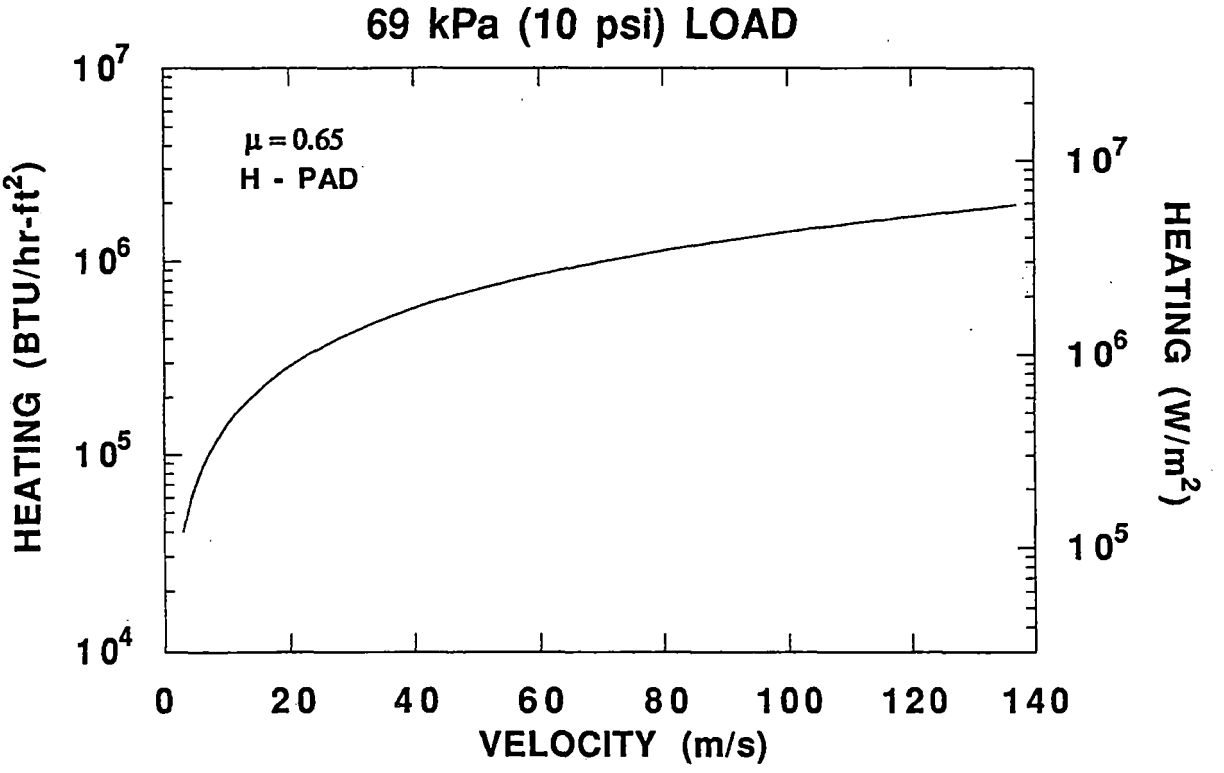

Figure 71 Heating in magway surface due to passage of one vehicle on its emergency brakes

3.2.1.e. BANKING CAPABILITY

This section describes the vehicle's mechanism for controlling banking in horizontal curves. Magneplane has no mechanical tilt mechanism; instead, banking is a passive effect mainly due to the weight distribution of the vehicle. Forces from the magnetic keel and the aerodynamic control surfaces can also come into play during a banked maneuver.

Sections 5.3.7.a.4., 5.3.7.a.6., and 5.3.7.a.9. give more information about the benefits of a self-banking system.

3.2.1.e.1. BANKING CONTROL APPROACH

A vehicle traversing the magway at velocities greater than 30 m/s is elevated at 15 cm. To control the vehicle in this mode of flight, both the aerodynamic surfaces and propulsion magnetic fields are adjusted to keep the vehicle in a stable path. In straight sections of magway forces acting on the vehicle are primarily gravity, opposed by the magnetic levitation, and acceleration in three planes. Forces acting on the vehicle which result in the acceleration moments are a combination of intentional actions and unintended disturbances. The vehicle must be controlled to minimize the propagation of the unintended acceleration forces to the passenger load, to maximize ride comfort. Any deviation of the magway from the straight and true, required to negotiate the terrain of the route, will induce acceleration forces which must be permitted to insure tight coupling of the vehicle to the magway. The magway will be designed to provide smooth adaptation to the intended accelerations. For optimal passenger comfort, minimal variation from the benign stationary forces are desired. There are two aspects to achieving this, the route must be designed not to induce excessive forces for any period, and the variation in these forces must also be minimized.

At the high velocities achievable with the Magneplane system, curved sections of the magway can be negotiated in relatively short periods. A 60° curve of 4 km radius can be negotiated at 134 m/s. However, such a curve is approximately 4 km long, hence a vehicle traversing it at that speed is in the curve for less than 30 seconds. If a section of the route consists of a sequence of curves, the passenger will continuously experience alternating left and right forces which will be a tiring experience. Coordinated banking of the vehicle into curves reduces the effect on the passenger considerably. The coordinated banking leans the vehicle into the curve at a speed optimal for that curve to maintain all effective downward force inside the vehicle. Hence a passenger in a seated position will only experience slight increases in apparent weight going through this maneuver. The Magneplane concept optimizes the coordinated banking maneuver by having a free motion vehicle in the roll axis, and a center of gravity lower than the roll moment. The vehicle will naturally adopt the optimum roll angle when negotiating curves, and by designing the curves with smooth transition, the passenger comfort levels will be maintained. To this end, the vehicle roll angle while coordinating the curve should not exceed that at which ride quality degrades. A 25 degree roll is at the limit for BEST ride quality, which limits the curve radius to 4 km for a vehicle speed of 134 m/s. Curves of smaller radii will have to be traversed

at lower vehicle speed to maintain the prescribed BEST ride quality levels. If the passengers are seat belted, a 45 degree roll is considered acceptable, which permits a minimum radius of 2 km to be negotiated at 134 m/s. Curves of a radius less than 2 km must be negotiated at lower speed.

The coordinated curve design avoids sideways force variation on the passenger, however it is equally important to minimize forward force variation (jerk). Forward force variations are incurred when the vehicle is required to change speed to negotiate sections of magway. Speed changes will be primarily enforced to negotiate tight radius curves. Coordinated banking of a vehicle into a curve requires an increasing bank angle for reducing radius curves and higher traversing velocities. Coordination of curves is effective at bank angles up to almost 90°, however public acceptance will reduce permissible angles to less than 45°, and 25° angles are preferred where possible.

Curves of less than 2 km radius have to be traversed at less than 134 m/s. As the maximum velocity a curve can be traversed is dependant on its radius (see section 5.3.3.2.e.), it will be necessary to continually change the velocity of the vehicle as it negotiates the various radii.

It is important for the vehicle to have knowledge of the magway projection in three planes at all times. The vehicle on-board stabilization system will counteract any induced forces that deviate from true, unless it is aware that these forces are intentional. In a curve, for example, the accelerations that occur are intentional. The vehicle will have mapping data of the route so that it can separate intentional forces from disturbance forces, and only take action to correct for the disturbances.

3.2.1.e.2. BANKING CONTROL STRATEGY

For the purposes of mapping, the magway is partitioned into linear elements (chords) of a fixed length (N), with independent input (X_i, Y_i, and Z_i) and output (X_o, Y_o, and Z_o) coordinate references. A single element is depicted in Figure 72. The output coordinates have both rotational and translational displacement from the input coordinates, and form the input coordinate reference for the next linear element. The relationship between the entry and exit coordinate structures is described by the length N, and angles α_X and α_Y (spherical coordinate structure). The angles α_X and α_Y are re-referenced to an absolute coordinate structure (B_X and B_Y) to avoid errors accumulating from this type of incremental description. The length N is chosen to be 11 meters, which is the spacing between position markers on the magway. Figure 73 depicts a two dimensional example of a curve, with end cross-sections for each element interface. As the magway goes into the curve, the elements rotate about the X-axis. Once into the curve, the elements adopt a constant rotational offset, with a gradual reduction when returning to the straight section. The figure does not depict the vertical rotational component, that is included to fully describe the three dimensional transformation. This coordinate reference scheme forms a compact description of the curvature of the magway, and is retained in the on-board map database of the vehicle as described in section 3.2.1.

A vehicle will enter and exit a magway element at different velocities. Each magway element is designed for optimal entrance and exit velocities. This simplifies the control problem to the local element. Elements are designed so that the combination of translational and rotational displacements follow the optimal path for maneuvering the vehicle from point A to point B with controlled roll and acceleration forces acting on the passengers. As an example, to translate from a straight section into a curve, a

sinusoid path will be followed in the X and Y axes, and a coordinated sinusoid roll will occur about the X axis. The in-going transition elements will be designed with increasing displacement and rotation, such that the forces acting on the passenger will gradually increase in the downward axis of the passenger, when the curve is optimally negotiated. Likewise the outgoing elements will be designed with decreasing displacement and rotation to gradually decrease the force acting on the passenger. Individually, each element is fully described by the length and B_X and B_Y angles.

An element is designed for optimal entrance and exit velocities, with a linear transition (acceleration) through the element. The mid-point of the vehicle is used as the second reference to place the vehicle in the element. When a vehicle normally traverses an element, it does so at those optimal velocities. In this mode of operation, control of the vehicle is routine. The only varying conditions seen by the vehicle are forces in the downward (Z) axis of the vehicle, when negotiating a curve. The increase in downward force, due to the combination of gravitational and centripetal forces in the direction of the coordinated bank, is counteracted by amplitude and phase shifting of the propulsion travelling magnetic wave, with respect to the vehicle (dynamic) position. This is achieved in the vehicle control by monitoring the vehicle clearance from the magway with the on-board height sensors. As the vehicle anticipates the curve maneuver (from the map), it commands the local controller to provide an increase in propulsion magnetic field density to compensate for the increase in Z force, and maintained constant clearance. In addition, the vehicle will experience acceleration about the X axis due to the curve. The normal response of the vehicle is to compensate for such acceleration forces, but as it anticipates the curve the vehicle will not try to correct for it.

3.2.1.e.3. BANKING CONTROL FOR NON-OPTIMAL SPEEDS

The reasons why a vehicle enters an element at the non-optimal speed, are varied. The vehicle maybe performing a maneuver to open up a time slot for introducing another vehicle into the traffic. The vehicle maybe slowing to negotiate a turn-off, in a section designed for 134 m/s velocity, versus the 100 m/s required for turn-off. A global decision to slow the traffic may have been initiated due to an upstream problem, or the vehicle itself may be experiencing a problem due to communication or power loss. In these circumstances the vehicle may experience non-optimal coupling with the LSM and command increased amplitude of the propulsion winding to compensate. In severe conditions, the vehicle may be travelling on momentum and have no acceleration forces at all. In all of these instances the vehicle will attempt to maintain optimal orientation in all three planes, using aerodynamic stabilization. In extremes circumstances, initiated by a global or on-board decision, the vehicle may instigate the landing gear or even emergency brakes to support and control the vehicle. At all times, by use of the route mapping, the vehicle has knowledge of what to expect in deviation in the magway, to base the control decisions on.

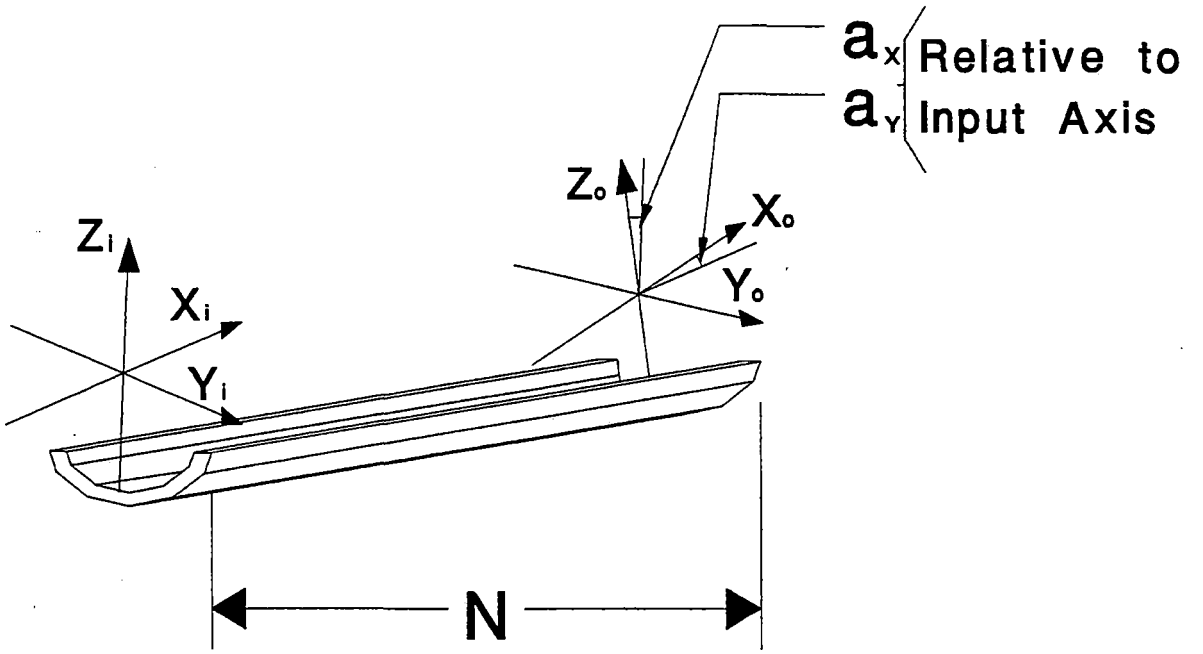

Figure 72 Linear magway element for mapping purposes

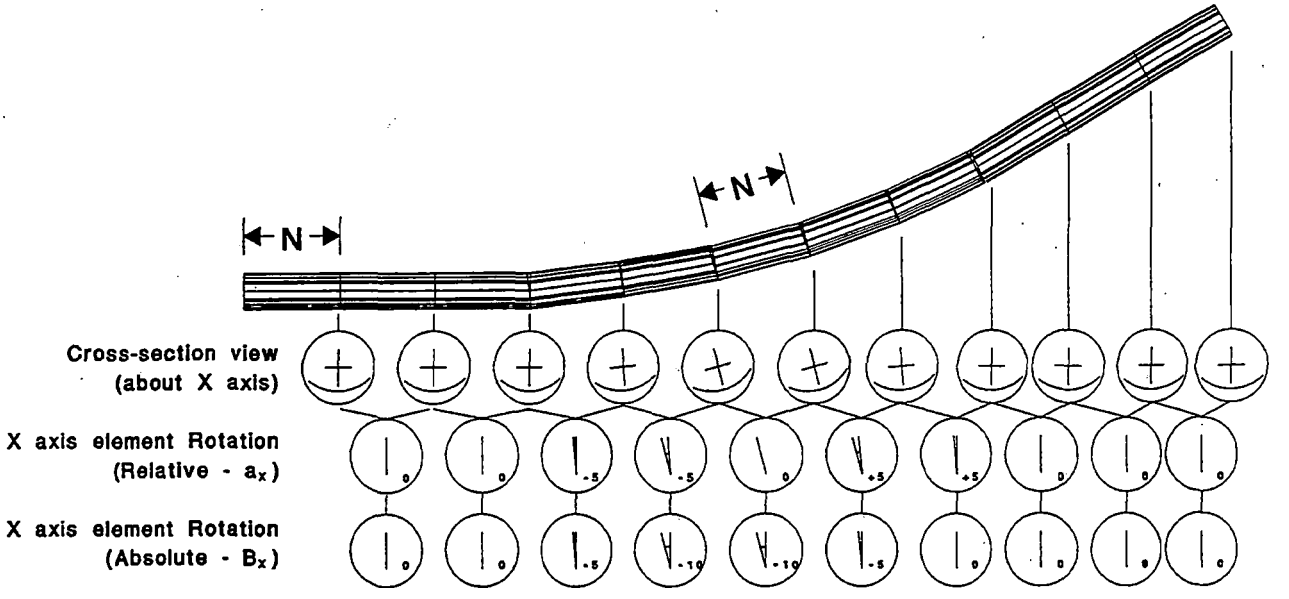

Figure 73 Example of map database for a curve with end cross-sections at each magway element interface

3.2.1.f. AERODYNAMIC CONTROL SYSTEM

3.2.1.f.1. VEHICLE AERODYNAMIC PROPERTIES

At Magneplane operating speeds, the aerodynamic characteristics of the vehicle become important from several viewpoints. In particular, the aerodynamic drag gives the largest single contribution to the propulsive force and power requirement. In this section, the aerodynamic properties are discussed under the following topics:

1) Drag
This determines the propulsion and magway design loads

2) Body Normal Forces and Moments
These are required for assessing the vehicle lift and pitching moment, and determining the loads in steady side winds.

3) Control Surface Forces and Moments
This is needed for control sizing to meet stability augmentation and guidance requirements.

4) Unsteady Aerodynamics
These effects are important in aspects such as vehicle behavior in gusts and turbulence, in transient situations such as vehicle passing, and in assessing aerodynamic damping properties.

5) Noise Emission

A detailed aerodynamic design of the vehicle has not been undertaken, but initial assessments have been made using the proposed vehicle layouts, and budget values established for items such as component drag coefficients. Lack of precision is not a design driver at this stage; for a demonstration or prototype design, computational fluid dynamic calculations and wind tunnel testing will be required to optimize the aerodynamic layout.

3.2.1.f.1.1. DRAG

The vehicle drag is composed of body drag and control surface induced drag. The drag force D is related to the vehicle configuration and operating conditions through the relationships:

$$D = C_D q_0 S_F$$
$$q_0 = \rho u^2/2$$

where C_D is the total drag coefficient, q_0 is the dynamic pressure, ρ is the air density, u is the vehicle speed and S_F is the vehicle frontal area. The components of the total C_D are:

$$C_D = C_{DFB} + C_{DB} + C_{DG} + C_{DI}$$

where

C_{DFB} = fore-body drag
C_{DB} = base drag
C_{DG} = ground interference
C_{DI} = control surface induced drag

The fore-body drag consists of a pressure drag contribution from the nose, and skin friction from viscous action on the vehicle body. The forms used for the drag coefficients are:

$$C_{DFB} = 4.4\ C_f L_D + 0.02$$
$$C_{DB} = 0.029\ (S_B/S_F)1.5\ C_{DFB}\text{-}0.5$$
$$C_{DG} = 0.02$$
$$C_{DI} = 0.38\ C_L 2\ S_C/(S_F A_R)$$

where

C_f = flat plate turbulent skin friction coefficient
L_D = body length-to-diameter ratio
S_B = effective vehicle base area
S_F = vehicle frontal area
C_L = root mean square control surface lift coefficient
S_C = control surface area
A_R = control surface aspect ratio

The parameters used to develop the budget drag components shown in Figure 74 are:

$C_f = 0.0016$
$C_L = 0.5$
$S_F = 7.1$ m2
$S_C = 5.3$ m2
Body diameter = 3 m
Base diameter = 2.4 m

The drag coefficient increases in a cross-wind because of vortex generation and an estimate of the effect with a steady side-wind of 15 m/s is included in Figure 74. A steady head-wind also increases the drag through an increase in the dynamic pressure rather than the drag coefficient. Aerodynamic drag values were estimated using the data in Figure 74 to determine worst case propulsive force demands.

It is well known that for a streamline shape the drag coefficient based on frontal area has a minimum when the body length/diameter ratio is in the range of three to five. For bodies with lower ratios than this the pressure drag is large and for bodies with larger ratios the skin friction drag dominates and increases linearly with length/diameter ratio. However, for a fixed vehicle diameter the number of passengers carried reduces with vehicle length, and although the drag coefficient may be optimal the number of passengers will not meet the headway and system passenger rate requirements. Alternatively, if the number of passengers per vehicle is regarded as a constant, then the floor area, vehicle surface and skin friction drag are also constant to a first order. In this case, the pressure drag contribution can be

reduced proportionately by increasing the length/diameter ratio. Therefore, there is no optimal length/diameter ratio from an aerodynamic drag viewpoint, and cabin dimensions are determined more by seating layout and floor plan requirements.

A similar argument is used in assessing multi-vehicle performance. There is a drag reduction because the nose and base drag contributions can be largely eliminated with suitable faring between adjacent cars. Based on the values presented earlier in this section, the total train drag coefficient can be determined as a function of the number of vehicles linked. This is presented in Figure 75 in the form of total C_D and C_D per vehicle.

The reduction in aerodynamic drag ranges from 20 to 30% and in total drag from 12 to 18% at 150 m/s vehicle speed. However, there are some aerodynamic disadvantages in linking vehicles. In particular, control surface effectiveness will be impaired.

3.2.1.f.1.2. BODY NORMAL FORCES AND MOMENTS

Because the vehicle is constrained magnetically to align itself closely in pitch and yaw with the track center-line, the aerodynamic normal forces and moments tend to be small compared with the vehicle weight and magnetic moments. However, a cross-wind induces a lateral angle-of-attack or side-slip angle ß given by:

$$\tan ß = v_C/u$$

where

v_C = cross-wind velocity
u = vehicle velocity

The side-force and yawing moment coefficients C_Y and C_N are defined as follows:

C_Y = side force / $(q_0 S_F)$
C_N = yawing moment / $q_0 S_F l_B)$

where q0 is the dynamic pressure, SF is the frontal area and lB is the body length. The major contributions to CY and CN are generated by the vehicle nose and control surfaces when the side-slip angle is small, and by vortex separations over the whole length of the body when the side-slip angle is large (high cross-wind or low vehicle speed). For low to moderate values of ß the coefficients become:

Body contributions:

$$C_Y = 1.7 ß + 0.71 L_D ß^2$$
$$C_N = 0.85 (1 - 4/L_D) ß$$

Control surface contributions:

$$C_Y = 3.8 S_C ß/S_F$$
$$C_N = 4.0 S_C ß/S_F$$

For the case where the vehicle is stationary in a steady side wind, the side-force takes the form:

$$\text{Side-force} = 0.71\ L_D\ S_F\ q_C$$

where

$$q_C = 1/2\ v_C^2$$

Because the side-force acts close to the center-of-gravity in this case, there is only a small contribution to the yawing moment. These relationships were used for estimating magway loads and a typical result is shown in Figure 76. Because the control surfaces are more efficient at generating lift than the body, they do contribute significantly to the cross-wind force. However, the force magnitude shown in Figure 76 represents an upper bound because no allowance has been made for the shielding of the lower portion of the vehicle by the magway.

The speed range in Figure 76 covers operations up to the peak gust value of 21 m/s for the Threshold I or Operational Wind Threshold,as proposed by J. Lever, memorandum dated 14 March 1992. Under the action of a steady cross-wind induced side-force, the vehicle will adopt a trim roll angle and will be displaced sideways from the track centerline. The data in Figure 76 and the magnetic stiffness properties of the suspension system were used to generate the results presented in Figure 77. These roll angles have little effect on passenger comfort and the lateral displacements have small effects on levitation height, propulsive force or magnetic drag.

The aerodynamic lift and pitching moment are produced by the flow over the upper surface of the vehicle, by the flow between the lower surface and the magway, and by the horizontal control surfaces. The upper surface flow and control surfaces produce forces and moments which are small compared with the vehicle weight and the magnetic forces and moments. The nose shape gives a small nose-down trim pitching moment while the aerodynamic interaction between the vehicle underside and magway involves both viscous and inviscid flow properties. Both effects result in a static pressure gradient from front to back when the vehicle is pitched-up with a resulting moment tending to increase the pitch-up. However, because of the relatively large levitation height, there is low resistance to lateral flow into the gap. This three-dimensional flow effect will reduce the pressure gradient and the aerodynamic pitching moment.

3.2.1.f.1.3. CONTROL SURFACE FORCES AND MOMENTS

The aerodynamic control surfaces are essentially lifting wings located and oriented so that they can be operated in combinations which control each of the six vehicle degrees-of-freedom independently or with a minimum of cross-coupling.

The force FC produced by the control surface takes the form:

$$F_C = q_0\ S_C\ C_{Lh}$$

where C_{Lh} is the lift curve slope for the control surface deflection h. The control surface may be either the whole wing or a trailing edge control. For the complete wing C_{Lh} is typically 4 per radian, while it is 3 per radian for a trailing edge control. Pitch, yaw and roll control moments are obtained using the appropriate moment arm lengths, measured from the vehicle center-of-gravity.

3.2.1.f.1.4. UNSTEADY AERODYNAMICS

The generation of unsteady aerodynamic loads by gusts or turbulence are modelled by using the vector combination of their velocity components and the vehicle speed. This provides instantaneous values for the angle-of-attack, side-slip angle and dynamic pressure so that forces and moments can be calculated, together with vehicle response to these loads. A typical initial lateral acceleration response as a sharp-edged side-gust is encountered is shown in Figure 78. The vertical control surface will again provide a significant contribution but the acceleration levels over the gust velocity range are not uncomfortable.

Unsteady aerodynamic forces and moments are also produced by the small movements of the vehicle about its steady state motion. Those resulting from the rates of movement such a pitch rate,yaw rate & roll rate tend to resist the motion and provide passive damping to the system. These were estimated for motion in each of the six rigid body degrees-of-freedom and used in determining the suspension system performance.

3.2.1.f.1.5. NOISE EMISSION

The main sources of noise emission external to the vehicle are:

1) Boundary layer flow on the vehicle body.

2) Aerodynamic flow separations.

3) Wing/control surface motions.

4) Aerodynamic ground interactions.

5) On-board equipment such as compressors, hydraulic pumps, etc.

The single most important contribution at the design operating speed is expected to be (1), the turbulent boundary layer. Several methods exist for estimating sound pressure levels using normal dipole representations for the turbulent boundary layer. The method used here was the one presented by King (Journal of Sound and Vibration, vol. 54 No.3, 1977). The features of this model include variations of sound pressure level with:

a) inverse square of distance

b) 5.5 power of speed

c) aspect angle.

d) vehicle Mach number.

The model also incorporates an acoustic dipole distribution to represent the base flow separation and wake. The distribution was selected to fit the noise measurements made during Transrapid TR07 runs at a speed of 120 m/s and a side-line distance of 25 m from track centerline. The calculated time history

using this approach is compared with the measured data in Figure 79. Results are also shown when the same model is applied to the Magneplane configuration. The noise levels are 3 to 5 dB lower because of the smaller radiating surface area.

The applicable noise emission regulations are FRA 49 CFR ChII Part 210 and EPA 40 CFR Ch. I. Part 201. These require the maximum sound pressure level to be no greater than 90 dBA at a distance of 30 m from the track. This is compared with the predications for the 145 passenger vehicle in Figure 80, where the maximum overall sound pressure level variations with vehicle speed and distance are presented. This shows that the regulation is exceeded for train speeds in excess of about 110 m/s.

Noise mitigation techniques that might be employed include:

a) Aerodynamic noise control such as:

    1) clean aerodynamic shape
    2) boundary layer transition control
    3) flow separation control using the aerodynamic surfaces.

b) Sound propagation control by magway barriers to produce:

    1) re-direction of the sound
    2) absorption through internal reflections

c) Vehicle operational procedures such as:

    1) speed reduction in sensitive areas.

The noise disturbance due to a single vehicle passing event is characterized both by the peak sound pressure level and by the duration of the sound pulse. The Sound Exposure Level (SEL) is a measure of the integrated sound energy from a single event, normalized to a one second duration. However, the noise regulations have no SEL requirement and, for a given peak value of the SPL, the higher the train speed the lower will the SEL value by. A more important aspect of the single event is the startle caused by the rapid build-up of the sound. The onset rate for the 140 passenger vehicle is shown in Figure 81 as a function of speed and distance from the magway. The rate is defined as the peak ASPL divided by the time to reach the peak from a 65 dB background. At this time there are no guidelines as to acceptable onset rates.

3.2.1.f.2. AERODYNAMIC CONTROL SURFACES

Please see section 3.2.1.c.1.7. (control surfaces) and 3.2.2.g. (vehicle/magway interactions).

	45 Passenger Vehicle	140 Passenger Vehicle
Length/Diameter Ratio, L_D	7.5	13
C_{DFB}	0.073	0.112
C_{DB}	0.055	0.044
C_{DG}	0.02	0.02
C_{DI}	0.018	0.018
Total, C_D	0.17	0.19
C_D in 15 m/s cross-wind	0.20	0.24

Figure 74 Drag coefficient components

Number of Vehicles	Total C_D	C_D per Vehicle
1	0.24	0.24
2	0.38	0.19
4	0.72	0.18
Large Limit	NA	0.17

Figure 75 Effect of multiple vehicles on total drag

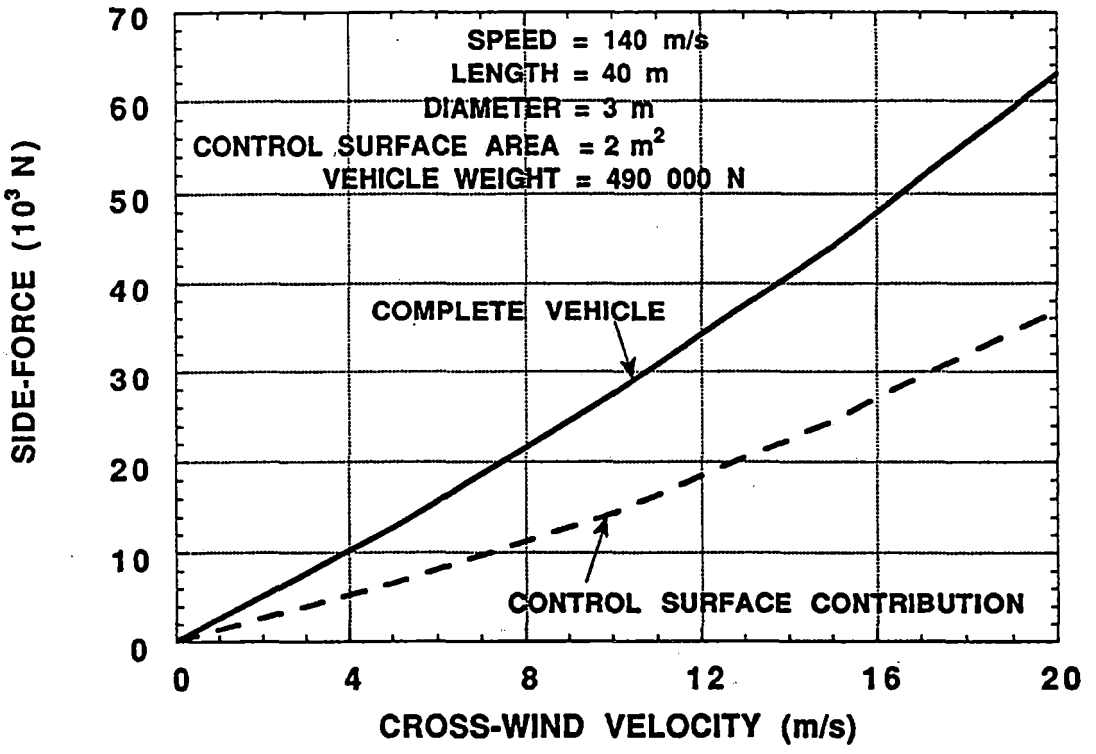

Figure 76 Side force caused by a steady cross-wind

Side-wind velocity	Roll angle	Lateral Displacement
(m/s)	(deg)	(m)
13.4	2.0	0.063
21	3.6	0.11

Figure 77 Vehicle roll angle and lateral displacement in a side-wind

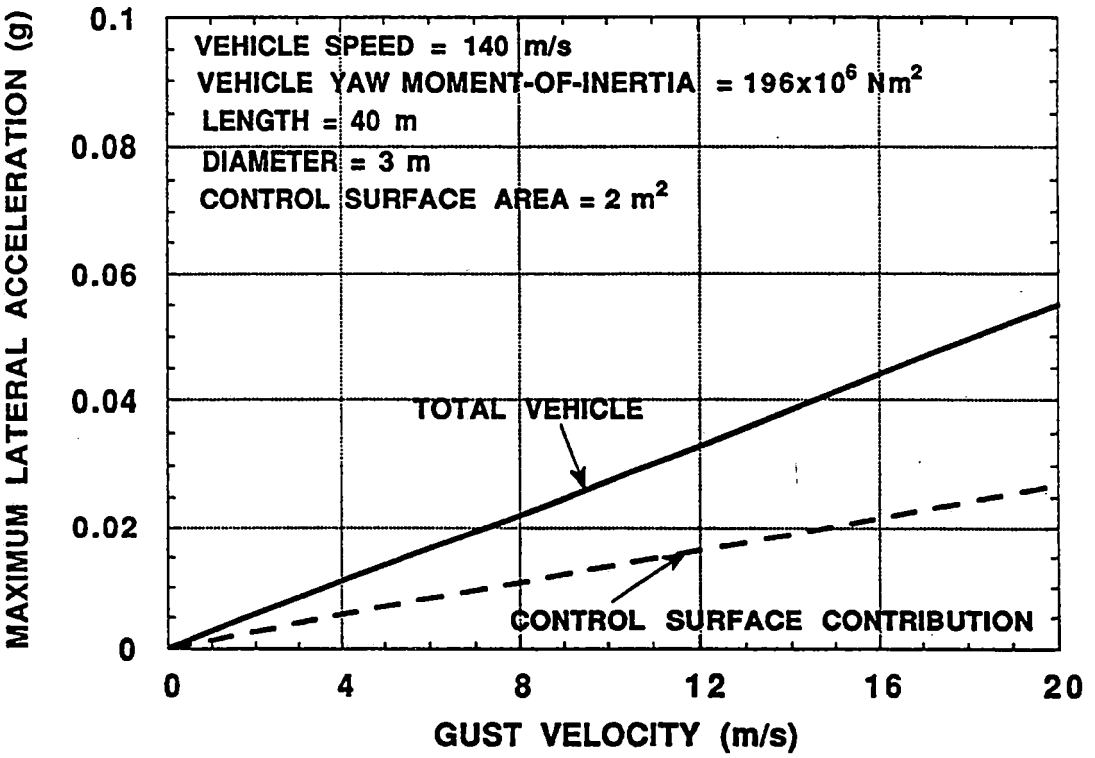

Figure 78 Maximum lateral acceleration during vehicle passing

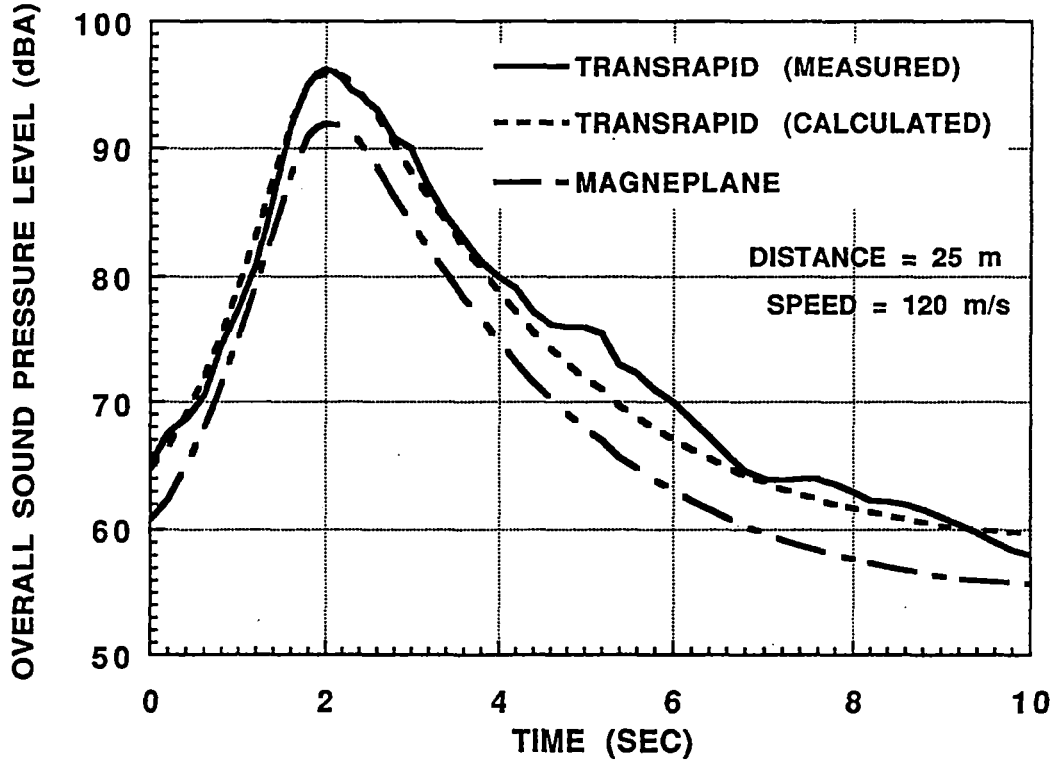

Figure 79 Noise time history

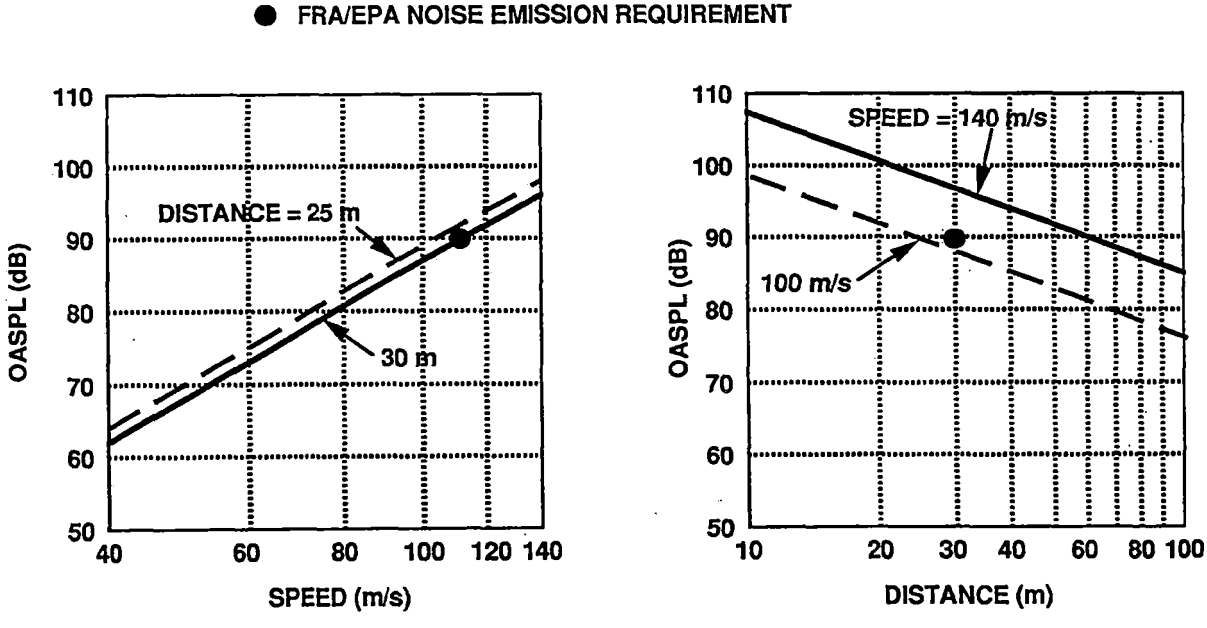

Figure 80 OASPL variation with distance

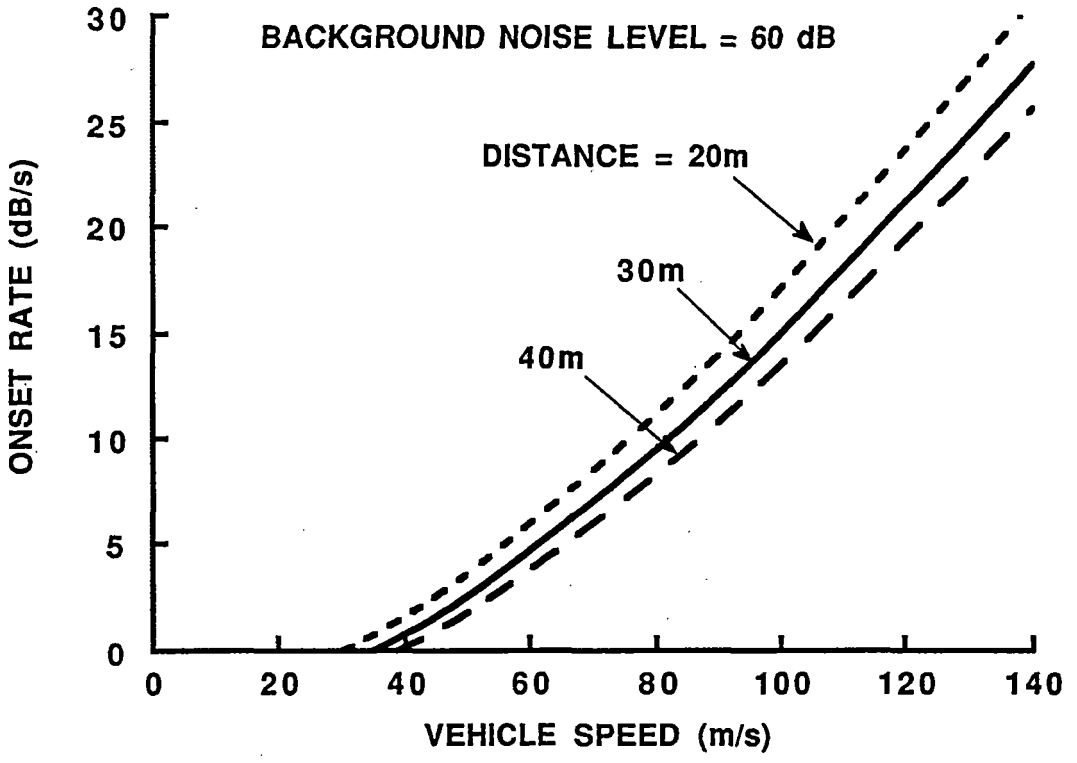

Figure 81 Noise onset rate

3.2.1.g. ELECTRICAL SYSTEM

The electrical system of the vehicle supplies normal operating and emergency backup power to ac and dc loads on the vehicle. A simplified block diagram of the electrical supply system is shown in Figure 82. AC power is provided from the magway by means of the inductive pickup coil, which is described in section 3.2.1.j.

The inductive pickup coil is divided into two halves which are connected to an input power bus on the left side of the figure. This bus supplies identical left and right side power conversion channels. At the front of each channel is an ac/dc converter (rectifier) to convert the pickup coil power to dc. The dc output voltage is typically 300 Vdc which may be maintained by a chopper incorporated in the converter. A 270 Vdc battery is charged from the dc bus which provides power to a dc/ac converter (inverter). The inverter will provide 208/120 V 3-phase ac power at either 60 or 400 Hz. Distribution buses provide connection points and circuit breakers for the individual loads. DC bus connections from the right and left sides may be joined to a common dc bus as shown or provided with separate buses as in the case of the ac systems.

Battery and power converter ratings will be selected to minimize the effect of a single battery or converter failure. An interlocked external power connection will be provided for operating from shop power.

The on-board vehicle loads are listed in Figure 83. The loads in the table are based on estimates for the 140 passenger and 45 passenger vehicles. The power requirements assume that the cryogenic cooling system will use an on-board supply of liquid nitrogen as a shielding gas for the superconducting magnets.

A brief description of the vehicle loads is as follows:

Cryogenic Cooling: Helium compressor and associated control apparatus.

Magnet Shielding: Active dc shielding coils for reducing propulsion and levitation coil magnetic fields inside the vehicle.

HVAC: Heating, ventilation and air conditioning loads.

Actuators: Aerodynamic control surface actuators.

Landing Gear and Emergency Brakes: Extension/retraction mechanisms and air pressurization.

Control/Communications: On-board computer processors for control functions and radio communications for voice and vehicle control functions.

Lights: Passenger compartment and exterior lighting.

Kitchen: Cooking and other food preparation facilities.

Spare: Contingency allowance.

A battery backup system is provided to supply power to the vehicle loads under several abnormal operating modes which are listed in the table. These modes are defined as follows:

Mode 1: Primary power source failure or major failure of on-board power conversion system. Vehicle loads are supplied by battery through on-board dc/ac converters.

Mode 2: Loss of magway power. Vehicle loads are supplied by battery through on-board dc/ac converters. Vehicle loads are selectively reduced. Normal operation resumes when magway power is restored.

Mode 3: Major loss of vehicle function, such as complete loss of levitation or propulsion coil functions. Vehicle loads are reduced to minimum levels for passenger comfort. Magnet shielding and cooling functions are reduced if magnets have been quenched. This increases the time the battery can provide power to critical functions.

The battery operating time for these three modes is shown in Figure 83. The battery subsystem is also divided into left and right side sections for fault tolerance. Conventional lead-acid batteries have been selected for the design. Alternative battery technologies should be investigated to determine whether they are more desirable when considering safety, cost and weight.

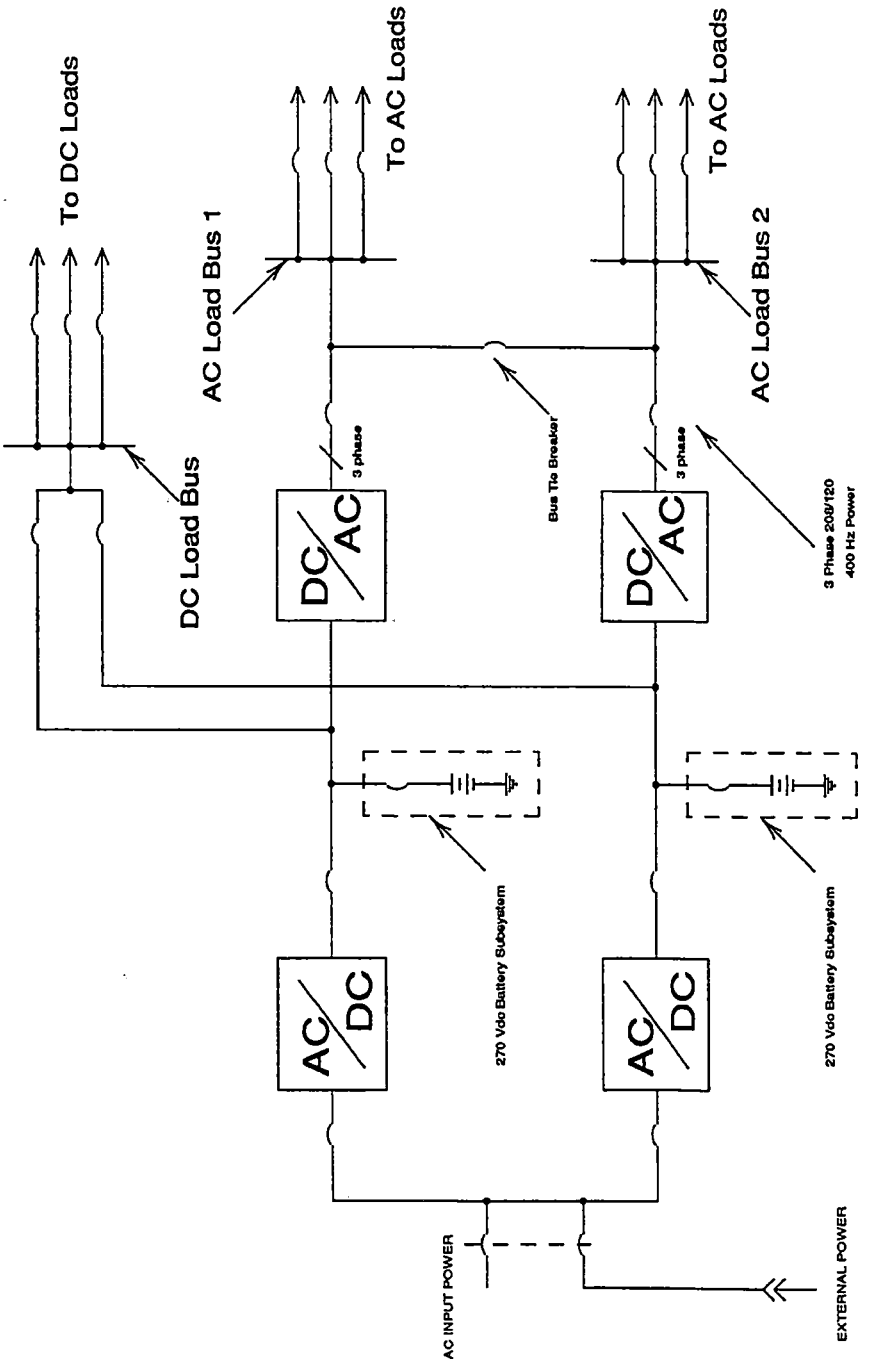

Figure 82 Block diagram of vehicle electric power system

140 Passenger Vehicle

Vehicle Loads	Vehicle Power Operating Modes: Normal	Reduced Performance Modes: Mode 1	Mode 2	Mode 3	
1 Cryogenic Cooling	60	2	2	0	kW
2 Magnet shielding	23	23	23	0	kW
3 HVAC	30	5	5	5	kW
4 Actuators	20	20	0	0	kW
5 Control/Communications	2	2	2	2	kW
6 Lights	5	5	5	5	kW
7 Kitchen	5	0	0	0	kW
8 Battery Charging	5	0	0	0	kW
9 Spare Capacity	35	0	0	0	kW
Total	185	57	37	12	kW
Battery running time	n/a	35	54	165	min

Battery system		
1 Type	Sealed Lead-acid	
2 Capacity	33	kWh
3 Mass	1801	kg
4 Volume	0.93	M^3

45 Passenger Vehicle

Vehicle Loads	Vehicle Power Operating Modes: Normal	Reduced Performance Modes: Mode 1	Mode 2	Mode 3	
1 Cryogenic Cooling	60	2	2	0	kW
2 Magnet shielding	16	16	16	0	kW
3 HVAC	10	2	2	2	kW
4 Actuators	15	15	0	0	kW
5 Control/Communications	2	2	2	2	kW
6 Lights	2	2	2	2	kW
7 Kitchen	0	0	0	0	kW
8 Battery Charging	4	0	0	0	kW
9 Spare Capacity	24	0	0	0	kW
Total	133	39	24	6	kW
Battery running time	n/a	51	83	330	min

Battery system		
1 Type	Sealed Lead-acid	
2 Capacity	25	kWh
3 Mass	1365	kg
4 Volume	0.71	M^3

Figure 83 Vehicle electrical loads

Levitation Gap (m)	Frequency (Hz)
0.1	2.23
0.15	1.82
0.2	1.58
0.25	1.41

Figure 84 Plunge natural frequencies for various levitation gaps

3.2.1.h. SUSPENSION SYSTEM

The suspension system uses the low magnetic stiffnesses of the levitation modules characteristic of the image electro-dynamic system, to provide vibration isolation without the added complexity and weight of an independently sprung secondary suspension system. This suspension arrangement, when combined with absolute damping (e.g. aerodynamic control surfaces) has been identified as optimal for traversing a randomly irregular magway. (Young, J. W. and Wormley, D.N. "Optimization of Linear Vehicle Suspensions Subjected to Simultaneous Magway and External Force Disturbance", ASME Journal of Dynamic Systems, Measurement, and Control, June, 1973.

The vehicle has two bogies, each consisting of two suspension coil modules and one propulsion coil module. To illustrate the characteristic behavior, consider the vertical plunge or heave motion. The magnetic force varies approximately as the inverse square of suspension gap between coils and magway. At the design gap h_0, the total force is equal to the vehicle weight. For small variations in gap about h_0, there is an effective magnetic spring stiffness k given by:

$$k = 2mg/h_0$$

where m is the vehicle mass.

Design Suspension Height of 0.2m
Passive Aerodynamic Damping
Desirable Damping Factor Range = 0.2 to 0.7

Mode	45 Passenger Vehicle		140 Passenger Vehicle	
	Frequency (Hz)	Damping Factor	Frequency (Hz)	Damping Factor
Plunge	1.27	0.0077	1.27	0.0038
Pitch	1.37	0.025	1.46	0.012
Sway	0.92	0.0106	0.92	0.0052
Yaw	1.00	0.034	1.06	0.017
Roll	0.64	0.020	0.64	0.020

Figure 85 Suspension natural frequencies and damping factors

The plunge natural frequency f_P is given approximately by:

$$f_p = \sqrt{\frac{k}{m}} \frac{1}{2\pi} = \frac{\sqrt{\frac{2g}{h_0}}}{2\pi}$$

The frequency is determined uniquely by the design gap, h_0, and typical values are shown in Figure 84. The design operating gap is 0.2 m and the undamped natural frequency is about 1.6 Hz.

The magnetic spring constants can be related to the fundamental single module stiffness k using the configuration and notation summarized in Figure 86. The modes are considered separately and comprise the translations of and motions about the vehicle center-of-gravity. For a stable vehicle, the

center-of-gravity must be located below the effective magnetic center of the superconducting levitation coils. The lateral modes also involve side-force stiffnesses arising from the magnetic keel and relative motion between the superconducting propulsion and LSM coils. Using the vehicle geometry and the actual propulsion and levitation coil properties, the mode-by-mode natural frequencies were obtained more exactly, as shown in Figure 85. Also presented in Figure 85 are the modal damping factors arising from the passive aerodynamic damping. These are typically more than an order of magnitude lower than desirable, and active damping must be used.

In the complete dynamic response of the vehicle, the modes will be coupled and the natural frequencies will be slightly modified. The simulation discussed in Section 3.2.2.g. incorporates the full magnetic, aerodynamic and mode coupling.

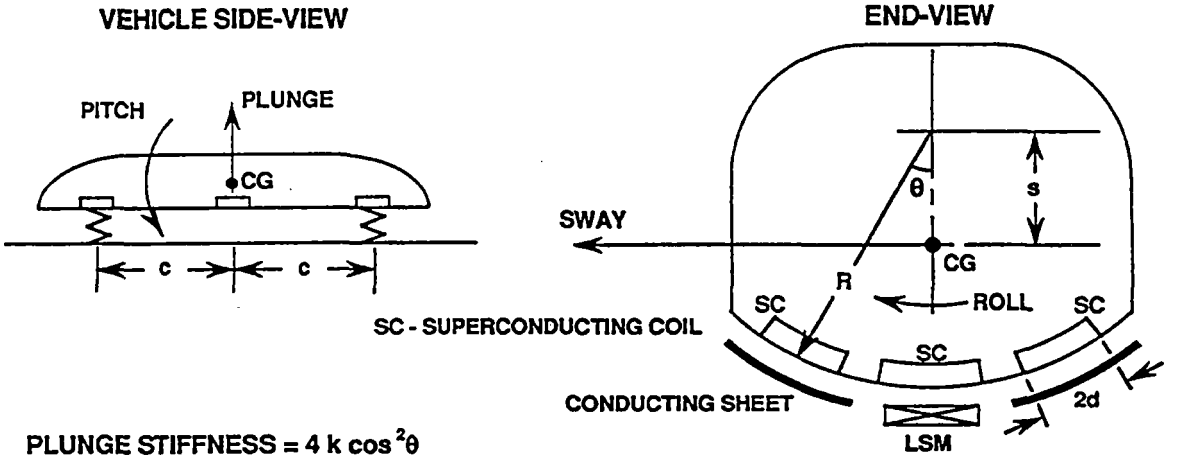

PLUNGE STIFFNESS = $4\ k \cos^2\theta$

PITCH STIFFNESS = $4\ k\ c^2 \cos^2\theta$

SWAY STIFFNESS = $4\ k \sin^2\theta + k_P + k_M$

YAW STIFFNESS = $(4\ k \sin^2\theta + k_P + k_M)\ c^2$

ROLL STIFFNESS = $4\ k\ d^2/3 + 2\ k\ s^2 \sin^2\theta + 2\ (k_P + k_M)\ (R - s)^2$

where k = SINGLE MODULE STIFFNESS
k_P = STIFFNESS FROM RELATIVE MOTION BETWEEN SC AND LSM COILS
k_M = MAGNETIC KEEL STIFFNESS FROM ITERACTION BETWEEN THE SC COILS AND THE EDGES OF THE CONDUCTING SHEET

Figure 86 Magnetic spring constants

Number of Passengers	Shield Coil Weight (kg)	Shield Coil Power (kW)
140	3400	33
45	2300	22

Figure 87 Shielding coil weight and power requirements

3.2.1.i. ELECTROMAGNETIC SHIELDING

3.2.1.i.1. WEIGHT AND POWER

The feasibility of an active coil shielding system for the Magneplane vehicle has been demonstrated. The results presented here are for the 140 passenger case. Shielding coils of similar geometry, but less power and weight would be required for the 45 passenger vehicle because the bogie coil geometry for this case is identical and the amp-turn requirements are reduced. The weight and power requirements for the shielding coils for both the 140 passenger and 45 passenger cases are given in Figure 87.

3.2.1.i.2. BOGIE SHIELDING COIL CHARACTERISTICS

Figure 89 shows an outline of the superconducting coils in a single bogie. They consist of two pairs of levitation coils and a set of six propulsion coils. The propulsion coils carry considerably more amp-turns than the levitation coils and are, therefore, somewhat more difficult to shield. However, the thrust developed by the interaction of the propulsion coils with the LSM windings in the magway is primarily dependent on the total ampere-turns in the propulsion coils and not on the distribution of the amp-turns among the six coils in the set. Hence, the distribution of the required total amp-turns among the six coils have been tailored to aid in the natural decay of the magnetic field. This approach is discussed in more detail in a trade study later in this report.

Limiting Field Level (gauss)	Distance from Centerline (m)
50	2.9
5	4.6
1	6.5

Figure 88 Summary of magnetic field

The idealized current distribution for the shielding coils can be found by first specifying planes on which the coils are to be located. Figure 90 shows a set of planes which overlay on the coils and coordinate system in Figure 89. Shielding coils in these planes would be located beneath the floor and in the walls of the bogie section of the vehicle, and would decrease the fields experienced by the passengers. The planes are located so as to allow a walkway that is 1.2 m wide over the bogie. Personnel access through the walkway would be restricted and passenger access would be prohibited.

Figure 91 shows an isometric view of an ideal shielding coil winding distribution on the selected planes for the baseline case of 2.42E+05 amp turns in each levitation coil, 7.8E+05 amp turns in the central four propulsion coils and 3.9E+05 amp turns in the end coils of the propulsion coil set. The contours are drawn such that the shielding coils should be wound with 1E+04 amp-turns between contours. A plan view of the ideal coil pattern is shown in Figure 92 .

Contours of constant field over the vehicle cross-section in a typical plane containing the bogie using an extended shield is shown in Figure 93. Contours are labeled and indicate that the bulk of the volume within the vehicle is below 50 gauss. However, this will be a restricted area with no passenger access and used for storage or location of selected items of equipment.

Figure 93 also indicates the extent of the field beyond the vehicle in the vicinity of the bogie. Figure 88 summarizes the distance in the transverse plane from the vehicle centerline to the field level listed as measured at vehicle floor level.

Depending on field exposure criteria to be applied in terminals, the figure indicates the area swept by the vehicle bogie fields as it enters a terminal and the area to have restricted access until the vehicle is stopped. Once stopped, these areas, which are only located near the bogies, could have no access or could be actively shielded by coils in the terminal.

The extent of the field along the vehicle length is indicated in Figure 94. It shows that the active coils on the vehicle result in a passenger compartment that is almost entirely below the 1 gauss level. The addition of localized shield coils may be necessary near the ends or around field sensitive equipment. We have allowed for this with a 50% contingency on shield coil weight and power in Figure 87.

More extensive discussion of fields, as well as plots of fields from the LSM may be found in the Supplementary Report on "Magnetic Field Analysis", which shows the fields from the bogies to be dominant.

The examples given in this section demonstrate the feasibility of shielding the fields from the levitation and propulsion coils in the Magneplane bogies to the 1 gauss level for the passengers in the vehicle. Further investigation might prove that these requirements can be achieved with less shielding coil weight and/or power, but it is clear that the goal can be achieved.

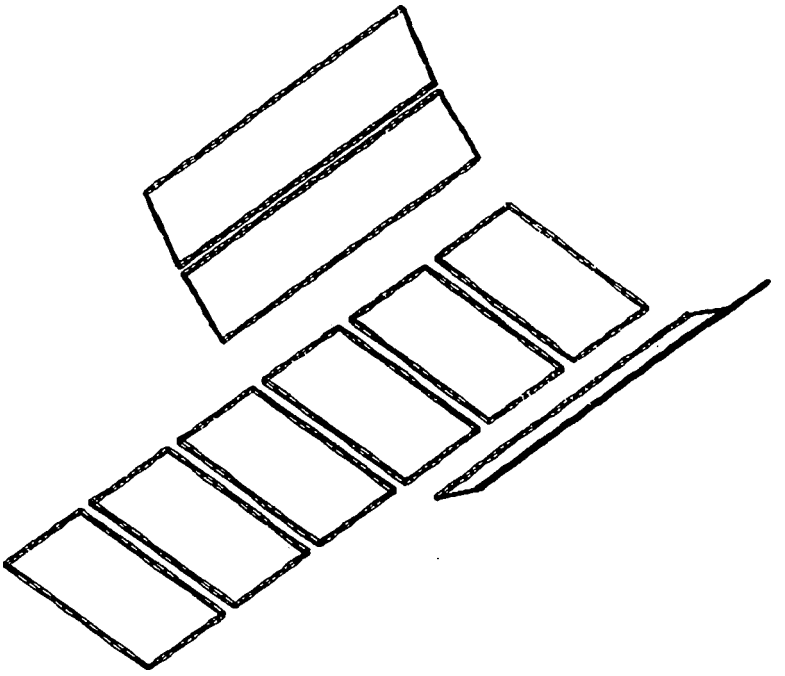

Figure 89 Outline of propulsion and levitation coils in bogie

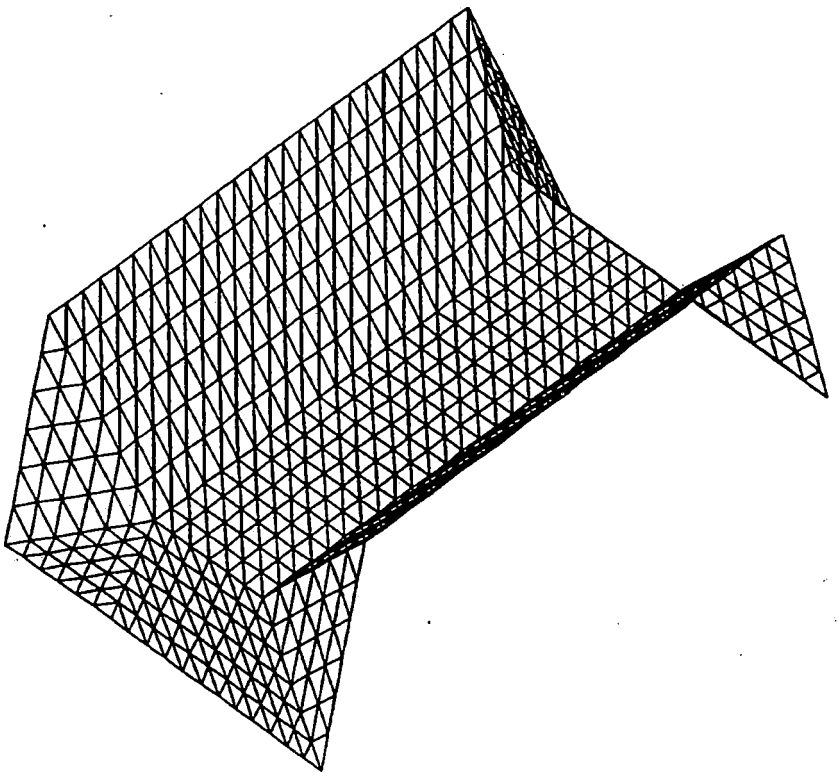

Figure 90 Surface in bogie region on which shielding coils are being located

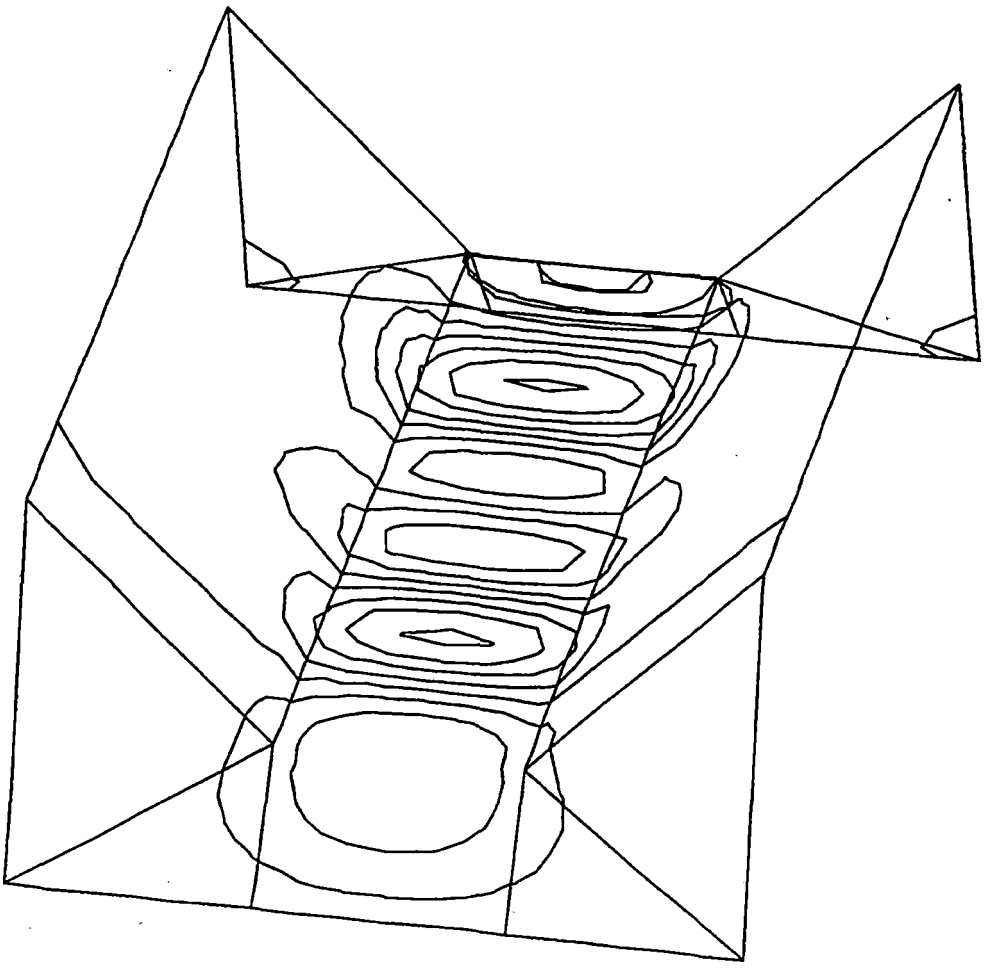

Figure 91 Isometric view of ideal current pattern for shield coils (propulsion coil currents: 390/4x780/390)

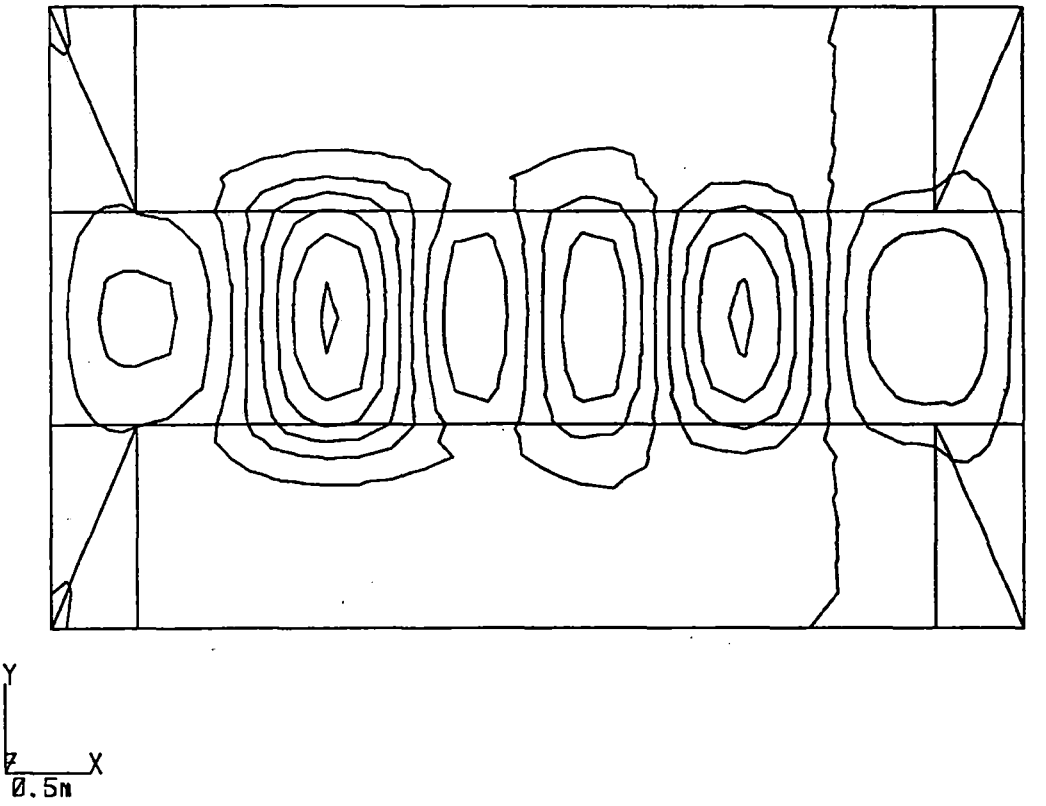

Figure 92 Plan view of ideal current pattern for shield coils (propulsion coil currents: 390/4x780/390)

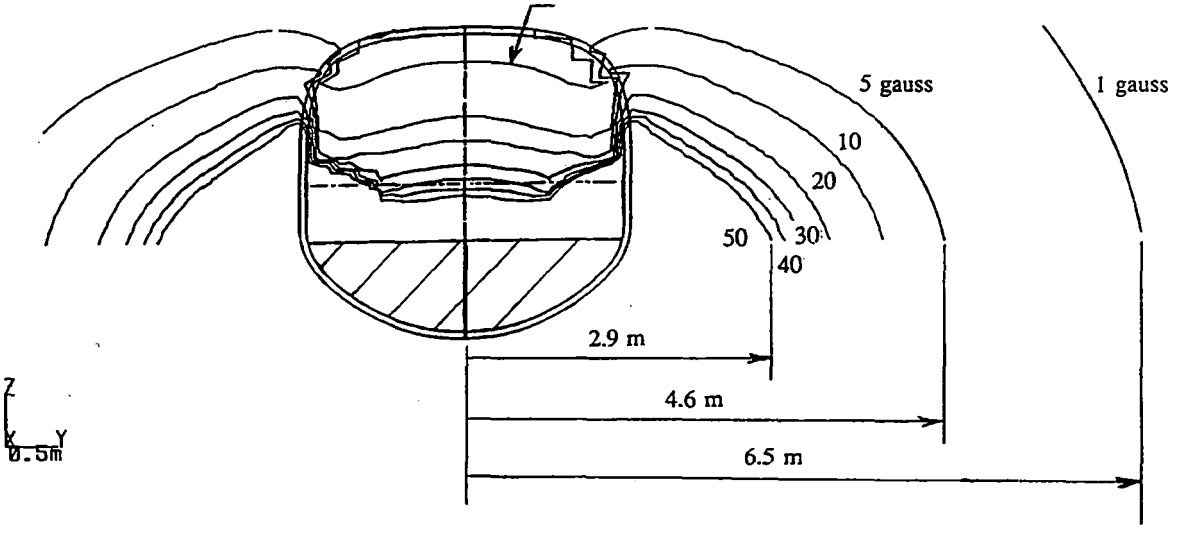

Figure 93 Contours of constant field magnitude in transverse plane over bogie with shields active (M07)

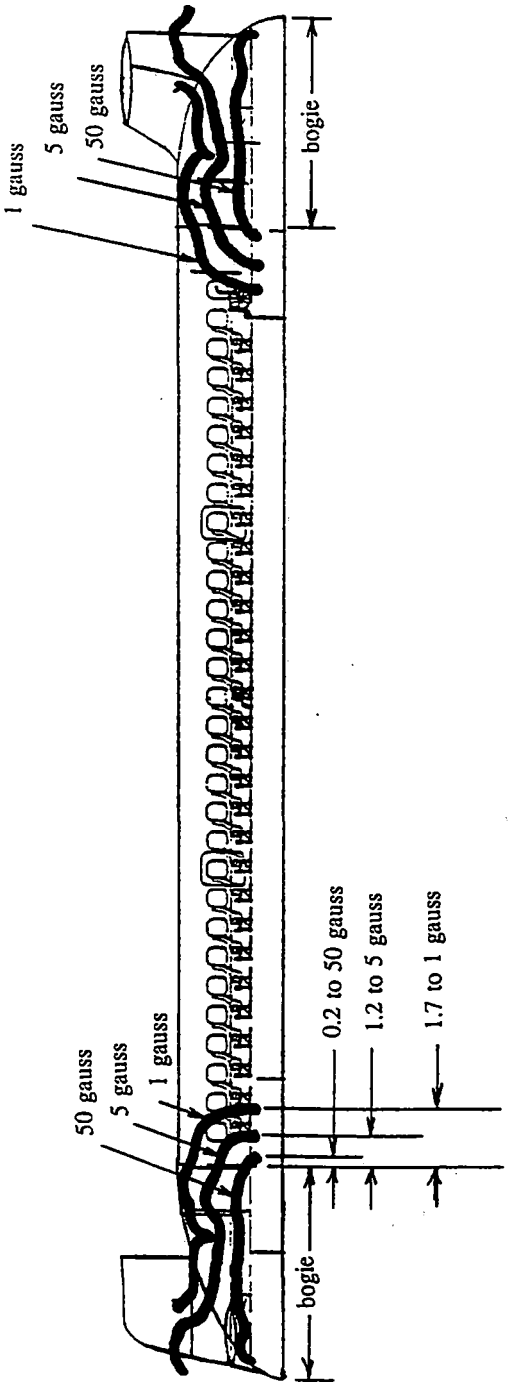

Figure 94 Magnetic field contour for 1, 5, and 50 gauss for the baseline 140 passenger vehicle with active shielding coils near bogies (M07)

3.2.1.j. MAGWAY TO VEHICLE ENERGY TRANSFER

3.2.1.j.1. INDUCTIVE PICK-UP COIL CONCEPT

Power for electrical loads on the vehicle will be transferred from the magway using an inductive pick-up coil in the lower fuselage of the vehicle. The coil will be magnetically coupled to the LSM winding and excited by an auxiliary (non-propulsive) frequency current. The auxiliary current generates a magnetic field which is not synchronous with the vehicle. This field induces a voltage in the pick-up coils and provides power to the vehicle.

To help visualize how the auxiliary current excites the pick-up coil, assume that the vehicle is travelling at the design speed of 150 m/s. The propulsion frequency is 100 Hz. If the auxiliary current is applied at 150 Hz the pick-up coil will perceive an ac field at 150-100 or 50 Hz. This difference between the propulsion and auxiliary frequencies is called the "slip" frequency.

Power transfer to the pick-up coil can be improved by reversing the direction of the auxiliary power travelling wave with respect to propulsion. With three phase power, the direction of the travelling wave is reversed simply by reversing the phase rotation - equivalent to interchanging two leads on a three phase motor. To see how this helps improve the power transfer, assume the vehicle is travelling in the +X direction at an equivalent frequency of 100 Hz. Auxiliary current at 100 Hz applied in the -X direction will produce a slip frequency of 200 Hz. This improves power pick-up without increasing the magway voltage. The Magneplane system uses this principal to improve power transfer to the pick-up coil.

This improvement is not without some penalty however. Since the extra slip frequency is generated by the vehicle, a mechanical load occurs. In effect, the vehicle coils act as an induction generator. The faster the vehicle goes, the more power is generated. But the fraction of power that comes from the vehicle motion needs to be supplied by the propulsion system. Fortunately this load is relatively small compared to the propulsion power. At 134 m/s every 100 kW supplied by vehicle increases the drag by 1500 N - less than 3% of rated thrust for a 7.5 MW system.

The pick-up coil will be constructed with the same pitch and width as the LSM winding. The 140 passenger vehicle has approximately 20 meters between propulsion bogies. A coil approximately 18 meters long has been designed to fit this space and is shown in the sketch of Figure 95. The sketch shows a single layer of a coil which spans 24 pole pitches of the LSM winding. One phase of a three phase coil will consist of several layers stacked on top of each other. The phases will be staggered in the X axis so the entire coil structure becomes a replica of the LSM winding but with multiple layers.

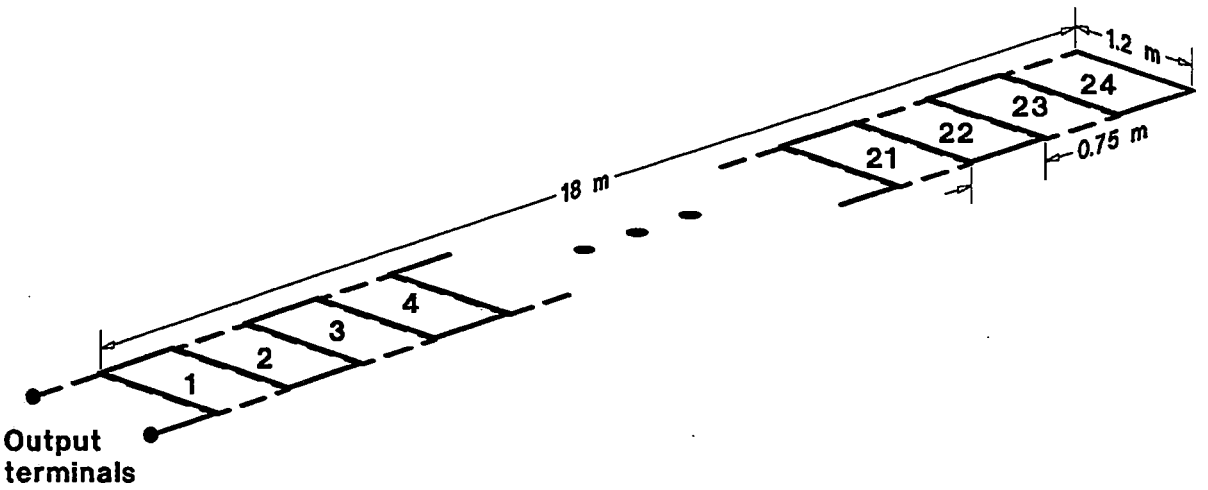

Figure 95 Simplified diagram of power pick-up coil

3.2.1.j.2. CIRCUIT ANALYSIS

Once the slip frequency is known, the inductive pick-up circuit can be modeled as an air-core transformer. The coupling equations for the transformer are:

$$V_1 = (R_1 + j\omega L_1)I_1 - j\omega MI_2$$

$$V_2 = j\omega MI_1 - (R_2 + j\omega L_2)I_2$$

where subscript 1 refers to the primary (magway) circuit and subscript 2 refers to the secondary (pick-up coil) circuit. ω is the slip frequency in rad/s.

The coupling between the pick-up coil and the LSM winding is expressed in terms of the mutual inductance M. R_1 and L_1, and R_2 and L_2 are the resistance and self inductance of the LSM winding and pick-up coil respectively. When ω, I_1 and I_2 are given, V_2 is maximized by maximizing M and minimizing R_2 and L_2. This observation defines fundamental design tradeoffs. M is increased by decreasing the distance between the coils. R_2 and L_2 are reduced by increasing the physical size of the pick-up coil.

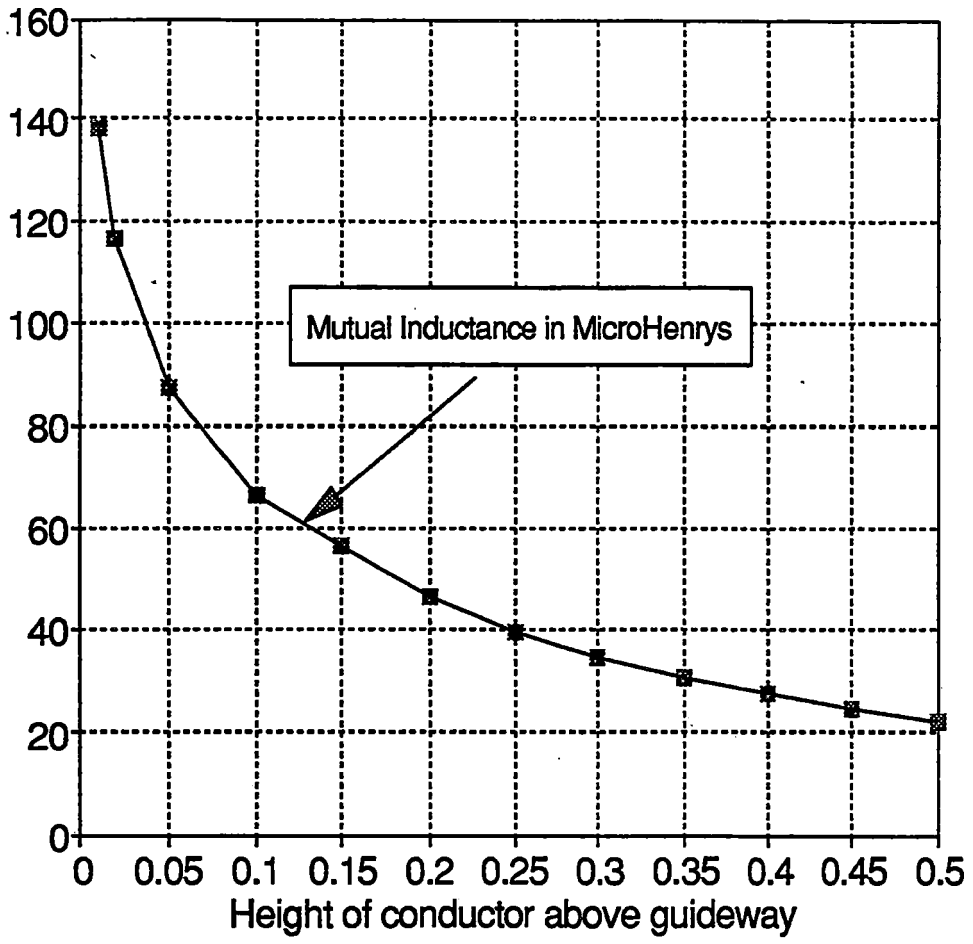

Figure 96 Mutual inductance of pick-up coil to LSM winding

Although M cannot be controlled directly it is an important parameter in the design. Figure 96 shows the mutual inductance between a one layer coil and the LSM winding as a function of height. Preliminary designs presented later in this section are based on a nominal coil height of 0.3 m to allow for coil build.

Power transfer to the load is improved dramatically if the self inductance of the coil, L_2, is cancelled by an external compensating capacitor as shown in Figure 97. When compensated this way the power in the load becomes

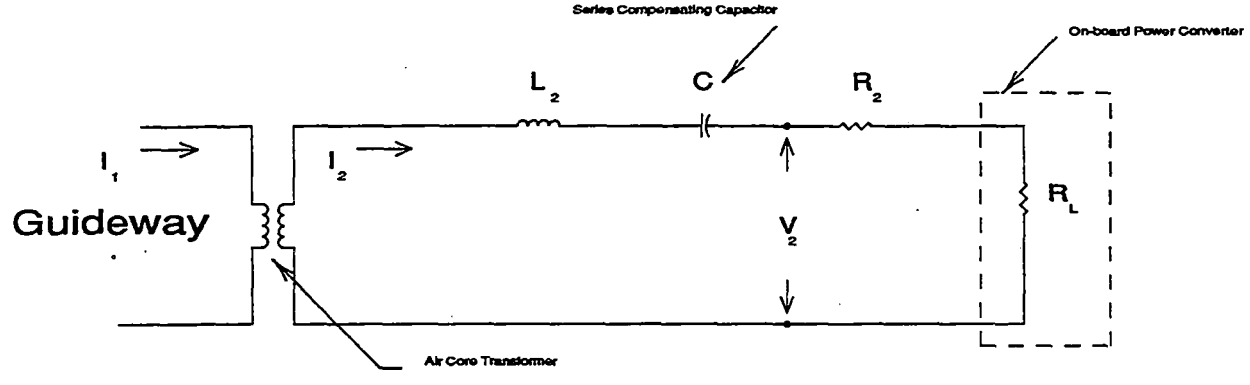

Figure 97 Equivalent circuit model of the pick-up coil

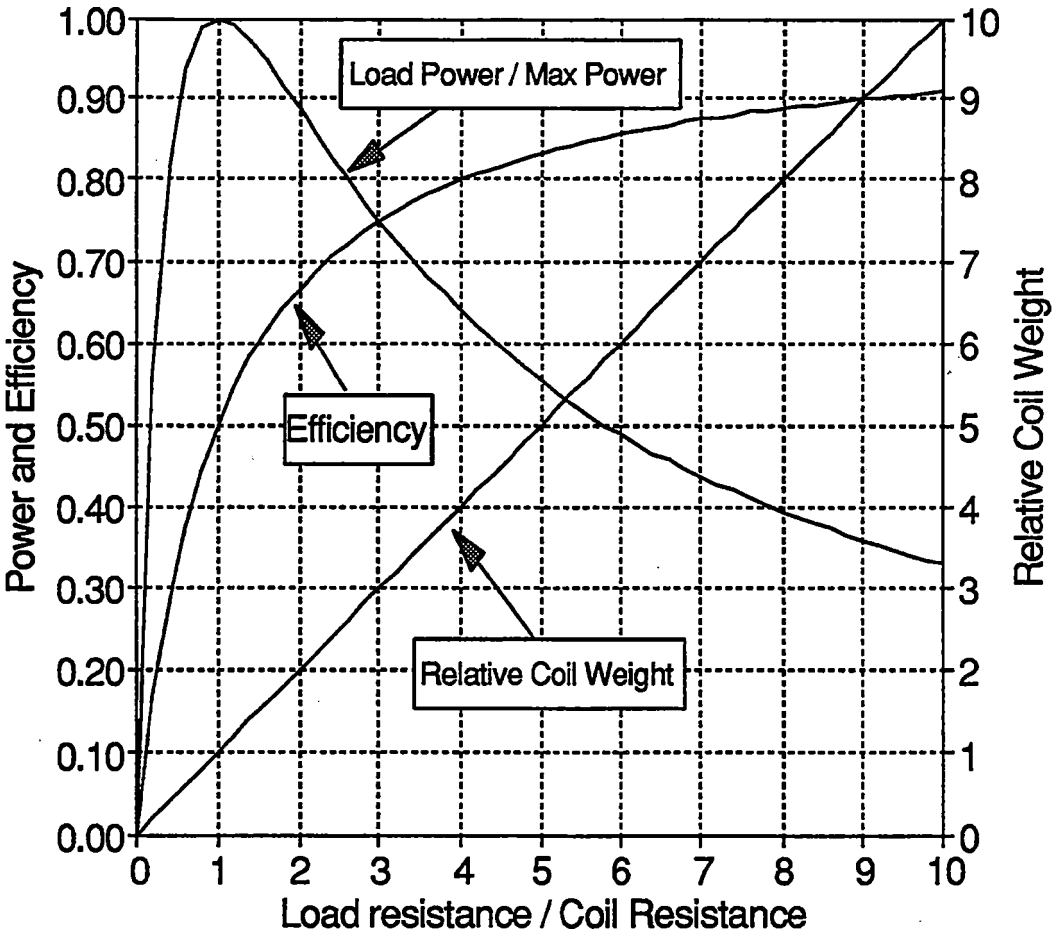

Figure 98 Efficiency, power, and weight of the pick-up coil

$$P_L = \left[\frac{V_2}{R_2 + R_L}\right]^2 \cdot R_L$$

The power dissipated in the coil is

and the efficiency becomes

$$P_2 = \left[\frac{V_2}{R_2 + R_L}\right]^2 \cdot R_2$$

$$\eta = \frac{R_L}{R_2 + R_L}$$

The maximum power that can be delivered is:

Some of the resulting relationships are shown in Figure 98. Maximum load power occurs when the load resistance equals the coil resistance ($R_L = R_2$). At this point, the efficiency is 50% since the power used by the load equals the thermal dissipation in the coil itself. Thus maximum output can be achieved only with significant coil power loss. Increasing coil weight by 5 times improves efficiency to 83% but at a significant weight penalty. Another trade-off in the design.

A preliminary design for the pickup coil is shown in Figure 99. Additional design constraints and detailed design issues need to be considered to finalize the design. This concept can be made to deliver power for all on-board loads but modification to the following operating parameters will be needed:

1. Auxiliary current
2. Auxiliary frequency
3. Vehicle load requirements

Sufficient flexibility exists to modify these parameters but experimental work will be required to finalize the design. Modifications should not compromise present cost or weight estimates.

Standard Layer Definition		
Conductor length	93.6	m
Conductor area	1	cm^2
Resistance	0.02677	Ohms
Volume	0.00936	m^3
Mass	25.3	kg
Mutual inductance to Guideway	36	uH
Mean coil height	0.3	m

Operating Characteristics		
Guideway frequency	-500	Hz
Vehicle speed	150	m/s
Coil frequency	600	Hz
Guideway aux current	167	A
Guideway prop current	1075	A
Guideway total current	1088	A
Guideway aux voltage	7450	V
Guideway prop voltage	9591	V
Guideway total voltage	12145	V

Layer characteristics		
Layer OC voltage	22.7	volts
Max layer output power	4797	Watts
R load/coil	6	
Layer power dissipation	392	Watts
Layer power output	2350	Watts
Efficiency	85.7	%

Coil system characteristics		
OC Voltage	579	V
FL Voltage	496	V
Output Current	121	A/phase
Total output power	180	kw
Total coil power dissipation	30	kw
Efficiency	85.7	%
Number of layers	26	/phase
Total Coil Mass	1936	kg
Percent of 50000 kg	3.9	%
Total Coil Volume	0.72	m^3

Figure 99 Preliminary design of pick-up coil

3.2.1.k. INSTRUMENTATION AND CONTROL

Instrumentation and control functions within the Magneplane vehicle are implemented by a computer system employed within a multi-controller architecture. This architecture implements various computer based sub-systems for managing the internal/external communications, the internal environment, the flight recorder as well as vehicular control operations. The vehicle control system consists of two computer subsystems, the flight control processor and the vehicle flight I/O processor. Communication between these two subsystems, and the other subsystems is via a digital serial ethernet link. The two subsystems that make up the vehicle control system are called the Integrated Flight/Propulsion Control System (IFPC). This system is used to implement two primary functions; Propulsion Control and Vehicular Stabilization.

The system features a computer architecture which provides fault-tolerant operation through hardware and software failures. The hardware topology insures that any critical operations can be sustained during a system or sub-system failure, thus ensuring fail-safe operation. Software reliability and robustness is enhanced by the non-dependance on interrupt driven events which in turn permits critical functions to be serviced sequentially.

To implement the control functions, the IFPC System integrates every device on the vehicle which can sense or produce a force or moment on the vehicle. This includes inertial sensors, aerodynamic control surfaces, the propulsion thrust, and the landing gear braking functions. A summary of these available control effectors is presented in Figure 100.

3.2.1.k.1. PRIMARY IFPC FUNCTIONS

The IFPC provides the required capabilities for performing the inertial control functions which are necessary to operate the Magneplane. These include propulsion and aerodynamic measurement and controller operations for implementing propulsion and stabilization servo loops, along with various emergency and backup operations. For the propulsion control loop, the system is used in conjunction with on-board communications and propulsion components, along with the wayside control processor. The IFPC is used to acquire and process sensor data to generate frequency, phase and magnitude data for the linear synchronous motor (LSM) magway winding. These commands are sent to the wayside control processor across an RF link, to affect the LSM winding excitation as part of the propulsion control loop. Figure 101 depicts the data flow of the IFPC.

Velocity commands and route information is received at a 12 Hz rate across an RF link from the wayside control processor. Motion and displacement sensor data is derived from sensor platforms distributed within the vehicle. Optical height sensors and three axis accelerometer groups are positioned inside the vehicle to measure these parameters. Magnetic field sensors are configured as an array inside the vehicle to derive data on the magnetic wave that the vehicle 'rides'. Air data is derived from sensors located on the outside surface of the vehicle to measure the angle of attack and yaw forces. The propulsion

SENSOR	AERODYNAMIC	PROPULSIVE	LANDING GEAR
Height Detector (6) Inertial Sensors (6) Position Markers (2)	Forward Left Stabilator Forward Right Stabilator Forward Yaw Canard Aft Left Elevon Aft Right Elevon Aft Rudder	Gross thrust	Normal brakes Emergency brakes

Figure 100 Summary of available control effectors

parameters are based on the vehicle static and dynamic response, which is dependent on the size of vehicle and its load. This data is acted upon to derive the control of the aerodynamic surfaces to stabilize the vehicle, and the propulsion commands which are returned to the wayside processor for implementation, across the RF link at a 96 Hz rate. Additional control functions include the landing gear, which is activated at low velocities, and the emergency braking.

The IFPC performs all facets of the control function which include: acquiring sensor measurements, implementing the control laws, and operating the aerodynamic surfaces to induce the proper response. The control laws for the system must consider the interactions of all various control effectors in response to various inputs as well as to the input feedback response from any effector. This shall include any cross-coupling effects. The vehicle response to a particular effector will vary with flight conditions. The control law processor computes the overall force or moment to provide the desired response, then parcels the control command among the available effectors to optimize their usage.

3.2.1.k.2. IFPC ARCHITECTURE

The resulting architecture used on the Magneplane vehicle is depicted in Figure 102. Using state-of-the-art equipment, the IFPC maintains the necessary flying and ride qualities for all required modes.

New, but proven, technologies will be utilized for the force-motor controlled surface actuators and microprocessor based controllers. All actuators and sensors that are critical for a safe flight default to fail-safe operation (first failure produces no significant degradation in safety) using a combination of cross channel and in-line monitoring. Aerodynamic control surfaces have redundant sources of electrical supply.

The following summarizes the electrical redundancy levels for the IFPC system components:

Flight controller - Two channels with identical software in both channels

Vehicle-to-magway Height Sensors - Six sensors feeding two channels

Magway Position Sensors - Dual Channels

Magnetic Field Sensors - Thirteen sensors feeding two channels

Inertial Sensors - Duplex Accelerometer Packs (Three-axis)

Angle-of-Attack Sensors - Dual inputs for both pitch and yaw

Stabilator, Elevon and Canard Actuators - Duplex force motor

Air Data Sensors - Static and dynamic air pressure and speed

RF Transceivers - Dual Transmit/Receive units

In addition, a Global Positioning System (GPS) is provided to accommodate special situations.

The IFPC consists of the Flight Path Control Set (FPCS), the vehicle control I/O set, the vehicle aerodynamics actuators, the flight control sensors, the propulsion control sensors, the attendant interface, the maintenance interface and backup hardware. The FPCS contains two (2) digital Flight Controllers (FC), resulting in duplex-synchronous system operation.

The FPCS interconnection pathway diagram is shown in Figure 103. The command chain for the FC's is such that one channel is designated as the primary channel. A second, shadow FC processor duplicates the operations of the primary FC using independent transducers. Internal performance monitoring software routines running on each FC permit the shadow FC to take over partial or total system control should problems develop with the primary FC channel. Use of a combination of dedicated and shared sensors provides the necessary FPCS inputs to meet the safety, computational and mission reliability requirement. Command inputs, vehicle motion/displacement and air data sensors, as well as surface actuators, are supplied with transient resistant electrical excitation/power. The actuator servo loops are digital, with the FC closing the loop, thus providing maximum rejection of radiated and conducted noise effects that would impact more sensitive analog loops. Vehicle dynamics are monitored by analog sensors which are converted and transmitted to the controllers over redundant digital busses. All data transfers for an FC channel or between the individual FC's are digital for increased data accuracy, flexibility, and reliability.

The vehicle I/O control set are dual processors that operate in a similar primary and shadow manner to that described for the FPCS, and provide the interface between the non-flight hardware and the FPCS. The interface to the FPCS is via the ethernet link. The non-flight hardware includes the RF link, the attendant displays, the voice channels, GPS, and the maintenance interface.

The system architecture is structured for flight safety as well as redundancy with one-half the system physically separated from the other. This is true of both the communications and power distribution busses such that a single catastrophic failure of a sub-system has minimal effect on overall system performance and passenger safety. The IFPC interface block diagram is shown in Figure 104 and clearly defines the redundant functionality and data highways.

The system is partitioned into two major functional blocks; Flight Control and Vehicle Communications I/O .

For the Flight Control function, digital computations based on the flight control laws are made by a Flight Control (FC) processor. Each channel of the FPCS contains a single FC, each supporting electrically erasable programmable read only memory (EEPROM) for storage of the Operational Flight Program (OFP). The EEPROMS's containing the control laws can only be re-programmed by authorized personnel through a series of protection and password schemes. This capability is only available while in the maintenance depot and access is restricted while the vehicle is in service.

Vehicle sensor outputs are converted into digital form and transmitted simultaneously on redundant busses. Multiple sensors are used to measure the vehicle-to-magway displacement, to detect encoded magway position data, and to measure the vehicle's acceleration and air speed/direction at various locations. Duality is implemented with the sensor arrays where required to augment the duplex nature of the flight control function. Critical flight data is transmitted on two (2) separate digital serial busses, one link going to each channel of the FPCS.

Aerodynamic control surface actuators are state-of-art designs developed for military programs. All actuators are fly-by-wire with various levels of hydraulic and electrical redundancy as required for the specific location on the vehicle.

Vehicle Communications I/O processing is performed by dual redundant communications processors with a similar architecture to that of the Flight Control processors. A VME architecture is adopted for this function with duality retained for the data highways. All external vehicle communication I/O are processed via this pathway and passed to/from the FC shared memory area. The interface supports the vehicle duplex RF link for Voice and data (Propulsion loop processing), decoded GPS time and position reference data, attendant display I/O and off-line maintenance I/O. The VME environment ensures that the data processing capability exists to meet the computational throughput required to adequately perform these functions in the context of normal and abnormal vehicle operations. The fault tolerant VME processor design uses a Reduced Instruction Set Computer (RISC) architecture, similar to the Global center hardware (see section 3.2.3.a). The prime criteria for adopting a dual redundant approach is passenger safety. Failure of the communications processing function will isolate the RF link to the wayside controller from the flight controllers. This results in loss of vehicle control by the Global center, and loss of propulsion winding control by the vehicle. The dual I/O processor insures that one failure can be tolerated without affecting the system performance, and permits the vehicle to travel to its destination prior to a repair being required.

3.2.1.k.3. PROPULSION CONTROL ACTIVITIES

Prior to a Magneplane departure, the vehicle's GPS system will be used to provide position data as necessary to the wayside and global controllers. The global controller will generate a trip profile consisting of coordinate descriptions of eleven (11) meter sections of the magway that the vehicle must follow along its path. Sufficient mapping data is transmitted to the vehicle for the immediate magway. This mapping data is appended as the vehicle proceeds along the magway, by the Global Center, enabling dynamic re-routing to be instigated without corrupting this database.

When the Magneplane departs, the initial function is to propel the vehicle towards the main pathways. A starting sequence is employed to synchronize the power excitation to the vehicle's position while accelerating the vehicle along the magway. After synchronization, a normal propulsion control loop will be invoked for this purpose. Once the vehicle is underway, propulsion control parameters are computed by the vehicle and sent to the wayside controller which adjusts the LSM winding excitation for frequency, phase and amplitude. The landing gear will be withdrawn when the Magneplane achieves flight velocity. Control of the vehicle requires that the relative position of the magway field and the vehicle's field be maintained. Phase command words for the LSM excitation are sent to the wayside control processor across the RF link at a 96 Hz rate. The phase data is derived from the magnetic field phase of the LSM coil with respect to the vehicle. The required frequency and amplitude of the LSM winding excitation field is also sent to the wayside control processor. These are derived from the vehicle's relative velocity and position along the magway, and the height between the vehicle and the magway.

3.2.1.k.4. LSM FIELD DETECTION

The LSM field strength will be measured on the vehicle using fluxgate magnetometers located between the bogies on the vehicle above the propulsion windings. These sensors depend for their action on saturation in magnetic material, usually a toroidal
coil, which maintains a closed flux path for the excitation and sensed fields. External fields coupling into the core introduce odd harmonics in the sensed output winding on the core, directly proportional to the magnitude of the external field. This method of sensing is more linear than conventional Hall effect sensors and does not suffer from the temperature sensitivity found with semiconductor sensing devices. Since the distance of the sensor array from the magway windings has an effect on the magnetic field strength measured, vehicle to magway height and orientation displacements must be factored into the readings. Similarly, to reduce any interference effects due to the levitation magnets in each bogey, the sensor array is located at a midpoint location on the underside of the vehicle at an equal distance from each bogey. Measurement errors introduced by magnetization of local ferrous materials in the vehicle and distortion effects of the vehicle structure can be compensated by performing periodic calibration of the sensor array in a sterile magnetic environment.

An array of 13 sensors arranged as shown in Figure 105 will be used to detect the magnetic field strength of the magway windings. The arrangement of the sensors in the array is chosen to provide at coverage over at least two pole pitch's (1.5 m). This configuration improves the accuracy of the LSM waveform reconstruction from the sampled data points by ensuring that at least two sensors will be detecting flux transitions near the zero crossing point of the waveform. The relative position of sensors in the array is derived from the physical relationship of the phase coils in the magway which are offset from each

other by 1/3 of a pole pitch (0.25 meters). The composite magnetic field generated by the three phase coils has a wavelength of 1.5 meters, as do the individual phase components. The sensor arrangement is such that the sinusoidal LSM field pattern can be reconstructed from the individual field strength data points with a high degree of accuracy. The number of sensors in the array permits single failures to occur without significant reduction in the accuracy of the reconstructed waveform. The phase offset between the vehicle propulsion coils and the LSM magway coils is computed using the reconstructed flux waveform, knowledge of the vehicle to magway height and the index offset of the sensor array to the vehicle propulsion coil geometric center. Calculations indicate a flux-gate sensor with a dynamic range of 76 dB shall be sufficient for this application, which is within the capability of current commercial technology.

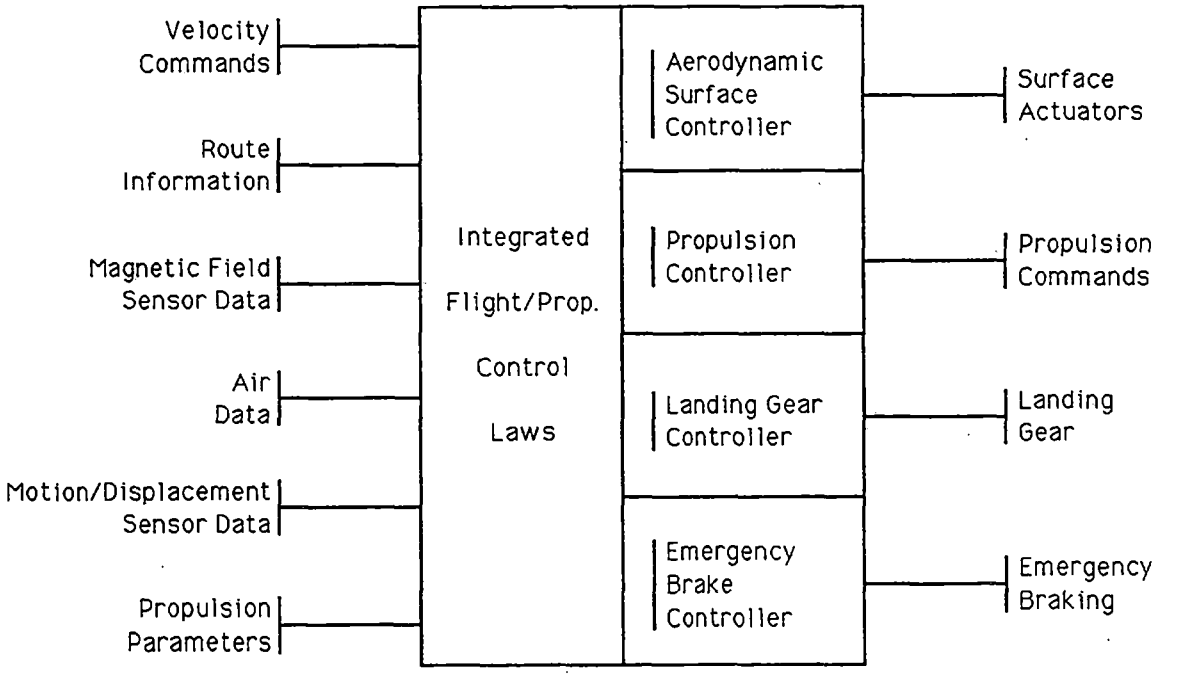

Figure 101 IFPC data flow

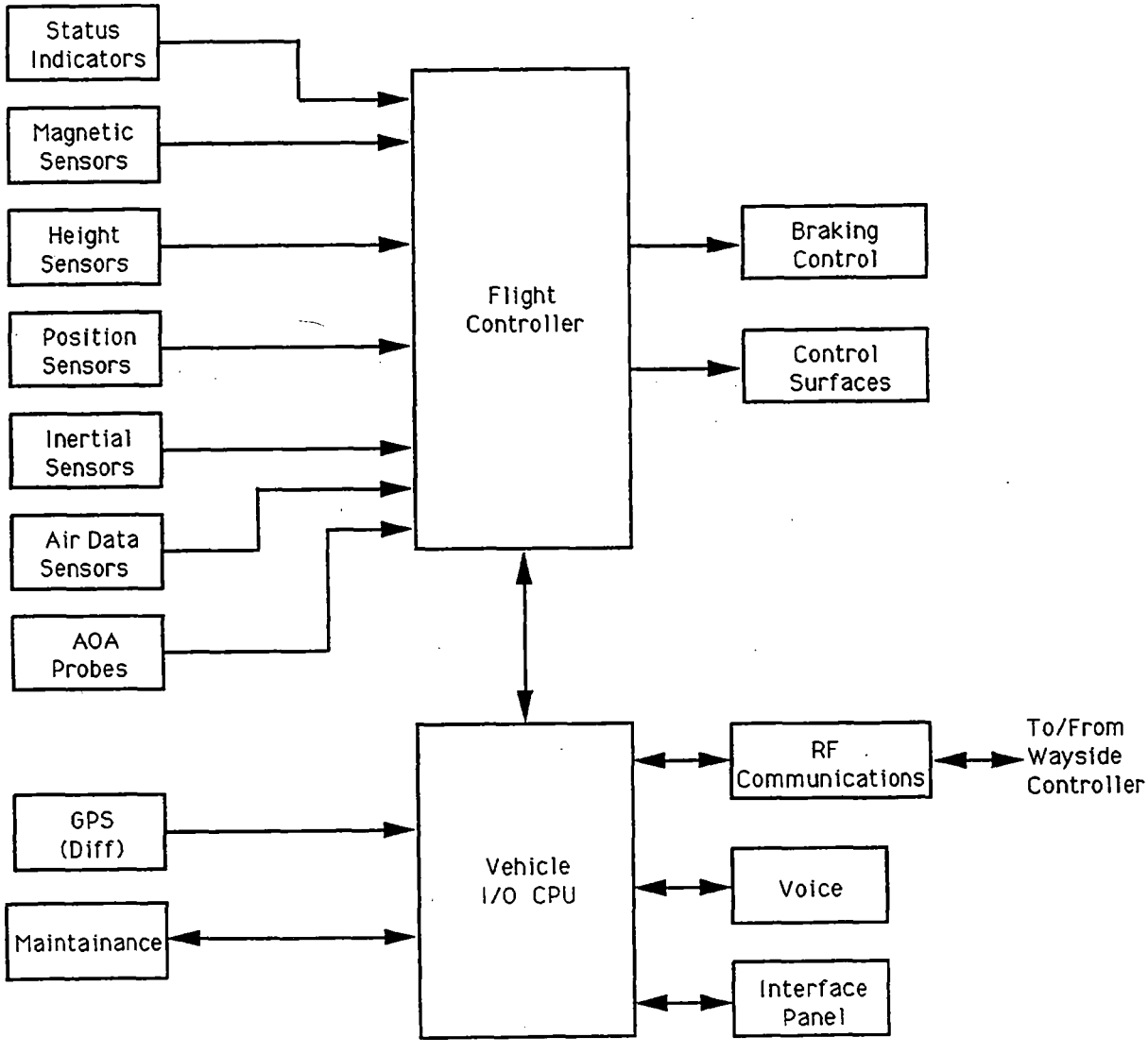

Figure 102 IFPC system diagram

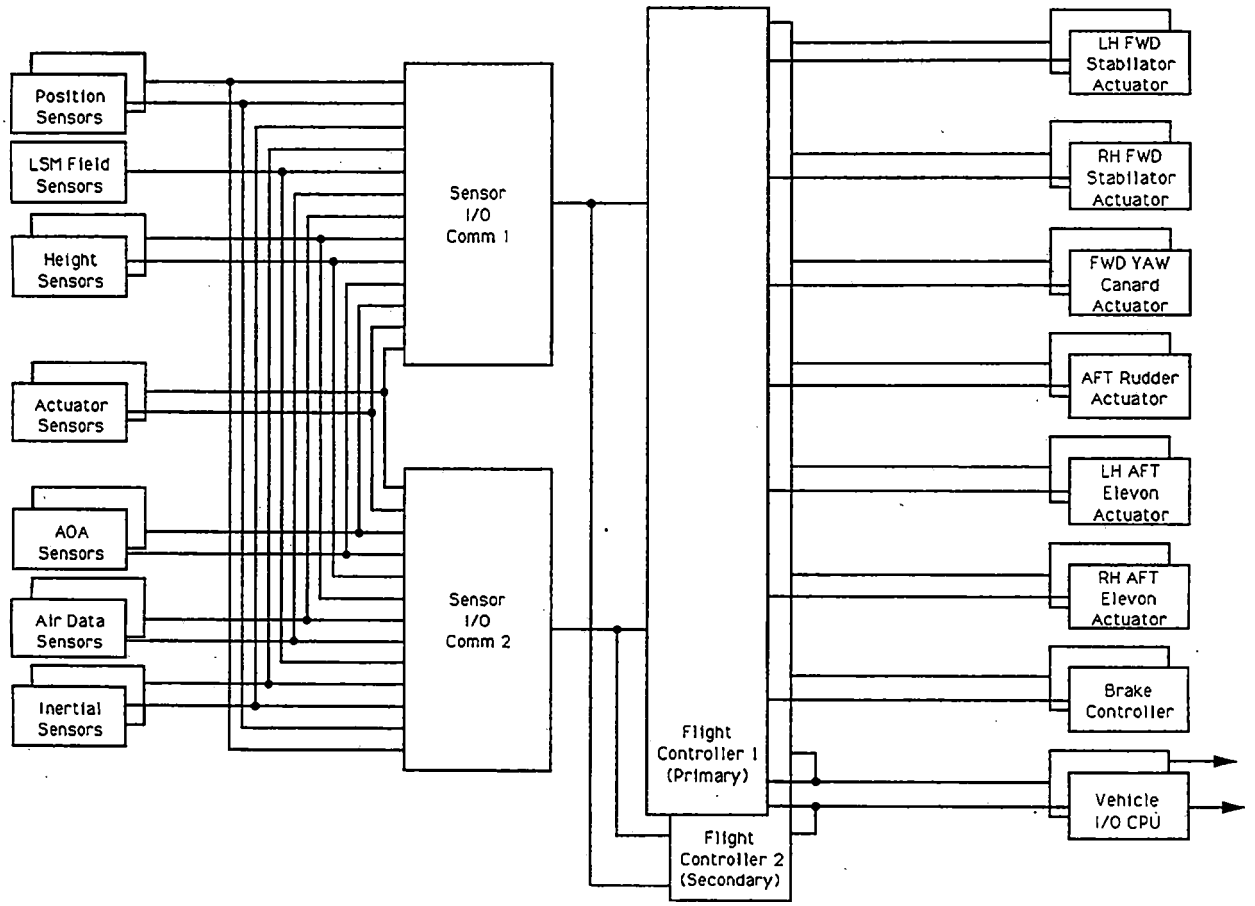

Figure 103 FPCS interconnection pathway diagram

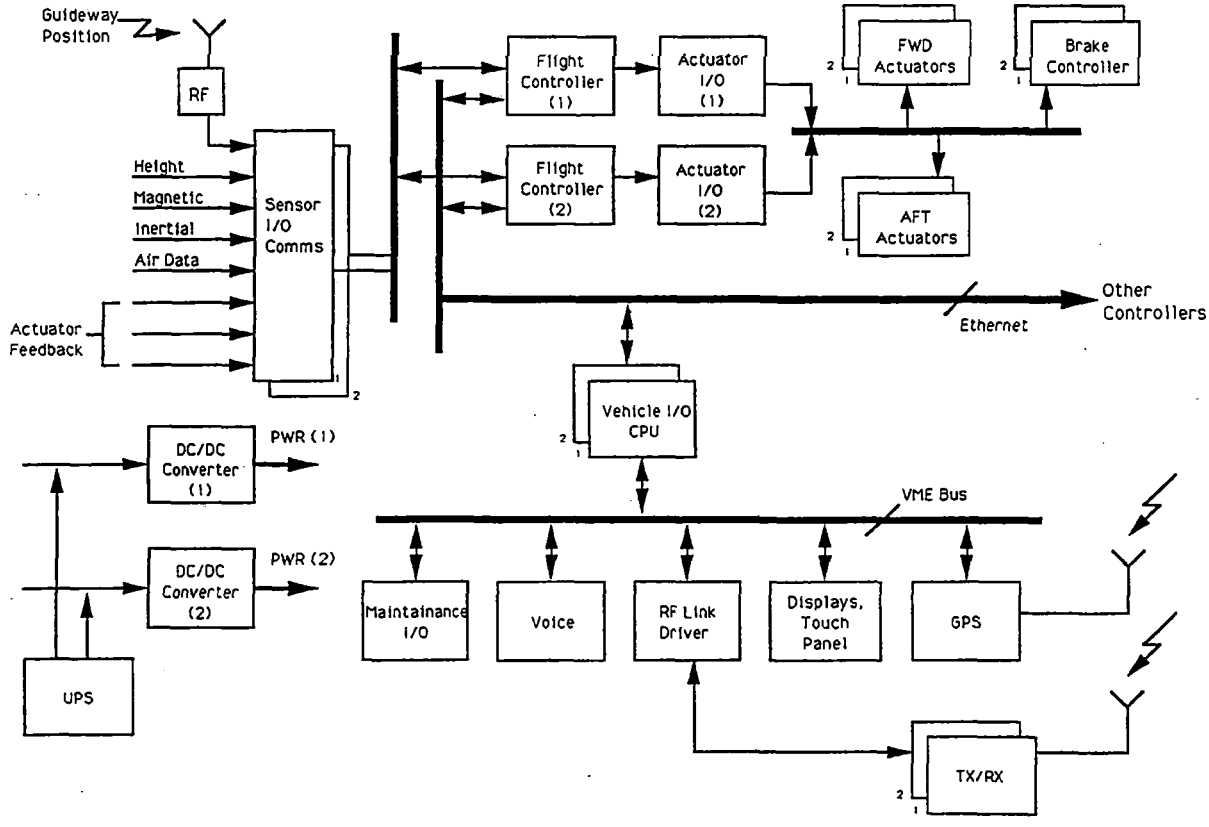

Figure 104 IFPC interface block diagram

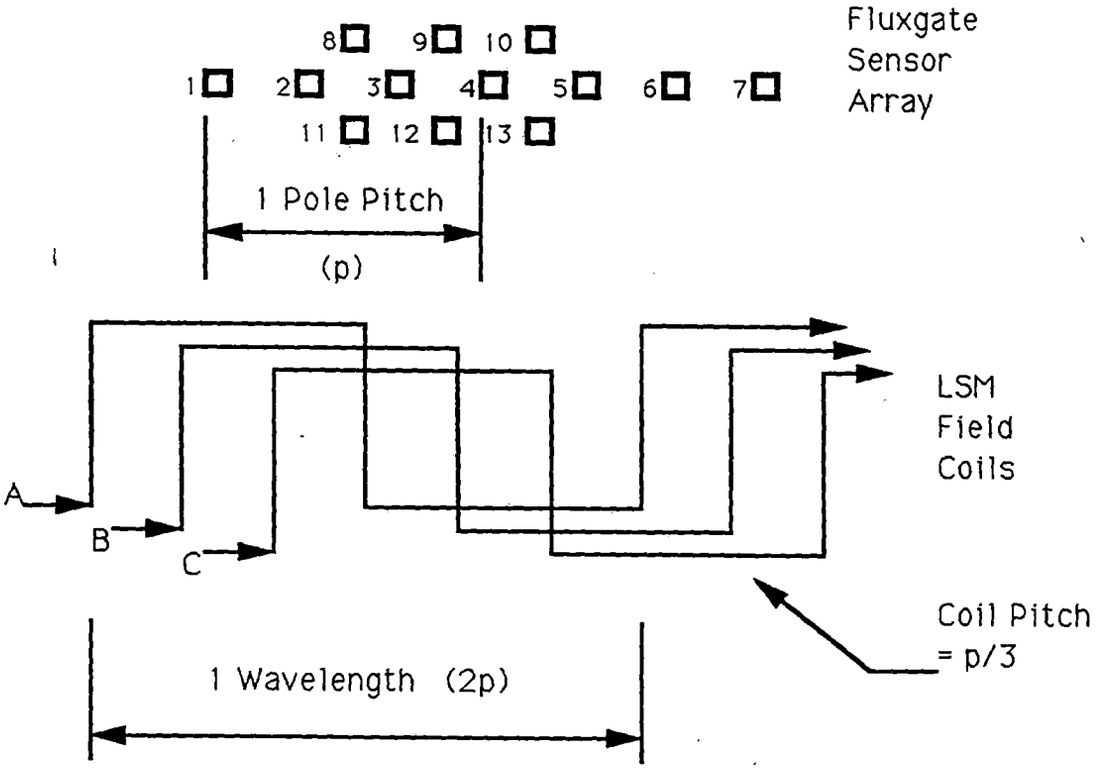

Figure 105 Fluxgate sensor array diagram

3.2.1.k.5. VEHICLE-TO-MAGWAY HEIGHT DETECTION

In addition to magnetic field strength measurements, the distance between the Magneplane and the magway must be acquired. This will be accurately performed by a sensor that uses an optical scheme to triangulate a pulsating photolight source transmitted from the vehicle to the magway.

The sensor provides a infrared light pulse at a repetition rate of 20 kHz which illuminates a field covering 5 to 7 mm. The pulse is reflected into a lens system on the vehicle and focused onto a photo-detector. The detector produces a current depending on the light's intensity and position to the center of focus. The signal is processed by the electronics which produces an linear analog output as a function of the height between the sensor and the surface (25 mV/mm). The measuring range for this device is specified at $\pm$ 125 millimeters with at an offset distance of 400 millimeters. The linearity performance is less than 1 percent.

The device will automatically adjust itself to the reflected light intensity. So, only some amount of reflectivity is required on surfaces to perform measurements. The levitation plates will be used for this purpose. Any transient light intensities, such as those experienced in the transition into or out of tunnels, do not effect the sensor performance. The sensor receiving element has a peak response tuned to that of its internal light source and is insensitive to the relatively low ambient light content at the internal light source wavelength. Sensor signal jitter is filtered by electronics which provide a detector bandwidth of 30 Hz.

This sensor is a commercial product that has been used in other high speed applications up to 250 miles per hour, which represents the limit for today's surface vehicles. The manufacturer is confident about operating the device beyond this speed and indicates that adjustments to the design to achieve higher performance will be straightforward.

Six (6) height sensors will be used to perform the height measurements. Three sensors will be mounted along the vehicle on each of the right and the left sides. This will provide coverage of the vehicle regardless of the misalignment from the center of the magway coils. Data from all six sensors is shared by both channels of the FPCS. The redundancy provided insures a gradual degradation in data if one or more of the sensors fail during flight.

3.2.1.k.6. POSITION/VELOCITY MEASUREMENTS

The primary method for detecting the velocity and position of the magneplane along the magway will employ the use of RF markers placed along the magway. The Magneplane implements RF receivers so that the unique marker codes can be captured and processed as the vehicle passes a transmitter which continuously emits a code. The transmitters are spaced eleven (11) meters apart and emit a unique code to represent the position along the magway. Peak detection will be used to determine when a marker is passed. The velocity will be derived by computing the frequency at which the markers are passed.

To receive the code, two receivers will be mounted on the magneplane near or at the center line height of the vehicle. The position of the receivers will insure detection over a 45 degree orientation of the magneplane along the magway. The second receiver provides a fail-safe operation for the function.

One of the benefits of this approach is that it allows operation throughout various environmental conditions. Passive detection schemes which depend on visual recognition of light/dark patterns can become defective from environmental conditions and general wear.

3.2.1.k.7. PROPULSION LOOP PROCESSING

The input processing of the flight controller integrates sensors of each type and produces results that are crosschecked for expected and reliable operation based on the vehicle's current status. The reliability of the data provided by a sensor is assessed by verifying it against other data acquired both temporally and spatially from other sensors. This provides measurement coverage for various orientations of the vehicle for achieving the required performance. It also permits failed sensors to be taken off-line to prevent continued corruption.

The communications between the vehicles and the wayside control processors is achieved with an RF link which accommodates the transmission of the vehicle's propulsion commands, the vehicles position and velocity along the magway, and the voice communications between the vehicle and the wayside. The position and velocity data will be provided at a sample rate of 12 Hz. Voice communications will be provided with a 3.5 kHz bandwidth, consistent with modern telecommunications standards.

Negotiating a turn-off is considered no different from a coordinated curve, hence it has no impact on the propulsion control activities implemented by the FC.

For arrival sequences, the controller will reduce the velocity of the vehicle until the landing gear can be employed. Braking activities are performed by the FC using the Braking Controller. The function of the Brake Controller is to provide control of the landing gear in order to obtain controlled vehicle deceleration. For the normal braking mode, deceleration is obtained through use of the propulsive magnetic fields, essentially by creating a negative thrust through the magway/wayside control loop. The Brake Controller is also capable of providing independent braking control for both forward and rear landing gears. Both modes are dependent on information from the Flight Path Control Set (FPCS). The Brake Controller interfaces with the FPCS via a digital bus. Failure monitoring for the FC employs monitoring of the brake control servos, both speed sensors, input power and autobrake. Also, a completely separate emergency braking system is provided through the extension of the emergency skids. The emergency braking system is a direct two-state system, and no linear control is employed to stabilize the emergency brakes.

3.2.1.k.8. STABILIZATION CONTROL ACTIVITIES

The Magneplane's ride quality depends on two factors. The first one defines how well the vehicle can be controlled with respect to the correct roll angle in the magway, and the second one establishes how

well inertial disturbances can be dampened by the vehicle. For stabilization, the aerodynamic control features of the Magneplane are used. These features are implemented as part of the IFPC. This includes the inertial sensors, the air sensors (velocity, pressure, and direction), the FC's, and the surface actuators, which interface with the controlled surfaces. The Magneplane design is naturally stable, but underdamped. The vehicle will inherently adopt a centered and coordinated position in the magway, rolling to align in curved sections when traversing at the (curve) design speed, and returning to an upright position in straight sections. The vehicle shape, center-of-gravity, moment of roll and interaction with the magway are all designed to provide this stability. Perturbations due to acceleration, wind gusting, magnetic keel and magway misalignment will result in a decaying oscillatory motion, which is undesirable for passenger comfort. These perturbations can occur more frequently than they can be dissipated unless an active control scheme is incorporated.

When the vehicle is in flight, aerodynamic stabilization is performed by the FC for controlling roll through the magway turns and switches. These maneuvers are coordinated by the FC which utilizes route information cross-referenced by the vehicles known position on the magway. In this way, the vehicle attitude can be modified prior to entering a switch or curve, thus maintaining its optimal trajectory for the maneuver. Stabilization is also used for controlling the vehicle from external disturbances, such as those caused by wind velocities and imbalances of levitation forces on curved sections. The role of the stabilization control function is to null out any tendency that would cause the Magneplane not to follow its assigned profile.

3.2.1.k.9. INERTIAL MEASUREMENTS

Acceleration disturbances will be measured using linear accelerometers which compose an Acceleration Sensor Assembly (ASA) using three orthogonal sensors. Each channel of the FPCS receive a normal lateral acceleration sensor signal from one (1) of two (2) identical dual ASA's. Each of the dual ASA's will be located in the Fwd and Aft of the vehicle and displaced about the horizontal center line of the vehicle. The instruments are DC powered by the appropriate FC channel to maintain continued operation through periods of transient or emergency operation. The ASA's are fully developed operational units currently in use in production aircraft.

3.2.1.k.10. AIR/PRESSURE MEASUREMENTS

Directional sensors will include Angle-of-Attack (AOA) sensors, for both pitch and yaw, and pressure sensors. Each FPCS channel interfaces with one AOA transducer input for each of the axes. This provides independent data to the primary and shadow FCs to permit sensor data verification to be implemented.

Static and dynamic air pressure sensors are maintained by the Air Data Sensor Assembly (ADSA). The ADSA is a dual unit which supplies signals to the FPCS primary channel. These signals are then supplied to the internal FC cross channel data link to the shadow FC element. They are used within the FC along with the AOA signals to derive differential air speed, from which the vehicle velocity can be

established. The ADSA is DC powered by the corresponding FC channel as with the ASA's described in section 3.2.1.k.9.

3.2.1.k.12. STABILIZATION LOOP PROCESSING

Input data from the inertial instruments and the air/pressure sensors will be processed similarly as described for the magnetic field strength measurements and the vehicle-to-magway height measurements. All inertial measurements will be filtered and used to extract the six inertial moments of the vehicle; thrust, pitch, heave, roll, sway and yaw. The results, along with the air/pressure measurements, the vehicle's profile commands, and the magway curvature computations, will be used by the FCs control laws. These laws use six (6) degrees-of-freedom to provide directional and lateral control for various maneuvers required by the Magneplane. Similarly, as in traditional aircraft applications, for example, coordinated turns require roll control of the vehicle. However, adverse yaw effects may be induced which require rudder deflection in the direction of the roll. The FC control routines will also be used to null disturbances that would cause pitch, roll, yaw, sway, heave or thrust. The results of these computations will command the actuators of the various surface control devices (stabilators, elevons, rudder and canard). The actuators are arranged in a duplex configuration to drive each of these assemblies. Each actuator within a duplex is driven by separate channels of the FC across a digital interface. The duplex arrangement will provide the required fault coverage for these assemblies (Fail-safe). Although the stabilization scheme has much similarity in concept with aircraft, the natural confinement of the magway, the limited suspension forces of the levitation scheme and the specific placement of the control surfaces fore and aft of the vehicle yields a unique set of control laws (see section 3.2.2.g).

3.2.1.k.13. POWER CONDITIONING REQUIREMENTS

Power for each FPCS is supplied from two different buses. Both buses are tied together during normal electrical system operation through a current limiting device. An Uninterruptable Power Source (UPS) is included to provide emergency and transient suppression power to the FPCS. The transient suppression feature provides power to the FPCS via two dedicated bus channels to each FC. Emergency power is supplied to each FC as required, by automatic switching of UPS which is capable of sustaining FPCS operation for a minimum of 120 minutes.

3.2.1.k.14. ENVIRONMENTAL PROVISIONS

The vehicle will house separate and independent controllers to maintain the environmental conditions in the vehicle. This includes meeting requirements for air-conditioning, heat, overall lighting, local audio communications, and internal sensors/ actuators for passenger doors as well as local lighting. Environmental data will be collected and stored into the flight recorder.

3.2.1.k.14.1. DE-ICING AND ANTI-ICING PROVISIONS

State-of-the-art de-icing equipment will be used to automatically sense and correct any icing conditions on external aerodynamic surfaces of the vehicle. The system combines unique features for detection and elimination. Detection is accomplished using ultrasonic sensors whose resonance changes as ice forms on the exposed probes, the change in resonant frequency being detected by the control electronics. The actual de-icing mechanism is based on pneumatic inflation/deflation of flexible membranes on the leading edge of the control surfaces. Inflation pressure requirements for this type of scheme are low, in the range of 0.5 to 1 PSI. Similarly, the power requirements to operate the system are negligible since power is tapped from the compressor in the braking system. Under normal conditions, pressure loss in the braking system is compensated by action of the compressor. It is estimated that the operating power requirements for the entire de-icing system is equivalent to the small losses observed in the high pressure braking system. Once the vehicle has been placed in service, the continued operation of the de-icing elements provides an efficient anti-icing scheme that prevents ice build-up on the control surfaces while the vehicle is in motion or stationary.

3.2.1.k.15. DATA/AUDIO COMMUNICATIONS

Information will be shared among the various processors through a two-way digital interface bus tailored to the ARINC 629 standard. This is one of the most recent standards being implemented on commercial aircraft. The bus is specified to operate at a 2 Mhz bit rate using a fibre-optic data link.

The communications between the vehicles and the wayside control processors is an RF link which accommodates the transmission of the vehicle's position along the magway, velocity, LSM commands and voice communications. Voice information is routed directly to the Global control centers over the FDDI Wayside to Global voice and data links. The position and velocity data will be provided at a sample rate of 96 Hz whereas voice communications will be provided with a bandlimit of 3.5 kHz. Packet switching will be used to accommodate the RF coverage overlap for nearby wayside control processor transmissions such that LSM field synchronization can be accomplished for magway block transitions.

For the IFPS, redundant serial busses tailored to the ARINC 629 interface standard will be used for interfacing vehicle sensors and actuators to the FC's. Again, fibre-optic data links will provide the connections. For the interface between the FC and the surface actuators, the intention is to retain a bidirectional digital structure for command and feedback signals. All necessary D/A and A/D conversions shall be accommodated by the actuator interface electronics. This configuration eliminates the need to distribute sensitive analog control signals from the FC'c to the actuators.

3.2.1.k.16. GLOBAL POSITIONING SYSTEM (GPS).

Each vehicle incorporates a GPS receiver to provide both the vehicle and Global Control Center with vehicle position data during a system "Wake-up" or restart. Vehicles located in areas where GPS satellite coverage is not available (Tunnels etc.) will make a coordinated restart in conjunction with the wayside control processor which will move the vehicle toward the next block boundary at low speed. A transition

into the adjacent block provides the necessary position initialization for correct on-board systems operation. The GPS time reference data is also used for synchronizing LSM drive level commands issued by the vehicle to the wayside units.

3.2.1.k.17. TEST PROVISIONS

The FPCS will contain a comprehensive Built-In-Test (BIT), which consists of Periodic BIT (PBIT) and a manually Initiated BIT (IBIT). PBIT operates continuously whenever the FPCS is operating. It performs computer self-test and collects failure data from hardware and software monitors. PBIT sets the necessary cautions and warnings for display to the vehicle operator and central control and also collects status and maintenance codes for problem analysis and maintenance. Sufficient data ia contained in the status information to enable alternate route planning.

IBIT has a number of submodes: Preflight BIT, Dial-A-BIT, and special operator intervention submodes. Preflight BIT is used to determine that the IFPC system is mission ready by means of an end-to-end check of sensors, computers, and actuators. Dial-A-BIT is used to facilitate maintenance. The operator can select specific tests, single step through a test, or auto stop-on-failure.

Brake Controller (BC) BIT testing is not under the control of the FPCS and occurs with application of electrical power. The status is reported to the operator and Global Control via the FPCS.

3.2.1.k.18. EMERGENCY OPERATIONS

Ultimately, in the event of unforeseen failures within the transit system, it is critical that the Magneplane operates in a manner that maximizes the safety of the passengers. A more detailed appraisal of potential hazards to the vehicle is given in section 5.3.10. Global failures could affect such functions as vehicle-to-wayside control communications or LSM propulsion. These failures require emergency procedures that affect multiple vehicles over a wide area and utilize the coordinated response of adjacent Global centers. Likewise, certain failures within the vehicle may require safety measures that affect not only it, but other vehicles controlled by neighboring wayside control processors. In either case, the action taken by the system, wayside or vehicle elements should be a coordinated response that minimizes the impact the existing hazard without introducing additional dangers.

Communication failure with the wayside control processor will result in the vehicle not receiving velocity command at the anticipated 12 Hz rate. If the vehicle determines that a number of successive commands have not been received then it will automatically initiate a braking maneuver and stop. A vehicle will traverse less than 50 meters in the time required to determine four successive commands have been missed. As the wayside control processor and Global center are also aware that communications to a vehicle has failed, automatic procedures can be instigated to stop downstream traffic, anticipating that the affected vehicle will automatically deploy its brakes.

Gross propulsion failures due to LSM or vehicle failure will also require braking procedures to be invoked for coordinated stopping of the vehicle. The vehicle will broadcast such a failing to the wayside control processor across the RF link, so that appropriate coordinated action at a Global level is instigated.

Another situation may include the loss of the Magneplane's control over its surfaces. Emergency procedures would require that the vehicle operate at reduced speeds until it is within a safety envelope. Likewise, certain gross sensor failures may require the vehicle to operate at reduce speeds while using other sensors to interpolate for the missing sensors. For example, height detectors would be used to measure pitch and roll with some degraded accuracy. The profile data that was stored in the FC would be used in conjunction with the height measurements along the magway to interpolate the vehicle's inertial attitude. If the circumstances did not allow any of these approaches, emergency braking procedures would be used.

General power failures on the vehicle will be managed by switching over to the backup power system which has sufficient reserve to allow time for the vehicle to continue to its intended destination or an earlier exit, as determined by the Global controller.

In general, many safety and emergency features will be employed. The goal of all control functions performed by the Magneplane is to insure passenger safety regardless of circumstance.

3.2.1.k.19. VEHICLE ATTENDANT

It is anticipated that an attendant will be on-board every vehicle in transit. The prime responsibility of the attendant will be to insure passenger comfort, and notify/monitor the passengers to insure that they are seated and belted when required. The attendant has access to a display unit which provides a summary status of the vehicle operations, and any data/messages received across the RF link from the wayside control processor. This permits Global updates (via wayside), so that passengers can be kept updated on arrival time, weather conditions etc. Keyboard communications augmented with voice communications will be available across the RF link. The keyboard communications will be limited to reporting status of the vehicle/magway/passengers. The presence of an attendant insures that any passenger problems (illness etc) can be addressed in an appropriate manner, and any impending problems (local weather, excessive perturbations on a stretch of magway etc) can be reported in a timely manner.

The attendant has no control of the vehicle, other than requesting velocity or route changes via the RF communications in an abnormal event, to the wayside. The Global center will coordinate such changes in a safe manner, with human intervention to initiate the change in the scheduling, implemented by the Global center control system on all affected vehicles.

3.2.1.el. VEHICLE/VEHICLE DYNAMIC INTERACTIONS

In the Magneplane system, vehicles are not coupled. They do not normally fly on the same electrical block, so there are no vehicle\vehicle dynamic interactions.

For justification of vehicle/consist capacity, see section 5.3.2.3.

3.2.2. SYSTEM DESCRIPTION - MAGWAY

CONTENTS

FIGURES

3.2.2.a. CIVIL CONSTRUCTION

3.2.2.a.1. GENERAL

The magway consists of the magway trough and its supporting structure. See Figure 1. The magway trough is composed of two levitation plate box beams and a LSM winding as described in Section 3.2.2.b. Depending on the depth of the box beams, the trough is able to span up to 15 m (49 ft) between vertical supports as shown in Figure 2. If it is required that the distance between vertical supports exceed 15 m, the magway trough is supported by a horizontal structure that spans between vertical supports. Where it is required, the horizontal structure consists of a steel truss or concrete box beam which supports the magway trough at 4.57 m (15 ft) intervals. The depth of the aluminum box beams spanning 4.57 m is 0.41 m (16"). This depth increases to 0.8128 m (32") for a 9.14 m (30 ft) span.

The vertical supports are columns or piers that have crossbeams to support the trough or the spanning structure and are described in Section 3.2.2.a.4. The piers in turn are supported on concrete foundations as discussed in Section 3.2.2.a.5. Section 3.2.2.a.3. describes the spanning structure. The design criteria is given in the following section:

3.2.2.a.2. DESIGN CRITERIA

The civil structure (including the magway trough) is designed to meet the minimum requirement (MR) of a 50-year life. The entire structural system is also specifically designed for the following loading combinations:

$$D$$
$$D+S$$
$$D+L$$
$$D \pm W$$
$$D \pm E$$
$$\pm E_L$$
$$(D+L \pm E_v)x75\%$$
$$(D+L \pm E_L)x75\%$$
$$(D+L \pm B)x75\%$$
$$D+L \pm [(\frac{30}{85})^2 W + W_v]$$

Where,

D= Dead load includes weight of magway and structure and a 100 plf utility load

L= Moving live load due to vehicle (Includes impact)

S= Snow load of 40 psf on the horizontal projection of the magway and supporting structure

W= Design wind load against the structure. This load was calculated in accordance with input from the COE using ASCE 7-88 with a basic wind speed of 38 m/s (85 mph) and an importance factor of 1.10

W_V= 30 mph steady state wind load against the vehicle, 50 mph gust, with the vehicle traveling at design speed

E_t= Transverse earthquake based on Seismic Zone 2

E_L= Longitudinal earthquake based on Seismic Zone 2

B= Breaking force from vehicle = 0.65 g

The above loading combinations are consistent with U.S. Building Code requirements. The AASHTO bridge specification requirements have also been reviewed, however, they are not considered to be 100% applicable to maglev magways since, for example, Magneplane vehicle live loads are more predictable than highway live loads. As such, they should not require the same factors of safety.

In addition, the magway structure is designed for a delta T of 83°C (150°F) which is consistent with U.S. highway and railroad bridge criteria. The magway trough is designed to accommodate up to a 157°C (284°F) temperature delta (see Section 3.2.2.c.). The following additional requirements have been established by the system dynamic analysis in order to meet ride quality guidelines:

- The design natural frequency in hertz shall be greater than 160/L, where L is the span in meters
- The dynamic live load deflection shall not exceed L/2000 or 0.02 . (0.8")

3.2.2.a.3. SPANS

Several materials and many configurations were considered for the supporting structure spanning between columns. These options are discussed in Section 5.3.2.23. That section also discusses the preliminary screening and the results.

The optimum structural system for both at grade and elevated magways was found to consist of the aluminum box beams spanning between vertical supports. The at grade and elevated magways are shown in Figure 2 and Figure 3. When it is required to span distances longer than 15 m (49 ft), it is cost effective to provide a horizontal steel truss to support the magway. Concrete beams were also considered for this purpose but were found in this study to be more costly than the steel truss system. It is recommended, however, that designs for both steel and concrete supporting members be considered in the future as the relative costs of steel and concrete can change based on local situations and market conditions. Highway bridge designers traditionally provide both options to encourage competitions

between the two industries. The trade studies relating to the selection of these structural systems are presented in Sections 5.3.2.25. and 5.3.2.26.

The calculations included a dynamic analysis that indicate the dynamic load factor for the nominal span to be approximately 1.20. Allowable stress levels were based on fatigue considerations as required by applicable codes. The restriction on the natural frequency and live load deflection generally controlled the design of the spanning members. The present design for the steel truss or concrete beam members assumes simple spans between supports.

3.2.2.a.4. COLUMNS OR PIERS

The columns or piers have caps or crossbeams that support the ends of the spanning members. As noted in Section 3.2.2.c., which follows, the bearing pads at the ends of the spanning members shall be designed to provide 0.04 m (1.5") of adjustment to allow compensation for foundation settlement. The support columns have been estimated for the purpose of providing preliminary dead loads and costs for input to the tradeoff study in Section 5.3.2.23.. For the selected optimum spans a more detailed design was done which refined the sizing to efficiently and adequately support the magway structure under all loading conditions. The design shall be aesthetically pleasing and where practical be designed for a minimum footprint such as would be required in the median strip of an urban or suburban interstate highway. The present design of hexagonal columns and rectangular piers and their caps or crossbeams configured to support various structural systems are shown in Figure 4, Figure 5 and Figure 6.

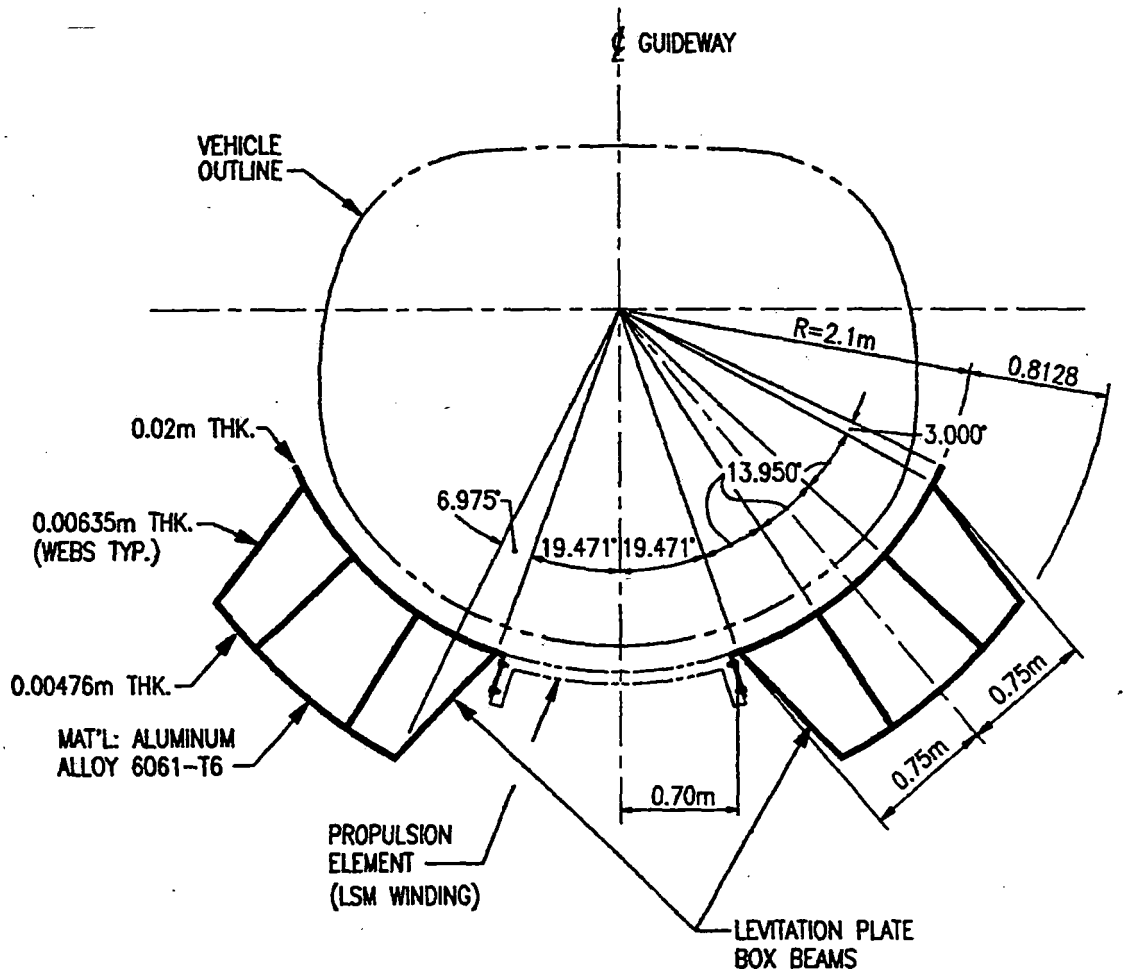

Figure 1 Magway trough

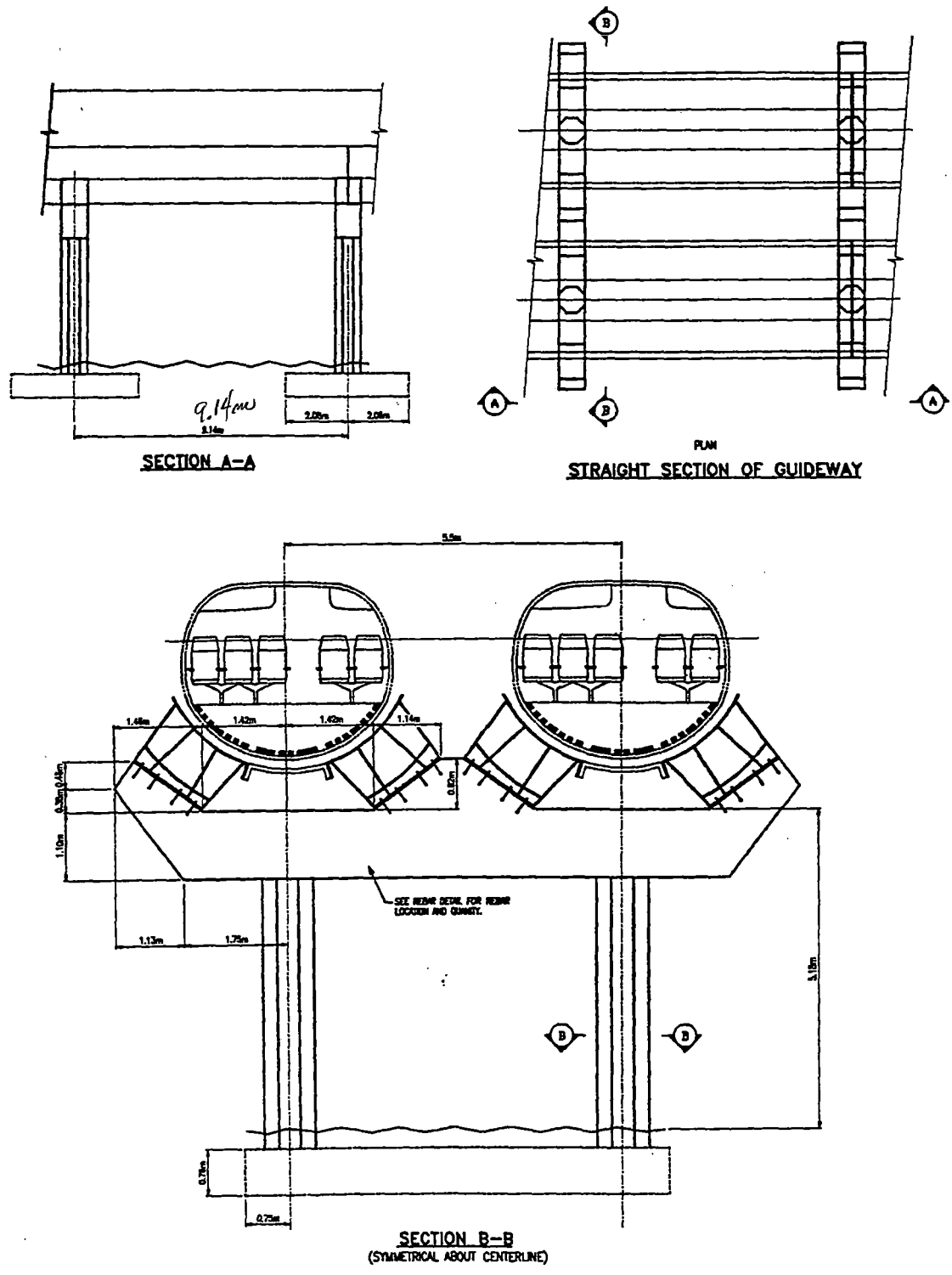

Figure 2 Elevated aluminum double magway

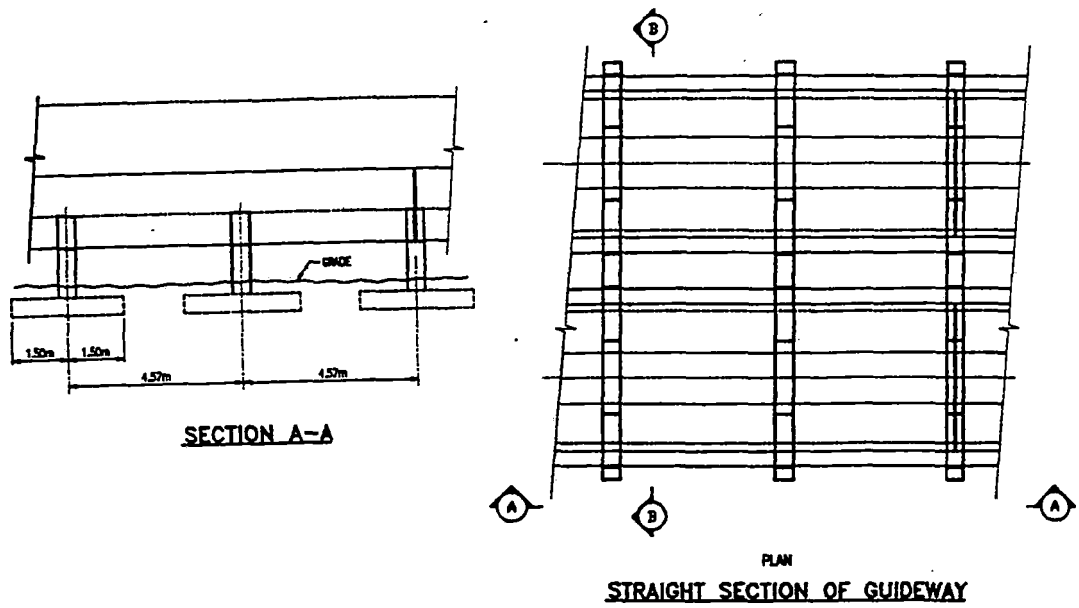

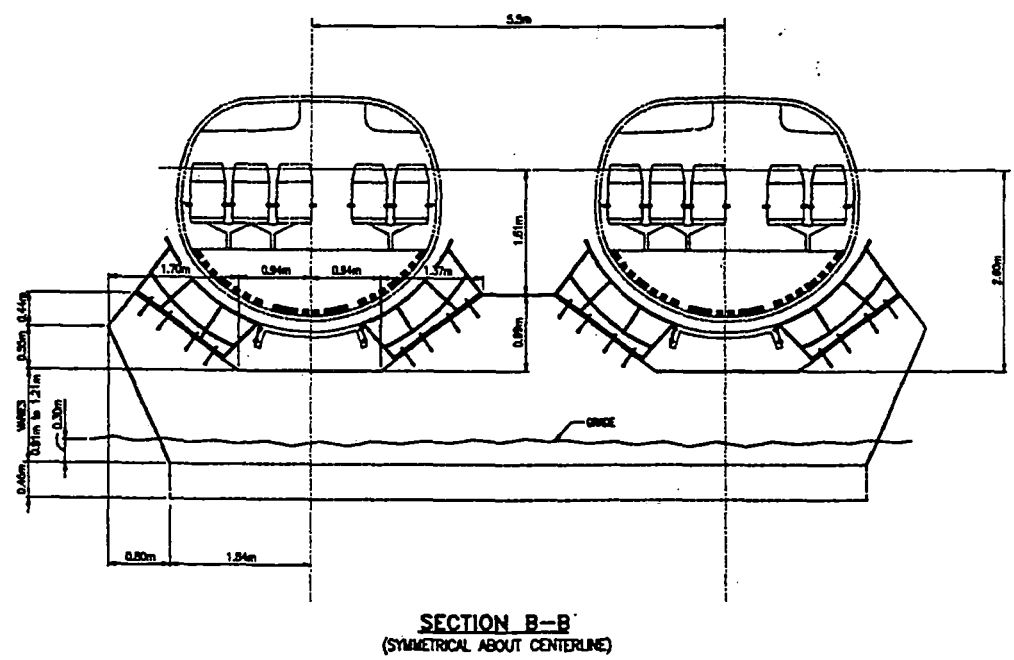

Figure 3 Aluminum double magway at grade

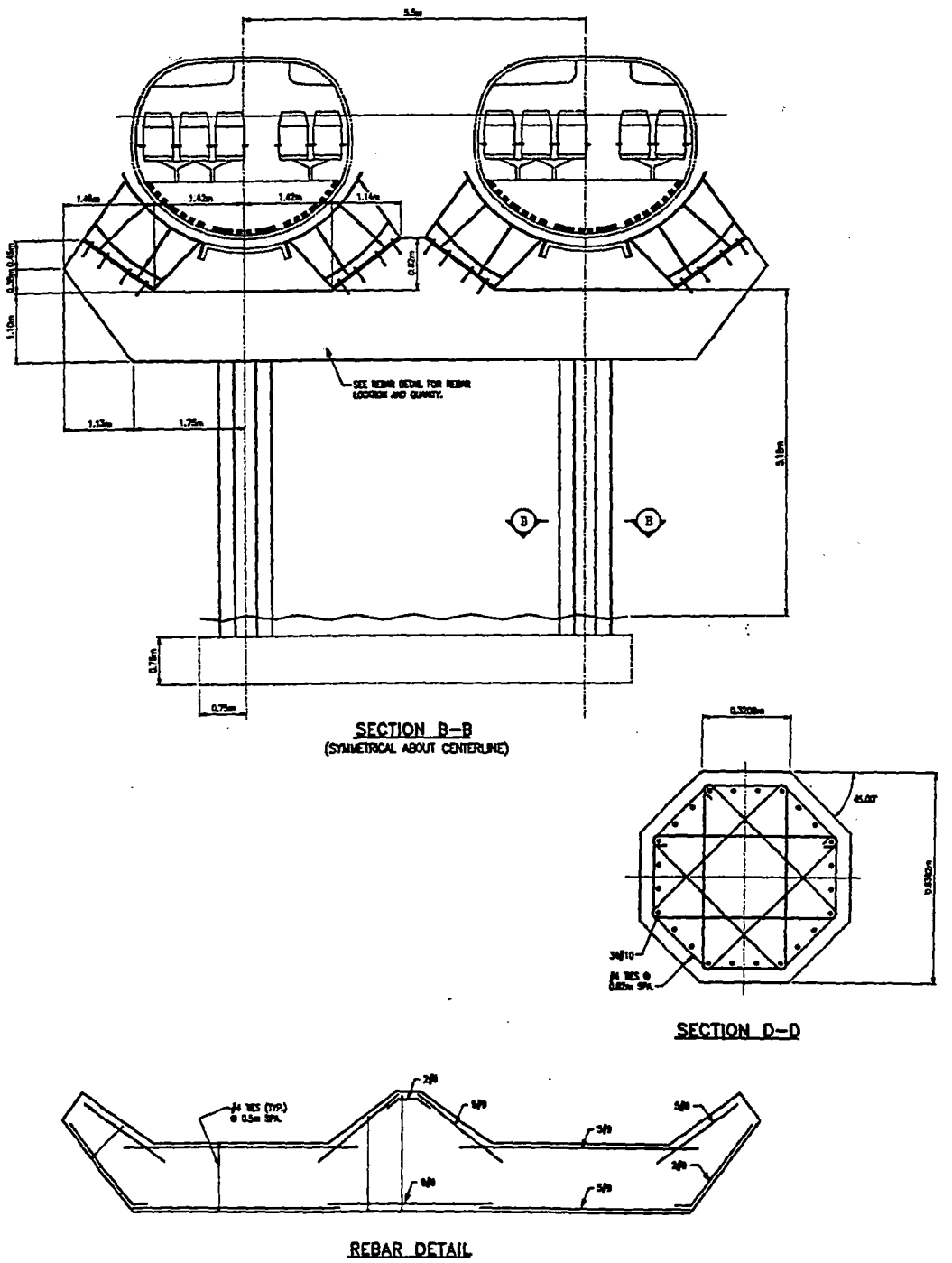

Figure 4 Concrete crossbeam and columns supporting an aluminum magway

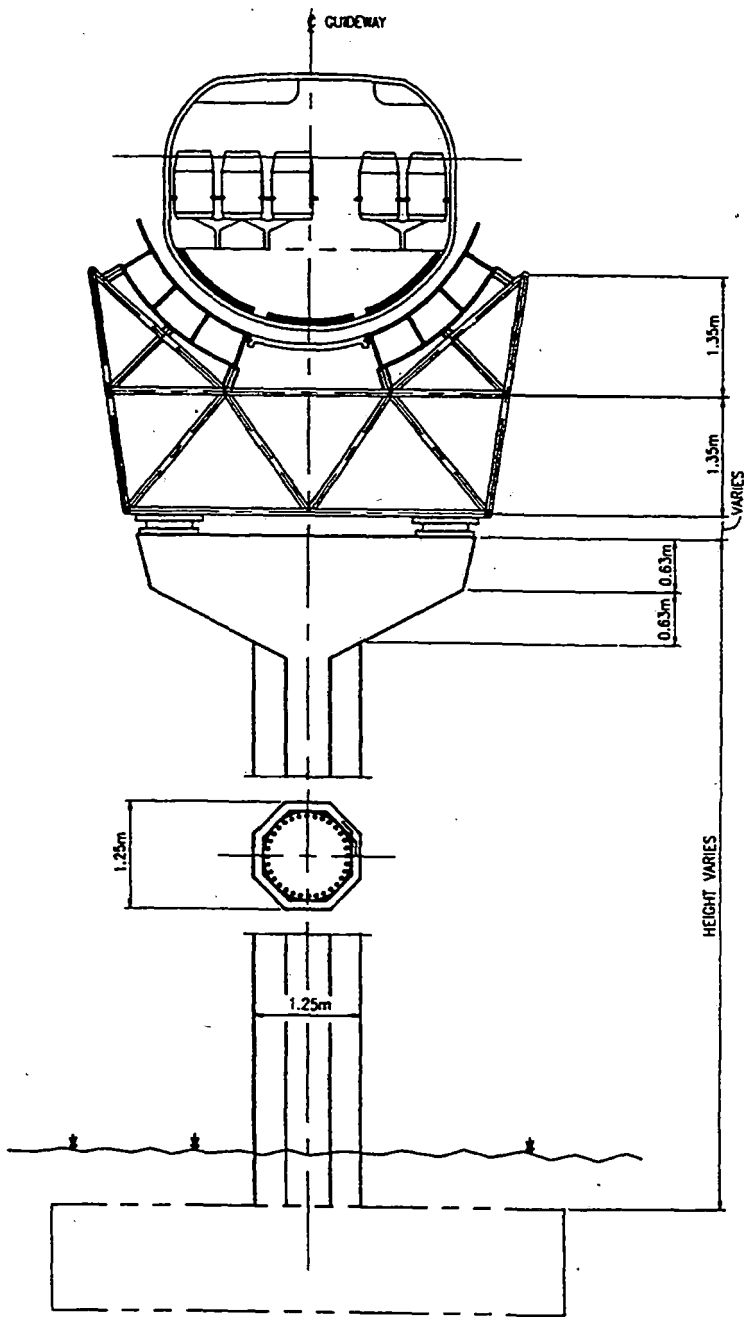

Figure 5 Concrete crossbeam and columns supporting an aluminum magway

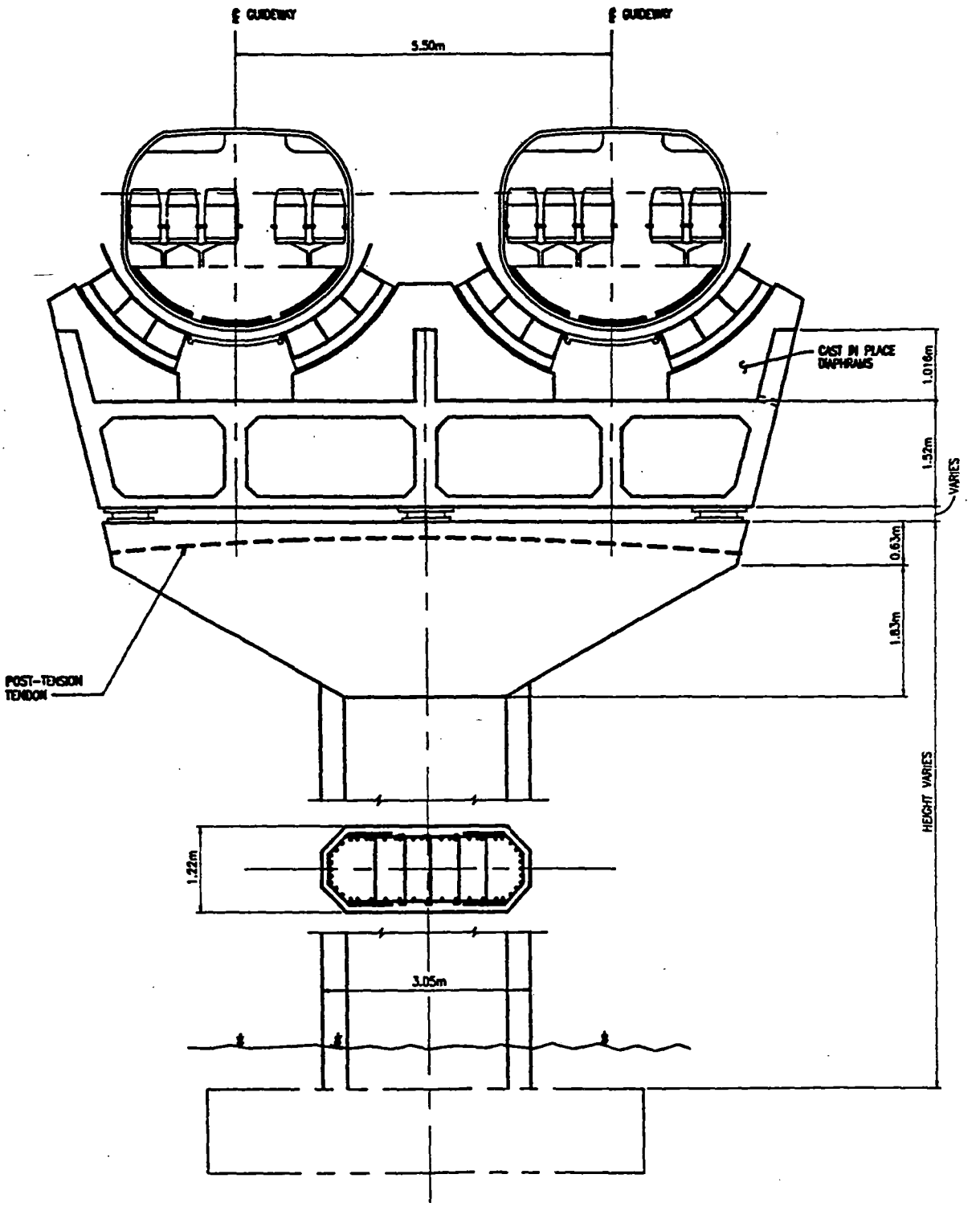

Figure 6 Column support for a double concrete box beam

3.2.2.a.5. MAGWAY FOUNDATIONS

Trade studies for various foundation types and sizes, including piles and spread footings, were completed by Bromwell & Carrier, Inc. (BCI). Foundations selected for the Magneplane magway will vary in size, type, and cost, depending on the following criteria:

- *Static and dynamic loading of the structure*
- *Soil or rock type encountered*
- *Variability of soil with depth and area*
- *Soil strength and compressibility*
- *Environmental constraints*

For purposes of this report, foundations were designed assuming static and dynamic loading information supplied by others of the MI team, a soil with uniform conditions as described below, and no major environmental constraints. These parameters are described in detail in the following sections. Spread footings were analyzed for bearing capacity, sliding, and settlement. Deep foundations were analyzed for both axial and lateral capacity.

3.2.2.a.5.1. LOAD CRITERIA

Foundation loads were determined for a variety of different cases during trade studies conducted by the structural engineers. Figure 8 shows a typical footing and column detail, which describes the direction convention and the various loading cases used in these analyses. Axial loadings consisted of the column, the contributory weight of the magway, utilities and ancillary components, snow, and the weight of the vehicle. Lateral loads and moments were induced at the footing by seismic, wind on the magway and vehicle, and emergency braking forces. An analysis was completed for each loading combination shown in Figure 8.

For a given magway type, span length, and column height, each of 10 load combinations were analyzed and a spread footing was sized for that load combination. Over 1000 load combinations were sized based on these parameters. Due to the eccentric loading conditions, each footing was initially designed to assure that the loading was within the kern (middle third) of the footing, and adjustments were made depending on the calculated minimum and maximum stresses on the soil beneath the footing. However, it was determined that for emergency loads, it is not necessary to keep the resultant in the kern. Footings were designed based on this assumption. Ultimately, the final size of the footing was chosen as the maximum dimensions of width and length based on the list of footings designed for each load condition, and rounded up to the nearest 0.1 m.

3.2.2.a.5.2. SOILS CRITERIA

Although trade studies could be completed to determine the best foundation type for each soil condition, this was not deemed appropriate for this report. Instead, uniform soil conditions similar to those presented by the Government for use in the Severe Segment Test were assumed, and trade studies were completed on various loading conditions.

Parameter	U.S. Units	S.I. Units
dry density	90 pcf	5.62 kg/m^3
total density	100 pcf	6.24 kg/m^3
angle of internal friction	29 deg.	29 deg.
cohesion	0 psf	0 kN/m^2
water table depth below footing	5 feet	1.5 m
SPT N value	10	10
allowable bearing pressure	3.0 ksf	150 kN/m^2
modulus of subgrade reaction	25 pci	6770 kN/m^3
modulus of subgrade reaction (saturated)	20 pci	5430 kN/m^3

Figure 7 Soil type parameters

In reality, varying soil conditions will exist, and will impact the selection of the appropriate foundation. For conditions which are environmentally sensitive, or for which conventional construction means are limited, the "end-on" construction may be employed to erect the Magneplane magways. The relationship between end-on construction, foundation installation, and cost is discussed in a later section of this report.

The soil type selected for analysis herein is a loose, slightly clayey sand. The detail parameters for the soil type are given in Figure 7.

It is noted that the allowable bearing pressure, above, is equal to the criteria given by the Government for the Severe Segment Test. Other parameters are correlated from the bearing pressure value.

3.2.2.a.5.3. FOUNDATION TYPE

Various foundation types considered in our preliminary trade studies as potentially appropriate to the Magneplane system include the following:

spread footings
drilled shafts (belled, straight)
driven piles
augercast piles
pullout anchors

pin piles
step-tapered piles
grout anchors in rock
in-place stabilization

Of these, augercast piles and pin piles were deemed to have limited capability to resist the high moments that are induced on the magway by wind and earthquake loadings. Pullout anchors and rock anchors could be used in conjunction with spread footings to take some percentage of the loads and thus reduce the size of the footing. In-place stabilization of poor soils may be the most cost effective way of improving soil conditions such that less conventional foundations are feasible for construction.

Detailed analyses of four foundation types - steel and prestressed concrete (PSC) piles, spread footings, and drilled shafts - are presented below. From these, the spread footing option was chosen for use in the cost and other trade studies on the Magneplane system, again to be consistent with the SST parameters.

3.2.2.a.5.4. SPREAD FOOTINGS

Spread footings which would support the Magneplane magway were designed and analyzed based on load and moment data obtained from UEC, Denver Colorado. A total of five different support structures were analyzed during trade studies.

Assumptions made for the analyses are listed below.

- The allowable bearing capacity of the soil is approximately 150 kN/m^2, or 3.0 ksf.
- The weight of the footing is neglected.
- The footing is rigid and the applied loads and moments are uniformly distributed throughout the foundation.
- Loads applied to the footing and footing dimensions are those shown in Figure 8. The bottom of the footing is at least 1 m below the ground surface to avoid frost penetration.
- Under normal loads (ie. dead loads, live loads, snow loads) the minimum soil pressure must be greater than or equal to zero, the maximum soil bearing pressure must be less than the allowable pressure and the resultant force must fall within the kern (middle 1/3 of the foundation base) as shown in Figure 9, Case 1.
- During transient loading conditions (ie. wind loads, emergency breaking loads, and earthquake loads) the resultant force is permitted to fall outside the kern.
- During transient loading conditions the minimum foundation bearing pressure may be less than or equal to zero providing that the maximum foundation bearing pressure does not exceed the maximum allowable bearing capacity as shown in Figure 9, Case 2 and Case 3.

The formula used to calculate the maximum and minimum loads exerted on the soil by the foundation is shown below.

$$q=\frac{Q}{A}\left[1\pm\frac{6e}{L}\pm\frac{6e}{B}\right]$$

where

q = load exerted on the soil
Q = summation of the forces in the vertical direction
e = eccentricity
L = footing length
B = footing base

Analyses of the typical magway section, i.e., the aluminum box beam double magway, with a span of 9.1 m and a height of 5.2 m, resulted in a footing base of 4.1 m and a footing length of 5.6 m. Footing sizes for other spans and magway heights for the aluminum box beam are shown in Figure 10. Footing sizes for the concrete pier single magway, concrete pier double magway, steel truss single magway, and steel truss double magway are shown in Figure 11, Figure 12, Figure 13, and Figure 14 respectively.

Immediate settlement was calculated from the Meyerhoff equation, using the assumptions listed above including the allowable net bearing capacity. The settlement was 0.025 m, which is the maximum allowable based on the preliminary Severe Segment Test criteria. A reasonable construction procedure would be to compact the soil before constructing the footings, which would increase the density of the foundation materials and decrease the amount of settlement which might occur.

3.2.2.a.5.5. PILE FOUNDATIONS

The pile foundations for the Magneplane magway were designed and analyzed using a static bearing capacity analysis computer program (SPT91) and a lateral capacity program (LPILE). These computer programs are commercially available. The pile foundations analyzed were 0.46 m square prestressed concrete (PSC) and 0.46 m diameter pipe piles.

Axial loadings consisted of the column, the contributory weight of the magway, utilities and ancillary components, snow, and the weight of the vehicle. Lateral loads and moments were induced at the footing by seismic, wind on the magway and vehicle, and emergency braking forces.

The design for the double aluminum box beam magway was analyzed using the braking load combination. This combination represented the highest load in the axial and lateral direction. The design for the steel single truss magway was analyzed using the braking and wind load combinations. The wind load combination was the controlling factor in the axial design of deep foundations. The braking load combination was the highest load based on the lateral analysis.

The axial column loads were equally distributed to a four pile group. The moment imposed on the column was distributed on the piles as an compressive or tensile axial load, depending on the magnitude of the moment. Figure 15 shows the distribution of the loads on the piles. The design was initiated by using the axial capacity vs. depth to determine the length of the pile assuming both skin friction and end bearing, along with appropriate safety factors. The next step was to determine the pile length required

for fixity against rotation/deflection based on the lateral load response. The final design of the pile length and size was determined by a comparison between the axial and lateral responses.

Figure 16 summarizes the results of the axial capacity analysis (SPT-91). The allowable pile capacity reached 1177 kN at 30.5 m depth for a 0.46 m square prestressed pile (PSC). The allowable capacity was 925 kN at 30.5 m for the pipe pile. Figure 17 and Figure 18 are examples of the lateral design response to the 5.2 m span aluminum box beam, on a 0.46 m square psc pile.

The axial capacity controlled the design of the double aluminum box beam and the steel single truss. For these two magway types, lateral fixity was achieved at a relatively shallow depth.

The final deep foundation configurations for various load conditions are listed in Figure 19. For each loading case, this table indicates the number, length, and diameter of piles/drilled shafts in the group.

3.2.2.a.5.6. DRILLED SHAFT FOUNDATIONS

Drilled shaft foundations for the Magneplane magway were designed and analyzed using a static bearing capacity analysis as outlined in the FHWA's *Drilled Shafts: Construction Procedures and Design Methods* (1988). Lateral capacity analyses were completed using the computer program LPILE (tm) which is commercially available. Drilled shaft diameters considered in our analyses ranged from 0.76 to 1.22 m.

The design for the double aluminum box beam magway was analyzed using the braking load combination. This combination represented the highest load in the axial and lateral direction. The design for the steel single truss magway was analyzed using the braking and wind load combinations. The wind load combination was the controlling factor in the axial design of the deep foundations. The braking load combination was the factor used in the lateral analysis.

The column loads were equally distributed to a four-shaft group. The moment imposed on the column was distributed on the piles as a compressive or tensile axial load, depending on the magnitude of the moment. Design consisted of determining the axial capacity vs. depth, including uplift capacity, and also determining the length of shaft required for fixity against rotation/deflection based on the lateral load response. A comparison between the two response curves was used to determine the length required to meet capacity.

Figure 20 summarizes the results of the axial capacity analyses for drilled shafts. The allowable/design capacities as shown are based on a factor of safety of 2.5.

Based on soil and loading conditions analyzed for this study, it was determined that 0.91 m is the optimum shaft diameter. The axial capacity controlled the design for the double aluminum box beam and the steel single truss span. The lateral fixity was achieved at a relatively shallow depth. The final drilled shaft dimensions for various load conditions are listed in Figure 19.

Given the lack of shallow competent rock or other suitable end bearing material within the subsurface profile used for this study, drilled shafts do not appear to be the most practical foundation alternative based on the hypothetical project conditions. Construction of drilled shafts within the soil profile used for this study would require the use of "wet-hole" techniques due to the shallow groundwater conditions and the generally loose somewhat sandy soil profile.

Among the conditions in which drilled shafts could be considered a cost-effective foundation alternative include loading conditions in which large uplift capacities or moments are possible. Also, shafts drilled into bedrock can carry very high loads which could eliminate the need for a "pile cap" since most loads can be carried on a single pier/shaft.

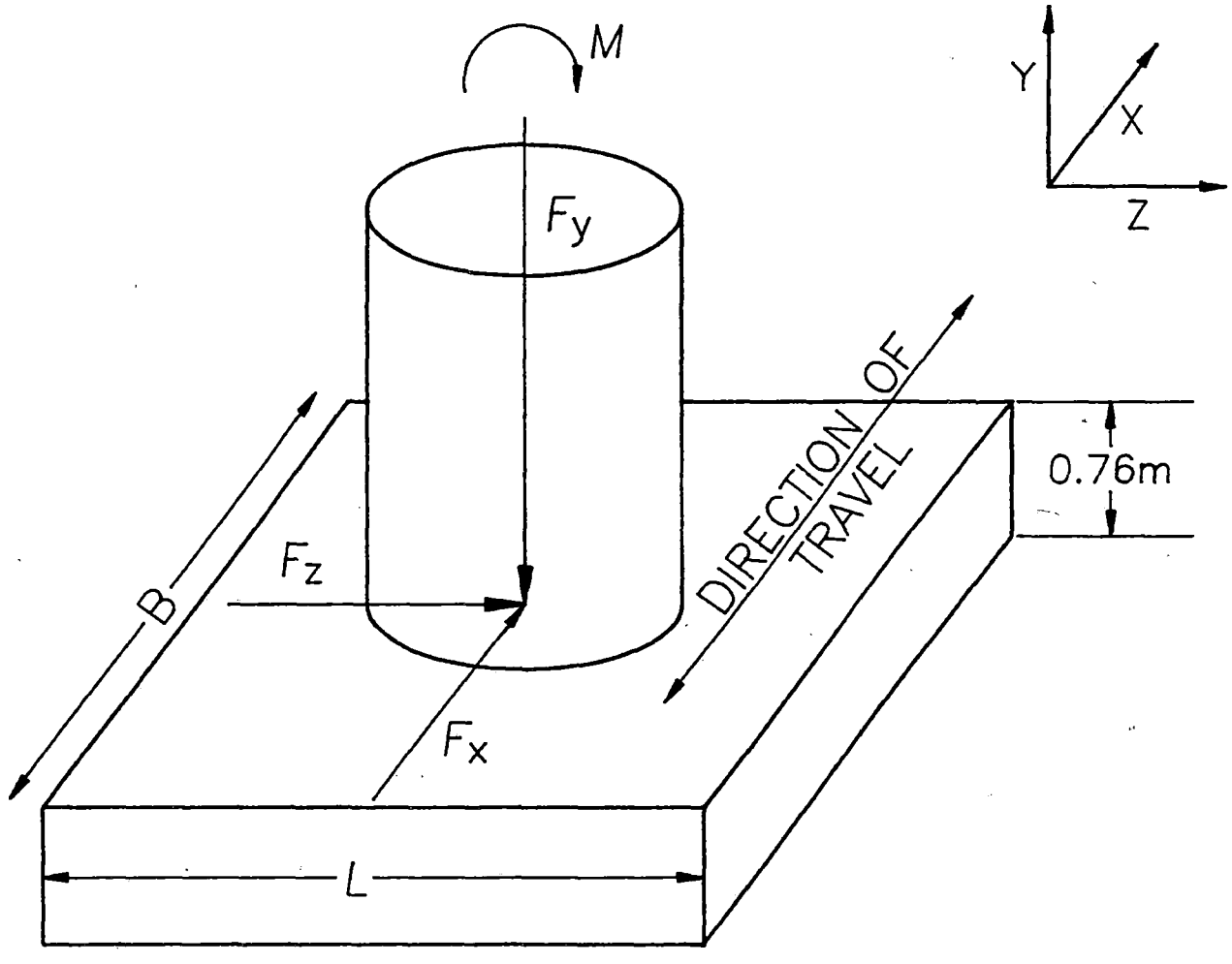

Figure 8 Magneplane foundation loading conventions

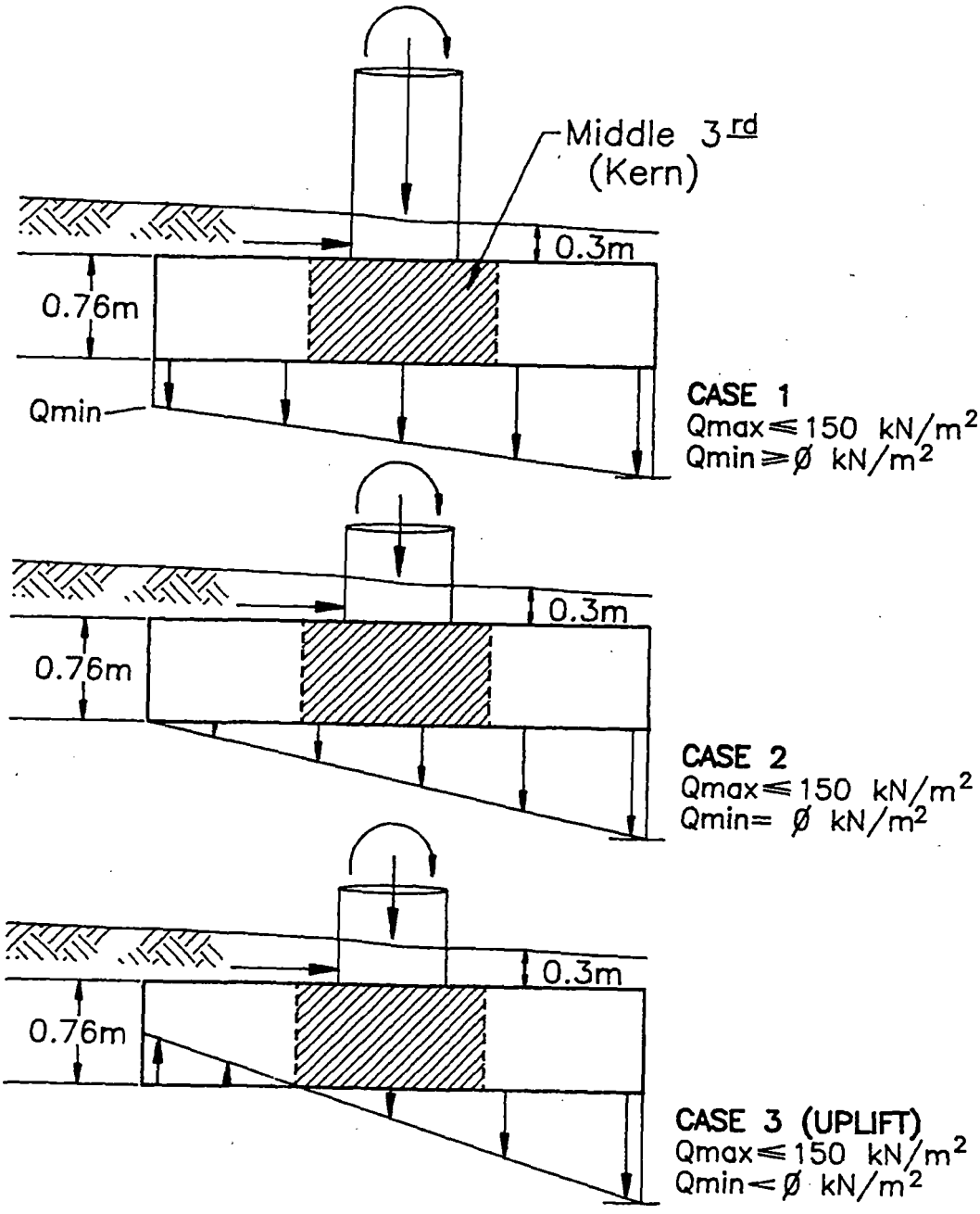

Figure 9 Magneplane footing load distributions

Guideway Span (m)	Guideway Height (m)	Foundation Base (m)	Foundation Length (m)	Excavation (m^3)	Form & Pour (m^3)	Backfill (m^3)
13.7	19.8	6.4	6.9	55.8	33.4	22.4
13.7	9.1	5.2	4.9	33.9	19.2	14.6
13.7	7.6	4.9	4.9	32.1	18.1	14.0
13.7	5.2	4.7	4.7	30.3	17.0	13.3
13.7	0.9	3.0	9.1	38.0	21.2	16.8
13.7	0.6	3.0	9.1	38.0	21.2	16.8
9.1	19.8	6.9	6.1	53.4	31.8	21.6
9.1	9.1	5.0	5.0	33.9	19.3	14.6
9.1	7.6	4.9	4.9	32.1	18.1	14.0
9.1	5.2	4.1	5.6	31.5	17.7	13.8
9.1	0.9	3.0	9.1	38.0	21.2	16.8
9.1	0.6	3.0	9.1	38.0	21.2	16.8
4.6	19.8	6.6	6.1	51.2	30.4	20.8
4.6	9.1	5.0	4.9	33.0	18.7	14.3
4.6	7.6	4.6	5.2	32.0	18.0	14.0
4.6	5.2	4.3	5.0	29.3	16.3	13.0
4.6	0.9	3.0	9.1	38.0	21.2	16.8
4.6	0.6	3.0	9.1	38.0	21.2	16.8
9.1	0.0	6.1	14.6	109.0	67.9	41.0

Figure 10 Footing spread summary - aluminum box beam double magway

Guideway Span (m)	Guideway Height (m)	Foundation Base (m)	Foundation Length (m)	Excavation (m^3)	Form & Pour (m^3)	Backfill (m^3)
33.5	19.8	11.1	11.1	146.8	94.3	52.6
36.6	9.1	9.0	9.0	98.3	61.6	36.7
36.6	7.6	8.7	8.7	92.1	57.5	34.7
36.6	5.2	8.2	8.2	83.3	51.6	31.7
36.6	0.9	7.9	7.3	72.1	44.1	28.0
36.6	0.6	7.9	7.3	72.1	44.1	28.0
22.9	19.8	7.3	7.3	67.0	40.8	26.2
22.9	9.1	5.5	5.5	39.6	22.9	16.7
22.9	7.6	5.3	5.3	37.7	21.7	16.0
22.9	5.2	5.0	5.0	33.9	19.3	14.6
22.9	0.9	4.3	4.1	24.6	13.4	11.2
22.9	0.6	4.3	4.0	23.8	12.9	10.9
9.1	19.8	6.1	6.1	47.9	28.3	19.6
9.1	9.1	4.3	4.3	25.4	13.9	11.5
9.1	7.6	4.1	4.1	23.8	12.9	10.9
9.1	5.2	3.8	3.8	20.8	11.1	9.8
9.1	0.9	3.5	2.6	14.0	6.9	7.1
9.1	0.6	3.0	3.0	14.3	7.1	7.2

Figure 11 Footing spread summary - concrete single pier

Guideway Span (m)	Guideway Height (m)	Foundation Base (m)	Foundation Length (m)	Exca-vation (m^3)	Form & Pour (m^3)	Backfill (m^3)
36.6	19.8	14.6	14.2	240.2	157.9	82.3
36.6	9.1	12.2	11.7	168.5	109.0	59.5
36.6	7.6	12.2	11.3	162.2	104.7	57.5
36.6	5.2	11.6	10.8	148.6	95.4	53.1
22.9	19.8	10.4	9.3	115.9	73.4	42.5
22.9	9.1	7.9	7.6	74.9	46.0	28.9
22.9	7.6	7.6	7.3	69.5	42.5	27.1
22.9	5.2	7.3	6.7	61.8	37.4	24.5
9.1	19.8	8.5	7.3	77.3	47.5	29.7
9.1	9.1	6.1	5.2	41.4	24.1	17.3
9.1	7.6	6.1	4.9	39.2	22.6	16.6
9.1	5.2	5.5	4.6	33.7	19.1	14.6

Figure 12 Footing spread summary - concrete double pier

Guideway Span (m)	Guideway Height (m.)	Foundation Base (m)	Foundation Length (m)	Excavation (m^3)	Form & Pour (m^3)	Backfill (m^3)
36.6	19.8	12.5	3.7	59.6	34.8	24.8
36.6	9.1	9.1	3.2	39.6	22.3	17.3
36.6	7.6	8.5	3.2	37.1	20.8	16.3
36.6	5.2	7.3	3.2	32.2	17.8	14.4
36.6	0.9	6.1	2.4	21.8	11.3	10.5
36.6	0.6	5.5	2.7	21.8	11.5	10.3
22.9	19.8	7.3	4.3	41.2	23.8	17.4
22.9	9.1	5.5	3.5	26.7	14.6	12.1
22.9	7.6	4.9	3.5	24.1	13.0	11.1
22.9	5.2	4.9	2.9	20.5	10.8	9.7
22.9	0.9	3.7	1.8	11.1	5.1	6.0
22.9	0.6	3.4	1.8	10.3	4.7	5.6
9.1	19.8	5.5	5.0	36.6	21.0	15.6
9.1	9.1	4.6	3.8	24.4	13.3	11.2
9.1	7.6	4.3	3.7	22.2	11.9	10.3
9.1	5.2	3.8	3.2	18.0	9.3	8.7
9.1	0.9	3.0	1.7	8.9	3.9	5.0
9.1	0.6	3.0	1.5	8.3	3.5	4.8

Figure 13 Footing spread summary - steel truss single magway

Guideway Span (m)	Guideway Height (m)	Foundation Base (m)	Foundation Length (m)	Exca-vation (m^3)	Form & Pour (m^3)	Backfill (m^3)
36.6	19.8	10.7	10.1	128.3	81.7	46.6
36.6	9.1	8.5	7.9	83.2	51.5	31.7
36.6	7.6	8.1	7.6	76.2	46.9	29.3
36.6	5.2	7.6	6.6	62.8	38.0	24.8
36.6	19.8	8.5	7.6	80.2	49.5	30.7
22.9	9.1	7.2	6.2	56.8	34.1	22.7
22.9	7.6	6.7	6.4	54.7	32.7	22.0
22.9	5.2	6.6	5.5	46.6	27.4	19.2
22.9	0.9	7.3	6.1	56.7	34.0	22.7
22.9	0.6	7.0	6.2	55.7	33.4	22.4
22.9	19.8	6.7	6.7	57.1	34.2	22.8
9.1	9.1	5.3	5.3	37.7	21.7	16.0
9.1	7.6	5.0	5.0	33.9	19.3	14.6
9.1	5.2	4.6	4.6	28.6	15.9	12.7
9.1	0.9	4.9	2.4	17.8	9.1	8.8
9.1	0.6	4.6	2.6	17.7	9.0	8.7

Figure 14 Footing spread summary - steel truss double magway

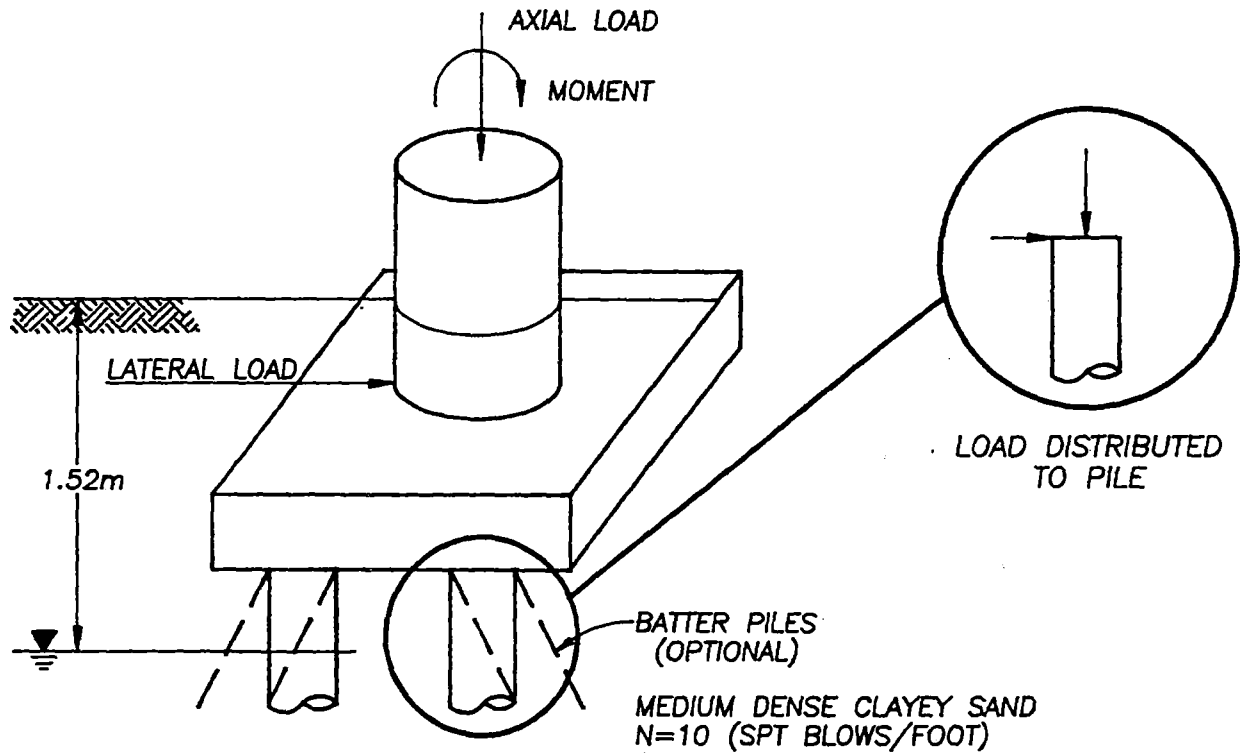

Figure 15 Load distribution to deep foundations

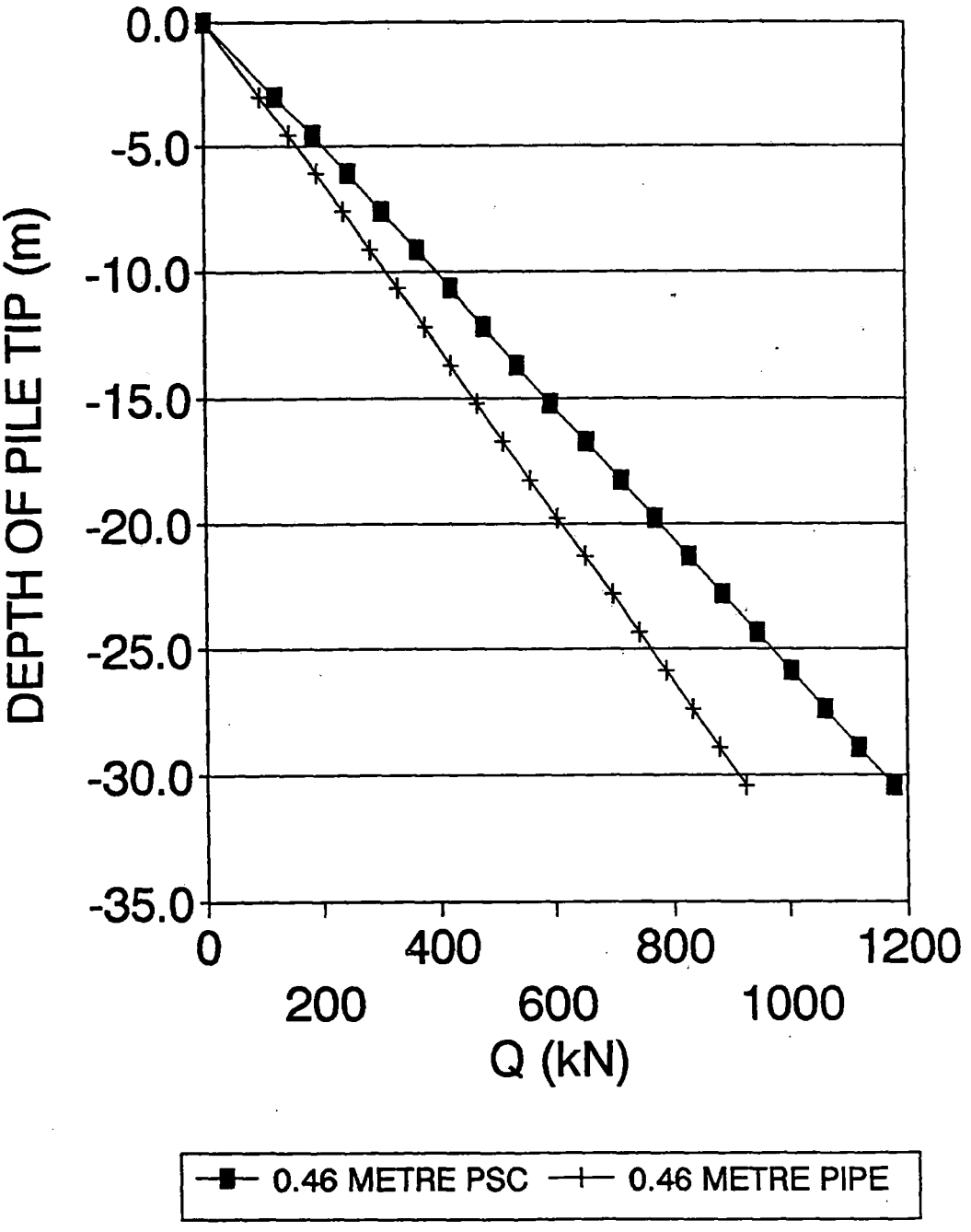

Figure 16 Axial pile capacity versus depth

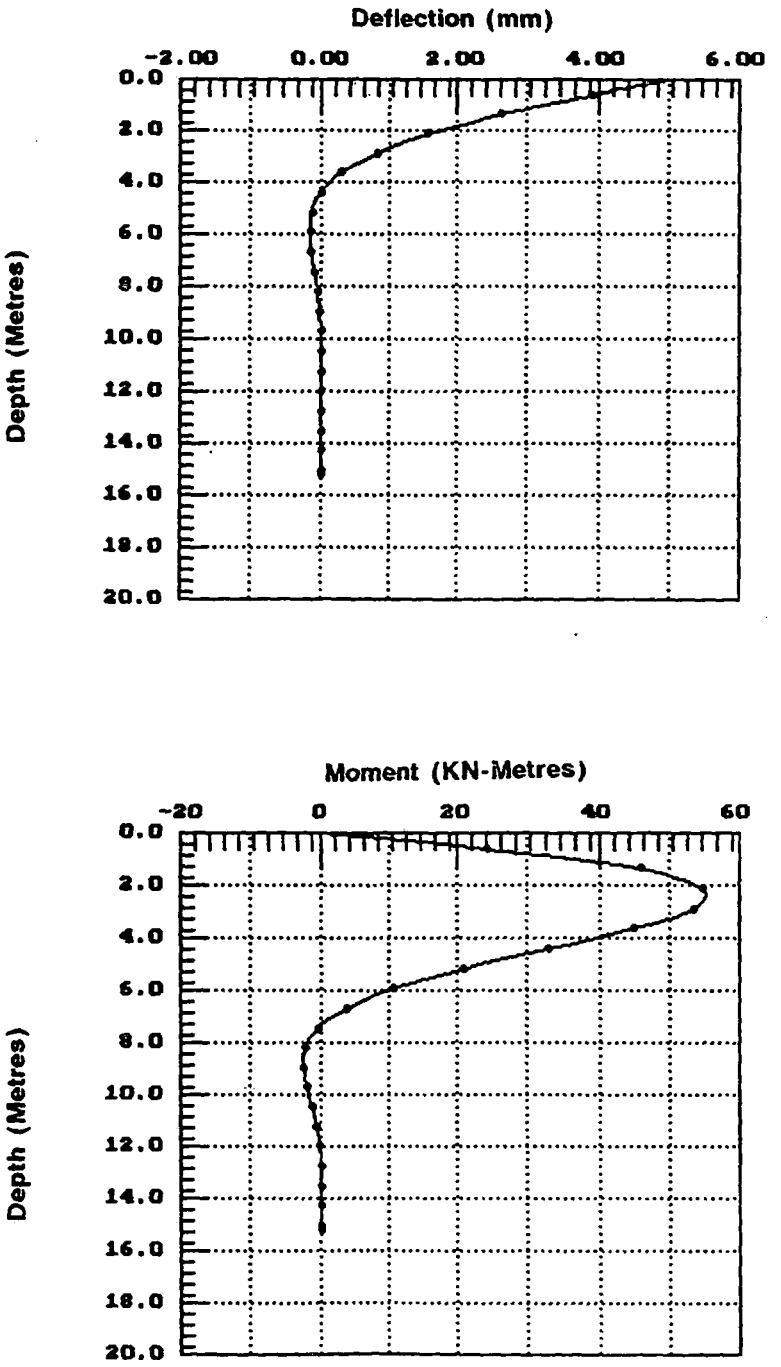

Figure 17 Lateral pile load response (deflection and moment)

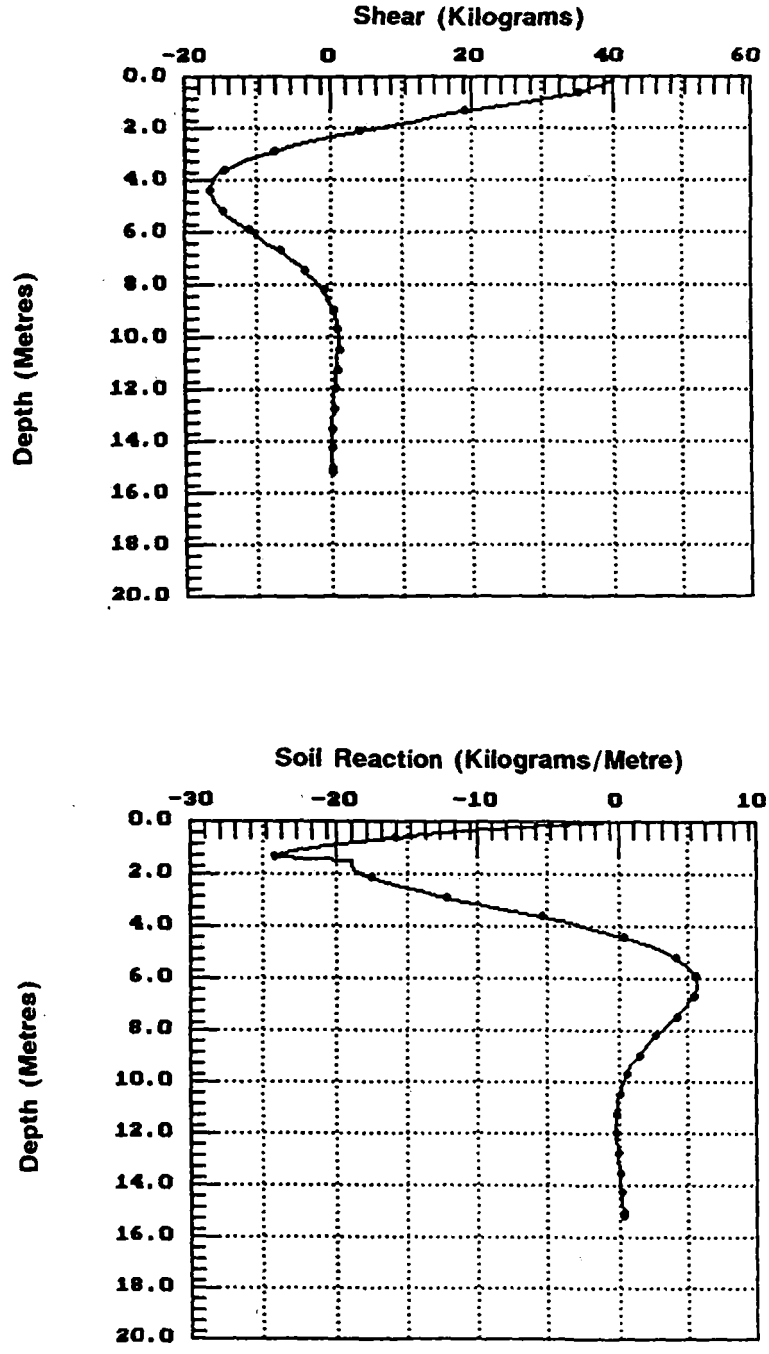

Figure 18 Lateral pile load response (shear and soil reaction)

GUIDEWAY TYPE	SPAN (m)	HEIGHT (m)	FOUNDATION TYPE	PILE GROUP NO./SIZE (m)	PILE LENGTH (m)
DOUBLE ALUMINUM BOX BEAM	13.7	9.1	STEEL PIPE	4 - 0.46	24.4
	13.7	9.1	PSC	4 - 0.46	19.8
	13.7	9.1	DRILLED SHAFT	4 - 0.91	12.2
	9.1	5.2	STEEL PIPE	4 - 0.46	19.8
	9.1	5.2	PSC	4 - 0.46	15.2
	9.1	5.2	DRILLED SHAFT	4 - 0,91	10.7
STEEL SINGLE TRUSS SPAN	22.9	5.2	STEEL PIPE	4 - 0.46	21.3
	22.9	5.2	PSC	4 - 0.46	16.8
	22.9	5.2	DRILLED SHAFT	4 - 0.91	10.7

Figure 19 Summary of Magneplane deep foundation design

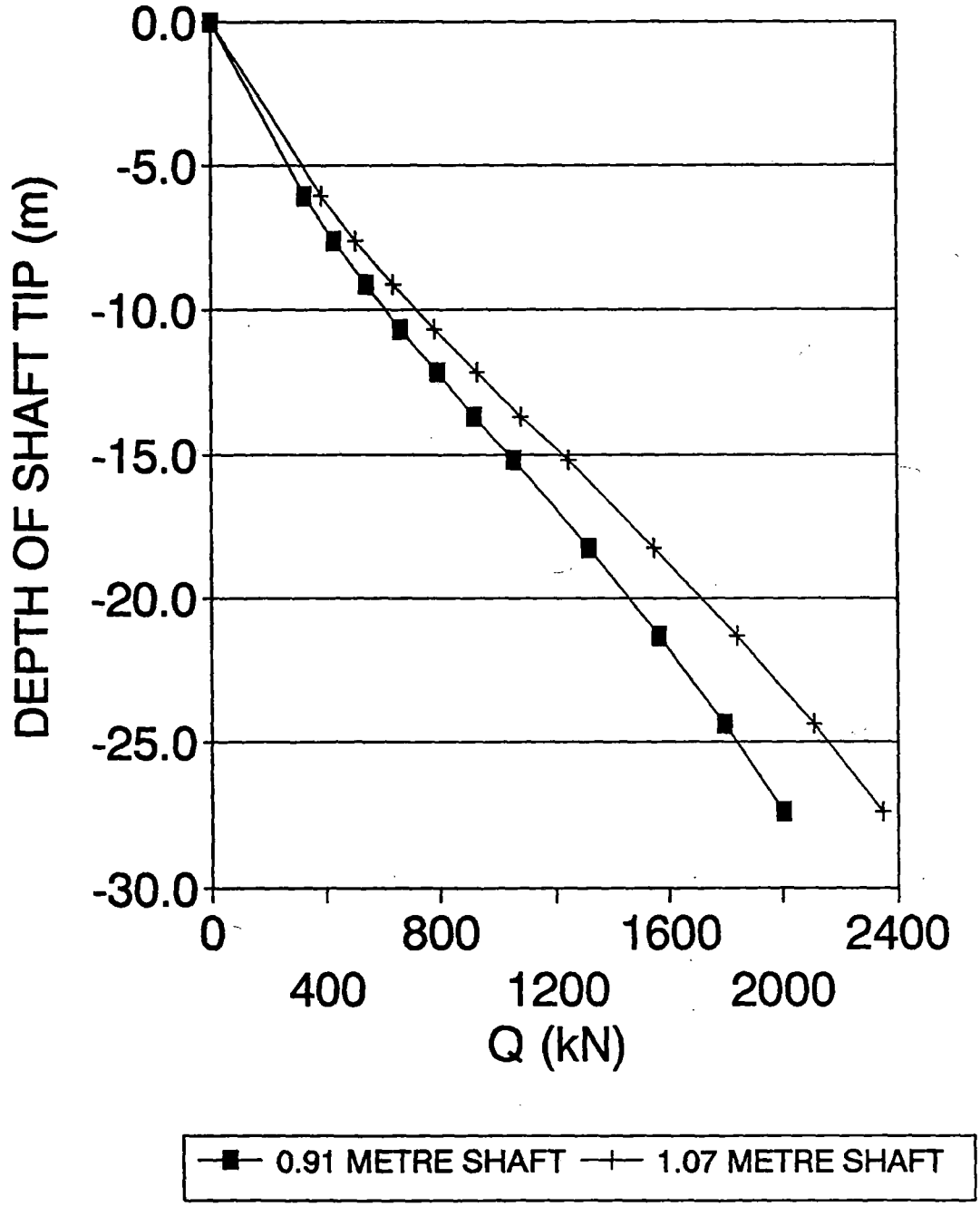

Figure 20 Drilled shaft axial capacity versus depth

3.2.2.b. MAGLEV ACTIVE/PASSIVE ELEMENTS

3.2.2.b.1. GENERAL

The magway trough is made up of the active/passive elements as shown in Figure 1. The sides of the trough are made up of passive aluminum levitation plates curved to conform to the shape of the vehicle; they form one surface of a box beam as explained below. The bottom section of the trough is the active propulsion element called the LSM winding in the Magneplane System.

3.2.2.b.2. LEVITATION BOX BEAMS

The levitation box beams, which are part of the magway trough, consist of a pair of three-celled box beams symmetric about the magway centerline. Referring to Figure 1 it can be seen that each box beam is made up of a curved upper sheet of 2.1 m radius, 45° arc length, and .02 m thickness. The bottom plate is a curved panel of .00476 m thickness, encompassing an arc of 28°. The two curved panels are held together by four equally spaced longitudinal stiffeners of .00635 m thickness. The overall depth of the box beam is designated as "d". This required depth "d" is a function of the span lengths of the levitation box beams. The box beam material is aluminum alloy 6061-T6.

The box beams have been designed to withstand loads imposed by the levitation bogies. Each passenger vehicle has two levitation bogies with a center-to-center spacing designated as "L". For the 45 passenger vehicle, L=13.11 m; for the 140 passenger vehicle, L=28.65 m. Each bogie consists of two levitation modules, one on each side of the magway centerline. Each module has two levitation coils which impart loads perpendicular to the curved .02 m thick magway sheet. The load footprint for the two levitation coils is shown in Figure 21. For design purposes this load footprint is assumed to move along the magway at 134 m/s (300 mph).

Three separate analyses were performed to insure the integrity of the levitation box beams. In the first analysis, the box beam was analyzed as a multi-span continuous beam subjected to moving loads (spanning in a direction parallel to the magway). In the second analysis, the top .02 m thick magway sheet was analyzed as a curved panel supported by the four stiffeners which are parallel to the magway. This analysis was performed to check the adequacy of the specified 0.02 m thickness. In the third analysis the box beam was checked for combined longitudinal stresses from the first analysis and from stresses due to the thermal heating of the levitation plate. Detailed calculations are provided in cupplement C.

The first analysis was performed using a modified version of the program DYNACB which was obtained from Paul Johnston of Failure Analysis Associates. The second analysis was performed using ANSYS-

PC LINEAR, Revision 4.4A. The third analysis was solved using ANSYS PC THERMAL, Revision 4.4A.

Acceptance criteria for the first two analyses were two-fold. For the case of the box beam acting as a multi-span continuous beam, the maximum dynamic deflection was limited to the span length divided by 2000. Secondly, since the dynamic loads produce considerable alternating stresses, the stresses were compared to allowable fatigue stresses as set forth in the Fifth Edition of the Aluminum Construction Manual issued by the Aluminum Association. Allowable stress ranges were determined assuming an infinite number of load cycles.

The overall depth "d" of the box beams was determined for the following span length conditions:

1. Four (4) - 4.57 m spans (18.29 m overall length).
2. Two (2) - 9.14 m spans (18.29 m overall length).
3. One (1) - 13.72 m span (13.72 m overall length).
4. One (1) - 18.29 m span (18.29 m overall length).

The thermal analysis was performed for two cases; one 9.14 m simple span, and two 9.14 m continuous spans. The 9.14 m span was chosen as the results of the first two analyses and the work documented in sections 5.3.2.23 and 5.3.2.26 indicated it to be near the optimum span length. The heat input from the electromagnetic drag was based on Magneplane vehicles traveling at 30 m/s at a 20 second headway as given in [fig 4, sect. 3.2.2.g.5]. The temperature distribution in the levitation box beam was solved using ANSYS with the aluminum and the enclosed air modeled using 3-D isoparametric thermal solid elements. Convective and radiant heat transfer was modeled with appropriate convection and radiation links. The temperature distribution thus obtained was input to a second program that calculated longitudinal stresses and deflection due to the temperature gradient. These stresses were then combined with beam stresses due to the moving vehilce and compared with the allowables as set forth in the Aluminum Association manual.

3.2.2.b.3. SUMMARY OF RESULTS

I. Required depth "d" of box beams
Figure 22 summarizes the results of the analysis for the 4 span length conditions.

II. Required thickness of magway sheet.
A dynamic analysis of the magway sheet was accomplished which indicated that the fluctuating bending stresses are within the allowable fatigue stresses for aluminum and that the thickness of the 2 cm sheet is adequate.

III. Results of the thermal analysis.
Based on an ambient temperature of 32 deg. C, the steady state temperature in the top plate was found to be 127 deg C, and the bottom plate was 51 deg C cooler at a temperature of 76 deg C. The upward deflection due to this thermal gradient is 0.01307 m and 0.00354 m for the simple and continuous span respectively. The combined stresses due to the thermal gradient and the moving load were found to be a maximum of 7.164×10^7 N/m^2 at the center support of the continuous span.

(and this is the evacuation platform!

LEVITATION COIL MODULES

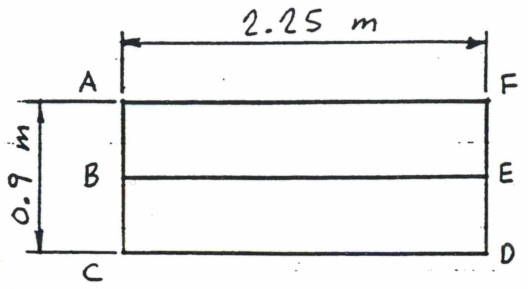

LOAD FOOTPRINT

THE LOADS ARE PERPENDICULAR TO THE GUIDEWAY ALONG EACH OF THE LINES ABOVE

THE LOADS ARE ASSUMED DISTRIBUTED OVER A WIDTH OF APPROXIMATELY 0.2 m ALONG EACH OF THE LINES.

140 PASSENGER VEHICLE

$F_{AF} = F_{CD} = 12706\ N$
$F_{BE} = 89548\ N$
$F_{AB} = F_{BC} = 9076\ N$
$F_{FE} = F_{ED} = 9076\ N$

$\Sigma F = 151264\ N$
$2(2 \times 151264 \times \cos 36^\circ) = 489500\ N$ (110000 LB)

45 PASSENGER VEHICLE

$F_{AF} = F_{CD} = 6353\ N$
$F_{BE} = 44774\ N$
$F_{AB} = F_{BC} = 4538\ N$
$F_{FE} = F_{ED} = 4538\ N$

$\Sigma F = 75632\ N$
$2(2 \times 75632 \times \cos 36^\circ) = 244750\ N$ (55000 LB)

Figure 21 Levitation coil load footprint on magway

	15 FT SPAN (4.57M)	30 FT SPAN (9.14M)	45 FT SPAN (13.72M)	60 FT SPAN (18.29M)
PROPERTIES FOR EACH BOX BEAM: (IE, ONE HALF OF THE GUIDEWAY THROUGH)				
DEPTH OF SECTION (M)	0.4064M (16″)	0.8128M (32″)	1.3208M (52″)	1.7272M (68″)
CROSS-SECT. AREA (M^2)	4.9228E-02	6.0964E-02	7.5634E-02	9.818E-02
MOM. OF INERTIA (M^4)	1.2834E-03	6.1918E-03	1.9785E-02	4.0888E-02
SECTION MODULUS (M^3)	3.7442E-03	1.0290E-02	2.2138E-02	3.7281E-02
NATURAL FREQUENCY (HZ)	61.2	30.19	21.53	15.281
RESULTS:				
MAX. DYNAMIC DEFL (M)	0.00219	0.00436	0.006517	0.009030
MAX. STRESS RANGE (N/M^2)	3.35E+07	3.24E+07	2.866E+07	2.789E+07
CRITERIA:				
ALLOWABLE LIVE LOAD DEFL (L/2000)	0.002286	0.004572	0.006858	0.009144
ALLOWABLE STRESS RANGE	4.14E+07	4.14E+07	4.14E+07	4.14E+07

MATERIAL PROPERTIES: (ALUMINUM 6061-T6)	DENSITY:	26600 N/M^3	(0.098 LB/IN^3)
	E:	6.895E+10N/M^2	(10E+06 PSI)
	ULT STRESS:	3.103E+08N/M^2	(45000 PSI)
	YEILD STRESS:	2.758E+08N/M^2	(40000 PSI)

Figure 22 Aluminum box beam section properties and summary of results

3.2.2.b.4. LSM WINDING SUPPORT STATIC LOAD STRUCTURAL ANALYSIS

A finite element analysis of the propulsion winding support structure was performed to ensure that, when subjected to various static load conditions, the stresses induced in the structure were of an acceptable magnitude. The structure's geometry was modeled using an inverted U-shaped cross section. The web and leg dimensions were 1.4 meters wide by 4 centimeters thick and 0.5 meters long by 2 centimeters thick, respectively. The 9 meter long section was modeled with its legs supported every three meters to simulate rigid bolted connections. The material was modeled as an isotropic, fiber-reinforced polyester (FRP), similar to Glastic's commercial product, UTS.

The structure was subjected to four separate loading conditions. The first of these was the dead load of the structure, including the weight of the FRP (2976 lbs), aluminum (1194 lbs) and epoxy (estimated to be 10% of the FRP weight = 297 lbs). The dead load was 4467 lbs (19,900 newtons) for the 9-meter-long structure. The second loading condition imposed was comprised of the structure's dead load with a uniform, 40 pound per square foot (1920 pascal) snow load (equal to 24,200 newtons).

The remaining two loading conditions were combinations of the structure's dead load with two unique vehicle loadings. Both of these cases imposed considerably higher loads on the support structure than the cases previously described. The assumed vehicle weight (491,000 newtons) and landing gear geometry (each 1.1 meters wide by 2 meters long) was that of the 140-passenger vehicle. The first vehicle loading condition considered a vehicle stopped in the magway and rotated 10.6° around the magway's longitudinal axis (see Figure 23). This orientation increases the landing gear area in contact with the web of the winding support structure, and results in a load of 46,000 newtons distributed over an area of 0.7 square meters (65,700 newtons per square meter). This loading is larger and, therefore, conservative when compared to the 5400 newton load distributed over an area of 0.1 square meter when the vehicle is in the "Normal Upright Attitude" (54,000 newtons per square meter).

In addition, a worst-case vehicle loading condition was considered. The vehicle was positioned in the magway as described above, however the load-carrying capabilities of the aluminum box beam were ignored. Thus, the winding support structure was assumed to carry the entire landing gear load. This loading condition resulted in a load of 122,780 newtons (approximately one-fourth the total vehicle weight), distributed over the same 0.7 square meter area of the support structure web.

Illustrations of the applied loads and contour plots of the resultant displacements (meters) and Von Mises stresses (newtons per square meter) associated with the two vehicle loading conditions can be seen in Figure 24, Figure 25, Figure 26, Figure 27, and Figure 28. The magnitudes of these stresses and displacements are highlighted in Figure 29, as is the tensile strength of the modeled FRP material.

The largest stresses reside around the "bolt" locations and are approximately 28% higher than the largest stresses experienced in the web (directly under the landing gear). Therefore, proper design of these connections appears to be especially important. Examination of principal and shear stresses resulting from the loading conditions indicated that they were less significant than the Von Mises stresses.

In summary, the analysis indicates that use of an FRP structure to support the propulsion windings is feasible. It should be noted, however, that several simplifying assumptions relating to the material have been made in this analysis. Therefore, additional investigation into the actual properties of the specific material to be used must be carried out to fully understand factors including, but not limited to, the material's isotropic/anisotropic characteristics, elastic/plastic behavior and environmental sensitivity, to ensure its success in this application. In addition, special care must be taken to ensure proper design of the "bolted connections," as supports generally experience higher stresses than the rest of the structure.

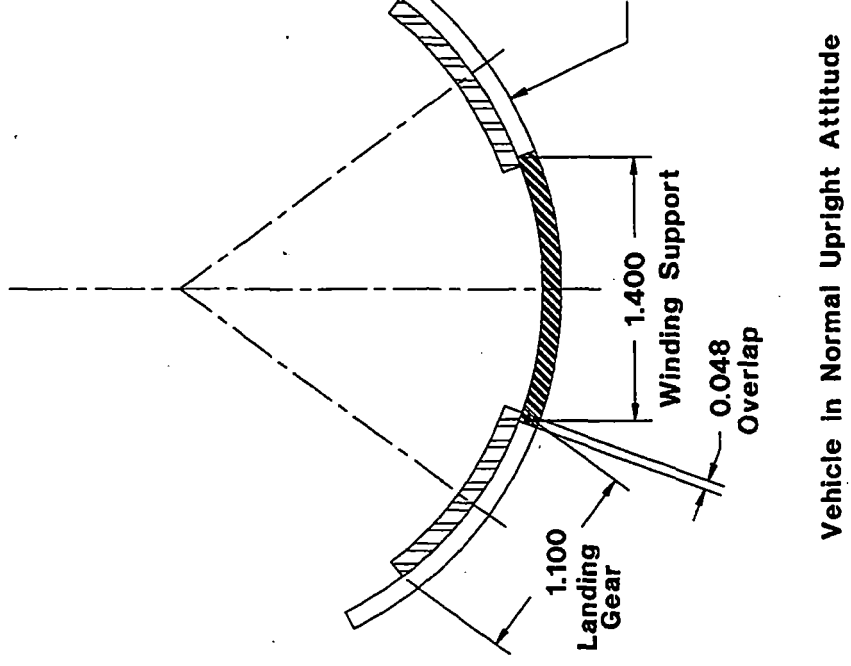

Figure 23 LSM winding support, rotated vehicle loading

Vehicle Rotated 10.6°

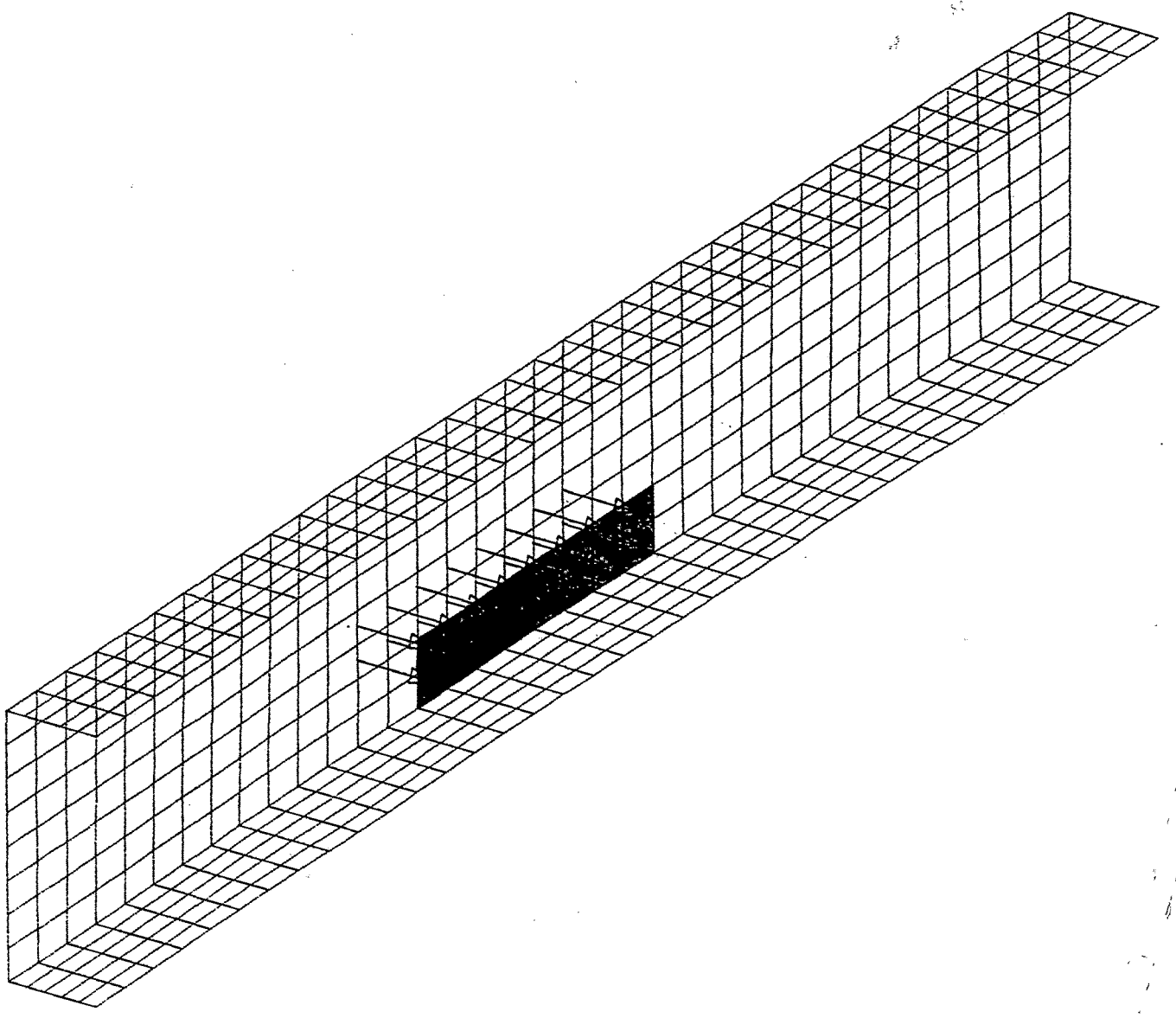

Figure 24 Location of application of vehicle load

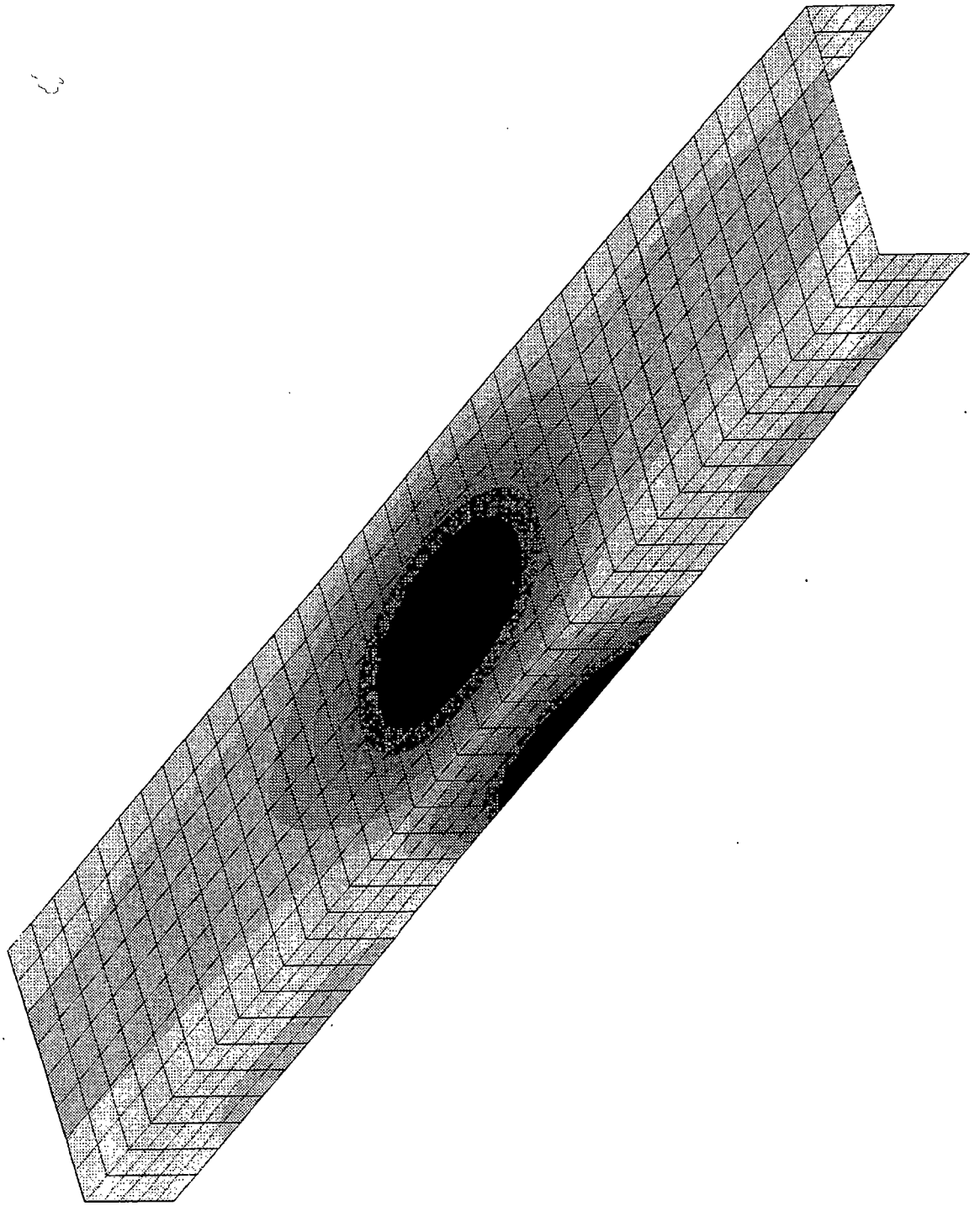

Figure 25 Dead load plus 10.6° rotated vehicle load: resultant displacements, stresses and FRP material strength

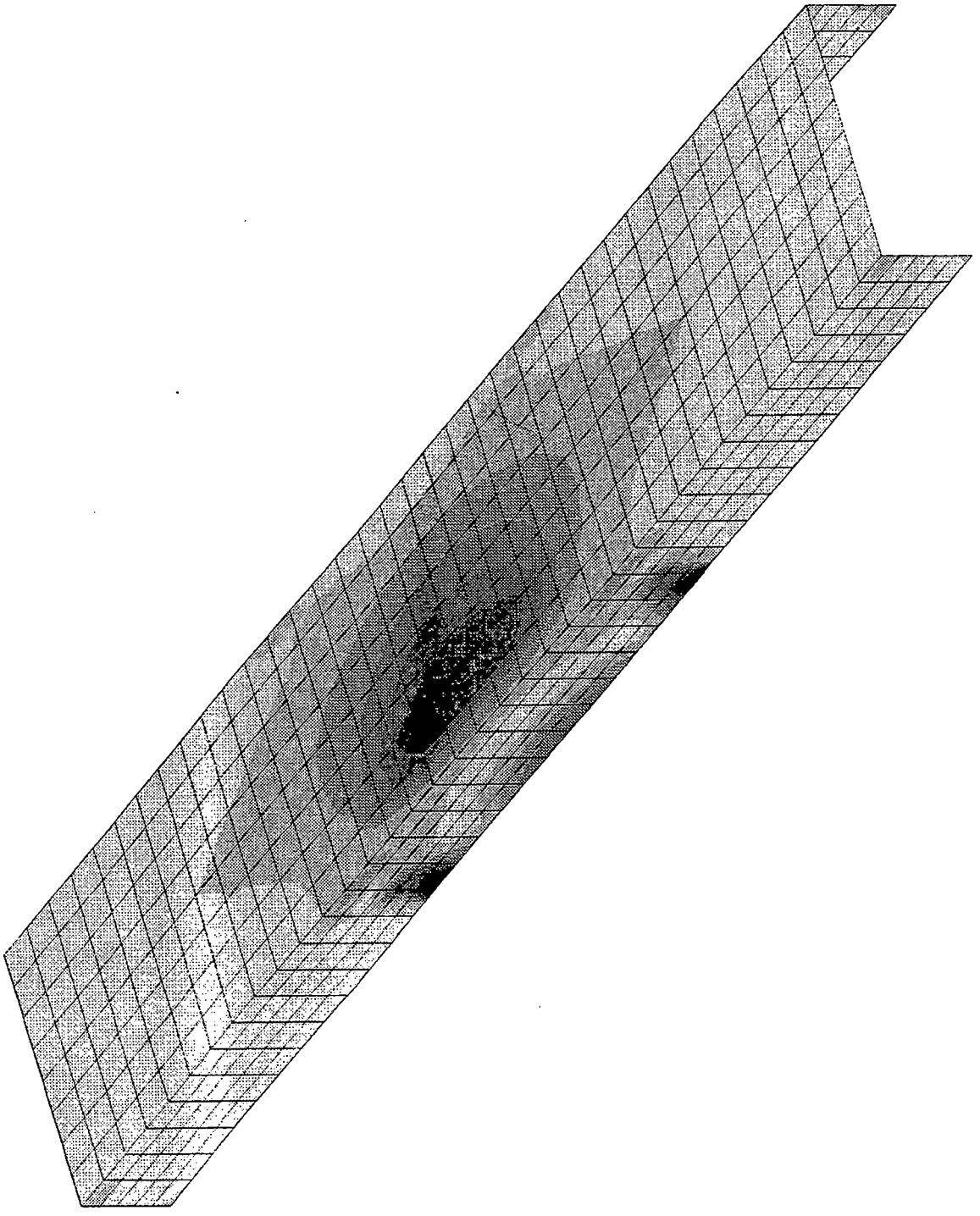

Figure 26 Dead load plus 10.6° rotated vehicle load: Von Mises stresses

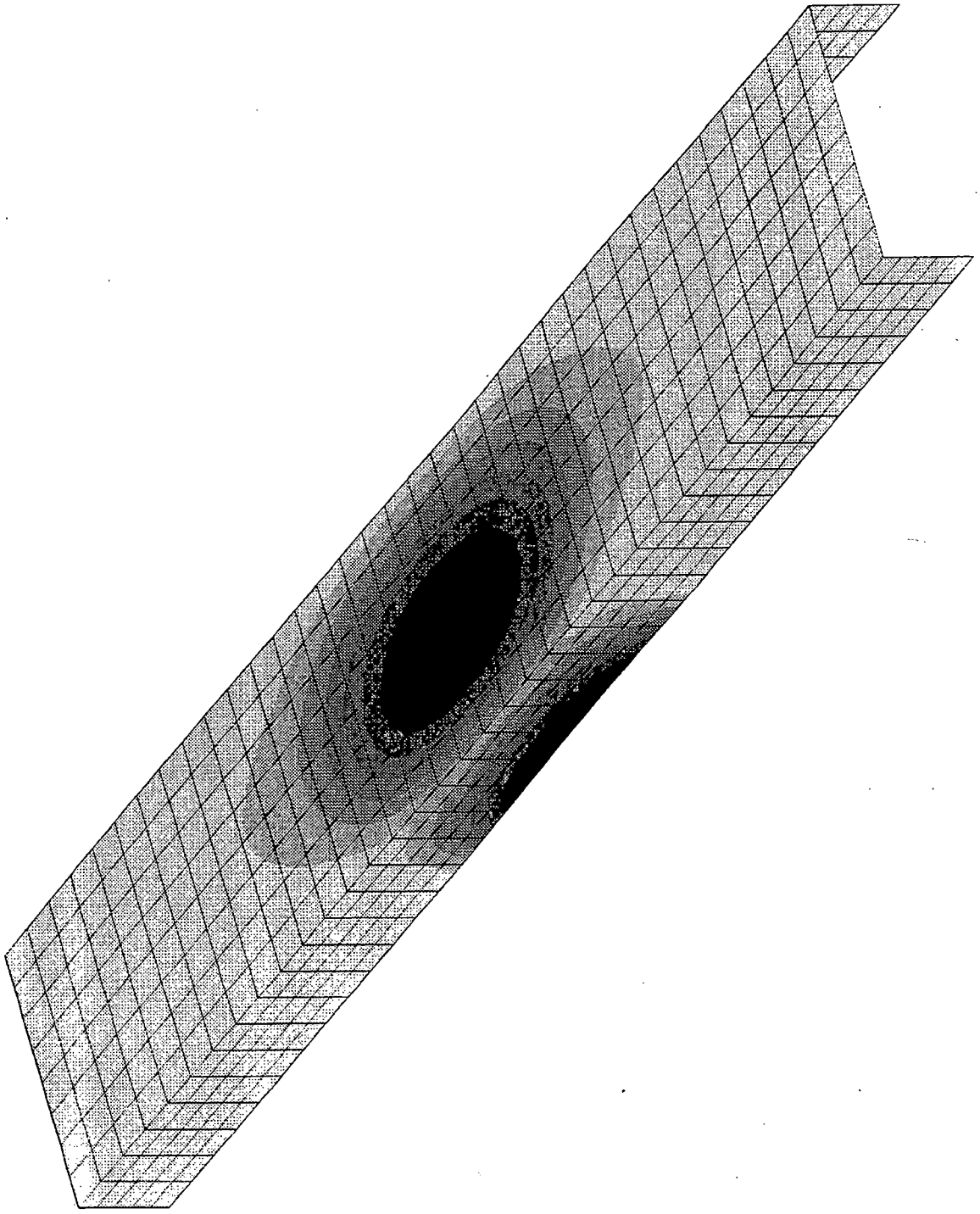

Figure 27 Dead load plus 10.6° rotated vehicle load, no box beam support: resultant displacement

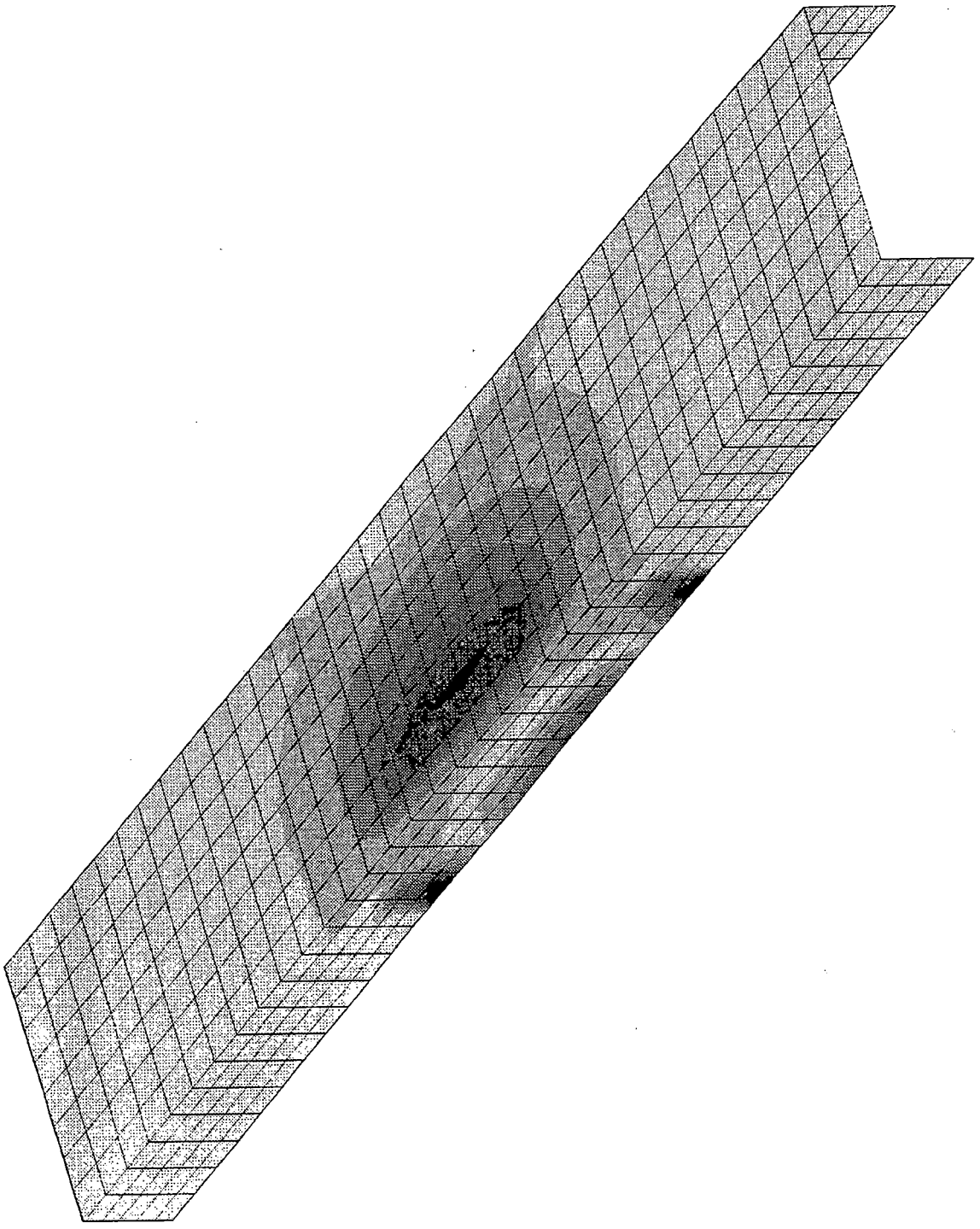

Figure 28 Dead load plus 10.6° rotated vehicle load, no box beam support: Von Mises stresses

LOADING CONDITION	MAXIMUM DISPLACEMENT	MAXIMUM VON MISES STRESS	GLASTIC UTS TENSILE STRENGTH
DEAD LOAD PLUS 10.6° ROTATED VEHICLE	7.346×10^{-3} m (0.289 inch)	145.8×10^5 N/m^2 (2115 psi)	6.14×10^7 N/m^2 (8900 psi)
DEAD LOAD PLUS 10.6° ROTATED VEHICLE, NO BOX BEAM SUPPORT	17.45×10^{-3} m (0.687 inch)	358.4×10^5 N/m^2 (5198 psi)	

Figure 29 LSM winding support; induced displacements, stresses and FRP material strength

3.2.2.b.5. LSM WINDING CONSTRUCTION

LSM winding construction is illustrated in Figure 31. The winding consists of a stranded aluminum conductor wound on slotted fiber reinforced plastic (FRP) structure. The primary means of insulation is epoxy impregnation of the wound form. Approximate dimensions are shown in the Figure. The end turn construction and conductor detail are shown in Figure 32.

A winding diagram is shown in Figure 33. Each phase uses two litz-wound aluminum conductors approximately 0.03 m in diameter. There are 12 conductor slots per phase. The pole pitch is 0.75 m and the active transverse width of the winding is 1.2 m.

3.2.2.b.6. LSM WINDING ATTACHMENT

The box beam segment length has been identified as 9.14 m. As long as the length of the box beam is near 9 m, the exact length can be changed with no detrimental impact on the design. One option under consideration is to reduce the box beam length to 9.0 m to coordinate the length with the 0.75 m pole pitch of the LSM winding. The remainder of this discussion presumes that this adjustment has been made.

LSM winding segments 9 m long will be attached to box beam segments using a spacer and bolt arrangement. The coefficients of expansion of aluminum and the FRP are sufficiently close (or can be made close by altering the FRP base material slightly) so that rigid attachment can be used over this length.

Thermal expansion of the box beams is accommodated by their mounting arrangement. One end of each beam is bolted to a concrete pier. The other end of each beam rests on a shelf which is part of the adjacent beam. The shelf plays a dual role. First, it allows for thermal expansion. Second, it provides a sufficient amount of aluminum so the electromagnetic interaction with the vehicle's levitation magnets is not disturbed near the expansion joint.

Thermal expansion of the box beam and LSM winding can be analyzed based on the coefficient of thermal expansion for aluminum. Figure 30 shows the total length change for the 9.0 m beam for various changes in temperature.

The variation in length of the LSM winding has the effect of altering the phase of the magnetic field perceived by the vehicle's propulsion coils. This phase alteration causes a change in the heave force. The spacing of the bogies determines the type of effect on the vehicle. If the center-center spacing of the bogies is a multiple of 9 m, then the force shows up as periodic heave variation. If they are spaced at 9 x N + 4.5 m, then it is a pitching variation with no net heave component. The forces are relatively small and well above the natural frequencies of the vehicle.

	Change in Temperature		Total Length	
	ΔT (in °C)	Variation (°C)	Change (CM)	Variation (CM)
Worst Case:	150	±75	3.12	±1.56
	100	±50	2.08	±1.04
Typical:	50	±25	1.04	±0.52

Figure 30 Thermal expansion in LSM

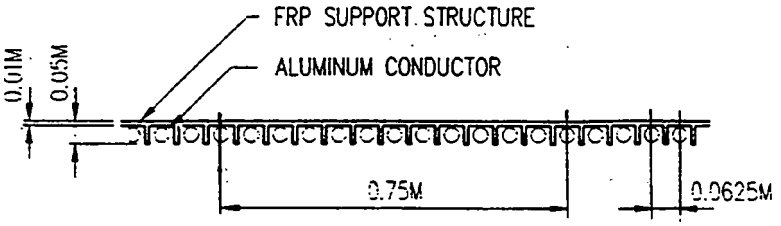

LONGITUDINAL SECTION

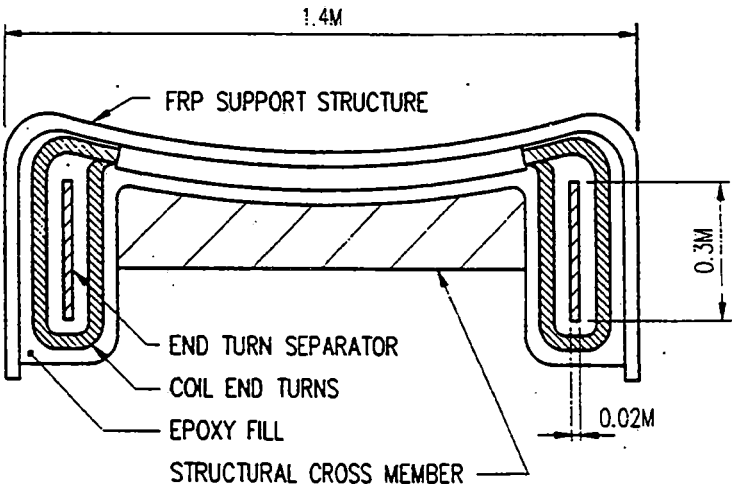

CROSS SECTION

Figure 31 LSM winding construction

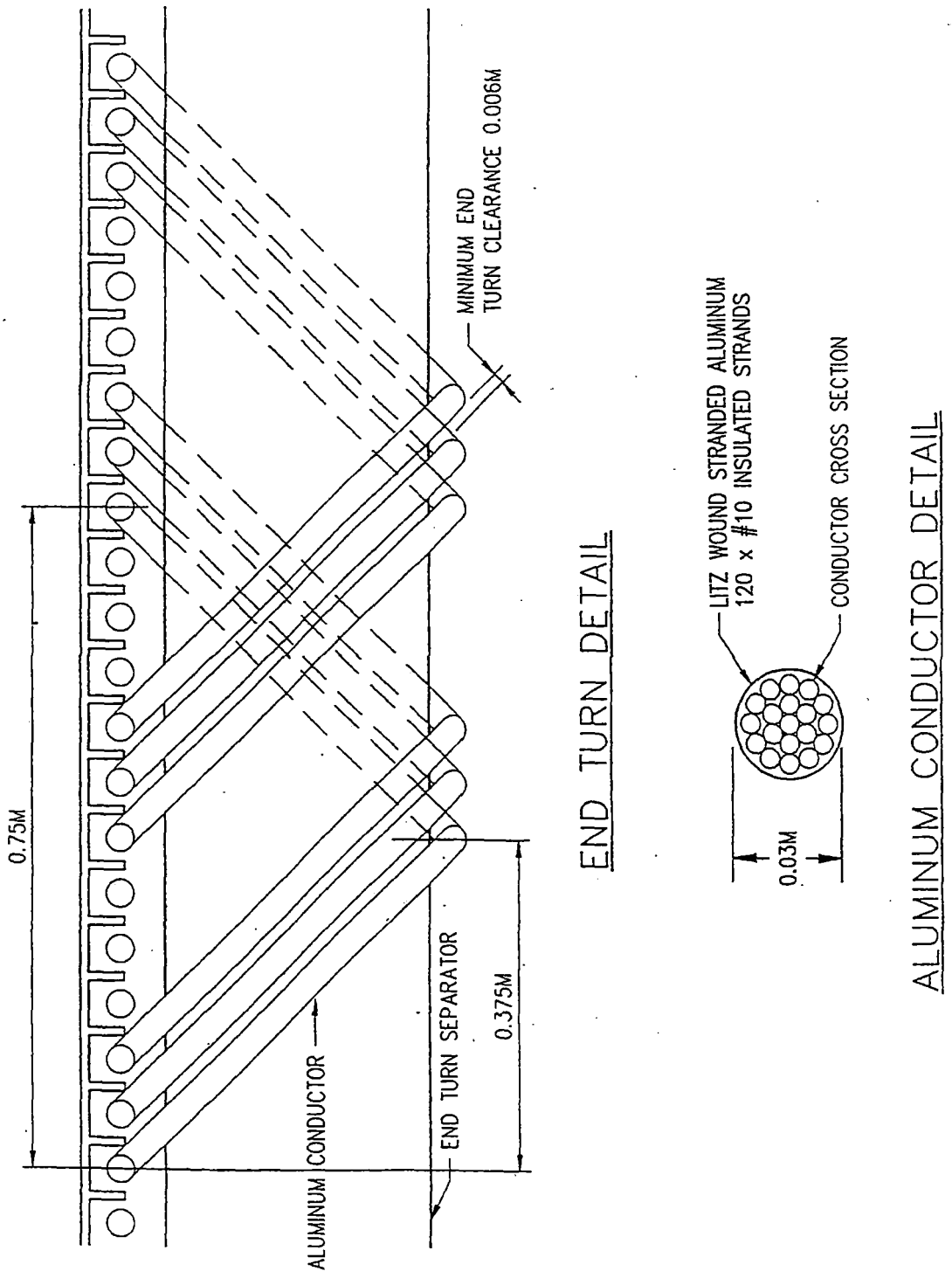

Figure 32 LSM winding end turn and conductor detail

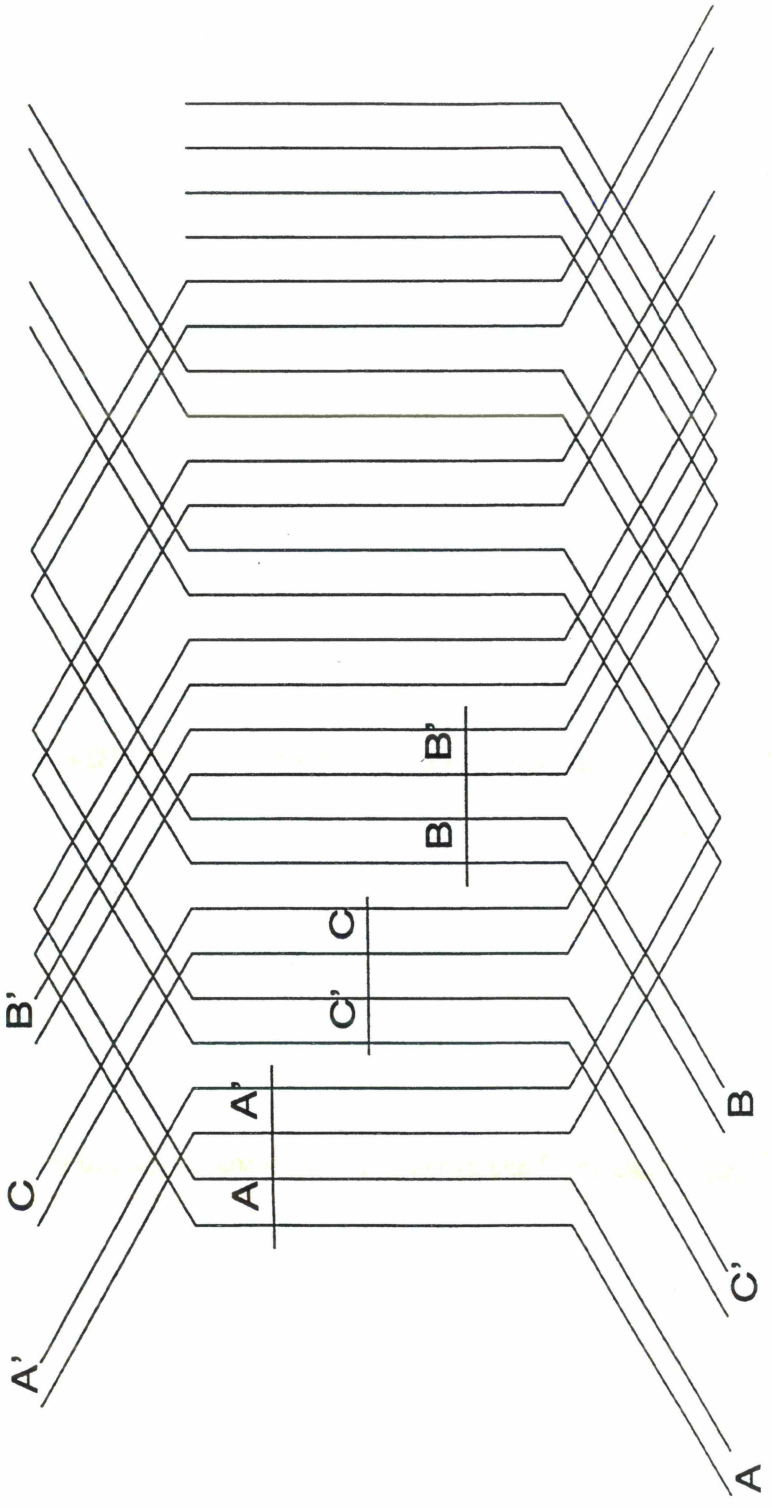

Figure 33 Winding electrical diagram

3.2.2.c. ALIGNMENTS

3.2.2.c.1. THERMAL EXPANSION

The baseline levitation plate box beam design as described in previous Section 3.2.2.b. includes thermal expansion joints to accommodate thermal expansion/contraction in the aluminum and preclude excessive warpage of the box beam. The joint design as shown in Figure 34 allows for up to 0.076 m (3") of travel. It incorporates a 1 m long backing plate that straddles the joint region underneath. One box beam is fixed at the support while the other is supported by and allowed to slide over the backing plate. Alignment guides are incorporated to prevent uplift or movement transverse to the vehicle travel. Temperature fluctuations in the magway can be caused by ambient temperature swings, the suns rays, emergency braking, and electromagnetic drag. The sum of the first two effects has been taken at 83°C (150°F) which is consistent with U.S. highway and railroad design requirements. The heating effect of emergency braking has been calculated in Section 3.2.1.d.2. to cause a temperature rise of 2°C (3°F). The thermal calculations described in section 3.2.2.b.2. indicate that the heat buildup in the aluminum levitation plate due to vehicles traveling at 30 m/s at a 20 second headway could cause a temperature rise of up to 95°C (171°F). Conservatively, the sum of the above effects is a 180°C (324°F) temperature delta. Using a coefficient of expansion for aluminum of 0.0000131 per degree F, the maximum length between expansion joints would be 18 m (59'). This joint spacing was also checked to not be a multiple of the bogie spacing for either size vehicle.

3.2.2.c.2. SETTLEMENT AND DEFLECTIONS

The Magneplane system is not a close tolerance system as it operates with a nominal separation of 0.15 m between the vehicle and the surface of the levitation plates. Misalignments in excess of 0.02 m (0.8") would, however, adversely affect ride quality. The total vertical or horizontal misalignment due to the combination of construction "out of tolerance" and dynamic deflection shall be limited to 0.02 m. The supporting structural members will be specified to be cambered to reduce dead load deflections. Any remaining out of tolerance deviations in the supporting structural member can be mitigated by the shim adjustments provided at each magway trough support point. The supporting structural members will be designed to limit live load dynamic deflection to less than the span length divided by 2000. Foundations will be designed to limit settlement to 0.025 m (1"), however, the end bearing of each spanning member will be designed to accommodate adjustments of up to 0.04 m (1.5").

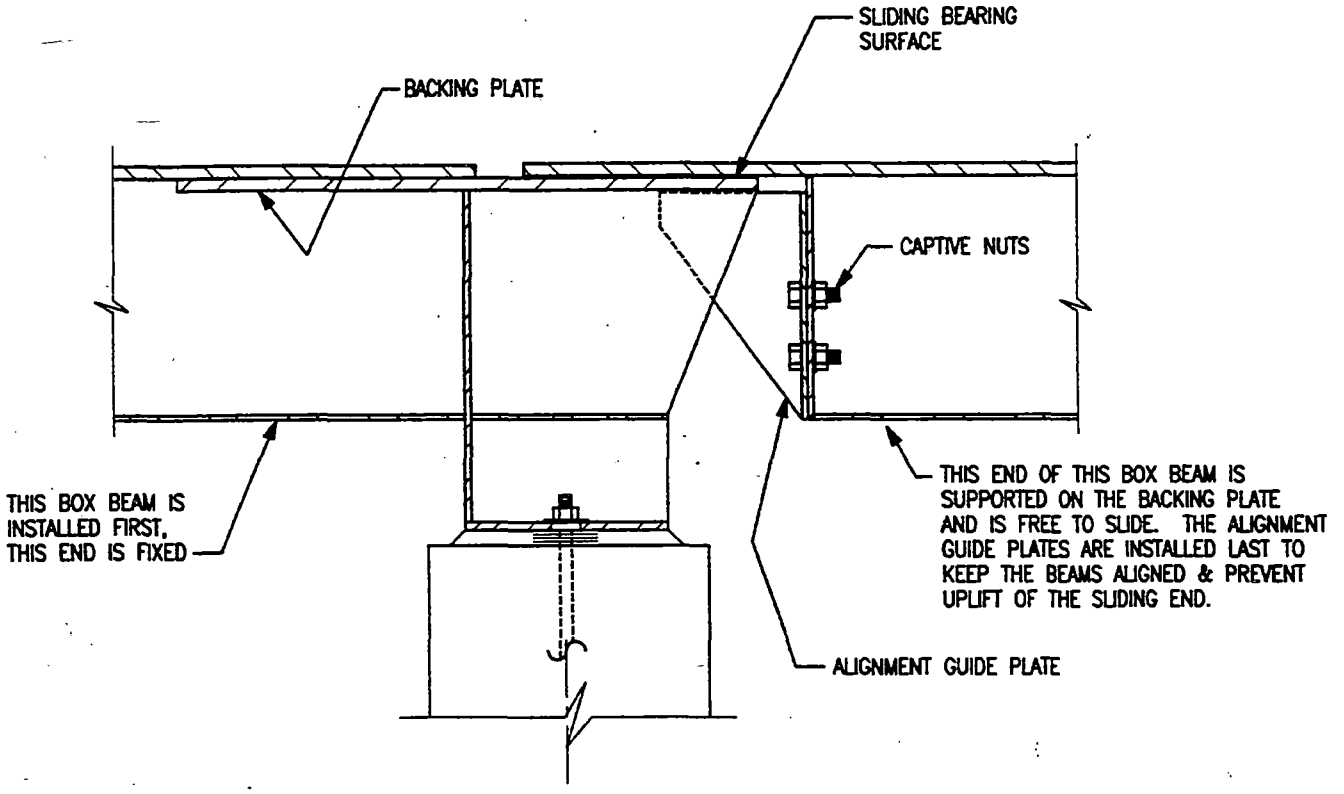

Figure 34 Levitation plate longitudinal section showing joint design

3.2.2.d. MAGSWITCH

Several switching options have been considered in the course of the Magneplane study. The present baseline is an electromagnetic switch that has been investigated sufficiently to show concept feasibility. The back-up alternative is a mechanical switch that was developed earlier in the program. The baseline is expected to provide a faster cycle time and to be less expensive. See section 5.3.2.22. for the tradeoff analysis.

The magswitch depends on the use of the propulsion coils on the vehicle and null flux coils on the magway to provide lift and guidance while traversing the main body of the switch surface which is flat. Speed control during the process is provided by the LSM. The baseline speed is 134 m/s straight through and 100 m/s for the branch, but there is no inherent speed limitation. The latter is governed by ride quality considerations and the availability of real estate for the particular switch location. In addition, the baseline clearance to the vehicle of 0.15 m has been maintained.

Sufficient computations have been performed to establish the dynamic equilibrium of the vehicle for a particular coil configuration. This has allowed us to provide data for cost estimation purposes. Optimization of the configuration and studies of the vehicle stability are yet to be done and will be pursued in a future phase of the program. This section begins with a description of the switch and then continues with some of the analyses performed in the process of the concept development.

3.2.2.d.1 CONFIGURATION

The switch configuration is shown in Figure 36. Upstream and downstream of the switch the magway configuration is the usual baseline as illustrated in section A-A. In the central part of the switch, it is flat as shown in sections C-C and D-D. There are also transition regions on entry and exit from the central sections in which there will be a transition from the double sheet curved magway with 1.4 m gap for the LSM to a single sheet magway with LSM and null flux coils mounted over the magway. The regions in between will use a smooth transition as the gap narrows. In the transition process, the vehicle will rise from a clearance of 0.15 m above the standard section to a distance of 0.415 m above the single aluminum sheet in the central flat sections. The clearance in the latter, however, will still be 0.15 m because the LSM and null flux coils will be mounted within the 0.265 m distance over the single aluminum sheet. The space on each side of the windings will be filled in with concrete to assure a flat surface. This is necessary for low speed operation when the air pads would be extended or if the vehicle must stop in the switch.

Figure 36 also shows that structural sections have been included along the sides of the switch. These are not used during the usual switching operation, but are included for safety purposes.

Figure 37 shows the cross-over variant of the switch, formed by two single switches.

Normalized Lift (g's)	Height (m)
1.97	0.385
1.00	0.465
0.43	0.565

Figure 35 Normalized lift vs. height of propulsion coil centerline over single sheet aluminum magway

3.2.2.d.2. LEVITATION AND GUIDANCE IN THE SWITCH

Analyses to date show the feasibility of providing the necessary levitation and guidance forces by using a narrowing gap between the two levitation sheets to lift the vehicle higher as the single sheet flat section is approached. They also show the availability of sufficient guidance forces through the use of the "keel" effect with the two magway sheets in combination with null flux coils as the two sheets become one. The operational selection of "straight through" vs "branch" is made by short circuiting the passive null flux coils in that direction and also operating the LSM in the desired direction. This concept is illustrated in Figure 38.

Two figures in section 3.2.1.a.1. illustrated the source of the "keel" effect by showing the differences in the eddy current patterns in the two parallel magway sheets if the vehicle centerline was aligned with or offset from the centerline of the magway sheets. The interaction between the propulsion coils and the edge of the magway is dramatic and gives rise to guidance forces that tend to keep the propulsion coils centered over the space between the magway sheets. It is also obvious that the propulsion coils could provide lift if the magway sheets were to extend under the propulsion coils. This would lead to a loss of some of the interaction with the LSM, however, which would be compensated in the switch area by increasing the LSM current if necessary.

The level of the electromagnetic lift and guidance interactions that can be achieved with the "keel" effect is indicated in the table in Figure 39. The table was generated for the baseline set of propulsion coils traveling at the given height (column 1) above two flat magway sheets, each having the baseline width of 1.5 m, but with different gaps (column 2) between the sheets that are under the coils. The interaction with the levitation coils was not included and is small because they are relatively high above the flat sheets. The column labeled "offset" is a specified horizontal distance between the centerline of the propulsion coils and the centerline of the magway system. The lift and guidance for each of the conditions is given in columns 4 and 5, respectively, with the values normalized to the weight of the vehicle. The result is, therefore, equivalent to force as a fraction of gravitational force.

The first 4 rows in the table give the lift and guidance variations for several gaps between the sheets, no offset, and a height of 0.2 m. The latter is consistent with other sections of this report in which the baseline is a clearance from vehicle to magway surface of 0.15 m plus an allowance of 0.05 m for the distance from the outside of the cryostat to the centerline of the propulsion coils. Results indicate that the gap width controls the lift. Specifically, sufficient lift can be generated to levitate the entire vehicle with a gap width of about 0.85 m, and the lift decreases to zero at about 1.25 m. (Note: along curved, standard sections of magway, the gap is 1.4 m, hence there is no lift provided by the propulsion coils.) The guidance force is zero in this section of the table because the offset is zero.

The second set of results in the table are for the same height of 0.2 m, a gap of 0.85 m, and selected offset values. Results indicate that both lift and guidance forces increase with offset at this gap value. Furthermore, since guidance forces will be limited to about 0.1 -0.2 g's from the ride quality standpoint, sufficient guidance will result with only a few centimeters of offset.

The last three rows in the table indicate the variation of lift and guidance forces with height for a gap of 0.85 m and an offset of 0.1 m. It shows that large guidance forces are retained with the height change, thus implying that the height and offset will adjust for the constant lift condition for the vehicle and for the guidance forces required by the dynamics of the situation.

Calculations to date indicate that the interaction with the narrowing gap may provide sufficient forces for levitation and guidance, but that the restoring moment for roll may not be sufficient. Hence, we have included null flux coils and the use of a single magway sheet in the flat section of the switch.

Figure 35 shows the normalized lift that can be achieved as a function of the height of the propulsion coil centerline above a single aluminum sheet due to the interaction of the propulsion coils with the induced currents in the magway. Lift is normalized to vehicle weight. The table, therefore, indicates that the levitation height above the single sheet magway section will be 0.465 m. Since there is 0.05 m between the coil centerline to the outside of the cryostat, the distance from the outside of the vehicle to the aluminum sheet will be 0.415 m as indicated earlier for the baseline switch.

Figure 40 shows a schematic of the six coils in a propulsion coil set moving over the magway at the clearance of 0.465 m. The vectors on the coils represent the local forces of electromagnetic origin on the coils. The end view shows that the coils are moving at a slight angle relative to the plane of the magway in this case and that the lift force distribution is non-uniform. Furthermore, it is clear that there is a restoring moment on the vehicle that will tend to decrease the angle and restore the vehicle toward parallelism with the magway. The figure also indicates that the lateral (y-directed) force on the coils is unbalanced in this situation, primarily because there is now only a single sheet and no "keel" effect. This leads to the need for the null flux coils in the section of the switch that has only a single sheet.

Figure 41 illustrates the case where there is a single aluminum sheet under the vehicle. This provides sufficient lift to raise the vehicle to a height of 0.465 m relative to the sheet and allows enough space to mount the LSM windings and a set of null flux coils under the vehicle. The result is that the clearance to the vehicle of 0.15 m. can still be maintained. The space on either side of the magway coils can be filled with non-conducting material (e.g., concrete with non-ferromagnetic reinforcement) to provide a flat surface as may be required for abnormal operations.

Each of the null flux coils in magswitch is equipped with a contactor so that it can be in an open or short circuited state. The selection of branch vs straight through operation is done by activating the proper line of switches as indicated earlier in this discussion and schematically indicated in Figure 41 by selecting either the "solid" or "dashed" null flux coils.

The shape and dimensions of the null flux coils have not yet been optimized. However, calculations have been performed for a specific set to show that the lateral and vertical shifts of the vehicle centerline that will be necessary to achieve dynamic equilibrium, are within reasonable bounds.

The top sketch in Figure 42 is a schematic, end view (i.e., motion perpendicular to paper), of the propulsion coils moving relative to the null flux coils and the magway. The turn associated with the switching action will require that the plane of the propulsion coils shift relative to the plane of the null flux coils and these displacements are defined by the increments dy and dz. The lower sketch also shows an angle defining the mounting of the plane of the null flux coils relative to the plane of the magway. This may be unintentional and related to tolerances, or intentional if future studies show that there is sufficient benefit to a non-planer mounting arrangement.

The dynamic equilibrium results for dy and dz as a function of the mounting angle are shown in Figure 43 for several speeds and for a fixed lateral g force of 0.1 on the vehicle. The results indicate that the displacements are relatively small and acceptable even if the tolerances for mounting the null flux coils are as much as a few degrees. The stability of the passage through the switch requires analysis and further optimization of null flux coil geometry is no doubt possible. This will be pursued in future design activities. The calculations done thus far, however, show the feasibility of the fully electromagnetic switch.

3.2.2.d.3. MAGSWITCH LENGTH

The length of the magswitch depends only on the speed and ride quality desired. Figure 44 shows the relationships involved. Nine options are given - the one actually chosen depends on route-specific considerations. For our baseline system, 100 m/s at MIN-B ride quality is used. Since switching is done mostly for take-off and landing, the best ride quality possible is not necessary. (In fact a lower ride quality requirement for a switch greatly reduces the cost of a magport, because it reduces the cost of the necessary entry and exit ramp lengths.)

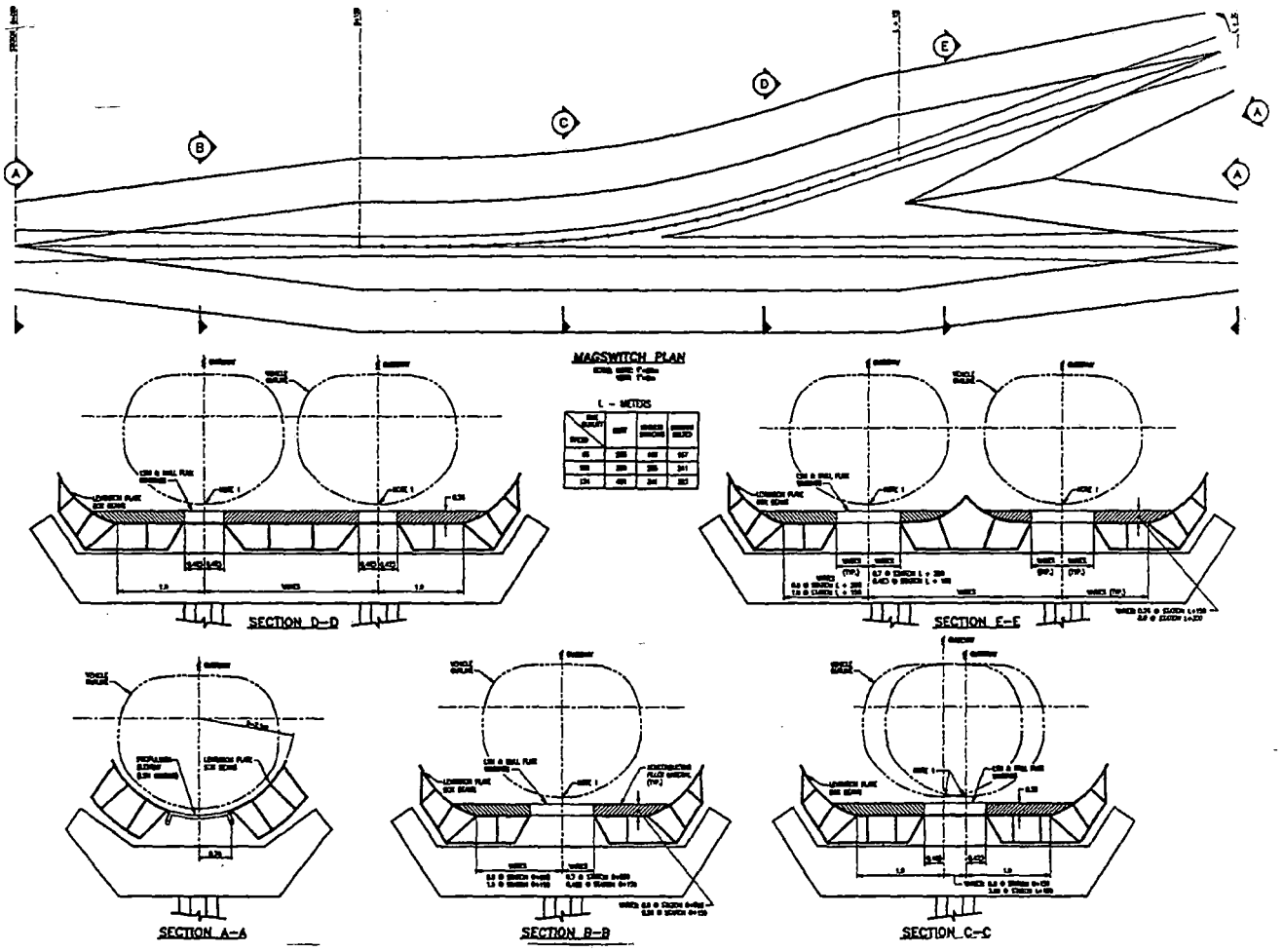

Figure 36 Magswitch configuration

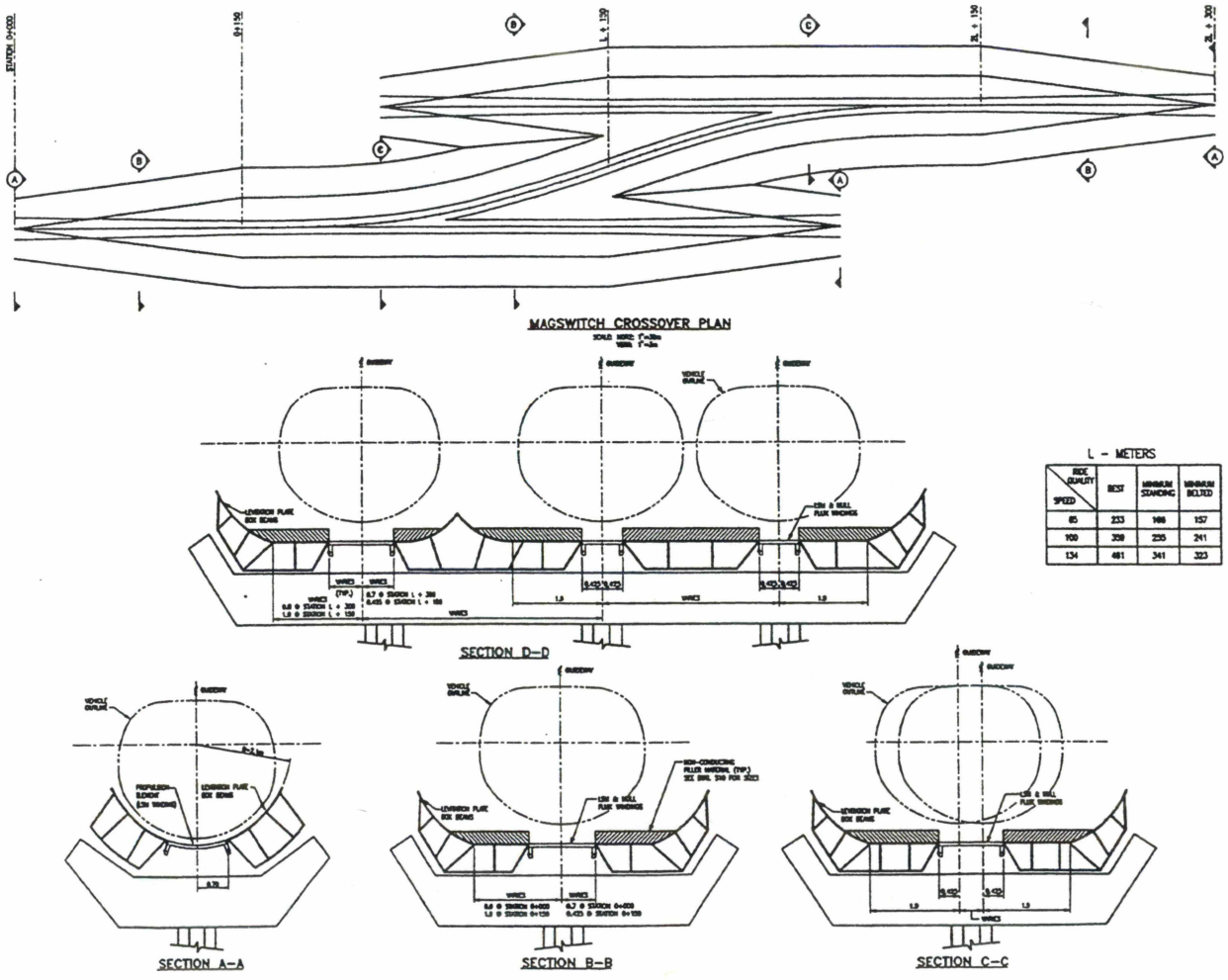

Figure 37 Cross-over variant of the magswitch (two magswitches combined)

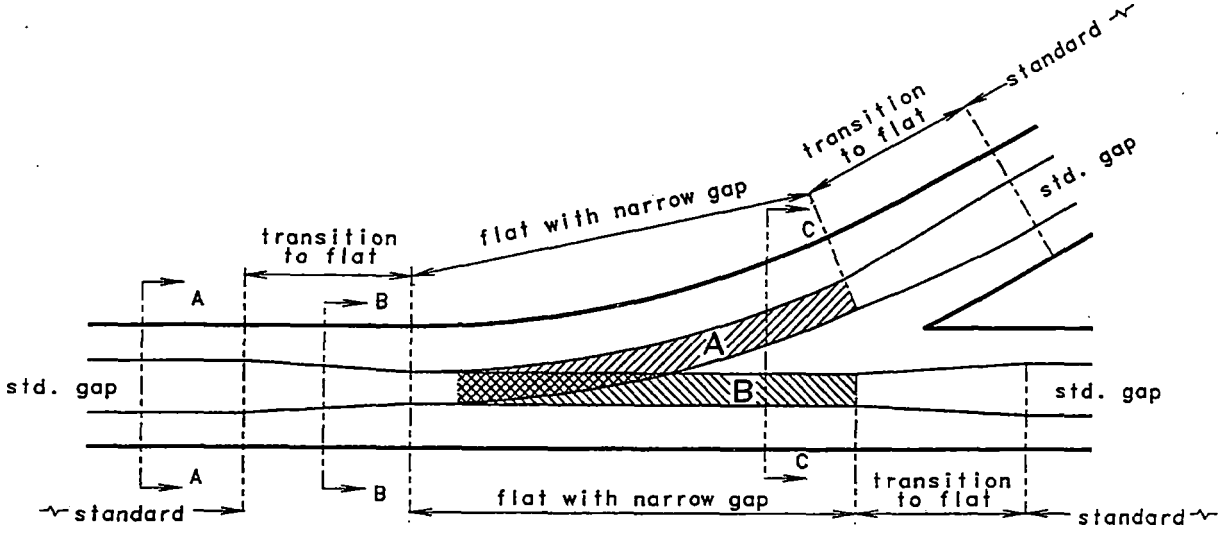

Section A-A

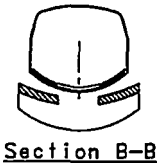

Section B-B

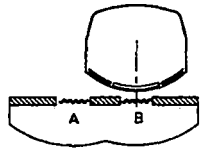

Section C-C

OPERATION	passive coils shorted	passive coils open
STRAIGHT THRU	B	A
SWITCH LEFT	A	B

Figure 38 Concept for magswitch operation

"Keel Effects" Due to Propulsion Coil & Guideway Interactions						
Height [m]	Gap [m]	Offset [m]	Norm Lift	Norm Guidance		Notes:
0.20	0.75	0.00	1.75	0.00		Gap Width Controls Lift
	0.85		1.02	0.00		
	1.00		0.26	0.00		
	1.25		0.00	0.00		
0.20	0.85	0.00	1.02	0.00		Offset Provides Guidance
		0.10	1.34	0.64		
		0.2	2.19	1.03		
0.2	0.85	0.1	1.34	0.64		Height & Offset Will Adjust for
0.23			0.99	0.48		Constant Lift & for Required
0.26			0.71	0.34		Guidance

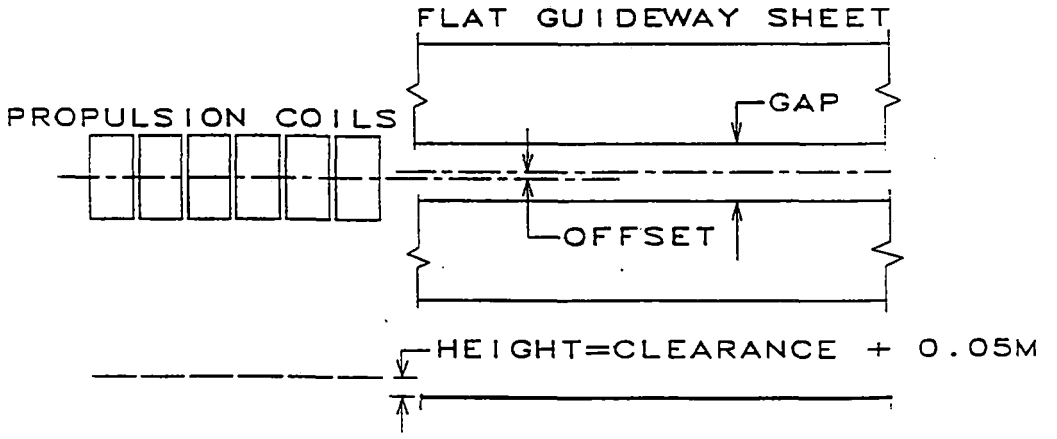

Figure 39 Level of lift and guidance forces that can be achieved with "keel" effects for the baseline propulsion coil set over a flat magway

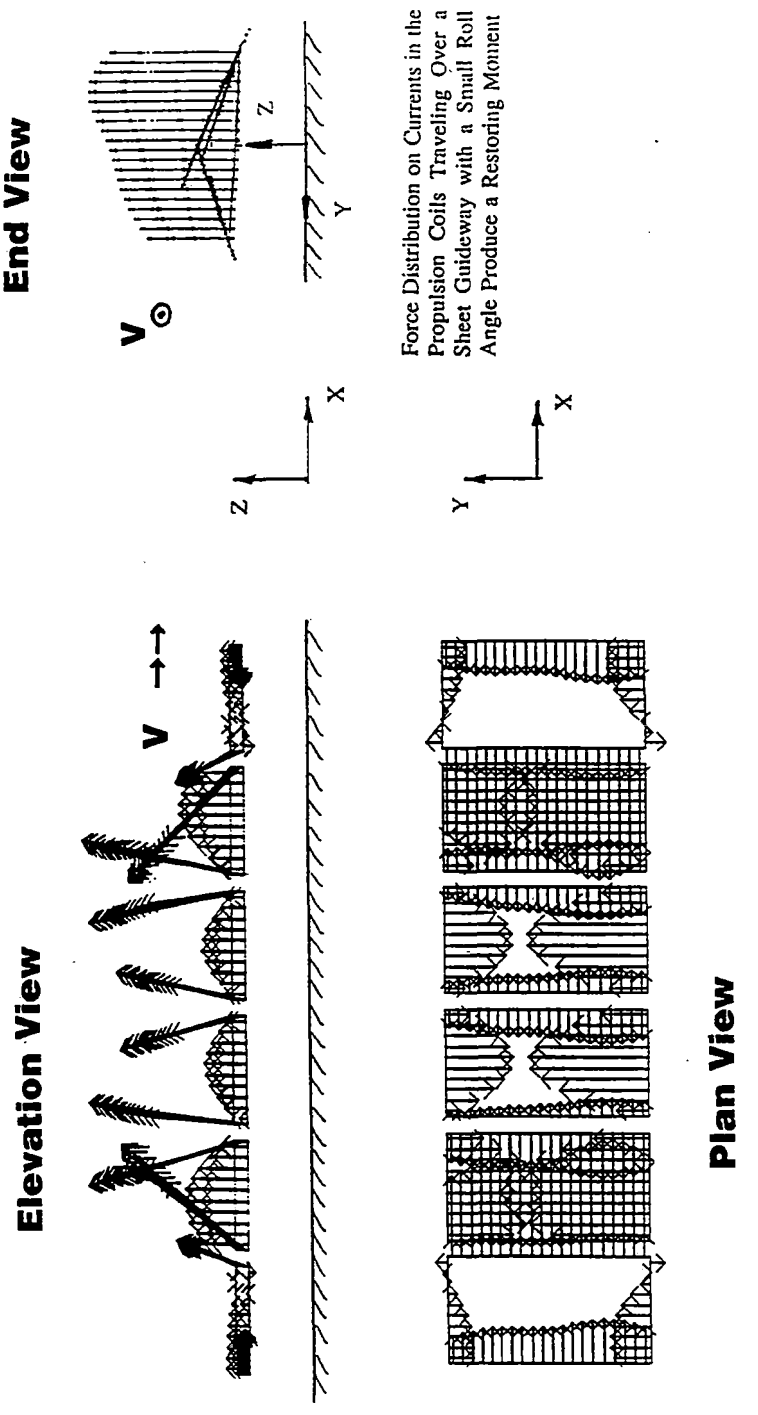

Figure 40 Local electromagnetic forces in a six coil propulsion coil set

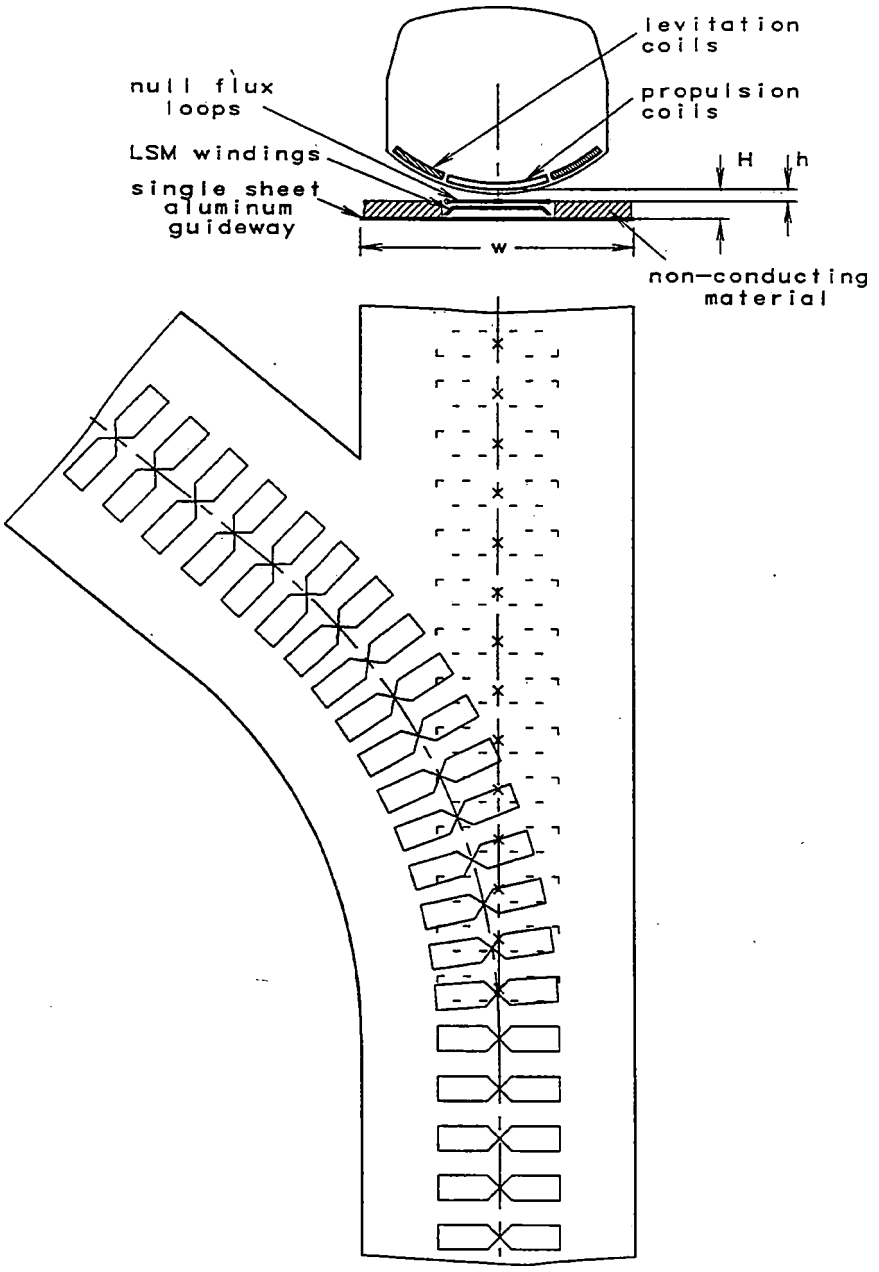

Figure 41 Concept for a single sheet switch section with passive null flux loops

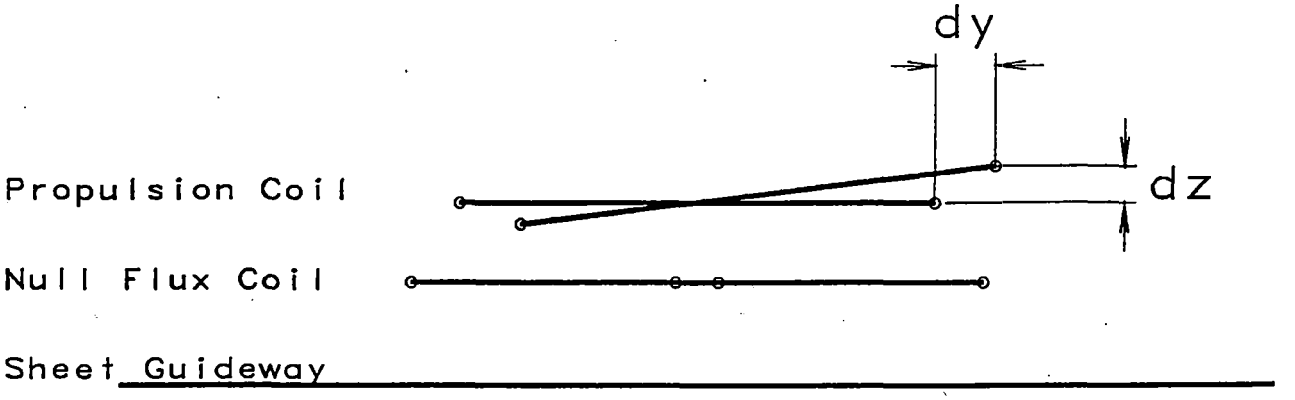

Dynamic Equilibrium Requires a Shift (dy, dz)
of Propulsion Coil Relative to Null Flux Coils

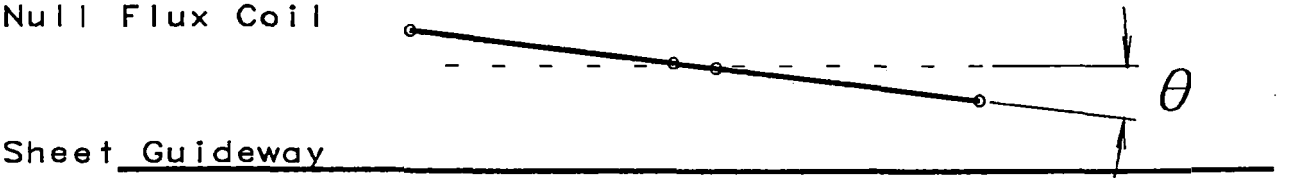

Sensitivity of Equilibrium Position (dy, dz) to Small
Angle of Null Flux Coil Relative to Guideway

Figure 42 End view of propulsion coil lateral and vertical shift relative to null flux coil and magway

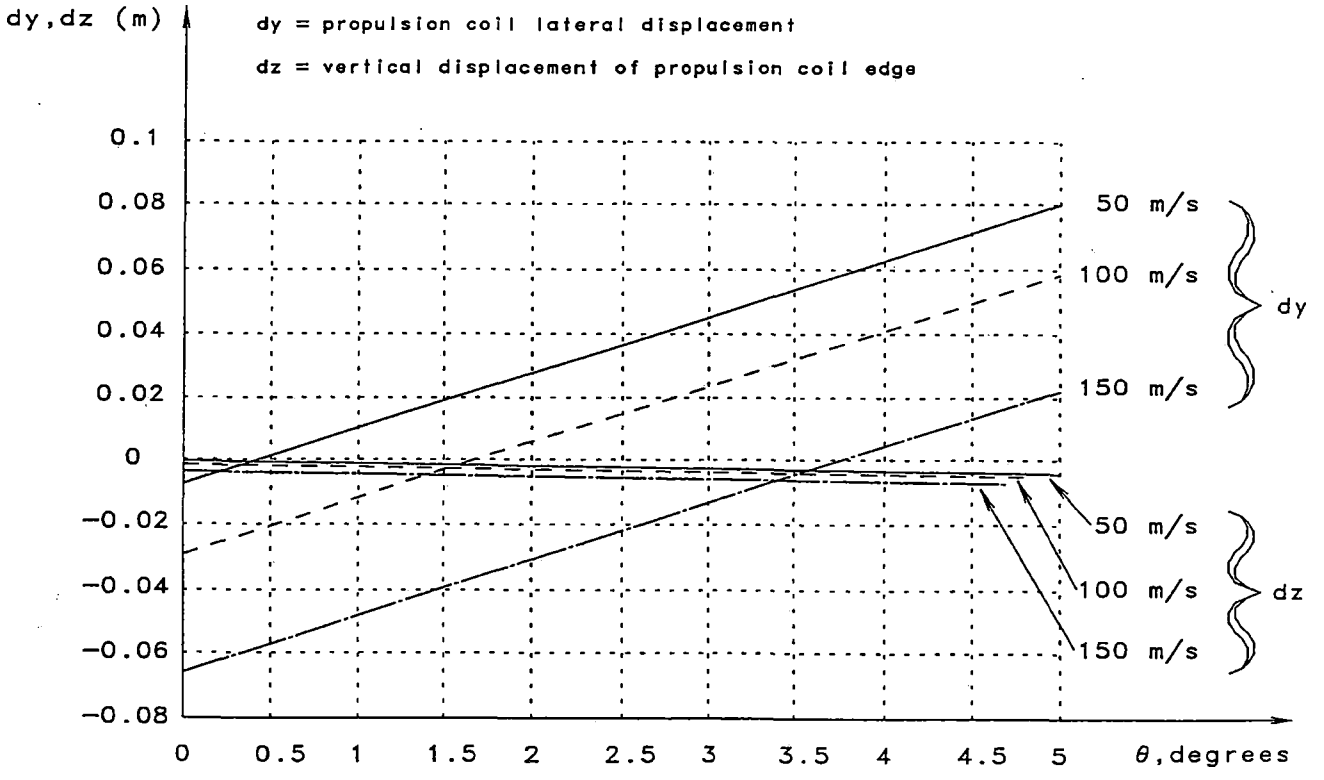

Figure 43 Propulsion coil displacement for equilibrium as a function of null flux coil angle for several speeds

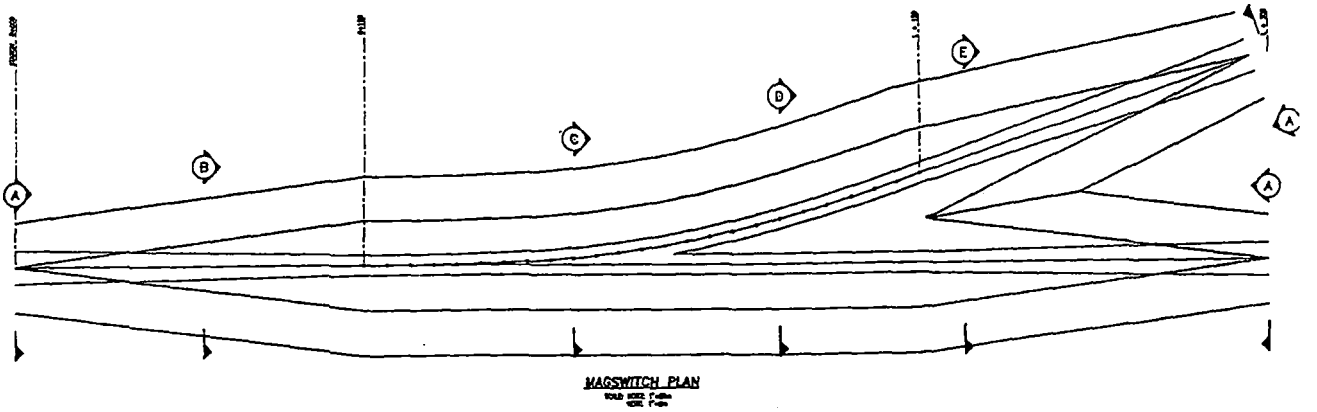

MAGSWITCH PLAN

L – METERS

SPEED \ RIDE QUALITY	BEST	MINIMUM STANDING	MINIMUM BELTED
85	233	166	157
100	359	256	241
134	481	341	323

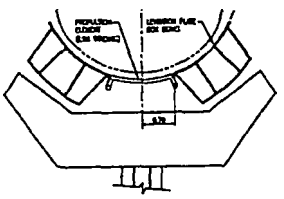

SECTION A–A

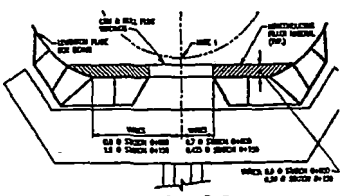

SECTION B–B

Figure 44 Magswitch geometry as a function of vehicle speed and ride quality

3.2.2.e. CONSTRUCTION TECHNIQUES

It is imperative for the success of this project that all phases of design consider ease of fabrication and constructibility to minimize costs and mitigate environmental impact. In many cases techniques can be implemented that serve both goals, i.e. maximizing shop fabrication which reduces field labor thereby both minimizing costs and reducing the impact of construction on the environment. On the other hand, mitigation of the construction impacts on a wetlands area may require the more expensive alternative of top down construction as explained later in Section 3.2.2.e.2. In all cases, however, the design must consider and be responsive to fabrication and constructibility issues.

3.2.2.e.1. GENERAL

The following are specific examples of techniques to be considered for reducing cost (and environmental impacts):

- The fabrication of the aluminum levitation plate box beams is being researched to maximize the amount which can be extruded thereby reducing the welding requirements. This not only reduces costs of welding itself but increases the allowable stress in the member since stress reductions are specified in areas adjacent to welding.
- The use of metal saddles to permit the joining of the two box beams and the LSM winding in the shop for transportation and erection as a unit.
- Provide simple means of adjustments between the magway trough and the structural supporting members to that expensive overly restrictive tolerances need not be specified.
- Design a jig to permit alignment of the magway trough use of laser instrumentation.
- Keep both steel and concrete designs in competition as much as practical as is done for highway bridge projects.
- Further investigate the use of prestressing for the concrete box beams and the crossbeams over the columns.
- Design should take advantage of repetition and the economies of scale.

3.2.2.e.2. END-ON CONSTRUCTION

National and state government concerns for wetlands impacts from construction of the Magneplane magway will become a factor in choosing alignments and construction methodology. The crossing of isolated wetlands and littoral or tidal zones along lakes, rivers and estuaries will probably be unavoidable for any real Magneplane route, except in areas with arid climates. Traversing these sensitive areas will require that the contractor avoid any major disturbance of the vegetation and the typically soft substrate.

Conventional wetland area crossings are typically done by first constructing a temporary haul road. These roads are often built with the aid of a geotextile material which is placed on a cleared but ungrubbed surface. The geotextile provides a working surface that can be subsequently buried with imported granular fill. The haul road surface is then used to provide access for material delivery vehicles, cranes and temporary structure support, such as shoring or scaffolding.

This type of construction access is detrimental to the wetland environment in the following ways:

1) The natural vegetation is removed and the substrate covered with a granular fill. This linear feature causes breaks in the vegetative canopy.

2) The haul road changes sheet flow drainage patterns in the wetland areas. These drainage pattern changes can impact the hydroperiod of receiving or downstream areas, which in turn would affect the survival of certain wetland vegetation species and cause flooding in upstream areas.

3) Even if the haul road is removed after final superstructure construction, the exposed ground/muck surface will likely be revegetated voluntarily by exotic or undesirable species that are difficult to control or eradicate.

Considering these impacts, governmental permitting agencies will often deny wetland crossing projects that involve even temporary haul roads, unless existing parallel features are already impacting the environment and watershed characteristics.

In response to these concerns, recent elevated roadway (low height bridge causeways), similar to the Magneplane magway, have been constructed using a process called end-on construction. Projects in Louisiana and South Carolina have recently been designed and constructed (or under construction) using this end-on construction. Articles about these projects were featured in Engineering News Record (ENR) in the November 4, 1991 and February 24, 1992 issues see Figure 45.

As discussed in the ENR articles, three different approaches to the end-on method have been selected by each of the contractors to complete the building of the superstructures over the sensitive wetland areas. However, the basic concept of working from a temporary superstructure, followed by installation of the final surface without intruding on the sensitive lands except for foundation, has been used in all of these projects.

The basic steps of the end-on construction are as follows:

1) Working from a barge or temporary ground surface platform at the edge of the wetland area, construct two bents or piers, on driven piles.

2) Place temporary steel and/or wood beams or trusses between the first two piers to form the first span of the elevated structure.

3) Relocate cranes and other lifting and pile driving equipment to rest on temporary first span beams or trusses.

4) Install the third bent and the second temporary span.

5) Move foundation equipment to second temporary span, remove first temporary span and replace it with the first permanent superstructure members. Install the fourth bent and third temporary span using the temporary beams from the first span.

6) Begin final construction of permanent spans and use advancing permanent spans to transport materials to the equipment working on the temporary spans.

7) Continue "leap-frogging" temporary and permanent spans across wetland area.

The system as described above and ENR utilized heavy steel beams for temporary spans and precast, prestressed concrete beams for the final spans. The width and capacity of the superstructure was designed for commercial truck and car traffic but had to be built to handle the heavier live loads of the cranes and trucks delivering long prestressed concrete piles and precast bridge deck panels.

The magway of the Magneplane will likely have a different final geometry than the flat bridge type structures currently being built using the end-on method. However, this concept may very well have application. As shown by other contractors, the end-on method can be modified to use temporary rails supporting overhead cranes, rather the temporary steel beam decking.

End-on construction has some built in higher costs as compared conventional low-bridge construction. Based on discussions with the contractor and Louisiana DOT officials, their cost differential was primarily due to using precast concrete bridge deck panels versus cast-in-place. The costs of precast versus cast-in-place panels were estimated to be $290/cy and $180/cy, respectively.

End-on projects involving temporary piles to support the working platform or overhead cranes would have higher costs than the Louisiana project, where the same piles were used for both temporary and permanent support.

The Louisiana contractor also reported that pile installation production and costs were similar for both end-on and conventional land-based foundation construction. They were able to install concrete driven piles up to 150 feet long in one piece, without major difficulty, from the temporary bridge spans.

Wetland areas typically have a soft, substrate of silts, clays and organic soils. In coastal areas these soft deposits can often be more than 100 feet thick. Therefore, support for temporary and permanent foundations for magway or roadway construction in a wetland environment will include driven piles and/or drilled piers. Use of pile or pier foundations also generally limits the amount of wetland surface area impacted by the foundation footprint.

Designing foundations for these wetland areas also requires special knowledge of the local conditions and techniques to determine the subsoil properties. Environmental permitting agencies often discourage or prevent access with drilling and sampling equipment to wetland areas, due to potential vegetative cover damage and water quality impacts. Design parameters may have to be extrapolated from nearby upland or fringe wetland areas. The choice of foundation types and load bearing and settlement criteria should be flexible, allowing the contractor design alternates. Once he has mobilized the foundation equipment and built the temporary platforms for end-on construction, deep foundation installation procedures and performance criteria can be finalized.

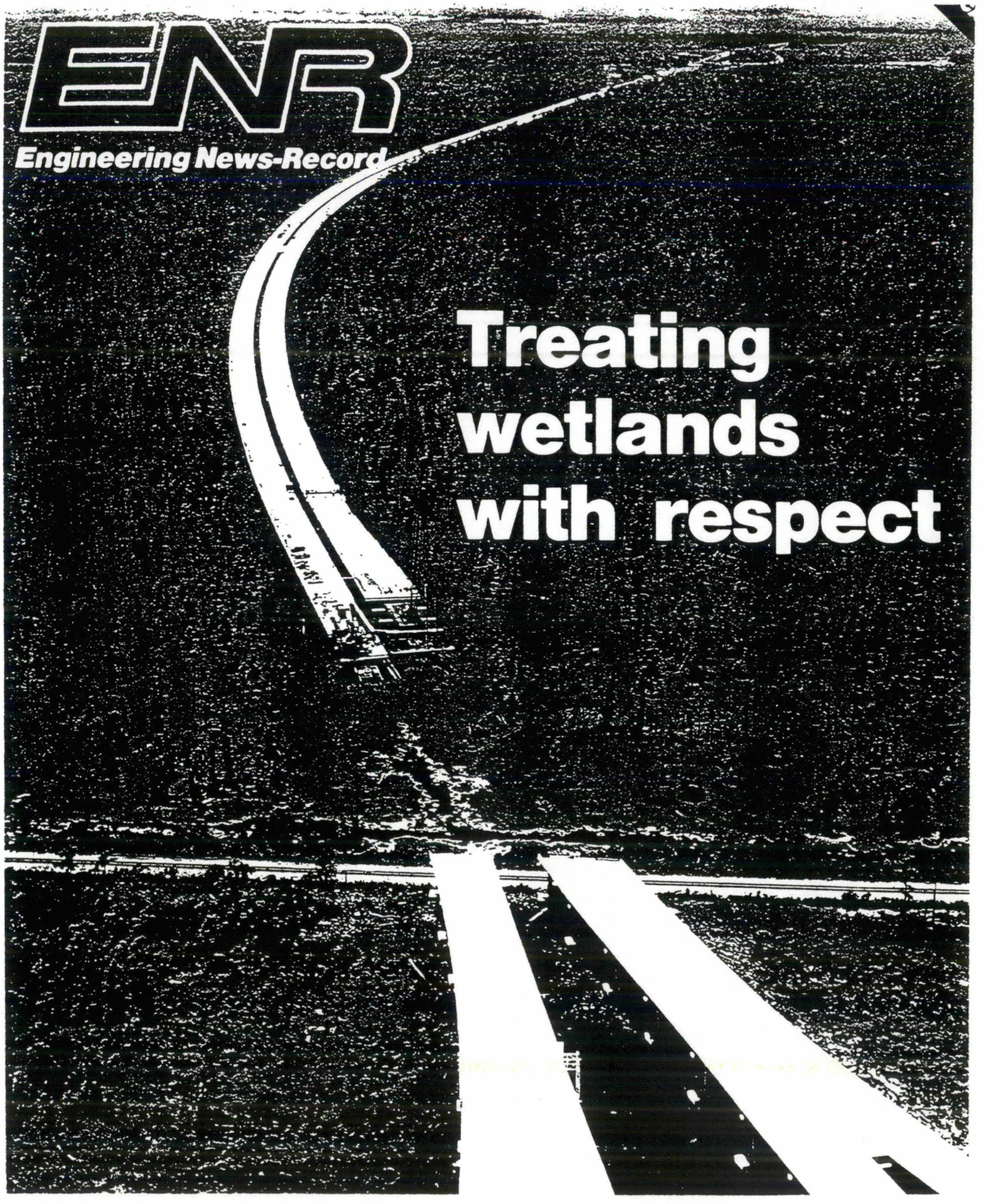

Figure 45 Example of end-on construction

3.2.2.f. POWER

3.2.2.f.1. LINEAR SYNCHRONOUS MOTOR OPERATION

The per-phase equivalent circuit model shown in Figure 46 is used to analyze the linear synchronous motor (LSM). The circuit represents one phase of the three-phase circuit and is analyzed assuming symmetrical operation of all three phases. E_1 is the voltage applied to the LSM winding and E_2 is voltage induced in the winding from the motion of vehicle propulsion coils. R and L are the resistance and inductance of the LSM winding. Electrical parameters for the motor are listed in the figure. Detailed inductance calculations for the LSM winding are included in Supplement E.

The phasor diagram shown in Figure 47 is used to analyze the LSM circuit model. δ is the angle between E_1 and E_2 and is normally called the torque angle in rotating machinery jargon. Thrust and levitation forces are controlled by the "thrust angle" α which is the angle between E_2 and the current. The LSM will produce peak thrust and no levitation force when $\alpha = 0$. Attraction or levitation can be developed at the expense of thrust when $\alpha > 0$ or $\alpha < 0$ respectively. $\alpha = 0$ is assumed in the following analysis.

3.2.2.f.2. POWER REQUIREMENTS

Electric Power Requirements for the LSM are based on the thrust speed requirements of the propulsion system.

Thrust is proportional to winding current in an air-core LSM and is limited mainly by the allowable resistive loss in the winding. The magnitude of the induced voltage E_2 is proportional to vehicle speed. Operating frequency is established by vehicle speed. Thrust and speed thus determine I, E_2, and the frequency. The remaining electrical quantities can then be determined by the geometric relationships established in the phasor diagram.

Figure 48 shows operating data for the LSM computed from the phasor diagram and the relationships described above. Data in the table are based on the designed thrust speed characteristic - constant thrust of 150,000 N from 0 to 50 m/s and constant power of 7.5 MW above 50 m/s. An LSM winding with reduced resistance will be used to improve efficiency in low speed sections. This is reflected in the table.

3.2.2.f.3. SELECTION OF BLOCK SIZE

The life cycle cost impact of block size is covered in the trade-off report. Block sizes for minimum life cycle cost are generally between 1 and 2 km. In addition block length will generally be limited to 2 km to keep the LSM winding voltage below about 20 kVac line-to-line.

3.2.2.f.4. POWER FACTOR COMPENSATION

Series capacitor compensation may be used to improve the LSM power factor and reduce the reactive power requirements. The basic concept is illustrated in Figure 49. The reactance of the series compensating capacitor matches that of the LSM inductance. This creates the electrical effect of canceling the magway inductance, dramatically improves power factor and reduces the voltage needed to drive the LSM.

Since fixed capacitors will only compensate the LSM winding inductance at a specific frequency, it will be necessary to have switched banks that can be selected as needed. Capacitor values will be selected for some range of frequencies corresponding to the expected speed range of a given block. It will not generally be necessary for each block to be equipped for compensating the worst case conditions.

Vehicle speed variations will generally require that the capacitance be matched more or less continuously to a value within some range of the ideal. This will be accomplished using the principle of circuitry now used in static VAR (Volt-Ampere-Reactive) compensators. Operation is illustrated in the simplified schematic of Figure 50.

The basic circuit consists of capacitor C_1, thyristor T_1, and diode D_1. If T_1 is ON the circuit will behave just as if the C_1 is directly connected across the ac line. If T_1 is OFF the capacitor is effectively disconnected. There is no transient involved in attaining the steady state current through C_1 because T_1 is always turned ON at the minimum value of the line voltage.

A number of capacitor elements can be connected in parallel and electronically controlled to provide any combination of the capacitor values. Large commercial static VAR compensators use a binary arrangement of capacitor values (e.g. 1,2,4,8) to provide an economical range and resolution of the effective capacitance value.

3.2.2.f.5. MATCHING THE THRUST-SPEED ENVELOPE

A more detailed examination of LSM operation shows how the desired thrust-speed performance is achieved with the minimum converter rating. It is useful to consider the required LSM terminal voltage if ideal reactive power compensation is assumed. This is not the general case, of course, but can be approached in practice and is useful in illustrating the converter rating process. Figure 51 shows the uncompensated and compensated LSM voltage assuming the thrust-speed characteristics presented earlier. Notice that although the compensated voltage increases with speed, the uncompensated voltage is constant

over a wide range. The thrust-speed curve, current and (compensated) LSM voltage are shown in Figure 52.

The range of current and voltage shown in Figure 52 cannot be supplied by a single fixed rating converter unless it can supply both the maximum current and the maximum voltage. The required rating would then be slightly over 24 MW even though no more than 10.7 MW is required at any single operating point. Transformer matching can be used to select a converter rating only slightly higher than 10.7 MW in our example and achieve the required thrust-speed curve. The matching transformer is connected to the converter output as illustrated in Figure 53.

The principle of transformer matching is illustrated in Figure 54. As an example, assume that the base rating of the converter is 1400 V, 3225 A and 13.5 MW. The converter alone can supply 3225 A corresponding to 150,000 N up to 50 m/s. The thrust falls off above 60 m/s where the converter voltage is less than the required winding voltage. This is shown on the line labeled "converter alone." Operation can be extended from about 70 to 110 m/s by using a transformer to increase the output voltage of the converter. This is shown on the line labeled "Transformer 1." The current reduction due to the transformer is consistent with the reduced current requirements of the thrust-speed envelope. Operation on the thrust-speed curve above 110 m/s can be accomplished using a second transformer. This is shown on the line labeled "Transformer 2."

In concept the transformer matching scheme discussed above works the same way field-weakening does on dc traction systems. In dc systems operation above base speed is achieved by reducing the field current. This reduces the induced voltage at base speed so the motor operates above base speed to match the maximum voltage of the armature supply. Torque decreases with the field current and the motor operates on a constant power curve as shown in our example.

The two sets of output voltage ranges for the transformer matching scheme discussed above may be obtained with two distinct transformers or a multi-winding transformer. The difference is primarily a cost, not performance, issue. The range of needed transformer voltages depends primarily on the expected speed ranges for a particular block.

3.2.2.f.6. POWER CONVERTER

Magneplane will use GTO (Gate Turn-Off thyristor) PWM (Pulse Width Modulated) inverter technology for the LSM power conversion. A greatly simplified schematic of a GTO PWM converter is shown in Figure 55. AC utility power is converted to dc by an input rectifier and filtered by an LC filter circuit which is sometimes called a dc-link. The dc is converted to ac by an inverter circuit consisting of 6 power switch devices. The switch devices are turned ON or OFF by control signals to connect the output to the positive or negative side of the dc link. The pattern of the control signals is used to synthesize a sinusoidal voltage waveform which is supplied to the output circuit.

GTO PWM converters are commercially available in the power range needed for the Magneplane system. They have efficiencies above 95% and can provide output frequencies up to 200 Hz.

3.2.2.f.7. PWM WAVEFORMS AND HARMONIC CURRENT REDUCTION

Pulse width modulation (PWM) will be used to synthesize the ac sinusoidal waveshape in the inverter of the power converter. The simplest form of PWM waveform generation is illustrated in Figure 56. This method is sometimes called the sine wave intersection method because the output is switched at points in time when a reference sine wave intersects a triangular "carrier" waveform.

The example shows the worst case for the Magneplane converter which will have a maximum output frequency of 100 Hz and a typical switching frequency of 500 Hz. Operation at lower frequencies will be synthesized more accurately. In fact, the converters will have "neutral point clamped" inverter output stages which have three levels of output instead of two. This allows better sine wave synthesis and reduces harmonics.

Typical voltage harmonics for the example are shown in Figure 57. The dominant harmonic is at the 500 Hz carrier frequency with significant components at all odd harmonics. The LSM circuit itself plays an important role in preventing these voltage harmonics from causing large harmonic currents. The impedance of the LSM and compensation circuit at 100 Hz is shown in part B of the Figure. Part C of the Figure shows how the harmonic currents are attenuated by the impedance characteristic of the LSM. Harmonic currents in the LSM winding will not be a significant problem due to the attenuation provided by the LSM circuit.

3.2.2.f.8. HEAVE DAMPING CONSIDERATIONS

Heave damping requires that the wayside power converters be able to make changes in the phase angle of the LSM current in response to commands from the wayside control equipment. The overall response needs to support a closed loop bandwidth of 2-5 Hz to coordinate properly with the natural frequencies of the vehicle body.

Preliminary simulation studies were conducted to address two questions relative to heave damping requirements: (1) can the LSM circuit be controlled to provide phase change responses consistent with the bandwidth target and (2); does the converter rating need to be increased to support the control loop requirements.

Simulation studies were conducted using the standard per-phase equivalent circuit model of the LSM and assuming series capacitor compensation at 150 m/s. Converter dynamics were not included as these should be well above the frequency range of interest. The vehicle speed was assumed to be constant while phase angle changes in current (measured in terms of α) were made. Steady state relationships and other data were developed at this stage and are presented in a more detailed discussion included in Supplement H. Simulation results are presented here to facilitate the discussion relative to converter capability.

A simple phase angle control loop was constructed around the dynamic model of the LSM to investigate the ability to make phase changes. The control loop alters the phase of the converter voltage in response to phase errors while keeping the magnitude of the voltage constant. The results from a closed loop step

response test are shown in Figure 58. In this test a 10 degree phase change was commanded and the phase response and converter current were observed. The results show an effective bandwidth between 2 and 3 Hz even though little work was done to optimize the closed loop response. The maximum converter current during this response is within 5% of the steady state value.

Simulation results presented here show that the converter and series compensated LSM can support the heave damping requirements presented in this report. In addition, wayside power converter ratings should not need to be significantly increased to support operation in a closed loop heave damping system.

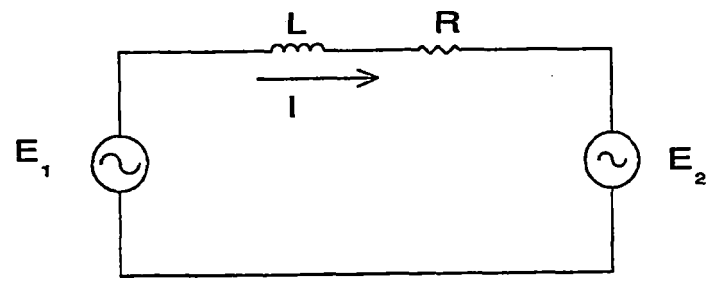

Motor Parameters

1. L : 7.1 mh / phase / km
2. R : 0.1 Ohms / phase / km
3. E2 : 2326 Volts rms per phase at 150 m/s
4. Design Current : 1075 A rms/phase
5. Design Thrust : 50000 N at 150 m/s
6. Design Speed: 150 m/s
7. Pole Pitch : 0.75 m
8. Nominal block size 2 km

Figure 46 Equivalent circuit model of the linear synchronous motor

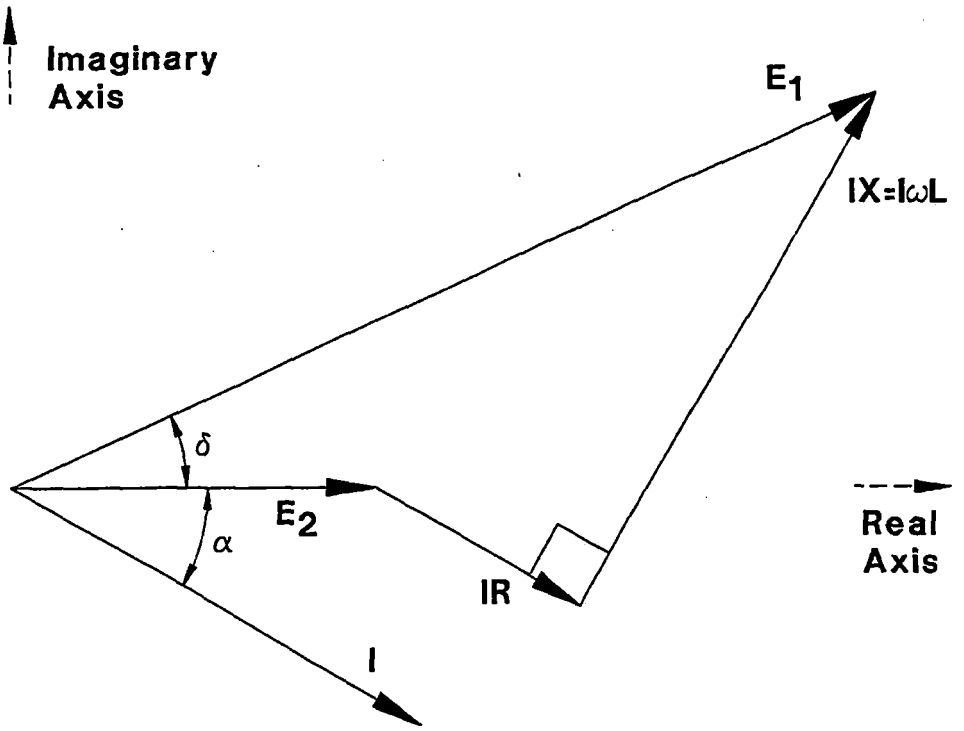

Figure 47 Phasor diagram for the linear synchronous motor

Speed m/s	Thrust N	Current A	E1 V	E2 V	Resistance Ohms	Output Power MW	Resistive Loss MW	Input Power MW	Efficiency %	Power Factor
0	150000	3225	323	0	0.10	0.0	3.1	3.1	0.0	1.00
10	150000	3225	1977	155	0.10	1.5	3.1	4.6	32.5	0.24
20	150000	3225	3888	310	0.10	3.0	3.1	6.1	49.0	0.16
30	150000	3225	5808	465	0.10	4.5	3.1	7.6	59.1	0.14
40	150000	3225	7731	620	0.10	6.0	3.1	9.1	65.8	0.12
50	150000	3225	9654	775	0.10	7.5	3.1	10.6	70.6	0.11
60	125581	2700	9710	930	0.10	7.5	2.2	9.7	77.5	0.12
70	106977	2300	9700	1085	0.20	7.5	3.2	10.7	70.2	0.16
80	93953	2020	9752	1241	0.20	7.5	2.4	10.0	75.4	0.17
90	83721	1800	9794	1396	0.20	7.5	1.9	9.5	79.5	0.18
100	75349	1620	9817	1551	0.20	7.5	1.6	9.1	82.7	0.19
110	68372	1470	9824	1706	0.20	7.5	1.3	8.8	85.3	0.20
120	62791	1350	9869	1861	0.20	7.5	1.1	8.6	87.3	0.22
130	57674	1240	9852	2016	0.20	7.5	0.9	8.4	89.0	0.23
140	53488	1150	9873	2171	0.20	7.5	0.8	8.3	90.4	0.24
150	50000	1075	9922	2326	0.20	7.5	0.7	8.2	91.5	0.26

Energy intensity > $\frac{8.3\,MW}{134\,m/s \times 140\,peak} = 442\,J/peak\,m$

$= 737\,J/pass\,m$

$\times 3 = 2210\,J/pass\,m$

not 1546

Figure 48 Operating data for the linear synchronous motor

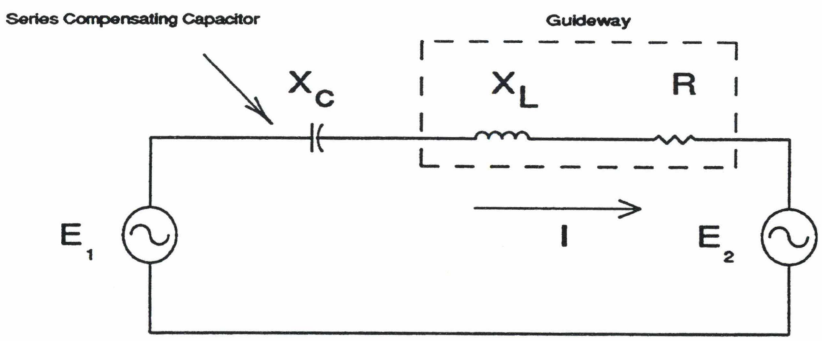

Figure 49 Capacitor compensation of the linear synchronous motor

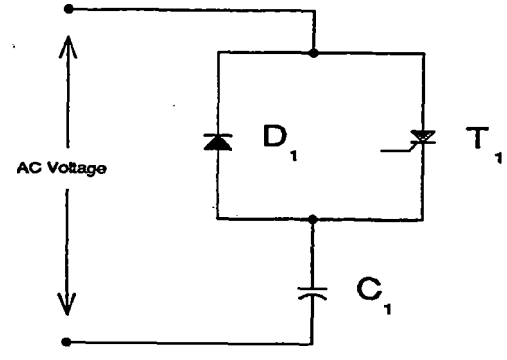

Figure 50 Simplified schematic of a static VAR compensator

Speed m/s	Current A	Required Voltage Uncompensated (E1)	Compensated V	Capacitance microFarads
0	3225	323	323	none
10	3225	1977	478	40136
20	3225	3888	633	10034
30	3225	5808	788	4460
40	3225	7731	943	2509
50	3225	9654	1098	1605
60	2700	9710	1200	1115
70	2300	9700	1545	819
80	2020	9752	1645	627
90	1800	9794	1756	496
100	1620	9817	1875	401
110	1470	9824	2000	332
120	1350	9869	2131	279
130	1240	9852	2264	237
140	1150	9873	2401	205
150	1075	9922	2541	178

Figure 51 Uncompensated and compensated LSM winding voltage

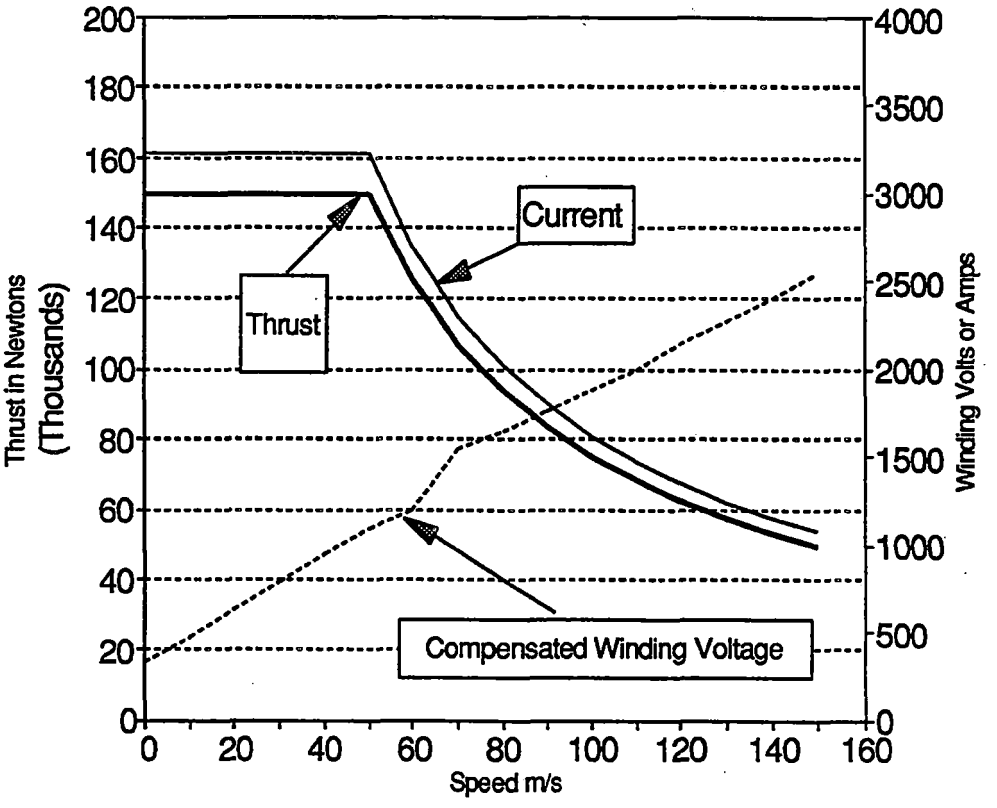

Figure 52 LSM thrust-speed curve, current and compensated voltage

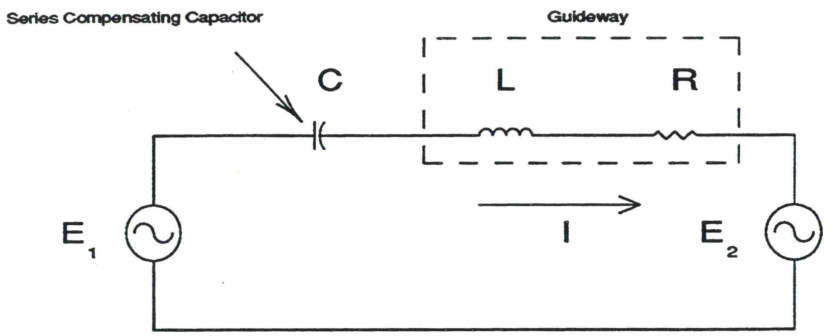

Figure 53 Schematic of LSM with transformer matching

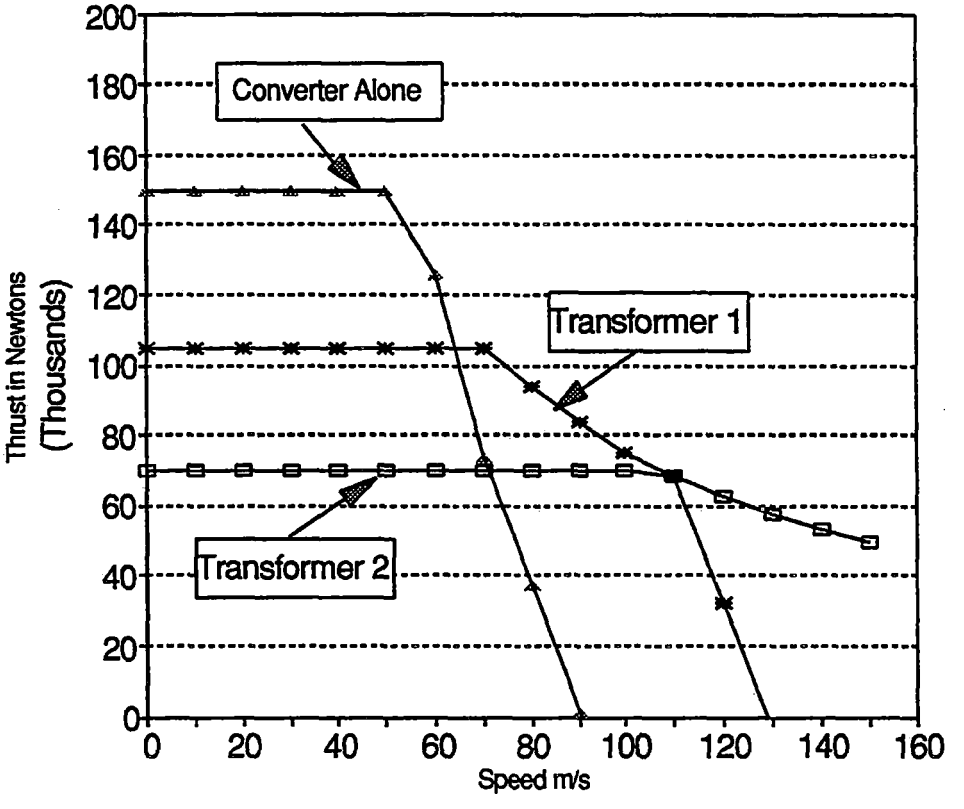

Figure 54 Piecewise construction of the thrust-speed curve

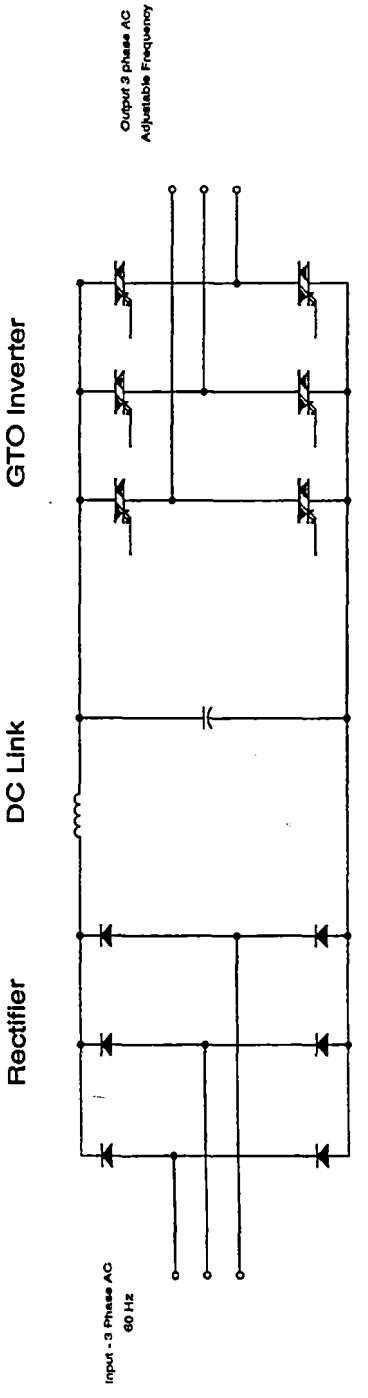

Figure 55 Simplified schematic of GTO PWM power converter

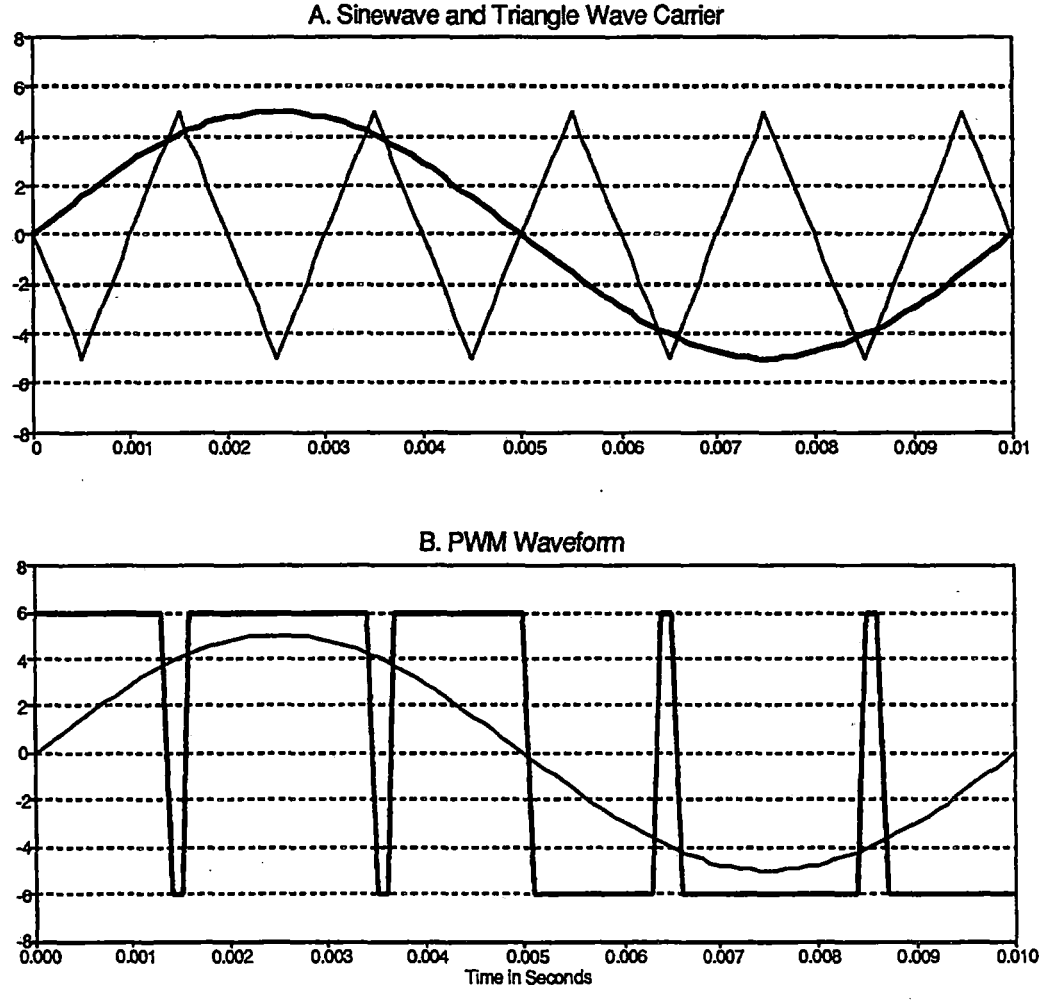

Figure 56 PWM waveform generation

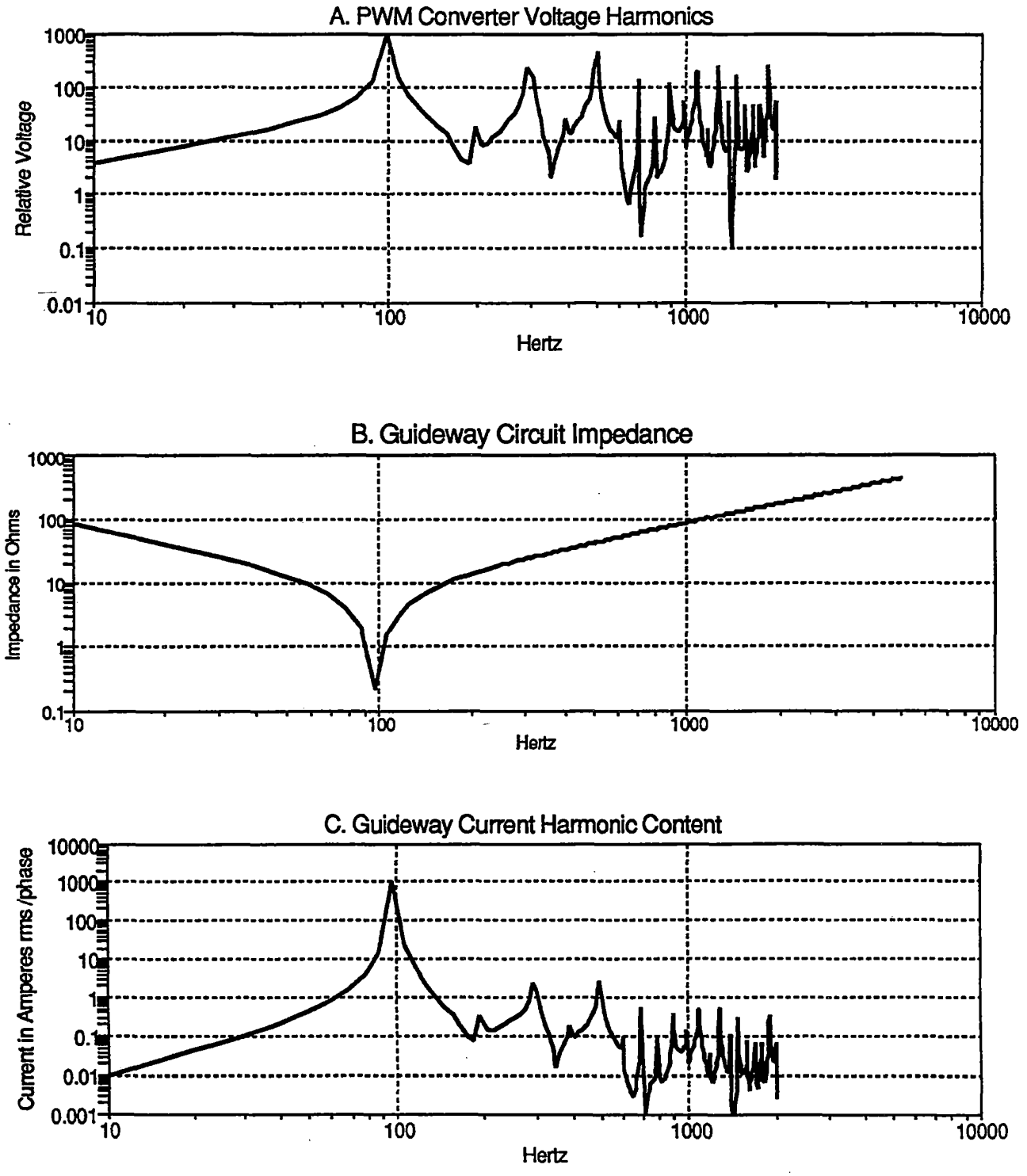

Figure 57 Reduction of current harmonics from PMW waveform

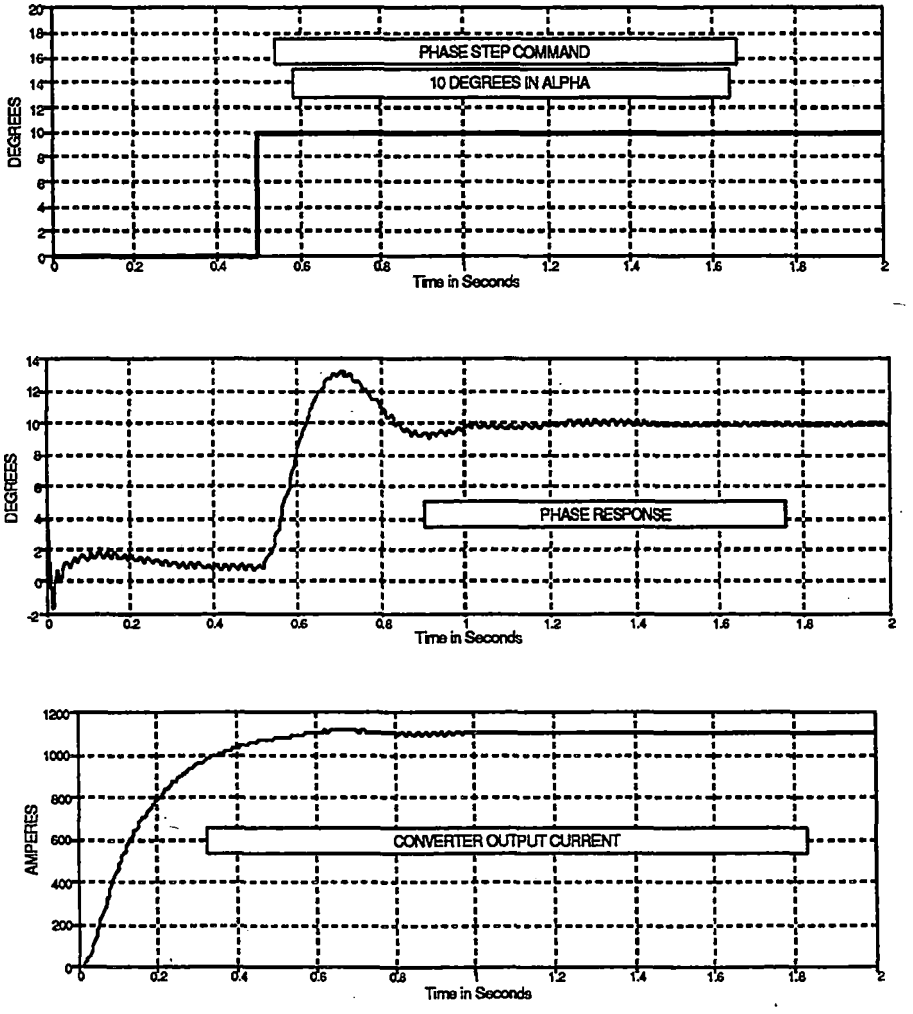

Figure 58 Simulation of LSM thrust angle control (heave)

3.2.2.f.9. AUXILIARY POWER TRANSFER

Power for electrical loads on the vehicle will be transferred from the magway using an inductive pick-up coil in the lower fuselage of the vehicle. The coil will be magnetically coupled to the LSM winding and excited by an auxiliary (non-propulsive) frequency current. The auxiliary current generates a magnetic field which is not synchronous with the vehicle. This field induces a voltage in the pick-up coils and provides power to the vehicle. A detailed discussion of the coil design is presented in section 3.2.1.j.

The supply of auxiliary power to the vehicle is a complex problem that requires two separate power frequencies be supplied on the (single) LSM winding. Two primary design constraints are: (1) that the propulsion and auxiliary power source do not feed power into one another and; (2) that power system components be as simple as possible. Power filter circuits were identified as the solution to the problem and considerable experience with these circuits was applied to this problem. Several circuit topologies were investigated to meet the design constraints and evaluated in detail. The preferred solution is illustrated in Figure 59.

The central leg of the schematic represents the LSM winding and its series compensation capacitor. P1 and P2 are the propulsion and auxiliary power converters respectively. P1 operates from 0 to 100 Hz while P2 is fixed at 500 Hz. The two filter circuits consisting of Lf1/Cf1 and Lf2/Cf2 provide the needed power separation. The filter Lf1/Cf1 is parallel resonant at 500 Hz and tends to pass power from P1 to the LSM but rejects 500 Hz power from P2. The filter Lf2/Cf2 is series resonant at 500 Hz so that it passes 500 Hz power from P2 but prevents propulsion frequencies from entering the P2 branch.

The fundamental metrics for the success of the design are the power transfer characteristics from P1 and P2 to the LSM. Figure 60 shows the propulsion power transfer to the magway. Power in the central leg of the circuit is denoted PG. PG/P1 is plotted as a function of frequency and is practically 1.0 at 100 Hz when the propulsion frequency is 100 Hz and the LSM is appropriately compensated. Figure 61 shows the auxiliary power transfer characteristic PG/P2 and is about 0.9 at 500 Hz. Together these curves show that power from P1 and P2 is reaching the LSM circuit and not being dissipated in the opposing circuit branches. The second constraint discussed above is met by using a fixed auxiliary frequency. None of the components aside from the LSM compensation capacitor needs to be adjusted with vehicle speed.

We are not aware of any operating or experimental system using this method to supply significant amounts of power.

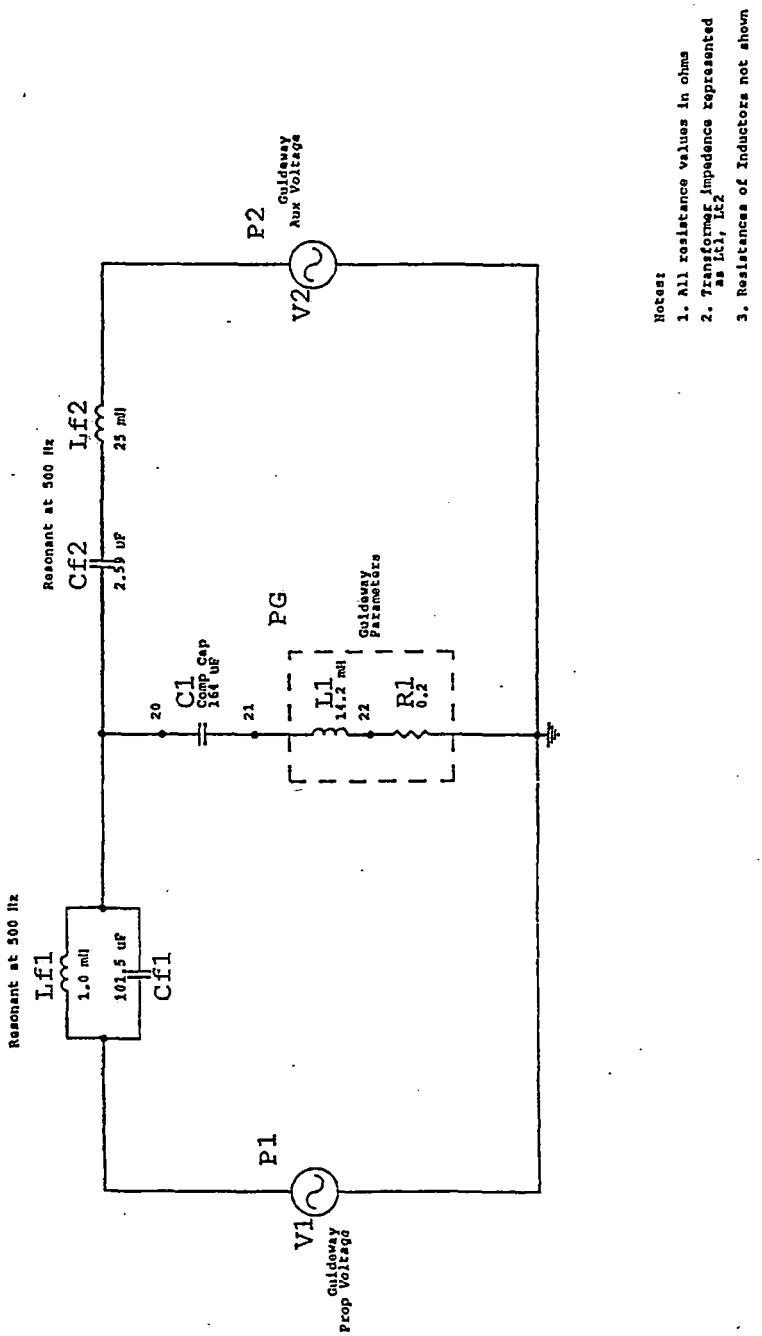

Figure 59 Power filter circuit for supplying auxiliary power

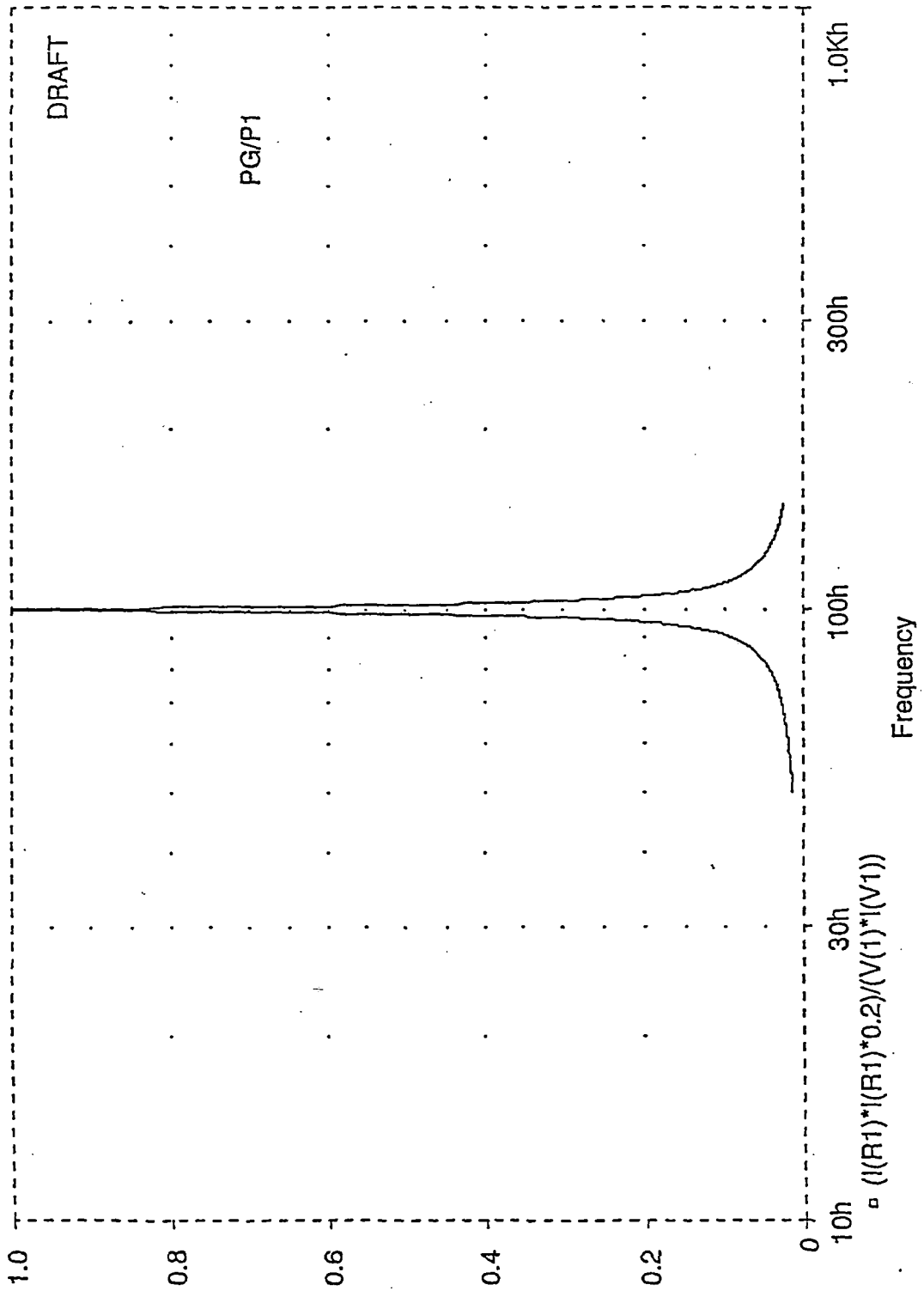

Figure 60 Propulsion power transfer characteristic

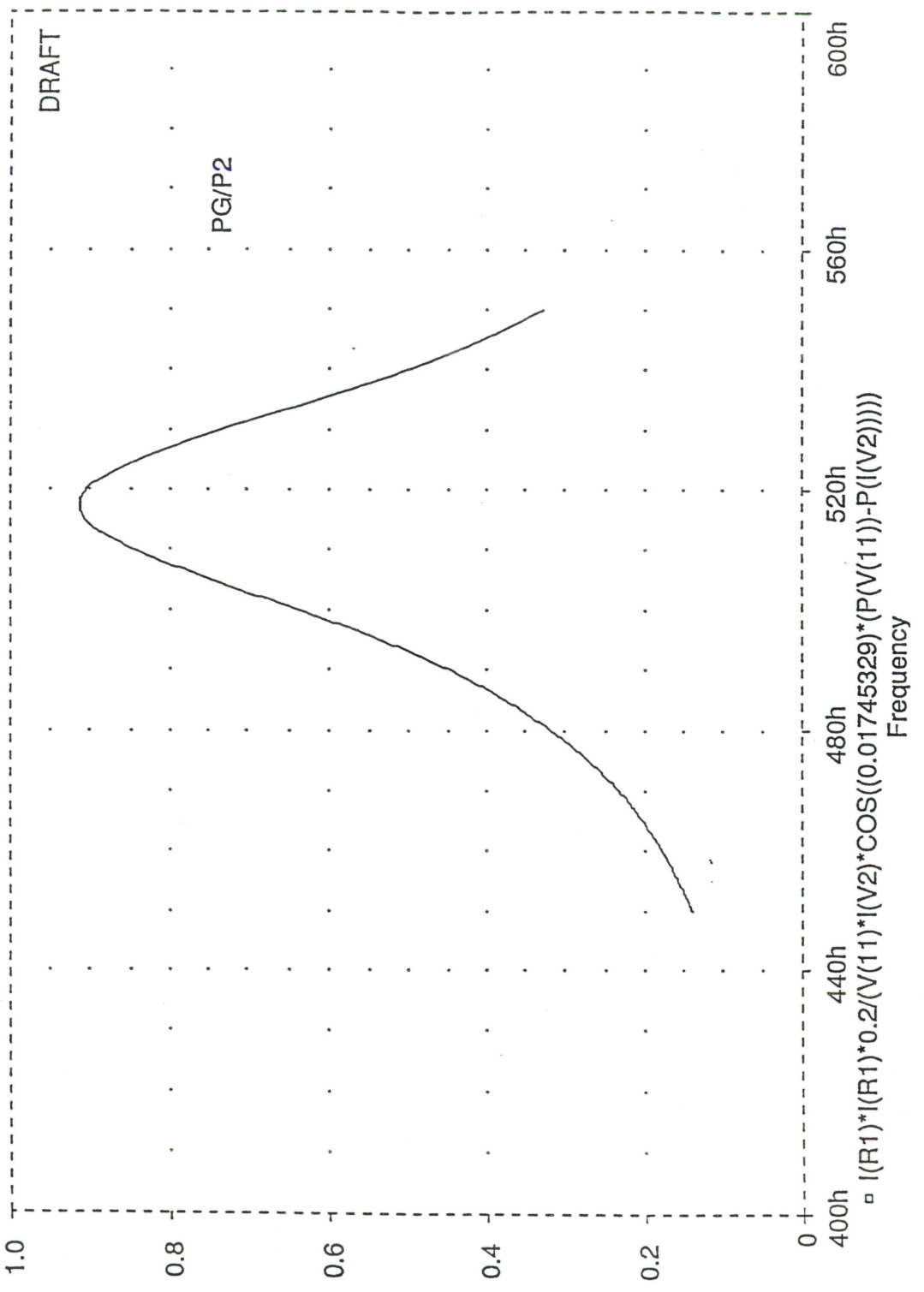

Figure 61 Auxiliary power transfer characteristic

3.2.2.g. VEHICLE/MAGWAY INTERACTIONS

3.2.2.g.1. VEHICLE DYNAMIC SIMULATION

3.2.2.g.1.1. CONTROLLER DESIGN

The non-linear, six degree-of freedom computer simulation of the Magneplane was developed using the equations in Supplement F. The model includes twelve states: the three linear degrees of freedom (surge, heave, and sway), the three rotational degrees of freedom (roll, pitch, and yaw rates) and their time derivatives. The lift and propulsion magnets are modelled as non-linear springs of the following form:

$$F_m = F_0 [h_0 / (h_0 + h)]^e \qquad \text{(TVI 1)}$$

where

F_m is the magnetic force
F_0 is the reference force
h_0 is the reference height
h is the deviation from the reference height
e is the non-linear spring exponent (= 1.6 for lift, 1.0 for propulsion)

The magnetic drag takes a similar form, but D_0 varies as a function of velocity as follows:

$$D_0(v) = D_{0,ref} [v_0 / (v_0 + v)]^{0.5} \qquad \text{(TVI 2)}$$

where

$D_0(v)$ is the reference drag as a function of velocity
$D_{0,ref}$ is the reference drag at the reference height and velocity
v_0 is the reference velocity
v is the velocity deviation

The lateral force due to the "magnetic keel" effect is modelled as cubic polynomial of the lateral displacement of the bogies.

The aerodynamic forces take the conventional form:

$$F_{aero}(v) = 1/2 \; r \; C_d \; S \; (v_0 + v)^2 \qquad \text{(TVI 3)}$$

where

$F_{aero}(v)$ is the aerodynamic force as a function of velocity
r is the density of air

C_d is the coefficient of drag (or of lift for the lift force)
S is the reference cross sectional area of the vehicle
v_0 is the reference velocity
v is the velocity deviation

Similar forms of the above equations are used to calculate the torques on the vehicle which cause roll, pitch and yawing motions.

The pitching moments due to the unequal forces on the fore and aft bogies are now included in the model. Vertical magway disturbances now correctly excite both the pitch and heave modes of the vehicle.

The primary disturbances which affect ride quality are the aerodynamic gusts, the magway roughness, and the periodic deflection of the magway support spans. The gust spectrum is based on the Davenport model of horizontal gusts near the ground (as specified in the memorandum of Jim Lever, dated 14 March 1992):

$$nS(n) = 4.0\, x^2\, u_t^2 /(1 + x2)4/3 \qquad \text{(TVI 4)}$$

where

S(n) is the gust velocity spectrum
n is the gust frequency, Hz
ut is the friction velocity, m/s
$x = 1200\, n / U_{10}$
U_{10} is the 1 hour average wind speed at a 10-m height
u' is the standard deviation, assumed to be $= 2.5u_t = U_{10}/5.7$

In the above equation, the bulk velocity, U_{10}, gets replaced by the velocity of the Magneplane to shift the gust frequency spectrum to that seen by an observer on the vehicle. The friction velocity, u_t, is still based on the bulk velocity, U_{10}. In this way, the gust intensity remains the same, while the frequency gets shifted upward. The gust spectrum is converted from the frequency domain to the time domain to be used in the time domain simulation of the system.

Although this equation was specified primarily for structural load calculations, we believe that its use is valid for the average gust intensity seen by the vehicle. More detailed gust definitions may provide a more accurate description of the instantaneous gust forces on the vehicle, but we believe this definition is suitable for determining the average ride quality in the vehicle.

The magway roughness spectrum is modelled as filtered white noise[1] with the following spectrum:

$$S_{td}(w) = A\, u / w^2 \qquad \text{(TVI 5)}$$

where

$S_{td}(w)$ is the magway disturbance spectrum

---

[1]D. N. Wormley, et. al., *Magnetic Levitation Vehicle-Suspension Guideway Interaction*, January 1992

w is the disturbance frequency, rad/sec
A is a constant, = 6.1×10^{-8} m (based on welded rail smoothness)
u is the vehicle velocity

Although the roughness parameter, A, used above was defined for welded steel rail, we contend that the roughness of the aluminum magway sheets will be of at least comparable smoothness. A representative of a major aluminum producer concurs with this contention.

The periodic deflection of the magway spans is modelled as a quasi-static sinusoidal deflection with amplitude $a_{deflect}$:

$$S_{deflect}(t) = 0.5 * a_{deflect} * \sin(2p\ u\ t / l_{span}) \qquad \text{(TVI 6)}$$

where

$S_{deflect}(t)$ is the magway deflection disturbance as a function of time
$a_{deflect}$ is the deflection amplitude = 0.0046 m
u is the vehicle velocity
l_{span} is the span length, = 9.14 m

The use of the quasi-static load solution is justified by the separation of the maximum vehicle passing frequency, which is less than 15 Hz, and the natural frequency of the magway span, which is greater than 20 Hz. The deflection amplitude is specified by the structural engineers to be no more than the span/2000. The exact solution to the distributed load on the beam agrees with the sinusoidal approximation to within 4%. Since the last report, the span length was decreased to 9.1 m. This had a beneficial effect on the ride quality by lowering the deflection amplitude and increasing the deflection frequency.

The magway roughness time domain disturbance and quasi-static deflection disturbance are combined to form a time domain magway disturbance. Figure 62 shows a typical magway disturbance plotted versus magway position. Note the effects of both the sinusoidal disturbance, with the 9.1 meter span period, and the random disturbance due to roughness and misalignment.

The actuators which control the response of the vehicle are the linear synchronous motor (LSM) amplitude and phase, which give direct control of propulsive and vertical forces, and the aerodynamic actuators. Aerodynamic actuators are treated as individual actuators for this simulation. It is assumed that the aerodynamic actuators give us direct control over pitch, roll, yaw, heave, and sway. The six degrees of freedom are thus controlled by seven actuators, with the heave mode being controlled by both the LSM and the aerodynamic actuators.

The magway motions are defined external to the simulation and appear in the equations as commands which the vehicle must follow. This allows the magway geometry to be computed off-line, based on route planning or other considerations. The equations of motion are computed using body centered coordinates, so all magway motions are defined relative to the vehicle, making post-processing of passenger ride quality a simpler task. The magway shapes of the four Severe Segment Test (SST) zones were defined as inputs to the simulation. In addition, a section of straight and level magway was simulated while varying the major disturbance parameters (i.e. magway roughness, span deflection, and wind gusts).

Since all curves for the Magneplane are designed to be coordinated, there is (ideally) no lateral acceleration in the vehicle coordinate system. The vehicle rolls to whatever angle is required for a coordinated turn and the vertical acceleration is the vector sum of gravity and the vehicle centripetal acceleration. The lateral roll rate limit of 5 deg/sec (for best ride quality) creates an implicit vertical jerk limit due to the (self imposed) coordinated turn requirement, although this limit did not seem to adversely impact the route planning for the hypothetical route. In fact, we could argue that the coordinated turn philosophy provides a more comfortable ride than non-coordinated turns. That having been said, the coordinated turn requirement is our own, and could be relaxed for curves with special requirements without violating the specified system ride quality requirements (e.g. vertical jerk limits), although we would not expect this to be necessary.

The aerodynamic and LSM motor control law is a linear, constant coefficient, full-state feedback controller. It is designed by first creating a linearized model of the nonlinear system equations. In the most general form, system equations developed in Supplement F can be expressed in state-space form as follows:

$$d/dt(x) = f(x,t,u) \qquad \text{(TVI 7)}$$

where

d/dt(x) is the time derivative of the state vector
f is the non-linear function which defines the entire system
x is a vector containing the twelve states of the system
t is time, also used to specify the external disturbances in time u is the state of the control actuators

The linearized form of the system equations is used to design the controller. The linearized equations are developed by disturbing the system about the reference state and using the first term of a Taylor series expansion. The linearized equations thus become, in state-space form:

$$d/dt(x) = Ax + Bu \qquad \text{(TVI 8)}$$
$$y = Cx$$

where

d/dt(x) is the time derivative of the state vector
A is the linearized state matrix
x is a vector containing the twelve states of the system
B is the linearized controller matrix
u is the state of the control actuators
y is the system output vector
C is the system output matrix (in our example = identity matrix)

The linear quadratic regulator (LQR) design methodology is used to create a controller. The LQR methodology can be found in many basic control system texts.[2] The control system designer chooses

[2]W. J. Palm III, *Modeling, Analysis and Control of Dynamic Systems*, John Wiley & Sons, 1983.

weighting matrices for the states of the system, x, and the controller outputs, u. An optimal control gain matrix is selected which minimizes the weighted cost functional, J, defined as follows:

$$J = 0.5 * \text{integral}(x'Qx + u'Ru)dt \qquad \text{(TVI 9)}$$

where

J is the cost functional
x is a vector containing the twelve states of the system
u is the controller state
Q is the state weighting matrix
R is the controller weighting matrix

The optimal gain matrix, K, comes from the solution to the Riccati equation which minimizes J above:

$$A'S + SA + Q = SBR^{-1}B'S \qquad \text{(VTI 10a)}$$

$$K = R^{-1}B'S \qquad \text{(VTI 10b)}$$

The optimal gain matrix, K, thus forms a closed loop control system. The control actuator states are found by multiplying the gain matrix times the states of the system (a minus sign is used by convention):

$$u_{feedback} = -Kx \qquad \text{(TVI 11)}$$

where

$u_{feedback}$ is output of the actuators
K is the LQR optimal gain matrix
x is the system state vector

Substituting this into the original linearized set of equations defines the linearized closed-loop system:

$$d/dt(x_{cl}) = (A - BK)x_{cl} \qquad \text{(TVI 12)}$$

where

x_{cl} is the closed loop system state vector
K is the optimal gain matrix
A is the system state matrix
B is the system controller matrix

The controller is a linear state-space controller, although the full non-linear system equations are used in the simulation. The non-linear, closed loop system equations that are solved in the simulation thus become:

$$d/dt(x) = f(x,t,-Kx) \qquad \text{(TVI 13)}$$

where

d/dt(x) is the time derivative of the state vector
f is the non-linear function which defines the entire system

x is a vector containing the twelve states of the system
t is time, also used to specify the external disturbances in time
-Kx is the command to the control actuators, using the feedback controller K

The LQR design methodology provides a guaranteed stable control system for a linear system. Typically, the designer varies the diagonals of the Q and R matrices (the off-diagonal terms are generally zero) and the effect on the output states and actuator authority is observed. Although LQR designs are guaranteed to be stable, they are not guaranteed to be robust in the presence of unmodelled system dynamics. More powerful designs, such as H∞ and direct covariance control system design tools can be used when the model uncertainty and the model disturbances and desired outputs can be characterized. In spite of these shortcomings, the LQR method, when used carefully, can give a good and quick indication of the achievable results.

The nonlinear simulation was performed for the Severe Segment Test zones with the specified disturbances. The controller was derived from the linearized model of the system. The ride comfort is calculated according to the Peplar composite model:

$$C' = 1.0 + 0.5w_r + 0.1[dB(A) - 65] + 17a_T + 17\,a_V \qquad \text{(TVI 14)}$$

where

C' is the ride comfort index
w_r is the rms roll rate (deg/sec)
dB(A) is the interior noise
a_T is the rms transverse acceleration (g's)
a_V is the rms vertical acceleration (g's)

We assumed an interior cabin noise of 70 dBA for our simulations when calculating the Peplar ride comfort index. Software tools for the ISO ride quality specification were developed which transform the time domain simulation results into the frequency domain for comparison with the 1/3 octave ISO vibration limits The Peplar index is calculated for the center of gravity of the vehicle, while the ISO spectral plots are calculated for the worst-case seat at the end of the vehicle.

The control system bandwidth is chosen implicitly by the choice of the parameters in the weighting matrices, Q and R. To verify that the system is not being designed for unrealistic actuator bandwidths, Bode plots of the closed loop response of the vehicle can be plotted based on the linearized closed-loop system defined by equation TVI 12. The values used in the Q and R matrices were chosen iteratively by comparing the desired values of the state errors and the desired values of the actuators outputs. Figure 63 shows the closed loop response of the twelve states of the system versus the pitch axis command. This plot is typical (in terms of closed-loop bandwidth) of all of the states of the system. Note that the closed loop response of all of the states begins to roll off at about 2 Hz, which indicates that a reasonable bandwidth for the aerodynamic actuators and the LSM should provide satisfactory control. Even if the 5 Hz first bending mode of the vehicle is included in the controller dynamic model, which may be necessary for additional stability and to prevent excitation of this mode, the required actuator bandwidths should be quite feasible.

3.2.2.g.1.2. SIMULATION RESULTS

The results of the simulations of the four Severe Segment Test zones are shown in Figure 64, Figure 65, Figure 66, and Figure 67. Figure 64 is a tabulation of the Peplar ride quality index for these four simulations. Note that the ride quality has improved considerably since the preliminary results seen at the June IPR. A Peplar ride quality of better than 2 (comfortable) is achieved for all four test zones.

Figure 65, Figure 66, and Figure 67 are the 1/3 octave spectral plots versus the ISO standard for the X, Y, and Z axis accelerations for SST test zones 1. This is representative of all four of the SST zone simulations. Note that all of the spectral plots are well below the ISO 1 hour comfort standard.

Actuator authority for the four test zones is shown in Figure 68. This table shows the rms actuator values for the seven actuators over the four test zones. This shows that the actuator values are within acceptable and achievable limits, with the notable exception of the value of the LSM vertical force per bogie. The rms LSM vertical bogie force is nearly the same as the LSM forward force. This is due to the coupling of the various system states as you will see in the following figures.

Figure 69 shows the forward and vertical LSM force for the SST zone 1 simulation. Notice how the vertical force, which has the sawtooth shape to damp out the pitch/heave motions, tracks the forward force, due to the coupling of the forward force and the vertical and pitch position errors. As the forward force varies, based on acceleration demands on the vehicle determined by the route, the equilibrium states vary from the nominally commanded positions. Thus, the vertical force couples with the forward acceleration. If we altered our state commands to match the new equilibrium condition, or if we high pass filtered the position errors in the states that we prefer to go to the equilibrium position (i.e. pitch, yaw, vertical, and lateral position) this coupling in the DC level of the LSM forward and vertical force commands will be eliminated. We will still wish to directly control the forward and roll positions of the vehicle for safety and ride comfort reasons, as well as damp oscillations of the velocity errors in all the states.

Figure 70 shows the LSM vertical and forward forces with this coupling removed, and the vertical force is much more reasonable and achievable. It can be achieved by modulating the phase angle by approximately +/- 5 degrees, considerably less than our available value of at least +/- 20 degrees. The values in Figure 68 are retabulated shown with the LSM vertical/forward coupling removed in Figure 71.

The preceding discussion describes the major results of the simulation which validates the controller concept in terms of ride quality and actuator authority and bandwidth. An additional topic which relates to the advantage of using the 15 cm levitation gap can be seen in a step response of the vehicle for a vertical step in the magway. The simulation of the vehicle was performed for vertical magway steps of 2 and 5 cm, which, although a rather extreme condition, could occur after an earthquake. Figure 72 shows the time response of the vehicle travelling at 100 m/s as it travels over the step. Note the double bump in the rise, which is due to the front and the back bogie passing over the step. Figure 73 shows the vertical acceleration of the vehicle center of gravity as it goes over the step. Note how small the maximum acceleration is: approximately .25 and .1 g's for the 5 and 2 cm steps respectively. The maximum aerodynamic actuator deflections are 13 and 37 degrees in the pitch actuator for the 2 and 5 cm steps respectively. Although we would not chose to intentionally drive a vehicle over a curb at 224 mph, this suggests that such an occurrence would not damage the vehicle, and would cause minimal discomfort to the passengers. We doubt that such a claim could be made for the other maglev systems which are now being proposed.

This is only possible because of the large levitation gap which provides resiliency to the suspension. The resiliency lowers the natural frequencies of the oscillation modes, allowing them to be controlled directly using the electromagnetic and aerodynamic actuators. By controlling these oscillations directly, we eliminate the need for a secondary suspension, while the resiliency of the suspension decreases the effect of magway irregularities on the motion of the vehicle.

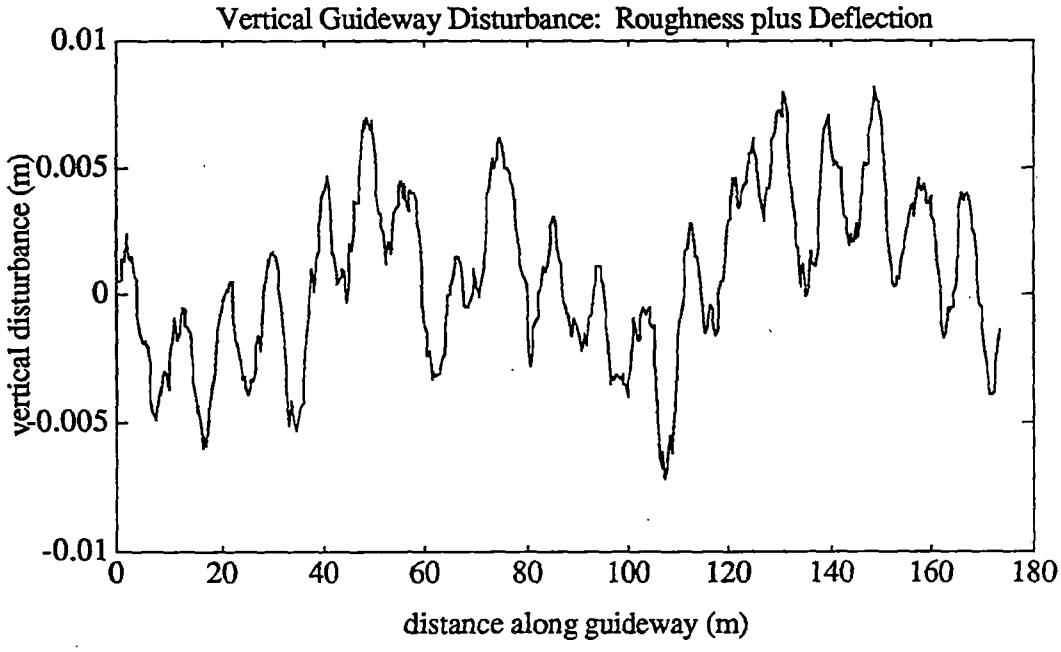

Figure 62 Typical magway vertical disturbance due to roughness and magway deflection

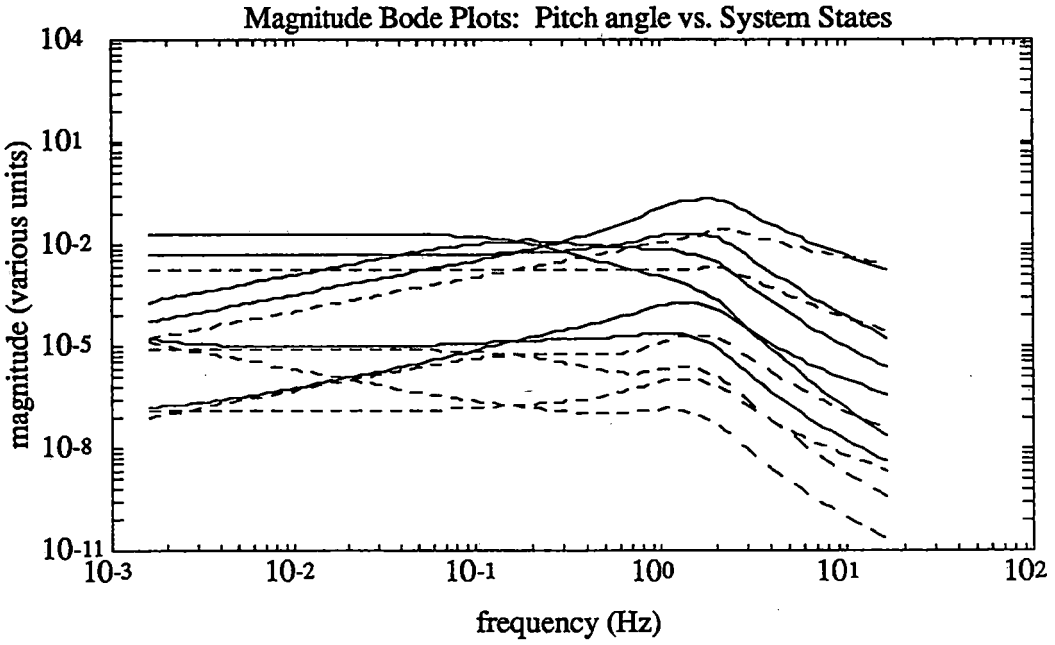

Figure 63 Bode plots of pitch angle versus the 12 system states

SEVERE SEGMENT TEST NUMBER	PEPLER RIDE QUALITY INDEX
1	1.83
2	1.84
3	1.82
4	1.77

[1 = very comfortable; 2 = comfortable; 3 = somewhat comfortable]

Figure 64 Peplar ride quality for the four Severe Segment Test zones

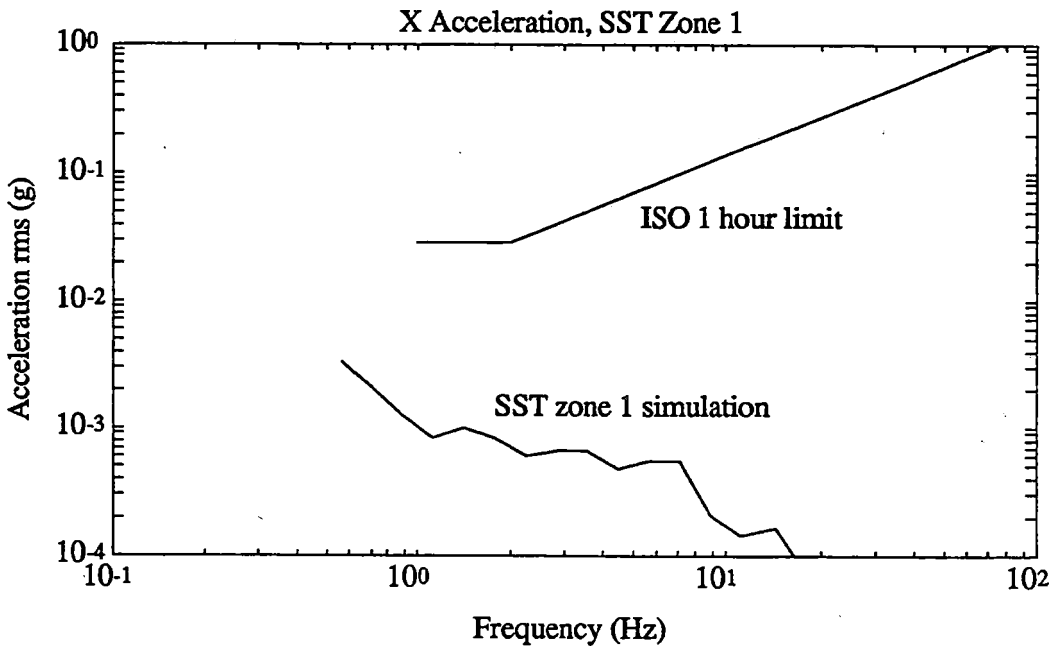

Figure 65 ISO forward acceleration and SST zone 1 simulation

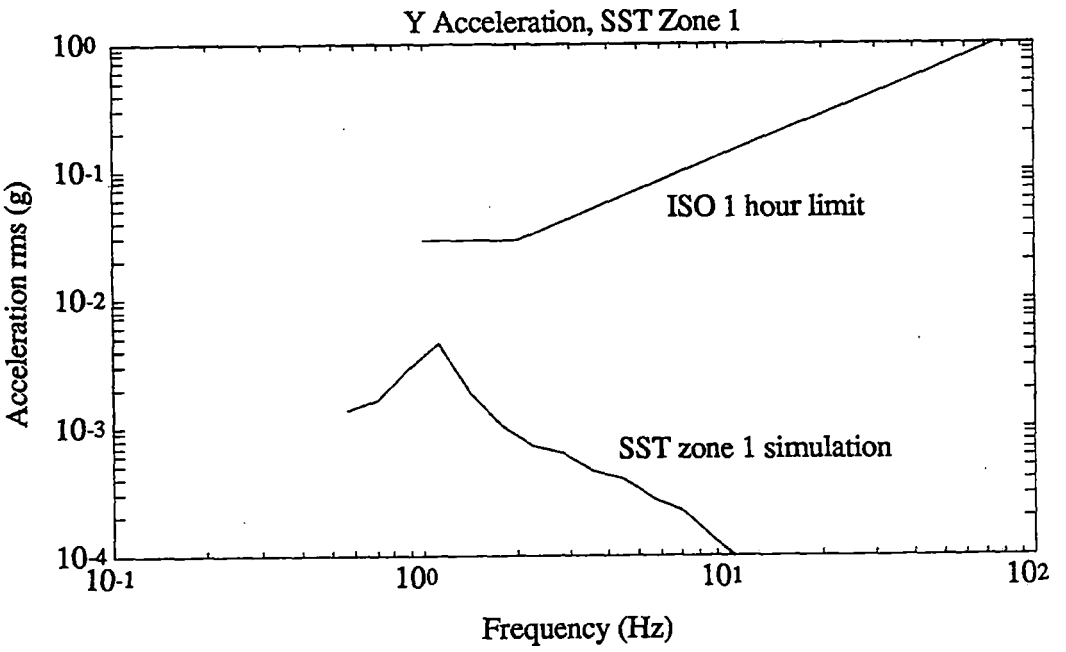

Figure 66 ISO lateral acceleration and SST zone 1 simulation

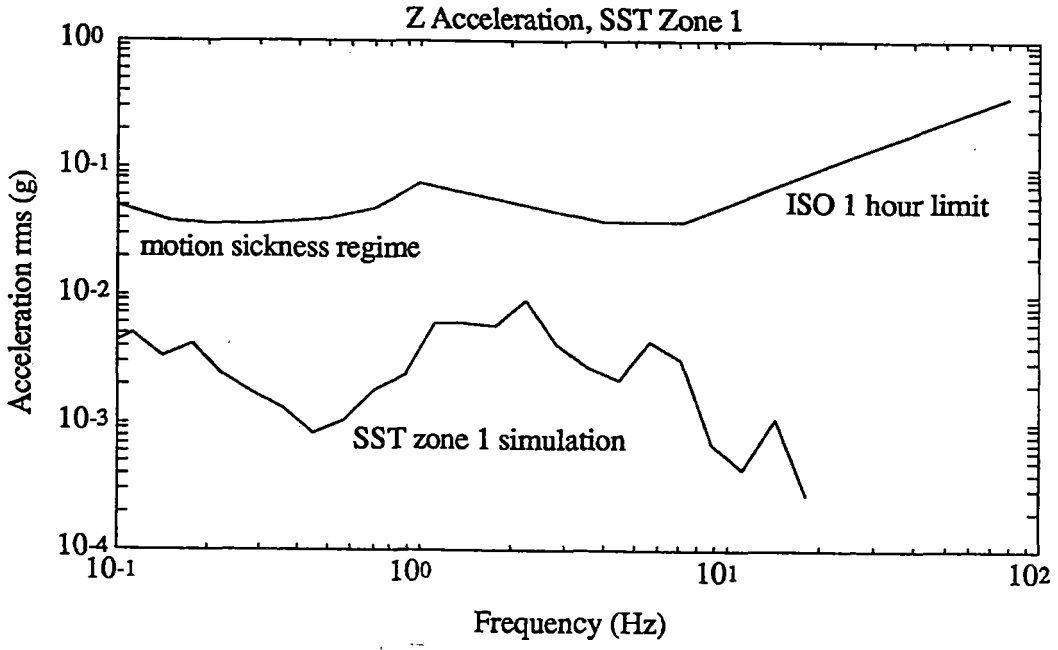

Figure 67 ISO vertical acceleration and SST zone 1 simulation

RMS ACTUATOR VALUES FOR THE SEVERE SEGMENT TESTS

ZONE #	SPEED RANGE (m/s)	LSM FWD (N)	LSM VERT (N)	AERO VERT (deg)	AERO SWAY (deg)	AERO PITCH (deg)	AERO YAW (deg)	AERO ROLL (deg)
1	53 - 91	34,000	33,000	9.4	5.1	10.8	5.9	10.2
2	38 - 90	37,000	36,000	10.2	4.9	9.8	5.7	9.1
3	61 - 97	23,000	23,000	6.4	5.0	7.1	5.8	6.3
4	134	3,300	4,500	1.3	2.6	3.2	1.8	3.9

Figure 68 Rms actuator values for the Severe Segment Test zones

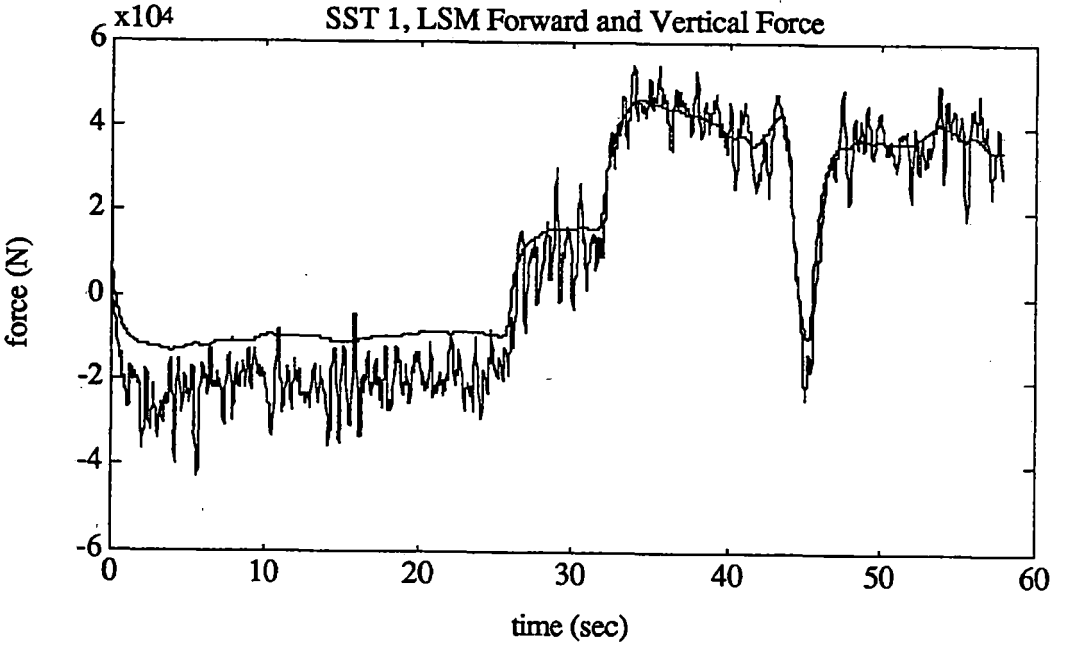

Figure 69 LSM forward and vertical forces, SST zone 1

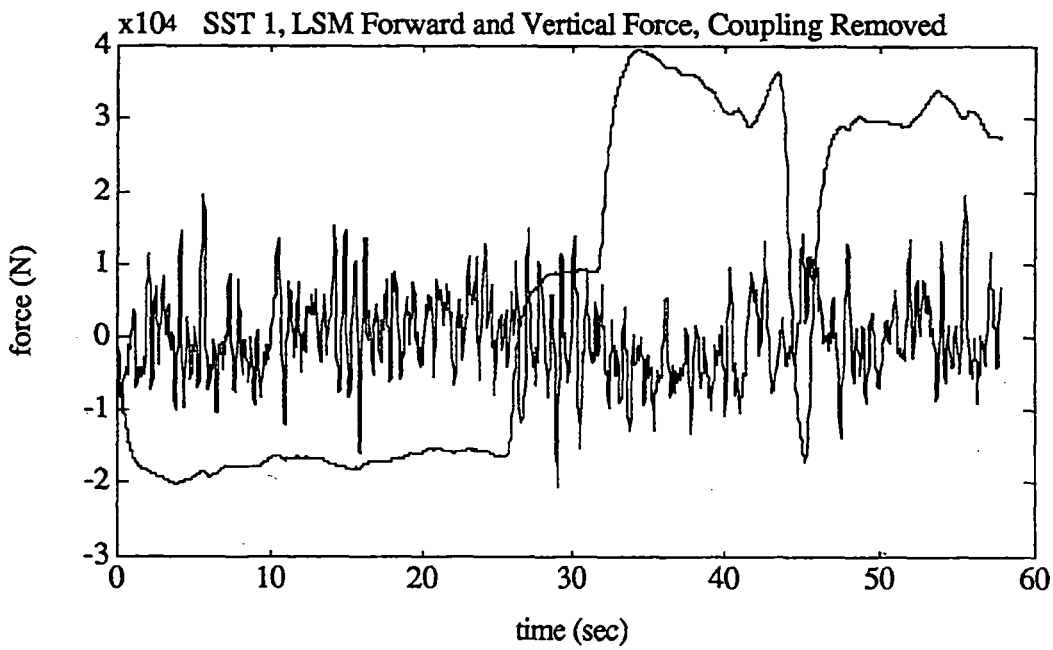

Figure 70 LSM forward and vertical forces, SST zone 1, Forward/vertical coupling removed

RMS ACTUATOR VALUES FOR THE SEVERE SEGMENT TESTS
(* CORRECTED FOR FORWARD/VERTICAL LSM COUPLING)

ZONE #	SPEED RANGE (m/s)	LSM FWD (N)	LSM VERT* (N)	AERO VERT (deg)	AERO SWAY (deg)	AERO PITCH (deg)	AERO YAW (deg)	AERO ROLL (deg)
1	53 - 91	34,000	4,000*	9.4	5.1	10.8	5.9	10.2
2	38 - 90	37,000	4,100*	10.2	4.9	9.8	5.7	9.1
3	61 - 97	23,000	3,600*	6.4	5.0	7.1	5.8	6.3
4	134	3,300	4,500	1.3	2.6	3.2	1.8	3.9

Figure 71 Rms actuator values for the Severe Segment Test zones

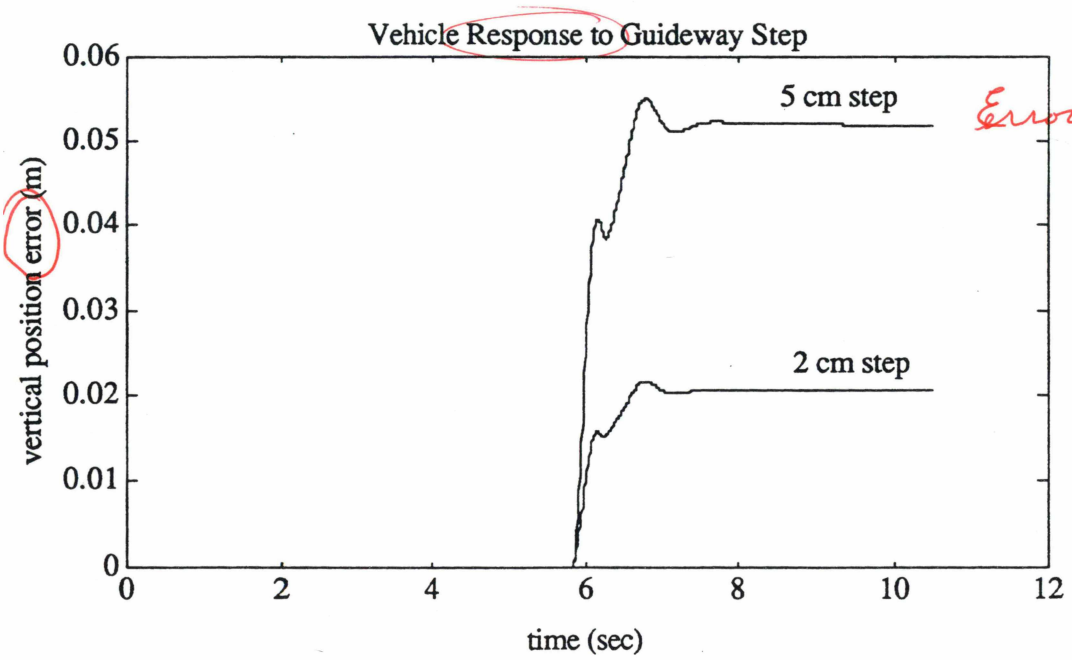

Error persists ?

Which is it ?

Figure 72 Vehicle response to step in magway

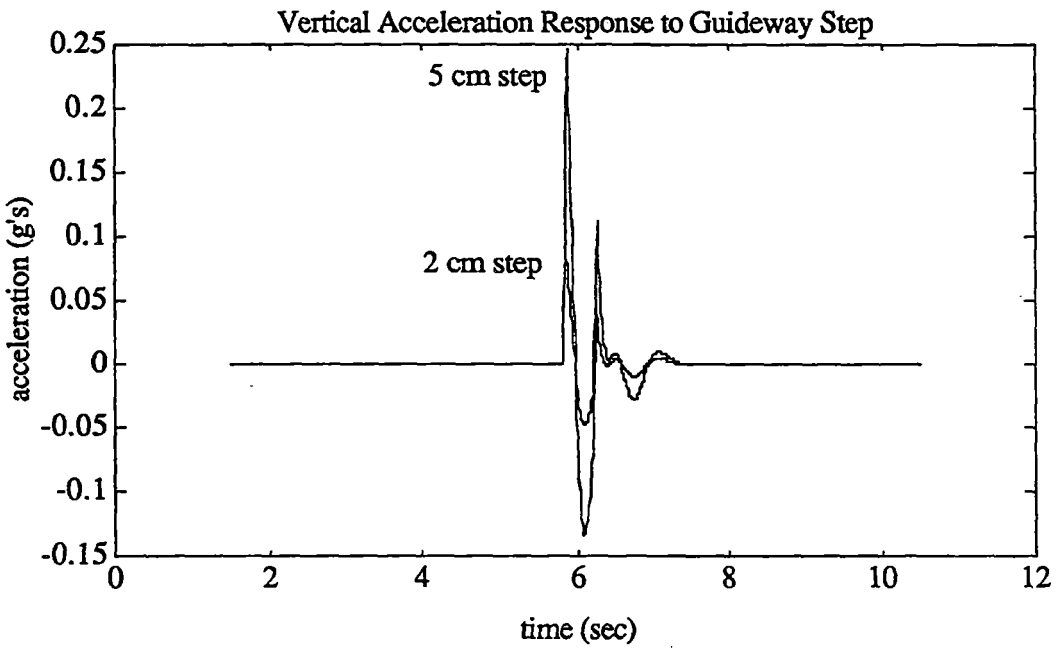

Figure 73 Vehicle acceleration response to step in magway

3.2.2.g.2. DISTURBANCE PARAMETER VARIATIONS

The dynamic simulation was used to determine the sensitivity of the system to variations in the disturbance parameters: the magway span deflection; the magway roughness, and the wind gusts. A section of straight and level magway was simulated using the disturbance baselines values defined in the previous section. Subsequent simulations varied the three disturbance variables separately to determine the sensitivity of controller and the ride quality to the varied parameters. The Peplar ride quality index was calculated for the simulations, along with the rms control actuator values.

The Peplar ride quality index did not vary sufficiently between the different simulations to use this as an index for the system sensitivity to the varied parameters. It appears that the control system successfully rejected the increased disturbances with increased actuator control. It seems more likely that saturation of the actuators rather than ride comfort would be the limiting factor to system performance, or alternatively, ride comfort would only deteriorate significantly when the actuators reached saturation. Therefore, the rms actuator values were plotted versus the varied disturbance parameters as an indication of the limits to system performance.

3.2.2.g.2.1. MAGWAY SPAN DEFLECTION

Figure 74 shows the rms control value of the pitch, roll, and yaw actuators plotted versus the magway span deflection. Span deflections 1, 2 and 10 times the baseline value were used in the simulations. Notice that the rms control values increase with the increasing disturbance amplitude, but at much less than a less than 1:1 correspondence. This is most likely due to the fact that the several disturbances which affect the vehicle add in an approximately root sum squared (rss) manner. Unless the disturbance being varied is the dominant (or only) disturbance, the actuator authority will not increase as rapidly as the varied parameter.

The required actuator authority for the largest span deflection simulated does not seem excessively large. Therefore, the structural engineering considerations which are used to design the span deflection will be the driving factor in determining the allowable span deflection. The actuator authority and hence ride quality does not appear to increase dramatically if the span/2000 maximum dynamic deflection requirement is loosened. This is due primarily to the fact that the disturbance frequency at the baseline velocity of 100 m/s is high relative to the natural frequency of the vehicle, and is not the major disturbance affecting actuator authority and ride quality.

3.2.2.g.2.2. MAGWAY ROUGHNESS

Figure 75 shows the rms control value of the pitch, roll, and yaw actuators plotted versus the magway roughness parameter, a. Magway roughnesses of 1, 2 and 10 times the baseline value were used in the simulation. The rms control values increase nearly 1:1 with the increasing disturbance amplitude. From this we can infer that the magway roughness is the major disturbance parameter which affects rms actuator usage. This parameter could perhaps be increased by a factor of 2 without significantly affecting overall control system performance, but this parameter has a major influence on ride quality. This is most likely due to the fact that the frequencies which can most easily disturb the vehicle (the natural

frequencies of the magnetic suspension) are represented more in the magway roughness than in the other disturbances

3.2.2.g.2.3. WIND GUSTS

Figure 76 shows the rms control value of the pitch, roll, and yaw actuators plotted versus the wind gust parameter, u10. Wind bulk velocities of 1, 2 and 5 times the baseline value were used in the simulation. Notice that the rms control values generally increase with the increasing disturbance amplitude, but at much less than a less than 1:1 correspondence. Again, the wind gust does not appear to be the major parameter which drives the response of the control actuators. The decrease in the Yaw actuator between the 2 and 5 times the baseline value may be a result of the random element used to create the time domain gust disturbance. One may notice the apparently anomalous behavior of the system at high wind gusts: the sensitivity actuator response increases less rapidly as the wind gusts get larger. This may be due to the shift in the frequency peak of the gust power spectrum at higher bulk wind speeds. Perhaps a better test would have been to vary the gust velocity as a fraction of a constant bulk wind velocity rather than to vary the wind bulk velocity.

3.2.2.g.2.4. SUMMARY

The non-linear dynamic system equations of Supplement F were linearized in order to design a multiple-input, multiple-output (MIMO) controller for the dynamic system using the Linear Quadratic Regulator (LQR) control system design methodology. The linear controller was combined with the non-linear system, and the resulting closed-loop system was simulated for the four Severe Segment Test (SST) zones, a vertical step in the magway, and parametric variations of the disturbances. The dynamic model included the non-linear magnetic forces, the non-linear aerodynamic forces, the magnetic keel effect, the magway curve and speed demands, the fore/aft distributed suspension, and the disturbances due to the span deflection, magway roughness, and wind gusts. The controller bandwidth and actuator rms values were within reasonable limits for the four SST zones. The ride quality for the four SST zones was better than "comfortable" as defined by the Peplar ride quality standard, and the spectral vibrations were well below the required ISO 1 hour standard. The results of the step response simulation indicate that the vehicle could withstand and continue to operate normally after a 5 cm vertical step in the magway, due to the primarily to the 15 cm levitation gap.

Of the three disturbances which were varied (span deflection, magway roughness, wind gust), the magway roughness had the greatest influence on the control actuator response and hence had the most influence on the vehicle ride quality. This conclusion is valid only for the variations about the chosen baseline disturbance values, and a different conclusion could be reached for a different set of baseline values.

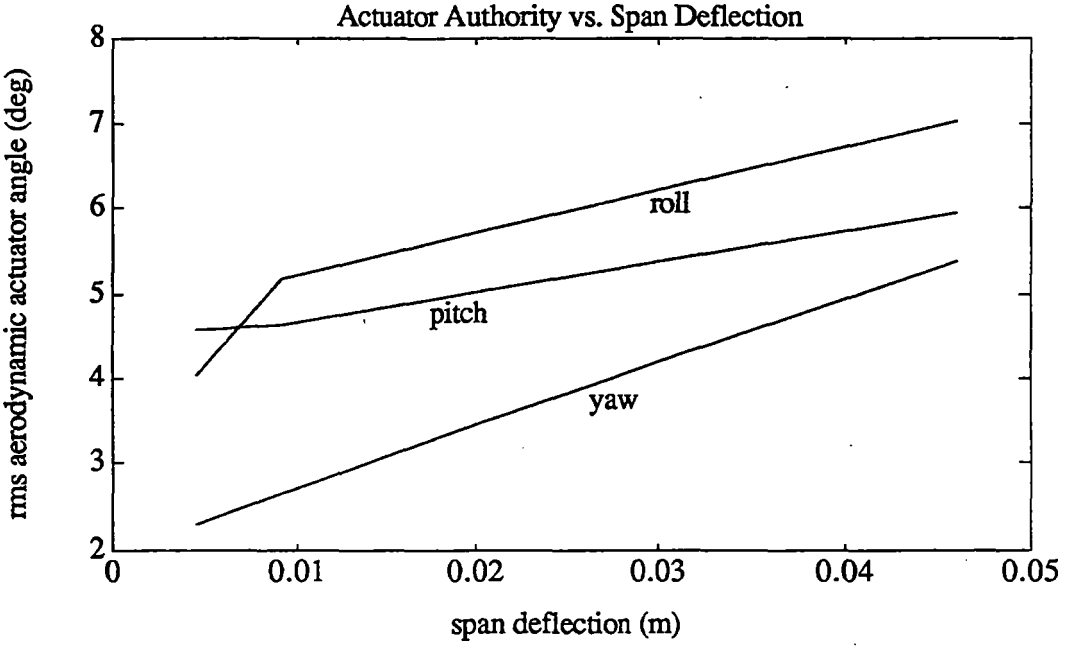

Figure 74 Rms aerodynamic actuators versus span deflection

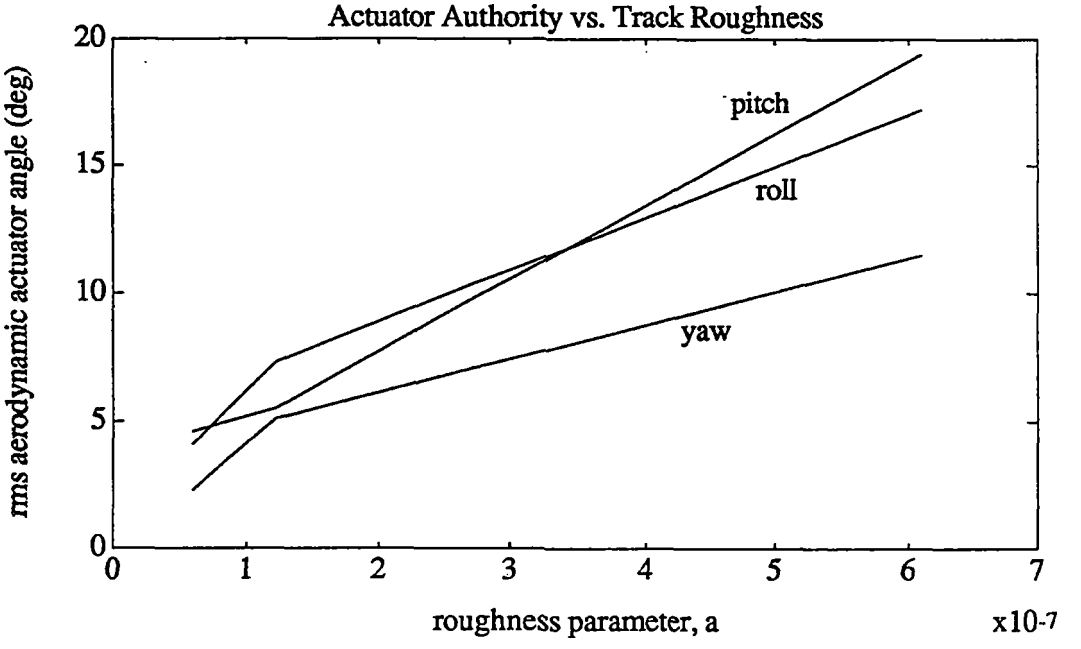

Figure 75 Rms aerodynamic actuators versus magway roughness

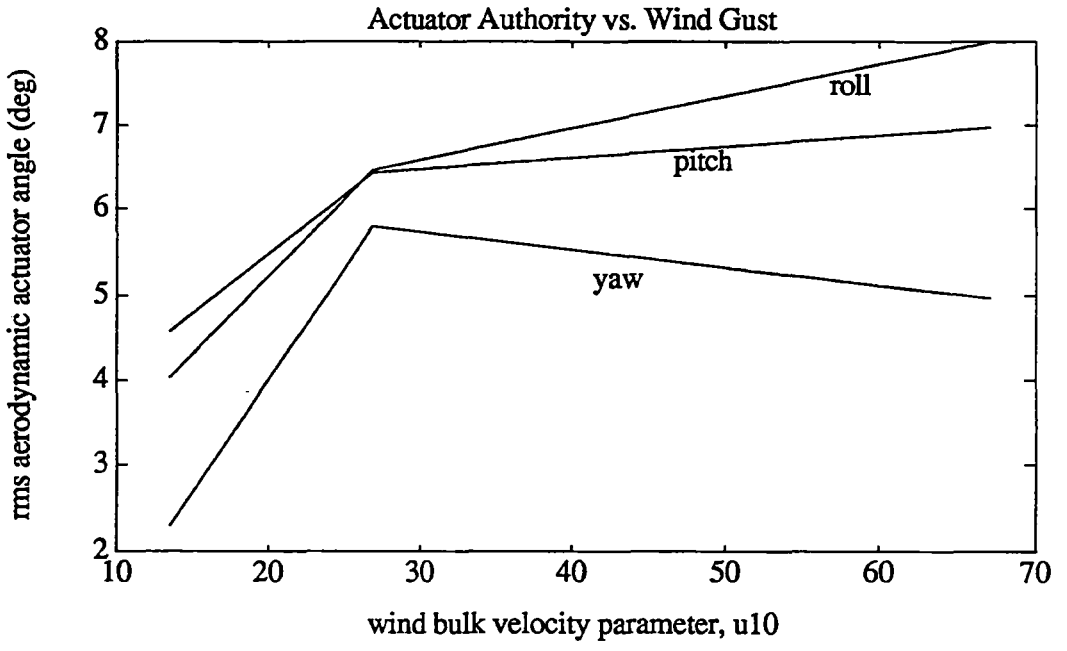

Figure 76 Rms aerodynamic actuators versus wind gusts

3.2.2.g.3. SUSPENSION CHARACTERISTICS

The suspension system approach and characteristics were discussed on a mode-by-mode basis in Section 3.2.1.h, and their incorporation in the dynamic simulation model in Section 3.2.2.g.1 and in the equations of motion in Supplement F. In the full simulations, all the mode couplings are incorporated. These result from the rigid body dynamics, from the aerodynamic forces, from the control surfaces and from the interactions between magway, LSM, levitation and propulsion coil sets.

The coupled modes are statically stable provided the vehicle center-of-gravity is positioned well below the effective magnetic center of the levitation coils, as shown in Figure 79. However, because of the coupling between the plunge, pitch and forward speed modes, a negatively damped oscillatory motion can occur, requiring active stabilization through LSM heave control. Moreover, the remainder of the modes are only lightly damped leading to unacceptable ride quality. It is therefore necessary to use active stabilization in all the rigid modes. The adequacy of the aerodynamic control in providing this stabilization has been demonstrated in Section 3.2.2.g.1.

The vehicle flexible mode with the lowest frequency is the first bending mode. It is probable that this frequency will lie in the control system bandwidth. To prevent coupling problems with this mode, it will be necessary to increase the number of state variables used in the control system to include the bending mode. The control system design described in Section 3.2.2.g.1 does not incorporate the flexible modes.

3.2.2.g.4. KEEL EFFECT

When the vehicle is travelling in its stable upright position along a straight section of track, there is no net side force on the bogies because of the cross-sectional symmetry of the superconducting coils and magway. Moreover, the cross-sectional dimensions of the levitations plates, LSM and on-board coils are such that individual side-forces on the coils are small. This situation also pertains in a banked coordinated turn. However, when the vehicle is displaced from the symmetric equilibrium configuration, side-forces are generated at the coils as follows:

1) An attractive force as a levitation coil moves towards the edge of the conducting sheet.

2) A restoring force between the propulsion coils and the LSM.

3) A repulsive force as the propulsion coils approach the edge of a levitation sheet.

Eddy current model calculation show that the forces in (1) and (2) are small, and that mechanism (3) dominates and is largely responsible for the vehicle keel effect or tendency to remain aligned with the slot between the conducting sheets. The keel effect is an extremely important feature of the Magneplane concept and is the prime mechanism for guidance through turns. The eddy current calculations also show that, for the normal magway/coil configuration, the force interaction is highly non-linear. The vehicle can roll through about 3° relative to the track before any significant keel effect occurs. Side-forces then build-up rapidly and can be as high as 0.25 to 0.5 of the vehicle weight.

ΔV= Speed difference from the curve design speed as a percentage.

	Lateral acceleration =+0.16g		Lateral acceleration =-0.16g	
Track Bank Angle (deg)	ΔV(%)	Vehicle, roll angle (deg)	ΔV(%)	Vehicle, roll angle (deg)
10	+72	19.4	-100	0.6
15	+52	24.4	-100	5.6
20	+42	29.4	-81	10.6
25	+37	34.4	-53	15.6
30	+31	39.4	-42	21.6
35	+29	44.4	-35	26.9

Figure 77 Vehicle dynamics in a horizontal curve at off-design speeds

The distribution and size of the levitation coils is such that the footprint pressure loading is essentially equal for all the modules during normal operating conditions, including coordinated turns, although the magnitude of the loading increases in the turn. During transient situations such as curve entry or if the vehicle is operating at off-design speeds in a horizonal curve, the load will no longer be distributed evenly. If the speed is lower than design, the inside levitation modules will have a higher load proportion; at speeds higher than design the modules on the outside of the turn will be more heavily loaded. Magway, coil and vehicle structures are designed to meet these enhanced loading cases.

The keel effect also comes into play when banked turns are negotiated at speeds other than the design coordinated turn speed. In this case, the vehicle roll angle will not be the same as the track bank angle and the passengers will be subjected to a lateral acceleration. Provided this acceleration can be kept within ride comfort levels, it is possible to use the keel effect to limit the maximum track bank angles, resulting in lower constructions costs and reduced roll rate demands.

The keel effect is also important at off-design speeds in the determination of the operating speed envelope in banked turns. In this case also, the turns will be un-coordinated and the allowable departure from the design speed condition is determined by the ride comfort limits on lateral acceleration. For acceleration levels of +0.16g and -0.16g, the corresponding vehicle roll angles and percentage difference in curve speed from the design speed are shown in Figure 77 as functions of guideway bank angle. The

hc	ΔT (°F)	(30)	(100)	(300)
	°C	16.7	55.5	166.7
w/m²°C		3.86	5.79	8.35
(BTU/hr/ft²°F)		(0.68)	(1.02)	(1.47)

Figure 78 Turbulent heat transfer coefficient

results presented are for a separation of 1.8m between levitation plates, compared with 1.4m for the straight guideway. The gap was increased to reduce the magnetic keel effect but this does not represent an optimized dimension and further study of the control of magnetic keel stiffness is required. The results in Figure 77 show that there is no low speed limit to operation with track bank angles of 15° or less. The smallest range of operating speeds occur at the maximum bank angle.

3.2.2.g.5. MAGWAY SURFACE WEAR AND HEATING

Magway surface wear will be minimal by using non-contacting air bearing pads operating at a nominal of gap of 0.008 mm (0.3 mil). Experience with soft graphite fiber reinforced Teflon indicates that it should not damage the magway under these conditions but because the material is new and has not been tested under the required conditions the following development program tasks should be carried out concurrently with detailed vehicle design.

1) Develop laboratory size test bed to test friction and wear of sample materials under operating conditions.
2) Optimize material composition for best performance.
3) Perform test of single air bearing pad at full curved speed and load conditions.
4) Test full module array of pads with pneumatic support and design air flow rates.

While braking does not produce appreciable magway heating as discussed in Section 3.2.1.d, the magnetic drag of many vehicles does. Even though the temperature rise from one vehicle is small, at short headway of 20 to 120 seconds, after a hundred or so vehicles have passed the magway must be at an equilibrium temperature at which it can dissipate the heat by natural convection and radiation.

The magway can be modeled as a 3 m wide (2 x 1.5 m) sheet of aluminum forming a horizontal surface. The heat transfer coefficient for turbulent free convection is given in Figure 78, and this was used to estimate the convective dissipation terms in Figure 80.

If the magway is above ambient temperature it will radiate energy as well. Assuming it radiates like a gray body the radiative dissipation is:

$$w=\alpha(T^4-T_a^4)\epsilon$$

where ϵ is the Stefan Boltzman Constant and ϵ is the emissivity. The emissivity is taken to be 01 for polished and 0.4 for anodized aluminum. For T_a=32°C(550°R) the radiative heat loss per unit area Q/A is given in Figure 80.

The effect of including radiation is estimated in the last line of Figure 80. These results indicate that the temperature rise is reasonable but significant compared to ambient temperature. These values are big enough that even at 40 or 80 sec. headway ice formation should not be a problem on operating magways. Detailed thermal modeling of the complete assembly including surface should be included in a future detailed design study.

To allow for magway heating resulting both from vehicles passing and from solar loading, thermal expansion joints or mechanisms must be provided in the levitation sheets. If these interrupt the induced currents in the sheet, magnetic lift and drag perturbations will occur at the passing frequency. The suspension characteristics are such that the vehicle response to these perturbations will be largest at the lowest operating speeds. A typical sheet discontinuity can lead to a magnetic lift reduction of 3% while the levitation module is passing over the gap. The corresponding magnetic drag change is a positive impulse followed by an equal negative impulse with total pulse length equal to the module passage time over the gap, and a pulse magnitude of 0.3 of the drag. At 30 m/s, these produce a peak acceleration of about 0.01g and a root mean square level of 0.0002g. These have a minimal effect of ride quality. Similar perturbations are expected because of LSM dimensional changes caused by thermal effects.

3.2.2.g.6. VEHICLE DYNAMIC RESPONSE UNDER EMERGENCY BRAKING CONDITIONS

The dynamic braking behavior of the vehicle under emergency braking was analyzed using the following assumptions:

1. Small perturbations with respect to a uniform acceleration.
2. Linearized equations
3. Friction coefficient as a linear function of speed.
4. Each H-pad was modelled as a damped independent spring with the spring force acting through the magnetic center.

The following combinations of motions were analyzed:

1. Longitudinal plane consisting of heave, pitch, and fore-and-aft motion
2. Lateral plane consisting of sway, yaw, and fore-and-aft motion
3. Sway and roll combined in a mode with motion about the magnetic center

For motion combinations (1) and (2) there were three modes in each case. Two of the modes were damped oscillations. The third was neutrally stable and was associated with the fact that there is no equilibrium speed condition. There was no evidence of the kinetic energy of forward motion being fed into the pitch or heave oscillations. No use was made in the analysis of the positive damping capability of the LSM even under braking conditions. The vehicle roll motion (3) was also a damped oscillation because the frictional force at a pad acts along the relative velocity direction to the track.

The stable state results apply even if the frictional force is being applied unevenly, if, for example, one side of the track has a lower coefficient of friction than the other. The braking effectiveness will be reduced and the distribution of normal forces at the pads will be modified in this case. The condition of stability also holds for emergency braking in a turn because this only represents a modified initial equilibrium, with enhanced frictional and breaking forces.

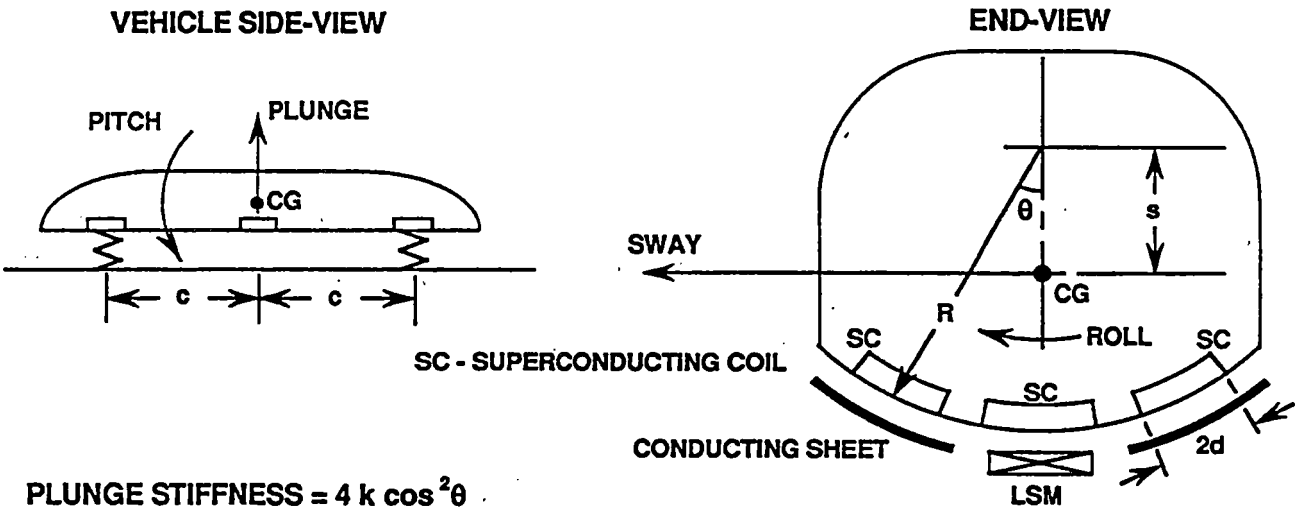

PLUNGE STIFFNESS = $4\,k\cos^2\theta$

PITCH STIFFNESS = $4\,k\,c^2\cos^2\theta$

SWAY STIFFNESS = $4\,k\sin^2\theta + k_p + k_M$

YAW STIFFNESS = $(4\,k\sin^2\theta + k_p + k_M)\,c^2$

ROLL STIFFNESS = $4\,k\,d^2/3 + 2\,k\,s^2\sin^2\theta + 2\,(k_p + k_M)\,(R - s)^2$

where k = SINGLE MODULE STIFFNESS
k_p = STIFFNESS FROM RELATIVE MOTION BETWEEN SC AND LSM COILS
k_M = MAGNETIC KEEL STIFFNESS FROM ITERACTION BETWEEN THE SC COILS AND THE EDGES OF THE CONDUCTING SHEET

Figure 79 Magnetic spring constants

Magnetic Drag Guideway Heatloads for 20 Second Headway (others by inverse proportion)

Velocity m/s	150	100	50	30
Magnetic Drag Newtons (lbs)	15052 (3384)	21368 (4804)	40868 (9188)	68107 (15312)
Guideway ΔT Per Vehicle °C (°F)	0.09 (0.17)	0.13 (0.24)	0.25 (0.45)	0.42 (0.76)
Energy Input to 3.05 m (10 ft) of Guideway kw (BTU/hr)	2.29 (2820)	3.26 (11,132)	6.23 (21,275)	10.38 (35,447)
Q/A Convective kw/m^2 ($BTU/hr\ ft^2$)	0.25 (79.5)	0.36 (113.1)	0.68 (216)	1.13 (360)
ΔT (Convection Only) °C (°F)	52 (93)	61 (110)	89 (160)	136 (244)
ΔT est Convection + Radiation at ∈=.4 for Anodized Aluminum °C (°F)	42 (75)	50 (90)	61 (110)	72 (130)

Figure 80 Magway heating

3.2.2.h. MAINTENANCE REQUIREMENTS

Please see sections 3.2.3.i. (Operations and Maintenance) and 5.3.5. (Maintenance Plan) and 5.3.11. (Life Cycle Cost Report).

3.2.2.i. MAGWAY MONITORING

3.2.2.i.1. GENERAL

Magway integrity, which includes the major components such as levitation sheets, propulsion winding, and joints, will be continuously monitored by a number of different methods. The monitoring methods and the magway components being monitored are listed below:

Closed Circuit TV
Joint integrity, debris in magway, and other abnormal conditions at critical areas only

Power Distribution
Propulsion winding integrity (open or shorted)

Vehicle Ride Quality
All components. Indicate via "G" level of on-board sensors where further/additional inspection is required.

Visual
Normal maintenance inspection of all components

Structural
Prohibit people, animals and debris on the magway

Vehicles travelling on the magway are typically elevated by 15 cm. This clearance insures that small irregularities or obstructions in the magway are of no concern. Typically, due to the air displacement of a vehicle travelling at 134 m/s, the magway will immediately be cleared of small objects, preventing build up. It is important, to insure safe transportation of passengers and freight, that a means of continuously monitoring the state of the magway is available.

3.2.2.i.2. BLOCK INTERFACE MONITORING STRAPS

One method of monitoring the magway to insure its integrity for safe operation will be via continuity straps. The continuity straps will be a flexible conductor with sufficient length that will accommodate the small expansion and contraction, and heave changes, of the magway, which are associated with the environmental, namely weather. The location of the continuity straps will be at the boundaries or joints between magway sections. A top view illustration is shown in Figure 81, titled "Magway Continuity Strap Locations." The continuity straps (four (4) per magway section) will connect adjoining sections

of magway sheet levitation. A major physical separation (vertical or horizontal 1 ft.) will cause a loss of continuity, which in turn will automatically trigger a magway monitor alarm. The magway monitor alarm will be sent to wayside and global control for initiation of emergency (shut down) procedures.

One method of locating the fault can be determined by the reflectometry method; a technique used by the communications industry. The reflectometry method sends a signal towards the open fault, which reflects (in-phase) the signal back to the source. The time interval for the signal to travel to and be reflected at the open location back to the sending source, determines the fault location.

3.2.2.i.3. CLOSED CIRCUIT TV SURVEILLANCE

A catastrophic failure, such as loss of prime power, will disable the system. The vehicles are equipped with on-board power capability to safely come to a coordinated stop if such a condition occurred. The vehicle will also remain active for a significant period, entering a lower power drain standby mode to maintain just the critical support systems such as the control and communications equipment. This permits continuous communication with the wayside controller for the block the vehicle is occupying, and coordinated re-start of the system once power is re-established. The Global center requires knowledge of vehicle location to initiate a coordinated recovery. If the magway mounted markers were active during the entire deceleration maneuver of the vehicle, true position is inherently retained and can be communicated to the Global center via the wayside controller RF interface. GPS on board the vehicle is also available, hence if the markers were disabled prematurely, the vehicle can still report its absolute position, enabling the Global controller to correlate the reported coordinates to a magway section and re-establish mapping of all vehicle locations. This will permit the (networked) global centers to develop a restart procedure, moving those vehicles forward that have upstream clearance to complete their journey or turn-off at the nearest station. As this frees up clearance for the preceding vehicles they can also be synchronously brought back up to some speed that permits them to continue or turn-off.

Continuity Monitoring of the magway; will be performed by remote control surveillance cameras spaced at critical locations (curves, stations, etc). Each camera will have a view in two opposite directions for 305 m (1000 ft.) to detect excessive joint heave or settling, debris, etc. An illustration (top view) of the proposed camera location for monitoring a dual magway section is shown in Figure 82. The anticipated magway surveillance covered by CCTV is approximately 10%.

Remote controlled closed circuit television equipment (CCTV) is commercially-off-the-shelf available to perform this task. Suppliers such COHU, Inc. of San Diego, CA currently have Microprocessor Camera Control (MCC) systems applicable for use in the Maglev scheme. The MCC uses state of the art technology with flexibility of expandability up to 255 camera sites, 32 monitors, and 32 master and remote stations located up to 8 km (5 miles) apart. See Figure 83 for a typical MCC System configuration. Digital control for the pan, tilt, zoom,and focus functions are performed by digital control signals transmitted from the MCC using a serial format (RS-232 or RS-422) and twisted shielded pair wiring. Also, the equipment contains power and data line surge protection, preset control for camera positioning, and autoscan, color and bright light limiting controls. Other major system specifications are:

Use of a the high performance monochrome CCD (Series 4910) camera with a 1/2" HAD Interline Transfer Imager.

Field of View at 305 m (1000 ft)
Horizontal = 22.9 m (75 ft)
Vertical =15.2 m (50 ft)

Using a 15" high resolution raster scan monitor with greater than 60,000-hour-or MTBF reliability; the capability or resolving a four (4) inch joint discontinuity (up, down, or canted) is determined as follows:

15" Monitor diagonal = 13.86"
Resolution = 800 lines at corner
Aspect ratio = 4:3

therefore:
No. of horizontal lines = 800 X 4/5 = 640
No. of vertical lines = 800 X 3/5 = 480

Horizontal line detection at 1000 ft. is defined by:

$$line\text{-}detection = \frac{horiz\text{-}view\text{-}at\text{-}1000\text{-}ft}{no\text{-}of\text{-}raster\text{-}horiz\text{-}lines}$$

$$= \frac{75.0ft}{640}lines = 1.4\frac{inch}{line}$$

thus approximately three (3) raster lines will equate to a four (4) inch displacement of the magway at 1000 ft. distance.

This time to scan a straight 305 m (1000 ft) section of magway using a wide angle lens (approximately no horizontal motion is required) using a pan/tilt camera mount, capable of 6°/sec in the horizontal and 4.5°/sec in the vertical is;

Total vertical distance = 90° (straight down to horizon)

$$time = \frac{total\text{-}travel\text{-}angle}{rate} = \frac{90^0}{4.5^0/s} = 20s$$

(Focus and zoom times are negligible to the overall vertical time)

Time to monitor 1000 ft. of magway is determined as follows: (rotate 180°, vertical will move from horizon to -90° during 180° rotation in azimuth)

$$T_{total} = 2T_{vertical} = T_H$$

$$= 2(20s) + \frac{180^0}{6^0/s}$$

$$= 40s + 30s$$

$$= 70s$$

The target scheme to enhance detection of magway joints (see both sag and elevated position) is shown in Figure 84. The circular reference targets shall have a diameter of eight (8) inches with darkened opposite quadrants to enhance visual perception, and when used with the reference pointer/marker will define the integrity of the magway joint being inspected. Analysis to date indicates a vertical joint discontinuity of less than four (4) inches will not damage the vehicle, but will be noticeable in the ride quality. Greater than a four inch vertical displacement may cause vehicle damage. In addition to continuity straps and camera monitors at critical locations, the vehicle motion sensors in conjunction with the magway position markers will be recorded on-board the vehicle, and thus provide a off-line ride quality data source to indicate where addition magway monitoring or magway maintenance is required.

Three monitors per global center will provide a dual redundant operational mode with the third camera available as a spare, but utilized off-line as a training or maintenance unit. The breakdown of the 160 km magway into critical viewing sections facilitates (1) Mean-time-to-repair; travel distance for maintenance is optimized from source of detection to on-site/location inspection and/or repair, and (2) time to complete the critical area of magway scan/monitoring is more optimal in terms of operator function and fault detection. The global control center magway monitors (3) will have the capability of viewing all critical sections of the total (160 km) distance.

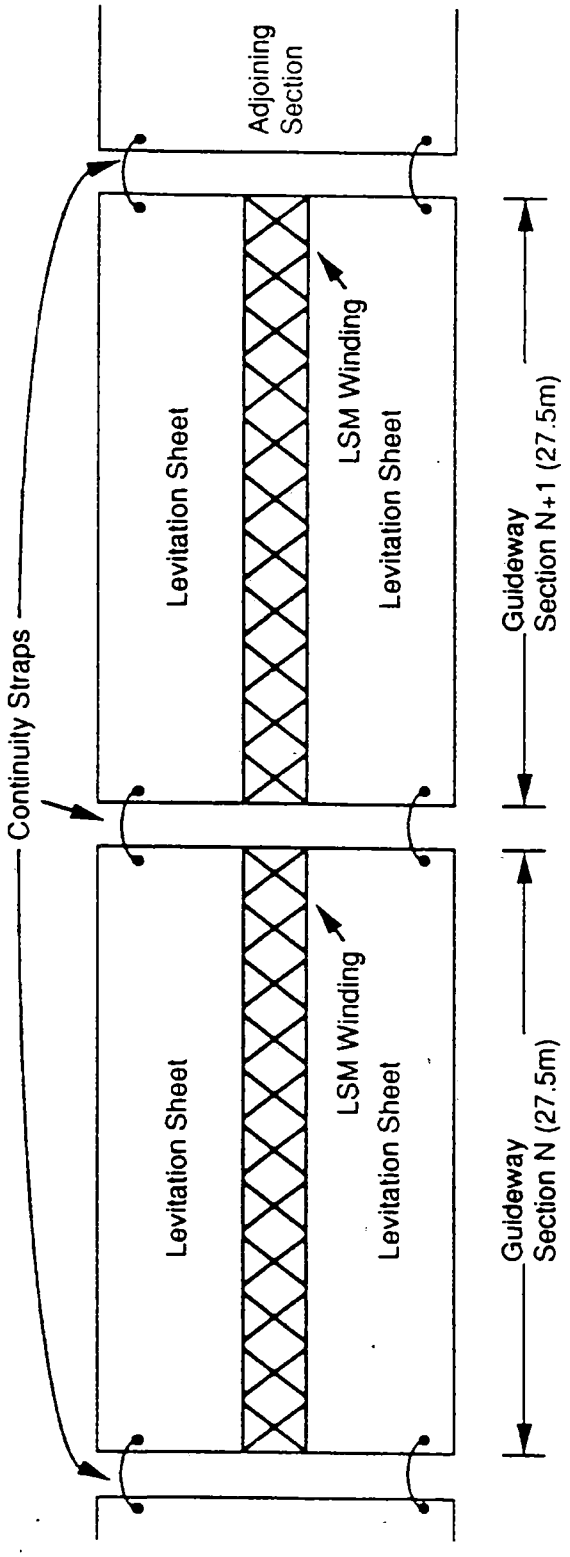

Figure 81 Magway continuity strap locations

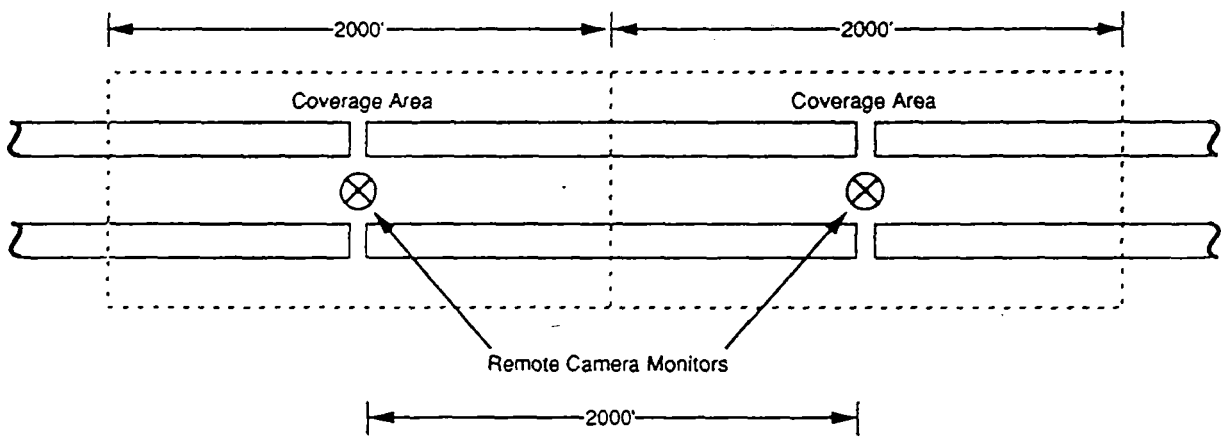

Figure 82 Dual magway CCTV monitoring

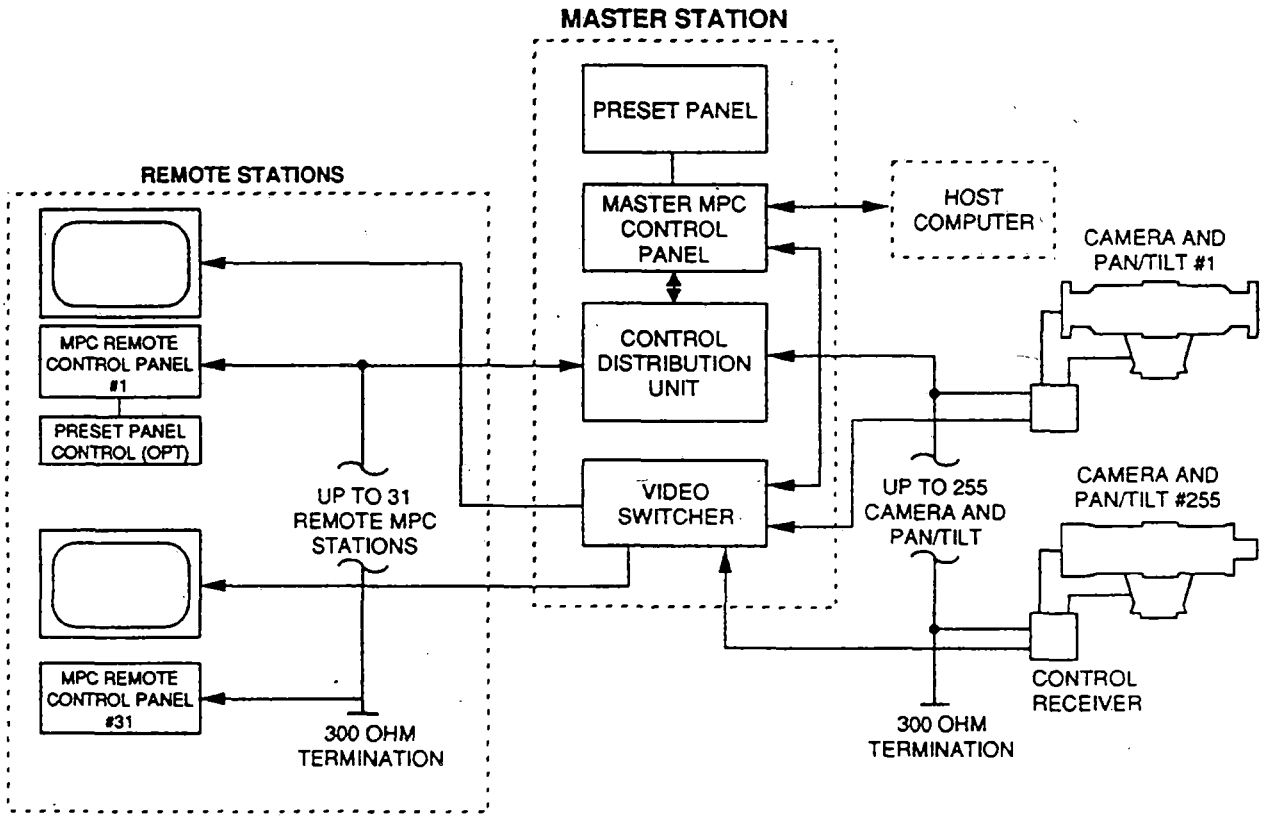

Figure 83 Typical micro-processor camera control (MCC) system

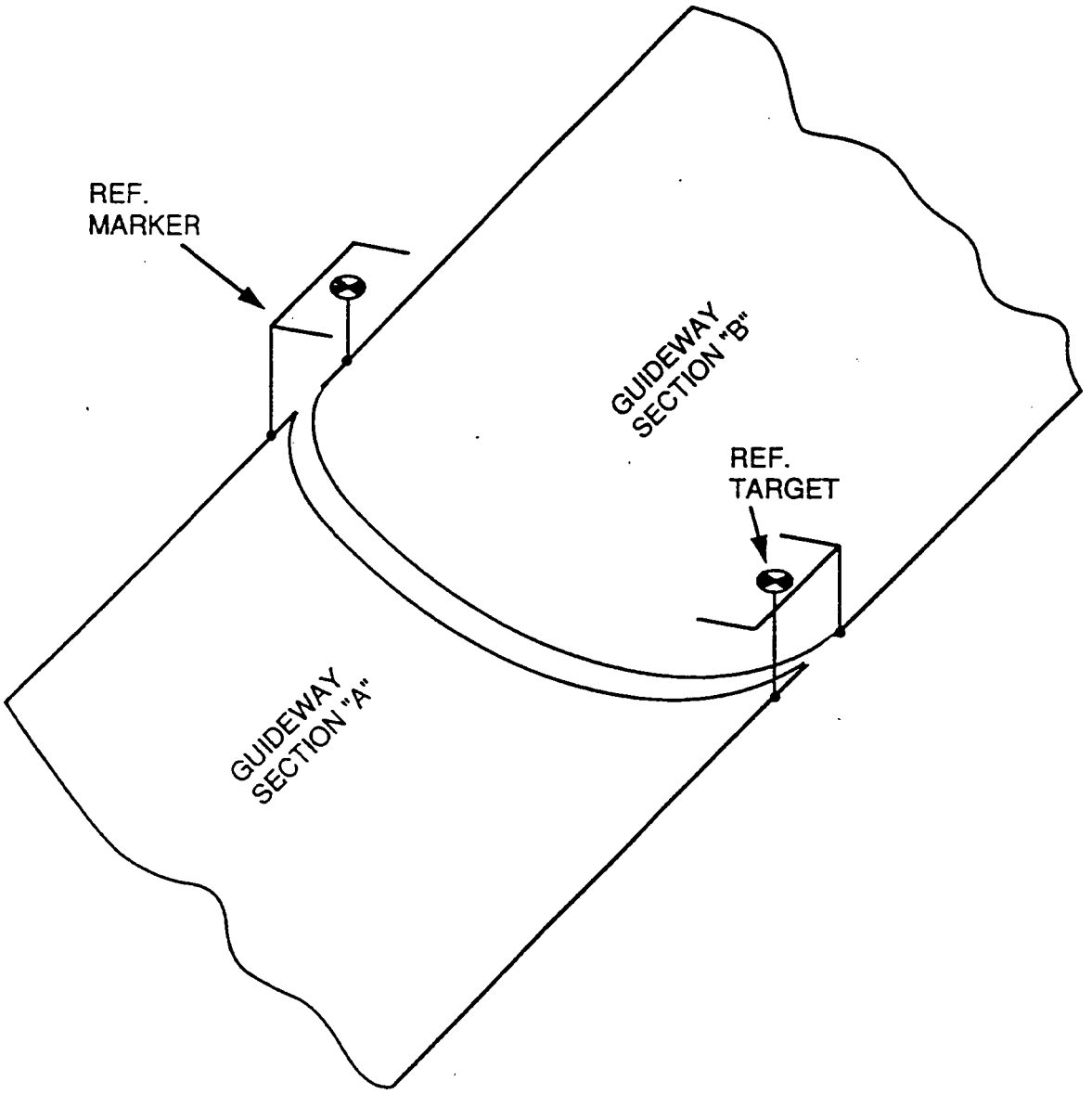

Figure 84 Joint alignment target

3.2.2.j. ANCILLARY STRUCTURES

3.2.2.j.1. MAGPORTS

Major magports - those at ends of corridors in particular - will contain the following:

1. Passenger ticketing (automatic and manual)
2. Baggage handling
3. Vehicle control area
4. Global control center
5. Vehicle loading area (passenger, baggage, freight)
6. Passenger areas (toilet, food, stores)
7. Automobile parking area

Many magports will be smaller.

3.2.2.j.1.1. VEHICLE CONTROL IN MAGPORTS

The global control system will be responsible for the control and operation of the vehicles when they are on the magway, exiting or making crossovers. When the vehicle has reduced its speed and is entering the magport area the magport control system will take control of local operations. At this time the vehicle will have deployed its landing gear and will be powered by the LSM and travel at low speeds. The magport controller will position the vehicle at the loading dock. The magport controller will also bring up vehicles from the storage area when directed by the global controls. When required vehicles may be turned around by the magport controller.

3.2.2.j.1.2. PASSENGER LOADING AREA

The ticketed passengers will proceed through controlled entrances to the appropriate gate and enter the vehicle for their destination. Baggage that has been checked through will be mechanically transferred from the ticket area to the gate where it will be loaded into the baggage compartment by the attendant.

3.2.2.j.1.3. FREIGHT AREA

A freight receiving and loading area will be provided for freight. The freight will be transferred into a special container, loaded into freight vehicles and shipped to their destination.

3.1.2.j.1.4. GLOBAL CONTROL AREA

The global control center will consist of the Operations Room, Communication Room, Equipment Room and the Electronics Shop.

The major magport is shown on the following drawings.

MPT-1 Yard Layout
MPT-2 Loading Level
MPT-3 Passenger Level
MPT-4 Parking Level

3.2.2.j.2. MAINTENANCE FACILITY

The maintenance facility will be configured to provide routine daily maintenance and major repairs to the vehicles.

The routine maintenance areas will contain the following systems:

1. Vehicle washing (exterior)
2. Vehicle cleaning (interior)
3. Septic removal
4. Food service
5. Levitation magnet charging bay
6. Liquid gas

Major repair area will contain the following repair systems:

1. Levitation module repair shop
2. Propulsion module repair shop
3. Cryogenic system repair shop
4. Body shop (exterior and interior)
5. Instrument repair shop (global, local and vehicle)

Also see section 3.2.3.i., Operations and Maintenance.

3.2.2.k. TUNNELS

3.2.2.k.1. AERODYNAMIC PROPERTIES

For the same speed, the vehicle aerodynamic drag is higher in a tunnel than in free air. This occurs because the flow velocity between the vehicle and the tunnel wall is larger than the forward speed and the skin friction is increased. The velocity increase is a function of the ratio A of vehicle frontal area to tunnel cross-section area. The corresponding drag increase for incompressible flow is given to first order by:

$$\frac{\Delta D}{D} = \frac{1}{(1-A)^2} - 1$$

The tunnel size should be as large as possible to minimize the drag increase, which would be accompanied by increased propulsive force and energy costs, both operational and capital. However, increasing tunnel size causes a large increase in construction cost. To aid in the choice of tunnel size, the drag increase was estimated using the equation presented above. Its applicability was assessed by comparison with Japanese data for Shinkansen type tunnels and maglev style trains. (Matsunuma et al, Maglev '89, July 1989). The predictions are presented in Figure 85 for a range of area ratios. The results show that the first order incompressible flow estimate is slightly conservative but is adequate for cost parameter studies. For a vehicle diameter of 3 m and a circular tunnel with a flat floor 9 m wide, the drag increase as a function of tunnel diameter is presented in Figure 85.

3.2.2.k.2. TUNNEL CONFIGURATIONS

Two tunnel configurations are provided for the Magneplane magway. The first configuration is for a single magway tunnel bored in rock (a double magway would consist of two single bores). This configuration is shown in Figure 86.

Based on the tradeoff study in section 5.3.2.30., the tunnel diameter will be 10 m (at most) in most locations. See section 5.3.3.2.h. for the cost effect of various tunnel diameters. Obviously tunnel construction is extremely sensitive to local site conditions and there are a variety of soil conditions that would be encountered even throughout the length of a given tunnel. For purposes of costing tunnels of different diameters, it was assumed that the rock would require rock anchors to provide stability and that the tunnel would be lined with an average 4" thickness of pneumatically placed concrete. This concrete would be placed over reinforcing mesh which is anchored to the rock surface. In accordance with input from the COE, a 12" base slab was assumed. The cost estimate includes provisions for ventilation, lighting and drainage. Additionally, an elevated walkway is provided for maintenance and emergency egress. For completeness, the cost of the magway trough and supports to provide 0.61 m (2') height were also included.

Comparison of Tunnel Drag Data

Tunnel Area Ratio	0.14	0.11	0.092	0.079
% Drag Increase (Matsunuma)	31	21	7	13
% Drag Increase (Magneplane)	34	27	21	18

Drag Increase as a Function of Tunnel Size

Tunnel Diameter (m)	10	12	14
Drag increase (%)	28	16	11

Figure 85 *top:* Comparison of tunnel drag data; *bottom:* Drag increase as a function of tunnel size

The second tunnel configuration provided is a cut and fill type tunnel that would be used in an urban or suburban setting where it is desired to place the magway below grade. This tunnel is rectangular in cross-section with a separating wall between two magways and is shown in Figure 87. The inside cross-sectional area of each half of the tunnel matches the area of the 10 m diameter bored tunnel described in the previous paragraph. This tunnel size is the smallest and most cost effective of three sizes investigated (10 m, 12 m, and 14 m). Note that the net amount of concrete is reduced by adding the separation wall as the addition of the wall halves the span of the top slab thereby reducing its thickness. It is assumed there will be 1 m (3') of cover over the tunnel. The reinforced concrete floor will act as a footing for the magway and is assumed to be .61 m (2') thick. Sizes of the top slab and wall as shown in the figure is based on preliminary design. The costs estimated for the tradeoff study include the excavation, backfill, vertical shoring, ventilation, lighting, drainage, concrete and magway installation, but do not include such items as: street demolition and replacement, utility relocation, temporary covers, underpinning of adjacent structures, etc. The later costs are not included because they are extremely site specific and are unrelated to the concept under study. The aerodynamic effect of tunnel entry is discussed in 3.2.3.c.

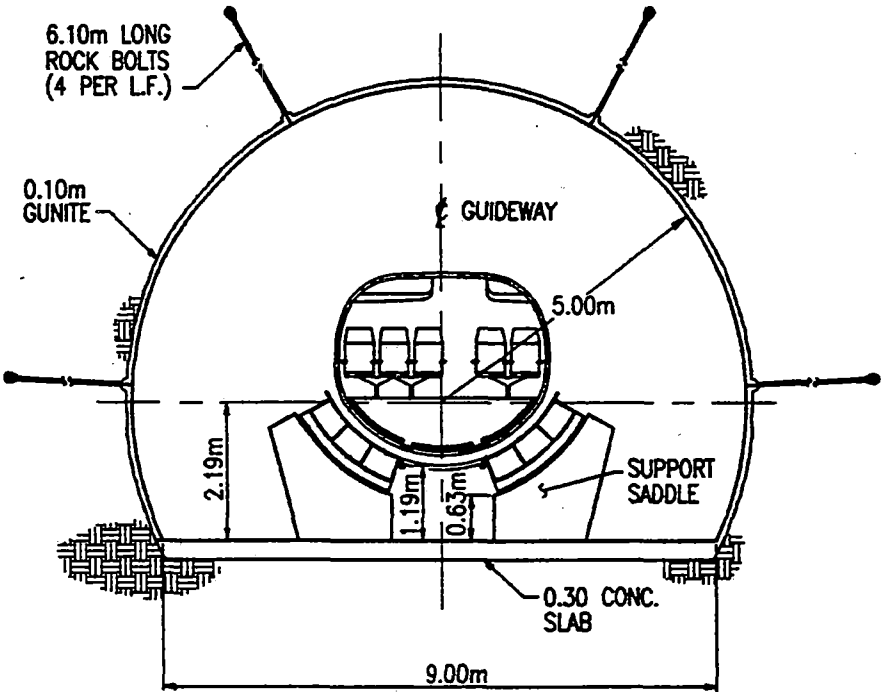

Figure 86 Bored tunnel

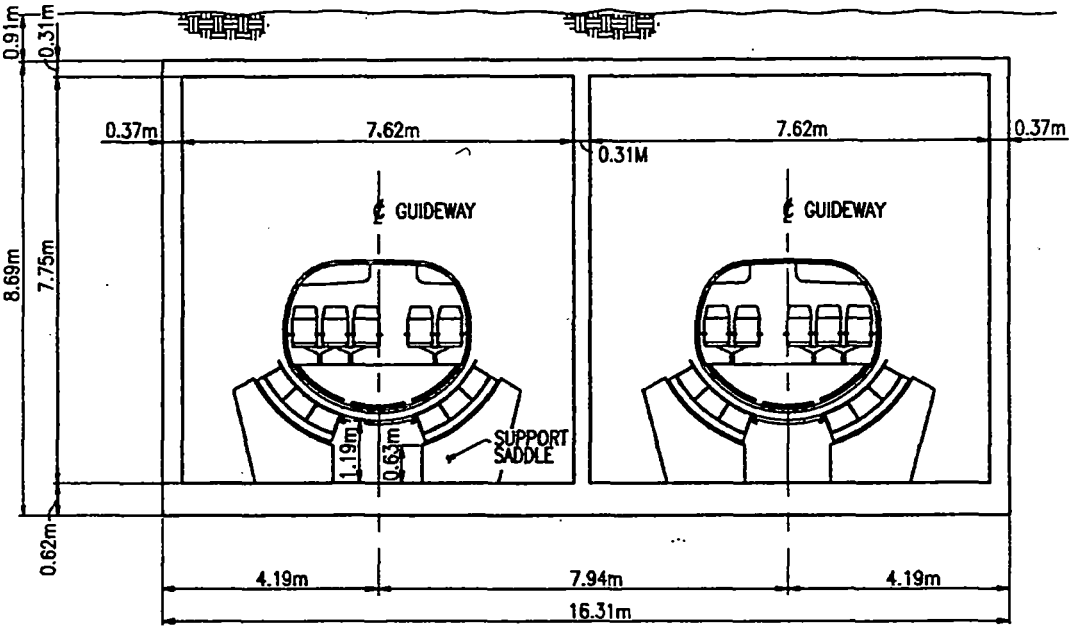

Figure 87 Cut and fill tunnel

3.2.2.el. MAGWAY SEPARATION

The costs of magway separation will vary with several factors. The most practical double magway at grade is actually two (separate) single magways. In this instance, the cost of increased separation would primarily be due to increased Right-of-Way costs. However, establishment of Right-of-Way costs are not within the scope of this report as no site specific information was provided.

For elevated magways, the cost of separation is the length of the crossbeams at the top of the columns and the width of the spanning steel trusses or concrete box beams.

The separation distance between vehicle centerlines has been established as 5.3 m minimum based on ride quality considerations. The present design provides a 5.5 m vehicle centerline separation.

3.2.3. SYSTEM DESCRIPTION - SYSTEMWIDE

CONTENTS

FIGURES

3.2.3.a. COMMUNICATION AND CONTROL

3.2.3.a.1. OVERVIEW

The Global Control System/Center shall be modeled after an Air Traffic Control (ATC) Center due to the similar role/function that is performed, namely controlling the vehicle traffic within a large geographical area. The design shall merge proven techniques with state-of-the-art technology to achieve the specified performance with minimum cost. The Global Control System requirements so closely parallels the design of an ATC system that much of the experience, hardware, and software which Raytheon has spent over 40 years acquiring and developing is directly beneficial to the National Maglev Initiative program.

3.2.3.a.1.1. SYSTEM OPERATION OVERVIEW

3.2.3.a.1.1.1. GLOBAL CONTROL AND COMMUNICATION

The command, control, and communication (C^3) scheme for the Maglev system primarily involves three areas; namely the global control center, wayside controller, and the on-board vehicle controller. This three layer system uses a distributed control architecture, permitting continued safe operation of the rest of the system when localized areas are non-operational.

The global control center has C^3 function jurisdiction over a maximum area of 160 km (100 mile) area, which contains Magports (stations), dual magway (two direction), wayside controllers, and a maximum of 160 vehicles (80 in each direction) in active use with others in standby (sidings). The maximum number of vehicles is based upon a 2 km magway section containing one vehicle. The primary mission of the global control center is to provide the most expedient passenger/freight travel within its jurisdiction while maintaining the highest level of safety possible. This involves minimum of station stops, with minimum delay time at station stops, and wait time between trains. The global control center performs its mission by collecting passenger and freight travel requests through the number of tickets and/or freight billings purchased at stations and in conjunction with route history (date, time, traffic load, etc) performs via a computerized traffic flow algorithm (see section 3.2.3.a.4.) the dispatching and control command needed to operate each vehicle in its system/jurisdiction.

Initially, the global control center will perform a start-up/monitor sequence to determine where all the vehicles are physically located int he system, and determine vehicle status (health). This normally is performed at the start of daily operation, or after an emergency shut down by interrogating each vehicle to report its location and status back to the global control center. The global control operator may also initiate this position reporting and status request at any time. Normally, vehicle position location is performed by the vehicle noting its location via active magway markers. In addition, each vehicle, active or standby, will have a Global Positioning System (GPS) receiver/monitor on-board, which will be continuously monitoring their respective location and forward this location data via an RF link to the

wayside controller, which in turn relays the data to global control over a fiber optic interface data link. The system control loops are shown in Figure 3.

As incoming passenger data (number of destination requests via ticket purchases) from the route Magports arrive; the traffic flow control algorithm/process within global control begins to dispatch and schedule vehicles into the system. Each vehicle has a unique identification number so that particular C^3 data can be sent from the global control center to each vehicle. C^3 data is sent to each vehicle via a data packet switching scheme between the global control center and every wayside controller's along the particular route. An analogy to this scheme is the airline flight plan being broken down in to 2 km intervals (blocks), which require a particular velocity, acceleration, position and time profile. Thus, the vehicle transition profile (real time velocity commands) from its origin to final destination is computed by the global controller, and sent in piecemeal (2 km) segments to the appropriate route wayside controllers. Due to changes in passenger and/or freight loading throughout an operating period; the traffic flow algorithm processor (computer) will be modifying various or all vehicle travel plans; thus updates will be forwarded automatically to the wayside controllers. This process (traffic flow) will be continuously on-going and interactive to insure safe and expedient passenger/freight throughput.

All vehicles in the system shall be under continuous electronic surveillance and control by the global control center, which issues travel orders and monitor each vehicle/s progress via wayside control, thus insuring that global control/commands are being performed by the particular/designated vehicle in the magway block (2 km). The primary function of the global control center operator is to monitor the system and provide technical management of its resources; initiate start-up or shut-down, and modify/select various automated modes of traffic flow operation including emergency shut-down. Each operator can also initiate emergency measures as a back-up mode of operation. Primary responsibility of emergency (stop) initiation will be the responsibility of the computerized fault tolerant and redundant control, command, and monitor/sensor systems, which are automatically updated and monitoring the vehicle velocity, acceleration, magway position plus magway status. Emergency status can also be initiated by the vehicle attendant in the vehicle. A summary of fault and emergency scenario's (what if's) are listed in the safety plan section 5.3.10 with the appropriate corrective/back-up action to be utilized.

3.2.3.a.1.1.2. WAYSIDE CONTROL AND COMMUNICATIONS

Since a Global Center (GC) is responsible for control of approximately 160 km of magway and converter stations are spaced every 8 km, and each Global Center is in communication with 20 converter stations. At low system capacities (less than 12,000 seats/hour), each converter station contains four power converters, two used for westbound, and two used for eastbound traffic. Switching contained in the converter station building, directs each power converter to one of two magway blocks, to implement the leap-frogging switching described elsewhere. At system capacities of 12,000 seats/hour or more, each block has a devoted power converter, with a total of eight power converters residing at each converter station. Consequently each converter station is always driving eight blocks of the magway, four west bound and four east bound, as well as any turn-off functions contained within a block. The converter station contains one wayside control processor system, which controls two vehicles at one time, one in each direction at the low system capacities, and up to eight vehicles at the maximum capacity. The single wayside control processor has the inherent capacity to control up to eight power converters, and the associated switching.

The communication structure is primarily Global to vehicle, with the Wayside Control providing the power to the propulsion drive and verifying/repeating the communication data as required. The Global Controller in a region is responsible for maintaining the correct and synchronized velocities of the vehicles, commanding turn-out switches as required to divert vehicles to magports or alternate routes, and providing transfer of vehicles as they leave the region and come under the command of a neighboring Global Center. Maneuvers, such as compressing traffic to move a vacant time slot, or changing velocity to accommodate an upstream problem can be initiated by one Global Center and continued by the neighboring Global Centers as required.

The Global Center communicates with each wayside control processor in its region, sending commands for each block/vehicle, and receiving updates and status of each block/vehicle in regular intervals. Each vehicle is addressed at a 12 Hz rate by the Global Center. The Global Center provides velocity commands and mapping data to the vehicle. In return it receives an update of the actual vehicle velocity and position within a block, and the status of the vehicle. By knowing the vehicles position and velocity, the Global Center can command velocity adjustments to negotiate curves and insure correct headway between the vehicle and its neighbors. Knowledge of the vehicles status can be a modifier in determining the route of the vehicle (it may have to be diverted to the next Magport if certain safety functions are failing), its ideal velocity and the rate at which the velocity should be changed. In extreme cases, where communication with the vehicle is lost, the Global Center will assume the vehicle initiates an emergency braking procedure, hence all vehicles downstream will be commanded to brake also, so that collision is avoided.

The functional flow from the Global Center to control one vehicle is depicted in Figure 1. In normal operating mode, the Global Center determines the desired velocity of each vehicle at 12 Hz increments by evaluating the required headway from the next vehicle upstream, the maneuvers in process, such as negotiating a curve at a lower velocity, forthcoming maneuvers based on position or external traffic needs, and weather conditions. The calculated desired velocity is normally a small change from the current velocity, and checking is performed to insure no unreasonable acceleration profile is required to adopt the new velocity. Modifiers to the acceleration profile include incline of the magway at the vehicle position, the size of the vehicle, and its cargo. Freight vehicles may experience different acceleration profiles to passenger carrying vehicles. The resultant output is a legal velocity command to the vehicle. Due to the distances involved (up to 80 km from the Global Center), and propagation delays, the issued command is time tagged to the **next** command slot. That is the velocity command should be adopted by the vehicle 83.3 ms (at 12 Hz) after it is issued by the Center. This requires that the GC extrapolates the velocity commands based on anticipated position of the vehicle(s).

The single Fiber Data Distributed Interface (FDDI) communication loop requires that each Wayside Controller and respective vehicle is addressed in sequence by the Global Center. This can result in a maximum skew of an additional 42 ms (half the period of the 12 Hz command rate). This skew is distributed across the distance between the Global Center and one boundary of the region, or a total of 10 Wayside Controllers. Adjacent Wayside Controllers are consequently subject to a data skew of approximately 2 ms, insignificant with respect to the minimum 20 second headway between vehicles.

In addition to sending velocity commands, the GC also sends mapping data to the vehicle. This is required by the vehicle to avoid trying to correct for curves in the magway, as the control system would otherwise adopt a straight line profile by aerodynamic and magnetic field correction. Each map section represents the linear angular relationship of 11 meters of magway to a reference axis, defined by two

angles B_X and B_Y. The mapping data is sent sufficient sections in advance of the vehicles current position to allow the vehicle to process the mapping data, prior to it being required for control correction. Initial mapping data is downloaded to the vehicle prior to launch, at the magport, and the updated mapping information received on route is appended to this database.

The vehicle interprets the velocity commands, in conjunction with the mapping data, to develop an acceleration profile. This profile, along with measured inertial disturbances made by sensors on the vehicle, are used to derive phase, magnitude and frequency commands back to the wayside controller. These commands are sent at a 96 Hz rate, and are used as a reference for the power converter to modify the magnetic wave that propels the vehicle along the magway.

The vehicle 'rides' the magnetic wave generated by applying three phase AC power to the propulsion windings. The windings are spaced 0.75 m apart in the magway, and generate a magnetic sine wave rotating 360° over 1.5 m. This wave propagates down the magway at a velocity proportional to the AC frequency of the power source. 0 Hz (DC) provides a zero velocity field, and the velocity is directly related to the frequency by the equation $v=1.5f$. This results in a frequency of 100 Hz relating to a velocity of 150 m/s. The vehicle is always synchronized to the travelling sine wave, and is positioned approximately at the peak of the thrust component. Adjustment to the magnetic wave permits correction to both the thrust and lift forces. The vehicle travelling at a constant velocity requires a constant thrust force to overcome opposing magnetic and aerodynamic drag. If the aerodynamic resistance increases, the thrust force has to be increased to maintain the velocity. Likewise, if the vehicle negotiates a curve or incline, the magnetic drag and component of vehicle weight opposing the vehicles thrust will change, requiring compensation. In addition, the height of the vehicle above the magway can be modified by inclines, curves and air turbulence, requiring correction by modifying the lift force derived from the magnetic wave. Description of the travelling wave takes the general form:

Magnitude x sin(Frequency x Time + Phase)

The thrust and lift forces can be controlled in combination or independently, by altering the phase angle the vehicle 'rides' on, as well as the magnitude. The lift component offered by the magnetic propulsion drive is just one correcting function used to stabilize the vehicle during flight. The other functions, primarily aerodynamic, are contained within the vehicle, hence the vehicle implements the control algorithms to determine the required phase and magnitude of the wave, as part of the overall stabilization process.

The fact that the vehicle is always synchronized to the travelling wavefront produced by the wayside controller, permits derivation of the vehicle position at all times, to within a few degrees of the wave, or a few millimeters in linear measurement. This knowledge is used to enhance the accuracy of the vehicles calculated position and derived velocity, prior to reporting them back to the Global Center at a 12 Hz rate.

The frequency, phase, and magnitude commands are issued at a 96 Hz rate across the RF link by the vehicle, to the wayside controller. The frequency command is a representation of the required net velocity. The phase command is typically 0°, with variations dependant on the dynamic requirements of the traversing vehicle. The magnitude command is defined as an absolute value. All three use 32 bit word structures to provide resolution better than 1 ppm.

The frequency, phase, and magnitude commands received from the vehicle are evaluated with respect to other parameters prior to being implemented. The controller performs cross-checking of the information to verify that the impending modifications to frequency, phase and magnitude of the magnetic propulsion field are reasonable. If the controller receives an irrational or zero response from the vehicle it tags a fault status word to warn the Global Center and takes appropriate action to maintain safe conveyance of the vehicle, based on knowledge of the current vehicle velocity and position. The LSM power drive takes the frequency and phase commands and modifies a generated sine waveform to adopt the new phase position. This is fed to the phase locked-loop control of the power converter, along with the scaled magnitude command, which tracks both with a nominal 10 Hz bandwidth.

Prior to a vehicle making a transition between blocks of magway, the forward block must be frequency, phase and magnitude synchronized with the preceding one. This requires internal synchronization when the two blocks are driven by one Wayside Controller, or external synchronization when the two blocks are controlled by separate Wayside Units. Based on a vehicle weight of 50,000 kg, and a maximum thrust of 50,000 N at the peak thrust operating point, synchronization accuracy must be better than 3° between the power converters to induce less than a 0.001g disturbance. This is achieved within 0.25 seconds with a converter bandwidth of 10 Hz. Magnitude control must be within 0.1% to induce a disturbance of less than 0.001g. Both of these parameters are achievable with conventional design techniques.

Internal synchronization is performed by applying the same (verified) frequency, phase, and magnitude commands 0.5 seconds prior to the vehicle entering the new block, to both frequency synthesizers and LSM Power Converters. External synchronization is achieved by transmitting the frequency, phase and magnitude commands across the dedicated fiber optic link. This induces a fixed (approximately 50μs) propagation delay due to the communication link, that would result in a phase shift at the next block by up to 1.4°. The receiving wayside controller performs a phase correction computation to correct for this known latency. This transmission also commences 0.5 seconds prior to the vehicle entering the next block.

A typical wayside control processor receives commands from four sources, from the Global Center across the FDDI interface, from the two neighboring wayside controllers via the direct fiber-optic communication links, and from the vehicles occupying the controller blocks. The prime function of the converter station is to provide the propulsion drive magnetic field for each of the eight blocks it controls. In addition, the blocks may contain turn-outs, which also require control commands. At boundaries between regions, the wayside controllers communicate directly via the dedicated fiber optic interfaces, and an FDDI bridge provides communication access between Global Centers. This provides the mechanism to coordinate the required transition of vehicles between Global Centers, as well as direct communication between neighboring Global Centers.

The wayside controller provides for eight blocks of magway, and a vehicle entering one block will typically traverse the four blocks of one traffic direction, unless diverted by a turn-out. Prior to the vehicle entering the first block, the wayside controller downstream transmits time tagged data over the devoted fiber optic link to synchronize the propulsion windings at the boundary for a smooth transition. While the vehicle is in the four blocks, the controller receives commands from the vehicle over the RF link to appropriately modify the time referenced frequency, phase and magnitude of the magnetic field. The controller synchronizes the second of the two blocks prior to the vehicle transitioning from the first block. As the vehicle proceeds to the block boundary for the second and third blocks, the switching

process is initiated to re-route the power converter originally driving the first block, to start driving the third block. The third block is then synchronized with the second prior to the vehicle transitioning. This is repeated, re-routing the converter driving the second block, to the fourth block, and synchronizing appropriately, for the vehicle to traverse the final block controlled by the converter station. As the vehicle traverses the fourth block, the first power converter is re-routed back to the first block, in preparation for the next vehicle. As the vehicle reaches the boundary of the fourth block, the power drive parameters are transmitted to the next converter station across the fiber optic data link, so that the next block can be bought into synchronization.

Another task required some wayside controllers is to activate turn-outs to switch traffic as required. A turn-out is activated while the vehicle is in the block containing the switch, and consists of activating appropriate sections of the magway windings to direct the traversing vehicle. The switch time is approximately 5 seconds, and the switch is physically at the end of the block, such that a vehicle traversing 100 m/s has a minimum traverse time of 10 seconds prior to encountering it. If a switch transition is detected to have failed, there is sufficient time to reset it prior to the vehicle using the affected section. The Global Center issues the commands to transition a switch as it coordinates the vehicle through the block, and reset it once the vehicle(s) have turned-off. The switch function is coordinated by the wayside control processor in response to the commands from the Global Center.

An FDDI bridge router provides access between the FDDI links of adjacent Global Centers. Each Global Center is in communication with at least two neighboring centers, requiring two bridge routers. Where a more complex route exists, with turn-offs accessing different regions, more bridge routers are introduced to provide communication from on Global center to its many neighbors. A vehicle proceeding to exit a Global center region enters the transitional block controlled by a boundary wayside control processor, which communicates directly to the neighboring wayside control processor in the next Global region across the dedicated fiber optic link. This process is identical to that administered at any other wayside to wayside interface. Communication between global centers is maintained through the FDDI bridge.

3.2.3.a.1.1.3. VEHICLE CONTROL AND COMMUNICATION

The vehicle communicates to the Wayside Unit that is operating the block the vehicle occupies via a dual RF link. Two data rates are used for transfer of commands and responses, 12 Hz and 96 Hz. Velocity commands and mapping data are received from the wayside processor at a 12 Hz rate, and vehicle measured position and velocity, as well as status, is returned as a response at the same rate. This information is used by the controlling Global Center. Frequency, phase and magnitude commands for the propulsion windings in the magway block that are driven by the converter station are transmitted at a 96 Hz rate. The function of controlling the magnetic wave that the vehicle 'rides' on is a closed loop, that is driven by sensors on the vehicle, and the external velocity command. This higher communication rate of 96 Hz is required to avoid the 10 Hz response of the power converter in the control loop.

Figure 2 depicts the functional flow of the controls process on board the vehicle. Velocity commands ($\dot{\varnothing}_G$) received from the Global Center (via the wayside control processor) are compared with the current velocity ($\dot{\varnothing}_V$), and an eight point acceleration profile is generated, based on mapping data and the status (health, load etc) of the vehicle. This acceleration profile normally achieves the commanded velocity just prior to receipt of the next velocity command. In abnormal conditions, the vehicle may not reach the

commanded velocity. As actual velocity of the vehicle is known by the Global Center, it is able to make corresponding adjustments to downstream traffic if necessary, to prevent loss of headway.

Actual velocity is derived by determining the frequency at which stationary position markers are passed by the vehicle. RF position markers are placed at 11 m intervals along the side of the magway. The spacing insures that a minimum of two markers are inside the length of the vehicle at all times. The markers emit continuous signature streams, which are received by sensors on the side of the vehicle. An amplitude peak detection scheme is used to determine when the marker coincides with the vehicle mounted receiver, achieving accuracies of better than one meter. This provides an indication of coarse position (P_{COARSE}).

This data is enhanced by using the magnetic field sensors distributed along the length of the vehicle. The magnetic field sensors sense a stationary wave of 1.5 m cycle length from the propulsion field. By spacing the sensors appropriately, the waveshape can be accurately established inside the vehicle. The vehicle 'rides' this wave at a nominal phase angle of 0°, modulated to provide heave and thrust control. As the waveshape is re-created inside the vehicle, the physical relationship of when it crosses zero can be determined within a few degrees. A 2°accuracy will yield position sensing with respect to the magnetic wave to within 8 mm. This knowledge of the fine position is used to modify the coarse measurement. As long as the coarse measurement is known within one magnetic wavelength (1.5 m), the position of the vehicle can be accurately determined to within a few millimeters.

This position data is communicated back to the wayside control processor at a 12 Hz rate. By time referencing the position and differentiating it, the velocity ($\dot{Ø}_V$) of the vehicle can be extrapolated. This velocity is used to derive the required frequency (w_C), based on the winding pitch of the magway LSM. The velocity estimate can be further improved by using the accelerometer data to determine the acceleration profile of the vehicle (not shown). The velocity of the vehicle is communicated back to the wayside control processor across the RF link at a 12 Hz rate. The desired propulsion frequency (w_C) is transmitted back at a 96 Hz rate.

The measured velocity ($\dot{Ø}_V$), and commanded velocity ($\dot{Ø}_G$), are interpolated to derive the required acceleration profile. This profile is subdivided into eight acceleration commands which are then acted on at a 96 Hz rate.

The two on board accelerometer packs are used to provide a measure of the thrust acceleration currently experienced by the vehicle ($\ddot{Ø}_{MM}$). Mapping information is used to modify the interpretation of the accelerometer data. When the vehicle is negotiating an incline, the accelerometer will also measure a component of gravity. As the mapping provides knowledge of the incline, this component can be corrected for when calculating the vehicle acceleration relative to the magway. Mapping information is used to modify the desired acceleration profile, as inclines will limit the thrust force capability of the propulsion drive system. This results in a modified acceleration term, $\ddot{Ø}_{CM}$. Mapping data, held in memory, describes 11 m sections of the magway in terms of two referenced angles, B_X and B_Y. The memory buffer contains a description of the next 2 km of magway and is updated at a 12 Hz rate by the Global Center (via the wayside control processor), history is discarded to save memory space. The buffer size requirement is limited to just under 1 KB, based on 182, six byte map references.

The measured thrust acceleration ($\ddot{Ø}_{CM}$), and the commanded acceleration ($\ddot{Ø}_K$), are used to derive a thrust acceleration error ($\ddot{Ø}_E$). This acceleration error can be converted to a thrust force error (F_{PE}) based

on the dynamic parameters of the vehicle. This force, error, modified by any aerodynamic coupling terms required, drives an integrator to provide the correcting thrust driving element F_{TE}.

A similar process is used to derive the heave component, F_{HE}. Heave acceleration is also measured by the accelerometer platforms. The two platforms, mounted fore and aft of the vehicle, permit rotational and translational motions to be distinguished, hence the component of heave acceleration ($\ddot{O}_{MH}$) can be extrapolated. This is also modified by the mapping data, to exclude components of heave due to inclines, providing the heave component $\ddot{O}_{CH}$ that requires compensation.

The heave compensation is provided through two mechanisms, modulating the phase and magnitude of the magnetic propulsion wave, and aerodynamic control. The aerodynamic control has more authority at higher velocities, and the magnetic wave more authority at lower velocities. The measure velocity ($\dot{O}_V$), is used in a function to apportion the measured heave error between the magnetic and aerodynamic controls. The component apportioned to the magnetic compensation ($\ddot{O}_{MH}$) is converted to the equivalent force error F_{HM}, based on the vehicle dynamic properties. The difference of this component, and the measured heave force component (F_H) (along with any required aerodynamic modifiers), is used to derive the correcting force.

The measured heave force (F_H) is derived from the magnetic sensors on the vehicle. These sensors measure the magnitude of the magnetic field produced by the propulsion windings in the magway , as seen at the vehicle. Height sensors, also distributed throughout the vehicle provide a measure of the clearance of the vehicle from the propulsion winding. The knowledge of the vehicle height, and the measured magnetic field strength, are used in combination to extrapolate the magnitude provided by the magnetic wave (M_M). This magnitude, along with the known phase (P_M), are acted on to extract the component of the field that produces the heave force (F_H).

The heave correcting force is integrated to provide a heave driving element F_{HE}. This, in combination with the thrust driving element (F_{TE}), is used to derive the new phase (Φ) and magnitude (M) commands that are sent to the wayside control processor at a 96 Hz rate.

Figure 2 represents a simplified control process to demonstrate the normal control flow. The combination of height, magnetic and inertial sensors permit additional cross-correlation of vehicle operation. As an example, the spacing of the height sensors permits verification of when a vehicle is negotiating a curve (the center of the vehicle is at a different height with respect to the magway than the extremes), to augment the accelerometer data. These secondary mechanisms enhance the fault tolerance of the vehicle operation, and permit alternate derivation of dynamic parameters when individual sensors fail. The status of the vehicle is a measure of the operating state of each of the subsystems, sensors and controllers on board. Certain faults (partial loss of height detectors etc) may invoke reduced acceleration profiles for safety reasons. This is taken into account by modifying the control process to re-route parameter data as required.

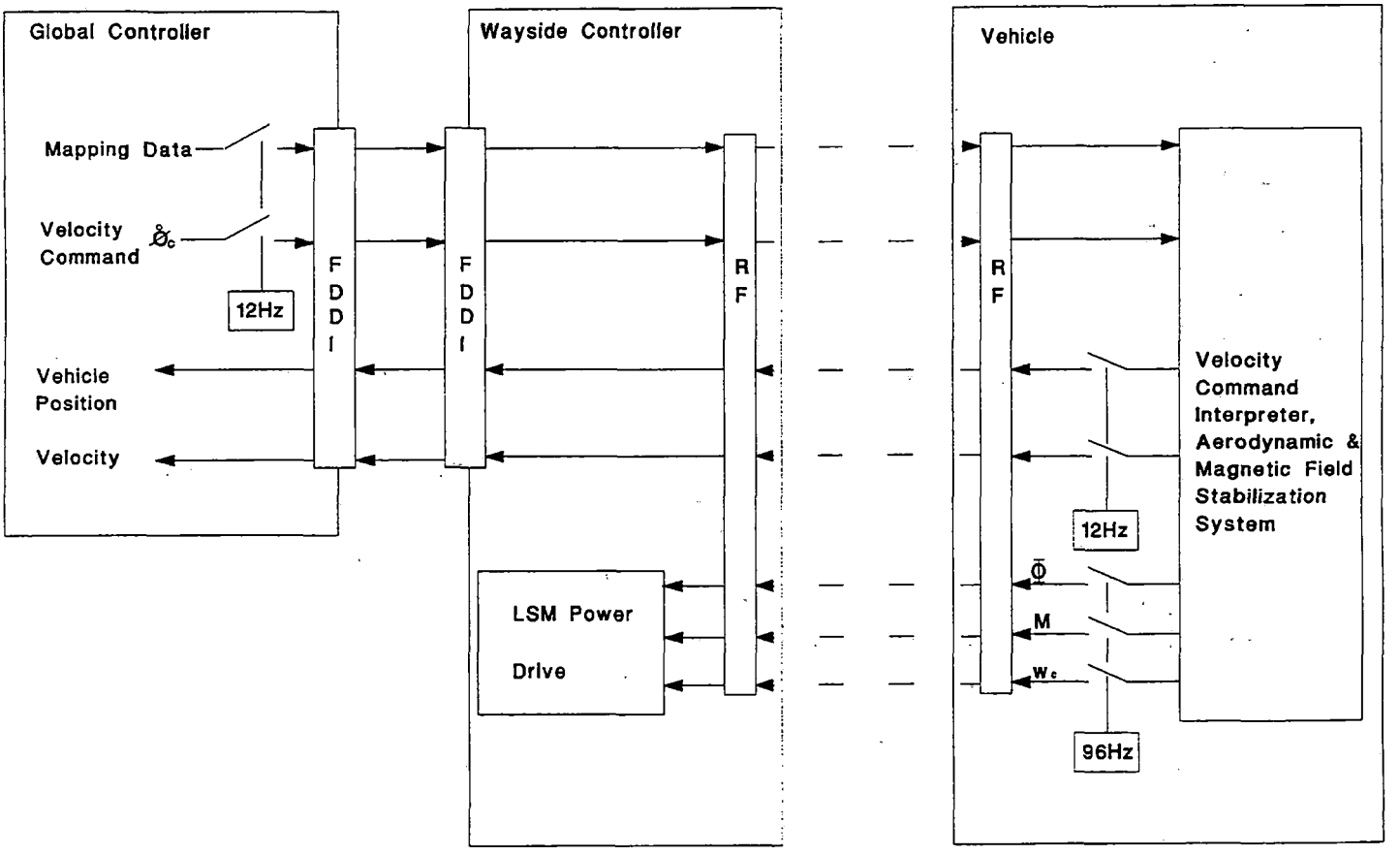

Figure 1 System data flow

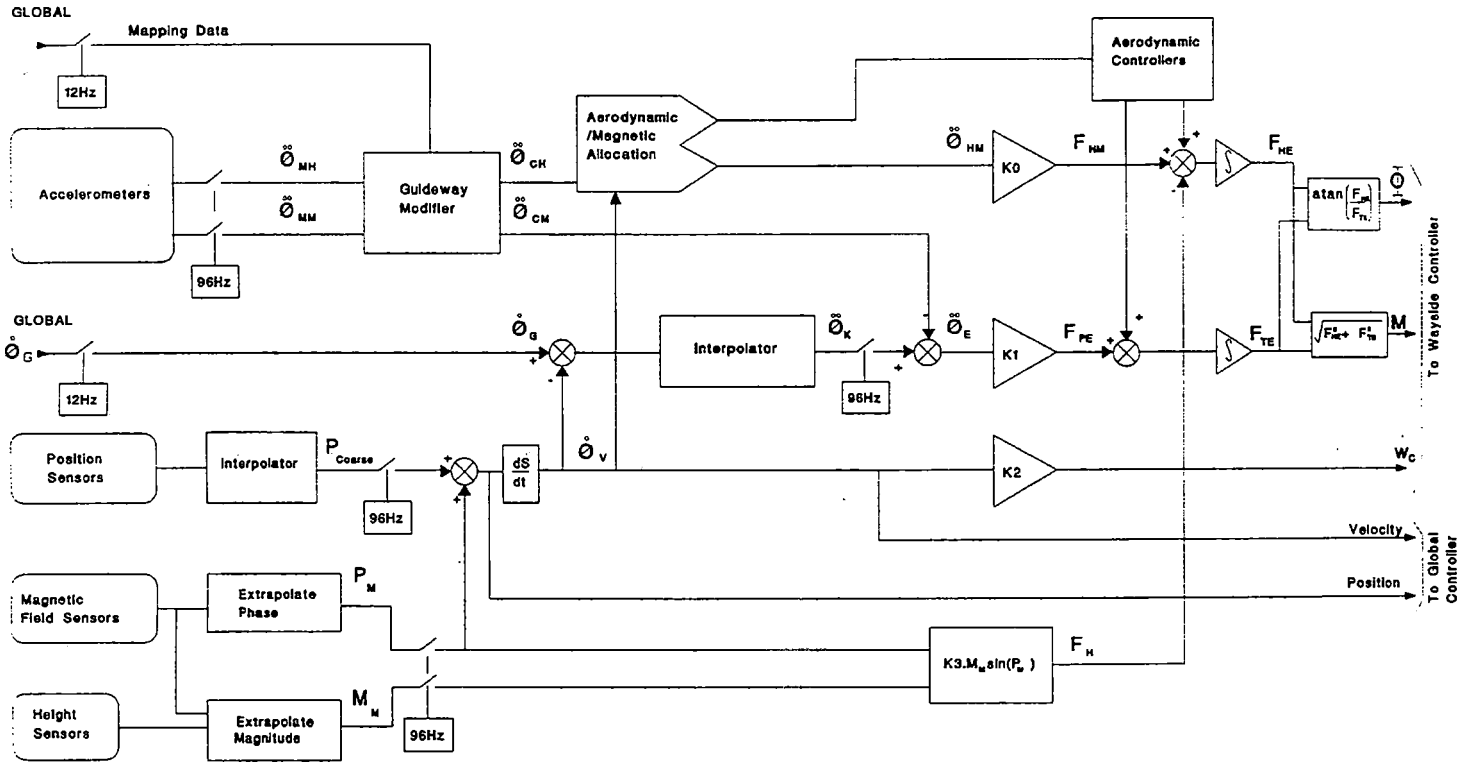

Figure 2 Vehicle functional control flow

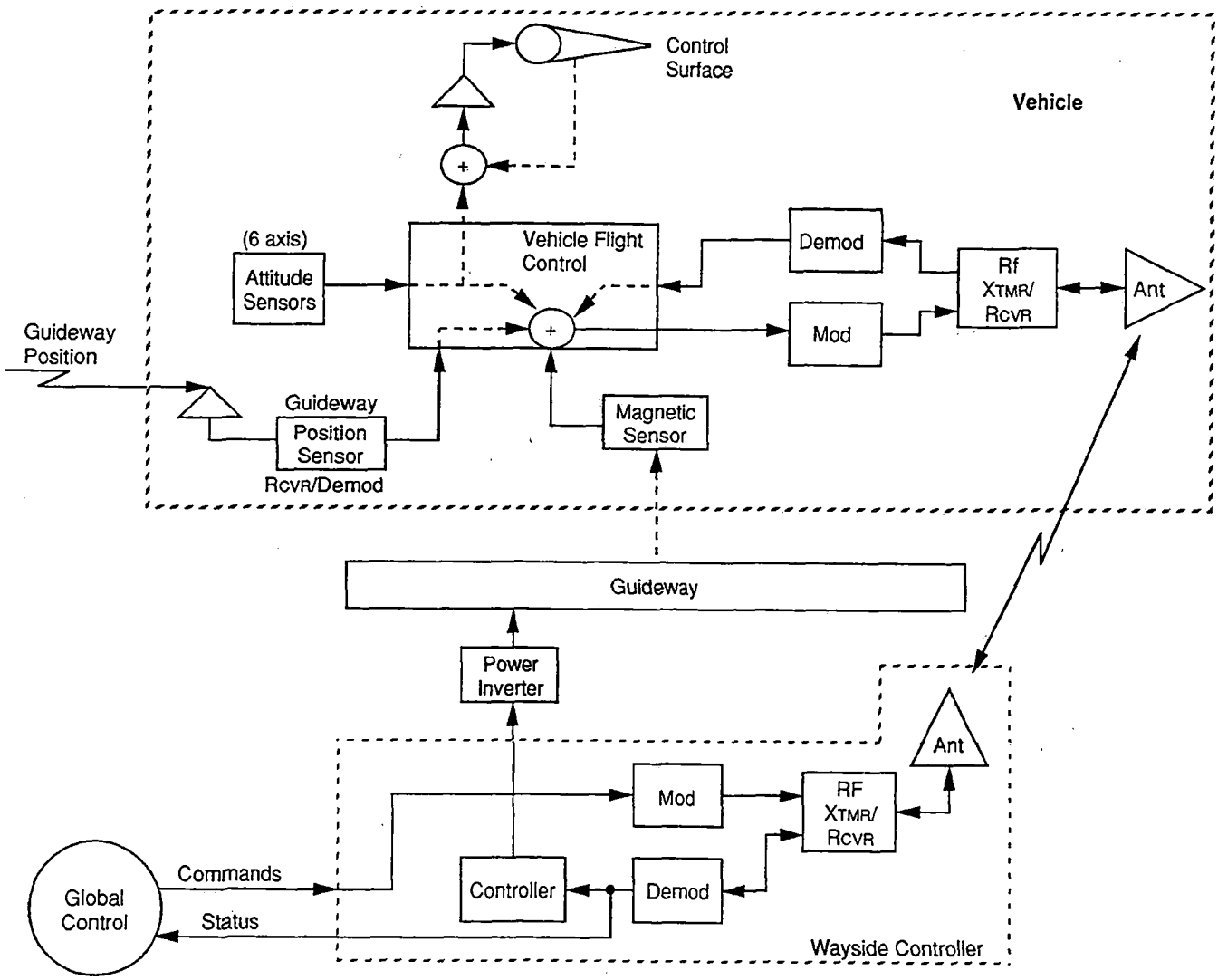

Figure 3 System control loops

3.2.3.a.2. KEY FEATURES - GLOBAL CONTROL SYSTEM

The proposed Global Control System will provide each traffic controller with a situation monitoring system that presents him with a total picture of vehicle traffic in his area. The system will facilitate his assessment of the traffic and enable him to make the right decision concerning each event that requires his intervention. In addition, various vehicle control sensors will provide the safety and operational effectiveness while simultaneously reducing the ownership costs. See Figure 4 for a summary of features.

Safety has the highest priority of any vehicle traffic control system requirement. The system must not only meet today's safety needs but be capable of the growth needed to maintain these high standards as traffic densities increase in the future. Raytheon's system will provide the traffic control efficiency through increased coverage, data reliability, system availability, and target capacity.

Data reliability is as important as coverage for maintaining safety. When too many false alarms or false replies accompany the desired sensor data the system effectiveness is degraded. The system Raytheon proposes incorporates all the proven methods of controlling false alarms.

High system availability is also essential for safety. This is achieved through the greatest possible use of redundancy so that single failures cannot interrupt the data to the vehicle traffic controllers. Extensive use of built-in test equipment and automatic fault detection and isolation further improves availability by minimizing the time required to repair a fault.

Excess vehicle capacity is vital for safety because only in high density situations are the limits of system capacity and the margin for safety approached. In this regard, the Raytheon design fully complies with the vehicle capacity and data requirements set forth in the specification. Furthermore, it has a modular architecture that allows the system capacity to be matched to the needs of individual sites and to be increased as needed in the future. As more system (vehicle) capacity is needed, prime power reserve, power supply reserve, space card slots, and space for additional modems are available for future expansion.

3.2.3.a.2.1. TECHNOLOGY

Raytheon's design includes: Global Control Center (GCC) consoles derived from the consoles we are supplying to the Federal Aviation Administration (FAA) for this Advanced Automation System (AAS);RISC processors, with UNIX operating systems; GPS subsystems produced by CAST; software evolved from RAMP, DERD, and Raytheon's Automatic 2000 product line and mapping systems produced by Intergraph; sensor signal processing and communication systems design by Raytheon engineers and configured with state-of-the-art off-the-shelf equipment.

3.2.3.a.2.1.1. TECHNOLOGY UPGRADE IN PROVEN SYSTEMS

While proven technology is essential in safety-oriented, mission critical, GCC systems, use of state-of-the-art technology is also important. Raytheon has evolved its system to take advantage, where prudent, of emerging and stable technologies. The ability to up-grade to the latest hardware platforms is a key element of Raytheon's overall system design. Modular, microprocessor based architecture, local area

network (LAN) connectivity, and use of industry standard interfaces are integral to our overall design. This, combined with software written using industry standard software development and testing methodologies, results in a highly reliable and flexible system compliant with individual customer requirements.

3.2.3.a.2.2. OPEN ARCHITECTURE DESIGN

Raytheon's designers have built "openness" into the proposed system. The concept of an open system revolves around an open environment design philosophy that, rather than create barriers with proprietary hardware and software architectures, follows industry wide standards. Our open system allows interconnection with other open systems without requiring a significant redesign or reintegration effort. It is based on the mutual recognition and support of applicable standards, without forcing a particular implementation or technology. This idea is central to Raytheon's system design.

3.2.3.a.2.2.1. MICROPROCESSOR

The selection of SUN and Motorola processors assures compatibility with industry-standard software, networking, an systems technology.

3.2.3.a.2.2.2. UNIX OPERATING SYSTEM

Raytheon's software system is built on a standard implementation of the UNIX operating system. The UNIX operating system and development environment is the fastest growing in the computer industry. UNIX offers a number of significant advantages to both system developer and customer including: simplified development and training; minimized maintenance costs; software which is readily portable to other hardware platforms; and compatibility of software and development tools from third parties.

3.2.3.a.2.2.3. "C" HIGH ORDER LANGUAGE

Raytheon has selected the "C" language, one of the world's most widely used standard high order programming languages. The "C" language has a very large userbase and is designed to be easily portable to other hardware platforms.

3.2.3.a.2.2.4. TCP/IP COMMUNICATION PROTOCOLS

Raytheon has given careful consideration to the choice of the communications protocol that provides the logical link between the computers on the local area network. The industry standard Transmission Control Protocol (TCP) and Internet Protocol (IP) suites have been selected because they offer a mature working set of protocols that provide high levels of interoperability and functionality. In addition, TCP/IP enjoys a solid position in the commercial marketplace with a high degree of acceptance by vendors providing communications products.

3.2.3.a.2.2.5. VME and SCSI BUS TECHNOLOGY

Raytheon's use of VME bus, the leading 32-bit bus standard, allows access to a large and expanding set of controllers and system components implemented on VME modules. The system designer may select from a range of system configurations for the storage and I/O expansion required.

3.2.3.a.2.2.6. ETHERNET LOCAL AREA NETWORK (LAN)

The computers that form the GCC system are all linked via a powerful (10 million bits per second) LAN. The LAN is compliant with the Ethernet standard (IEEE 802.3) and is replicated for fault tolerance. The use of a standard local area network allows the system to be upgraded and expanded to include a network of computers of arbitrary complexity and size.

3.2.3.a.2.3. SOFTWARE ARCHITECTURE

Raytheon's software architecture is characterized as distributed and layered. It is organized as discrete tasks, distributed among subsystems which are all linked by redundant LANs. The entire system is message driven, with intertask communication and synchronization also via messages. This assures modularity in which functions can be added or removed to adapt to large and small systems by adding or removing the associated software modules. It also assures the easy integration of software modules originally developed for different systems. To ensure maximum software maintainability, the application tasks are isolated from the communications tasks by layering the application tasks on top of the industry standard network protocol (TCP/IP). A commercially available operating system (UNIX) provides the interface between network protocols and the application tasks.

Workstations are driven by software developed by Raytheon for the Federal Aviation Administration's (FAA's) Advanced Automation System (AAS). The workstations include the Silicon Graphics, Inc. (SGI) graphic library which has been enhanced by Raytheon to provide high-level support for air traffic control functions, which are directly applicable for Maglev.

Raytheon's systems are configured so that no single path failure can interrupt the flow of data to the displays or the operation of any vital function. High availability is achieved with a reconfiguration strategy is which all subsystems report their status to a central processor which then provides optimum configuration commands to the subsystems.

3.2.3.a.2.3.1. SOFTWARE FEATURES

1. Open architecture, extensive use of standardization.
2. UNIX operating system, high level language code.
3. Algorithms and software proven in U.S., Canada and Germany.
4. High availability achieved through proven automatic reconfiguration software.
5. System functional and capacity growth accommodated without hardware or software throw-away.
6. Comprehensive on-line diagnostics throughout support control and monitoring system.
7. System management, error detection, and health monitoring performed continuously.
8. The use of an industry standard network protocol (TCP/IP), a distributed architecture, and flexible software allow new nodes to be easily added to meet future expansion requirements.

3.2.3.a.2.3.2. SOFTWARE ESTIMATE

The Maglev system concept design consists of three processing subsystems referred to as Global, Wayside and on-board Vehicle Control and Communications.

The information presented below is an initial estimate of the software lines of code required for each processor type in the various subsystems. The Estimated Lines of Code is based on estimates of like functions in the Raytheon DERD-XL (D) or RAMP (R) ATC systems, or simply rough order of magnitude estimates for new (N) functions that don't have a similar counterpart in the ATC systems.

The criteria used to estimate Critical Lines of Code is based on a subjective estimate of total code which is

(a) critical to proper control of the vehicle, and
(b) code execution frequency.

3.2.3.a.2.3.2.1. GLOBAL CONTROL AND COMMUNICATIONS SUBSYSTEM

The purpose of the Global Control and Communications Subsystem is to provide a central position from which human operators can monitor and control the vehicle activity on a given 160 kilometer section of two-way maglev track. The basic inputs to this subsystem are from the operators (3) and Wayside Control and Communications subsystems (80 max). Operator inputs consist basically of vehicle route plans and display commands and device control commands. Wayside inputs consist of vehicle progress status, local status, and configuration.

The Global Control and Communications Subsystem consist of a dual redundant channel processor and three display processors interconnected via dual redundant LANs.

The channel processor software components are shown in Figure 5. The display processor software components are shown in Figure 6.

3.2.3.a.2.3.2.2. WAYSIDE CONTROL AND COMMUNICATIONS SUBSYSTEM

The function of the Wayside Control and Communications Subsystem is to control the power distribution to a two (2) kilometer section of the magway in order to propel the vehicle along this section. The basic inputs are the route data from the Global subsystem and performance and status data from the Vehicle Control and Communications Subsystem. The basic outputs are the controls to the Power Inverter Interface and status data to both the Global Control Center (via LAN) and Vehicle (via RF) subsystems.

This subsystem is made up of dual redundant control processors and an arbiter processor interconnected to each other and to the Global Subsystem via a dual redundant LAN.

The software components are shown in Figure 8.

3.2.3.a.2.3.2.3. VEHICLE CONTROL AND COMMUNICATIONS SUBSYSTEM

The purpose of the Vehicle Control and Communications Subsystem is to control the "motion" characteristics of the vehicle as it traverses the track. Its basic inputs are "motion" data from the vehicles various sensors and data from the Wayside subsystem via an RF link. Its outputs are commands to the vehicle's motion control units and current vehicle status and "motion" parameters to the Wayside subsystem.

The Vehicle Control and Communications Subsystem consist of a dual redundant flight control processor.

The software components are shown in Figure 7.

3.2.3.a.2.4. CONTROLLER CONSOLE DESIGN

The single most critical system feature is the GCC display consoles' human-computer interface (HCI) for non-fatiguing, error-free operation by traffic controllers.

Raytheon's GCC consoles provide unique HCI features derived from the United States FAA Advanced Automation System (AAS) program and from proprietary Raytheon display management software.

Raytheon has designed and will deliver over 5000 AAS Common Consoles. Each console contains a 20-inch square, 2048-line, color raster monitor and a state-of-the-art Raytheon display controller.

Raytheon's AAS display controller is proposed for the GCC console. It provides exceptionally rapid responses to controller. Actions and display requests together with exceptionally clear data presentations. Flexible windowing allows situation presentations to be combined with vessel data presentations. Each window can be independently scaled, scrolled, and set up with presentation formats and data-color associations.

The AAS display is ideally suited primarily because of the close similarity of the ATC controller and GCC controller tasks. Also, the console was designed with a great span of adjustability in order to accommodate controllers (watchstanders) from the 5% female to the 95% male.

Raytheon's proprietary display management software also is incorporated within the GCC console. Display set-up features normally found only in so-called "Rapid Prototyping" experimental test bed workstations are incorporated into the operational GCC console. Colors, color-data associations, font types and sizes, data block formats, preset windows, and a wide variety of other settings can be established using pop-up and pull-down menus and the track ball.

Display settings which need to be standard for all consoles can be stored by the supervisor and password protected against unauthorized change by the watchstanders. Other settings are available to the controllers and can be stored by the different controllers to become available automatically when they log on to the system.

This unique combination of fully developed and mature state-of-the-art hardware and software provides the GCC system with exceptional opportunities for matching the human-computer interface to the operational requirements of the GCC controllers. It also provides unique opportunities for minimizing the training impact of the initial transition to GCC.

GLOBAL CONTROL CENTER (GCC) **GPS Reference Station (GPSRS)** 1. Communicates GPS corrections via FDDI to wayside controller for broadcast to vehicle. 2. GPS receiver tracks all visible satellites $\geq 10^0$ above the horizon. 3. Once initialized, the GPS initializes itself automatically at power-up. 4. Alert messages generated when satellite track not achieved. **GPS Performance Monitor (GPSM)** 1. Measured position accuracy evaluated 2. Alarm issued when position error exceeds 10 meters.	**Data Communication System (DCS)** 1. DCS implemented with open systems (IEEE 802.3 LAN, RS232C serial interfaces, Internet LAN protocols (TCP/IP), VME-based computer products). 2. LAN performance monitoring software. 3. Each LAN has enough bandwidth to support the traffic among all nodes. 4. Network security provided using limited access via log in and password protection. 5. Router/gateway uses same processor at GCC consoles to maximize commonality.
DECISION SUPPORT SYSTEM (DSS) **Digital Selective Calling (DSC) Management System** 1. Controller able to initiate DSC communications with any vehicle, set the reporting interval time, and terminate periodic DSC transmissions from any vehicle. 2. Uses queuing to keep channel utilization minimal. 3. Passes ID of vehicle requesting initiation of tracking to the TIPS. 4. Adaptive sampling rate based on predicted encounters. **Target Information Processing System (TIPS)** 1. Open standards - "C" language and UNIX operating system. 2. Mosaic tracker using guideway position sensor and GPS position reports. 3. Record/playback **Vehicle Traffic Information Systems (VTIS)** 1. Multi-user Data Base Management System (DBMS) supports VTIS. 2. Generic interface to DBMS provided by an ANSI standard	**Geographic Display System (GDS)** **Electronic Charts** 1. Charts generated/edited with software. 2. 6 resolutions used to retain readability. **Display Unit/Consoles** 1. Image update 4 times per second. 2. 20-inch-square color displays. 3. Graphics Library enhanced by Raytheon. 4. GCC console driven by standard VME bus and 17 MIP Motorola Delta series 8000 system running UNIX. 5. Suitable for use with ambient background lighting of 10 foot candles. 6. User friendly software permits relatively unskilled personnel to align the display. 7. Symbols for each vehicle type are oriented to heading and scaled to chart size. 8. Color coding of tracking status. 9. Automatic target symbol as well as tag deconflicting. **Alarms** 1. Queue overflow causes error message to be sent to operator. 2. Prioritized.

Figure 4 Global control system features

	Total Lines of Code		Critical Lines of Code
Startup			
Initialize applications	250	D	0
Establish database/retrieve from redundant channel	500	D	50
Performance Monitoring (PM)			
Confidence Checks	250	D	100
External/Internal status processing	200	D	50
Self assessment	300	D	300
System Configuration/Control			
Redundant channel reconfiguration	300	D	50
Redundant LAN Status/Control	200	D	50
Display Processor init./startup coordination	300	D	0
Wayside Configuration Status	250	N	50
Input/Output Control/Routing			
LAN Message Routing	300	D	150
Redundant Channels			
Display Processors			
Wayside Controllers			
GPS	200	N	50
Data Recording/Display Playback	1500	R	100
Target Information Processing (TIPS)	2400	N	600
Sensor Input			
Maintain Tracks			
Fuse Track Data			
Route Generation			
Route Conformance			
Encounter List			
Danger Area			
Alarm Detector			
Vehicle Status			
Digital Selective Calling Management			
Handoff Control			
Track re-route processing			
Vehicle Traffic Information (VTIS)	2000	N	500
Database Management			
SQL I/O			
Archive			
Reports			
Total Lines of Code	8950		2050

Figure 5 Channel processor software components

	Total Lines of code	Critical Lines of code
Start-up	500 D	0
Performance Monitoring	1500 D	300
Input/Output Control/Routing	300 D	150
Operator Input/Output Command Processing	4000 D	400
Geographic Display System		
Zoom/Pan	100 D	0
Video Processor	500 N	50
Status/Alarm Display	100 D	50
Track Display	200 D	200
Chart (Map) Display	300 D	0
Graphic Editing	200 N	0
Record/Play Control	300 R	0
Tag Deconflicting	200 D	0
Display Playback	500 R	0
Diagnostic Terminal Processing		
Chart Generation	500 N	0
Maintenance	1000 N	0
Availability Statistics	200 N	0
Data Recording Analysis	2000 R	0
Total Lines of Code	12400	1150

Figure 6 Display processor software components

	Total Lines of Code		Critical Lines of Code
Startup			
Initialize applications	300	D	0
Establish database/retrieve from global channel	500	D	50
Performance Monitoring (PM)			
Confidence Checks	200	D	100
External/Internal status processing (20 Devices)	2100	N	500
Self assessment	300	D	300
System Configuration/Control			
Redundant processor reconfiguration	200	D	50
Redundant External Device Control (20 Devices)	2000	N	1000
External Interface (20 Devices)	4000	N	2000
Integrated Flight/Propulsion Control Function	5000	N	2500
Total	14600		6500

Figure 7 Vehicle control software components

	Total Lines of Code		Critical Lines of Code
CONTROL PROCESSOR			
Startup			
Initialize applications	300	D	0
Establish database/retrieve from Global channel	500	D	50
Performance Monitoring			
Confidence Checks	200	D	100
External/Internal status processing	300	N	150
Self Assessment	300	D	300
System Configuration/Control			
Redundant processor reconfiguration	200	D	50
Redundant LAN Status/Control	100	D	50
External Interface			
Vehicle RF Comm	300	N	300
Telecom Interface	200	N	50
Position Marker Monitor	200	N	100
Power Inverter Interface	300	N	150
Vehicle Drive Function	500	N	200
Route Plan Processing	500	N	200
Total Lines of Code	3900		1700
ARBITER PROCESSOR			
Startup			
Initialize applications	50	D	0
Establish Database	100	D	0
Performance Monitoring			
Confidence Checks	200	D	100
External/Internal status processing	100	D	50
Self-assessment	100	D	100
System Configuration/Control			
Redundant processor selection	100	D	100
Redundant LAN Status/Control	100	D	50
Maintenance Interface/Control	500	N	0
Block Strap Monitor	200	N	50
Total Lines of Code	1450		450

Figure 8 Wayside controller software components

3.2.3.a.3. OPERATIONAL REQUIREMENTS

This section presents the Magneplane International team view of the operational scenario of a Global Control Center as would be operated in a regional area using sensor information from vehicles and large-screen, high resolution raster displays portraying vehicle magway position data and chart data in a cohesive manner.

The Global Traffic Control system must provide each operator with a useful collision and conflict assessment capability, at a glance, via a decision-making tool that fuses all necessary information into a logical and easy-to-understand format. This concise and timely information must be displayed to the operator for performance of the traffic advisory role or, when necessary, to support the decision/information requirements needed to direct or, as a last resort, control the safe movement of vehicle. See Figure 9.

The proposed solution is based upon Raytheon's experience in building traffic control systems throughout the world and by our experience in marine/vessel tracking, air traffic control, and weather monitoring systems worldwide. Thus, Raytheon will draw on its extensive knowledge to support the National Maglev Initiative objective for safe, economical and expedient movement of traffic in commuting corridors and surrounding feeder lines.

Each Global Control System shall co-ordinate and control on a continuous basis all vehicle traffic within 160 km (100 miles) distance. This corresponds to approximately eighty (80) wayside control blocks. The primary function of the global control center will be maintaining headway and speed limits for all vehicles, route planning, vehicle availability (scheduling) based on passenger and freight loading, and continuous monitoring of the magways. In addition, the global control center will be the central hub for all voice and data communication within its control boundaries as well as the point of communication and data hand-off to adjacent (neighbor) global control centers.

The selection of a large-screen, high-resolution and Electronic Chart Display and Information System (ECDIS) databased cartographic reference with vehicle magway position data will allow the Global Controller/operator to have confidence to monitor and direct traffic. Information will be clearly and correctly presented in sufficient detail and flexibility of scaling so that the controller can look up any vehicle or vehicles in any area by simply selecting an appropriate zoom or display centering. The Global Control Center Display (GCCD), based on the Raytheon AAS display, has been proven in a similar air traffic environment. Use of windows, flexible keyboard, in conjunction with a database system, will positively identify all vehicles in the geographic control area via vehicle identification and reporting of position, direction, and speed via the wayside controller to the GCCD. In addition, extensive graphics capabilities will allow the controller/operator to add notations that will augment the vehicle symbology and tagging provided by the Geographic Display System. A background chart will be overlaid with the information provided by the Global Positioning System (GPS). The operator will the capability to create and edit an overlay for the addition of routing and/or danger/caution areas. Permanent edits maybe accompanied only with the proper access privileges and password.

Each Global Control center/site will support a GPS reference site and the associated performance monitoring equipment. Site locations will be surveyed to an absolute accuracy. This reference station

will check on the health of the satellites in view, provide accurate UTC (Universal Time Coordinated) time, and determine the necessary differential - correction information for the area routes being controlled. The differential correction and almanac information will be constantly used to correct the GPS information received for each vehicle. The accuracy of the GPS and the appropriate correction factors are automatically fed to the Decision Support System (DSS) for alarms and statistical recording. The reference station and performance monitor shall be reconfigurable for fault tolerance; thus any monitor may also serve as a reference, should that unit fail or develop excessive errors in any measured parameter.

3.2.3.a.3.1. DECISION SUPPORT SYSTEMS (DSS)

The DSS consists of three subsystems namely; the Digital Selective Calling (DSC), Vehicle Traffic Information (VTI), and Geographic Display System (GDS). The DSS is the information interface and support system that the operator uses to monitor traffic and prepare advisories to participating vehicles. All the graphic information, vehicle magway position, and the data-base information is available to the operator through the DSS. Information gathered from the communications system is entered to the DSS to augment the decision-making capability. However, it is the manipulation of the data and how the operator decides to process and display the data and graphics that determines the operator's effectiveness in performing the global control function. The operator becomes an important factor in deciding just how much and what information will be used from the DSS. The DSS will assist the operator in making correct and timely use of the information in the DSS and it will relieve the controller of some of the time-consuming repetitive functions that can detract from individual performance and/or reduce system capabilities.

The information for the remote (local) sensors is gathered in the DSS for processing and display. The wayside control units continually send vehicle position information to the VTI. The VTI captures this constant stream of data and allows the DSS to display it in an operator-selected format. All the tracked target data is displayed on the GDS with information and windows of other information as selected by the operator.

At this point the operator will have available, either graphically on the chart, or through alphanumerics in displayed windows the situation of all known vehicles movements in the global coverage area. He will be able to project vehicle movements for scheduling purposes and conflict analysis. As more information is gathered and/or displayed and decision-making features energized, the operator can conduct management of vehicle encounters by critical analysis through fast forwarding of the present situation to see when and where conflicts can be minimized. Projections of routes and speeds along the routes provides this capability. Deviation requests can be checked and proper strategies established.

Data logging functions have been automated to relieve the operator of many duties. Position logging, status information of the external sensors, automatic acquisition vehicles are a few key areas handled for the Controller. Statistical information will be stored and available for processing, training may be automated by using the optional embedded training to exercise and test trainees, and area familiarization will be completed faster due to the electronic charting. All of these feature will enhance cooperation in performance of the duties of a Global Controller.

The Raytheon AAS console selected for the Global display role features a flexibility to allow each operator great latitude to mold the console to his own ergonomic choices. The entire main display monitor assembly may be rotated ±45 degrees in azimuth.

At the normal viewing distance of 20 in., the corner of the display is exactly 35 deg off-axis as permitted by MIL:STD-1472C and the required minimum 16 minute-of-arc character size (93 mil) is bracketed by the capability to simultaneously display 10 character sizes ranging from 80 mil (5 by 7) up to 280 mil. The brightness and contrast of the monitor are suitable for subdued ambients of typically 5 to 10 ft-candles of white-light incident normal to the cathode ray tube (CRT). Raytheon has developed optional features which enhance the performance of the 2048 by 2048 pixel Sony monitor. In order that all monitors look alike and that color tracks correctly when display brightness is adjusted, the gamma characteristics of each monitor are determined and stored on-line. This is used operationally to adjust the drive signals to achieve correct color. Raytheon has also developed user-friendly software which permits relatively unskilled personnel rapidly (one-half to one-tenth the time of commercial procedures) to align a monitor for any of its maintenance adjustments.

The keyboard is a standard QWERTY keyboard with 109 keys and additional features. In addition to the alphanumeric section, there is a cursor control pad, a numeric pad, and a function key area with 36 keys. The keyboard has standard features such as: auto-repeat. N-key rollover and multiple key operation. The key characteristics are per MIL:STD-1472C. In the MMI design development in conjunction with the FAA, six of the function keys have LED feedback, 18 of the function keys have dedicated functions, and 12 of the function keys are softkeys, whose function is determined by a set of labels displayed on the monitor. The audible alarms which are programmable in frequency, duration, duty cycle, and volume are also contained within the keyboard.

3.2.3.a.3.2. NETWORK MANAGEMENT

Network management, performance monitoring and reporting, fault recognition, configuration control and security for LAN are all features that are built into NOS, the Raytheon LAN Network operating system. These feature separate automatically and report to the supervisor and watchstander through routine warning and alarm messages and through a small number of data files or reports that the system will automatically generate. Due to the high level of automation of these functions, we estimate that the network security office (NSO) will require less than two hours per week to perform his duties. The duties that the NSO will need to perform will include looking at the reports that the system prepares and thereby judging the integrity of the network and calling for assistance if necessary according to stated operational criteria.

3.2.3.a.3.3. SOFTWARE

Raytheon corporate policy calls for the use of the CASE tool, Software-thru-Pictures (StP) on major software developments. We have used StP with great success on a number of large projects such as TDWR (Terminal Doppler Weather Radar) and ROTHR (Relocatable Over The Horizon Radar). One of the more desirable consequences of the use of StP interfaced with a desktop publishing system such as INTERLEAF is that the production of documentation conforming to complex standards is largely automated. With these tools, the designer/developer is left free to dwell on design architecture and development issues while the development system itself produces high quality, accurate and guaranteed complete documents.

This page is blank.

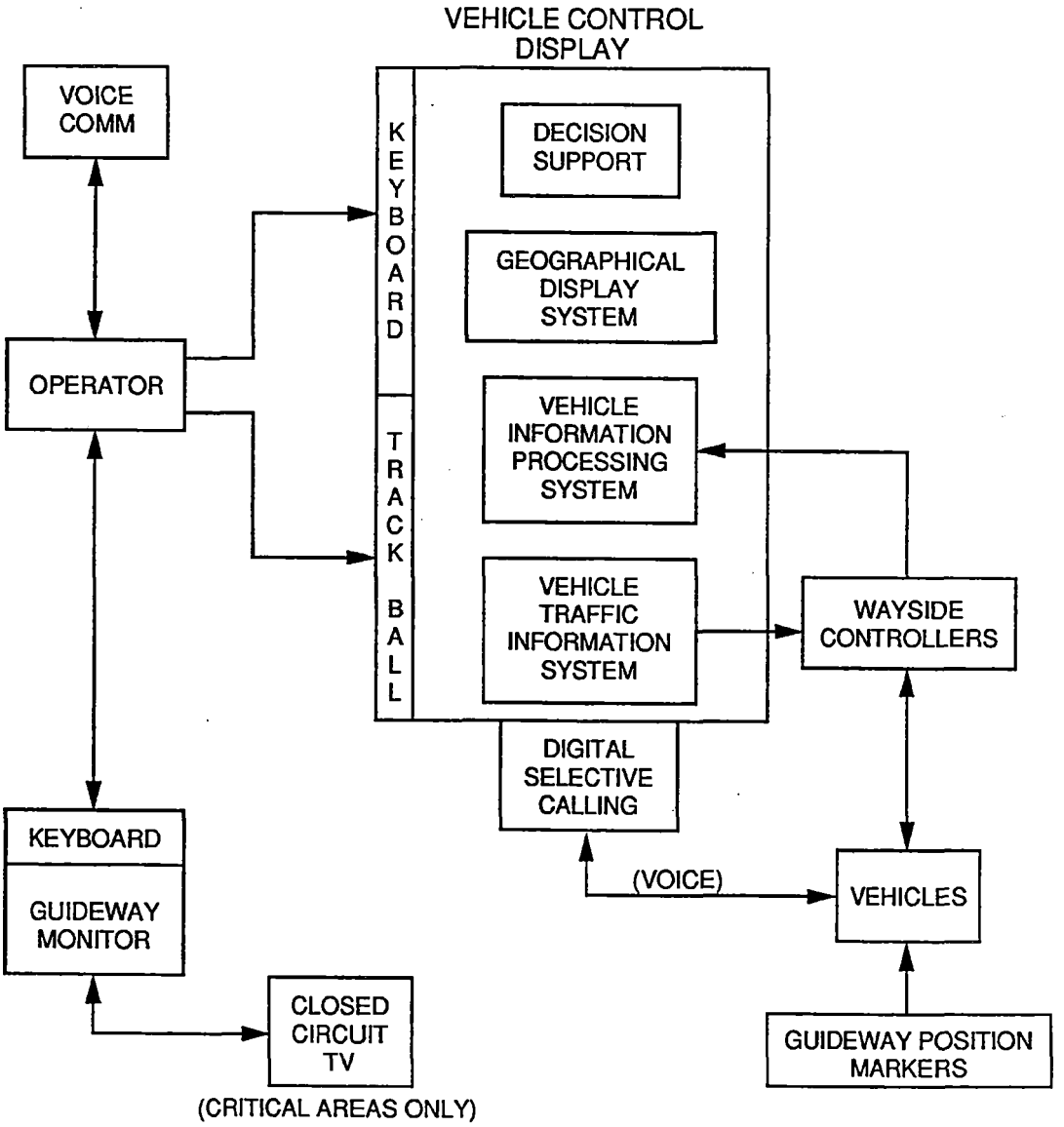

Figure 9 Global control information flow

3.2.3.a.4. SYSTEM CONFIGURATION - GLOBAL CONTROL CENTER (GCC)

The Global Control Center (GCC) system configuration is detailed in this section along with our technical approach towards its design and implementation. This approach, built upon a foundation of maximal reuse of existing commercial hardware and proven infrastructure and application software, made possible by strict adherence to open-system concepts and standards,has been repeatedly proven in our Raytheon ATC system developments. We are poised to apply the same techniques and components towards the GCC.

3.2.3.a.4.1. GENERAL SYSTEM REQUIREMENTS

A illustration of a hypothetical geographical Maglev system routing and Global Control area coverage is shown in Figure 10.

The primary mission of the global Control Center is to maintain safe and expedient vehicle routing within its boundaries and process vehicle hand-overs (transfers) to neighboring Global Control Centers.

Each Global Control Center will generate commands and communications to all vehicles via eighty or more wayside (local) controllers. The wayside controllers are situated a maximum of 2 Km spacing and may be located at shorted intervals due magport exists, switches, and magway profile such as curves, tunnels, etc.. This provides the necessary vehicle spacing and headway for achieving maximum thru-put capacity with a minimum of time between destinations. A general Transportation Flow Block Diagram is shown in Figure 11. This flow diagram portrays the interaction between passenger and/or freight, magway usage, and vehicle inventory required to obtain the best overall utilization of the system The particular control algorithm used will be based on the demographic features and requirements of the area under Global Center control.

Each Global Control Center will communicate, voice and data, via a dual redundant Fiber Distributed Data Interface (FDDI) to the wayside (local) control stations. The American National Standards Institute (ANSI), has defined this 100 MHz fiber optic link FDDI LAN.

A Global Positioning System (GPS) reference station will be located at each Global Control Center to receive at least four satellite signals for computing a differential location correction by comparing this measurement against its precisely surveyed location. This correction signal will be broadcasted via the wayside controller to all vehicles in the coverage area to be applied against their received GPS satellite signals, to achieve accurate rate time, location, and velocity estimates, which are

displayed on-board the vehicle as well as returned to the Global Control Center for system usage. Each GPS station will have a performance monitor for complete and continuous accuracy operation in a failure or degrade performance occurs in the primary GPS.

A block diagram of the Global Control Center configuration is shown in Figure 12. This block diagram depicts the major subsystems/groups within the Global Control Center, namely Data Processing, Data Storage, Graphics Displays, Communications Control, GPS', Magway Monitors, and various LANs need

to interface with other GCC's and wayside controllers. A more detail block diagram of a GCC is shown in Figure 13. This diagram shows the internal bus structure and a more detailed breakdown of the equipment in a Global Control Center.

3.2.3.a.4.2. GLOBAL CENTER CONCEPT DESIGN

The Global Control Center (GCC) generates commands and communications to all vehicles within its area of control via forty or more Wayside Control Units (WCUs). For the Global Control Center the design goal is to achieve an open, commercial off the shelf (COTS) solution as far as possible, while maintaining adequate safety, high system availability, and adequate performance margins to adapt to future enhancements.

The GCC is designed for flexibility in adapting to a wide variety of system configurations. The system is conceived as a set of GCCs each with a sphere of control corresponding to the magway blocks associated with its WCUs. Cooperation among GCCs and WCUs allow vehicles to traverse freely and safely throughout the system.

Redundancy in the GCC was chosen primarily based on three system factors, passenger safety, system availability, and cost. The discussion of the system trade is found in section 3.2.3.a.4.10.

The following paragraphs discuss the following functional areas of the GCC; communications, processing, workstations, graphics displays, data storage controllers and media, magway monitoring, uninterrupted power supply and GPS interfaces.

3.2.3.a.4.2.1. COMMUNICATIONS

Cooperation among GCCs and WCUs depends heavily on high availability of the communications system and timely transfer of critical data. The selected communications system shown in section 3.2.3.a.7.1. provides two fiber optic Local Area Networks (LANs), one in each direction from the GCC along the magway. The selected LAN is the Fibre Distributed Data Interface (FDDI).

FDDI design concepts include a dual fiber optic ring architecture, 100 Mb/s data rate, and distributed clocking to support a large number of stations on the ring. Two types of fiber optic media are classed as multimode fiber and single mode fiber. Multimode fiber has a maximum length between adjacent stations of 2 km while the less widely used single mode fiber can support up to 40 Km between stations. The FDDI for Maglev will use single mode fiber as adjacent WCUs can be up to 4 Km apart. This is because each WCU controls four blocks of magway, two blocks up to 2 Km in length in each direction. Note that the WCUs have two connections to the network. The connections are distributed on both sides of the dual fiber optic rings. This evenly distributes stations around the ring and reduces the maximum distance between stations on the ring. The two WCU connections to the network provide redundancy and with appropriate fault detection, isolation and recovery will minimize the possibility that any single failure will bring the network down.

Communications are required over the FDDI network between the Global Center and WCUs and among Global Centers. Global Centers each interface to two FDDI LANs, one spanning to the "East" and one spanning to the "West". They form part of a Wide Area Network (WAN) made by bridges or routers that link adjacent networks as shown in section 3.2.3.a.7.1. This allows Global Centers to communicate

with each other without requiring a separate WAN for the GCCs. Fault tolerance is also enhanced by allowing adjacent Global Centers to be substituted for a failed GCC. The network can reconfigure itself by distributing the critical functions to adjacent Global Stations. The bridges/routers are dual units so that the ability of GCCs to communicate will not be degraded by failure of a bridge/router. Two bridge/routers are allocated to each GCC to allow up to four interfaces between a GCC and its adjacent GCCs.

One communication requirement that is not supported by the FDDI LANs relates to communications between adjacent WCUs. Adjacent WCUs require a low-latency (less than 50 microseconds) communication path to pass power converter phase and magnitude status from one WCU to the next as a vehicle transitions between a block controlled by one WCU to a block controlled by a second WCU. The proposed solution is a separate point-to-point fiber optic interface between adjacent WCUs to enable messages to be transferred within 50 microseconds. This will ensure a smooth phase and magnitude power converter control for vehicle transitions between magway blocks of adjacent WCUs.

The hardware used to interface to FDDI is of common design in Global Centers and WCUs. The GCC FDDI interface is composed of an FDDI controller module (MVME385) and optical bypass switches. The bypass switches allow the GCC or a WCU to be optically bypassed if it loses power or it detects an internal failure that could compromise the data on the bus. A bypassed GCC interface on a LAN does not degrade the fault tolerance on the LAN (dual rings are maintained) so the adjacent GCC can take over control over the vehicles on the affected LAN.

The Motorola MVME385 (designed by Interphase Corporation as the V/FDDI 4211) can perform much of the communications protocol processing, as well as certain network management functions required by FDDI. It can maintain FDDI's 100 Mbit/s data rate. It provides 1 MB of dual ported VMS Bus accessible communications buffer. The buffer operates as a high-speed First-In-First-Out (FIFO) and decouples internal activity from the 32A/32D VME bus.

The MVME385 fully supports both Class A Dual Attachment Stations (DAS) and Class B Single Attachment Stations. The Maglev FDDI LAN design is fully configured and offers the fault tolerance of having two fiber rings. In the event one of the rings fails or is broken, the FDDI network can automatically reconfigure itself to compensate for the failure and remain operational.

Should the FDDI Controller fail in such a way as to disable with both rings of one of the networks, the GCC can still maintain control over both rings by using its interface to the second ring. As shown in section 3.2.3.a.7.1., failure of the Global Center's interface to the A ring (on the left) can be bypassed by transferring critical data to Wayside 1B. Wayside 1B can then retransfer the data to the appropriate Wayside station on FDDI Ring A (Wayside 20A) via the point-to-point interface between adjacent WCUs. Wayside 20A then can retransfer the data to the specified WCU on FDDI A. This technique allows the GCC to maintain limited control over both networks even when its interface to one network is down. The critical timing constraint for high speed travel cannot be maintained so vehicles within the affected network will have to be slowed and/or brought to a safe stop.

The FDDI hardware and software support the Open Systems Interconnection (OSI) model. The FDDI set of standards define the LAN interfaces, protocols and topologies at the Physical and Data Link layers of the OSI model. FDDI divides the Physical layer and the Data Link layer into sublayers as listed:

Physical layer:
PMD or Physical Layer Medium Dependent
PHY or Physical Layer Protocol (upper layer)

Data Link layer:
MAC or Media Access Control
LLC or Logical Link Control (upper layer)

The FDDI SMT (Station Management) defines how to manage the PMD, the PHY, and the MAC - the three lower layers.

3.2.3.a.4.2.2. PROCESSOR SELECTION AND IMPLEMENTATION

Raytheon has adopted a common processor design for the processors of the GCC and the WCU. Using a single processor in multiple applications can have life cycle cost advantages. Other processors available in the market can provide the processing speed and memory size required in the Maglev applications. Some of the discriminators used to select the baseline processor are listed below:

1. The architecture of the processor must have potential for a long life in the marketplace.
2. The processor must be a standard in industry and support both the VME bus and Unix.
3. The design must support multiprocessing with multiple processors sharing the same bus.
4. The manufacturer must have a long-term commitment to provide opportunity for technology insertion as technologies advance.

These criteria are all met by the selected baseline processor for Maglev, the Motorola MVME187 RISC Single Board Computer (SBC). Selection of the newer Reduced Instruction Set Computer (RISC) architecture over the traditional Complex Instruction Set Computer (CISC) design will avoid the concern of architectural obsolescence by the time the design is implemented and fielded. The selected RISC design is based on the 88100 CPU and offers scalable and upgradeable migration paths should future requirements expand beyond anticipated levels. The MVME187 is available with options in clock speed, cache size, shared DRAM size (4MB to 64MB), and capability for startup/diagnostic memory (four ROM/PROM/EPROM/EEPROM sockets). The processor supports industry standards of the 32A/32D VME Bus, the 88open Consortium, and the industry's first UNIX application binary interface for Binary Compatibility Standards/Object Compatibility Standards. Through the Interoperability Test Suite (ITS/88), 88open certification assures compatibility in three main areas: UNIX, networking, and X/Windows. The architecture allows multiple processors to operate out of shared memory on the VME Bus. The MVME187 can be set up so that some on-board memory can be private and some can be made available to the VMS Bus. Motorola has a history of consistency in supporting its computer architectures and is committed to extending its 88000 RISC family of products in the future.

The single board MVME187 provides a variety of additional resources that can reduce the number of VME boards required. The capabilities that are included are listed in Figure 14. Although all these resources may not be needed for the GCC they provide capabilities that may prove useful during the life of the system. Options selected for the baseline system are 25 MHz clock and 4MB of ECC RAM.

The GCC provides two SBCs that share the VME Bus, on-board memory and peripherals on the bus. One SBC performs all mission functions. These functions include managing communications with its

WCUs and with other GCCs. The second SBC performs health monitoring functions of the GCC and its assigned WCUs, stores critical data on separate tape and hard disk units, and keeps itself ready to take over the primary functions in the event of a primary SBC failure.

The MVME187 SBC includes 4MB of shared dynamic RAM, arbitrates the VME bus, interfaces with the GPS and GPS Performance Monitor, interfaces with the FDDI controllers operating as Dual Attachment Stations (DAS), interfaces with the hard disk and tape controllers via an SCSI bus, interfaces with the printer, and interfaces with the graphics display stations via an Ethernet bus. In the event of a processor failure the second SBC assumes the processing responsibilities of the first processor. Single bit errors in memory are corrected by means of error correction code on the memory.

In the next design phase, detailed loading of the processors will be performed including identification of critical performance requirements, including time criticality.

3.2.3.a.4.2.3. DATA STORAGE

The data storage portion of the Global Center provides capability to store digital data in non-volatile memory (both tape and hard disk), to record voice data, and print video screens and reports as required. The digital data storage stores program and data, including archived history data. On system initialization, program data is transferred to the memory of the SBCs from hard disk. Tape storage is for secondary storage and for archived data. Voice recording capability is also provided.

A second data storage system is provided connected to the second SBC via an SCSI bus. This storage provides critical data backup capability and provides storage capability in the event of a failure of the primary system. The second storage system provides an on-line capability to continue with tape storage while the first unit is having the tape replaced. It also gives a continuous recording capability while servicing the first system. The printer is non-critical and is not provided in the second data storage system.

3.2.3.a.4.2.4. GRAPHICS DISPLAY STATIONS

Within the GCC the most critical system feature is the graphics display consoles' human-computer interface for non-fatiguing, error free operation by area controllers. Three graphics display stations provide the human interfaces to the GCC. Two controllers and a supervisor each have a station that allows the status of vehicles to be displayed and gives the controllers capability to control the system. The two controllers activities are normally partitioned so that each has control over the WCUs and vehicles associated with one of the two FDDI LANs.

Raytheon's consoles provide unique human-computer interface features derived from the United States FAA Advanced Automation System (AAS) program and from proprietary Raytheon display management software. Each console contains a 20-inch square, 2000-line color raster monitor and a state-of-the-art Raytheon display controller. This console is proposed for the primary controller interface in the Global Control Center. These graphics display stations provide the following characteristics:

- Image update 4 times per second
- 20-inch-square Sony color displays
- Silicon Graphics Library enhanced by Raytheon

- Console driven by standard VME bus and 17 MIP Motorola Delta Series 8000 system running Unix
- Suitable for use with ambient background lighting of 10 foot candles
- User friendly software permits relatively unskilled personnel to align the display
- Polygon filled areas accurately portray detailed weather areas but do not obscure magway and vehicle legibility
- Fully adaptable track, map and other symbols
- Color coding imparts specific meaning
- Color coded updates reduce scan time and alert controllers to changes in data

The keyboard design and layout provide a logical, easy to understand means of interfacing to the system with category keys, "soft" keys, dedicated keys, a cursor/numeric/parameter keypad and a standard QWERTY layout.

Should one of the operational graphics display stations fail the supervisor station can take over until a repair is made, assuring high availability.

3.2.3.a.4.2.5. WORKSTATION

A workstation is also included to provide capability for non-control activities such as report generation, system maintenance, system upgrading etc.. The workstation selected is the SPARKstation-IPX by Sun. The IPX supports fast color graphics, windowing, and text scrolling. The selected IPX has 16MB of memory and is connected to both Ethernet buses allowing it to communicate with either SMC. It provides a 40-MHz SPARC integrated integer and floating-point unit and an integrated graphics accelerator. The Sun IPX capabilities will yield cost-effective, reliable workstation power for the GCC.

3.2.3.a.4.2.6. MAGWAY MONITORING SYSTEM

The Magway Monitoring System allows controllers at the global center to monitor high risk and/or critical sections of the magway. Typical locations for monitors are entrances to tunnels, tight magway turns, Magports, etc.. The monitoring system is based at the GCC with two independent fiber optic communications systems that control and monitor an average of ten cameras, typically five in each direction along the magway. Cameras are strategically placed along the magway with overlapping monitoring space. As long as consecutive cameras do not fail the ability of the system to monitor critical areas will not be compromised. The cameras are under full remote control from the GCC including lens control (iris, focus and zoom functions) and pan/tilt controls.

The system is based on the Cohu Microprocessor Camera Control (MPC) System except using communications via fiber optic cable rather than RS-422 or RS-232. Each camera can be controlled from the GCC SMC. The fiber optic cable uses single mode fiber for long distance communications. Even with single mode fiber a repeater is included to allow coverage over the entire 160 km of magway.

3.2.3.a.4.2.7. UNINTERRUPTABLE POWER SUPPLY

The uninterruptable power supply (UPS) proposed for the GCC is a redundant solid-state online system designed to provide high-quality, continuously-filtered and conditioned ac power to the critical loads. The GCC will be powered by a 15 kVA UPS. The battery system is sized to supply a full critical load

for 15 minutes. If one channel of the UPS fails the second will take over. The UPS will allow the system to continuously operate despite temporary loss of prime power. If prime power fails permanently, the battery backup will give the system adequate time for safe shutdown.

The UPS system is a dual-conversion system (i.e. ac-to-dc then dc-to-ac). The redundant UPS configuration proposed is shown in Figure 15. A single string UPS is comprised of the following components:

- ac input filter
- Rectifier/charger
- Invertor
- Static bypass switch
- Maintenance bypass breaker
- System control logic
- Digital monitoring panel
- dc disconnect
- Battery system

The ac input filter reduces ac input harmonics to 10 percent THD maximum at nominal conditions and full load. The rectifier/charger converts the ac input to filtered, regulated dc voltage used to power the invertor. The invertor changes the dc bus voltage to a precision ac voltage through pulsewidth modulated inversion. Should the utility power fail the battery system powers the invertor.

3.2.3.a.4.2.8. GPS INTERFACES

The SBCs interface to the GPS system by serial interfaces, one for the primary GPS system and one for the monitor. The interfaces are serial EIA-232-D interfaces. A backup set of interfaces are provided with the second SBC.

3.2.3.a.4.2.9. VOICE INTERFACES

The SBCs also provide interfaces to voice channels for weather and emergency access. Redundant channels are provided, one for each SBC.

3.2.3.a.4.2.10. REDUNDANCY SELECTION

As noted earlier, redundancy allocation in the GCC was based on three system factors, passenger safety, system availability and cost. (Cost is a factor in selecting among alternate redundancy options, as long as each meets system goals for safety and availability.) The methodology for this selection is given below. It should be noted, that the current allocation is based on a concept design of the system. As more accurate data is developed the trades for redundancy may alter the final selection.

Of the three selection criteria, passenger safety is the most important. The first operation in selecting redundancy for the system is to assess the relative criticality of the system operations. One of the first activities is a fault modes and effects criticality analysis (FMECA). Level I is the most critical category. Once the safety issues have been identified for a given system design, then alternative approaches are analyzed to determine if critical safety issues can be avoided by modifying the baseline design. The

analyses are performed hierarchically, first at the highest level and once the high level issues are resolved at a lower level. During this period allocations among the Global Control Center, the Wayside Control Unit and the Vehicle are made. Functional redundancy is also addressed during this period. Functional redundancy refers to providing redundancy by differing means than the primary approach. It does not refer to providing multiple copies of the same design. The Category I safety issues that remain are then addressed with more standard redundancy approaches, including providing multiple copies of a resource so that passenger safety is assured.

Once the minimum set of redundancy is selected to insure passenger safety, then the next step is to assess the system availability and to allocate additional redundancy to increase availability to that required. In this case preliminary allocations are made among the GCC, the magway, the WCUs, and the vehicle. Redundancy is added as necessary to achieve the needed system availability. In this effort care must be taken to ensure that the system is partitioned into appropriate fault containment units with fault containment boundaries so that the effects of a fault cannot cause passenger safety risks prior to fault detection, isolation and recovery or safe system shutdown.

To select the appropriate subunits of the GCC, WCU, or vehicle to be made redundant, each partitioned subunit is prioritized in terms of failure rate. A spare is provided for the highest failure rate item first, the resulting availability is then evaluated, if the system meets its allocated goal for availability (with adequate margins) the task is complete. The process is then repeated for the next highest failure rate subunit until the allocated availability goal is met with adequate margins. Figure 16 lists the redundancy provided for the GCC.

3.2.3.a.4.2.11. FAULT TOLERANCE ISSUES

Fault tolerance issues must address both permanent faults and transient faults. Transient faults historically have occurred much more often than permanent faults. Transient faults do not cause permanent damage to the system, but can change the state of individual storage cells (i.e. individual bits in memory words or in logic registers). If the stored data that is altered is critical the data may be corrupted and may cause errors in control data which could be a hazard the passenger safety. More likely, the faulty data would be detected and a false alarm would occur. For instance, a vehicle may be shutdown because of a false alarm.

One primary goal for handling potential transient failures is to design the system to avoid false alarms to the greatest extent possible. By far, the largest number of storage cells are in the CPU memory. We have provided single-bit-error correction in the memory to allow the system to continue in the presence of transient errors. If however, the transient faults are allowed to accumulate, the possibility of two bits within the same word increases with time. We propose to avoid this by periodically "scrubbing" memory. Memory scrubbing is performed during CPU idle time. Each word in memory is read in sequence, if a single-bit-error is detected the data is corrected and written back to memory. A corrected word is read again, if the data is still in error, a permanent fault has been detected. The address and bit are then recorded and the GCC is notified. Note that a single bit permanent fault in a memory word does not mean that the system has to be halted until repair is performed.

In order for the predicted availability to be realized, the fault detection coverage of the system must be high. The system uses multiple means to achieve high coverage. In all cases, the channel being used continuously monitors its own operation as well as the operation of the resources with which it interfaces.

Several independent means are employed. Error detecting and correcting codes are used in memories, disks, tapes and serial communications over FDDI. All data received by processors is tested to determine its reasonableness. Also communications data generated by processors will be tested by independent software to verify the reasonableness of the data. Excess computation capability will be used to perform Kalman filters (or other filters) to identify commands sent or received that are not reasonable. All transient failures are identified and reported to the GCC where analysis is performed to identify subunits that may have caused or where a high rate of transients have been observed. In general, defensive software techniques are planned to detect faults before they are communicated.

The GCC has two CPUs, each capable of performing all necessary processing tasks. The secondary processor provides a means for monitoring the actions of the primary CPU on-line as the system is operating. The secondary CPU has access to data being generated and received by the primary CPU by means of shared memory. It can independently test communications on the FDDI Networks, and between the primary CPU and its tape, disk, and voice recorder. The second CPU also provides access to the secondary SCSI Bus where independent copies of critical data can be stored and interrogated.

Both CPUs also periodically issue keep-alive messages to each other via shared memory indicating the current status as each sees it. In addition to detecting faults within the CPUs, the both processors also continuously perform background tests to verify the health and status of all peripherals. It is important to test periodically all key features of the system. This allows test software to detect faults in little used areas of the system and allows these faults to be detected by test software rather than during critical system operation.

In the event that a failure in a CPU is detected, the failed CPU is disabled. By itself if it has detected the failure, or by the secondary CPU if it detected the failure first. In either case, the failed CPU is held reset so that it can no longer take part in the system and the secondary CPU takes over primary functions, and notifies the operator that a failure has occurred.

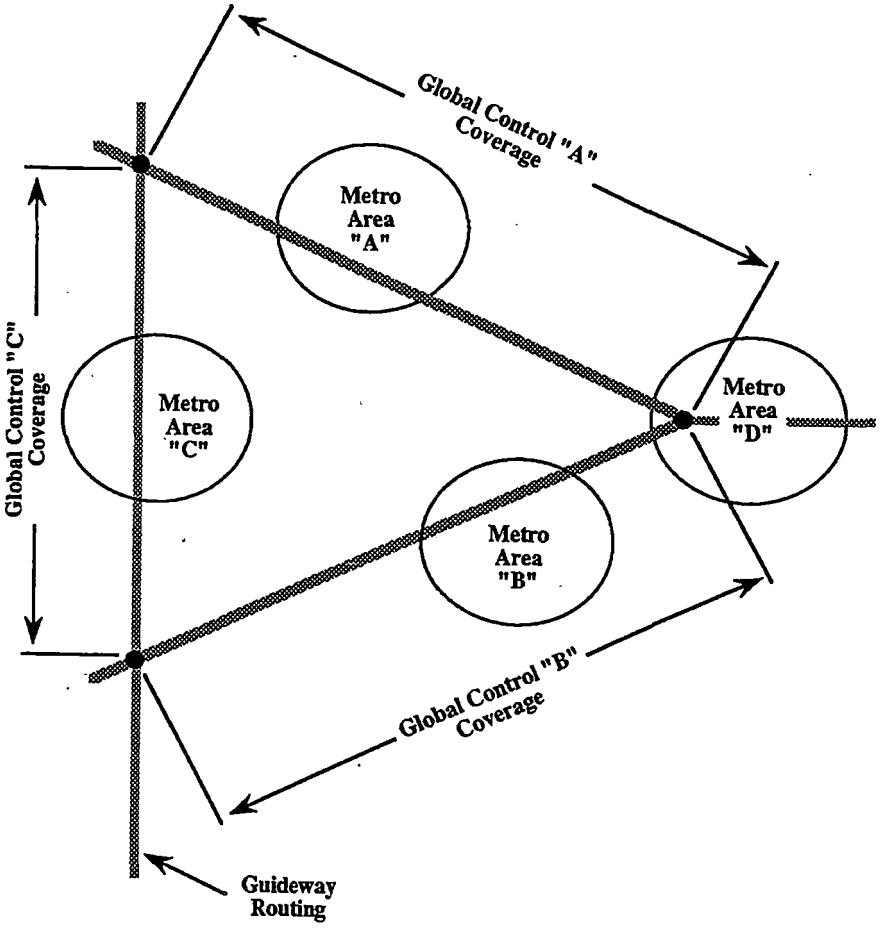

Notes:

- Global Control coverage approximately 160Km
- Guideway Routing maybe "N" multiple lanes
- Global Control coverage may include one or more Metro areas

Figure 10 Hypothetical geographical routing and global control

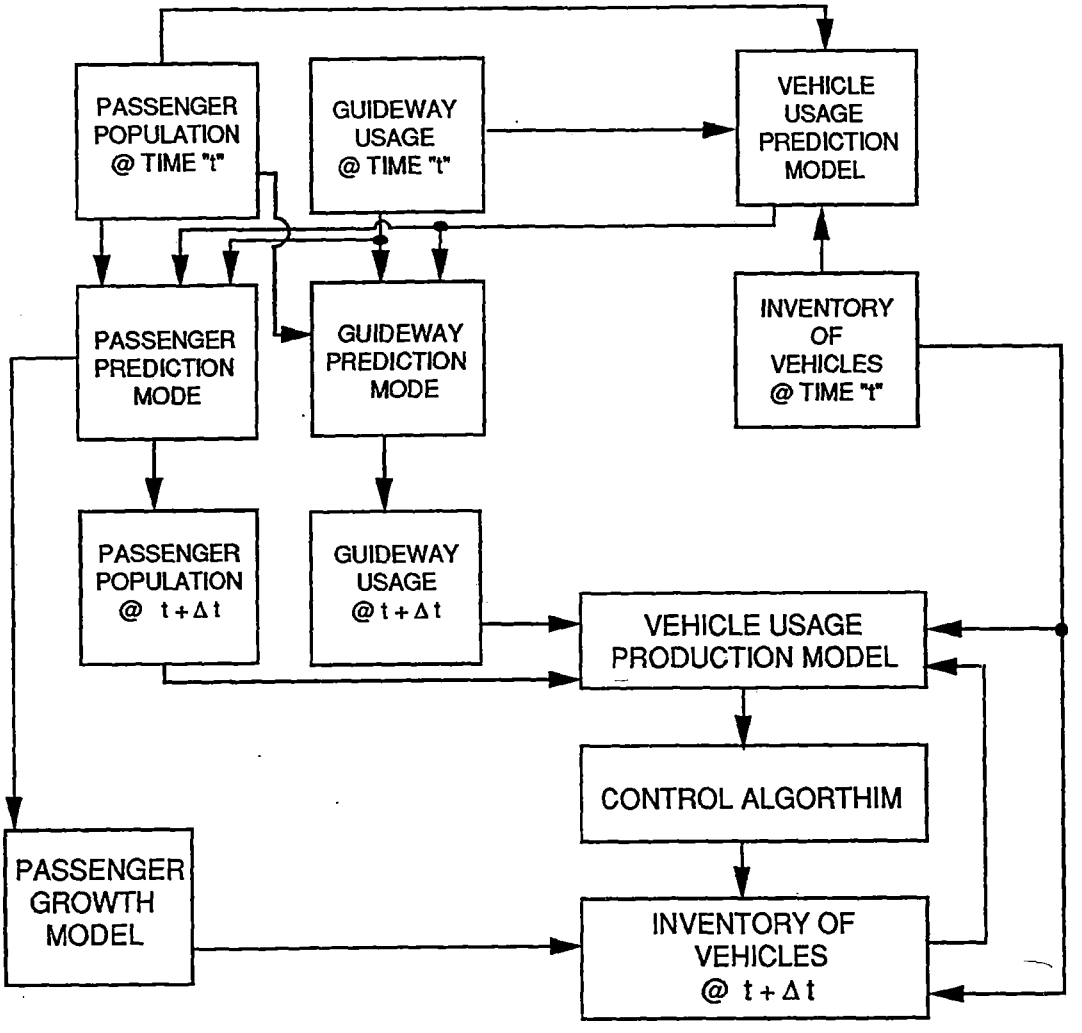

Figure 11 General transportation flow block diagram

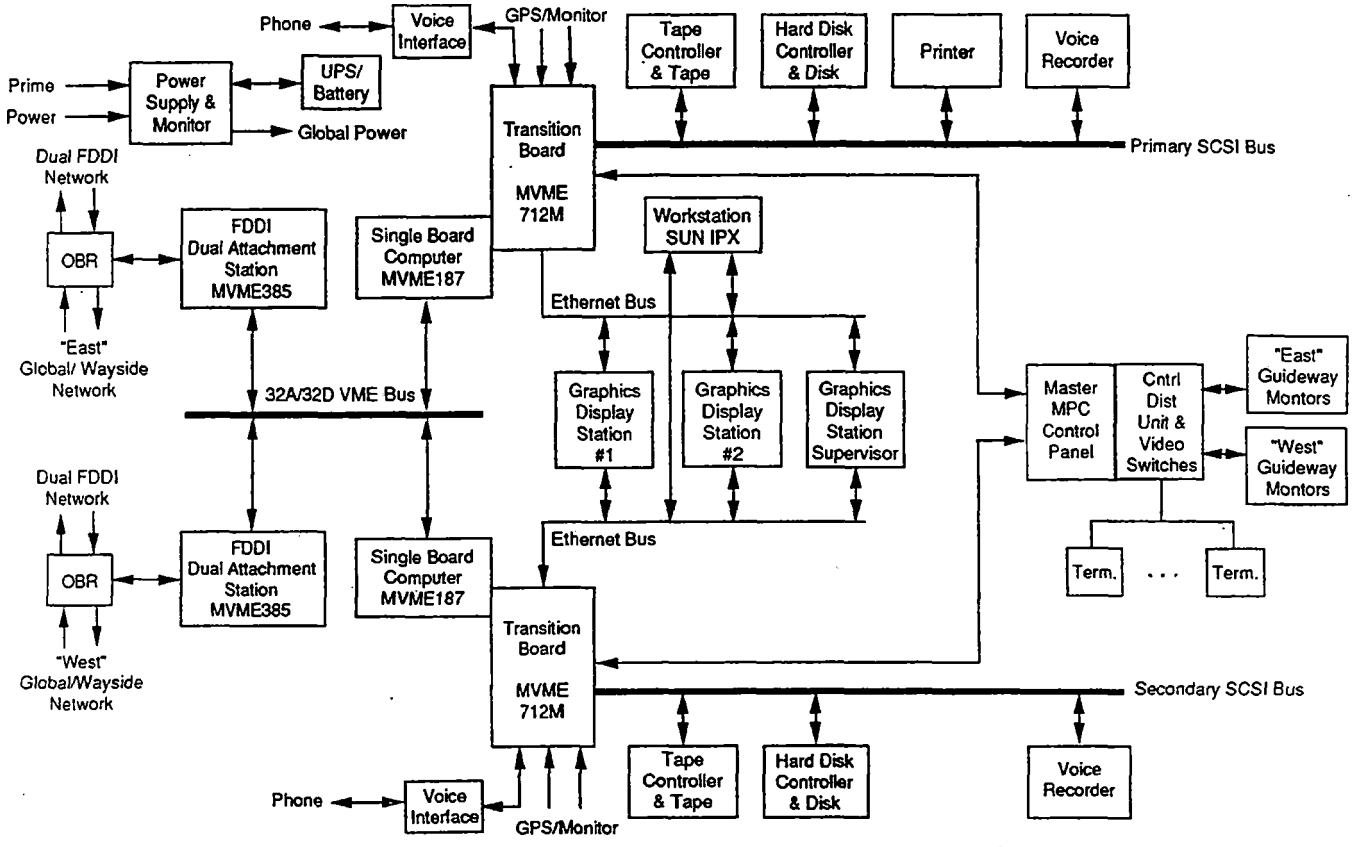

Figure 12 Global control block diagram

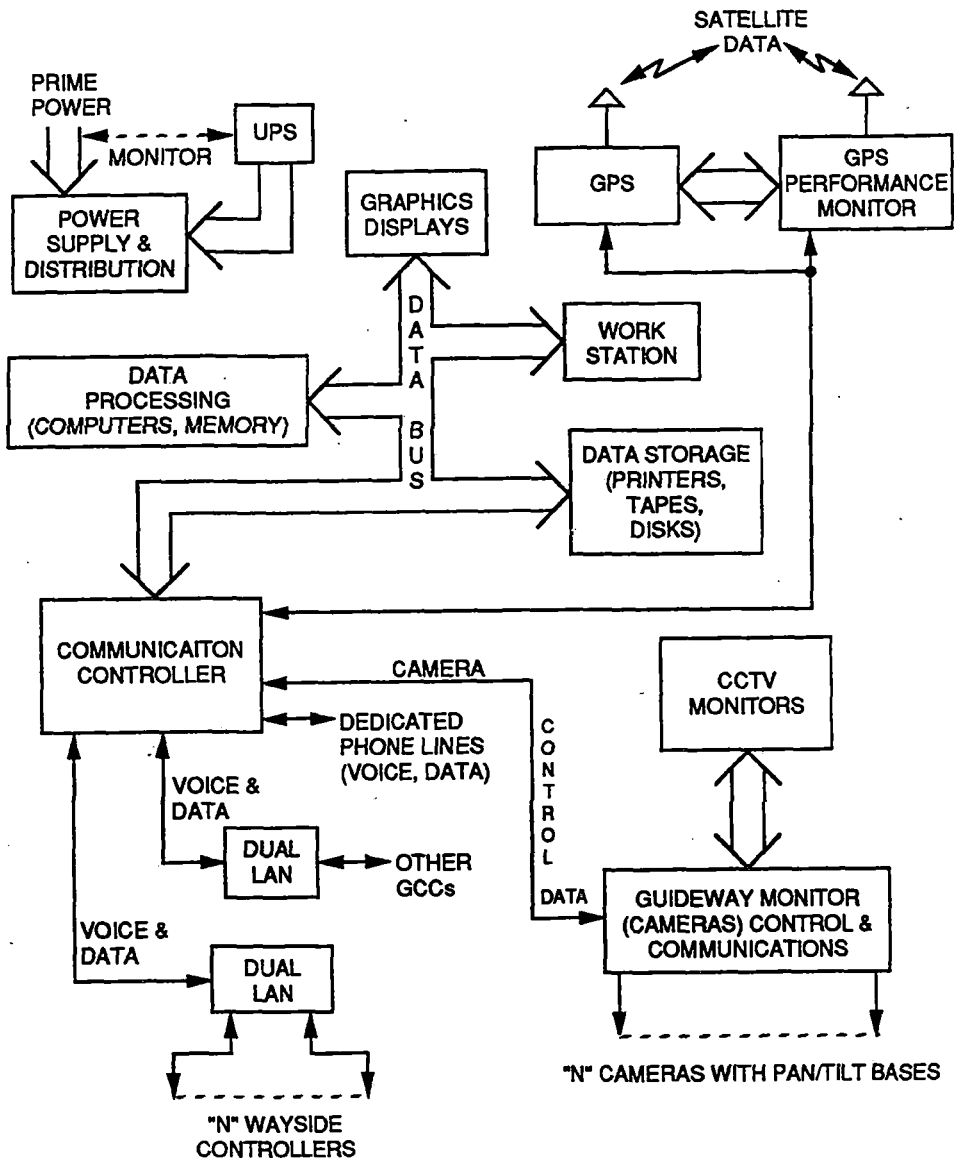

Figure 13 Global control center system configuration

Quantity	Description
1	RISC MC 88100 (25 MHz or 33 MHZ)
2	Memory Management Units and Cache (16KB or 64KB)
4 to 64	MB of Shared Memory (Memory Protection Options; None, Parity, ECC)
4	44-Pin ROM/PROM/EPROM/EEPROM Sockets
1	Time-of-Day Clock, 8KB of NVRAM, Oscillator, Power Fail Detection, Memory Write Protection and Battery Back-up
1	A32/D64 VME Bus Interface with DMA
4	EIA-232-D Serial Communications Ports
1	Parallel Printer Port
4	32-bit Timers (and one Watchdog Timer)
1	SCSI Bus Interface with DMA
1	Ethernet Transceiver Interface with DMA
1	Set of Interrupt Requester/Handlers
1	On-Board Debugger and diagnostic Firmware Included (Requires 2 of 4 PROM Sockets)

Figure 14 Characteristics of the single module computer

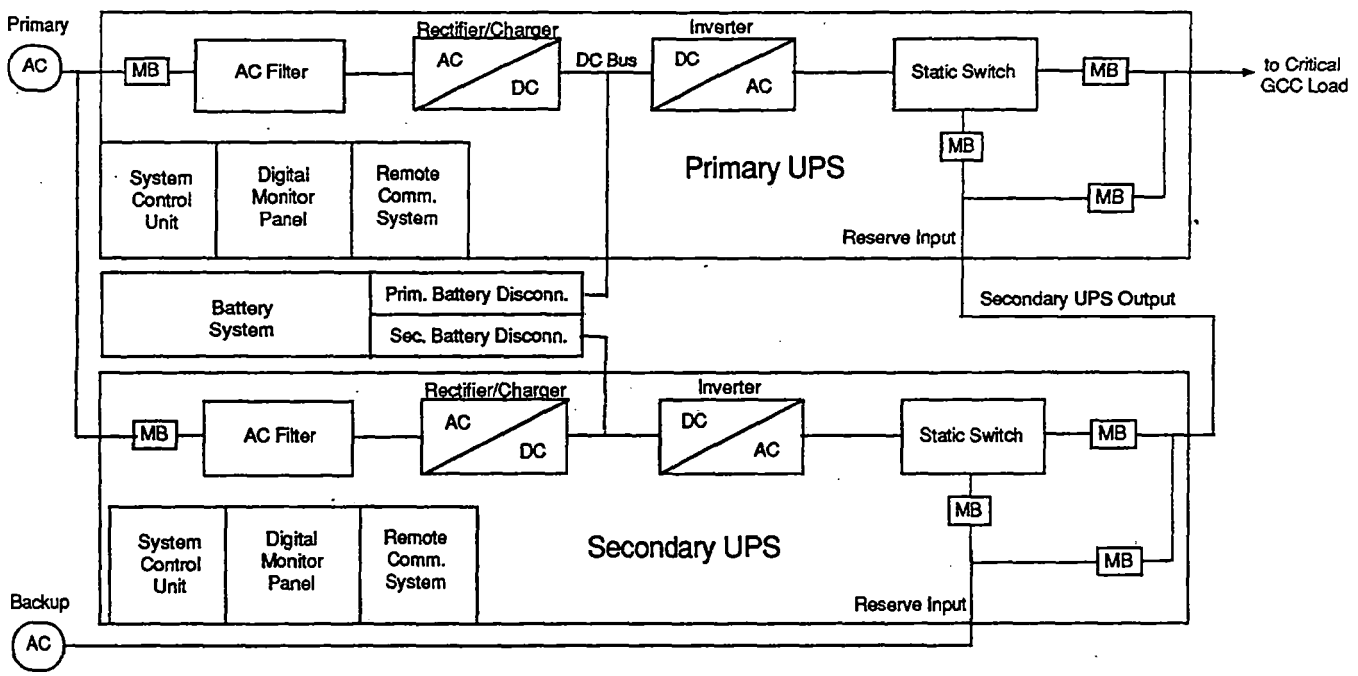

Figure 15 GCC redundant UPS block diagram

Global Control Center Redundancy Provisions		
Subunit	Type of Redundancy	Comment
Data Processing	1 of 2	
GPS System	1 of 1	Not Critical
FDDI System	1 of 1	Functional Redundancy by WCU /WCU Interfaces
Camera System	1 of 1	Internal Redundancy (at Camera Level)
Graphic Displays	2 of 3	Supervisor also Functions as a Spare
Workstation	1 of 1	Not Critical
Data Storage	1 of 2 for all Except 1 of 1 for Printer	Printer not Critical
Power System	1 of 1	Internally Dual Redundant

Figure 16 Global control center redundancy provisions

3.2.3.a.5. SYSTEM PERFORMANCE

The time delay between a time tagged vehicle position marker data transmission and the appearance of the track on the Global Control Center display will be approximately 4.5 seconds. This time can be broken down as follows; (1) vehicle detection, processing and transmission to wayside controller, (2) processing, and retransmission to Global Control Center, (3) time to relay the data through the wayside to Global LAN, and (4) time to process and display the data at the GCC. Figure 17 shows a detail breakdown of the time budget from reception to display of the data.

The major contributors to the delay are; (1) relay from vehicle to wayside control, (2) wayside to global link transmission/reception, and (3) the display processing time, which may be further minimized through the use of efficient scan-conversion techniques developed by Raytheon.

The number of display updates for a vehicle operating at max. velocity (150 m/sec) traveling in a block length of 2 KM is determined as follows:

$$time\text{-}in\text{-}2km\text{-}block = \frac{velocity}{distance}$$

$$= \frac{150m/s}{2000m}$$

$$= 13.11s$$

$$time\text{-}to\text{-}update\text{-}display = 4.53s$$

Updates (Min) per block length is thus defined by:

$$updates = 13. \frac{33}{4} . 53 = 2.94$$

Therefor the number of display updates per block length (2 km) shall be approximately three (3).

3.2.3.a.5.1. HUMAN COMPUTER INTERFACE

For the controller consoles, Raytheon has chosen its ergonomically-proven design for the AAS (Advanced Automation System) common console, which is currently in production for the Federal Aviation Administration (FAA). There are several reasons why this console design is right for the Maglev application. First, the tasks of an Maglev Controller and an ATC controller are very similar in nature and this console was designed with this type of application in mind using a 20 by 20-in. main display with 2048 by 2048 pixels. Second, the FAA has already studied its' population of ATC controllers to

determine the anthropomorphic characteristics which are slightly different from those in MIL-STD-1472C, but which are more typical of this type of population. Third, the console has been designed with a great amount of adjustability in order to accommodate controllers from the five percent female to the 95 percent male.

The controller enters data and commands into the system using a MIL-STD-1472C-Compliant 109-key keyboard plus numeric pad. The combination of these devices has proved effective for the ATC systems which Raytheon has installed throughout the world. The keyboard contains 18 fixed functions switches. These will be used to implement single-key functions and a mutually determined set of other routine tasks. A preliminary set of Direct Functions is proposed as Auto Entry: Alarm Acknowledge, Display Mode (submenu), screen print, vehicle entering, vehicle exit, Help, Idle, Loading, etc. Less than four key strokes or three menus are needed to change system state, exclusive of password verification when required. An additional twelve keyboard function keys are available to be programmed by the supervisor or the controller. Each of these twelve keys can be reassigned at any time to execute any one of the primary Decision Support System (DSS) functions, including Pulling Internal (submenu), DR enter, Target Leaving Area (submenu), and Encounter Lists. The currently assigned function for each of these keys is shown immediately above the key in an area along the bottom of the situation display. This key function label is updated whenever the key is reassigned, so that all keys always remain clearly and correctly identified.

Of primary importance is the situation display in which vehicle tracks must be clearly presented. A vehicle track is represented by a present position symbol together with tag information, leader line, velocity vector and histories. The present position symbols are designed using sets of vector strokes so that each individual symbol may be scaled to correspond to the current position setting and may also be rotated to match the vehicle heading/direction.

Data other than the situation display is contained in windows. These windows, may be placed in areas of the display which do not obstruct the control/monitoring of vehicle traffic. Windows containing data associated with alarm conditions or system errors may not be deselected but may be relocated to permit continued operation. Raytheon is proposing display hardware and software which have the performance capability to update the display with no breakup and to meet a system response time of 0.1 sec for menu or keystrokes response with 100 percent margin. Graphics updates, such as a window requests are readily accomplished within one second with 20 percent margin. For pan or zoom, response time is 3.0 sec with 20 percent margin.

One window is set up as the input preview area where messages are composed and reviewed prior to their being sent into the system. It is in this area that travel advisories are generated, either form scratch or from templates which only require a few inputs, or from a set of entirely canned messages. Graphical entry tools are provided so that temporary route lines and symbols, etc. may be easily added, edited, saved or retrieved as an overlay to the selected chart. This overlay data is available to all console positions within the system.

3.2.3.a.5.2. LOCAL AREA NETWORK (LAN)

This section describes the communication controller and other equipment, which interfaces the Global Control Center to its wayside controllers and other Global Control centers via dual fiber optic transmission media.

The dual-LAN architecture is well proven and a standard architectural feature for all Raytheon ATC systems. The connection between all computer subsystems is the redundant LANs, included to improve reliability and availability. Each LAN is realized using the 10BASE5 physical layer characteristics as defined in ANSI/IEEE Std 802.3 - 1988. The data link layer, and the interface with the physical layer for each LAN are in accord with ANSI/IEEE Std 802.2 - 1985 (Logical Link Control Layer Specification). Each subsystem is a distinct network node with its own address on each LAN at the 802.3/Ethernet level. The protocol employed is the TCP/IP. System performance monitoring software automatically reports any detected problems via control and monitoring software while the affected LAN is configured out of service.

Each LAN has sufficient bandwidth to support the required traffic among nodes, so that failures disabling one LAN can be tolerated without interruption of normal operations.

Network security will be realized using limited access via login and password protection as well as administrative and physical security.

A Motorola 88K Series 8000 computer, similar to that used as the operational display processor (ODP) in the graphics display system is proposed for the router (which may function as a bridge or gateway) to maximize hardware commonality. Dual-redundant machines are proposed to provide high system availability.

3.2.3.a.5.3. Section deleted

3.2.3.a.5.4. DECISION SUPPORT SYSTEM (DSS)

The DSS display is based on the Raytheon AAS ATC display and has undergone extensive testing required by the FAA. The 2048 by 2048 pixel display, in color and with the system controls fully-integrated in the DSS, is the latest technology in both man-machine interface and capability.

The DSS, is similar to ATC systems presently provided by Raytheon. It contains redundant and secure hardware and software designs. Software configuration is controlled by adaptation to each site so that expansion or modification of the system may be made with minimum impact to existing software. Raytheon's extensive work in the field of ATC, missile guidance control, and marine traffic control provides an understanding of the human-machine interface requirements of real-time traffic control systems.

The proposed configuration, shown in Figure 18 (hardware view) and (software view), provides three workstations each containing a copy of the GDS module which may be used by a supervisor, controller, trainee, and/or administrator. Any of the workstations may perform any of the above functions, as determined by a password-controlled access. LAN monitoring and data recording are performed by separate processors. In addition, there is a diagnostic console which is used for the editing of chart data and preprocessing of chart images. The DSS hardware is tied together via a dual-LAN, assuring LAN availability through redundancy. All centralized equipment essential to availability is also redundant. The data recording facility is connected directly to the LAN monitor so that LAN status will be recorded even in the unlikely event that the LAN is not operational. A terminal server is provided to coordinate processor startup before the LAN is available.

3.2.3.a.5.4.1. MONITOR VEHICLE TRAFFIC

The DSS is the heart of the Global Control system, providing control and monitoring of all system elements. Data from all sensors is processed and fused to provide accurate and timely display of area traffic against a background of chart graphics. Vehicle position updates on the situation display will be seen at least once per sec except during zoom or pan while charts are being redrawn.

3.2.3.a.5.4.2. SECURITY AND USER ACCESS CONTROL LIST

The GCC, operating under Unix, provides password access control and maintains a list of users who have accessed the equipment. By utilizing the standard login procedure of Unix, procedures and adaptation files may restricted to specific group use. In this way, we will provide the appropriate access capabilities to Controller, Trainee, Supervisor, and System Administrator. The time to change operators is typically less than 30 seconds (logout - login - warm start).

Additional security is provided by the fact that non-application controlled access to the LAN is restricted to outgoing calls only. Outgoing calls which connect to the LAN may only be initiated by the Supervisor.

3.2.3.a.5.4.3. UNIX SYSTEM

Each processor in the DSS operates under the Unix operating system. Raytheon would write the DSS software in the C-language to take advantage of existing software.

3.2.3.a.5.4.4. DSS MANAGEMENT EQUIPMENT

As defined, the DSS equipment contains all hardware and software needed for normal maintenance. Equipment furnished will contain built in test equipment to report and diagnose problems.

3.2.3.a.5.4.5. DSS AUDIT TRAIL

All history data including operator actions, vehicle and track data are recorded on the same media. All track and operator state control records from-to information so that it can be played back in reverse. Periodically, state data is recorded so that excessive amounts of data do not have to be scanned to reestablish system state. Playback of data may be performed on the redundant recording equipment while operational data is being processed and recorded on the operational recorder. Recording of the training audit may also be done on the redundant equipment without interfering with operational recording. Spooling is used for all cases where the recording media might need to be changed.

3.2.3.a.5.4.6. DDS REBOOT

The DSS system will start the boot process as soon as the power switch is turned on. The DSS system will also automatically start the reboot process after a power failure. A given workstation will not, however, provide an interactive environment to the operator until he/she has provided a user name and password. The current system needs about 1.5 min before the user is asked for a user name.

The time from completion of the password until the terminal has a full display and will respond interactively is less than 15 seconds. The current positions of participating vehicles will only be available in this time frame for a warm start. In the case of a power failure, vehicles will be shown as "coasting" until verification of position can be made.

3.2.3.a.5.4.7. DSC MANAGEMENT SYSTEM (DSCMS)

The DSCMS controls all DSC functions. The Controller will be able to initiate DSC communications with any vehicle or group of vehicles, set the reporting interval time for any vehicles in one sec increments from a minimum of one-sec. to one hr, and modify/terminate periodic DSC transmissions from all vehicles or any vehicle. Unsolicited messages from vehicles will be handled by DSCMS.

The DSCMS will control broadcasting to all vehicles, groups of vehicles and individual vehicles. By using periodic response messages rather than requesting each response,the channel will be able to handle more messages. Periodic responses will be limited to 10 repetitions in order to guarantee positive control.

The DSCMS will not keep track of polling times or intervals. This function will be performed by the Target Information Processing System (TIPS), which may use a combination of operator-selectable and software-adaptive reporting interval times.

The DSCMS will estimate channel utilization and attempt to keep below a set value by queuing and delaying output messages. A table of all vehicles which have been commanded to transmit periodic report messages must be maintained by the DSCMS so that the amount of communication bandwidth remaining for other purposes can be estimated. If it is projected that channel utilization will exceed the set value, a warning message will be displayed and the TIPS will be informed of this condition.

The DSCMS will also respond to an incoming vehicle (other global control area) which requests initiation of tracking. The current position and ID of the requesting vehicle will be passed to the TIPS, which will initiate tracking of the vehicle.

3.2.3.a.5.4.8. TARGET INFORMATION PROCESSING SYSTEM (TIPS)

The TIPS proposed for use in the GCC will employ a very substantial reuse of the software that is developed by Raytheon for AutoTrac 2000 ATC systems. The AutoTrac 2000 system was written in the C-language and operates under the UNIX operating system thus giving TIPS the advantage of open standards and automated network management during development and thereafter during system operation. This tracker will easily handle 80 or more vehicles. The tracker will automatically or manually accept new vehicles which will be identified and linked to the database. If the database link is not found, default tagging will be employed. Labels may be modified by the operator.

AutoTrac 2000 employs a multisensor mosaic tracker system as is needed for GCS to unify the controller's view of the situation before him. Vehicle position track update reports are periodically sent from the wayside control sites to the GCS. Vehicles will report their positions, velocity, and ID to the GCC. At any moment, a system track may be supported by any combination of position data, GPS data, or manual controller inputs.

The GCC tracker and track-prediction function must be able to predict vehicle positions accounting for the irregular availability of sensor data. Raytheon's AutoTrac 2000 tracking system routinely makes such predictions and will serve as a very good basis for GCC.

The off-line vehicle function will be added to the AutoTrac 2000 software since nothing like it now exists in ATC systems. The requirement to accept, retain and display unique vehicle identification information is supported by the AutoTrac 2000-based TIPS. This is done both in the form of tabular lists (arrivals, departures) and in the form of the data block displays linked to position symbology on the GDS.

The AutoTrac 2000 function to cover comparison of all tracked vehicles simultaneously, enables the controller to be warned about future encounters and congestion sufficiently ahead of time for the controller to take corrective action. On the other hand this function will also, by its predictive power, show when situations that appear to be overly congested will clear up, thereby allowing the controller to avoid introducing unnecessary traffic delays.

The track history function required by GCS is in close correspondence to the playback function available in the AutoTrac 2000 software. All target data is recorded as required. All display manipulation features that are available in real-time are also available as is the ability to start the history/playback display at a operator-specified time.

3.2.3.a.5.4.9. VEHICLE TRAFFIC INFORMATION SYSTEM (VTIS)

Raytheon will provide a multiuser database management system to support the VTIS. Supplying quality software while minimizing the costs and risk factors associated with its development will be achieved by adapting software from existing Raytheon tracking control programs where applicable.

The complete database for GCC will consist of a combination of data structures programmed in C and a commercial-off-the-shelf software. The current Raytheon approach to traffic control systems uses specifically-designed data structures for high-performance access to the program's internal data.

VTIS will provide for the management of three major data types in the database. These data types and their associated elements will consist of:

- Static data including vehicle particulars and participation summary records for all participating traffic. Procedures will be provided for extracting these participation summary records for a given vehicle and formatting the records into a report summary.

- Semistatic data including vehicle, radio call sign, and a 10-character alphanumeric ID code assigned to the operator. A history of the semistatic data, which captures the two previous values and a time stamp for the changes, will be maintained.

- Dynamic data including target-track-derived information.

VTIS will also manage all data required for the VTS operator to communicate with participating vehicles using the digital selective calling management system as described.

3.2.3.a.5.4.10. GEOGRAPHIC DISPLAY SYSTEM (GDS)

The workstations contain software and hardware to present both text and graphic type information to the operator. Raytheon avoids distractions caused by blanking of individual images when they are moving by writing data to a back refresh-buffer and then swapping buffers. Keyboard echo and cursor movements write directly to the front buffer. Movement of the cursor position device and keyboard entries provide a visual response which appears in less than 0.03 seconds. For a normal surveillance display, the image will update to show changes about four times per second.

Zooms (and pans) may be defined by choosing one of the preselected zoom windows, defining two corners of a zoom window with the cursor-positioning device, or by selecting the previous zoom window. When zooming or panning, the current screen will freeze until the display is ready (typically less than 2.0 sec) and then present the latest update.

All data is sent to the display generator as part of a hierarchy of objects. Each vehicle is defined as an object with position, rotation, velocity vector, leader, and textual data block. Once loaded into the display generator, the system need only edit position, rotation, velocity, and occasionally text information. Histories which are time-dependent may be loaded into timed objects for automatic aging and discarding. Histories which are event-count-dependent are handled as separate objects are regenerated between buffer swaps.

3.2.3.a.5.4.10.1. GENERAL

Chart data incudes physical features, traffic lanes, separation zones, traffic aids, emergency response locations/capabilities, danger areas, and magway obstructions. The dedicated bit plane for chart data, as well as vehicle position data, acts as a background frame of reference for other dynamically changing data.

A number of physical and menu keys are predefined by adaptation to perform graphic functions. For example, a single key may specify display at a predetermined position and scale. Temporary additions or changes may be made to chart data for display on operational workstations. These additions may be transferred to the off-line workstation for editing and merging with chart data.

3.2.3.a.5.4.10.2. DISPLAY OF DATA

The display system will display all chart data including land mass, traffic aids, magway lanes, safety bypasses, masking areas, danger areas, waypoints, and named reference points within the three planes reserved for chart data. Dynamic data is constantly updated according to fused track data and vehicle positions presented to the operator.

The operator may create, edit, save, retrieve, delete, or display traffic aids, magway lanes, traffic separation zones, safety lanes, danger areas, waypoints, and named reference points as well as manually entered vehicles. Manually entered data will not interfere with operation beyond highlighting and reporting of specific alarms created by such entries.

The operator may zoom to any scale from 3700m full screen to 237 km full screen with the pixel position accurate to one pixel of the appropriate Transverse Mercator projection of the chart data.

Each tracked vehicle is drawn over the chart data. The course and speed vector ride with the target and are updated as new data is processed by the tracker.

3.2.3.a.5.4.10.3. ELECTRONIC CHARTS

The Raytheon software provides chart information in Transverse Mercator cartographic projection form. The chart data is registered accurately (within 1 pixel) with the location framework for vehicles position. In addition, semi-static information such as traffic aids, sidings, magway lanes, traffic separation zones, safety lanes, danger areas, waypoints, named reference points, and other features may be created, edited, saved, deleted, and superimposed on the chart data.

3.2.3.a.5.4.10.4. DSS FUNCTIONS

The Raytheon AutoTrac 2000 system supports operator manipulation of aircraft vehicle data through the use of function keys, and an alphanumeric keyboard.

The AAS keyboard employs a large number of function keys in a manner designed by system and site-specific adaptation data. Thus, dedicated function keys are designated to meet requirements and other more dynamically-defined function keys are established.

The AutoTrac 2000 system generates alarms as new targets are entered into the system. These targets are blinked until they are acknowledged by a controller. Audible alarms are generated in response to designated events and the nature of the audible alarms can be established and controlled by system management by means of adaptation data sets. The ability to enable the supervisor to suppress the audio alarm was also provided within AutoTrac 2000. A context-sensitive help system is part of the AutoTrac 2000 system and will be adjusted to apply to GCC specific situations.

The AutoTrac 2000 system was designed to provide the controller with a large number of selectable display modes. Consideration will be given to the selection of color, brightness and the drawing sequence of layered displays so that the potentially busy video displays will not overwhelm the more delicate and critical displays of tracked objects.

3.2.3.a.5.4.11. ALARMS

Alarms are a vital element of the Raytheon system's emphasis on safety. The full range of alarms will be provided, by reusing and extending existing Raytheon software. These alarms will be flagged identically on all three types of GCS display consoles: controller, supervisor and training. Both audio and visual indicators will be enabled/disabled by the supervisor.

Existing Raytheon traffic control systems currently provide two classes of alarms: high priority and low priority. All of the identified alarm conditions will be assigned one of these priorities. High priority alarms are presented to the console operator before low priority alarms. High priority alarms are indicated by both a visual display and an audio signal. Low priority alarms receive only the visual display. For GCC Raytheon, will add the capability for the supervisor to enable or disable either the audio or visual signal or both.

To assure that no alarm is lost by the system, the software design uses queues for all newly created alarms, one queue for high priority alarms and another for low. A designated area on the display is maintained for visual presentation of one new alarm at a time. The oldest unviewed alarm message is displayed before newer ones, and high priority alarm messages are presented before low priority alarms. For each alarm, the time of occurrence and a brief message text are displayed. Different background colors are used in the alarm panel background for the two priorities. In addition, the panel also includes the total number of unviewed alarms in the queues, whether or not a high priority message is in the queue, and a soft key for the operator to acknowledge viewing the message currently displayed.

Once a given message has been acknowledged, it is deleted from the queue. It is entered into a message history disk file containing the most recent 1500 (nominal value; a variable system parameter) alarm messages. This list is accessible by the operator on a separate display form. It can also be printed

To make useful history reports more brief and logically grouped, Raytheon has implemented message categories. The user can define (nominally up to eight) categories of alarm messages. Example categories might be designated areas violations, loss of vehicle contact, or emergency calls. Recent message history reports can be printed by category. Since the console display is used as the visual indicator, no separate diagnostics are required for it. Built-in diagnostics will check the correct functioning of the audio alarm.

Raytheon systems provide a suite of tools to enable the console operator to create, modify, and delete polygonal designated areas without programmer assistance. These areas may be plotted on the charts and used in conjunction with the alarms.

3.2.3.a.5.5. CONSOLES AT THE OPERATIONS CONTROL CENTER.

The ergonomic and performance requirements for the consoles are implemented in proven, off-the-shelf hardware. There are two types of consoles: the graphic display subsystem console, and the smaller diagnostic workstation.

The geographic display is comprised of the components shown Figure 19. This basic design is used by Raytheon on all of its' latest generation controller workstations. Many specific features were added for the FAA on the AAS. Because the functionality of an ATC system and a GCC system are very similar, these features are a direct benefit to the GCS graphic display subsystem.

The Main Display Controller (MDC) is a high-performance 2048 line display generator developed by Raytheon for ATC applications and is currently being delivered to the FAA on the AAS. The design is based on the Silicon Graphics Inc. (SGI) product line and uses an enhanced version of the SGI graphics library. The MDC hardware features a pipelined processing architecture consisting of an M68020, an AT&T DSP32C and graphics ASICs. The refresh memory section contains eight video bit planes per pixel double-buffered and three eight-bit DACs for Red-Green-Blue (RGB) data. The refresh memory supports both the 2048 by 2048 pixel display at 60 Hz noninterlaced and an optional 1024 line by 1280 pixel auxiliary display. When updating dynamic data, the MDC first clears the background buffer, writes the new data in the background buffer and, when complete, the buffers are swapped. In this manner only valid stable data is presented without breakup or visible rebuild. The display processing portion communicates with the display processor via a SCSI bus which supports transfer rates of 2.5 Mbytes sustained and 5 Mbytes burst. Six 9600 baud serial ports are provided; one for the keyboard, one for

the MDM (main display monitor), one for the system monitor function, and three spares. A baseline of 4 Mbytes of display list/program memory is provided, which is expandable to 16 Mbytes. A feature of hardware antialiasing of vectors was added for two reasons. first, antialiased vectors appear smooth at any angle, enhancing the appearance of the display and, second, vectors drawn in this manner maintain uniform brightness at all angles, whereas normal vectors will have an inherent 2:1 brightness variation due to angle.

Some of the key performance parameters of the MDC may be summarized as follows: polygon fill rate - up to 220 M pixels/sec; block move rate - up to 12 M pixels/sec; vector writing rate (normal or antialiased) - 13 M pixels/sec minimum; character writing rate (12 by 12 font) - 150,000 characters/sec; simultaneous display of complete character fonts in 10 different sizes; and transformation of geometric coordinates at 86,000/sec. The net effect of these performance values is that any of the complete displays with area maps at any scale can be presented in about two sec. Similarly, update of dynamic data on the display without altering the maps (no pan or zoom) will be done four times/sec and response/acknowledgement of requests or keystrokes will typically take place in 30 ms.

The SGI graphics library is a very powerful three-dimensional graphics command language. Raytheon has developed several extensions to the language for enhancements to our ATC applications. Some of these enhancements are summarized as follows: Ability to display eight simultaneously independent graphical cursers-hardware enhancement also; intelligent display list using graphics variables - permits one word to completely alter the display; Timed objects-local control and display of track histories; Atomic text-writing of text directly in the foreground buffer for fast response; software hooks for legal recording of data; display of data in either transparent or opaque windows.

Fault detection/isolation software is provided in three levels. At startup, confidence tests are run to validate the integrity of the display subsystem prior to its being permitted to go on-line. Continuous fault detection software operates in the background cycling through hardware tests and looking for protocol and parity errors etc. Once a fault has been detected, off-line fault isolation software is employed to locate the failure to an line replacement unit (LRU). The fault isolation software is also run after repair to confirm the correction of the failure.

The Main Display Monitor is the Sony model DDM-2801CS. The key performance parameters for this monitor are as follows: Display addressability - 2048 lines by 2048 pixels per line; Active display size: 19.6 $\pm$ 0.4 by 19.6 $\pm$ 0.4 in.; 60 Hz noninterlaced refresh rate; White area brightness - 80 nits. This monitor meets all of the functional requirements of the GCS. Raytheon has considerable experience with this monitor and participated in the concept and detailed design reviews. We have developed proprietary alignment software which greatly eases the maintenance process and reduces the required skill levels and time involved.

The diagnostic terminal provides an off-line location to monitor and control the GCS without involving any of the controlled workstations. This workstation also functions as a print server for getting hard copies from the controller stations. The workstation is comprised of a Sun IPX with peripherals and the hard copy printer. The Sun SPARC station IPX is configured with 32 Mbytes of RAM, a single Ethernet interface, a 207 Mbyte internal hard disk, a 1.44 Mbyte 3.5 in. internal floppy drive, a 644 Mbyte desktop Sun CD Pack, a 2.3 Gbyte 8 mm tape module and a keyboard and mouse.

The monochrome printer requirements may be satisfied by a number of solutions ranging from a 300 dot-per-in. laser printer with an 8.5 in. wide image to a 32 grey shade thermal printer with a 20-in. wide image and 4096 total pixels per line. It is well understood that in any case the color image must be interpreted into a monochrome format for printing. The range of fidelity is large between the two solutions, but, depending upon the actual use, the 300 dot-per-in. black and white laser may be sufficient. In order to provide some grey scale capability we are proposing the Real Tech Laser 400 printer which provides 400 dot-per-in. resolution in each direction and a full print size of 11 by 17 inches. Therefore, each pixel on the CRT monitor will be represented by a 2 by 2 pixel matrix on the printer. This will permit the generation of five grey shades by dot densities of 0 to 4. The 10 basic colors on the display will be transformed into this grey scale resolution on a 10 by 10-in hardcopy.

Item	Time Reqd. (Sec)
Marker reception & confirmation @ vehicle	7.5×10^{-4}
Marker decode @ vehicle	27.7×10^{-4}
Marker Data + Vehicle ID & Status; 20 Instructions @ 5MHZ.	4×10^{-6}
RF Transmission to Local Control; Serial Data, 22 bytes/11 bits/byte @ 1.45µsec/bit	350.9×10^{-6}
Data Processing @ wayside control for transmission to GCC	
- Format 20 instructions @ 5 MHZ	4×10^{-6}
- Arbitrate Bus 120 vehicles @ 2 Bus cycles ea. @ 5 MHZ	48×10^{-6}
- Transmit @ 100 MB/Sec (FDDI) 22 Bytes X 11 bits/byte	2.4×10^{-6}
Transmission Time (max distance) - 100 miles = 160 KM ÷ 3×10^5 M/Sec	0.53
Data Processing @ Global	
- Decode/Process 20 instructions @ 5 MHZ	4×10^{-6}
- Bus Arbitration 120 vehicles @ 2 Bus Cycles ea. @ 5 MHZ	48×10^{-6}
Display Updates - Window Update } AAS' Display Capability - Ban/Zoom } @ 20% Margin	1.0
	3.0
TOTAL	4.53 Sec

Figure 17 Time budget table

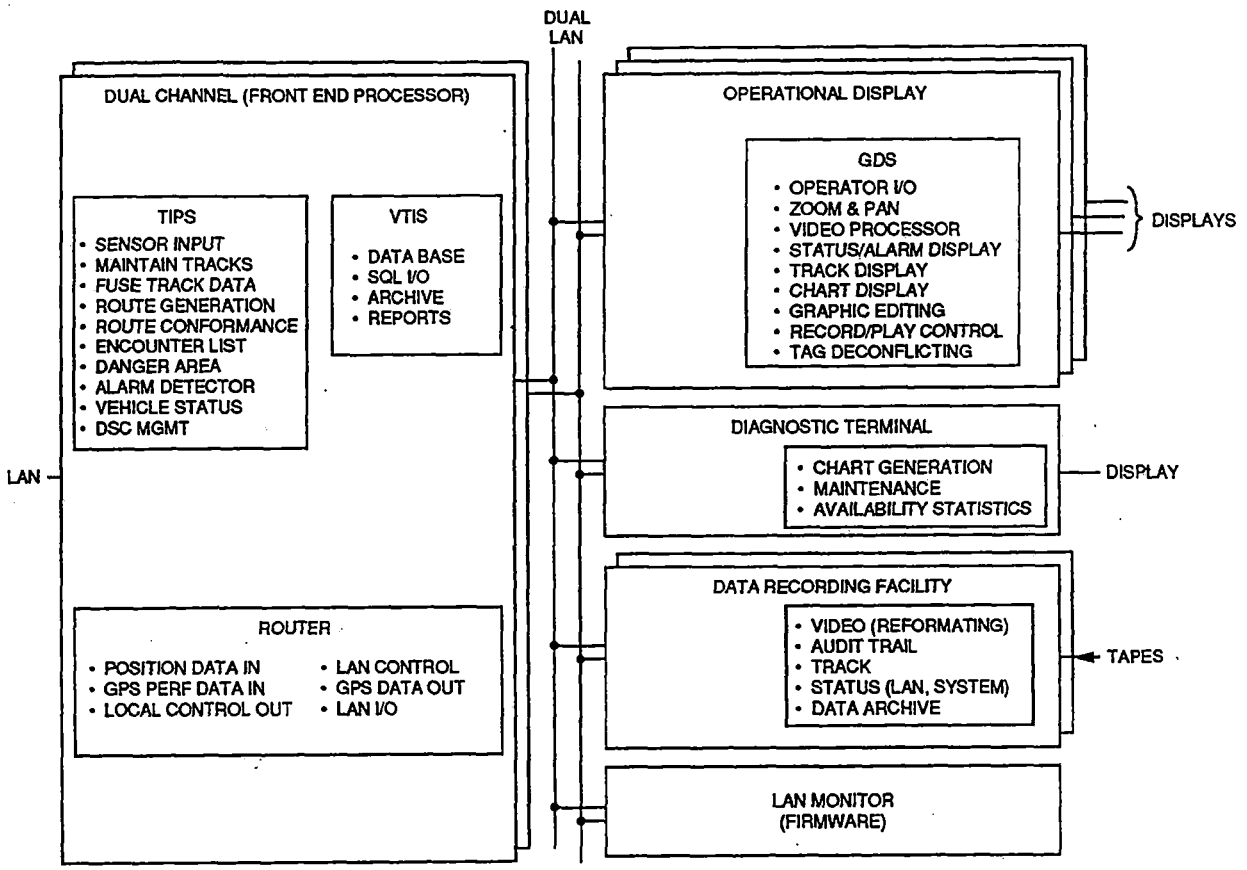

TIPS = TARGET INFORMATION PROCESSING SYSTEM
VTIS = VEHICLE TRAFFIC INFORMATION SYSTEM
DSC = DECISION SUPPORT CONTROL
GDS = GEOGRAPHIC DISPLAY SYSTEM
GPS = GLOBAL POSITIONING SYSTEM
LAN = LOCAL AREA NETWORK

Figure 18 Decision support system software architecture

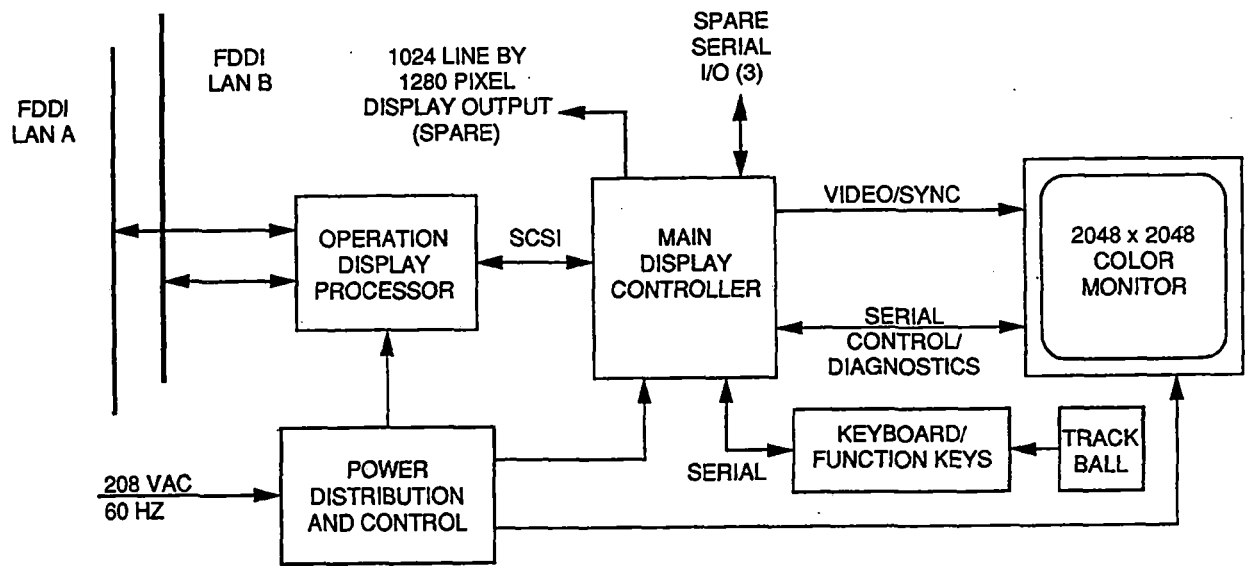

Figure 19 Geographical display block diagram showing the major funcitonal assemblies

3.2.3.a.6. EQUIPMENT LAYOUT

A preliminary layout for the Global Control and Communications Center is shown in Figure 20. The operations room has three manned operator positions and their associated equipment (hard disks, tape recorders, printer, etc.) plus various auxiliary equipment such as GPS, magway monitors, etc. The controller consoles (3) are placed in a row, typical of FAA configurations, to facilitate direct serial interface with each of its neighbors permitting control of any console from any position or keyboard. However, a more probable use in GCC is for a supervisor, using the multiple cursor feature; to be independently indicating something on either the controller or trainee's console with his unique supervisor cursor symbol.

The diagnostic workstation with printer is located in the electronics shop. this will facilitate easy repair and testing of line replaceable units (LRU).

Emergency power will be provided by an uninterruptable power source (UPS) or back up power generation depending on the needs and requirements of a particular site. All installed equipments will be protected by automatic reset source arrestor units which will be either rack- or bulk-head mounted.

Power and signal cables will be run to the equipment via cable trays. These cables will be run underneath the raised floor or along the wall and ceilings on a noninterference basis. All cables will be keyed and connectors arranged to insure correct, reliable interconnections of equipment.

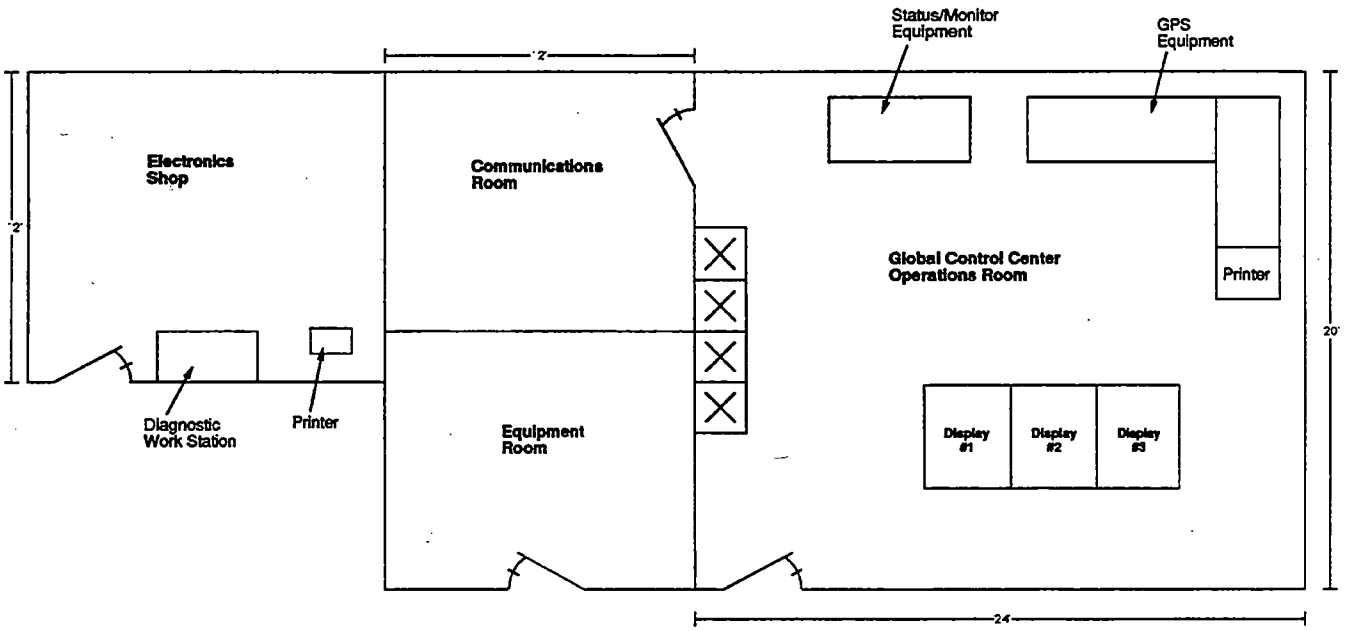

Figure 20 Layout of global control and communications center

3.2.3.a.7. LINK DEFINITION AND REQUIREMENTS

3.2.3.a.7.1 GENERAL

The communication and control systems for the Maglev configuration covers three distinct areas, namely global, wayside, and on-board. A top level Magneplane system control and communication block diagram is shown in Figure 24.

The global control/communication level is similar to a regional air traffic control center, which is the hub or center for dispatching commands and monitoring of vehicle traffic within a prescribed area. Also, each global control area communicates with adjoining global areas to facilitate a coordinated transfer of traffic between global jurisdictions or areas of control. A typical two-way distance of control for the global system is typically 160.9 km (100 miles). This distance has been selected based on the currently available Fiber Distributed Data Interface (FDDI) networking standard. This fiber optic network has ANSI and ISO approval, thus insuring a less difficult job of building a layered network system/architecture with communication functions sorted into logical groups (layers) so that they always perform in a peer-to-peer (non-hierarchical) relationship. Some of the major features of the FDDI are:

- Dual counter-rotating ring topology
- 100 Mbit/sec transmission rate
- Total fiber length of 200 Km (124 miles)
- Sophisticated encoding techniques to insure data integrity
- Distributed clocking to support a large number of stations (500 max) on the ring

The features listed above support the proposed global to global interface as well as the global to wayside interface. An illustration of the global to wayside interface is shown in Figure 25. Each global to wayside interface will utilize dual fiber optic links (FDDI) to provide the necessary redundancy and backup (fault tolerance) to establish an overall system availability of 0.97 or better. See Section 3.2.3.h tittled Reliability for System Analysis Data.

The spacing of global center to global center will be typically around 160 Km (100 miles), but due to geographic features, metro-center locations, etc. the spacing may extend to 199.5 Km (124 miles). Each global center will control and communicate with 160 Km of dual direction magway. Using a typical magway block length of 2.0 Km, will require a minimum of 160 wayside control stations (80 each direction). Since each FDDI link can service a maximum of 500 stations per 199.5 Km; the intended application is well with-in the proposed number of stations even if additional local controllers are needed at stations, service centers, etc.

The data flow for a typical global control station/center is shown in diagram form in Figure 26.

The global control generates all dispatch and docking commands for each station via wayside control, who in turn communicate these commands to the on-board vehicle control. Also, the global control generates emergency and failure management commands that can be forwarded to the vehicle and/or the wayside control. In addition, the global control transmits the vehicle travel profile (map) to the wayside control.

The wayside control forwards voice, velocity, and route commands to the on-board vehicle control, and in turn receives vehicle voice, position, and status. Vehicle position is obtained from two sensor subsystems, namely the magway position markers and the on-board Global Positioning System (GPS). All vehicle voice, magway data, and status is fed from the wayside control to the global control.

3.2.3.a.7.2. COMMAND FLOW

A typical command flow sequence (shown in Figure 26) for the vehicle velocity profile can be described as follows:

Global Center
-> Wayside Control
-> Vehicle
-> Wayside Control
-> Power Controller

1) Global Center originates and Wayside Controller communicates desired velocity to vehicle
2) Vehicle determines acceleration or de-acceleration required to achieve desired velocity
3) Vehicle determines phase of Linear Synchronous Motor (LSM) field and communicates back to wayside controller
4) Wayside controller directs Power Inverter to modify LSM field. (Power)

If a loss of communication between wayside and the vehicle occurs then the controller shall modify the LSM field directly.

A typical command flow for vehicle direction can be shown as follows:

Global Center
-> Wayside Control
-> Vehicle

1) Global center determines vehicle magway switching
2) Wayside Control communicates to vehicle and acts at switch point
3) Vehicle modifies control to anticipate left or right magway switching
4) Loss of communication will result in vehicle autonomous switching based on Map (Route)
5) Loss of communication will result in wayside action based on vehicle position (measured or predicted)

A typical command flow for vehicle braking can be shown as follows:

Global Center
-> Wayside Control
-> Vehicle

Vehicle

-> Wayside Control
-> Global Center

1) Global Controller determines braking for station pull-in
2) Global Controller determines braking required for optimum block velocity - ie, curves
3) Global Controller determines braking required for vehicle space compression - ie, re-entrant vehicle
4) Vehicle determines braking for communication or other failure
5) Loss of communication exceeding a predetermined period will result in emergency braking by vehicle
6) Loss of communication will result in Wayside Controller reporting emergency to Global Center

3.2.3.a.7.3. KEY SPECIFICATIONS

The requirements of the control and communication system are based largely on the major specifications are described in Figure 27.

The overall control and communication data and voice requirements will be reviewed by examining and establishing rationale for the global to wayside, global to global, and wayside to vehicle links.

The link requirements will be established in terms of message content, message rate, and data format.

3.2.3.a.7.4. GLOBAL TO WAYSIDE LINK

For the global to wayside control data link, the message content in terms of bytes is shown in Figure 28. In addition to the thirty-eight (38) data bytes the message will contain the following overhead bytes;

Sync = 2 bytes
Header = 2 bytes
Checksum = 2 bytes

for a total of six (6) bytes. The total number of message bits using eleven (11) bits (1 start + 8 data + 1 parity + 1 stop) per byte is calculated as follows:

Total message bits = (38 Data bytes + 6 Overhead bytes) x 11 bits/byte = 484 bits (global to wayside)

The global to wayside data message rate is established by the most demanding of the following criteria:

Data rate shall be 5X the vehicle servo closed loop bandwidth (-3 db);

$$5 \text{ X } (2 \text{ Hz}) = 10 \text{ Hz}$$

or the data rate shall be equal to the vehicle sensing magway markers,

$$\frac{134 m/\text{sec}(typ.velocity)}{11\ meter\ spacing} \approx 12Hz$$

Therefore, the required global to wayside message rate will be 12 Hz.

A digital voice channel requirement can be expressed by the following calculation;

$$Voice(bps) = 2\ x\ BW\ x\ N\ x\ (1 + \frac{\%OH}{100})$$

Where BW = voice bandwidth $\approx$ 3.5 kHz
N = quantization level = 8
%OH = percent overhead required for transmission $\approx$ 15%
bps = bits per second

The global to wayside voice communication shall be comprised of three bi-directional channels to satisfy two global controller positions plus a supervisory position. Using a voice bandwidth of 300 to 3.5 kHz to insure a good level of intelligibly at eight bits per sample and 2X samples equals $\approx$ 64.4 kHz per channel with approximately 15% overhead.

The total digital communication link (global to wayside to global) requirement is defined as:

Total Capacity = Data Message + Voice Messages

- DATA

Where the data message rate can be expressed as:

Data = N x message length x rate

where N = 2 x 80 = =160 {each of 80 vehicles receives and sends one message}

Message length = 484 bits

Rate = 12 Hz

Data (bps) = 160 (484)(12) = 0.93 Mbs

- VOICE

The voice capacity requirements can be expressed as:

D_{voice} = N x channel requirement

where N = number of channels = 2 x 80 = 160 (each of 80 vehicles using bi-directional voice)

Total digitized voice = 160(64.4 kHz) = 10.340 Mbs

Total link requirements = 0.93 Mbs + 10.34 Mbs = 11.27 Mbs

3.2.3.a.7.5. GLOBAL TO GLOBAL LINK

The global to global communication data message content is outlined in Figure 21.

The total data message capacity in bits/sec assuming a message overhead factor of 15% and a rate of 1 Hz can be determined as follows:

Total bits/sec
= (1,049,520 bytes x 11 bits/byte)1.15 x 1.0
= 13.277 Mbits/sec
(Global to Global)

The voice data message capacity is based upon three bi-directional channels for each of four FDDI fiber optic communication links. (Two links per input and output.)

Using the voice channel analysis of the global to wayside communication, where each voice channel uses 64 KB; the total voice capacity (global to global) is defined as:

Total Voice Capacity = 2 x 3 x 64 x 10^3 = 0.384 Mbs

Then total capacity
= Data Messages + Voice Message (Global to Global)
= 13.277 Mbs + 0.384 Mbs
= 13.661 Mbs

where total FDDI capacity link
= (global to global) + (global to wayside)
= 13.661 Mbs + 25.83 Mbs
= 39.491 Mbs

Using a FDDI fiber optic link with 85 Mbit/sec capacity (100 Mbit/sec less 15% overhead) provides a reserve link capacity for future growth and/or expansion, defined by:

$$Percent\ Reserve = \frac{85.0 - 39.491}{85.0} \times 100$$

$$= 53.5$$

3.2.3.a.7.6. WAYSIDE TO WAYSIDE LINK

The wayside to wayside direct communication data message content is outlined in Figure 22.

The total data message capacity in bits/sec is calculated as follows;

Using 11 bits/byte = 1 start + 8 data + 1 parity + 1 stop

Total Data bits = 28 bytes x 11 bits/byte = 308 bits

Using the FDDI message frame structure, which is comprised of a preamble, data, and cyclic redundancy check (CRC), the total number of bits/frame is;

Bits/Frame = Preamble Bits + Data Bits + CRC Bits
= 112 + 308 + 48
= 468 bits

A requirement of the wayside to wayside FDDI data link is to transmit, receive and process a message in 50μsec or less to satisfy vehicle control with the specified ride quality requirements. The total time budget for a message is shown in the table below, based on the assumed criteria:

- VME Processor data clock = 25 MHz
- FDDI mode requires 50 instructions @ 100 MHz bit rate to process messages
- Maximum distance between wayside stations is 4 km
- FDDI bit clock rate = 100 MHz = 1 x 10^8

Thus, the wayside to wayside FDDI data link transmission time is less than the 50μsec budget value.

The link capacity utilization base, on the following data, is determined as follows:

- FDDI effective bit rate = 95 Mb/sec
- Wayside to wayside message rate = 96 Hz

Total link capacity = 1 x 468 x 96 = 44.928 Kb/s

$$\% \ Capacity \ Utilized = \frac{44.928 \ X \ 10^3}{100 \ x \ 10^6} \ x \ 100 = 0.04\%$$

Reserve capacity is approximately 100%

3.2.3.a.7.7. WAYSIDE TO ON-BOARD VEHICLE LINK

The communication and control channel between the wayside controller and the vehicle on-board control will be a full-duplex RF link. A block diagram of the various communication interfaces between the vehicle, magway, GPS, etc., is shown in Figure 30.

The wayside controller will communicate to the vehicle in its magway block (2.7K m min.) via an RF link with control and voice data. The control data will basically consist of velocity, acceleration/de-acceleration profile, map updates, system status, etc.; eventually that information which is necessary to control the vehicle as part of the overall system operation. Figure 31 lists the various message contents and the anticipated number of bytes per each item. The rate the data will be transmitted to the vehicle is 20X the vehicle dynamic response of approximately 2 to 3 Hz minimum or 60 Hz.

Thus, the channel (wayside to vehicle) capacity can be calculated as follows:

Using 11 bits/byte = 1 stop + 8 data + 1 parity + 1 stop

Data Capacity = 216 X 11 X 60 = 142.56 Kb

The voice channel will be a 3.5 KHz bandwidth link with a 2X sampling rate using 8 bits (1 byte) of quantitization. Thus, the voice channel capacity requirement is 64.4 Kb using 15% overhead.

Then, the total link (wayside to vehicle) link capacity is:

Total Capacity Required = Control Data + Voice (Local to Vehicle)
= 142.56 + 64.4
= 206.96 Kb

RF Transceiver requirements can be established to accommodate the channel data capacity using the following assumptions/requirements:

$S/N_{(vehicle)} \geq +$ 15 db for error probability $> 10^{-6}$ using FM modulation

The wayside to Magneplane on-board RF link for voice and data communications would use the existing land mobile communications in the 450 MHz or 800/900 MHz band. These are presently assigned land mobile frequency bands by the Federal Communications Commission (FCC). For purposes of this study, the 450 MHz band has been selected. Final frequency operational assignments for Maglev will be negotiated with the FCC. THe 450 MHz band for land mobile communications is subdivided into 25 KHz FM channels. Each channel can transmit or receive data up to 9.6 kbps, clear voice or private digitized voice.

Air Traffic Control (ATC) and Vessel Traffic Control (VTC) both use clear voice RF links while many police and fire personnel are switching from clear voice to private digitized voice links. Both ATC and VTC have limited controlled arenas in which they operate most of their clear voice RF links. However, Maglev will operate throughout uncontrolled areas and consequently a voice privacy link should be incorporated. Also, the Maglev land mobile voice link is more like the police or fire usage in that very limited personnel would normally access the Maglev voice link. Using a private digitized voice link would prevent unauthorized users from intercepting and interfering with the Maglev voice link. The same Maglev land mobile voice link could be used for clear voice transmissions if this is preferred.

Land mobile radios are currently available that provide private digitized voice. The analog to digital voice conversion uses continuously variable slop delta modulation (CVSD) at a 12 kbps rate to send the digitized voice over each FM channel. The land mobile radios with modems will transmit data at 9.6 kbps over each FM channel. Following is an analysis that shows that with a one watt radio, an adequate RF signal path is provided over the expected wayside control unit to Magneplane vehicle radio frequency link.

3.2.3.a.7.7.1. FREE SPACE LOSS

The equation for free space loss (L) is as follows:

$$L = 32.44 + 20 \text{ Log } D + 20 \text{ Log } F$$

where

D = Distance in kilometers (km)
F = frequency in megahertz (MHz)

let

D = 4.7 km (Maximum distance between wayside control unit and Magneplane vehicle)
F = 450 MHz (land mobile communications band)

then

L = 94 dB

Consequently, the free space loss between the wayside control unit and the Magneplane vehicle is as great as 94 dB. The approval of the frequencies for Maglev land mobile operations is subject to Federal Communications Commission (FCC) approval. The 800 Mhz and 900 MHz frequency band may also be used for land mobile communications. If final FCC approval for maglev is in one of the higher land mobile frequency bands, then the free space loss would be approximately 6 dB more and L = 100 dB. Figure 23 shows the link budget per channel.

Therefore a one watt transmitter at the wayside control unit will provide an RF receive signal level with more than 46 dB of margin. RF fading due to multipath as well as path obstructions is helped by the large receive signal margin.

3.2.3.a.7.7.2. LAND MOBILE ANTENNA CONSIDERATIONS

For mobile antennas like those required on the Magneplane vehicle, antenna gain is very much limited by mechanical considerations. Larger land mobile antennas having the aperture to produce higher antenna gain may not be mounted on the Magneplane vehicle roof and still withstand the severe strain of environmental factors such as high wind velocity (i.e. 300 mph) and ice build-up. Consequently the wayside control unit mast-mounted antennas should be the primary source of wayside to Magneplane vehicle antenna gain. A standard antenna should be implemented for the Magneplane vehicle and any adjustments for antenna gain and antenna pattern would be made at the wayside control unit antenna. Center fed half-wave dipole radiator(s) antennas with vertical polarization are frequently provided for land mobile service as they give maximum gain in the horizontal plane which is a normal land mobile requirement. Figure 32 shows a typical vertical radiation pattern for the Maglev vehicle and wayside control unit antenna. The horizontal radiation antenna pattern is a horizontal Y axis rotation of the vertical pattern. These types of antenna patterns would help to provide good normal communications as well as when the Magneplane vehicle is banking around curves.

3.2.3.a.7.7.3. TUNNEL COMMUNICATIONS

Radiating leaky cable systems or leaky cables are a common mode of RF communications within tunnels due to the large loss of antenna-to-antenna RF signal power. A leaky cable is an open coaxial cable transmission line in which the electromagnetic wave may travel both inside and outside of the coaxial cable. The transmission of RF energy from a cable to the Magneplane antenna and vice versa is achieved with leaky cables.

A tunnel leaky cable system RF communications consists of a base station transmitter and receiver connected to a leaky cable. Line amplifiers or repeaters are installed at frequent intervals to compensate for leaky cable RF losses. The RF power radiated by the magneplane vehicle or fed into the cable can be one watt. When very long cable runs are necessary inside tunnels, the leaky cable system can be in sections and each cable section linked to its own base station. Base stations inside the tunnel would be interconnected via FDDI to the wayside control units. Leaky cable systems have been used successfully in the 400 MHz to 900 MHz range. The Maglev system would implement a leaky cable system within tunnels in order to maintain an uninterrupted land mobile communications link between the Magneplane vehicle and Global Control Center.

3.2.3.a.7.8. VEHICLE TO WAYSIDE CONTROL

The vehicle will communicate to the wayside control via a RF link with status and voice data. The status data content is shown in Figure 33 in terms of item description and number of bytes required. Using the same criteria, namely:

Message Rate = 12 Hz @ 11 Bits/Byte

the link data capacity can be determined as follows:

$$Data\ Capacity = \frac{47 bytes\ X\ 11 bits/byte}{1/12} = 6.2 kb/sec$$

The voice channel requirement is identical to the wayside-to-vehicle line; namely, the voice capacity equals 64.4 Kb.

Therefore, total vehicle-to-wayside control link capacity is:

$$\begin{aligned} \textit{Total Capacity} &= \textit{Data} + \textit{Voice} \\ &= 6.2 kb/s + 64.4 kb/s \\ &= 70.6 kb/s \end{aligned}$$

The RF transceiver requirements for the vehicle-to-wayside control will be identical to the wayside-to-vehicle channel. This will allow a commonality of equipment.

3.2.3.a.7.9. MAGWAY POSITION/LOCATION AND VELOCITY MEASUREMENT

The vehicle will determine its position from two independent sources that are conveyed via RF link to the wayside controller. One position determining source will be from position markers that are distributed along the magway at regular intervals (eleven (11) meters). The position markers will broadcast via a RF link a unique code, which establishes a particular location the vehicle is passing. The position markers and their RF broadcast will accommodate vehicles in curves, tunnels, and all other terrain features encountered. Each vehicle will have two or more position sensors on each side to receive, detect, and decode/process the marker code signal for determining vehicle position and velocity. A block diagram of the position marker scheme is shown in Figure 34. The on-board controller detects the position marker coded signal and time of intercept; thus, with an accurate position location and utilizing several different position marker receptions, the vehicle velocity is determined.

The vehicle magway position monitoring requirements (baseline) are:

Vehicle Velocity = 150 m/sec. (max.)
Measurement Accuracy $\approx$ 1%
Vehicle Length = 22.9 m (min.)
Global Control Length = 160.93 Km typical

In addition, the following assumptions were used in establishing the proposed concept:

Vehicle length spans two (2) location markers.

$$\textit{Number of Markers Required} = \frac{160.93 \times 1000}{11} = 15{,}373$$

ID Code for Identification = 14 bits minimum (16,384 positions)

Data transmission format similar to ATC Beacon
16 pulses at 1.45 μsec spacing

Transmission bandwidth > 3.5 MHz

Detection factors
Minimum transmissions received per location > 16
Error probability > 1 X 10^{-6}

RF azimuth beamwidth (-3 db) will be 10° minimum, elevation beamwidth = ±35°

Subsequently, the receiving antenna at a maximum distance of three (3) meters will be illuminated for 3.53 msec. for a vehicle velocity of 150 m/sec as calculated below;

$$\tan\theta = \frac{X}{3\ meters}$$

$$= 3(\tan^{-1}\ 10°)$$

$$X = 0.53\ meters$$

$$Illumination\ time = 0.539(\frac{1}{150})$$

$$= 3.53 milliseconds$$

The coded RF transmission will be similar in format to that used as an ATC beacon as shown in Figure 34.

with 16 pulses on 1.45 μsec leading edge boundaries. Pulse width = 0.4 to 0.6 μsec, and the rise/fall time ≈ 0.1 μsec. The bracket pulses are always transmitted with various combinations of the fourteen interior pulses. Using as code repetition rate (CRR) of;

$$CRR = \frac{1}{3\ X\ data\ length}$$

$$= \frac{1}{3\ x\ 23.2\ x\ 10^{-6}}$$

$$= 14.37 KHz$$

$$and\quad t_{CRR} = \frac{1}{CRR} = \frac{1}{14.37\ x\ 10^{3}} = 0.07 ms$$

Thus, the number of coded transmissions occurring for the RF beamwidth (10°) and the vehicle velocity equal 150 m/sec. is determined as follows:

$$\textit{Number of RF Transmissions Received} = \frac{\textit{Illumination x Time}}{t_{CRR}}$$

$$= \frac{3.53ms}{0.07ms}$$

$$\approx 50$$

Therefore, using detection criteria/factors as follows:

Error Probability = 1×10^{-6}
Constant False Alarm Rate (CFAR) loss $\approx$ 1 db
No. of transmissions required $\geq$ 16
S/N $\geq$ +10 db

we see the proposed illumination and detection scheme fulfills the intended application.

In addition, the Global Positioning System (GPS) will also be used as an autonomous and backup/redundant means by which the vehicle can determine its position. GPS will also be used as the means of locating (position) all vehicles in a start-up (awake) mode of operation. Currently, GPS equipment, such as receivers/processors and antennas, is available from leading electronic equipment manufacturers as Magnavox, Macom, CAST, etc.. Some typical/general data is as follows:

- Accuracy - typically 30 meters; 3 meters within seconds
- Coverage - all of continental U.S.A.; currently, 17 of 24 satellites in use
- Ultimate Usage - real time differential GPS broadcasts with local corrections being performed in the receiving equipment
- Frequencies:
  L1 = 1575 MHz $\pm$ 10 MHz (Commercial)
  L2 = 1228 MHz $\pm$ 10 MHz (Military)
- Receivers - 3 to 6 channels; can provide close to horizon (5°) satellite tracking
- Updates every second
- Most equipment has waypoint and travel plan (map) storage capability

MESSAGE ITEM	RANGE (based on 160.9 Km)	NO. OF BYTES
Vehicle Transfer (Global to Global Boundary)	Four vehicle transfers, (2 boundaries of dual track)	4x44 bytes = 176 bytes
Display Screen Transfer	2048x2048 Raster/ display (Transfer 2 boundary scenarios)	2x524,288 = 1,048,576 bytes (max)
Other data	Weather, Mgmt, System Status, etc.	800 bytes TOTAL = 1,049,552 bytes

Figure 21 Global to global message content

Message Item	Number of Bytes
Sending Wayside ID	2
Receiving Wayside ID	2
Vehicle ID	2
Magway Power	
- Frequency	4
- Phase	4
- Magnitude	4
Time Reference	4
TOTAL	**22**
Overhead	
- Sync	2
- Header	2
- Checksum	2
TOTAL	**6**
GRAND TOTAL = 28 bytes	

Figure 22 Wayside to wayside direct communication data message content

Frequency	450 MHz
Range	4.7 km
Free Space Loss	98.94 dB
Bandwidth	12 KHz
Receiver Sensitivity	-116 dBm
Transmit Power	30 dBm (1 watt)
Transmit Antenna Gain and Line Loss (1.0dB)	0 dBi -1 db
Receive Antenna Gain and Line Loss (1.0dB)	0 dBi -1 db
Required RF Receive Signal for 15 dB S/N Ratio	-116.2 dBm
Actual RF Receive Signal Level	-69.9 dBm
RF Receive Signal Level Margin	46.3 dB

Figure 23 Link budget per channel (wayside to Magneplane)

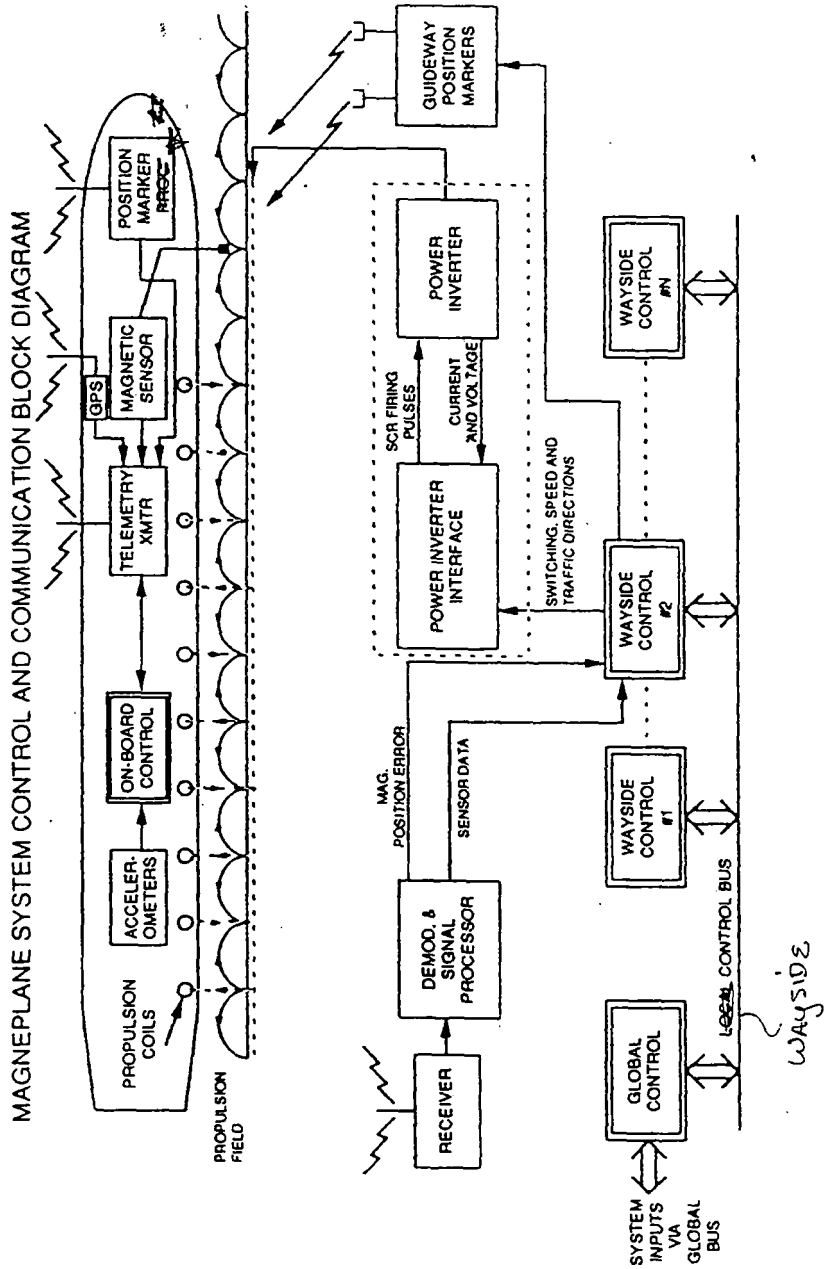

Figure 24 Control and communication block diagram

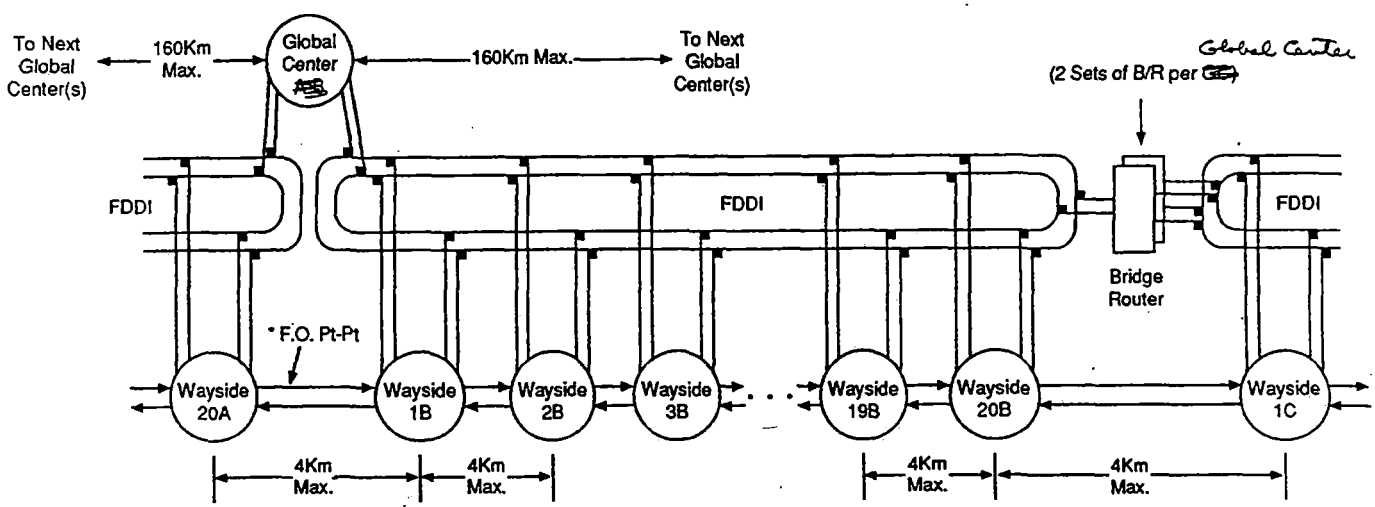

Figure 25 Global to wayside interconnection

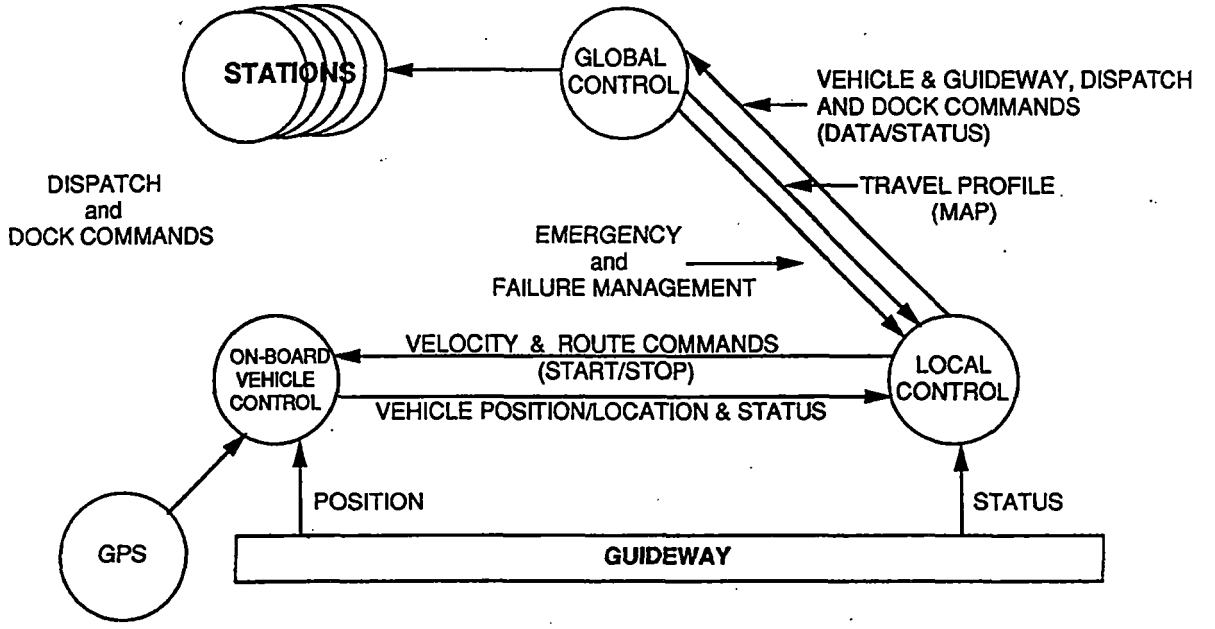

Figure 26 Control and communication data flow diagram

Total Distance	= 160Km (100 miles) Global to Global Station (typical)
Station Distance	≈ 14Km (15 miles) Metro Area
Vehicle Capacity	45 passenger and/or 140 passenger @ 40 sec. headway
Mix Ratio	Passenger vehicles or passengers plus freight
Venicle Speed	150 meter/sec (320 mph) maximum
Block Length	2.7Km typical
Capacity	= 4000 to 12,000 passenger/hour/direction
Braking	= 0.2G typical, 0.60 G maximum
Acceleration and de-acceleration	= 0.2G
Jerk (Δ accel)	= 0.1G
Mission Duration	= 3 hours typical
Station Stop Time	≈ 5 to 7 minutes (large complex) ≈ 1 minute (small complex)
Reliability (MTBF)	≥ 10° hours based on 18 hour day
Operating Temp. Range	= -25°C to +40°C
Vehicle Response	≥ 1.5Hz

Figure 27 Summary of major system control specifications

Message Item	Range (Based on 160.9 Km)	No. of Bytes
Vehicle Identification	>160	2
Track & Direction		2
Enter Slot Time	Day/hour/minute/second	4
Exit Slot Time	Day/hour/minute/second	4
Status	Major Subsystems (8)	2
Vehicle Origin		2
Vehicle Destination		2
Boundary	North, South, East West (degrees, minutes, seconds) Longitude/ Latitude (4 bytes)/ (4 bytes)	8
Location	GPS or Guideway Marker	12
	TOTAL	**38 Bytes**

Figure 28 Global to local data link message contents

Process	Time Required (μsec)
FDDI Message Time 468 bits x $1/10^8$	4.68
FDDI Instruction (50) Processing (send + recv) 2 x 50 (1×10^{-8})	1.00
FDDI Link Distance Delay $\frac{4 \times 10^3 \text{ meter}}{3 \times 10^8 \text{ meter/sec}}$	13.3
VME Processor Data Processing (send + recv) $2 \times 308 \times \frac{1}{25 \times 10^6}$	24.6
TOTAL	43.58 < 50.0μsec

Figure 29 Time budget for wayside to wayside FDDI data transmission

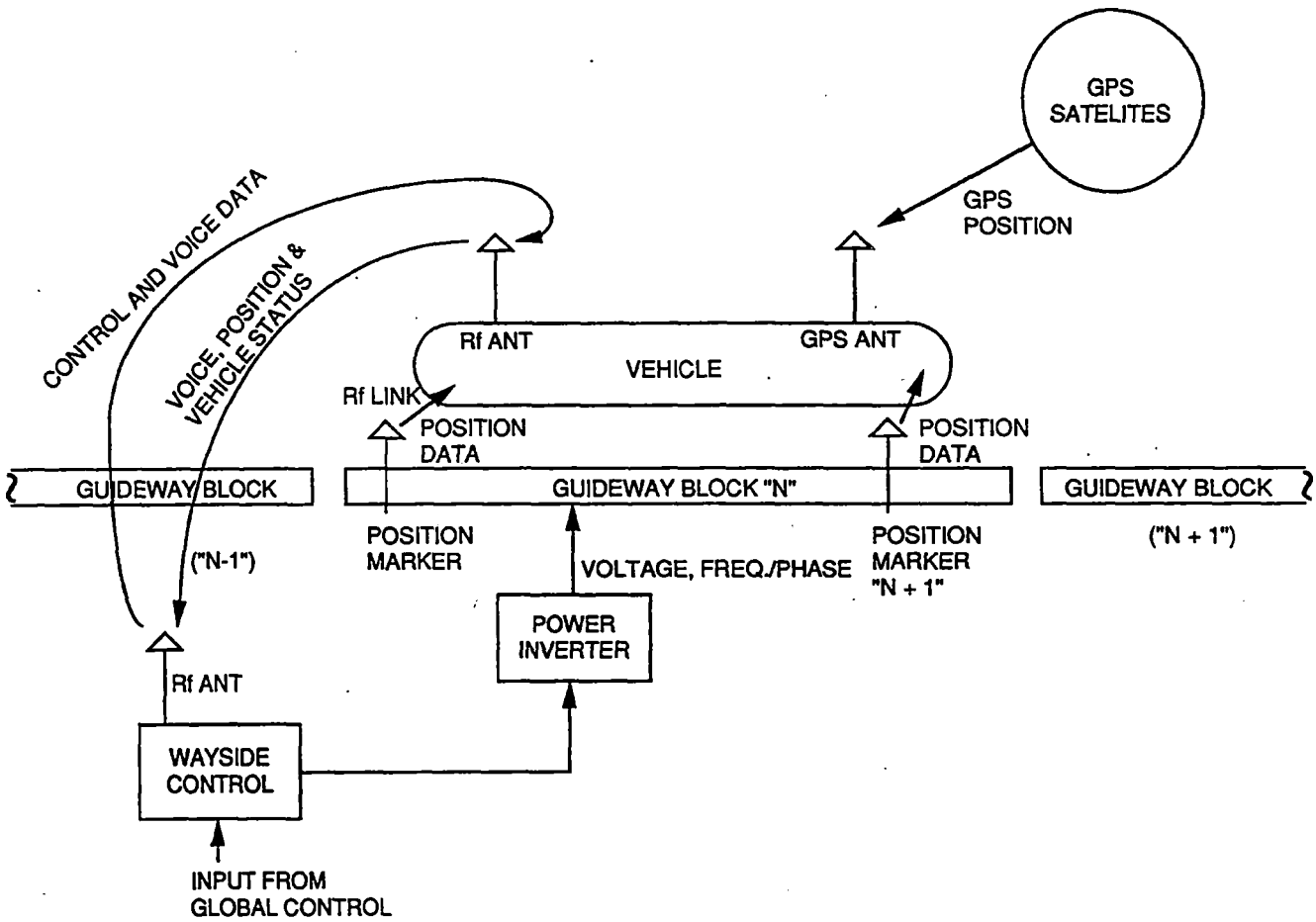

Figure 30 Wayside to on-board vehicle communication link

Message Item	No. of Bytes
Vehicle Identification	2
Wayside Identification	2
Time Reference	4
Velocity Command	2
Map Profile/Update	100
System Status (traffic, weather, etc.)	100
TOTAL	**210 bytes**
Overhead	
- Sync.	2
- Header	2
- Checksum	2
TOTAL	**6 bytes**
GRAND TOTAL = 216 bytes	

Figure 31 Wayside to on-board vehicle message data

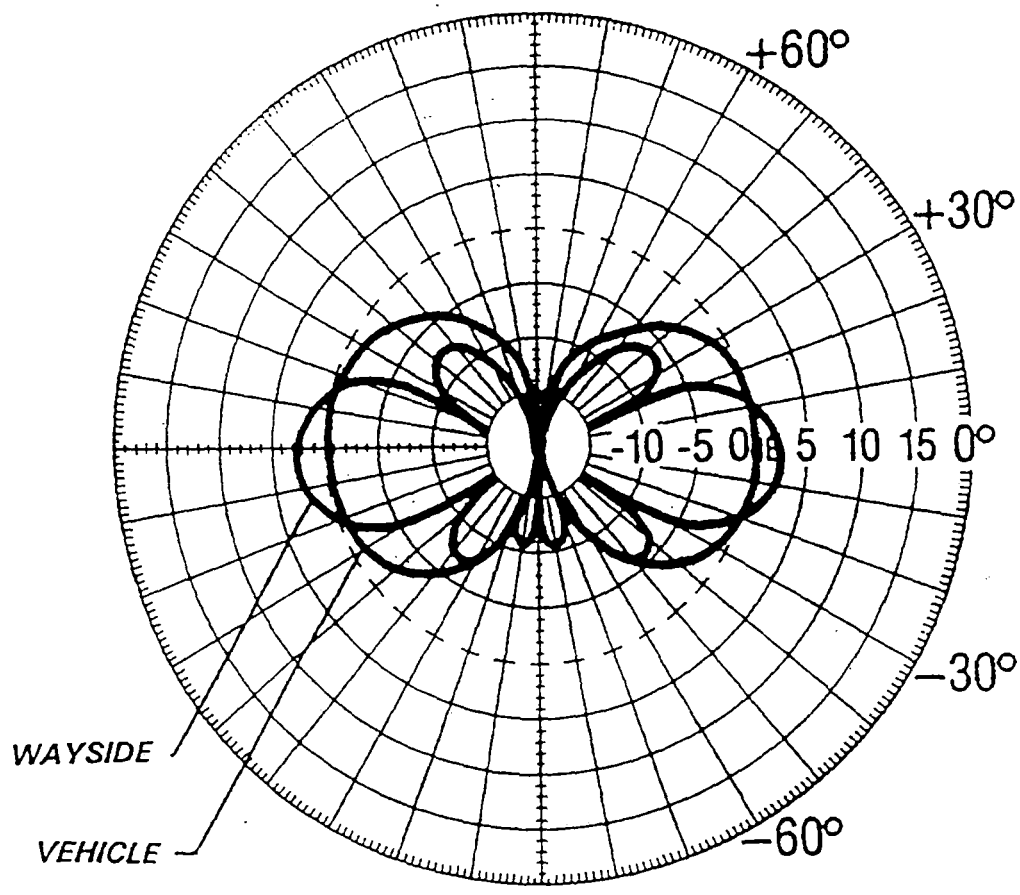

Figure 32 Typical vehicle vertical radiation patterns

Message Item	Range	Increment	Number of Bytes (8 Bits)
Velocity (Phase)	0 - 360° (0 - 150 Hz)	0.1°	2
Magnitude	1-100%	0.1%	2
Proximity Sensor Front, Middle, + Rear	0 to 0.5M	<0.1 cm	6
Accelerometers (3 Axis Each)	±5G	<0.06G	9
Braking	On/off	-	1
Aerodynamic Control Front + Rear (Four Surfaces Each)	±12° @ 4°/sec.	0.1°	8
Guideway Position	0 to 65,000	1	2
GPS Position	Deg./Min./Sec.	20 meters	7
Vehicle ID	60 - 300	1	2
Vehicle Subsystem Status	TBD		8
		TOTAL	47

Figure 33 Vehicle to wayside control message content

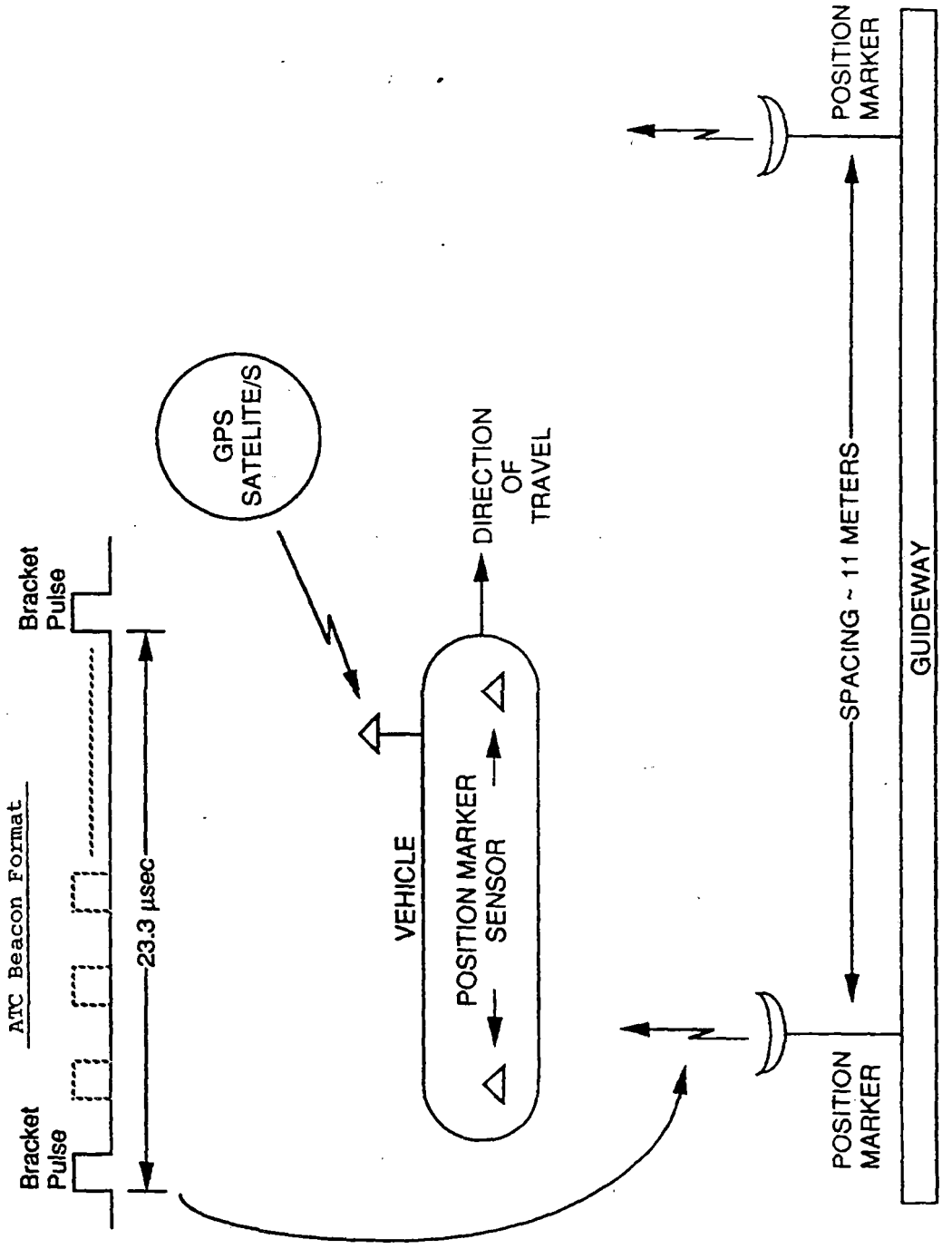

Figure 34 Magway position marker block diagram

3.2.3.b. CLIMATIC EFFECTS

Wind blown dust and debris should purge through the holes in the LSM windings in the bottom of the trough with the sweeping action of the moving Magneplane vehicles. Larger wind-blown items will be detected by the camera surveillance system and can be cleared by the self-propelled, balloon-tired maintenance vehicles.

Ice, snow, rain, fog and wind will affect the Magneplane system less than other transportation systems. Icing of the magway trough will be prevented by the heat generated through the electromagnetic drag of the system. This has been quantified in Section 3.2.2.c. Light snow will be blown off by the moving vehicle. Heavy snow accumulation may occasionally require clearing by a self-propelled snow throwing vehicle but this would be required with any transportation system. The magway has been designed for a snow load of 40 psf. Magneplane is not adversely affected by the visibility problems associated with snow or fog. Rain will drain through the holes in the LSM windings in the bottom of the trough. The system has been designed for the wind loadings specified by the COE. As stated in Section 3.2.2.a.2., this is presently based on a basic wind speed of 38 m/s (85 mph), however, the magway system can be designed for any wind speed as dictated by local requirements. Wind loads at various wind speeds have also been estimated for a stationary vehicle and a vehicle traveling at various speeds as described in Section 3.2.2.a.2.

Thermal cycling has been accounted for in the design of the support structure and the magway trough as explained in Section 3.2.1.f.1.

Seismic: The magway and supporting structure have been designed for seismic zone 2, however, the magway can be designed for any seismic zone as required by local codes.

3.2.3.c. AERODYNAMIC EFFECTS

Unsteady pressures and forces are produced when two vehicles pass, and to keep their effects at acceptable levels a minimum track separation distance must be established. Increasing the separation results in increased magway structure, ground footprint and magway cost. The qualitative behavior when the velocity and pressure fields of two passing vehicles interact is as follows. During initial approach, a pressure increase occurs and there is a repelling force between the two noses, the magnitudes of which are sensitive to the detailed nose shape. As the vehicles move alongside each other a second and stronger effect is to produce a suction and attractive force between the vehicles. Most of the published data on this phenomenon is based on two-dimensional analysis and wind tunnel tests. However, there is qualitative agreement with data from measurements from rail vehicle experiments.

Generally, the magnitude of the disturbances produced by three-dimensional bodies is significantly less than that of two-dimensional shapes. However, the disturbance falls off more rapidly with distance from the body. Both effects are shown in Figure 36, where the maximum velocity that a stationary observer would feel is presented as a function of distance in body diameters from the body center-line, for two and three dimensional bodies with circular or hemispherical noses. Using these results, the two-dimensional data for forces between passing vehicles presented by Johnston, et al (ASME 74-FE-22, 1974) was scaled in magnitude and for separation distance, and the maximum lateral accelerations calculated for the 140 passenger vehicle. The results are shown in Figure 37. An acceleration level of 0.04 g was felt to be acceptable and the corresponding separation distance between vehicles of 2.3 m (5.3 m between magway centerlines) was selected as the minimum for magway design purposes.

Vehicles passing each other inside a single tunnel experience a much larger perturbation than in free-air and the criterion for separation distance would have to be greatly increased over the 5.3 m requirement, resulting in large single tunnel diameters. It appears from Section 3.2.2.k. that it is better to construct separate tunnels for each magway direction and avoid the problem of passing in single tunnels. Therefore the problem was not analyzed further.

Another important unsteady aerodynamic effect is associated with tunnel entry. This involves two related aspects:

1) The build-up in aerodynamic drag to its steady value inside the tunnel.
2) The pressure and drag impulse due to compressible flow interactions between the vehicle nose and the tunnel at entry.

The steady drag increase in the tunnel is taken from Section 3.2.2.k. and takes place over a distance characterized by the vehicle length. The pressure and drag impulse magnitudes at entry were obtained from Gawthorpe (VKI Lecture Series 48, 1972) with a build-up and decay distance characterized by the length of the vehicle nose. The effect of tunnel diameter on the combined jolt ride comfort is presented in Figure 35, for an entry speed of 140 m/s and a flat tunnel entry face i.e. no entry shaping. The longitudinal ride comfort jolt requirements are 0.07 g/s peak-to-peak for the design case and 0.25 g/s as a minimum. For an acceptable jolt level in the case of a 10 m diameter tunnel the following measures

Speed = 140 m/s			
140 Passenger Vehicle			
Tunnel Diameter (m)	10	12	14
Entry Jolt (g/sec)	0.23	0.14	0.10
Drag rise jolt (g/sec)	0.07	0.04	0.03
Total jolt with no shaping (g/sec)	0.30	0.18	0.13

Figure 35 Tunnel entry ride quality

would be incorporated:

1) the propulsive force would increase with time to match the drag change.

2) the tunnel entry shape would be tailored over a distance equal to about two vehicle lengths so that the effective diameter at immediate entry is about 14 m.

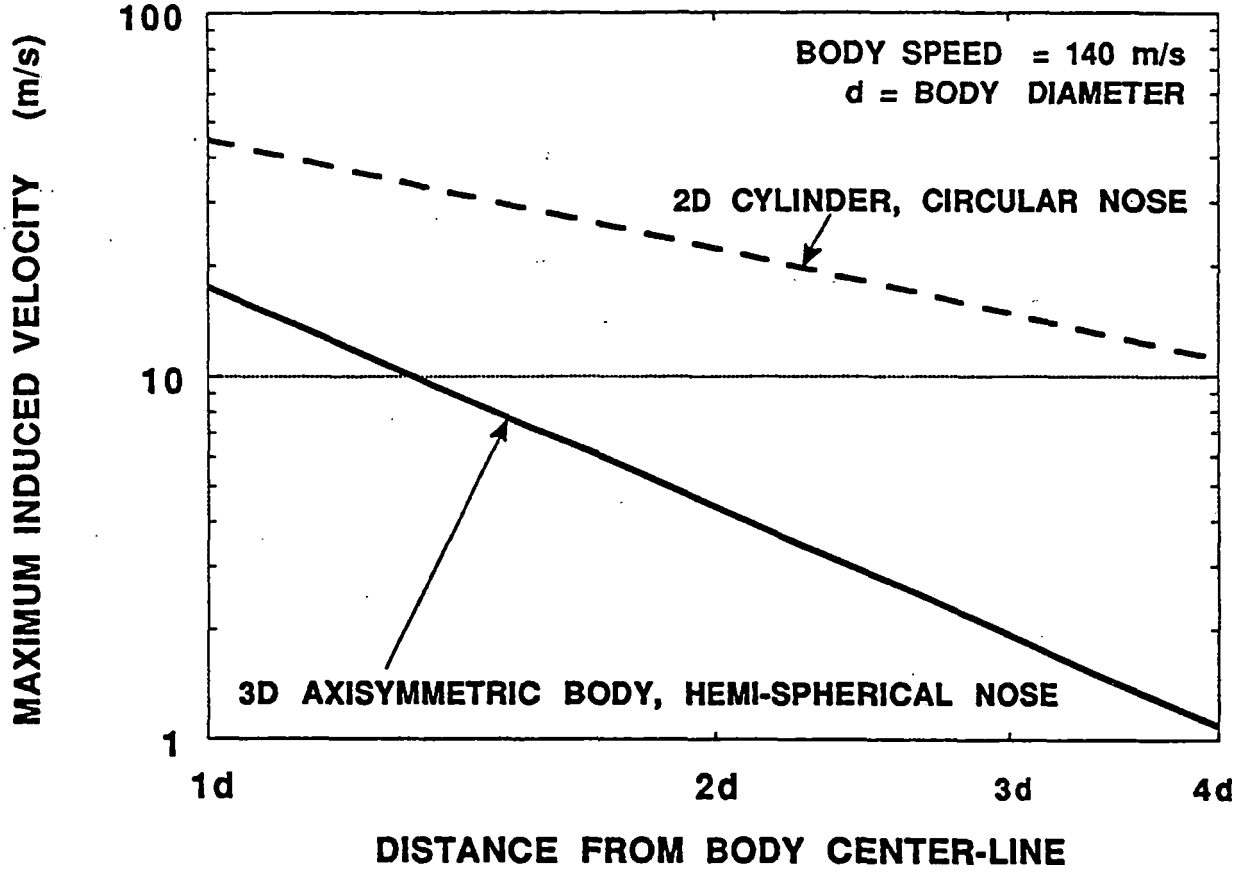

Figure 36 Maximum velocity induced at a stationary point by a passing vehicle

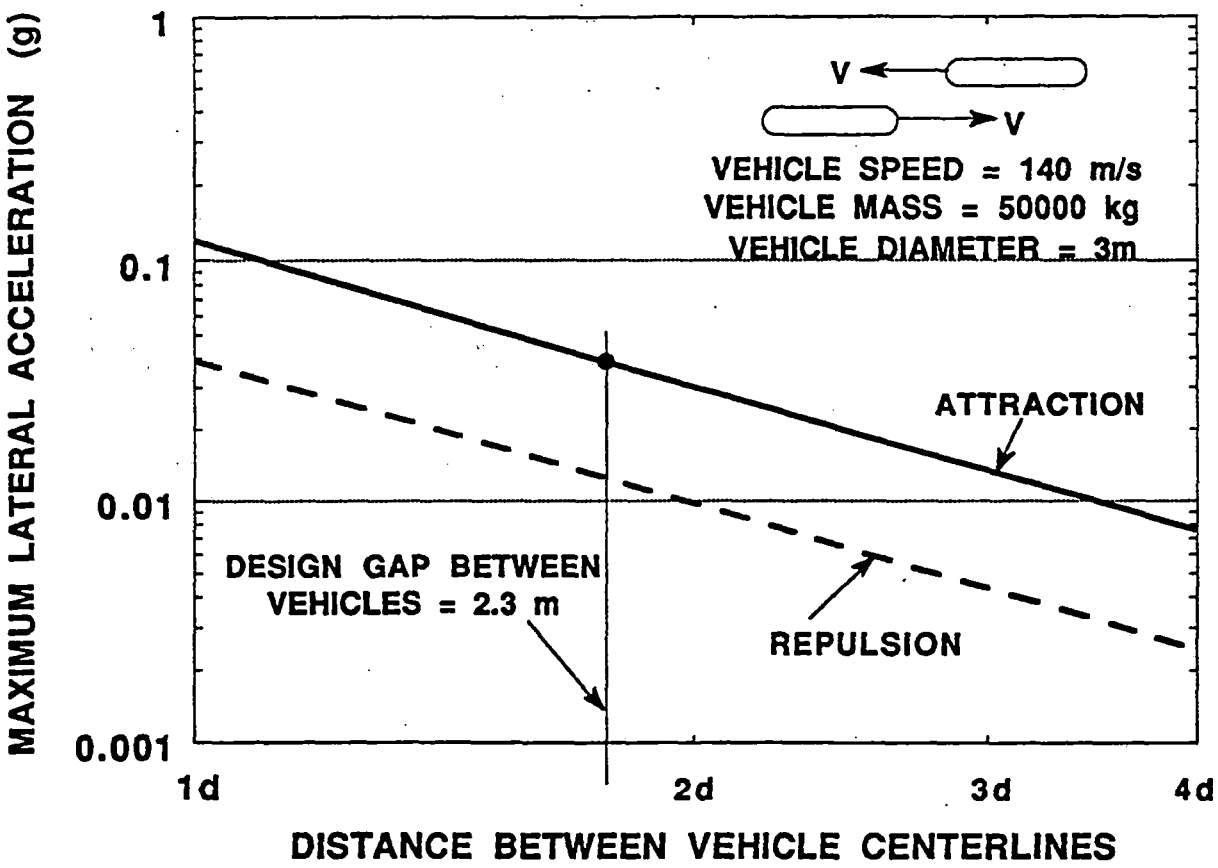

Figure 37 Maximum lateral acceleration during vehicle passing

3.2.3.d. PROJECTED ENVIRONMENTAL IMPACT

For the projected environmental impact, see the Preliminary Environmental Report, section 5.3.8.

3.2.3.e OTHER USERS OF ROW

This section discusses the methods used for allowing a highway and a magway to share a right-of-way. Detailed environmental impact information is found in the environmental report, section 5.3.8.

3.2.3.e.1. VISUAL IMPACT

There are many locations where highways are in close proximity to other transportation corridors. For example, Amtrak trains follow the Massachusetts Turnpike from Boston to Route 128, and airplanes landing in Portland and Brunswick Naval Air Station in Maine cross Route 95 at altitudes below 30 metres (100 ft). Warning signs which say "Low Flying Aircraft" have sufficed to prevent panic reaction among motorists.

Magplanes will travel faster and closer to automobiles, but there is no reason to expect that highway users will have difficulty getting used to this effect, particularly when magplanes become commonplace.

In the normal situation where magways are elevated directly above the median or the shoulder, the magway trough itself will screen view of vehicles from motorists below. The trough will also deflect the bow wave upward.

In the exceptional cases where magways are on-grade and 5 metres or less from the roadway, the magway will be fenced. The fencing should be opaque, or some visual screening will be provided in the form of shrubbery. Greenbriar would serve a dual purpose by preventing access as well as visual impact.

3.2.3.e.2. PHYSICAL IMPACT

To protect magway pylons from impact by trucks heavy enough to inflict structural damage, deflecting rail-barriers or sufficiently massive energy-absorbers will have to be provided, such as sand-filled containers screened by shrubbery, or large trees where space permits. In the exceptional locations where space is insufficient, the footings themselves will have to be extended high enough above grade and made sufficiently massive to withstand a worst-case impact.

3.2.3.f. COST SENSITIVITY ANALYSIS

3.2.3.f.1. APPROACH TO COST SENSITIVITY

Cost-sensitivity is largely a non-issue.

All previous studies of maglev economics, (Argonne, Charles River Associates, Parsons Brinkerhoff, Booze Allen, ICF Kaiser, etc), all based on Transrapid data, have concluded that maglev is not economically viable, with very few possible exceptions. This has caused maglev to be viewed as a luxury toy similar to the supersonic transport, a prestige technology dependent on perpetual government subsidy which it does not merit. In the words of Sam Skinner, former Secretary of Transportation: "...aside from being too expensive, a 300 mph railroad can't stop often enough to be useful!"

In a frantic effort to counter these condemnations, the NMI community has focused inordinate attention on "cost sensitivity" and tried to prove that cost, mostly magway cost, can be reduced substantially below Transrapid's exorbitant figure.

This effort is grossly misplaced!

A Transrapid type maglev will be an economic failure no matter how cheap its magway, and a Magneplane type maglev will be an economic success no matter how expensive its magway.

Success, in other words, depends far more on performance than it depends on cost.

A Transrapid type maglev can transport only 5,000 passengers/hour, half as many as a single highway lane. In addition, it can only compete with end-to-end services, air and rail, which handle less than ten percent of most corridor traffic.

A Magneplane type maglev can transport up to 25,000/hour, as well as priority freight. In addition, it can win a substantial fraction of the automobile passengers, which constitute more than 90 percent of most corridor traffic.

For this capacity to be used it will of course be necessary to provide intermodal connections. Private industry will soon provide connecting services when demand for them develops. Connections like Personal Rapid Transit (Taxi-2000) where density is high enough, minibus service where density is too low, and self-rental cars (public electrocars) where density is lower yet, as in rural areas. None of these services require new technology or government subsidy.

In other words: when 300 mph transportation is accessible at major malls, it will be used as certainly as the xerox machine was used. The cost of $40,000 (as compared to $400 for a Kodak copier) did not relegate the xerox machine to the status of a luxury toy! Nor did the cost of a Boeing 747.

3.2.3.f.2. CAPITAL AND OPERATING COST SENSITIVITY

The following ultra-conservative projections confirm the above assertion. Figure 38 shows the top-level breakdown of capital and operating expenses for the Magneplane baseline 160 km straight route carrying 4,000 seats per hour each way, 18 hours per day, 365 days/year. The source of the costs is given in detail in section 5.3.11. The figure shows the percentage of total cost for each cost component. So, for example, the figure shows that the cost of energy for propulsion accounts for 65.5% of the total annual operating costs.

Figure 39 shows the total annual expenses for capital and operations, assuming a levelized capital cost at 10.09% per year, as explained in section 5.3.11.4. Figure 40 (top) shows the annual expense breakdown graphically.

3.2.3.f.3. REVENUE POTENTIAL

Magneplane's potential for high revenue minimizes sensitivity to all costs. At the bottom of Figure 39, a possible budget scenario is given.

The Tampa Bay to Orlando corridor is about 150 km long, which happens to be approximately the same length as Magneplane's baseline straight route (160 km). It contains twelve population centers and two airports, which a Magneplane system could serve with off-line spurs. The corridor is presently served by a railroad (CVX), two airlines (Delta and US Air), a bus line, and an interstate highway (I-4) having between four and eight lanes. The highway carries a very high density of commuting traffic, particularly at its two terminal regions. It is also one of Florida's main tourist routes.

A study done by ICF-Kaiser Engineers for the Florida DOT, based on AMTRAK, TGV and Transrapid, assumes that they can service about four of the 16 population centers. It projects a ridership equivalent to 12,000 end-to-end trips each way per day. The trip-time for Transrapid is one hour. Present one-way fares are $80 by airline coach, $50 airline supersaver with advance purchase, and $20 by bus.

Magneplane could serve all fourteen stops, not just four. Trip time is only 26 minutes between the Tampa and Orlando airports, and it could therefore connect the two airports into a single hub. Magplanes could also serve a large fraction of the commuting traffic, and carry priority freight during off-peak and night hours. In addition, Magneplane fares would be subsidized by the State because it eliminates the need for highway expansion, and construction would be subsidized by the federal government under the ISTEA Act.

Neglecting most of these benefits, and considering that Magneplane carries only 2,000 passengers per hour each way, yet operates at 4,000 seats per hour (= 72,000 per day capacity), and charges one half the airline fare, $40, without any subsidy, it would produce revenue of $1,051,200,000 per year. Figure 40 (bottom) shows the annual budget for such a scenario.

If only 1,000 passengers per hour could be attracted, this scenario would still make a substantial profit with no government subsidy.

In other words, Magneplane would be self-supporting in a worst-case scenario without government subsidy and operating at a load ratio of only one fourth, charging one half of the airline fare, and serving only end-to-end traffic, without any freight service.

The system can be upgraded to carry twenty-five times more passengers and equivalent freight per day at only a very small increase in capital and operating cost.

160 km route

ITEM	COMPONENT COST	SUBTOTAL	PERCENT OF TOTAL
CAPITAL COSTS			
1211 magway contingency	$370,012,500		11.56%
1213 magway (double elevated)	$1,480,050,000		46.22%
121 total magway		$1,850,062,500	57.78%
151 electrical contingency	$131,210,000		4.10%
152 magway electrification	$656,057,000		20.49%
153 communication and control	$48,301,000		1.51%
15 total electrical/C3		$835,568,000	26.10%
18x vehicle (each)	$25,814,000		0.81%
18 total vehicle		$516,280,000	16.12%
total capital		$3,201,910,500	100.00%
ANNUAL OPERATIONS			
211 magway maintenance	$5,000,000		5.07%
212 vehicle maintenance	$6,570,000		6.66%
21 other maintenance	$12,636,000		12.80%
21 total maintenance		$24,206,000	24.52%
221 vehicle energy	$64,650,000		65.50%
222 fixed facility energy	$590,000		0.60%
22 total energy		$65,240,000	66.10%
23 on-board operations		$5,520,000	5.59%
24 other fixed facility operations		$3,738,000	3.79%
total annual operations		$98,704,000	100.00%

Figure 38 Cost sensitivity of Magneplane system to major components

ITEM	COMPONENT COST	SUBTOTAL	PERCENT OF TOTAL
COMBINED LEVELIZED ANNUAL CAPITAL AND OPERATIONS			
1211 magway contingency	$37,334,261		8.85%
1213 magway (double elevated)	$149,337,045		35.41%
121 total magway		$186,671,306	44.26%
151 electrical contingency	$13,239,089		3.14%
152 magway electrification	$66,196,151		15.69%
153 communication and control	$4,873,571		1.16%
15 total electrical/C3		$84,308,811	19.99%
18x vehicle (each)	$2,604,633		0.62%
18 total vehicle		$52,092,652	12.35%
211 magway maintenance	$5,000,000		1.19%
212 vehicle maintenance	$6,570,000		1.56%
21 other maintenance	$12,636,000		3.00%
21 total maintenance		$24,206,000	5.74%
221 vehicle energy	$64,650,000		15.33%
222 fixed facility energy	$590,000		0.14%
22 total energy		$65,240,000	15.47%
23 on-board operations		$5,520,000	1.31%
24 other fixed facility operations		$3,738,000	0.89%
total (annual cost)		$421,776,769	100.00%
REVENUE			
tickets (4000/hr/way at $40)		$1,051,200,000	100.00%
BUDGET			
pay off capital @ 10.09%		$323,072,769	30.7%
operating expense		$98,704,000	9.4%
profit		$629,423,231	59.9%
total budget		$1,051,200,000	100.00%

Figure 39 A possible annual budget and associated cost sensitivity (percent column)

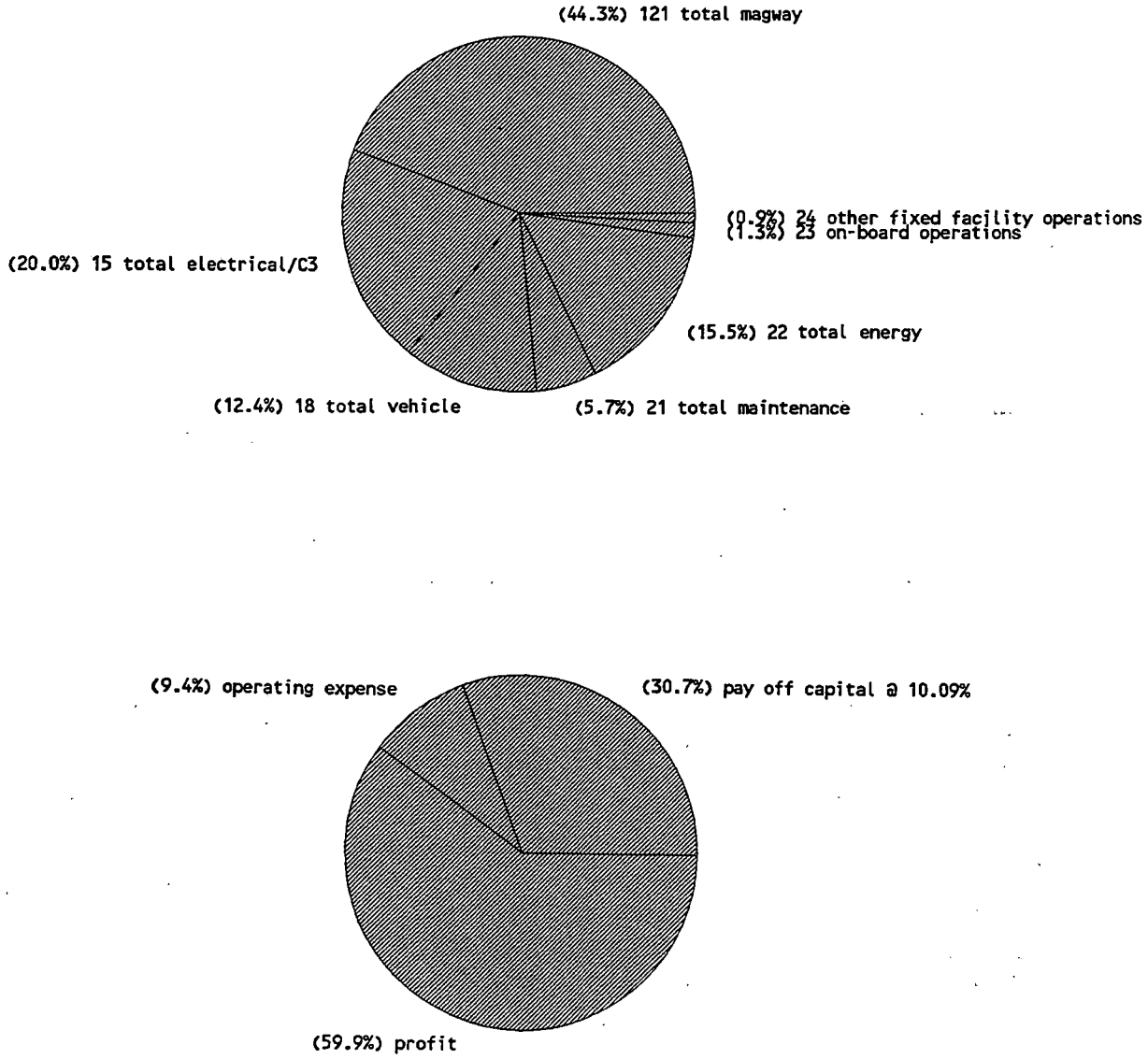

Figure 40 *top:* Annual expense pie-graph; *bottom:* Total annual budget pie-graph (according to previous figure)

3.2.3.g. POWER DISTRIBUTION AND CONTROL

3.2.3.g.1. POWER DISTRIBUTION

Power distribution from the utility system to the converter stations will depend on the geographic location of the system and the voltages and capacities of the serving utilities. For the purpose of the concept definition we have assumed that we will take power at a transmission voltage of 115 kV.

A one line diagram of the power distribution concept is shown in Figure 41. Power substations will be located periodically along the route to convert power from 115 kV to 34.5 kV for distribution to the converter stations. Each substation will include a 60 MVA oil filled transformer, high voltage and low voltage breakers, protective relaying and utility metering equipment.

Power will be delivered from the substations to the converter stations via a double circuit, 34.5 kV overhead distribution line built along the right of way parallel to the magway. The distribution line will consist of aluminum cable steel-reinforced (ACSR) conductors on 50 ft. steel poles. An overhead ground wire will be included for lightning protection.

A one line diagram for a typical converter station is shown in Figure 42. Each of the two 34.5 kV distribution line circuits will be tapped at each converter station to supply power to one half of an outdoor double ended, metal-clad switchgear lineup equipped with vacuum circuit breakers. The 34.5 kV switchgear will distribute power, through stepdown transformers, to the wayside power converters and to a low voltage substation for converter station auxiliary power requirements. On loss of one of the two 34.5 kV distribution circuits, a normally opened bus tie circuit breaker in the metal-clad switchgear will close enabling the remaining distribution circuit to supply the entire load of the converter station.

The floor plan for a typical converter station is shown in Figure 43. Each converter station includes the outdoor switchgear discussed above, 4 power converters, 4 auxiliary power converters, and 4 wayside controllers.

3.2.3.g.2. POWER CONVERTER HARDWARE

Figure 44 shows the arrangement of the equipment associated with each power converter. A circuit breaker and transformer are provided at the input and output of each converter. The output circuit breaker is the primary means of overcurrent protection. Switched compensation capacitors, or a static VAR compensator, will be used for LSM compensation. An optional bypass breaker is used to disconnect the matching transformer and series capacitor for low speed operation. A block selector switch connects the converter to one of two blocks in a leapfrogging arrangement.

Power from the output of the converters will be supplied to the magway by insulated power cables installed in cable tray. Each two km section of magway will be supplied by two 500 MCM cables per phase.

Magneplane will use GTO (Gate Turn-Off thyristor) PWM (Pulse Width Modulated) inverter technology for the LSM power conversion. A simplified schematic of a GTO PWM converter is shown in Figure 45. AC utility power is converted to dc by an input rectifier and filtered by an LC filter circuit called a dc-link. The dc is converted to ac by an inverter circuit consisting of 6 power switch devices. The switch devices are turned ON or OFF by control signals to connect the outputs to the positive or negative side of the dc link. The sequence of the control signals is used to synthesize the sinusoidal voltage waveform supplied to the output.

GTO PWM converters are commercially available in the power range needed for the Magneplane system. Efficiencies above 95% and output frequencies up to 200 Hz are standard. The arrangement of hardware in a typical converter is shown in Figure 46. The equipment uses closed-cycle water cooling and modular construction.

3.2.3.g.3. LEAPFROGGING

Magneplane uses the "leapfrog" connection for the power converters in the lower capacity system configurations. The principle is shown in Figure 47. Each converter is provided with a block selector switch connecting its output to one of two blocks. Converter 1 can be connected to blocks 1A or 1B which are separated by block 2A. When a vehicle is in block 1A converter 1 supplies power to the LSM. When the vehicle proceeds into block 2A the selector switch connects converter 1 to block 1B and begins synchronizing to match the new vehicle speed. This scheme can be used as long as the vehicles are separated by at least 3 block lengths.

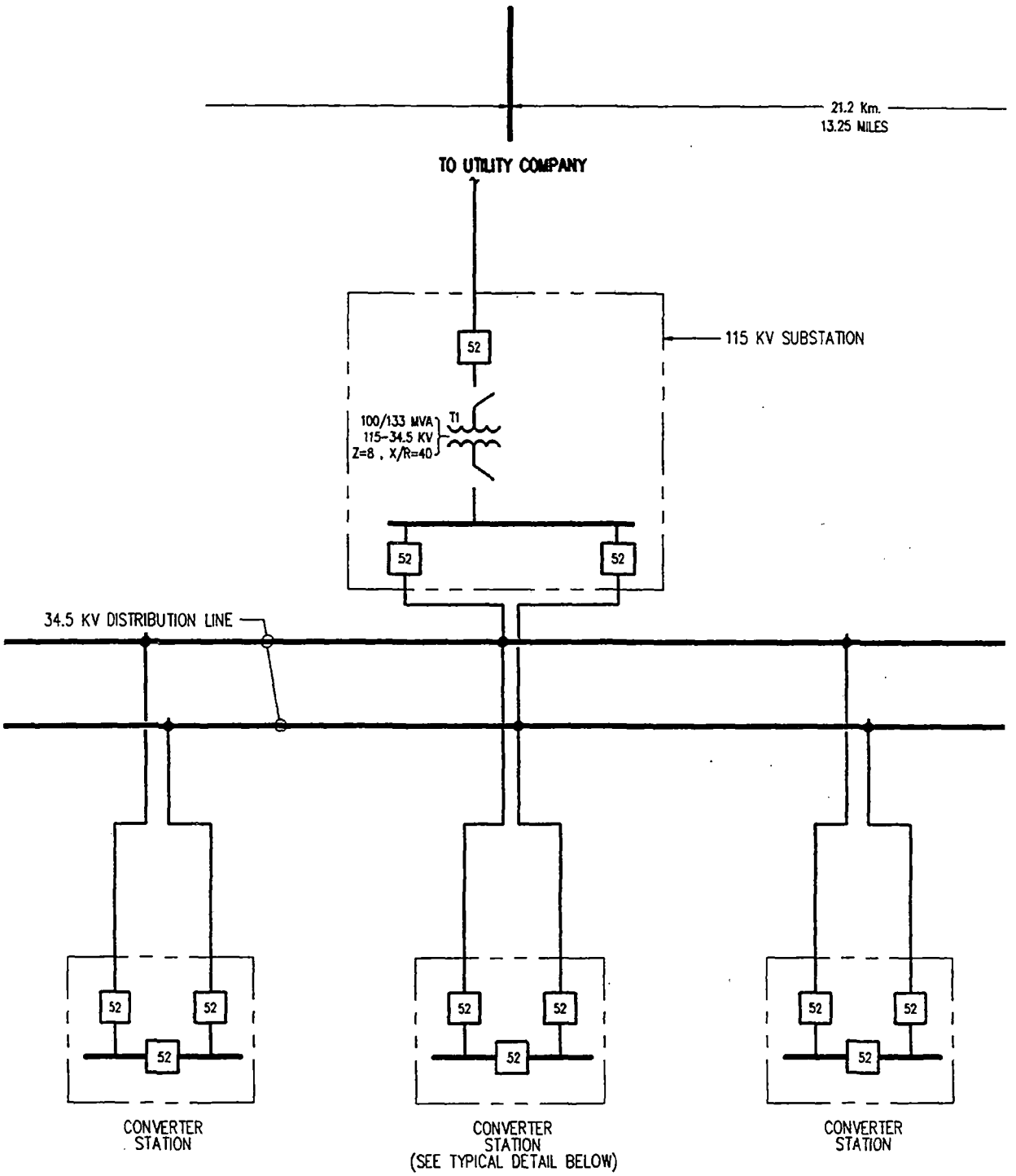

Figure 41 Power distribution one-line diagram

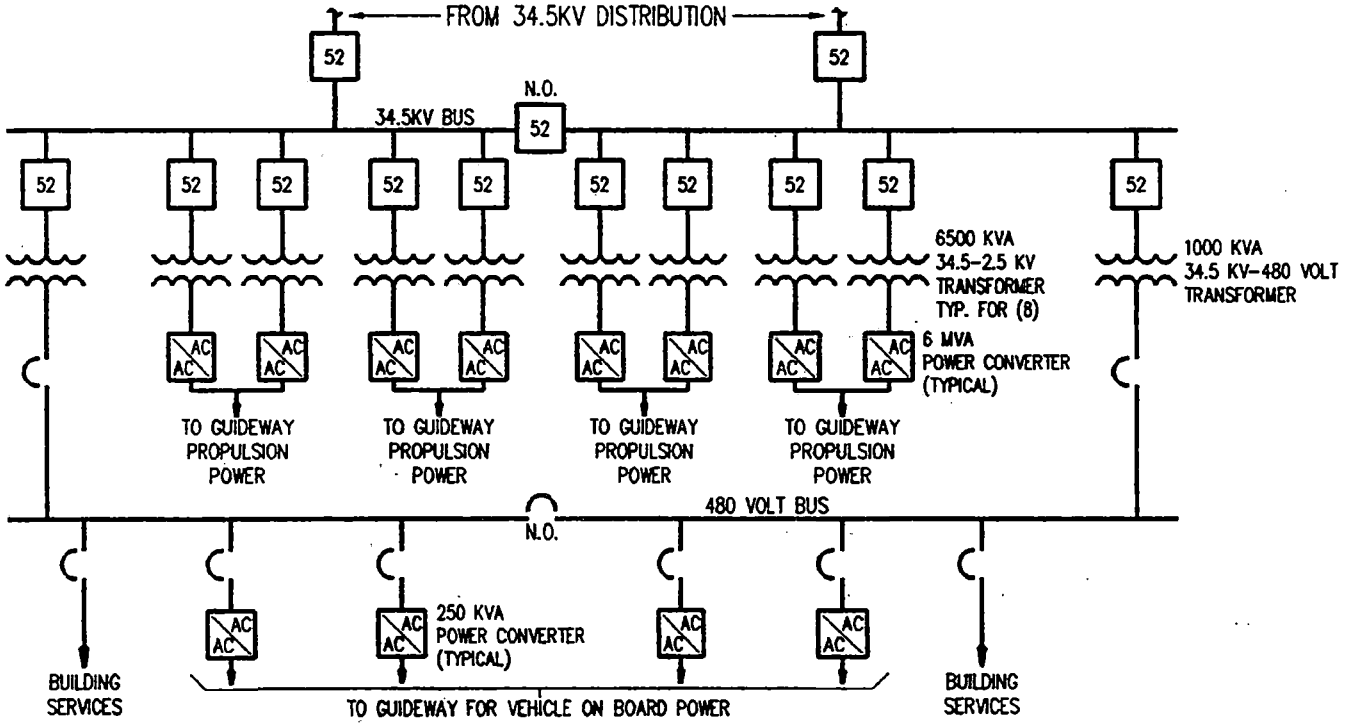

Figure 42 Converter station one-line diagram

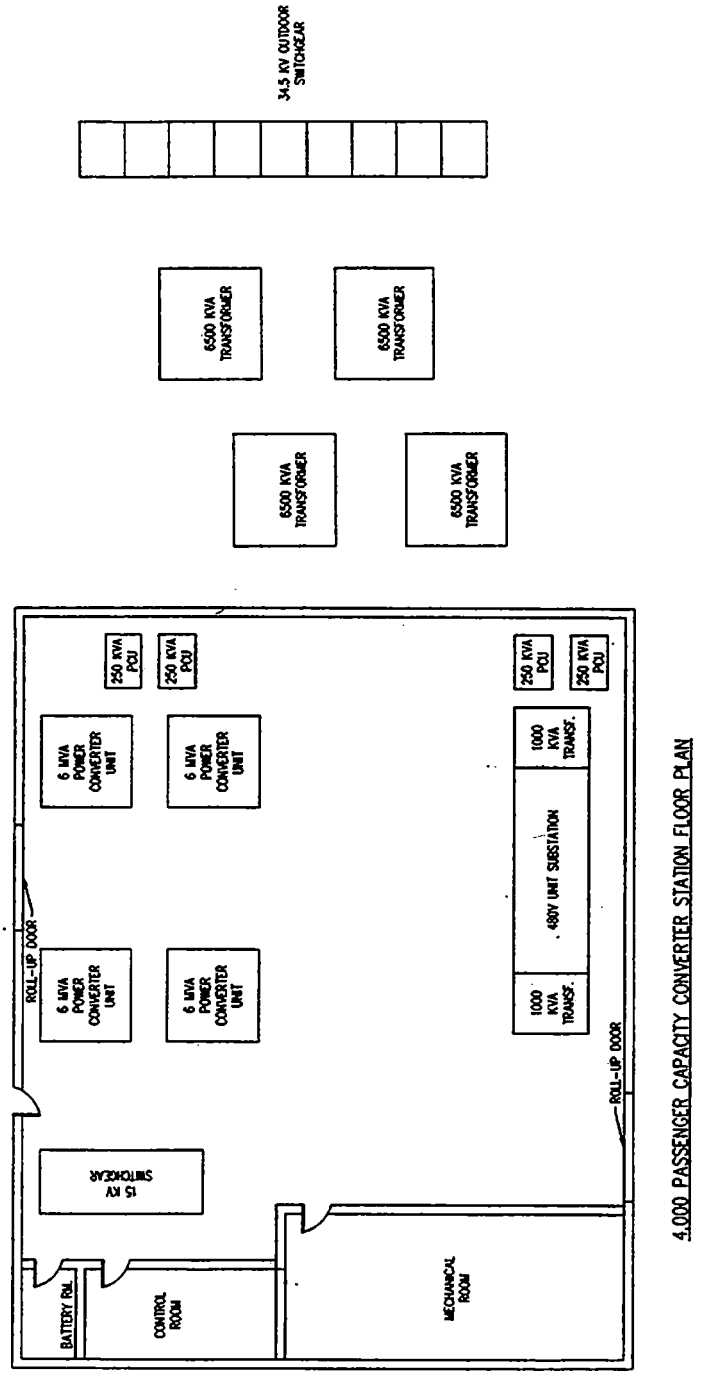

Figure 43 Converter station floor plan

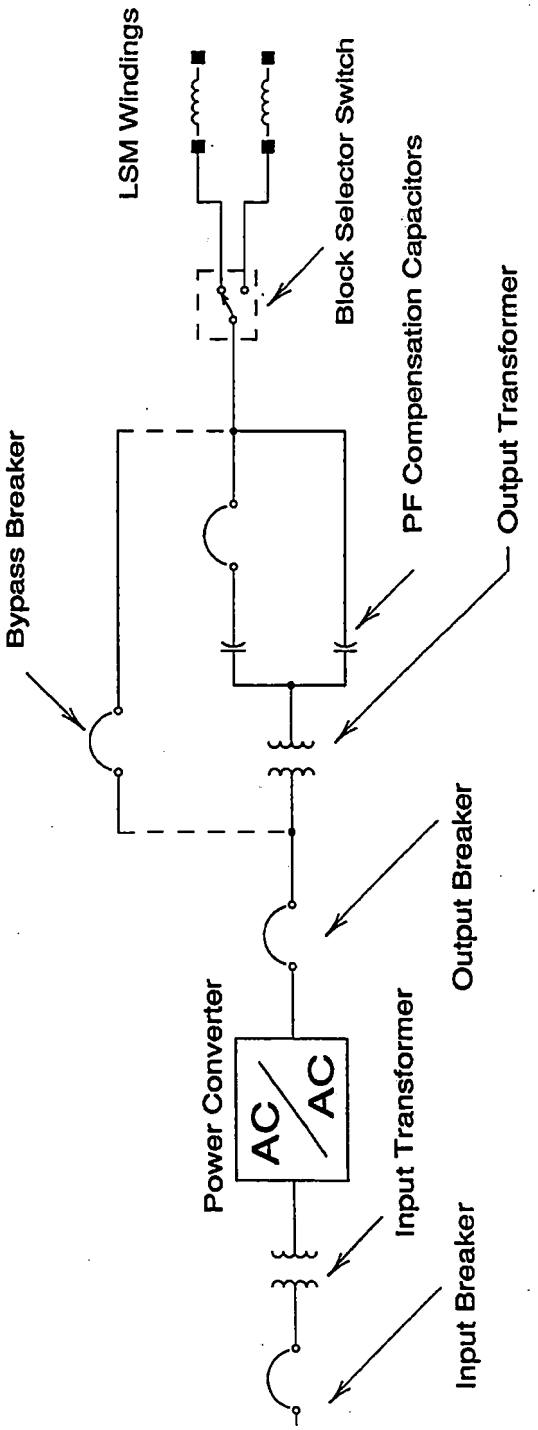

Figure 44 Diagram of power converter equipment

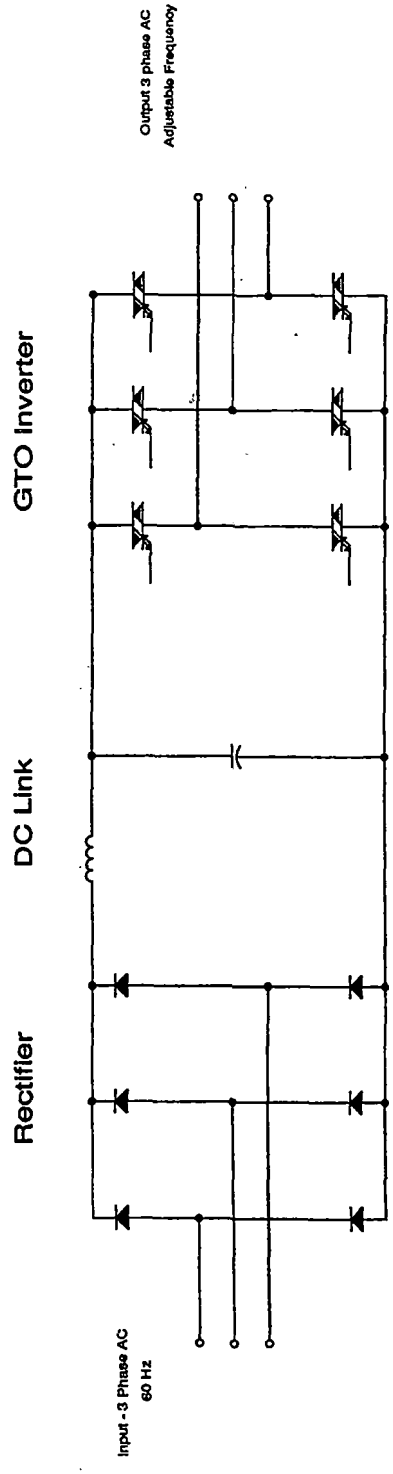

Figure 45 Simplified schematic of GTO PWM power converter

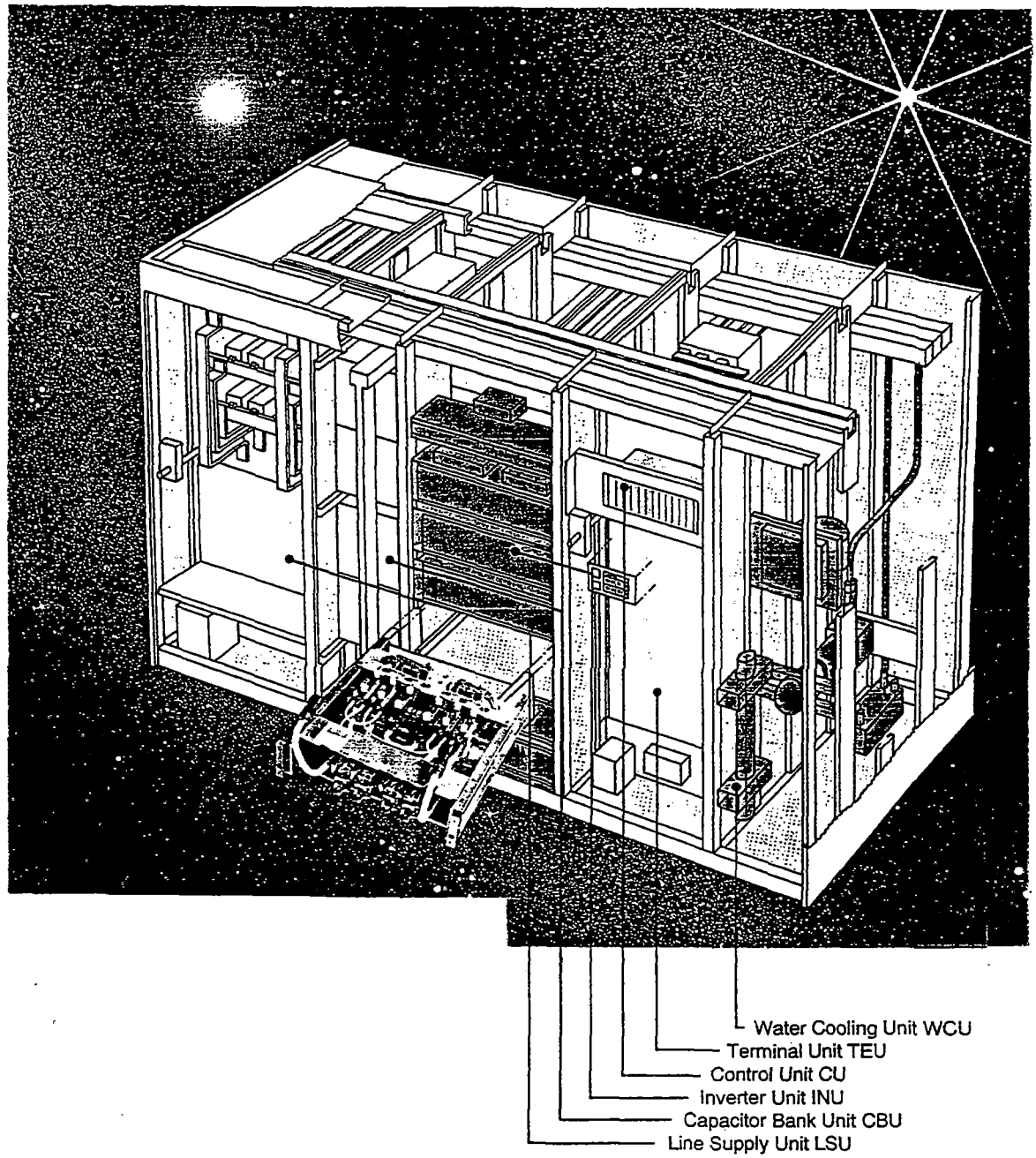

Figure 46 Power converter equipment

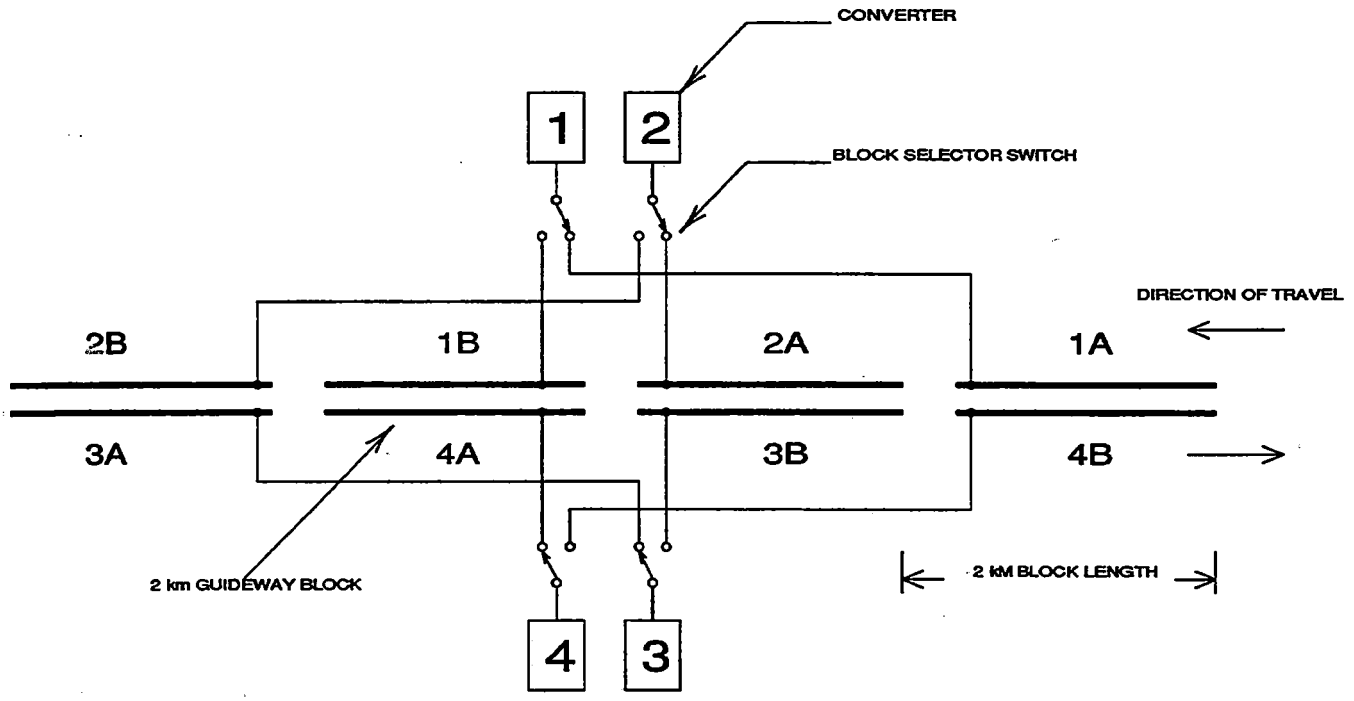

Figure 47 Leapfrog connection of power converters

3.2.3.g.4. WAYSIDE CONTROL PROCESSOR

3.2.3.g.4.1. CONTROL INTRODUCTION

The converter stations provide the propulsion power for the vehicles to the magway, and communication between vehicles occupying any one of the eight blocks driven by the converter station, and a Global center. They also provide the interface to activate turn-out switches contained in the blocks, as well as monitor the health of the block continuity sensors and position markers mounted every 11 meters on the magway.

The converter stations can have one of two configurations dependant on the system capacity required: At a system capacity of less than 12,000 seats/hour, the converter station employs a leap-frogging power drive scheme that effectively utilizes two power converters with four blocks of magway, in each direction. Active switching is used to coordinate powering the appropriate blocks of the magway as a vehicle traverses in one direction. Figure 48 depicts the eight blocks of magway driven by four power converters using the leap-frog switching strategy. At 12,000 seats/hour and higher, each block of magway has a devoted power converter as depicted in Figure 49.

When leap-frogging of the power converters is employed, vehicle spacing must exceed three blocks. This is evident from the switching process depicted in Figure 50. As can be seen from the four steps of the figure, it is not until the first vehicle has entered the fourth block that the first block can be powered, permitting a second vehicle to enter. The first vehicle must leave the fourth block, and enter a new converter station area, in sufficient time prior to the second vehicle entering the second block, so that the appropriate switching can be performed to energize the second block. The Magneplane concept of 2 km blocks and 134 m/s vehicle velocity permits this time to be 5 seconds with a minimum 20 second headway.

At the higher system capacities, when direct drive of the blocks is utilized, up to 4 vehicles can be occupying the blocks in one direction. A vehicle travelling with minimum headway from its neighbor will enter a block 5 seconds after the neighbor has cleared it.

Converter stations are located at four block intervals, nominally 8 km apart. The route design is bi-directional, that is parallel and opposing traffic magways are typically adjacent, resulting in eight blocks (four for eastward traffic and four for westward traffic) powered and controlled from one converter station. At maximum system capacity the converter station can be communicating with, and coordinating the flight of up to eight vehicles at any one time.

3.2.3.g.4.2. WAYSIDE PROCESSOR PRIMARY FUNCTIONS

The wayside control processor receives velocity commands for each of the vehicles it is controlling at a 12 Hz rate, from the Global center. These commands are transmitted to the appropriate vehicle using an RF communication link. The vehicle in turn determines what acceleration is required to match the commanded velocity. In addition, the vehicle determines what adjustment is required to the magnitude and phase of the LSM propulsion field to correct for disturbance motions detected by the on-board inertial system. The resultant processing yields time corrected frequency, magnitude and phase commands, which

are transmitted back to the control processor at a 96 Hz rate, using the same RF link. The processor instigates frequency, phase and magnitude correction of the power converter driving the propulsion winding, as commanded from the vehicle, and maintains that condition until the next command is received.

The processor also receives velocity, position and status data from each vehicle at a 12 Hz rate. The wayside processor will append to the status data and then communicate the information to the Global center.

The other responsibilities of the wayside processor include managing the power switching functions required to activate the leap-frogging scheme, as well as switching required to change the state of magway turn-outs in the jurisdiction of the converter station. In addition the processor monitors the health of distributed block continuity sensors and position markers. The block continuity sensors are located at each span interface in the magway structure, and permit detection of relative movement between the magway spans. Each span is nominally 9 meters long. The position markers are RF sources that line the magway at 11 meter intervals which communicate to a traversing vehicle, so that the vehicle can determine its position relative to the magway.

As a vehicle arrives at the boundary between two adjacent magway blocks, the LSM windings in the blocks must be synchronized in frequency, phase and magnitude to permit a smooth transition of the vehicle. In the jurisdiction of one converter station, a vehicle will traverse four blocks in one direction. All synchronization is handled internally by the Wayside control processor, insuring the magway blocks are synchronized no later than 0.3 seconds prior to a vehicle entering the new block. The synchronization between converter stations is achieved using dedicated fiber optic data links between neighboring converter stations. These links are used to transmit the vehicle drive parameters (frequency, phase and magnitude) to the neighboring converter station prior to the vehicle arriving. This permits the first block of a converter station to be synchronized with the last block of the previous. The dedicated fiber link is used to achieve a high speed interchange and avoid latency variations that are difficult to compensate for. The converter station controlling the vehicle instigates the communication to its neighbor autonomously, when the vehicle is close to the end of the fourth block. Communication is bi-directional between converter stations, as is the traffic flow.

Figure 51 depicts the data flow about the control processor.

3.2.3.g.4.3. WAYSIDE PROCESSOR SWITCH FUNCTIONS

The converter station, and consequently the attendant wayside processor may have jurisdiction of turn-offs within the eight blocks it is managing. The turn-offs are typically located at the third block of the four in one direction. The Global center is responsible for issuing a coordinated command of the state of the switch as the vehicle traverses the blocks. The default turn-off state retains the vehicle in the throughway. When commanded from the Global center, the wayside control processor instigates additional power switch functions to activate the turn-off.

A turn-off block is split into three sections, as depicted in Figure 52. The first section that precedes the turn-off is driven from one power converter. The point at which the transition of the two alternate magways commences is driven by a second power converter with a switch to direct which LSM winding

is energized. An additional null flux switch is required to activate the null flux coils that overlay the LSM winding that is activated.

Turn-offs are complemented by magway merges, which consist of an identical construction, in a mirrored image. Maintaining the symmetry permits the magway to also accommodate counter-direction traffic flow, and consequently has the same hardware and control requirements.

3.2.3.g.4.4. WAYSIDE PROCESSOR DATA MANAGEMENT

The wayside control processor evaluates the validity of all communications and particularly those that drive the power converters and power switching. The processor has knowledge of both the velocity commands issued to a particular vehicle from the Global center, and the parameter drive commands to be issued to a power converter. Consequently the processor can police the Global velocity commands to insure they are rationale, based on history, and police the responses from the vehicle to insure they are rationale and compliant with adopting the commanded velocity.

In the instance when the updated command exceeds the bounds of change determined reasonable by the wayside control processor, no modification will occur, and the discrepancy will be reported to both the Global center and vehicle, for corrective action. If the vehicle does not process and correctly command subsequent frequency, phase, and magnitude commands, the wayside control processor will continue to report the errors to the Global controller. The wayside processor will continue to ignore the vehicle command data and maintain the last valid frequency, phase and magnitude condition until the Global controller commands corrective action for the apparent loss of vehicle control. The action of the wayside processor is limited to maintaining constant conditions (velocity etc) when commands received are determined invalid, and to report the discrepancy. The Global center is always responsible for commanding and coordinating any traffic flow changes as a result of the reported discrepancy. If the vehicle does not receive valid data for a number of consecutive cycles, it will autonomously initiate a coordinated stop. Knowledge that any vehicle will adopt this action if the communication fails, permits the Global center to take appropriate action when it determines that the number of permitted consecutive command failures has been exceeded.

3.2.3.g.4.5. WAYSIDE CONTROL PROCESSOR CAPACITY

Figure 53 depicts the control processor interfaces for a typical converter station. This configuration employs leap-frogging (designed for a system capacity less than 12,000 seats/hour), and has turn-offs situated at the third block in each direction. The communication to the vehicles, Global center and neighboring wayside controllers is included. It should be noted that there are at least three neighboring converter stations to this configuration, as the turn-off function proceeds into the jurisdiction of a separate converter station to either the east or west bound throughways.

Figure 55 summarizes the interfaces required of a wayside control processor.

3.2.3.g.4.6. WAYSIDE CONTROL PROCESSOR HARDWARE

The hardware for a wayside control processor is depicted in Figure 54, showing interfaces and internal functional areas. The processing is centered about a dual configuration, primarily for system safety considerations. The failure of a wayside controller can result in loss of communication with up to 4

closely spaced vehicles in each of two directions, loss of synchronization between LSM windings for vehicles transitioning blocks and failure to coordinate the switching required to permit traffic turn-outs. The control of the LSM propulsion drive power converters is critical to vehicle safety. Fault tolerance of the operating software will mitigate the possibility of irrational commands being issued to a power converter, and the second (shadow) processor permits an additional command verification capability. Failure of one element of the configuration will not degrade the performance. Detection of the failure will permit the Global center to be notified that a service is required at the converter station without closing down the (serial) system. This topology is consistent with the vehicle configuration, described in section 3.2.1.k.

A central (VME structured) bus is used for all data handling by the two processors. Internal optical interfaces are used to drive critical hardware, providing a high degree of isolation so that there is no risk of the dual system being disabled by one half failing.

The controller incorporates two single board computers (SBC) that share the VME Bus and on-board memory. One SBC performs all mission functions. These functions include maintaining communications with the Global Center, with the vehicle, and with other wayside control processors. The second SBC performs health monitoring functions of the processor, ensures that the Global center continuously has up-to-date data; control data and well as health/status data. A major function of the secondary SBC is to maintain capability to take over the primary functions in case of a primary SBC failure.

The SBC includes 4 MB of shared dynamic RAM, arbitrates the VME bus, interfaces with the Global center via the FDDI controllers operating as Dual Attachment Stations (DAS), interfaces with up to eight vehicles via the RF transceivers, interfaces with the position markers and block continuity sensing sensors, interfaces with the power converters, interfaces with the turn-out and leap-frogging switch drives, and interfaces with other wayside control processors. In the event of a processor failure the second SBC assumes the processing responsibilities of the first processor.

Both SBCs periodically issue keep-alive messages to each other via shared memory indicating the current status as each sees it. In addition to detecting faults within the SBCs, both processors also continuously perform background tests to verify the health and status of all interfaces. It is important to test periodically all key features of the system. This allows test software to detect faults in rarely used areas of the system and allows these faults to be detected by test software rather than during critical system operation.

In the event that a failure in a SBC is detected, the failed SBC is disabled. By itself if it has detected the failure, or by the second SBC if it detected the failure first. In either case, the failed SBC is held reset so that it can no longer take part in the system and the other SBC performs the primary functions, as well as notifying the Global center that a failure has occurred.

Commands and data are received from the Global center via the FDDI communications loop. Both FDDI interfaces are active in the control processor, with the primary processor interrogating one, and the shadow processor interrogating the second, and validating the received data. Communication over these links is bi-directional, with the vehicle (and wayside appended) data returned via the primary FDDI interface (with fall back to the shadow if required). The communications medium is single mode fiber, required to communicate across the 8 km distances between neighboring converter stations.

The hardware used to interface to the FDDI is of the same design in the processor as in the Global center. The FDDI interface is composed of an FDDI controller module and optical bypass switches. The bypass switches allow a processor to be optically bypassed if it loses power or it detects an internal failure that could compromise the data on the bus. Failure of a processor interface on the network does not degrade the networks's performance as each processor has a second independent interface. Failure of a link between converter stations will cause the dual ring to be reconfigured to a single ring that loops back just before the failed link. All interfaces would still be accessible on the ring.

Dedicated communication between the neighboring converter stations employs a low-latency (less than 50 microseconds) communication path. This is used to communicate the power converter frequency, phase, and magnitude parameters from one processor to the next, as a vehicle transitions between a block controlled by one processor to a block controlled by the second. Dedicated communication for up to three neighbors is provided by the configuration. Separate point-to-point fiber interfaces are used to enable messages to be transferred within 50 microseconds. This will ensure a smooth vehicle transition between guideway blocks of adjacent converter stations.

Each processor maintains continual RF communications with each vehicle within the blocks controlled by the converter station. RF communication between the processor and vehicles is performed using packet switching. The processor can communicate with up to eight vehicles, one for every block under jurisdiction. Two independent RF transceivers are used. Normally, the primary channel is active and the secondary channel is passive. The secondary channel is connected to the secondary SBC and provides capability to monitor the primary channel by continuously being in receive mode. The secondary channel compares the received data from the primary transceiver with the data it would transmit if it were active and assesses the health of the primary channel. If the primary channel fails the secondary will be commanded to become active and take over communications control.

Although many converter stations may not have a magway turn-off within its jurisdiction, each wayside control processor has designed-in provisions for interfacing with up to two turn-off and two null flux switch drives. This approach insures a consistent configuration which minimizes logistics costs by reducing the number of types of designs and spares required. This strategy is also employed to provide interfaces for up to ten power converters and four leap-frog switch drives, permitting changes in system capacity to have minimal impact on the processor configuration.

The position marker interfaces are used to verify the health of the RF transmitters distributed along the magway. Over 1600 position markers are distributed along the magway controlled from one converter station. To minimize the interface overhead, markers status lines are serially connected within each block. 181 markers are distributed in one 2 km block and each marker has a unique digital signature which is transmitted along with its status at regular intervals to its neighbor. The neighbor appends is own status and signature and re-transmits the data forward. If a marker fails, the data stream is passively transmitted through that marker via internal default switching, hence its signature and status are not appended to the message. The wayside control processor receives eight channels of data streams reporting the health of the markers by block. Any marker that reports a problem via the status word is logged, as is any marker signature that is determined to be missing. The logged failures are reported back to the Global center across the FDDI interface, for appropriate service action to be instigated. The position markers are used by the vehicle, primarily for stabilization. They are spaced so that a passing vehicle can miss one marker without degrading performance, and miss two adjacent markers with minimal

impact on ride comfort. If multiple position marker failures are reported to the Global center, it may become necessary to modify traffic flow and routing accordingly to accommodate the problem.

Block continuity sensors are located at each span interface of each magway, to determine the static alignment integrity of the span interface. If a permanent shift is measured in alignment an alarm is triggered in the sensor. A similar scheme to monitoring the position markers is used for the 2000 block continuity sensors, reducing the interface overhead to analyzing eight channels of nominally 222 serial signatured messages.

Control interfaces are required to enable the wayside control processor to reliably command the frequency, phase, and magnitude of the (up to 10) power converters at one converter station. Two redundant fiber optic interfaces are used for this function, and each interface is driven by one of the two SBCs. The shadow SBC will not initiate commands unless it has determined that the primary SBC is at fault, where by it will take over the function of controlling the converters.

A maintenance interface permits external diagnostic tools to be used to evaluate the health of the wayside control processor. This interfaces directly into the VME bus, to provide access to both SBCs. The SBCs also provide interfaces to voice channels for communication during maintenance back to the Global Center.

In the event of a Global Center failure, it is desirable to have access to the FDDI link at a converter station, so that (minimal) computer facilities can be bought on-line to control the traffic. This is particularly significant for a single Global center configuration, where neighboring centers are not available to pick-up the traffic flow. This access is provided via the VME bus, to the FDDI interfaces so that limited traffic control is viable from the remote sight. The actual Global emulator would be installed at the location, only when required. Access to the FDDI link at any converter station by this means also insures continued communication is possible even when the FDDI link is broken at a number of locations simultaneously.

The uninterruptable power supply (UPS) is a solid-state on-line system designed to provide high-quality, continuously-filtered and conditioned ac power to the critical loads. The back-up battery system is sized to supply a full load for 30 minutes. Should the utility power fail, the battery system powers the control processor for enough time to insure that all vehicle stock is safely coordinated, and provides a continued communication path between the vehicles and the Global center.

The wayside control processor electronics is housed in a temperature controlled area of the converter station. The environment is maintained to insure maximum reliability of the hardware. The hardware is rack mounted, providing easy access, and serviceability. The electronic control modules are commercial-of-the-shelf items with a standard form-factor. They are modular and connectorized to minimize the use of tooling to perform maintenance and repairs.

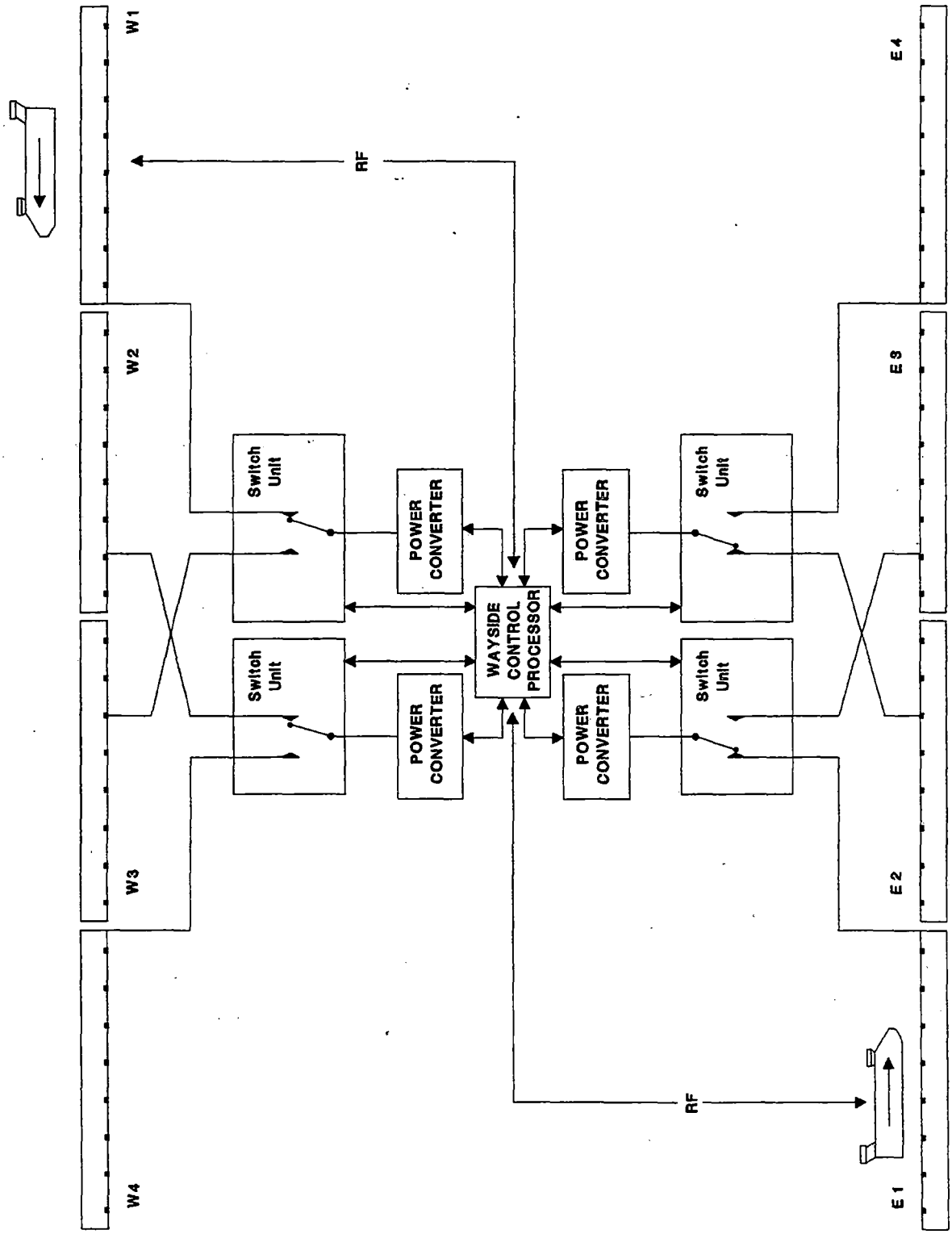

Figure 48 Leap-frog Power Converter Configuration (2 vehicles traversing)

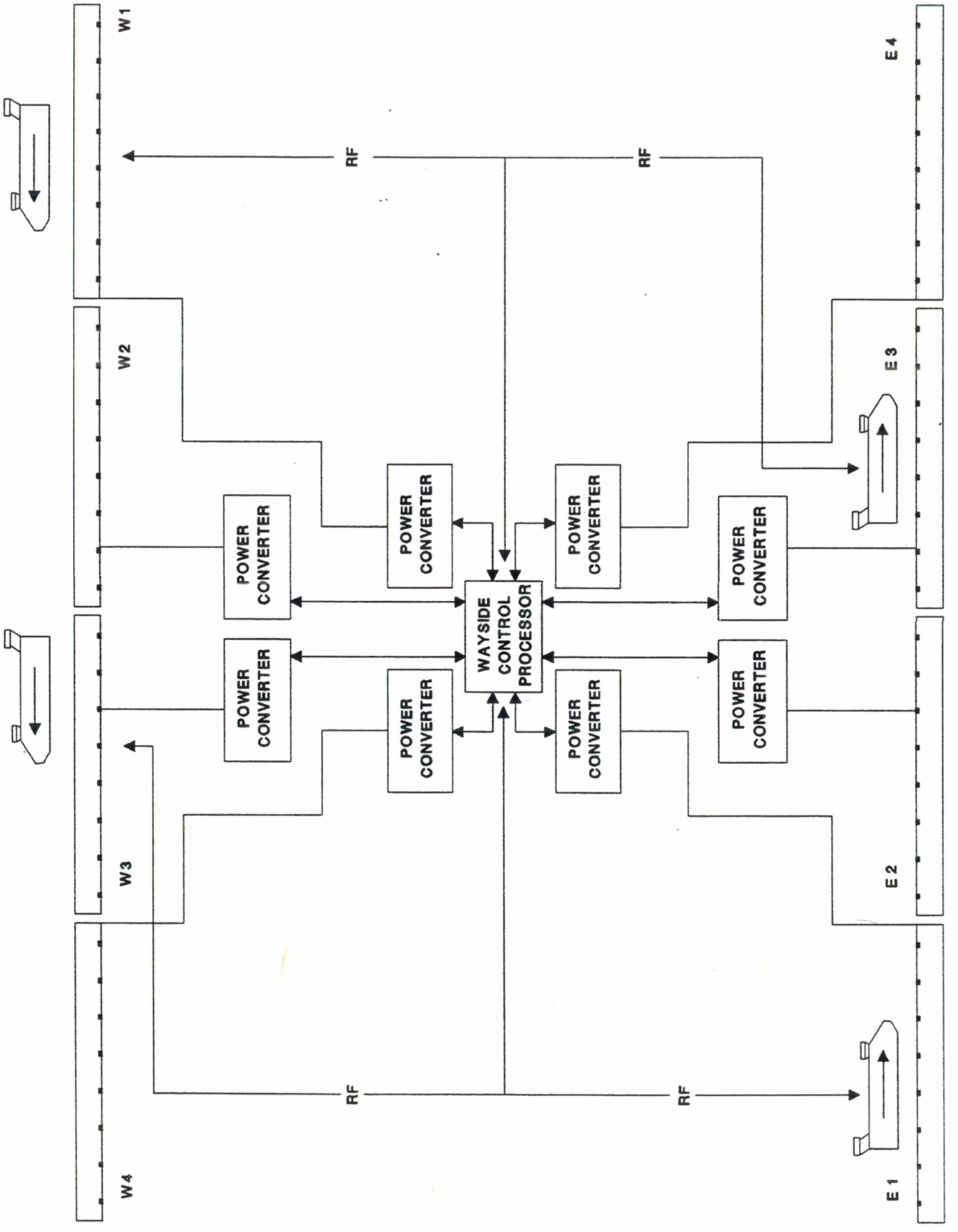

Figure 49 Direct Drive Power Converter Configuration (4 vehicles traversing)

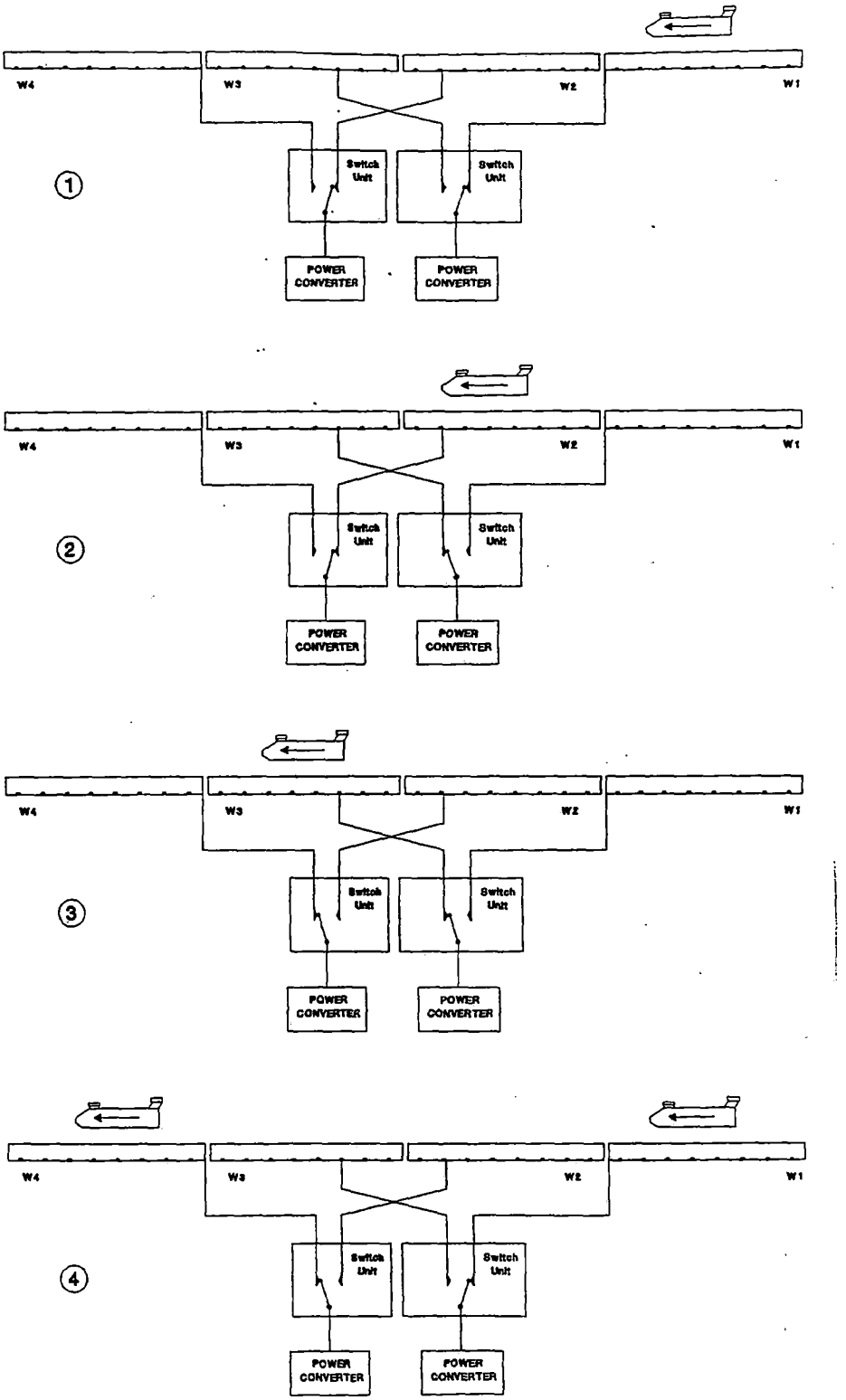

Figure 50 The leap-frogging power converter switching process

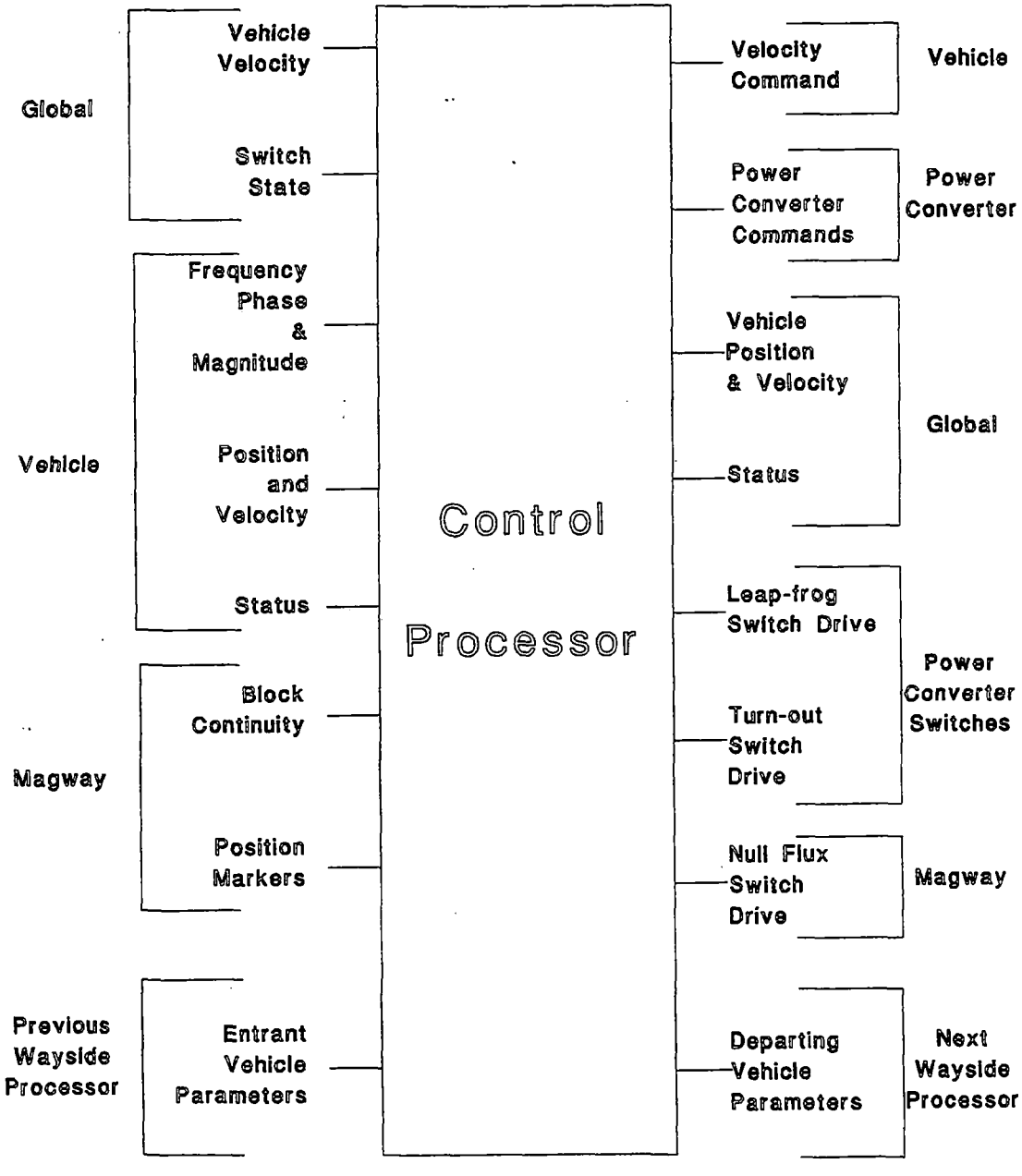

Figure 51 Wayside Control Processor Data Functions

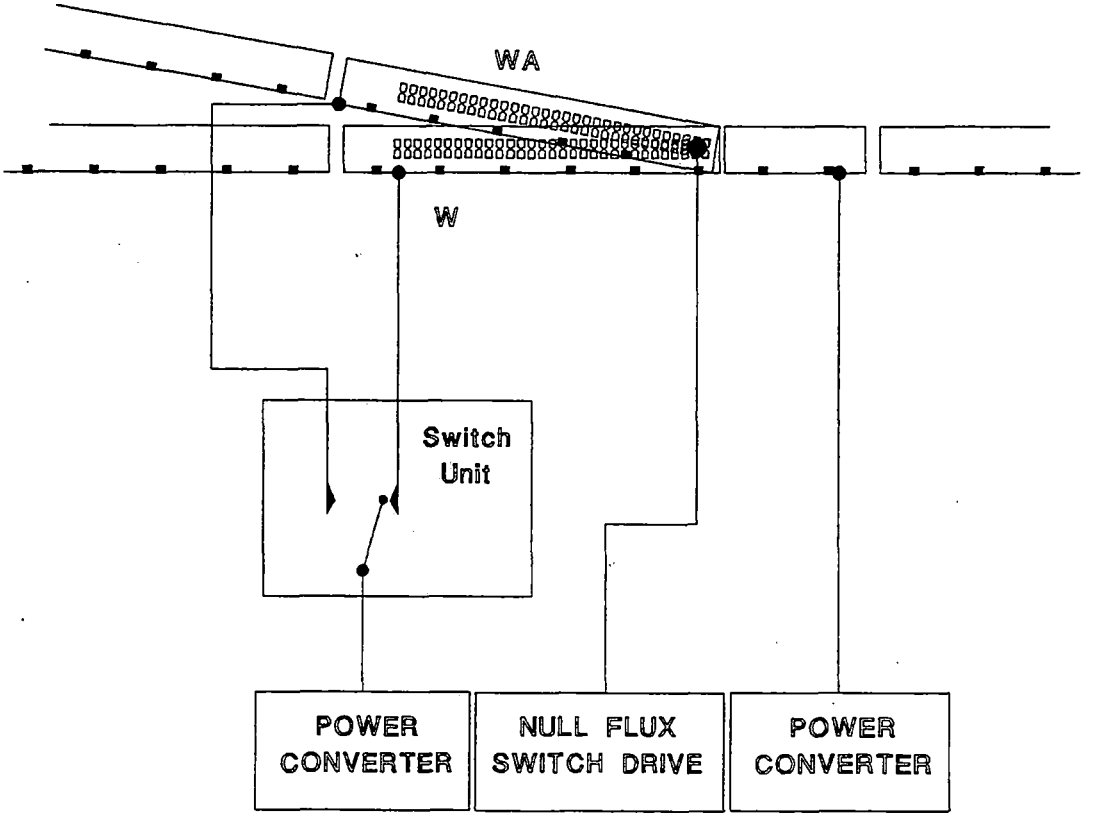

Figure 52 Turn-off Hardware Configuration

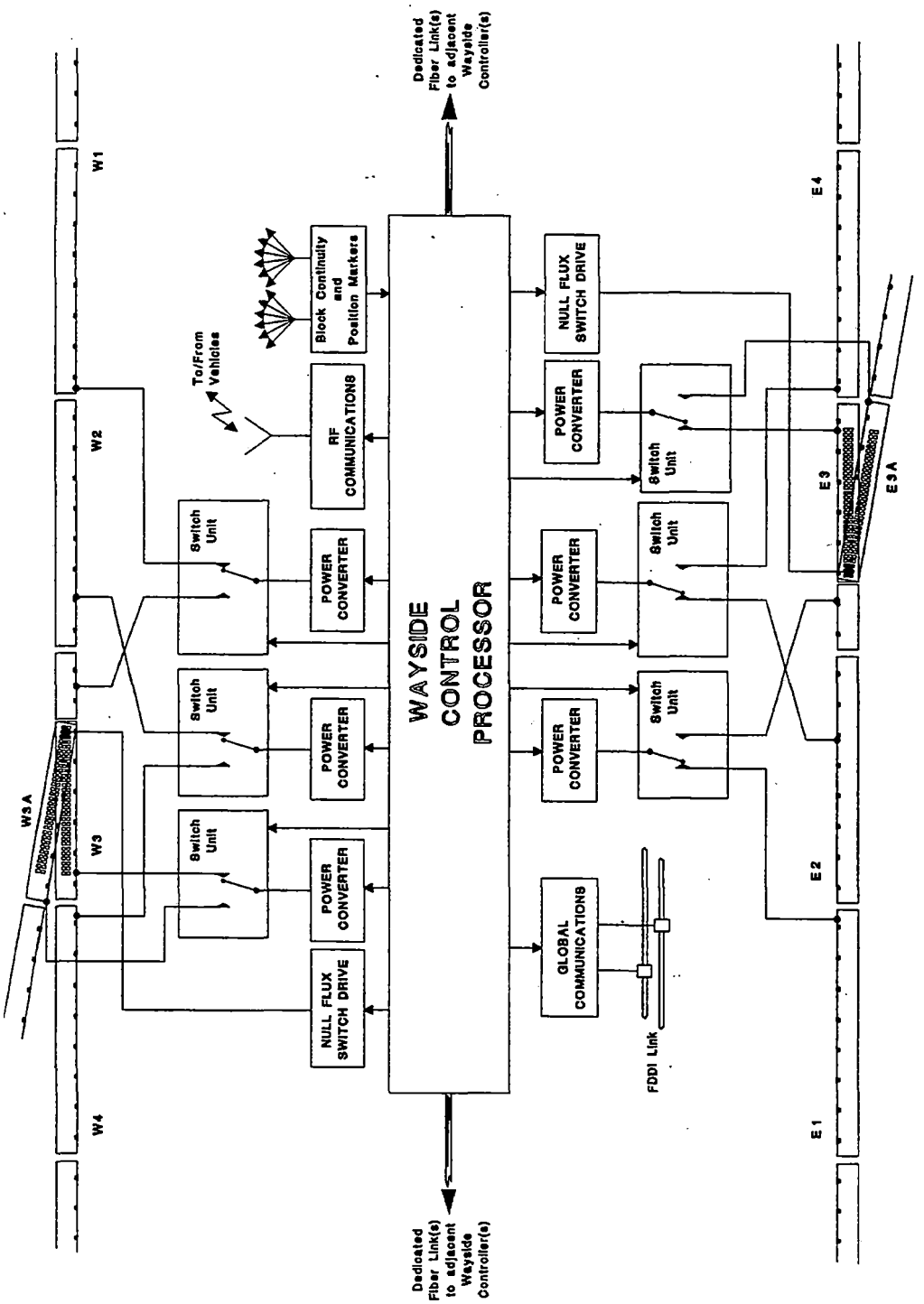

Figure 53 Typical control processor configuration

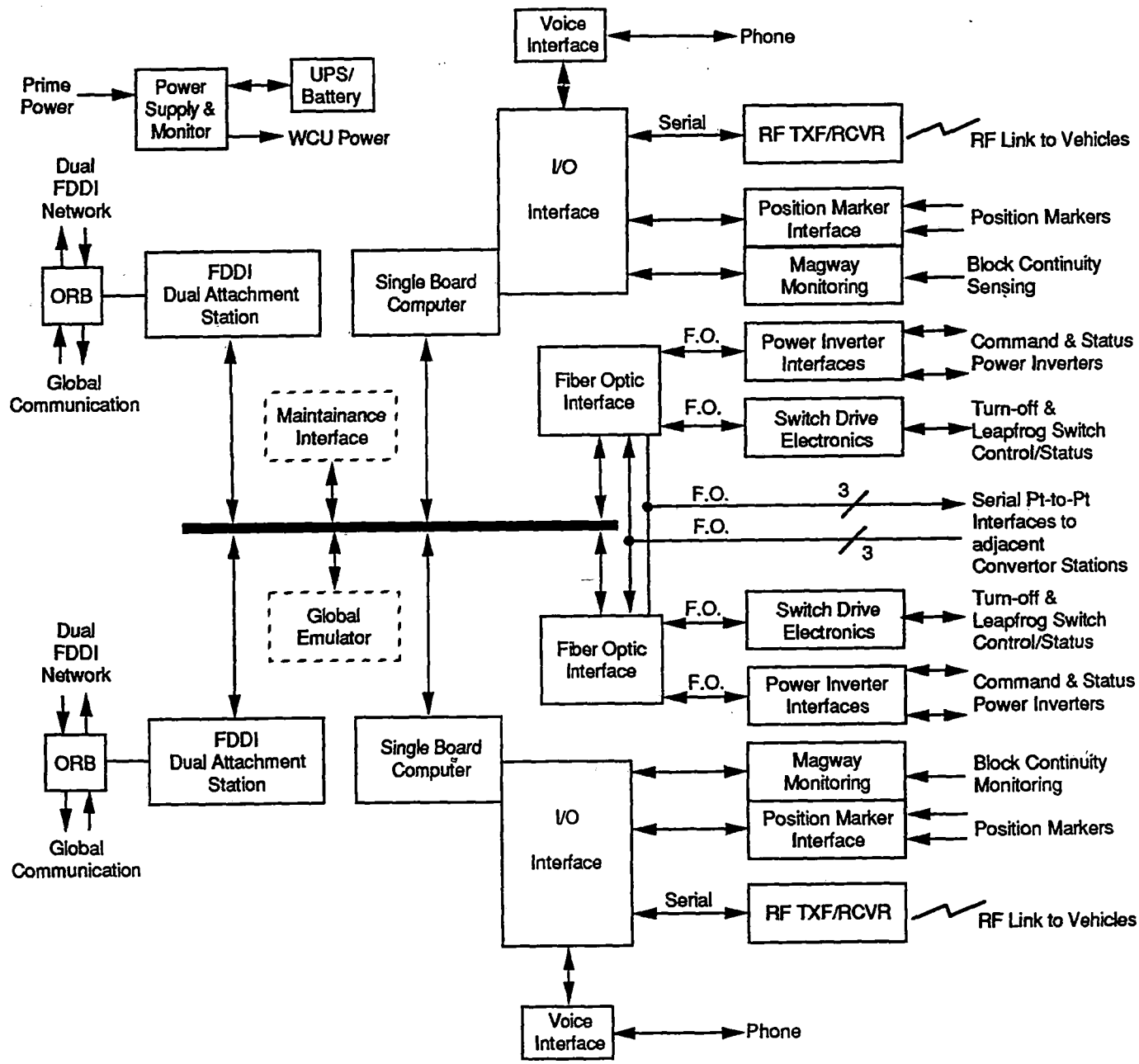

Figure 54 Wayside Control Processor Hardware

Function	Quantity	Comments
Control Processor	1	
Power Converters	4 to 10	Dependant on system capacity and if turn-offs are required.
Leap-frog switches	0 or 4	Dependant on system capacity.
Turn-off switches	0 to 2	If turn-offs are required.
Null flux switch drive	0 to 2	If turn-offs are required.
Global Communications	1	Dual FDDI loop
Wayside Communications	1 to 3	Dependant on location and if turn-offs are required.
RF Communications	1	One RF system services up to eight vehicles.
Block Continuity Sensors	8	Typically 222 serially connected sensors in each block.
Position Markers	8	Typically 181 serially connected sensors in each block.

Figure 55 Wayside control processor required interfaces

3.2.3.h. RELIABILITY/ AVAILABILITY/MAINTAINABILITY (RAM)

3.2.3.h.1. INTRODUCTION

RAM features have been incorporated into the system concept definition study in order to enhance system readiness and to provide a cost effective solution for the MAGLEV System. RAM analysis has been performed on design candidates to provide a measure of operational effectiveness for each and to establish a means for controlling system support costs. Operational Availability allocations have been levied against all major system components. These allocations are based on achievable equipment reliability and maintainability parameter values for the concept design configuration.

The high degree of fault tolerance built into the design has enhanced system operational availability. The result of this - in addition to providing the desired safety features - will be a potentially higher utilization of system services. The implementation of fault tolerance employs the use of functional redundancy or operation of equipment in an acceptable casualty mode. The method of approach for RAM assessment in considering the impact of system fault tolerance provisions on Availability is discussed below.

3.2.3.h.2. RELIABILITY/AVAILABILITY DEFINITION

For the MAGLEV Program, reliability can be considered as the probability that the system, defined below, is performing all critical functions without interruption due to a malfunction of equipment hardware or software. An additional consideration is that of malfunctions caused by human error. This probability is evaluated by modeling the states that MAGLEV equipment can experience any time during its mission. For MAGLEV the set of states include equipment casualty mode which are not system failure modes as a result of the fault tolerant architecture designed into the system.

The reliability parameter used in this concept phase is the equipment hardware or software failure rate. Its value is based on an accumulation of data collected on similar equipments over a period of time.

Availability is considered in a similar fashion as reliability. The appropriate state space is evaluated to determine the percent of time the MAGLEV System is operational. Considered time includes the time that the system is operational, down time for repairs or down time awaiting for repair resources to arrive at the repair site.

Figure 56 illustrates a state space, transitions between states and the general process for evaluating availability. The system depicted, much simplified for this example, is a fault tolerant computer composed of redundant CPU's.

STATE SPACE DEFINITION:

State 1 all equipment operating
State 2 one CPU failed - failure detected and repair action immediately begun
State 3 system failed

In performing an availability assessment, the following conditions are presumed:

- maintenance personnel have had adequate training and are qualified to perform repairs and preventive maintenance on the equipment being analyzed.

- spares and support test equipment are available at the designated supply point

As shown in the example, the availability parameters include the equipment failure rate and the equipment mean down time, which accounts for both active repair time and logistics delay time. The result of the analysis is the calculation of operational availability which, for the example above, is the probability of being in state 1 or state 2.

3.2.3.h.3. ANALYSIS APPROACH

A comprehensive procedure was implemented in performing the RAM analysis for MAGLEV which included the following steps:

- Determine RAM requirements and constraints
- Review system/equipment design characteristics
- Develop definition of system failure
- Develop system block diagram showing equipment functional dependencies
- Develop reliability/availability state space/ models for each major equipment
- Generate equipment failure rates/repair rates based on data from similar equipments
- Exercise RAM models to determine conformance to requirements and to trade off design options
- Use results to allocate acceptable RAM parameter values to equipment
- Revise allocations as design evolves

This procedure was implemented for the hardware design. Software reliability allocations were established based on the following process:

Step 1

Initially, we develop HW reliability model, predictions, and allocations such that specification requirements are satisfied with some margin to spare.

Step 2

Then, the difference between the HW reliability prediction/allocation and the specification requirements is allocated to SW.

Step 3

After the SW allocation is determined, a prediction value and test period is sought to support the allocation. Steps 1, 2, and 3 are repeated until a satisfactory HW/SW allocation is achieved.

SOFTWARE RELIABILITY PARAMETER ESTIMATION:

$$\text{Fault Density} = \frac{\text{Number of S/W problems reported}}{\text{Number of executable source lines of code}}$$

$$\text{Failure Rate} = \frac{\text{Number of failures observed}}{\text{Total time spent in testing}}$$

Cumulative % of faults:

$$F = 100\,(11\text{-}0.56^{t})$$

"t" in years after release

The relationship between hardware and software reliability is shown in Figure 57.

3.2.3.h.4. RAM EQUIPMENT EVALUATION

3.2.3.h.4.1. SYSTEM DEFINITION

The system analyzed is composed of the following components.

a) one vehicle
b) 7040 sections of magway
c) 40 Wayside Power and Control Stations
d) one Global Control Center

The system baseline parameters considered were as follows:

Length:
160 km (100 mi)
22 m (75 ft.) span,
5.2 m (17 ft.) elevation,
steel truss
Route: straight
Stations: 2-one at each end
Block Length: 2 km.
Number of blocks: 160
Speed: 134 m/sec
Vehicle spacing: 5.3 km

Number of vehicles: 60
Throughput: 12,6500 pph
Headway: 40 sec
Vehicle size: 140 Passenger
Converter Station spacing: 4 km
Number of substations: 40
Total converters: 160
Operating hours/day 18 hours
Operating hours/year: 6570 hours
Life: 50 years
Global controller: 1
Mission time: 3 hrs.
Substation Spacing: 21.5 km

3.2.3.h.4.2. SUBSYSTEM EQUIPMENT RAM ANALYSIS DISCUSSION

The major system components identified above were analyzed. The features of each component significant to the RAM analysis are discussed in the following paragraphs.

3.2.3.h.4.2.1. VEHICLE

Both the Flight Control and Control Surface Actuator Subsystems have incorporated a significant amount of redundancy in their designs. A dual redundant Flight Control System, including sensors and control system, is being used. The mechanisms controlling the forward stabilizers, canard, rudder and aft elevons are also redundant. On-Board vehicle communications, including the RF link to Wayside Stations and Voice were also redundant. The vehicle was considered to be required for a three hour mission. No on-board repair was assumed. Following the mission conclusion, necessary repairs could be performed. The beneficial effect of scheduled maintenance, which will be performed on the vehicle, was never-the-less disregarded as far as reducing equipment stress related failures. The average corrective maintenance time was estimated to require two hours of active maintenance. The average maintenance delay time was estimated to be four hours.

3.2.2.h.4.2.2. MAGWAY

Analysis for the magway considered the trough (7040 sections), associated instrumentation to monitor track health and safety condition and fiber optic equipment physically located in the general area of the elevated magway.

The instrumentation systems included four monitoring straps per section of magway to determine track continuity, a CC TV Camera system placed strategically along the track to warn of potential unsafe traffic conditions and position markers placed every eleven (11) meters along the trackway to track vehicle travel progress. Each system has redundant features; the monitoring straps by the multiplicity per section; the camera system by the incorporation of redundant cameras at each location; and the position marker system was that as long as less that than three transmitters in a row had not failed, the control system could respond to vehicle problems in adequate time.

Maintenance of magway equipment was considered. Both preventive and corrective maintenance will be performed. Corrective maintenance tasks were estimated to require four hours of active maintenance on the average. The average maintenance delay time was estimated to be eight hours.

3.2.3.h.4.2.3. WAYSIDE STATION

Each Wayside Station includes processing and power subsystems. The processing subsystems have been designed for considerable fault tolerance(stations are not manned). Trade offs performed on the interfaces to the processing equipment showed, in some cases, that a redundant interface was not needed. The following
interfaces fell into this category.

Fiber Optic Interface to the TV Camera System
Power Inverter Interface
Position Marker Interface
Wayside Station point-to-point Interface
Switch Drive Electronics Interface

The redundant elements of the processing subsystem benefitted from the fault tolerant architecture since fault annunciation is planned to be rapid and the repair process can be expedited and completed long before system failure is theoretically a remote possibility. The operational availability of the Wayside Processing Subsystem is calculated to be in excess of 0.99999.

Redundancy was also incorporated in elements of the Power Subsystem to increase its operational availability. All power groups except the LSM Converter Group have one spare (5 instead of 4) converter sections. The redundant configuration relieved the need for more rapid repair actions, resulting in an expected repair turnaround time averaging 32 hours instead of 8 hours. The operational availability of the Power Subsystem exceeds 0.9999.

3.2.3.h.4.2.4. GLOBAL CONTROL CENTER

Due to the significance of the Global Control Functions, a great deal of fault tolerance to equipment failure has been incorporated into this system. Data processing and system control functions are all backed up at major equipment levels. Rapid fault detection, isolation and repair capability have been designed priorities. Since the center is manned, estimates of corrective maintenance times approach that of an Air Traffic Control Center.

High (equipment) level redundancy has been incorporated in the Data Processing, Workstation and Data Storage Subsystem. Trade-offs determined that the TV Camera System Control, FDDI LANs and GPS equipments did not require a backup. The average corrective maintenance time for the redundant subsystems is approximately 0.5 hours. The average system down time has been estimated to be 2.4 hours. The operational availability is in excess of 0.999.

3.2.3.h.4.2.5. MAGLEV SYSTEM/SUBSYSTEM ALLOCATIONS

Based on the availability analysis, allocations for the system and its major components have been completed. Figure 58 shows the present availability allocations. The results of the availability analysis performed during this concept phase are summarized in Figure 59.

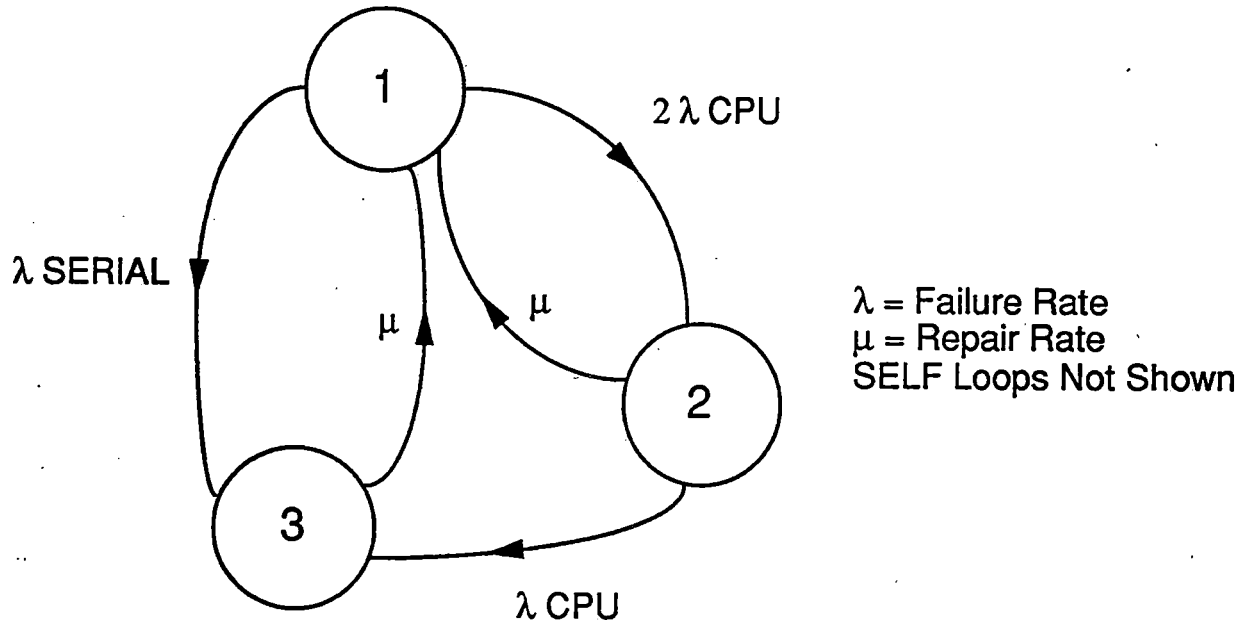

Figure 56 Availability transition diagram

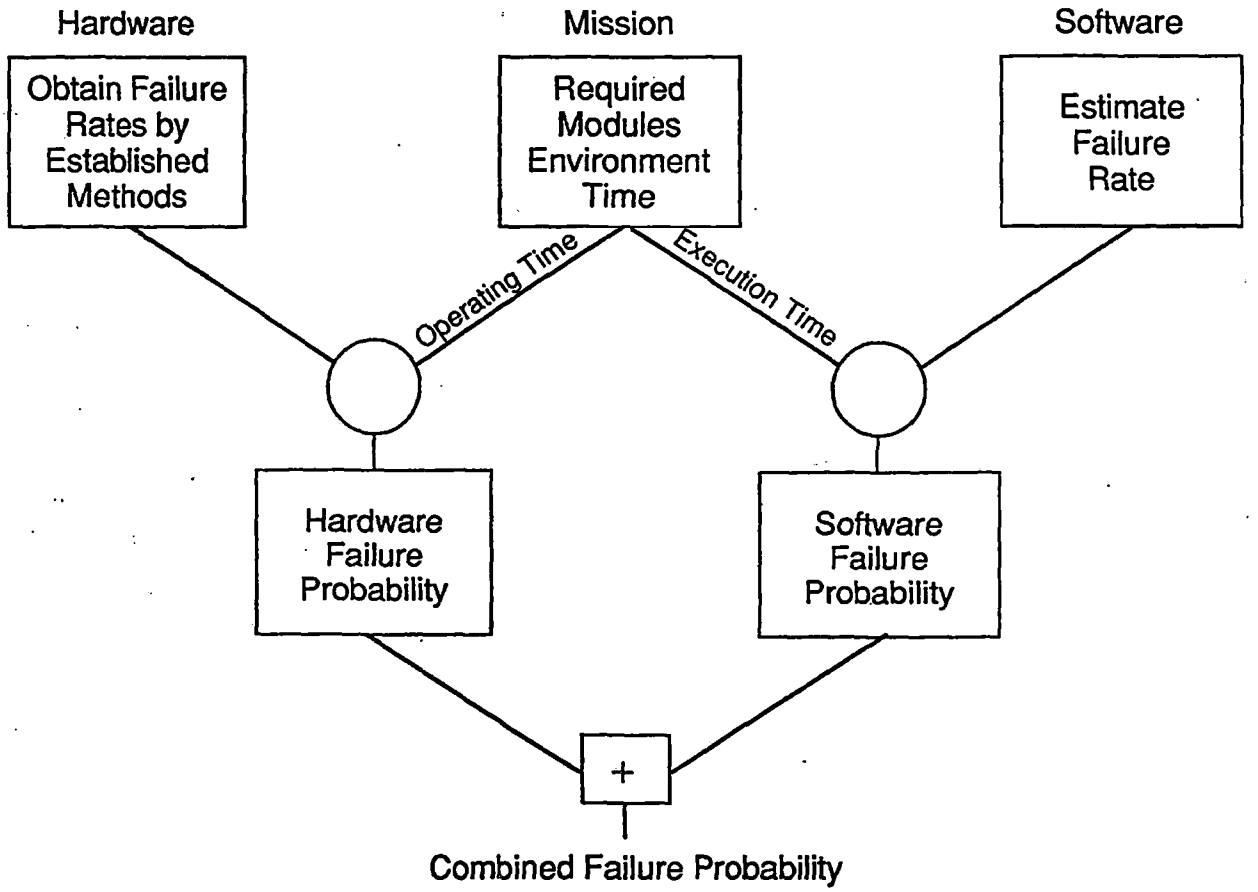

Figure 57 Relationship between hardware and software reliability

Subsystem	Operational Availability	Preventive Maintenance Constraints
Vehicle	0.985	Pre-operational checks daily, weekly inspections
Guideway	0.998	Daily inspection of track
Wayside Power & Control	0.987	Weekly inspection of power equipment, operational test of processing equipment
Global Control Center	0.9996	Monthly operational checks
Software	0.99998	
Human Factors	0.9995	
System	0.97	

Figure 58 Maglev operational availability allocations summary

SUBSYSTEM	FAILURE RATE (fpmh) Logistic	Effective	MAINTAINABILITY (hrs MTTR	Delay Time	UNAVAILABILITY Inheren	Operationa	COMMENTS Subtable	Prev. Maint	General
VEHICLE	3523.59	2366.326249	2	4	0.00471036	0.013999197	1	daily/weekly	
GUIDEWAY	28674.63	153.76	4	8	0.000614662	0.001841722	2	daily	switchover to selected redundant sections possible
WAYSIDE POWER and CONTROL	30337.2	2237.532855	1.755495207	3.95	0.00391261	0.012605311	3	weekly	on-line repair capability
GLOBAL CONTROL	2876.12	429.9591195	1.055734394	1.09	0.000453717	0.000921728	4	monthly	based on VTIS-2 system configuration
SOFTWARE	100	100	0.2	0	1.99996E-05	1.99996E-05	5		allocation
HUMAN FACTORS and EXTERNAL	-	-	-	-	0.0005	0.0005	6		allocation based on results of previous studies.
TOTALS	65411.54	FPMH			0.010211348	0.029887957			
AVAILABILITY					0.989788652	0.970112043			

Figure 59 Maglev availability analysis (summary page and following seven pages)

ITEM DESCRIPTION	# of ITEMS	LOGISTICS	SUCCESS	EFFECTIVE	MAINTAINABILIT		UNAVAILABILITY		NO
		F R (fpmh)	CRITERIA	F R (fpmh	MTTR	Delay Time	Inherent	Operational	
Flight Control System	1	1416.666667		350.7962492	2	4	0.002825328	0.002100357	
Sensors	2	253	1 of 2	84.33333333	2	4	0.000168638	0.000505744	CD Report - page 150
Height Sensors	3	23.4			2	4			
Air Sensors	2	34			2	4			
Magnetic Sensors	6	90			2	4			
AOA Sensors	2	34			2	4			
Yaw Sensors	2	14			2	4			
Accelerometers	2	12			2	4			
Position Sensors	2	45.6							
Flight Controller	2	431	1 of 2	143.6666667	2	4	0.000861258	0.000861258	
Control Surface Actu	2	48	1 of 2	16	2	4	3.1999E-05	9.59908E-05	dual redundant channels
Fwd Stabilizers	2				2	4			
Fwd Canard	2				2	4			
Aft Rudder	2				2	4			
Aft Elevon	2				2	4			
Communications	1	286	1 of 1	88.06958251	2	4	0.000571673	0.000528138	
GPS Receiver	1	8	1 of 1	8	2	4			
RF Link (To Waysi	2	54	1 of 2	5.402915843	2	4			
Vehicle Fiber Op	32	224	6*(1 of 2	74.66666667	2	4			
Attendant Displays	2	66	0 of 2	0	2	4	0.000131983	0	
Maintenance I/O	1	5	0 of 1	0	2	4	9.9999E-06	0	
Voice Interface	2	30	1 of 2	10	2	4	5.99964E-05	5.99964E-05	
Vehicle I/O CPU (MVM	2	26.18	1 of 2	8.726666667	2	4	5.23573E-05	5.23573E-05	
Power Sub-system	2	176.82		176.82	2	4	0.000353515	0.001059796	
Power Pick-up Coil S	2	0.4			2	4			six coils per set
AC/DC Converter	4	48			2	4			
Battery Backup Set	1	0.01			2	4			
DC/AC Converter	4	40			2	4			

ITEM DESCRIPTION	# of ITEMS	LOGISTICS		EFFECTIVE	MAINTAINABILIT		UNAVAILABILITY		NO
		F R (fpmh)		F R (fpmh	MTTR	Delay Time	Inherent	Operational	
Cryogenics Sub-system	1	363.11		363.11	2	4	0.000725693	0.002173924	
Cold Box	1	0.1			2	4			located at front and rear of
Heat Exchangers	6	8.3			2	4			
Turbo-expander	2	72			2	4			
Piping and Valves	12	6			2	4			
LNG Tank	1	0.07			2	4			
Helium Cooling Syste	1	83.07			2	4			
Helium Compressor	1	68			2	4			
Oil Cooler	1	15			2	4			
Primary Helium Tan	1	0.07			2	4			
Emergency Helium Tan	1	0.07			2	4			
Control Panel	1	14			2	4			
Levitation System	2	94.8		94.8	2	4	0.000189564	0.000568477	
Cryostat	1	20			2	4			each bogie has 2 levitation
Heating Element	4				2	4			modules of 2 coils each.
Superconducting Co	4				2	4			
Heater PSU	4	50			2	4			
Energising Coil	4	2.4			2	4			
Energising Coil PSU	4	2.4			2	4			
Control & Communicat	1	20			2	4			
Landing Gear	2	656.06		656.06	2	4	0.001310401	0.003920926	
Air Bearings									
Air Control Valves	4	428			2	4			
Low Friction Pads	4	80			2	4			Preventive Maintenance
Pressure Regulator	2	42.6			2	4			
Inflation Valve	2	84			2	4			
Capillary Tubes	2	1.46			2	4			

ITEM DESCRIPTION	# of ITEMS	LOGISTICS F R (fpmh)		EFFECTIVE F R (fpmh	MAINTAINABILIT MTTR	Delay Time	UNAVAILABILITY Inherent	Operational	NO
Control & Communicat	1	20			2	4			
Braking Sub-system	1	128.8		128.8	2	4	0.000257534	0.000772203	
High Friction Pads	1	20			2	4			Preventive Maintenance
Support Structure	8	0.8			2	4			
Pneumatic Drive	8	88			2	4			
Control & Communicat	1	20			2	4			
Propulsion System	2	412		412	2	4	0.000823322	0.002465904	
Cryostat									
Heating Element	6	28.8			2	4			
Propulsion Coils	6	3.6			2	4			
Heater PSU	6	75			2	4			
Energising Coil	6	3.6			2	4			
Energising Coil PSU	6	75			2	4			
Control & Communicati	1	20			2	4			
Control Surface Actuators		608		202.6666667	2	4	0.001214523	0.001214523	
Hydraulics	8				2	4			Preventive Maintenance
Power	8								
Pumps	8								
Valves	8								
Couplings	8								
VEHICLE TOTALS	1	3523.59		2366.326249	2	4	0.006640101	0.014279237	
AVAILABILITY							0.993359899	0.985720763	
NOTES * = insignificant due to scheduled maintenance activities.									

ITEM DESCRIPTION	# of ITEMS	LOGISTICS	SUCCESS	EFFECTIVE	MAINTAINABILITY		UNAVAILABILITY		
		F R (fpmh)	CRITERIA	F R (fpmh	MTTR	Delay Time	Inherent	Operational	
GUIDEWAY									
Guideway Trough	7040	704		1	4	8	4E-06	1.19999E-05	
Guideway Instrumentation									
TV Monitoring System	-	0		0	0	0	0	0	see Global Control Tabl
Monitoring Straps	35556	88.9		1	4	8	4E-06	1.19999E-05	
Position Markers	727	38.05		50	4	8	0.00019996	0.00059964	four straps per guidewa
									section
Guideway FDDI									
OPR	8	4	4 of 8	1.333333333	4	8	5.3333E-06	1.59997E-05	
Router	4	264.28	2 of 4	88.09333333	4	8	0.00035225	0.001056004	
Power Dist.	4	40	2 of 4	13.33333333	4	8	5.333E-05	0.000159974	
TOTALS		1139.23		154.76	4	8	0.00061887	0.001855618	
AVAILABILITY							0.99938113	0.998144382	
—									

	DESCRIPTION	# of ITEMS	LOGISTICS	SUCCESS	EFFECTIVE	MAINTAINABILITY		UNAVAILABILITY		NOTES
			F R (fpmh)	CRITERIA	F R (fpmh)	MTTR	Delay Time	Inheren	Operational	
Wayside Control Unit										
Processing		2	594.38	1 of 2	0.176591311	1	2	1.766E-07	5.29774E-07	
Processor/Memory	MVME187-01 RISC	1	13.09	1 of 1						
Transition Board	MVME712M	1	3.3	1 of 1						
Fiber Optic I/F	Lightwave ODL 50	7	77	7 of 7						
Power Converter I/F		4	60	4 of 4						
Switch Drive Electronics		1	12	1 of 1						
WCU pt-to-pt Interface		2	33.4	2 of 2		0.75	2			
Position Marker I/F		2	33.4	2 of 2						
Vehicle RF (Duplex)	STORNO CQF-9000	1	50	1 of 1		1	2			
Voice Interface		1	15	1 of 1						
Dual FDDI Ring		2	23.04	1 of 2	0.000130055	0.49	2	6.373E-11	3.23838E-10	
FDDI DAS	MVME385K-8	1	10.52	1 of 1						
OBR	DIPLEX	2	1	2 of 2						
Power Supply/UPS		1	44.01	1 of 1	44.01	1	2	4.401E-05	0.000132013	
AC/DC Converter		2	24							
Battery Backup Set		1	0.01							
DC/AC Converter		2	20							
Wayside Power Subsystem		1	97	1 of 1	11.7516	4.59621	4	5.401E-05	0.000101009	
250 KV MVA		5	57	4 of 5	1.6736	8	24			switchover FR=3 fpmh
LSM Converter		4	10	4 of 4	10	4	4			20% system duty factor
AC/AC Converter (PWR P/O)		5	10	4 of 5	0.026	8	24			20% system duty factor
AC/AC Converter		5	10	4 of 5	0.026	8	24			20% system duty factor
AC/DC Converter(WCE/FDDI)		5	10	4 of 5	0.026	8	24			20% system duty factor
WCU TOTALS		1	758.43		55.93832137	1.7555	2	9.819E-05	0.000233552	
WCU AVAILABILITY								0.9999018	0.999766448	
WCU System Total		40	30337.2		2237.532855	1.7555	3.95	0.0039126	0.012605311	
								0.9960874	0.987394689	

ITEM DESCRIPTION	DESCRIPTION	# of ITEMS	LOGISTICS F R (fpmh)	SUCCESS CRITERIA	EFFECTIVE F R (fpmh)	MAINTAINABILITY MTTR	MAINTAINABILITY Delay Time	AVAILABILITY Inherent	AVAILABILITY Operational	
Data Processing		2	93.26	1 of 2	0.001521901	0.7	1	1.065E-09	2.58723E-09	
CPU	MVME187-01 RISC	1	13.09	1 of 1						
Transition Module	MVME712M	1	3.3	3 of 3						
LVPS/Fan	96011210-	1	23.7	1 of 1						
SCSI Cable	96410754-	3	6	3 of 3						
ENET Cable	9303944-2M	1	0.54	1 of 1						
GPS System		1	33.33	1 of 1	33.33	0.75	1	2.5E-05	5.83241E-05	
GPS Receiver		1	20	1 of 1						
GPS Performance Mon.		1	13.33	1 of 1						
FDDI System		1	158.66	1 of 1	158.66	0.49	1	7.774E-05	0.000236348	
I/F FDDI Controller	MVME385K-8	2	10.52	2 of 2						
DPR	DIPLEX	4	2	2 of 2						
Router	TIME\LAN 100RB	2	132.14	2 of 2						
FDDI Controller I/O	MVME	2	4	2 of 2						
Power Dist.		1	10	1 of 1						
Camera System	COHU - MPC	1	1696.74	1 of 1	67.10787821	4	1.063958538	0.0002684	0.000339716	
Master MPC Con Panel	COHU - MPC	1	27	1 of 1	27	4	1			
Control Distribution	COHU - MPC	1	12	1 of 1	12	4	1			
Data Link (FO)		1	247.84	1 of 1	0.003837615	4	1			
Repeater	MVME-300	4	61.96	2 of 4	0.003837615	4	1			
Fiber Optic I/O		10	0	see notes	0					included in Camera data
Terminal	DL -VT420-AA	3	39.9	2 of 3	0.000202978	0.34	1			
Video Switcher	COHU - MPC	1	20	1 of 1	20	4	1			
Camera/Pan Tilt	COHU - MPC	10	1350	see notes	8.1	4	4			no two consecutive positions down
Graphic Display	RAYTHEON	3	437.7	2 of 3	0.024422071	0.34	1	8.304E-09	3.27256E-08	
AAS Display	RAYTHEON	1	145.9	1 of 1		0.294				
MDC	RAYTHEON	1		1 of 1						
Keyboard	RAYTHEON	1		1 of 1						
Trackball	RAYTHEON	1		1 of 1						
2Kx2K Monitor	SONY - 2801	1		1 of 1						

ITEM DESCRIPTION	DESCRIPTION	# of ITEM	LOGISTIC	SUCCESS	EFFECTIVE	MAINTAINABILI		AVAILABILITY	
			F R (fp	CRITERIA	F R (fp	MTTR	Delay Time	Inherent	Operational
Workstation	SPARCSTATION-IPX	1	117.68	1 of 1	117.68	0.49	1	5.766E-05	0.000175312
ENET controller	SUN -X450U	1	20	1 of 1					
16 MB RAM	SUN -X116U	1	12	1 of 1					
Keyboard	SUN X8307	1	5.18	1 of 1					
Terminal	DL -VT420-AA	1	13.3	1 of 1					
ENET Transceiver	DT500-03	1	1.6	1 of 1					
ENET Cable	9303944-2M	1	0.54	1 of 1					
Data Storage		2	341.9	1 of 2	0.014608205	0.5	1	7.304E-09	2.19123E-08
150 MB Cartridge Tape	MVME853F-8	1	21.8	1 of 1	0.000237612	0.5			
600 MB Disc Storage	MVME876F6	1	11	1 of 1	6.0499E-05	0.5			
Printer	THINKJET	1	38.15	1 of 1	0.00072767	0.5			
Voice Recorder		1	100	1 of 1	0.00499925	0.5			
Power System		1	35	1 of 1	15	0.4	1	6E-06	2.09996E-05
Power Supply/Distrib.	IPM-	1	30	1 of 1					
UPS	IPM BP-15	1	5	1 of 1					
TOTALS			2914.27		391.8184304	1.109831	1.09	0.0004348	0.000830757
AVAILABILITY								0.9995652	0.999169243

3.2.3.h.5. RELIABILITY PROGRAM PLAN

3.2.3.h.5.1. INTRODUCTION

3.2.3.h.5.1.1. OBJECTIVE

This plan describes the Reliability Program to be implemented for the Maglev Transportation Program. Reliability planning has considered passenger safety as the highest priority item. Program tasks have been selected based on achieving high system safety. Both candidate fault tolerant architecture and subsystem equipment designs will be examined for meeting safety criteria established for maglev. Reliability goals have been established to provide a safe and cost effective system.

3.2.3.h.5.1.2. SCOPE

The purpose of this Reliability Program Plan is to provide a detailed description of the tasks to be performed for the design and test of the maglev transportation system. The Reliability Program will be an integrated effort to define, analyze and achieve the reliability/availability requirements of the maglev system. The Reliability program has been structured to produce a significant contribution to the safety of the personnel, equipment, and environment.

3.2.3.h.5.1.3. TASK APPLICABILITY

The tasks specified herein have been tailored to provide a cost effective approach to meeting the proposed maglev requirements. The tasks were carefully selected from reliability and maintainability Military Program Standards to maximize the usefulness and applicability.

A summary of the maglev tasks are summarized in Figure 60. Additional details of each task are contained in the reliability plan paragraphs.

3.2.3.h.5.1.4. RELIABILITY ORGANIZATION

The Reliability engineering department is responsible for performing the R/M tasks at Raytheon's Equipment Division. An organization chart of the Reliability Engineering Department is shown in Figure 61. An R/M project engineer has been assigned to the maglev program. The maglev project engineer resides on the department technical staff and will report to the R/M section manager through a group leader for maglev tasks, as well as reporting functionally to the Maglev Program Office.

3.2.3.h.5.1.5. REFERENCED DOCUMENTS

The following documents of the issue shown below form a part of this plan to the extent specified herein.

MIL-HDBK-338
Electronic Reliability Design Handbook

MIL-STD-470

Maintainability Program For Systems & Equipment

MIL-HDBK-472
Maintainability Prediction

MIL-STD-756
Reliability Modeling and Prediction

MIL-STD-785
Reliability Program for System and Equipment Development and Production

44-5090-140
Failure Reporting and Corrective Action (FRACA) System 1 May 1987

MIL-HBK-217
Reliability Prediction of Electronic Equipment

44-1030-142
Raytheon Equipment Division "Circuit Stress Analysis Criteria" 01 June 1987

42-1007-210
Engineering and Research Policies and Procedures "Component 01 May 1987 Stress Derating Criteria"

3.2.3.h.5.2. RELIABILITY REQUIREMENTS

The quantitative requirements, as stated in the system requirements of the System Concept Definition Report will be derived to achieve the high availability, reliability, and ease to maintain and inspect. The Availability, MTBF, MTTR, and fault detection/isolation requirements are presented in Figure 62, and have been allocated to lower equipment tiers as explained in paragraph 3.2.3.h.5.3.7

3.2.3.h.5.3. RELIABILITY TASKS

The reliability program will be established to ensure timely achievement of the maglev requirements. The reliability program tasks will be planned, integrated, and performed in consonance with other design and development functions. Management and personnel resources will be allocated to the extent necessary to accommodate the tasks specified herein.

The reliability tasks to be performed are reliability math modeling, predictions, and allocations; internal and external design reviews; subcontractor guidance and review; specification inputs; reports; tolerance and circuit analysis; sneak circuit analysis'; failure reporting and corrective action; failure mode and effects; design guides; reliability demonstration testing and data analysis.

3.2.3.h.5.3.1. RELIABILITY PROGRAM PLAN

The Reliability Program Plan contained herein presents a description of tasks to be performed. The program was developed to address the specific reliability needs of the maglev system. The tasks selected were based on MIL-STD-785 and tailored to address the uniqueness of the maglev program.

This plan will be revised, approval obtained, and reissued as required during the maglev program.

3.2.3.h.5.3.2. MONITOR/CONTROL OF SUBCONTRACTORS AND SUPPLIERS

R/M and quality requirements will be included as appropriate in control drawings and purchasing specifications for maglev purchases of newly designed and/or modified parts and components. These inputs will include the following:

a. Component selection and application criteria
b. Quantitative reliability requirement as derived from subsystem allocations
c. Reliability analysis to be compatible with requirements
d. Verification data submittal requirements
e. Failure reporting, analysis and corrective action requirements
f. Organizational level repair time requirements
g. Electronic, electrical and electro-mechanical (EEE) parts derating requirements)

Each subcontract statement of work (SOW) will require approval of the appropriate support engineering function.

Prospective vendors will be surveyed to establish their experience/capability in complying with any burn-in/screening requirements and to explore the availability of valid, verifiable data on part failure rates in the maglev environment.

Subcontractors providing major assemblies will be required to generate and implement a reliability program as appropriate to the design and complexity of their respective equipment. These programs will be in accordance with the overall maglev Reliability objectives and requirements, and will require Raytheon approval.

Subcontractors and vendors will be required to schedule design reviews and provide for the monitoring of reliability program implementation and performance. These reviews will be used to identify problems and provide timely solutions to conditions which would effect reliability.

3.2.3.h.5.3.3. PROGRAM REVIEWS

3.2.3.h.5.3.3.1. INTERNAL PROGRAM LEVEL

Periodic program/design reviews will be held both at the program management level and at operating levels throughout the program to assure coordination of all disciplines affecting reliability, effect interchange of information on design development status, resolve problems, and assist design progress. Particular emphasis will be placed on the achievement of reliability and safety objectives.

Problem areas will be documented and passed on to the responsible disciples as action items for resolution. R/M engineering will participate in all trade-off reviews affecting the RMA and safety objectives.

3.2.3.h.5.3.3.2. CUSTOMER REVIEWS (FORMAL GOVERNMENT REVIEWS)

As a minimum R/M engineering will develop material for presentation at customer reviews for each task specified in Figure 60 including the following.

a. Rel. allocations and Rel. predictions versus system requirements
b. Trade-off study results and design changes
c. Parts and materials program
d. Conformance to design standards
e. Subcontractor design standards
f. Failure and repair data
g. Problems and solutions
h. Status of reliability critical items list
i. Circuit stress analysis status/progress
j. FMECA status/progress
k. Sneak circuit analysis
l. FRACAS status/progress
m. Subcontractor/supplier status/progress

3.2.3.h.5.3.3.3. EQUIPMENT LEVEL REVIEWS

The design review program has as its principal objective the assurance that a comprehensive and critical audit is made of all pertinent design parameters, including reliability/maintainability/safety, at key milestones in the design cycle. The review does not relieve the design engineer of responsibility for his design, but rather supplements his effort by assisting him in ensuring that he has considered every design requirement, including Reliability and Safety.

3.2.3.h.5.3.3.3.1. PRELIMINARY R/M DESIGN REVIEW ACTION

Informal internal design reviews will be held on a continuing basis by the responsible R/M engineers co-operatively with the design and system engineers. This continuing review program serves a twofold purpose: to ensure that each RMA task required by this plan is properly performed, and to identify RMA and Safety problems for resolution as early as possible in the design cycle.

3.2.3.h.5.3.3.3.2. INTERNAL DESIGN REVIEW PROGRAM

Raytheon will conduct internal design reviews at various levels of design. Planning and coordination of these design reviews is the responsibility of the System Design Task Manager in cooperation with the responsible design managers.

A review will be conducted on the new and modified major components of maglev to the line replaceable unit (LRU) level. The more complex LRUs may require subordinate reviews in order to conduct an

efficient review of the design. Reliability will be one of the principal design considerations at each review.

The following reliability design factors will be considered at each design review as appropriate:

a. Thermal derating and analysis
b. Functional concept
c. Electrical and mechanical
d. Reliability history of like or identical assembles/subassemblies in previous or parallel programs
e. Part selection
    1. Types and vendor QA provisions
    2. Special and/or critical parts review
f. Design analysis study
    1. Review of design calculations
    2. Review of computer-aided design studies
    3. Review of failure mode and effects analyses
    4. Review of testability

At the conclusion of each design review, the recommendations of the review board will be assembled in the minutes of the review and appropriate action items generated. The action item list will be reviewed by R/M engineering and the responsible design managers and corrective action determined and directed. Action items will remain open until satisfactory corrective action is taken and verified.

3.2.3.h.5.3.4. FAILURE REPORTING, ANALYSIS, AND CORRECTIVE ACTION SYSTEM (FRACAS)

Raytheon's policy on FRACA, featuring a closed-loop failure reporting, analysis and corrective action system, will be applied to maglev.

3.2.3.h.5.3.4.1. RAYTHEON FRACA SYSTEM

The aim of FRACA activity is to detect and correct deficiencies in order to maximize the inherent reliability and safety of the maglev design. The failure and maintenance data reporting, analysis, and corrective action program has provisions for collecting data on all failures and maintenance actions: failure, repair, delay and scheduled maintenance times. Raytheon's existing failure reporting system specifies that each failure remains an open item until closed by corrective action acceptable to the applicable R/M personnel. Data will be recorded on Raytheon TFR form No. 10-1571. The FRACA system will begin at the equipment level for the maglev system.

Physics of failure studies will be conducted,i when applicable, to determine intrinsic causes of failure. Microscopic analysis, photomicrography, chemical, metallurgical and spectrographic analysis, and other applicable and warranted techniques will be used. After comprehensive review and analysis, R/M engineers will submit recommendations to those activities responsible for corrective action.

An Failure Review Board (FRB), consisting of representatives from R/M engineering, parts engineering, materials, QA, program office and design engineering will review all failures, make corrective action assignments, and stimulate investigations, analysis and corrective action.

3.2.3.h.5.3.5. FAILURE REVIEW BOARD (FRB)

The FRB consists of the following representatives:

a. Reliability/Maintainability (chair)
b. Parts and materials engineering
c. Quality assurance
d. Design engineering
e. Maglev PMO (includes systems) engineering)
f. Maglev PPAM

The task of the FRB is to review significant failures, make assignments of responsibilities for investigation and corrective action, provide resources for investigative analysis, and maintain schedule control over the corrective process. In addition, the FRB validates closeout decisions and oversees the generation of management reports.

It will be the responsibility of the board chairman to ensure the comprehensive collection of data, analysis of discrepancies, and the initiation and follow-up corrective action recommended by the board. He will also assure the timely submittal of data items, and coordination with the government.

3.2.3.h.5.3.6. RELIABILITY MODELING

Reliability/Availability models were developed to address and define the requirements of Figure 62. These preliminary R/A Models were generated to ensure the proposed maglev design satisfies the required availability, reliability, safety, maintenance, and logistic support needed to comply with the overall maglev approach. The reliability models will be further developed and exercised as the equipment and approach evolve. The reliability models will utilize and verify the appropriateness of the maglev operational scenario's, as well as, to predict system and subsystem reliability parameters. The reliability models will instrumental in evaluating the effects of failure probabilities, use of redundancy and fault tolerance, maintenance policies (preventive, scheduled, and correctively), degree of fault detection/isolation and software maturity.

The reliability models will be exercised periodically and their outputs will be compared to their associated requirements. If the outputs indicate that the maglev design does not meet its requirements, then corrective action will be recommended until the requirements are satisfied. The reliability models have been used in conjunction with early/preliminary reliability and maintainability prediction values to provide an initial set of subsystem and lower tier equipment allocations.

3.2.3.h.5.3.7. RELIABILITY ALLOCATIONS

Reliability allocations for both the basic and the mission reliability requirements will be made. These allocations will be established in accordance with the subsystems complexities and the individual reliability math models developed as per paragraph 3.2.3.h.5.3.6. These allocations will be used as the

baseline for system, design, and subcontracts to establish reliability requirements. The initial allocations of quantitative reliability numerics, made at various equipment levels, will be an established set of goals that will meet overall program objectives. Periodically, all allocations are reviewed for a variety of reasons (program changes, equipment revision, etc.) and revised allocations may be generated. Review and documentation of progress made toward these goals will be a continuing reliability engineering task effort. The current and revised allocations will be included as a part of the formal design review meetings.

3.2.3.h.5.3.7.1. SYSTEM LEVEL

The reliability requirements have been analyzed to determine appropriate MTBF, MTTR, FD/FI value to be used as design requirements. The results of that analysis are contained in the technical proposal.

The derived MTBCF & MTBF values, θ_D, from that analysis will then be multiplied by 125% to obtain an MTBCF & MTBF value θ_A, to be used as a system MTBCF & MTBF allocations.

The 125% factor is Raytheon's policy for providing an MTBCF & MTBF margin to guard against any unanticipated increases in design complexity.

Thus, the allocated MTBCF & MTBF value for the maglev system are:

$$\theta_A = 1.25 \times \theta_D$$

3.2.3.h.5.3.7.2. SUBSYSTEM LEVEL

The maglev system consists of several subsystems (Vehicle, Magway, Wayside Power & Control, Global Control). Subsystem MTBCF & MTBF allocations are generated by using the preliminary reliability prediction values as weighing factors:

$$\theta_{iA} = [\,(\lambda_{ip} / \lambda_p) \times \lambda_A\,]^{-1}$$

where

N = *number of subsystems comprising MAGLEV* ($n \approx 5$)

$\theta_{i\,A}$ = *MTBCF & MTBF allocation for the ith subsystem*

$\lambda_{i\,p}$ = *preliminary failure rate prediction for the ith subsystem*

$$\lambda_p = \sum_{i=1}^{N} \lambda_{i\,p} = \textit{system level failure rate prediction}$$

$$\lambda_A = [\theta_A]^{-1} = \textit{system level failure rate allocation}$$

The current allocated MTBCF & MTBF for each subsystem and subsequent revisions will be included as part of the progress reports.

3.2.3.h.5.3.7.3. LOWER TIER EQUIPMENT ALLOCATIONS

Allocations to lower tier equipment will be generated as presented in paragraph 3.2.3.h.5.3.7.2 The current allocations to lower tier equipment and subsequent revisions will be included as part of the progress reports.

3.2.3.h.5.3.7.4. DESIGNATION OF REQUIREMENTS

The allocated values have been designated as a designer/supplier MTBCF and MTBF requirements on subsysteims and lower tier equipment.

Preliminary reliability predictions were performed to support the reliability modeling task and to generate a set of reliability and maintainability allocations to meet the requirements.

The resultant predictions and allocations will be contained in the Technical proposal. The preliminary predictions will be refined and updated to determine if the allocations are being satisfied and to provide a baseline for corrective action if required. The preliminary and refined predictions were, and will continue to be either applicable operational field data complimented by MIL-HDBK-217 reliability predictions. The reliability predictions will be calculated using the following criteria:

a. Ambient Temperature	30°C
b. Data Source	MIL-HDBK-217
c. Environment	Ground Fixed
d. Part Quality	Actual from Parts Lists

Field data and existing prediction data will be used after appropriately modifying the data to account for the maglev operating temperature and environment conditions.

The prediction results will be used in the math model to assess reliability status, to update allocations if required, and to recommend design changes if needed. The current predictions and subsequent revisions will be included as part of the formal design review meetings.

3.2.3.h.5.3.9. FAILURE MODES, EFFECTS AND CRITICALITY ANALYSIS (FMECA)

The FMECA is a formal, disciplined evaluation of potential failure modes within the maglev system, and a qualitative/quantitative study of the effects of these potential failures at successively higher levels of equipment progressing to the system level. Each item along with its function in the maglev system, will be evaluated for effects caused by potential loss of functions. All failure modes of the function will be determined and documented onto FMECA forms and circulated throughout the design team. For each failure mode, the local, higher assembly, and system level effects will be determined and entered. Determinations will then be made regarding the impact on mission critical performance, safety, and testability (both on-line and/or test driven). Determinations will also be made of compensating provisions within the design (e.g. fault tolerant or redundancy features) and the degrees of severity within the system.

The FMECA will be used in trade-off studies to reduce the impact of or to eliminate failure modes. The FMECA will be performed concurrently with the design effort to ensure that the designer will consider recommendations resulting from the FMECA. The objective of the failure mode criticality assessment is to reveal design deficiencies and prioritized design action. FMECA will provide early reliability criteria for maintenance planning, test planning, inspection and checkout requirements, safety analysis and logistics support analysis. FMECA will be made available to all design disciplines, to logistics, human factors engineering, and system safety on a continuing basis to assure that FMECA results are considered. FMECA will also be addressed as part of all design review activity.

The FMECA and safety analyses will address various phases of operation (vehicle motion, magway operation, and global and wayside control) to indicate failure effects and fault coverage probabilities critical mission phases. The outputs of the FMECA will be used in constructing and verifying the reliability models.

3.2.3.h.5.3.10. ELECTRONIC CIRCUIT ANALYSES

Raytheon will perform circuit stress analysis on all new and modified designs and perform tolerance analysis on a sample number of critical circuits. The circuit stress analysis will be performed using work case conditions, will include a thermal analysis, and will be conducted in accordance with Raytheon EDL Procedure 44-1030-142, "Equipment Division Circuit Stress Analysis Criteria".

3.2.3.h.5.3.10.1. CIRCUIT STRESS ANALYSIS

Design engineering will use the derating criteria and requirements contained in Equipment Division Standard 42-1007-210, "Component Stress Derating Criteria".

The design engineers will perform circuit stress analyses on all newly designed and modified circuits, recording the rated, recommended derated and actual stresses on forms provided by reliability engineering. Computer aided analysis techniques will be used wherever cost effective. results of the analyses will be compared to the referenced standard.

Reliability engineering will determine by audit that circuit stress analyses are properly performed on new designs and design modifications. As a minimum, 15% of the circuit stress analysis performed by Design Engineering will be verified by Reliability Engineering. If derating guidelines are exceeded, the reliability engineer will review his findings and the corrective action that is required with the design engineer. He will then select an additional 15% of the designs for audit. This process will continue until the audit shows that the sample complies with the derating guidelines.

Reliability engineering will log, index, and approve stress analysis worksheets which will then be archived with the drawing package.

3.2.3.h.5.3.10.2. CIRCUIT TOLERANCE ANALYSIS

Raytheon will perform analyses of critical circuits on a sampling basis to examine the effects of part and circuit electrical tolerances and parasitic parameters over the range of specified operating temperatures. The effort of this task will be performed primarily by design engineers as an integral part of the design effort. The role of reliability engineering in this effort is to assure a consistent and coordinated selection

of circuits for analyses, assure that analyses are reviewed and documented in a timely manner consistent manner, and assure that analyses are reviewed and documented in a timely manner consistent with their performance completion, and presented at design reviews as an agenda item.

Circuits will be selected for electronic circuit tolerance analyses if they are deemed marginal and if a failure (out-of-specification operation) of a circuit would potentially have the following effect:

a. Jeopardize the safety of the system operators, passengers, maintenance personnel.

b. Cause a degradation in availability (e.g., due to erroneous failure indications during test, or increase in overall maintenance actions).

The effects of circuit out-of-tolerance conditions identified in these analyses will be correlated to the corresponding "effects" column in the FMECA.

Circuit tolerance analyses will verify that, given reasonable combinations of within specification characteristics and parts tolerances buildup, the circuitry being analyzed will perform within specification requirements. The analyses will examine the effect of component parasitic parameters, input and power tolerances, life drift, and impedance tolerances on electrical parameters, both at circuit nodes (component interconnections) and at input and output points. Worst-case operations will be included for:

a. Maximum input signal variation
b. Maximum line voltage variation
c. Maximum part parameter variation
d. Maximum performance demands
e. Maximum and minimum temperatures
f. Fail-safe provisions
g. Redundancy provisions
h. Known transient conditions

3.2.3.h.5.3.10.3. SNEAK CIRCUIT ANALYSIS (SCA)

A Sneak Circuit Analysis (SCA) will be performed on selected electronic circuits that control the maglev operations. The SCA is used to determine if any conditions exists which are detrimental to passenger safety or can be caused to occur by equipment anomalies or operator error. The SCA will identify sneak paths, sneak timing, sneak indications, and sneak labels by addressing unexpected paths or logic flows which can initiate an undesirable function or inhibit a desirable function.

3.2.3.h.5.3.11. PARTS PROGRAM

Part quality levels will be selected consistent with the reliability requirements.

All parts used on the Maglev Program will receive sufficient controls to ensure acceptable reliability of hardware developed, fabricated, or procured for the program.

Reliability/maintainability engineering will participate in those parts activities necessary to define reliability design requirements for parts, ensure procurement specifications with adequate reliability

requirements, approve reliability test data for the maglev parts, materials and processes list, and verify sufficient baseline control to prevent purchase and use of parts with unapproved design/construction or insufficient screening data.

3.2.3.h.5.3.12. RELIABILITY CRITICAL ITEMS (RCI)

An RCI list will be generated and controlled to minimize the impact to maglev reliability and minimize the risks to safety. Control plans will be developed and executed on the critical items.

3.2.3.h.5.3.12.1. CRITERIA FOR INCLUSION ON LIST

The following criteria will be used to determine if an item belongs on the list:

a. Failure effects safety, causes loss of essential mission data or causes system shutdown.
b. Difficulty or expense to repair
c. Stringent performance requirements
d. Stress beyond specified derating criteria
e. Limited operating or shelf life
f. Sensitivity to handling, transporting, storage, or environmental conditions
g. Difficult to procure or manufacture
h. Design complexity with a high failure rate
i. No or unsatisfactory history to provide confidence in its reliability
j. Hybrids (RF, digital, analog) or complex monolithic circuits

k. Item requiring special handling or special support or maintenance task times in excess of the system specification
l. Item shown to be critical by FMECA
m. High quantity devices

3.2.3.h.5.3.12.2. RCI CONTROL

The RCI list will be generated by parts engineering in cooperation with reliability engineering. It will be controlled by a procedure titled, "Reliability Critical Item List Control Procedures" that defines the actions that will be necessary to add and remove items from the list. Justification for retaining an item on the list will be provided to all engineering personnel, including the special procedures needed to control the items.

Parts that remain on the list at the date of the PDR and CDR will be discussed at the review.

Each item on the list will be identified by name and number. Where the item is used (with quantities) and the critical item rationale will be included.

Reliability critical parts will be identified as such on the corresponding parts list for each maglev assembly.

3.2.3.h.5.3.13. RELIABILITY TESTING

Reliability testing will be conducted on selected items of the maglev system. These key items, will be evaluated to determine the appropriate reliability testing approach. The reliability testing plan provides a method of minimizing the risk to achieving the reliability requirements. The reliability testing will comprise of qualification testing to ensure the item meets technical and reliability performance requirements. The testing plans for each item will be based on the reliability performance demonstrated during the FRACAS data collection process.

The FRACAS program of paragraph 3.2.3.h.5.3.4 will provide data to assess the reliability performance of the system as well as the subsystems and components. The database of failure information will be analyzed to determine the reliability growth and current MTBF's of the system and sub-items. This failure tracking system will provide the means of minimizing the design risks by utilizing actual MTBF data.

3.2.3.h.5.3.14. REPORTING

3.2.3.h.5.3.14.1. RELIABILITY ANALYSIS

A reliability analysis report will be generated summarizing the reliability analysis. Each edition of the reliability report will present the latest update of the reliability models, along with the reliability allocations and predictions. Comparisons of design achievements versus specified reliability requirements will be included, along with any recommendations for design changes and progress related to past recommendations. The report will be written and formatted in accordance with Raytheon's format. In addition to the items previously mentioned, the report will include the following as applicable:

a. Derating policy and requirements for EEE parts
b. results of reliability trade studies
c. Reliability block diagrams
d. Basis for analysis including mission profiles and data sources
e. Summaries of Failure Modes, Effects, and Criticality Analysis (FMECA)
f. Summaries of electrical and thermal stress analyses

3.2.3.h.5.3.14.2. STATUS REPORTING

Discussions of reliability problems, investigations, solutions recommendations, corrective actions, and the status of all reliability activities will be included as part of the program stratus report to be generated quarterly.

Para.	Title	Activity
3.2.3.h.5.3.1	RELIABILITY PROGRAM PLAN	Update as required
3.2.3.h.5.3.2	MONITOR/CONTROL OF SUBCONTRACTORS AND SUPPLIERS	
3.2.3.h.5.3.3	PROGRAM REVIEWS	Includes internal, customer and equipment level reviews.
3.2.3.h.5.3.4	FAILURE REPORTING, ANALYSIS AND CORRECTIVE ACTION SYSTEM (FRACAS)	In-house and on-suite
3.2.3.h.5.3.5	FAILURE REVIEW BOARD (FRB)	During in-house testing
3.2.3.h.5.3.6	RELIABILITY MODELING	Update Refine models
3.2.3.h.5.3.7	RELIABILITY ALLOCATIONS	Update prelim. allocations
3.2.3.h.5.3.8	RELIABILITY PREDICTIONS	Detailed predictions
3.2.3.h.5.3.9	FAILURE MODES, EFFECTS, AND CRITICALITY ANALYSIS (FMECA)	To circuit level
3.2.3.h.5.3.10.1	ELECTRONIC STRESS ANALYSIS	Electrical/Thermal stresses
3.2.3.h.5.3.10.2	CIRCUIT TOLERANCE ANALYSIS	Combined tolerance effects
3.2.3.h.5.3.10.3	SNEAK CIRCUIT ANALYSIS	Critical control circuits
3.2.3.h.5.3.11	PARTS PROGRAM	Selection and control
3.2.3.h.5.3.12	RELIABILITY CRITICAL ITEM	Identification and control
3.2.3.h.5.3.13	RELIABILITY TESTING	Selected Items
3.2.3.h.5.3.14	RELIABILITY REPORTING	Status Reports

Figure 60 Maglev reliability tasks

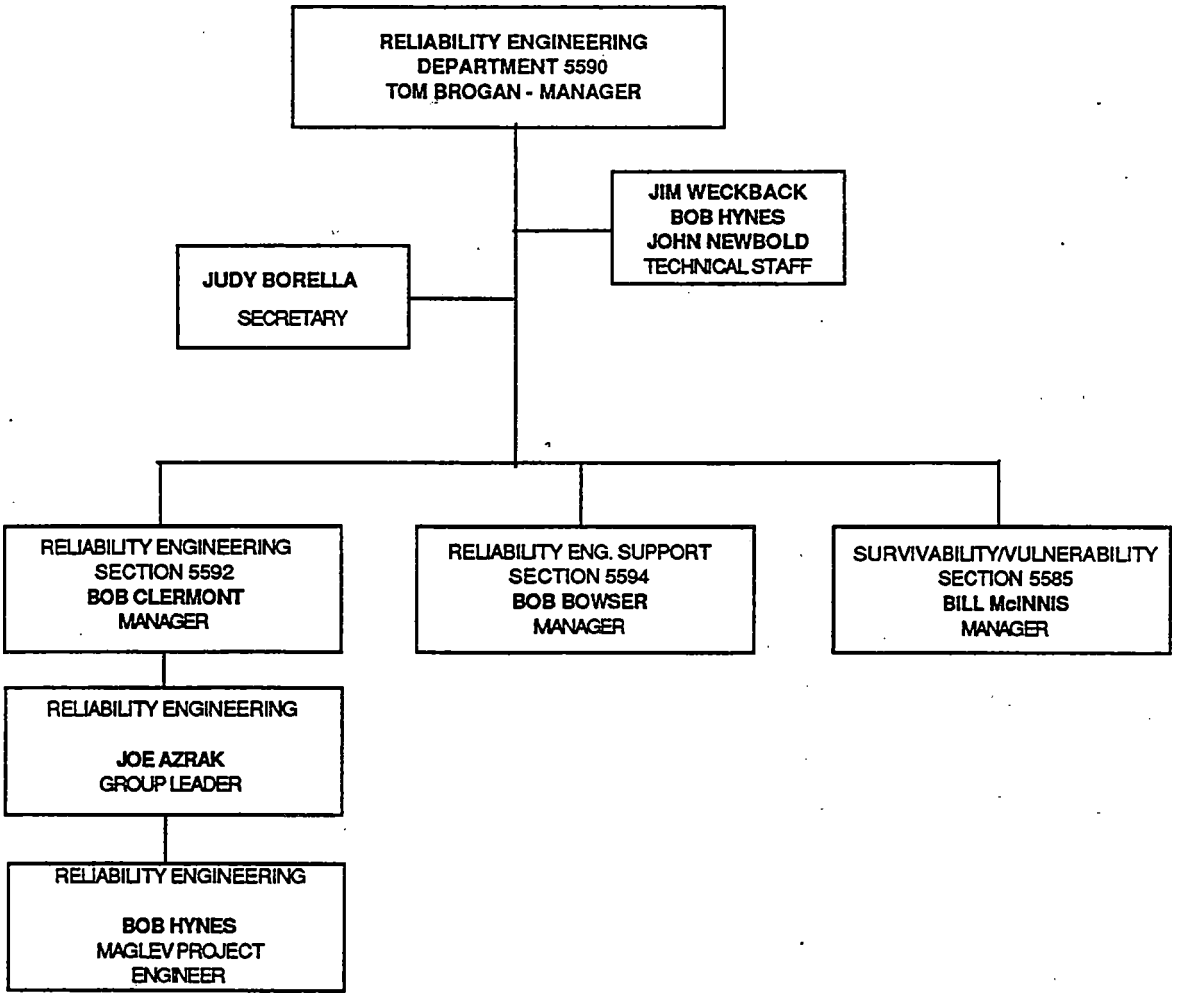

Figure 61 Reliability/maintainability department organizational chart

System Availability	$A_0 = 0.97$
System Mean Time Between Failure	MTBF = 1×10^{-9} hrs or greater
Global Center Fault Detection	FFD = 0.95
Fault Isolation	FFI (1 LRU) = 0.85 FFI (3 LRU) = 0.90

Figure 62 Maglev reliability requirements

3.2.3.i. OPERATIONS AND MAINTENANCE

This section includes descriptions of the procedures for operations and maintenance. The operations and maintenance cost details are provided in section 5.3.5.

3.2.3.i.1. LSM ACTIVATION

3.2.3.i.1.1. INITIAL ACTIVATION

The sequence of operations for energizing the LSM with a stationary vehicle in the block is outlined in the following discussion.

Step 1.

At zero speed, the LSM is supplied directly from the converter without any interposing capacitors or matching transformer. The converter supplies a low level of dc current to the winding which produces a sinusoidal field pattern in the space above the magway. Since it is being supplied at dc, the field is sinusoidal but is not moving. The magnitude of the field can be adjusted to provide enough field strength for the vehicle sensing apparatus but below the level that would ordinarily move the vehicle against skid friction.

Step 2.

Magnetic field sensors on the vehicle locate the field pattern and begin providing magnetic field angle data to the wayside controller.

Step 3.

Once the magnetic field angle has been determined wayside control commands the block power converter to adjust the magnitude and angle of the propulsive field.

Step 4.

Closed loop operation of the magnetic field orientation begins. Attitude control and thrust control on the vehicle respond to commanded velocity profiles from the global controller and requests the local control to begin advancing the phase of the power from the wayside converter. Heave control uses phase modulation once the vehicle is levitated.

3.2.3.i.1.2. RE-SYNCHRONIZATION OF VEHICLE MOVEMENT

This condition can arise under abnormal operation of the vehicle or after certain kinds of emergency conditions. Basically, the situation is that a vehicle is moving in the magway but may not be synchronized to the traveling field.

Magway power is reduced to a minimal level when this condition is first detected. Vehicle speed information transmitted to the local controller is used to estimate the required frequency. This frequency is applied to the magway until the magnetic sensing mechanism on the vehicle is able to estimate the difference in frequency and begin locking to the wave. The controller automatically locks to the traveling speed of the vehicle and begins closed loop operation.

In the absence of vehicle speed information, the induced voltage on the magway can be sensed to determine the phase and frequency needed to match the vehicle. This normally requires that at least one phase of the LSM winding be allowed to "float" electrically to make a measurement of the induced voltage.

3.2.3.i.2. HORIZONTAL CURVES

The traversal of horizontal curves implies two operational considerations:

1. The velocity envelope for normal ride quality is limited in curves, whereas in straight magway, good ride quality is achievable at all velocities. Therefore it is essential to plan the routes of all vehicles such that they do not have to slow down below the lower limit of the velocity envelope in a curve. The global control center does this. In unusual circumstances where slowing down is required, ride quality may suffer, but full control is still available.

2. The aerodynamic control surfaces must provide roll acceleration just before entering the curve, so that the vehicle begins its roll in unison with the beginning of the magway bank. This facility is integrated in the control system.

3.2.3.i.3. MAGPORT-MAGWAY TRANSITION

3.2.3.i.3.1. OPERATIONAL ISSUES

There are several interrelated issues involved in the transition period between zero and cruising speed. From the first motion of the vehicle to normal cruising, all this has to happen:

- departure from any adjacent magport structures
- gradual magway transition from flat to curved trough
- transition from paved surface to aluminum surface
- retraction of landing gear
- traversal of magswitch in merging direction

The relationship, order, and timing of these events is important. In particular, note that:

- the aluminum magway surface must not start abruptly near the drag-peak speeds (15-25 m/s) because this would produce a strong jerk that probably could not be compensated for.

- the vehicle must be going fast enough over an aluminum surface to provide magnetic lift to an adequate height before retraction of the landing gear.

- high speeds on flat surfaces are less stable, so the transition to a curved trough should be made at as low a speed as possible.

- the electromagnetic lift and drag are higher in the curved aluminum trough than they are on the flat aluminum surface because the levitation sheets are closer to the vehicle levitation coils. The transition to a curved trough can be made slowly so that there is a gradual increase in lift and drag, rather than a sudden increase.

- the landing gear can lift the vehicle up to 0.45 m (levitation plate to levitation coil center), which eliminates most of the electromagnetic lift and drag.

- the coupling between the LSM windings and propulsion coils drops off as the separation exceeds the design point of 0.25 m (center to center). This separation can remain constant if the landing gear could retract at the same rate as the appearance of curvature in the trough.

3.2.3.i.3.2. RIDE QUALITY IN MAGPORT AND ADJACENT AREAS

In accordance with the contract, any deviations from the "design goal" (ride quality standard BEST) must be justified.

We propose not to attempt to meet BEST ride quality in the magport environment and on the entry and exit ramps. For these areas, we have created the LAND ride quality standard, which is fully detailed in 3.1.1.c. Under the LAND standard, passengers would be seated and belted, and they could experience short periods of acceleration and jerk in excess of the normal cruising ride quality standard. This is how airplanes operate, and it is reasonable to assume that passengers will accept a similar situation in magplanes.

The particular advantage to a relaxed standard in magport areas is that the entry and exit ramps would not have to be nearly so long as they would have to be if longitudinal acceleration were limited as it normally is. LAND allows 0.6 g longitudinal acceleration while BEST allows only 0.16 g.

In fact, the current Magneplane concept definition allows the vehicle to accelerate at a maximum of 0.4 g due to power availability, so the acceleration value of 0.4 g (3.92 m/s^2) will be assumed for the rest of this discussion.

3.2.3.i.3.3. TIMEWISE DESCRIPTION OF ZERO-TO-MAX ACCELERATION

3.2.3.i.3.3.a. ZERO SPEED TO TAKE-OFF

At the magport platform, while loading, the vehicle is supported on fully extended landing gear. The separation between the vehicle skin and the flat floor of the magport is 0.15 m at the center of the vehicle and about 0.40 m at the location of the levitation coils. The magport floor is paved, with LSM windings installed (flush with the floor surface) along the centerline of vehicle paths.

levitation mode	I	II	III
lift mechanism	landing gear	landing gear and magnetic	magnetic
height is controlled by	landing gear position	landing gear position	velocity
distance on entry ramp	0-96 m	96-331 m	331+ m
time on entry ramp	0-7 s	7-13 s	13+ s
velocity on entry ramp	0-27 m/s	27-51 m/s	51+ m/s
approximate drag as used for energy calculations	mode I: landing gear plus aerodynamic	straight line connecting mode I at 30 m/s to mode III at 50 m/s	mode III: constant lift EM plus aerodynamic

Figure 63 Levitation mode specifications table for normal takeoff

The entry ramp is a section of magway 1 - 1.5 km in length that is flat on the magport end and has a curved trough on the other end. There is a gradual transition area between the flat and curved sections. The trough end typically connects with a magswitch that joins the entry ramp to the main corridor.

Approximately the first 100 m of the entry ramp are flat. The aluminum levitation sheets begin just short of the 100 m mark, while the magway is still flat. The ends of the two levitation sheets are tapered so that the lift and drag increase on a vehicle are not sudden, as shown in Figure 64. In the first 200 m the vehicle reaches the take-off velocity of 40 m/s. See the tradeoff analysis on the take-off velocity (section 5.3.2.5.) for further justification.

3.2.3.i.3.3.b. TAKE-OFF

In the area from about 100 to 300 m from the magport end of the entry ramp, the flat surface changes gradually to a curved trough. In this transition section, the landing gear retract, allowing the vehicle to settle slightly. Note that the vehicle does not actually "take off" but rather drops *down* a little when the landing gear retract. During the transition, the LSM coupling remains almost constant because the center of the vehicle remains at a nearly constant clearance from the centerline of the magway surface.

The shape of the transition area is made according to the distance D as shown in Figure 65. D is a measure of the vertical height of one side of the magway surface, in the line of the center of the levitation coil. The distance D is not in linear proportion to the distance along the magway; it varies rather in proportion to the square root of the distance along the magway. This is because D should increase linearly

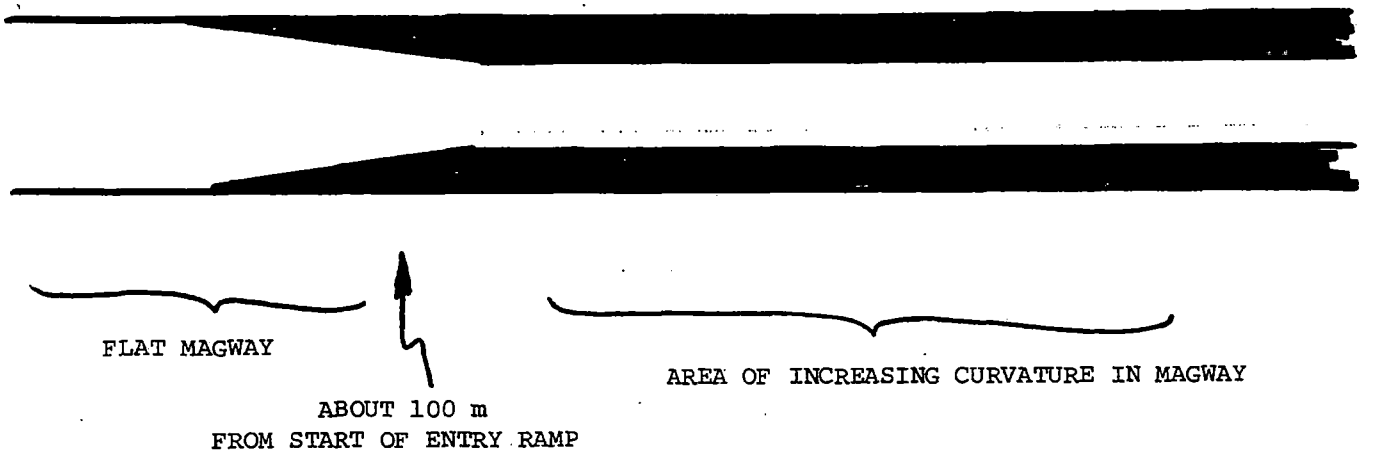

Figure 64 Configuration of tapered ends of levitation sheets on entry ramp

with time as a vehicle traverses the transition section. As the landing gear is retracted at a constant rate, the sides of the magway trough approach the vehicle at a constant rate, the pressure on the landing gear decreases in a controlled way, and electromagnetic lift and drag increase.

The Magneplane levitation modes are detailed in section 3.2.1.b. A table listing how the three modes are used in this context is given in Figure 63.

Mode I levitation is the starting mode and lasts until the levitation sheets begin at about 100 m into the entry ramp. Mode II levitation is used from the point where the levitation sheets begin until the point where the landing gear lose contact with the magway surface at about 300 m. Mode III is used thereafter.

The amount of lift and drag in mode II is determined by velocity and the separation between the levitation coils and the levitation plates. This separation is a function of the position of the landing gear and the shape of the magway, both of which change in the course of a normal take-off.

At the onset of mode II levitation when the magway is flat and the vehicle is travelling at about 27 m/s, the levitation separation is 0.45 m. Any drag experienced at this time is due to landing gear friction.

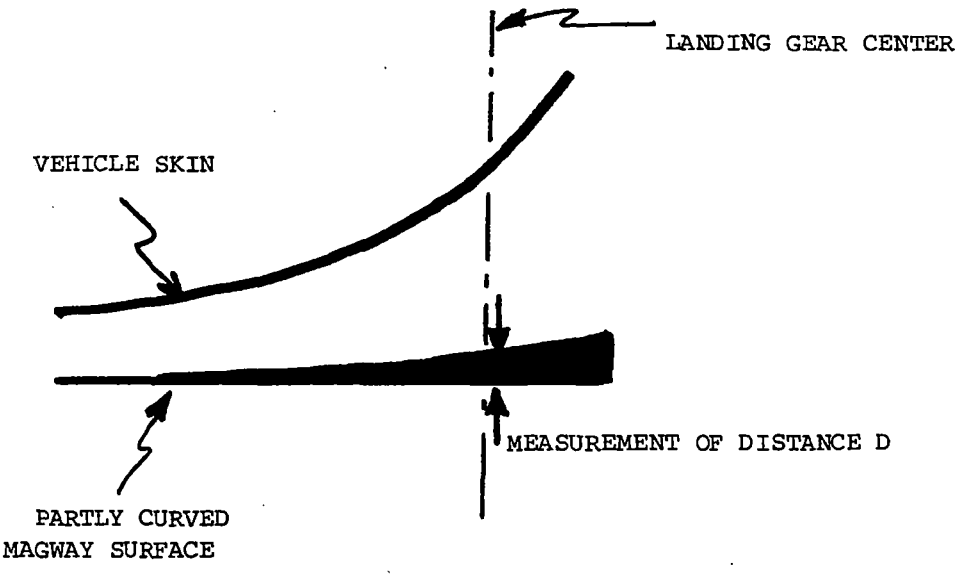

Figure 65 Cross section of magway trough showing distance D

At the end of mode II levitation, just before the landing gear retract enough to let the vehicle settle below its design height (0.15 m separation), the magway trough is fully curved and the levitation separation is 0.20 m (coil center to levitation plate surface). Refer to the 0.20 m drag curve in Figure 67 for the drag experienced at this time.

Through the whole take-off process, the actual drag experienced by the vehicle goes from the 0.45 m drag curve in Figure 67 to the 0.20 m drag curve, and then finally to the mode III curve as the landing gear retract and lose contact. This is the justification of the actual drag curve as shown in Figure 68. This actual drag curve is used for calculations of energy demand elsewhere in this report.

3.2.3.i.3.3.c. TAKE-OFF TO CRUISING SPEED

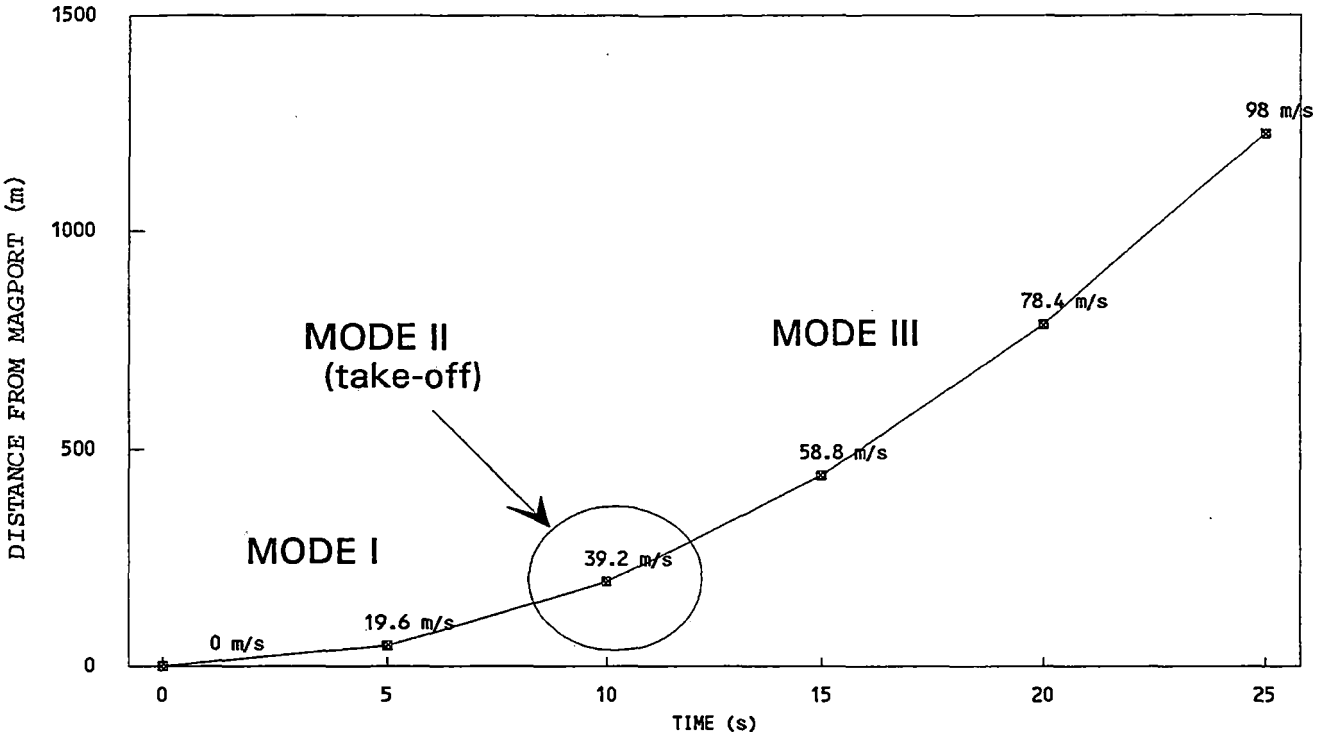

Figure 66 Graph of distance, velocity, and time during take-off, showing levitation modes

From about 300 m to about 1225 m the vehicle continues to accelerate, and reaches 100 m/s at the time of entry to the magswitch. The last part of the acceleration is done on the main corridor. Details on switching are given above in section 3.2.2.d.

The operation on the entry ramp is graphically summarized in Figure 66.

3.2.3.i.3.4. TIMEWISE DESCRIPTION OF MAX-TO-ZERO DECELERATION

Deceleration from cruising speed down to zero speed is essentially the same process as acceleration from zero to cruising speed, only backwards.

The vehicle slows to about 100 m/s before being switched onto the exit ramp. It slows to 51 m/s, at which time it is about 330 m from the end of the exit ramp. The landing gear are extended in the transi-

tion area to a flat magway. The vehicle reaches zero speed at a safe distance from the magport structure,

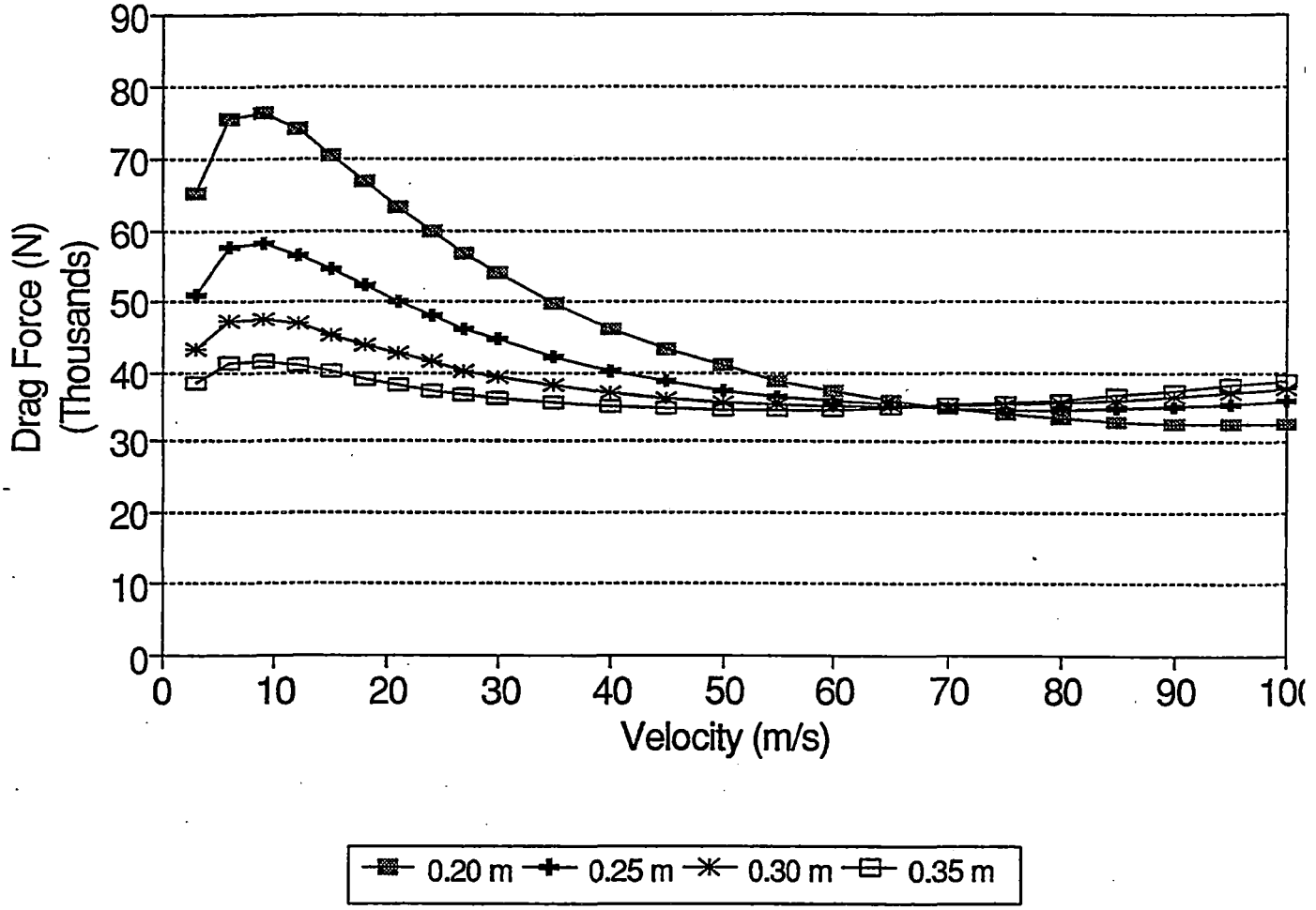

Figure 67 Total drag force of 140-passenger vehicle at various levitation heights

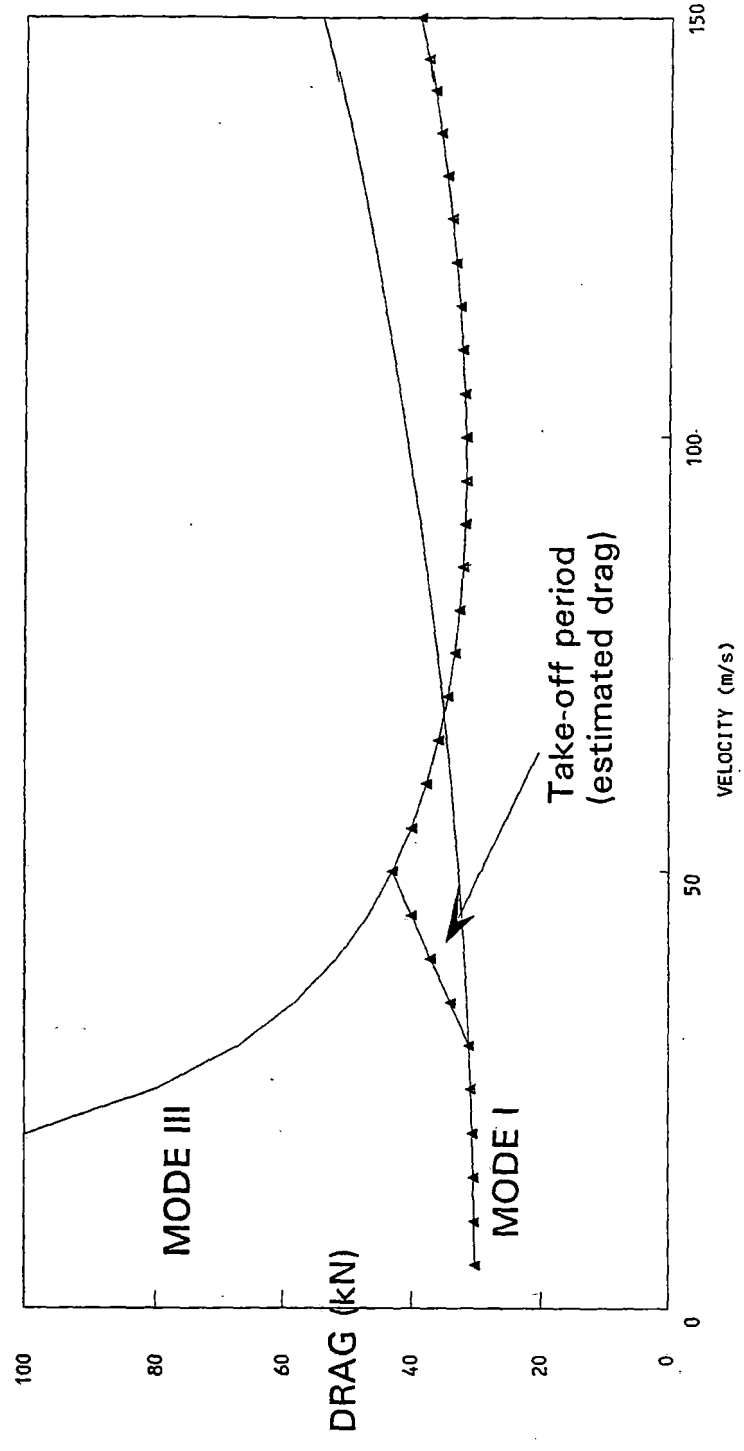

Figure 68 Composite drag curve showing estimated drag during take-off period

and then taxis to the platform for unloading.

3.2.3.i.3.5. ENTRY RAMP LENGTH

Although this discussion gave particular figures for the length of the various sections of the entry ramp, the actual lengths will be based on tradeoffs to be done for each magport. The design speed of traffic on the main corridor in the vicinity of the magswitch connecting to the entry ramp would be the main determinant of the length of the entry ramp.

The current choice of entry/exit ramp length is based on 0.4 g longitudinal acceleration, which is due to power availability limitations. As the ride quality standard LAND allows up to 0.6 g longitudinal acceleration and deceleration, the 0.4 g assumed in this description could be increased, and the entry/exit ramps could then be made shorter. The acceleration could only be increased with significantly more installed power, but the deceleration could be increased within the power availability currently assumed.

Guidance forces on the flat part of the entry ramp are sufficient to keep the vehicle going in a straight line during take off. See section 3.2.1.b.

3.2.3.i.4. NETWORK TRAFFIC MANAGEMENT

3.2.3.i.4.1. TRAFFIC MANAGEMENT REQUIREMENTS

Network traffic management is a topic that requires further study. In this contract, we have only outlined the general approach.

The global control center is primarily responsible for traffic management - getting magplanes to their destinations. The global management requirements include:

1. maintain safe distances between all magplanes (see below)
2. allow loaded, waiting magplanes to enter traffic flow
3. allow magplanes to exit traffic and dock at a magport
4. determine the route each magplane will take
5. respond to unplanned occurrences

As is explained below, there are methods for doing all of these five things effectively. Train schedules in use today can be complex; building a train schedule requires significant planning ahead, and foreseeing and avoiding all possible interferences. Magneplane proposes a system that will plan ahead and optimize routing in a similar way, but Magneplane's traffic management will plan ahead continuously on the basis of current demands, instead of just once.

3.2.3.i.4.2. SAFE HEADWAY DEFINITION

The safe headway is defined to be the separation in distance between successive vehicles so that the following vehicle can avoid colliding with the leading vehicle if the leading vehicle should come to an

instantaneous stop. This definition of safe headway is far more restrictive than allowable safe headways for highway travel.

Definitions:

leading vehicle	vehicle 1
following vehicle	vehicle 2
headway distance	d_h
stopping distance	d_s

If vehicles 1 and 2 are traveling at the same speed (v), then there is a time associated with the headway distance. We define headway time as follows:

$$t_h = \frac{d_h}{v}$$

This time should not be confused with the stopping time of vehicle 2 defined as t_s, and the associated stopping distance d_s.

In the following analysis we will assume that vehicle 1 stops abruptly at t=0 and that vehicle 2 must come to a stop as quickly as possible allowing for system delays and that vehicle 2 has a uniform deceleration capability of a_s.

We calculate the stopping time and stopping distance t_s and d_s.

$$t_s = t_c + t_d + t_{decel}$$

where

t_c = decision and communication time,
t_d = brake deployment time,
t_{decel} = time to decelerate vehicle 2

For uniform deceleration:

$$v = a_s t_{decel}$$

thus

$$t_{decel} = \frac{v}{a_s}$$

$$t_s = t_c + t_d + \frac{v}{a_s}$$

And the distance traveled during t_s is:

$$d_s = v(t_c + t_d) + d_{decel}$$

For uniform deceleration a_s:

$$d_{decel} = \frac{1}{2} a_s t_{decel}^2$$
$$= \frac{1}{2} a_s \left(\frac{v}{a_s}\right)^2$$
$$= \frac{v^2}{2a_s}$$

Finally

$$d_s = v(t_c + t_d) + \frac{v^2}{2a_s}$$
$$= v\left(t_c + t_d + \frac{v}{2a_s}\right)$$

The safe headway distance is:

$$d_h = d_s + d_m$$

where d_m = distance margin of safety

So

$$d_h = v\left(t_c + t_d + \frac{v}{2a_s}\right) + d_m$$

And then the expression for headway time is:

$$t_h = \frac{d_h}{v}$$
$$= t_c + t_d + \frac{v}{2a_s} + \frac{d_m}{v}$$

For a magplane traveling at 134 m/s we have the following values:

communication and decision time	t_c	0.25 s
brake deployment time	t_d	3.75 s
running velocity	v	134 m/s
deceleration capability	a_s	4.9 m/s^2

If we choose a margin of safety to be 300 m then we find

$$\begin{aligned} t_h &= 0.25s \\ &+3.75s \\ &+\frac{134m/s}{2\times 4.9m/s^2} \\ &+\frac{300m}{134m/s} \\ &=19.9s \end{aligned}$$

and

$$\begin{aligned} d_h &= vt_h = 134m/s \times 19.9s \\ &= 2667m \end{aligned}$$

For the 4,000 pas/hr (passengers per hour) configuration Magneplane will have the flexibility to use headway times as low as 19.9 s and as high as 126 s (depending on the vehicle size mix). To reach the ideal capacity of 25,000 pas/hr, 20 s headways must be used. The actual margin of safety is given by:

$$d_m = v(t_a + t_c + t_d) + \frac{v^2}{2a_s}$$

where t_a is the actual time between vehicles.

The margin of safety can range from 300 m in the 25,000 pas/hr configuration up to 14 km in the 4,000 pas/hr configuration.

3.2.3.i.4.3. VEHICLE TIME SLOTS

The prime Magneplane vehicle control strategy is based on vehicle slots. A vehicle slot is separated from its neighbors by the fixed headway time period. This headway is defined to be sufficiently long to insure that any action taken by one vehicle under any (emergency) circumstance will not jeopardize the action of vehicles ahead or behind. In routine negotiations vehicle slots are essentially fixed, and controlled by the Global centers. As each center controls approximately 160 km of magway, the transitions of the vehicle slots between centers is fully coordinated. A vehicle slot may not always be occupied.

In the instance of a catastrophic failure, such as the magway being damaged by an external event, no more than one vehicle should be at risk. It is obviously impossible to prevent damage to a vehicle travelling 134 m/s when the magway 100 m ahead of it collapses, however it is critical that the vehicle following it can stop safely. In such an event, the Global control center for the region will issue

emergency control commands to all wayside control units, and notify the Global centers downstream of the impending stoppage. The vehicle immediately following the incident will be commanded to apply braking at maximum. This will insure the vehicle stops well before the damage point, but invokes the risk of injuring standing passengers. The vehicles behind will also have to take action, as this is a serial event. Vehicles will be commanded into a coordinated stop, that is they will 'bunch', the vehicles will brake more gradually, the further away from the incident they are. Such decisions will be made dependant on which slots are occupied, to insure that no vehicle will be required to brake harder than necessary, or that any vehicle will make contact with another. Controlled braking and 'bunching' also insures that travelling passengers will arrive in a localized area, and not be dispersed along the length of the route. This is the only instance when more than one vehicle can be in the same wayside controlled block, whereby propulsion power is inactive, and the vehicle is supported and controlled on its landing gear.

Dynamic re-routing and exiting will also be activated to downstream traffic in an emergency, if the opportunity permits. This will be coordinated by the Global controllers, as will any traffic restart and reversal required to get as many vehicles as possible to their destinations or local stations.

3.2.3.i.4.4. EXITING AND MERGING WITH TRAFFIC

In a realistic corridor there are many stations, and vehicles negotiating only sections of the magway between their launch and their destination. This requires that vehicles leave the traffic (exit to a station), and join the traffic (enter from station). As either requires activation of the route switch to negotiate the maneuver, a number of slots will be left vacant about the vehicle of interest, so that the switch function can be completed in the time period between occupied slots. A vehicle leaving the main traffic will have one slot ahead of it empty. The Global control center will monitor progress of the vehicles ahead of the vehicle requiring exit, by means of the wayside controllers. When the Global control has report that the vehicles ahead are clear of the switch, it will activate the transition from ahead to turn-out, and monitor the progress of the switch mechanism. As the switch is designed to complete a transition in 12 seconds, one free slot insures sufficient time for the vehicle to take avoidance action and stop, if the switch fails in mid-travel. Monitoring of the active mechanism is continuous by the switch wayside control unit, and if at any point in the transition a failure occurs, the vehicle (and following ones) will be commanded from the networked Global centers to abort the turn-off procedure. If a situation occurs where the switch does not traverse because of complete failure, the vehicle will continue to the next station and the procedure repeated. Management of the failure mode in this manner does not impact the time slots of neighboring vehicles, hence does not corrupt the journey time of any vehicles other than the one intended to turn-off.

Assuming normal switch operation, the vehicle will traverse the switch section, decelerating to come to a stop in the station. An additional vacant slot will be allocated behind the vehicle so that the switch can reset after the vehicle has left the switch section and the following vehicle take safe action if the switch fails to reset.

A vehicle joining the traffic requires similar slot allocation for the maneuver. The switch will be activated to permit the vehicle to join the traffic as the vehicle leaves the station. Again sufficient time will be allocated in the main traffic flow for the switch to transition, and the vehicle to enter the flow. The allocation of one slot to do this is the same as a vehicle exiting, hence coordinated exit and launching at stations, under Global control is routine. Should a station not require to launch a vehicle coincident with receiving one, the two slots (vehicle slot plus vacant slot) are left vacant until the next station,

whereby an opportunity to launch into the vacant slots is available. These vacant slots can be used by any station upstream, and are accessed by priority decisions made by the Global controllers. Priorities are based upon passenger waiting time at stations and freight priority as well as destination of the passengers and freight.

3.2.3.i.4.5. VEHICLE BUNCHING

In some sections of the corridor, the opportunity to join the traffic by an available moving slot may not present itself in a timely manner. In this circumstance vehicle bunching is adopted. Vehicle bunching opens up a slot by slowing vehicles behind the desired opening (backward bunching) and if possible, advancing the vehicles ahead (forward bunching). A number of criteria, including local weather conditions, will be considered in deciding if a forward bunching maneuver is possible, as under no circumstance will vehicles be more closely time spaced than required for safe, non-interfering emergency braking. To instigate backward bunching, the Global controller will issue commands to the following wayside units to decelerate the vehicles in a coordinated manner to reduce their velocity by some value, and reduce the headway. As the velocity is reduced, so is the required stopping distance, hence emergency measures are not compromised. If the Global controller determines that braking efficiency of the vehicles in an area is adequate, the forward bunching maneuver will accelerate the vehicles ahead by some percentage of their current speed, in a controlled maneuver. This bunching will propagate backwards (and if implemented forwards), to the first free slot in the route. This slot will then be absorbed by the maneuver. When both backward and forward bunching are employed vehicle slots can be freed at twice the frequency compared with backward bunching only.

3.2.3.i.4.6. DESTINATION GROUPING

Vehicle management at a global level will be optimized to group vehicles by destination. A vehicle launched at one station with a specific destination will have one vacant slot ahead to accommodate the switching required to join the main traffic. Global slot management will invoke three slots behind it if another vehicle scheduled for the same destination is to join the traffic upstream. The second vehicle will join the mainstream in the second slot behind the first, in the coordinated launch sequence outlined above. This second vehicle will be operated at 10% higher velocity than the mainstream, to permit it to 'catch-up' with the first. The second vehicle will proceed at the higher velocity until it is one time slot behind the first. If additional vehicles can be picked up on-route that are also heading to the same destination, then three slots behind the second vehicle will be re-established (by bunching or vehicle exiting) so that these vehicles can also join the group in a similar manner. At the destination exit point, the switch is then activated to turn-off all the vehicles as one group performing a coordinated exit. This optimizes the number of switch transitions required to service the route, and maximizes the availability of slots otherwise used by the switch transition.

3.2.3.i.4.7. CIRCUMNAVIGATING DISABLED VEHICLES

As disabled vehicles disrupt traffic flow, they should be removed from the magway as quickly as possible.

While a disabled vehicle is stopped and is blocking traffic, an alternate route is used. There are two options for alternates: (1) use one magway for bi-directional traffic, and (2) use an entirely separate

corridor as a detour route. These are the options used in the event that a section of magway becomes unusual for any reason.

For option (1), crossovers spaced about every 25 km will be used. 25 km of magway will be bi-directional for the time that it takes to fix the problem (eg. remove the vehicle). The global control center will determine an optimal amount of time to run all westbound traffic in that section, then it will switch to eastbound for another period of time, and so on. This is equivalent to the system often used when repairing bridges when only one lane is available. The difference is that the traffic flow can be managed systemwide so that vehicles never have to approach the bi-directional section, stop, and wait for the direction to change. The delay (if a delay is required) would occur as far back as the previous magport stop. In other words, the magplane would not even take off until the global control center had projected a clear uninterrupted path through the bi-directional section (and perhaps all the way to the next stop).

3.2.3.i.5. PASSENGER/FREIGHT SCHEDULING

Scheduling is a topic that requires further study. In this contract, we have only outlined the general approach.

The global control center is primarily responsible for scheduling - the procedure of assigning particular passengers and units of freight to particular vehicles. The scheduling requirements include:

1. passengers must be serviced quickly (the allowed time variability being an issue for further study - probably 10 or 15 minutes)
2. passengers and freight (possibly on the same magplane) should be grouped such that those people and units going to the same place at the same time share the same vehicle

Requirement (1) implies short waiting time at the magport. Requirement (2) implies short trip time, because fewer stops would be required in a well-grouped system than in a system where passengers were not grouped according to destination.

These issues cannot simply be nailed down, since they affect the number of vehicles and average load, and they depend on the density of magports and patterns of demand for service - all of which are cost-related issued. For a discussion of determining the number of vehicles needed for a corridor, refer to the Hypothetical Route Report, section 3.6.

Requests for service (trip orders) will be incoming on a continuous basis. Trip orders are the result of passengers purchasing tickets or reserving a seat. A trip order consists essentially of the origin, destination, and allowable time window. Some trip orders will come in hours in advance of the requested departure time, while others will come in just at the requested departure time.

The scheduling system groups trip orders by origin and destination, and assigns them to vehicles in a way that maximizes vehicle load, minimizes stops, and minimizes waiting time. The relative importance of these goals depends on further study.

3.2.3.i.6. MAINTENANCE PROCEDURES

Please see the Maintenance Plan (section 5.3.5.) for costs of maintenance procedures. This section just lists the major maintenance procedures.

3.2.3.i.6.1. DAILY MAINTENANCE

The following maintenance will be required on a daily basis for each vehicle.

I cryogenic service
- fill nitrogen tank
- diagnostics

II electric system diagnostics

III control systems diagnostics

IV cleaning and interior

3.2.3.i.6.2. WEEKLY MAINTENANCE

The following maintenance will be required on a weekly basis for each vehicle.

I mechanical parts inspection
- aerodynamic controls actuators
- landing gear and emergency brakes

II cryogenic service
- pump vacuum system
- clean cryogenic traps

III recharge superconducting coils

IV check batteries

3.2.3.i.6.3. LONGER-TERM MAINTENANCE

The following maintenance procedures will be required on a term longer than weekly.

I cryogenic system overhaul - every six months

II vehicle overhaul - every year

III magway inspection - every six months

3.2.3.j. MAXIMUM SYSTEM CAPACITY

One measure of the capability of a transport system to perform its prime function of moving people is to calculate the systems' maximum capacity. System capacity is a measure of the number of passenger seats that can be moved passed a fixed point in one direction, in a one hour period. The simplest assessment of this rating can be performed based on the number of seats in a vehicle, and the maximum frequency at which the vehicles can occur. This assumes all the seats in every vehicle can be occupied without affecting the frequency. In practice this number of people is never achieved because of the limitations of scheduling and the actual load factor, or percentage utilization, of the facilities in any one time period.

3.2.3.j.1. MAGNEPLANE CONFIGURATION

For the concept definition, two vehicle sizes have been considered, a 140 seat vehicle and a 45 seat vehicle. The larger vehicle seating capacity was determined by rationalizing the maximum desirable length of a vehicle, considering its ability to negotiate curves etc. It is recommended that the 140 seat vehicle is the largest size used on Magneplane. The 45 seat vehicle was identified as an intermediate size that is attractive for prototype development. The only (imposed) restriction on the size of Magneplanes is that they do not exceed the length of the 140 seat configuration, and any intermediate size is possible. For the purposes of the system capacity evaluation, 140 seat vehicles are assumed, as they are the most cost effective from the aspect of system capacity.

The vehicles are used singularly, there are no consists. The vehicles are spaced on the magway such that they always have a safe stopping distance from their nearest neighbor. At 134 m/s, the maximum design speed, this is described in the time domain as a 20 second headway. A second consideration that evolves from the headway is the segmentation of the magway into discrete blocks. A maximum of one vehicle occupies a block of the magway at any time. A typical block length on the magway is 2 km, which has a nominal 15 second traverse time at 134 m/s. This magway length varies dependant on designed traverse speed, designed acceleration maneuvers, turn-off requirements and a number of other parameters. The spacing between vehicles is always longer than one block length.

A power distribution technique called leap-frogging is part of the Magneplane concept that provides cost efficiencies for lower system capacity use. Converter stations service four blocks in each direction, or eight blocks in total. Each block must be energized from a power converter. Just two power converters are used in each direction with the leap-frogging configuration, as opposed to four power converters. This reduces the total number of power converters required for a fixed length of magway, and the cost associated with their deployment and maintenance. Leap-frogging is effective when the system requirements are low, but requires that vehicles are separated by a minimum of three blocks for the power switching procedure to work. This three block length imposes a minimum 50 second headway requirement between vehicles.

Length	160 km
Route	Straight - one eastbound/ one westbound
Switches	None
Block Length	2 km
Converter Station Spacing	8 km
Converter Stations	20
Average vehicle velocity	134 m/s
Average propulsion power	6 MVA
Substation Rating	60 MVA

Figure 69 Baseline route used for capacity upgrade discussion

The Magneplane system ultimately has no limit of system capacity, although numbers much above 100,000 passengers/hour are increasingly difficult to achieve because of the logistics and wide right of way required. The solution to increasing the system capacity on Magneplane is identical to that used on automobile throughways, increase the number of available lanes. A configuration of four magways traversing in one direction will come much closer to realizing four times the throughput of a single magway, compared with the similar solution imposed on an automobile highway congestion problem.

The minimum configuration of two parallel magways for a particular route, one handling the 'westbound' traffic, and a second handling the 'eastbound' traffic satisfies the system capacity requirement defined in the contract, of 4,000 seats/hour, 8,000 seats/hour and 12,000 seats/hour.

For the purposes of evaluating the system capacity in a global manner a standard model is used. This model is the cost baseline, and is described in Figure 69.

3.2.3.j.2. MAGNEPLANE SYSTEM CAPACITY ANALYSIS

The contract requires Magneplane to accommodate 4,000 seats/hour, 8,000 seats/hour and 12,000 seats/hour. In addition the Magneplane can service up to 25,000 seats/hour with an increase in vehicle stock, hence this case is also described.

This evaluation is based on a simple model. Additional burdens of a real and more complex system include turn-offs and stations which result in the need for more vehicles as each vehicle is only active for some percentage of the time. The turn-off also introduces another parameter, as a vehicle must slow down from 134 m/s to 100 m/s to take an exit from the magway. This requires an additional 17 seconds of headway behind exiting (and entering) vehicles. Analysis of switching maneuvers and vehicle bunching to re-locate the 17 second period dynamically along the magway indicates that the 25,000 seats/hour limit is reduced to 22,900 seats/hour for a magway with turn-offs at 20 km intervals.

Doubling up the magway to four lanes permits direct doubling of the 22,900 seats/hour to 45,800 seats/hour.

The power distribution scheme of leap-frogging imposes a 45 second headway, as one vehicle must complete negotiating three of the four blocks in one direction that are driven from one converter station, before a second vehicle enters. The appropriate placement of turn-offs in the four blocks, permits the 17 second entry/exit burden to be absorbed into this 45 second limit of the leap-frogging configuration.

The power required of the magway propelling one vehicle at 134 m/s is approximately 6 MW. The designed capacity of the system, and whether or not leap-frogging power control is utilized, determines the duty cycle of a particular power converter. When leap-frogging of the power drive is employed, a converter station will be powering a maximum of one vehicle in each direction at any time, or two vehicles total. The four blocks require two 6 MW converter drives, which alternately propel the vehicle as it traverses each block. Each converter is active for two of the four blocks in the process. This results in each power converter being burdened for 50% of the time it takes a vehicle to traverse the blocks. When leap-frogging is not employed, a converter station will drive a maximum of four vehicles in each direction, or eight total, with a minimum 20 second headway. Each power converter is devoted to one block, and all the four blocks in a direction can contain vehicles at an instant. This mode of operation imposes close to a 100% burden on each power converter.

The power burden on the converter station determines the size and number of substations required to provide the 35 kV power from the 115 kV source. For this evaluation, each substation is 60 MVA, and additional substations are introduced when the system segment power requirements dictate. The substations are physically placed so that increasing the capacity of the system is achieved by locating new substations at intermediate positions. The substation power is distributed so that power is maintained at all converter stations all the time one substation is operational. A configuration designed for a system capacity utilizing a number of substations will continue to operate at a reduced capacity if one of the substations fail.

3.2.3.j.3. THE 4,000 SEAT/HOUR CONFIGURATION

A total of 10 vehicles are required to satisfy this system capacity in one direction. The vehicles are spaced a nominal 16.9 km apart and have an average headway of 128 seconds. 20 vehicles are required to satisfy the bi-directional traffic flow.

The leap-frogging power distribution scheme is utilized in the converter stations, requiring four power converters per station. A vehicle traversing along the 8 km section of magway requires two converters

to drive it through the four leap-frogged blocks. Each converter averages a 50% duty while a vehicle traverses the 8 km section, and the vehicle spacing of 16.9 km results in the 8 km sections being occupied for 50% of the time. This extrapolates to an average 25% duty cycle on each 6 MW converter, and a total of 6 MW per converter station to satisfy the bi-directional traffic.

The distributed 20 converter stations each requiring an average of 6 MW of power will be fed from three 60 MVA substations equi-spaced along the 160 km section. See Figure 70.

Because of the large headway between vehicles, the introduction of turn-offs in this configuration has no impact on traffic flow. The traffic management at this capacity is relatively static, and there is no interaction of traffic required for one vehicle to exit the magway.

3.2.3.j.4. THE 8,000 SEAT/HOUR CONFIGURATION

This capacity requires 20 vehicles for one direction, with 63 seconds average headway between vehicles. This headway permits continued use of the leap-frogging power scheme of the converter stations. In consequence the traffic management is also a minimal problem, as there is no traffic interaction.

The average vehicle spacing is 8.4 km which defines that the 8 km segment powered from one converter station will be propelling one vehicle with a 100% duty cycle, requiring a continuous 6 MW, and 12 MW total to satisfy the bi-directional traffic. The distributed 20 converter stations require six equi-spaced 60 MVA substations along the 160 km section.

3.2.3.j.5. UPGRADING FROM 4,000 TO 8,000 SEAT/HOUR

Doubling the throughput of the 4,000 seat/hour configuration requires doubling the number of vehicles available, from 20 to 40, and doubling the number of substations from 3 to 6. The converter stations are designed for 100% duty cycle, hence the increased burden on those units does not exceed the rating. The substations would be ideally equi-spaced, hence the increase from 3 to 6 results in allocating new land at intermediate locations to install the substations. Additional power cabling is required to connect in the new substations. The existing power cabling would be adequately rated so that it does not have to be replaced with a higher rating to reflect the 100% increase in loading. See Figure 71.

Planned maintenance of the converter stations would also be increased, to accommodate the reduced reliability of the hardware operating at the higher rating.

3.2.3.j.6. THE 12,000 SEAT/HOUR CONFIGURATION

This configuration requires 30 vehicles in one direction, with 42 seconds average headway between vehicles. The headway time of 42 seconds excludes the leap-frogging power scheme of the converter stations. In consequence there are eight power converters at each converter station, each one devoted

Number of vehicles	20
Vehicle spacing	126 s (16.9 km)
Number of Converter stations	20
Leap-frogging of magway blocks	Yes
Average power per Converter station	6 MW
Number of 60 MVA substations	3

Figure 70 Parameters for 4,000 seat/hour model

to a block of the magway.

Traffic management is straightforward at this capacity. A vehicle can perform a coordinated entry at 100 m/s into traffic flowing at 134 m/s and accelerate appropriately to match the traffic stream in a single 42 second time slot. The vehicle will maneuver within a 17 second window of this time slot, and never violate the safe stopping distance between its (new) neighbors during any part of the maneuver.

The average vehicle spacing is 5.6 km which defines that the 8 km segment powered from one converter station will be propelling two vehicles in one direction. Each of the four power converters will experience a average 35% duty cycle, requiring at total of 8.5 MW in each direction, or 17 MW total. Six 60 MVA substations are required to power the 20 distributed converter stations along the 160 km section.

3.2.3.j.7. UPGRADING FROM 8,000 TO 12,000 SEAT/HOUR

The upgrade from 8,000 seats/hour to 12,000 seats/hour requires that the converter switching hardware for leap-frogging is retired, and the number of power converters at each converter station is increased from four to eight. See Figure 72

The 50% increase in throughput from the 8,000 seat/hour configuration requires increasing the number of vehicles available, from 40 to 60. The number of substations required to provide the 35.5 kV power remains at six. The converter stations are designed for 100% duty cycle, hence the increased burden on those units does not exceed the rating. The existing power cabling would be adequately rated so that it does not have to replaced with a higher rating to reflect the 50% increase in loading.

Planned maintenance of the converter stations would also be increased, to accommodate the increase in the amount of hardware (power converters etc).

3.2.3.j.8. THE 25,000 SEAT/HOUR CONFIGURATION

This is the limit of the bi-directional two magway system, spacing the vehicles at a 20 second headway. It requires a total of 60 vehicles at any one time in one direction. Power leap-frogging is not feasible.

In a system with turn-offs, the 17 seconds additional time space required to perform an exit or entry maneuver degrades the throughput of the system to approximately 22,900 seats/hour, requiring 55 vehicles. This permits a floating time slot of 17 seconds every 20 km, which can be appropriately placed behind a vehicle exiting by instigating a vehicle bunching maneuver. This requires a more complex vehicle management control process compared with the other cases described.

The average vehicle spacing is 2.9 km which defines that each 2 km block will contain and propel a vehicle with a 70% duty cycle. This reflects as an average of 34 MW total per converter station containing eight power converters. A total of twelve 60 MVA substations are required to power the 160 km section model. See Figure 73.

3.2.3.j.9. UPGRADING FROM 12,000 TO 25,000 SEAT/HOUR

Upgrading from 12,000 to 25,000 seats/hour represents a doubling of the system capacity. This logically requires doubling the vehicle stock from 60 vehicles to 120 vehicles, and doubling the number of substations to service the 160 km stretch. The converter stations are unchanged, but experience an increase in duty cycle from an average of 35% to 70%. The converter stations are designed for 100% duty cycle, hence the increased burden on those units does not exceed the rating. The substations would be ideally equi-spaced, hence the increase from 6 to 12 results in allocating new land at intermediate locations to install the substations. Additional power cabling is required to connect in the new substations. The existing power cabling would be adequately rated so that it does not have to be replaced with a higher rating to reflect the 100% increase in loading.

Planned maintenance of the Converter stations would also be increased, as a consequence of the higher burden on the power converters and associated hardware.

3.2.3.j.10. COST IMPLICATIONS

Initial costs of implementing a system at a desired capacity, and upgrading an existing system to a higher capacity are summarized in Figure 74 and the several pages following. This is based on the simple cost model, as referenced in 3.2.3.j.1. This has been generated for the basis of comparison only, and specific cost evaluations are required based on an actual route, and analysis of scheduling and cyclic traffic demands.

Number of vehicles	40
Vehicle spacing	63 s (8.4 km)
Number of Converter stations	20
Leap-frogging of magway blocks	Yes
Average power per Converter station	12 MW
Number of 60 MVA substations	6

Figure 71 Parameters for 8,000 seat/hour model

Number of vehicles	60
Vehicle spacing	42 s (5.6 km)
Number of Converter stations	20
Leap-frogging of magway blocks	No
Average power per Converter station	17 MW
Number of 60 MVA substations	6

Figure 72 Parameters for 12,000 seat/hour model

Number of vehicles	120
Vehicle spacing	22 s (2.9 km)
Number of Converter Stations	20
Leap-frogging of magway blocks	No
Average power per Converter station	34 MW
Number of 60 MVA substations	12

Figure 73 Parameters for 22,900 seat/hour model

TOTAL ESTIMATED CAPITAL COST PER BASELINE ROUTE

Build 4,000 pph route	2,901,420	k$
Upgrade to 8,000 pph	407,396	
Upgrade to 12,000 pph	509,824	
Upgrade to 25,000 pph	1,219,215	
TOTAL (at 25,000 pph)	5,037,855	k$

DETAIL PAGES: Please refer to Supplement B.

Figure 74 Costs of the capacity upgrade plan (summary and detail pages following)

3.2.3.k. BAGGAGE AND FREIGHT

Section 3.2.1.c.3.3 describes space available for baggage storage on-board both the 45 and 140 passenger vehicles. There is additional space available in overhead storage bins.

It is anticipated that for long distance travel where significant luggage was brought on board the vehicle, additional time would be required for the loading of luggage over that needed for shorter trips where baggage would be minimal. Times to load and dispatch do not slow system operations since loading will occur off-line and not impede traffic flow on the corridor.

Passenger carrying vehicles will not carry significant amounts of freight. Express mail and overnight packages can be hauled without appreciable effect on station dwell time.

A freight version of the vehicle is described in Supplement D, Section B. Loading provisions are similar to containerized freight loading used in airlines. Times to load and dispatch freight vehicles are not relevant to system operations since loading will occur off-line and not impede traffic flow on the corridor. Freight vehicles may be mixed with passenger vehicles on the route when spaces are available in the traffic flow.

3.2.3.el. HUMAN FACTORS

Human factors are those that govern public acceptance of Magneplane. These are crucial, since Magneplane is intended to compete with the private automobile as well as railroads and airlines. The most important human factors are:

Access time (proximity of stations)
Access convenience (intermodal connections)
Space requirement
Waiting time (frequency of service)
Trip time (station to station)
Comfort (ride quality, amenities, luggage)
Cost

All of these considerations were foremost in the development of the original Magneplane concept, and they are still the driving forces behind design decisions. Because of our success in accounting for human factors, Magneplane will gain a major fraction of automobile ridership.

A more complete discussion of the advantages of Magneplane is given in section 5.3.7.

Access time is minimized by Magneplane's ability to locate multiple stations in every metropolitan area, and at frequent intervals along interstate highways. Individual vehicles can exit and enter the main magway without slowing the main traffic flow so as to service a large number of off-line stations located along loops and spurs.

Access convenience is maximized by small stations that can be located where travel and priority freight originates and terminates: at shopping malls, office parks, residential developments, downtown centers, and existing transit stations and airports.

Space requirements are minimized by multiple small stations in a city. Center-city stations need only be large enough to serve traffic originating in the city itself; suburban traffic will be served by suburban stations. This plan reduces the need to construct new parking and other facilities. It eliminates the need for new megahubs. Stations can be added easily, since vehicle switching will be done without the need for moving parts or major construction (when the passive switch design is completed).

Waiting time is minimized by dynamic scheduling. Traffic management is based on immediate demand, as continuously calculated by ticket purchases. Purchases by telephone several minutes in advance can reduce waiting time to nearly zero. A vehicle will be dispatched to provide non-stop or one-stop service between any station pair whenever a certain number of riders have purchased tickets between these stations, or whenever any smaller number of riders have waited at the origin station for some time limit (probably 5-10 minutes). This is made possible by the use of small, individually controlled vehicles operating at minimum headways as short as 20 seconds.

Trip time is minimized by non-stop or one-stop scheduling, and by Magneplane's ability to self-bank like airplanes, thereby making bank angles up to 45 degrees acceptable. In the case of the New York Thruway, for example, Magneplane can achieve an average speed of 130 m/s (295 mph), as compared to 80 m/s (182 mph) predicted for the Grumman system with a maximum bank of 24 degrees (all other conditions being equal).

Comfort is optimized by two of Magneplane's central features: (1) the ability to self-bank like airplanes, and the construction with zero unsprung mass. Self-banking permits high speed curves with no lateral forces on passengers. It may also permit three-dimensional (helical) curve transitions (chandelle maneuvers), which can almost eliminate both lateral and vertical acceleration forces. The use of chandelles is still under study.

Vehicle design using zero unsprung mass is important because it reduces magway stiffness and precision requirements and thus initial cost, minimizes fatigue loads on vehicle and magway structures, thus reducing life cycle cost, and improves ride quality very substantially over systems which require a secondary suspension. In fact, the ability to eliminate secondary suspensions is one of the leading advantages of maglev over wheeled systems, and we consider it irresponsible to ignore and discard this advantage.

Acceptable limits of ride quality remain to be determined as the public becomes accustomed to this new form of transportation. But whatever the limits turn out to be, the inherent resiliency and self-banking of Magneplane ensure that it will outperform any other system which requires a secondary suspension.

Cost is minimized by a combination of factors. The most important single factor is Magneplane's ability to attract and handle up to 25,000 passengers per hour on one magway. Each magway needs to carry only about 50 tons of live load, and requires wayside power stations rated at only 13 MVA in most places. A significant related factor is the very low requirement for stiffness and alignment precision: Magneplane can operate with beam deflections of span length over 1500, as compared to 4,000 for Transrapid type suspensions, and even more for wheeled trains. Other cost-minimizing factors are:

- High average load factors, made possible by the use of small, demand-scheduled vehicles
- Low energy loss in re-acceleration, due to non-stop or one-stop service, and power-regenerative braking, which returns a large fraction of kinetic energy to the power system.
- Resilient suspension with zero unsprung mass, which minimizes fatigue wear on vehicle and magway structures.
- The use of air-lubricated landing skids instead of wheels.
- The flexibility to take up any passenger slack with priority freight, both day and night.

INDEX

to the System Concept Definition Report, volumes 1-5

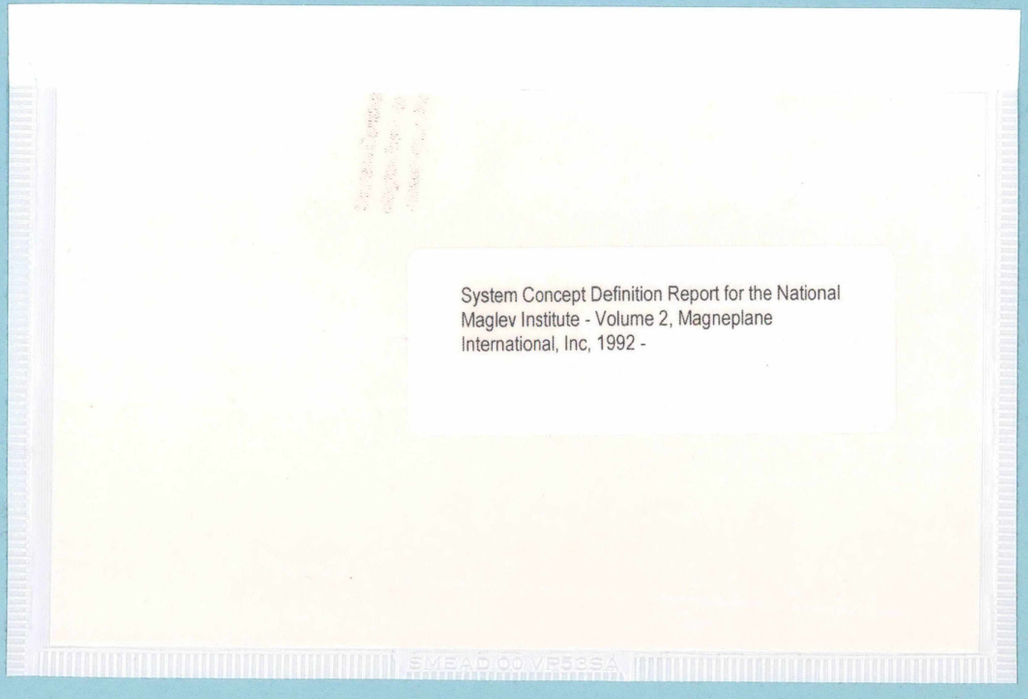

System Concept Definition Report for the National Maglev Institute - Volume 2, Magneplane International, Inc, 1992 -